PB 198 400

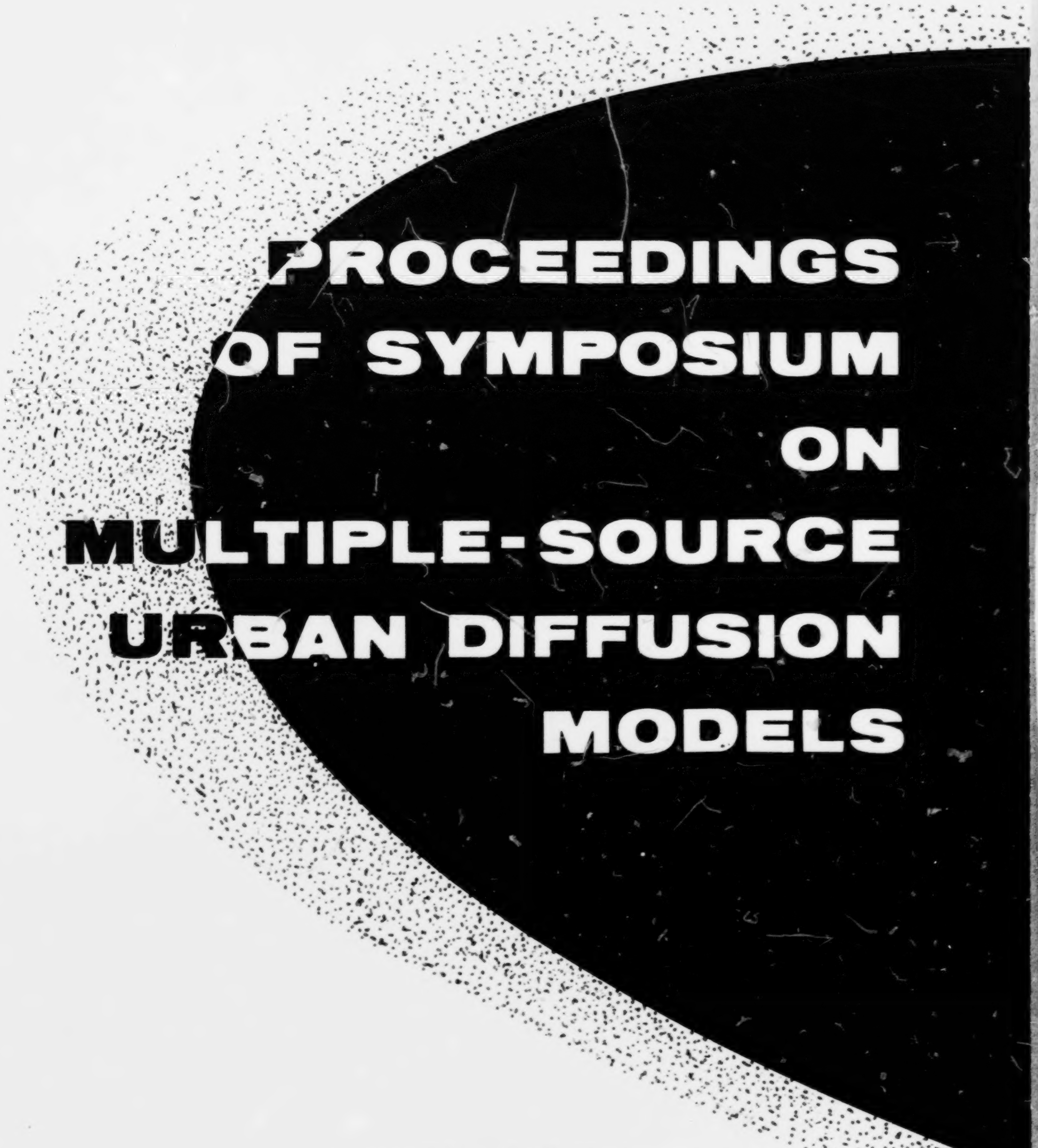

PROCEEDINGS OF SYMPOSIUM ON MULTIPLE-SOURCE URBAN DIFFUSION MODELS

Reproduced by
NATIONAL TECHNICAL
INFORMATION SERVICE
Springfield, Va. 22151

U. S. ENVIRONMENTAL PROTECTION AGENCY

416

PB 198 400

BIBLIOGRAPHIC DATA SHEET

1. Report No.
APCO-Pub-AP-86

2.

3. Recipient's Accession No.

4. Title and Subtitle
Proceedings of Symposium on Multiple-Source Urban Diffusion Models

5. Report Date
December 1970

6.

7. Author(s)
Arthur C. Stern (ed.)

8. Performing Organization Rept. No.

9. Performing Organization Name and Address
U. S. Environmental Protection Agency
Air Pollution Control Office
Research Triangle Park, North Carolina

10. Project/Task/Work Unit No.

11. Contract/Grant No.

12. Sponsoring Organization Name and Address
Same as above

13. Type of Report & Period Covered

14.

15. Supplementary Notes

16. Abstracts

A complete collection of thirteen papers presented at this symposium on urban diffusion models is provided in this volume. Also included those discussions that were subsequently submitted in writing.

17. Key Words and Document Analysis. 17a. Descriptors

Urban areas
Dispersing
Diffusion
Mathematical models
Carbon monoxide
Sulfur dioxide

17b. Identifiers/Open-Ended Terms

Diffusion models
Multiple source
Tracers (meteorological)

17c. COSATI Field/Group 13/B

18. Availability Statement Superintendent of Documents
Government Printing Office, Washington, D.C. 20402 - SOD No: FS2.300:AP-86

19. Security Class (This Report)
UNCLASSIFIED

20. Security Class (This Page)
UNCLASSIFIED

21. No. of Pages

22. Price
$ 1.75

FORM NTIS-35 (10-70)

USCOMM-DC 40329-P71

C

PROCEEDINGS
OF
SYMPOSIUM
ON
MULTIPLE-SOURCE
URBAN DIFFUSION
MODELS

Editor: Arthur C. Stern

Sponsors: National Air Pollution Control Administration
and North Carolina Consortium on Air Pollution

U.S. ENVIRONMENTAL PROTECTION AGENCY
Air Pollution Control Office
Research Triangle Park, North Carolina, 1970

For sale by the Superintendent of Documents, U.S. Government Printing Office
Washington, D.C., 20402 - Price $1.75

The AP series of reports is issued by the Air Pollution Control Office to report the results of scientific and engineering studies, and information of general interest in the field of air pollution. Information reported in this series includes coverage of APCO intramural activities and of cooperative studies conducted in conjunction with state and local agencies, research institutes, and industrial organizations. Copies of AP reports are available free of charge to APCO staff members, current contractors and grantees, and nonprofit organizations — as supplies permit — from the Office of Technical Information and Publications, Air Pollution Control Office, Environmental Protection Agency, Research Triangle Park, North Carolina 27709

Air Pollution Control Office Publication No. AP-86

PREFACE

This symposium was conducted under the terms of a contract between the Meteorology Division of the National Air Pollution Control Administration (NAPCA) and the Department of Environmental Sciences and Engineering, School of Public Health, University of North Carolina at Chapel Hill (UNC). The contract officer for the sponsor was Mr. Lawrence E. Niemeyer, Assistant Director, Division of Meteorology, NAPCA. The responsible officer for the University was Arthur C. Stern, Professor of Air Hygiene. The symposium was held from October 27 to 30, 1969, at the Carolina Inn on the University campus. On December 4, 1970, the functions of NAPCA were transferred to the Air Pollution Control Office (APCO) of the Environmental Protection Agency. All references to the former, therefore, now refer to the latter.

Although UNC was the contractor, it was agreed that the symposium would be sponsored by the North Carolina Consortium on Air Pollution, comprising: Duke University; North Carolina State University; the Office of Manpower Development, NAPCA; Research Triangle Institute; and the University of North Carolina at Chapel Hill. The detailed planning for the symposium was done by a steering committee representing the members of the Consortium and the contract officer.

All the papers, both invited and volunteered, that were presented during the symposium, are included in this volume. In addition to the invited participants, some attendees were selected from persons who responded to the public announcement of the symposium. Almost all papers were preprinted and distributed to participants in advance of the meeting. Although there was open discussion after every presentation except the Keynote and Banquet speeches, the only discussions incorporated in the Proceedings are those subsequently submitted in writing.

Questions from the floor and authors' responses do not appear unless those same questions and answers were also included in the written discussion. Every author questioned was given an opportunity to submit a rebuttal. The nature of such an arrangement made it necessary, for the sake of coherence, to incorporate all discussion in a separate chapter, divided into two sections: speaker-directed discussions and discussions submitted by the participants.

Particular thanks are given to the graduate students in Air Pollution in my department at UNC, who acted as floor monitors during the symposium – particularly to Harvey Jeffries and Douglas McKay, who managed the audio-visual arrangements throughout the symposium. The registration of participants and the preparation of the symposium program and information kits were ably handled by the Continuing Education Department of the School of Public Health, UNC. I am especially appreciative of the excellent services of my secretary, Martha Davis, for her help in the preparation and conduct of the symposium and in the coordination of these proceedings.

Arthur C. Stern
Chapel Hill, N. C.
November 1970.

STEERING COMMITTEE

Dr. Jay Apple, Director, Institute of Biological Sciences, North Carolina State University.

Dr. Robert Barnes, School of Forestry, Duke University.

Mr. James L. Dicke, Meteorologist, Office of Manpower Development, Air Pollution Control Office.

Dr. James S. Ferrell, Department of Chemical Engineering, North Carolina State University.

Dr. Kenneth Knoerr, School of Forestry, Duke University.

Dr. Harry Kramer, Director, Office of Manpower Development, Air Pollution Control Office.

Mr. Lawrence Niemeyer, Assistant Director, Meteorology Division, Air Pollution Control Office.

Professor Arthur C. Stern, Department of Environmental Sciences and Engineering, School of Public Health, University of North Carolina at Chapel Hill.

Mr. James J. B. Worth, Associate Director of Engineering, Research Triangle Institute.

SESSION CHAIRMEN

Mr. James J. B. Worth, Associate Director of Engineering, Research Triangle Institute.

Dr. Lester Machta, Director, Air Resources Laboratories, National Oceanic and Atmospheric Administration.

Mr. Robert A. McCormick, Director, Meteorology Program, Air Pollution Control Office.

Dr. Kenneth Knoerr, School of Forestry, Duke University.

Dr. Walter J. Saucier, Department of Geosciences, North Carolina State University.

Typed ——— copy [illegible]
only underlined
chapters

Contents :-

CONTENTS

1. *John T. Middleton*
Keynote Speech: Diffusion Modeling for Urban Air Pollution Abatement and Control 1-1

2. *Heinz H. Lettau*
Physical and Meteorological Basis for Mathematical Models of Urban Diffusion Processes 2-1

3. *Frank Pasquill*
Prediction of Diffusion over an Urban Area—Current Practice and Future Prospects 3-1

4. *Kenneth L. Calder*
Some Miscellaneous Aspects of Current Urban Pollution Models 4-1

5. *Warren B. Johnson, Francis L. Ludwig, and Albert E. Moon*
Development of a Practical, Multi-purpose Urban Diffusion Model for Carbon Monoxide 5-1

6. *John J. Roberts, Edward J. Croke, and Allen S. Kennedy*
An Urban Atmospheric Dispersion Model 6-1

7. *Glenn R. Hilst*
Sensitivities of Air Quality Prediction to Input Errors and Uncertainties 7-1

8. *Shin'ichi Sakuraba in collaboration with M. Mariguchi and I. Yamazi*
Elevation of Tracer Cloud over an Urban Area 8-1

9. *Heinz G. Fortak*
Numerical Simulation of the Temporal and Spatial Distributions of Urban Air Pollution Concentration 9-1

10. ***Liau J. Shieh, Ben Davidson, and J. P. Friend***
A Model of Diffusion in Urban Atmospheres: SO_2 in Greater New York 10-1

11. ***James R. Mahoney, William O. Maddaus, and John C. Goodrich***
Analysis of Multiple-Station Urban Air Sampling Data 11-1

12. ***Morris Neiburger***
Banquet Speech: Progress + Profits + Population = Pollution 12-1

13. ***Arthur C. Stern***
Symposium Summary: Utilization of Air Pollution Models 13-1

14. Discussions 14-1

15. Appendix: Attendance List 15-1

PROCEEDINGS
OF
SYMPOSIUM
ON
MULTIPLE-SOURCE
URBAN DIFFUSION
MODELS

AUTHOR

JOHN T. MIDDLETON, Acting Commissioner of the Air Pollution Control Office, was Professor and Director of the University of California State-wide Air Pollution Research Center where his pioneer studies of the environment as a regulating factor in disease development in agricultural crops enabled him to first recognize photochemical air pollution as an adverse economic factor to California agriculture in the mid-1940's.

Dr. Middleton has served in the past as: Chairman, California Motor Vehicle Pollution Control Board; member, Governor's Interagency Committee on Air Pollution, and Executive Task Force on Waste Management; consultant, U. S. Public Health Service, Office of Science and Technology, and the World Health Organization; and as a Director for the Air Pollution Control Association.

Dr. Middleton has a B.S. from the University of California and a Ph.D. from the University of Missouri.

Keynote Speech

1. DIFFUSION MODELING FOR AIR POLLUTION ABATEMENT AND CONTROL

JOHN T. MIDDLETON

Acting Commissioner, Air Pollution Control Office
Environmental Protection Agency

I am very pleased to be with you this morning, and to have the chance to talk to you about the urgent need for developing systematic solutions to one of the most ironic incongruities we face in this country today, the problem of air pollution.

Some months ago, we received from the National Aeronautics and Space Administration photographs of portions of the United States taken from Apollo 8 as it streaked toward the moon. NASA sent us these particular photographs because one of the more interesting phenomena they featured was the pall of air pollution hanging over a number of large urban areas. Here, it seems to me, is the irony for our time, a spaceship, carrying men to the moon and back, capturing with its cameras our tragic failure to prevent the contamination of the earth's most precious resource, the air that all of us breathe.

Of all the threats to our environment, air pollution is potentially the most dangerous; certainly it is the most difficult to solve. We cannot replenish the air as we replenish soil and trees; and we cannot purify the air, as we do water, before we use it. We must breathe the air as it comes to us—and each day it comes to us more heavily laden with the by-product wastes of our industrialized society.

Today, this Nation is paying billions of dollars each year for the dubious privilege of living with—rather than controlling—air pollution. Air pollution soils, corrodes, and damages a wide variety of structures in our cities and towns—from the despoiling of our homes to the corrosion of suspension bridges that span our rivers. It threatens forests and farmlands as well. It constitutes a national health hazard of greater significance than many may appreciate. It contributes to the rising incidence of such important respiratory diseases as lung cancer, asthma, bronchitis, and emphysema. Emphysema is the fastest growing cause of death in America today.

The ways in which we seemingly may be changing our environment through air pollution are endless; and they are international, as well as national, in their dimensions. An acid tongue of combustion products from the industrialized area of Western Europe is transported over the southern part of Scandinavia; and, particularly in the winter months when combustion activities are high, the acidity of rainfall in the area increases substantially. The ability of the soil to accommodate these international acid rains is certainly limited, and the consequent effects on vegetation and the ecosystem can only be guessed at.

Man introduces 10,000,000 tons of nitrogen into the atmosphere annually. This is comparable to the input of the natural nitrogen cycle. The main source of nitrogen contamination is inorganic agricultural fertilizers. The nitrates in the rivers and drinking water of some Illinois towns are now approaching the upper safe limit of 10 parts per million set by the Environmental Control Administration. As agriculture expands to keep the pace with world food needs, the problem of nitrates in water supplies will become more serious.

Although we are not sure of the health effects of the current levels of lead in our environment, we do know that a person's body burden of lead corresponds roughly to the levels in his environment and that those levels are going up as the use of the principal source of lead, the automobile, continues to increase. I have yet to see any data that show any useful purpose served by lead in the body.

The toxicity of mercury compounds has also been well established. The inhalation of only small amounts of mercury or its derivatives can result in exaggerated emotional response, muscular tremors, and gingivitis. This poisoning has occurred in most of the major industries that use mercury. Vegetation has been damaged when kept in a greenhouse painted with a mercury fungicide, and fish in some Swedish lakes have absorbed and concentrated methyl mercury from pesticides to such a high degree that fishing in those lakes has been prohibited.

Estimates differ about the potential effects on world temperature and climate due to increased atmospheric carbon dioxide and particulate concentrations. Estimates also differ on how much air pollution can affect precipitation and condensation. Questions are also being raised about the ultimate effect of man's conversion of energy to heat. The opinions differ about the details of processes involving temperature trends, climate, melting of polar ice caps, sea level, photosynthesis, and the distribution of fish, to name a few.

There are, of course, many other examples. The point is, that when man alters the balance of Nature, it is like tossing a pebble into a pond: the resulting ripples spread out concentrically from the entry point until they touch every point on the shore. Continued small alterations of our environment may have drastic effects later, effects we cannot foresee now.

Today we stand at a point in our scientific progress where our capacity to enhance—or to degrade—the quality of our environment is almost literally beyond reckoning. From the standpoint of our sheer survival as a nation and a people, it is essential that the talent and imagination of all of us—and especially of the scientific community—be engaged in enhancing it.

If it is obvious that one way to halt the contamination of the air we breathe is to prohibit automobiles, stop the generation of electricity, and shut down industry—it is just as obvious that this way is impossible. Air pollution is woven throughout the fabric of our daily lives. It is a by-product of the way we build our cities. It is a waste, left over from the ways we transport ourselves and our goods, and from the ways we generate the energy to heat and light the places where we live and work. It is part and parcel of the ways in which we produce and package a multitude of manufactured goods, and, among other things, the ways in which we use those goods and dispose of the remains.

The problem of air pollution, then, affects not one segment of society, but all segments. To deal adequately with such a problem has implications for thousands of daily decisions that are made in every activity of our busy modern life.

Air pollution is a direct threat to human health and welfare that no responsible person can put aside; but it is also a social, political, and economic problem. We will not truly come to grips with air pollution unless we derive our remedies from a careful consideration of what is truly in the public interest.

Here, then, is perhaps the most challenging frontier of our space-age society. Air pollution, like the other problems of our environment, is no longer the private preserve of the professional engineer, either in government or out. It is rather a problem that requires attention from all facets of our society if we and our institutions are to survive its solution. Governments at all levels must rise above their jealous disputes as to what jurisdictional rights are being violated by whom, and work together side by side as regional partners in a public enterprise that no single government possibly can carry off alone. The manufacturer will have to look beyond his assembly line and take responsibility for the performance of his product in the hands of the sometimes neglectful consumer. The industrialist is going to have to take responsibility for his use and misuse of those resources which sustain not only the industrial revolution in this country, but also our very lives. The scientist, hardly last and hardly least, must provide the technical solutions to those by-product problems that have unfortunately accompanied the modern miracles his science has created.

In the Clean Air Act, as amended, the Congress has attempted to give NAPCA* the legislative apparatus that we need to remove the malignancy of air pollution. This Act requires that we carefully consider all the ramifications of every step we take—and every step we do not take—in the control process. The Act charges us to protect the public in those places where air pollution has reached acute proportions and to prevent the problem from occurring in those places where fresh air is still enjoyed. On the other hand, the Act reflects an awareness that air pollution is the result of many of the activities that sustain our modern way of life. It says that we must optimize use of currently available technology to control and abate air pollution without disrupting these activities.

---

*Now APCO.

The Federal government has the responsibility for setting the machinery of the Clean Air Act in motion. Under the Act, the Department of Health, Education, and Welfare is required to draw the boundaries around each urban area of the country where we believe air pollution is a problem. So far we have drawn the boundaries around 20 major urban areas, and by the end of next summer we expect that we will have drawn the boundaries for a total of 57 air quality control regions, involving all the 50 states, the District of Columbia, Puerto Rico, and the Virgin Islands.

Last February we issued to the states criteria and control technique reports on two of the major families of air pollutants, the sulfur oxides and gross particulate matter. The states are now on notice to use this information in developing air quality standards for the regions we have designated and to design plans for implementing the standards.

It is at this later stage of the Clean Air Act procedure, the regional implementation plan, that the technique of diffusion modeling plays such an important role. I would like in the time remaining to me this morning to discuss that role in more detail.

In 1958, the year of the First National Air Pollution Conference, there appeared to be some element of doubt at least in the minds of some people as to whether there was indeed an air pollution problem... At that time, NAPCA's meteorologists were already engaged in developing an empirical diffusion equation. Weather Bureau wind summaries and an IBM 650 computer were used to furnish mean monthly sulfur dioxide concentration distributions for an entire urban area. The data from Nashville, Tennessee was used to test the model. Although the absolute magnitude of the concentrations could not be verified, patterns that were predicted and observed were generally similar for the 5-month test period. This was the first step by NAPCA scientists, indeed the first by any group following Frenkiel's pioneering effort in 1955, to delineate mathematically transport and dispersion processes on an urban scale.

We have come a long way since 1958, and NAPCA's Division of Meteorology has not been alone in its modeling efforts. In recent years its work has been complemented by modeling work conducted by meteorologists at New York University, the University of California at Los Angeles, the University of Florida, and ESSA's Air Resources Laboratory. Studies have also been conducted by Travelers Research Center and the Stanford Research Institute. Work also goes on abroad. There has been diffusion modeling by scientists in Germany, Hungary, Japan, England, and Canada. Some of their developments will, I understand, be presented at this symposium, and that is good. The need for abatement of air pollution is a strong international tie.

As we proceed with the implementation of the Clean Air Act, the meteorologist will be called upon more often to provide a mathematical description of the transport of air pollution in the research, survey, and operational phases of control activities. In essence, the meteorologist is charged, because of time limitations and paucity of air quality measurements, with the chore of presenting convincing evidence of the magnitude and frequency of pollution transport and dilution. The diffusion models we have been discussing are the yardsticks for furnishing quantitative determinations of ambient air concentrations of pollutants. These determinations must be credible enough to satisfy the members of other scientific and technical disciplines, as well as representatives of legal, economic, and political interests. These models should also be flexible enough to assimilate feedback from source emissions for obtaining solutions to both chronic and acute pollution problems.

Future diffusion models that incorporate air pollution climatology are expected to be used more frequently in long-range air-resource-management programs for the evaluation of future air quality and source locations with regard to projected emissions rates and population distributions. In order to interpret the relationships between proposed or existing source emission standards and ambient air quality standards, we need a quantitative account of the meteorological processes that cause pollutants to be diluted, chemically changed, or dispersed between source and receptor. Our hope is that by applying diffusion models to calculate the integrated effects of multiple sources of the same pollutant, we will be able to interpret the relationships between proposed or existing source emission standards and ambient air quality standards.

The advantages of this computer age technology have already been recognized by responsible segments of commerce and industry, and more recently by community planning agencies. In the words of Jimmy Durante, "everybody wants to get into the act."

Another application of diffusion models will come with the evaluation of the effectiveness of individual control or abatement procedures for a given source or complex of sources. By use of appropriately programmed models, such an assessment may be made without the need for an intricate and dense network of air quality measurements taken at the right place in the right time at the right season. Using diffusion models, the meteorologist can greatly reduce the time and cost of such evaluations by answering the questions of what actually constitutes "the right place, length of time and season." Moreover, under operating situations one may expect that the short-term-period diffusion model will be employed to determine the amount of emission decrease required to meet air quality standards. Such models will also be helpful in the strategic deployment of mobile air quality and meteorological monitoring units during air pollution alert situations.

So far as a warning scheme is concerned, the heart of any effective air pollution control strategy will be meteorological forecasts that can provide the necessary lead times and guidance required to deploy and implement abatement and control devices. The *sine qua non* of such forecasts is the capability of meteorological techniques to forecast meteorological conditions within the urban boundary layer on urban scales appropriate to the air pollution problem.

There are some meteorologists, and I must agree with them, who suggest that the utility of present diffusion models is limited by the inability to make accurate forecasts of wind and temperature profiles. I think it is abundantly clear that the accurate description within the planetary boundary layer of the profiles of wind, temperature, and moisture and their variability in time and space as a function of surface conditions and of synoptic-scale features is a fundamental requirement for improved meteorological services not only to air pollution problems, but also to many other interests. We have an urgent need, it seems to me, for greatly improved mesoscale forecasting from the national weather services.

I do not ask for a doctoral dissertation on a weather forecast; all I ask is that we be supplied with the facts that we need to do our job, the facts that you gentlemen need to make your diffusion models more efficient. I think we agree that the quality of your results depends upon the information you start with.

To alleviate to some degree the inadequacies in mesoscale observations and forecasts in the United States, we are supporting the Environmental Science Services Administration program of low-level soundings in five urban areas. The program provides for a full-time meteorologist to concentrate on mesometeorological-scale forecasts in these five metropolitan areas, particularly as they relate to air pollution. Hopefully, ESSA will be able to assume responsibility for such services in these five cities and to extend them to an additional 15 cities in the next fiscal year.

The programs that we are supporting in the National Air Pollution Control Administration to improve our knowledge in the atmospheric sciences area may seem to some of you at first glance to be a far cry from the usual business of a Federal regulatory agency. A closer look, I think, will reveal (1) that these and other research programs in NAPCA are a vital link in the control process and fully congruous with the fundamental thesis of the Clean Air Act and (2) that our efforts to control air pollution should be derived from a careful evaluation of the latest scientific evidence of the effects of air pollution on health and welfare. This systematic approach to control, this linking of the control effort to scientific evidence of the need for control, seems to me to lend a vitality to the research area that it might never otherwise acquire. I am hopeful that the research programs we have found it necessary to support in

NAPCA, in order to give us that information so vital to the planning of our control program directions, will stimulate other agencies and institutions to begin to explore this as yet largely untouched area of the meteorological sciences.

In this regard, diffusion models such as have been developed up till now, and the generations of models yet to come as we refine, expand, and develop our techniques, can play a vital role in our attempt to systematically apply air pollution control theory on a regional basis. For this reason, I wish all of you Godspeed in your deliberations at this symposium.

ABSTRACT

Diffusion processes in the volume of air above a geographical area can be described in spatial detail with two- and three-dimensional vector models drawn from boundary layer and fluid dynamics concepts. A simpler scalar model, in particular, can directly account for temporal trends in average pollutant levels due to simultaneous diffusion of mass, energy, and momentum from multiple sources.

By an application of climatonomy, the qualitative box model of scalar diffusion is expanded quantitatively with fluid dynamic equations. The theoretical model has been applied to prediction of both long-and short-range, thermal and particulate pollutant trends in large and small cities. The use of the box model to evaluate aerodynamic momentum drain over the built-up area of a city is also described. City types are specified in terms of their aerodynamic roughness parameter with a formula based on results of micrometeorological experiments. Knowing only the horizontal pressure gradient in the lower troposphere the model makes it possible to estimate the characteristic wind speed for a specific city type.

In comparison with Davenport's power law, a Universal Wind Spiral Theory described here has the advantages of yielding quantitative estimation of directional shear and surface roughness effect on the wind profile. Examples of scalar and vector application of the latter law to thermal pollution are discussed.

AUTHOR

HEINZ H. LETTAU is Professor of Meteorology and Civil Engineering at the University of Wisconsin, where his current research is directed toward modeling earth-air interaction processes. His model of the hydrological cycle for restoring the level in water sheds was one of the earliest attempts at environmental modeling. He has been a research scientist at the Geophysics Research Directorate U.S. Air Force, Cambridge, Massachusetts; Fellow of the American Meteorological Society; corresponding member of the Bavarian Academy of Science; member of the NAPCA Research Grants Advisory Committee, and is main editor of the two-volume **Exploring the Atmosphere's First Mile, 1957.**

Dr. Lettau received his Ph.D. in geophysics from the University of Leipzig in 1931.

2. PHYSICAL AND METEOROLOGICAL BASIS FOR MATHEMATICAL MODELS OF URBAN DIFFUSION PROCESSES

HEINZ H. LETTAU

University of Wisconsin at Madison

INTRODUCTION

I shall discuss some general aspects of processes taking place in the atmospheric boundary layer when wind passes over urban terrain. Emphasis will be on simultaneous diffusion of mass, energy, and momentum with special consideration of aerodynamic resistance due to roughness of urban surfaces and resulting feedback on the diffusion potential of the urban atmosphere.

I shall start with an illustration familiar to you. Figure 2-1 shows what I would like to call the "vector model" of diffusion from multiple sources. This illustration comes from a report by Moses[1] demonstrating the conventional approach that assigns one grid to the sources and another grid to the receptors, with a composite of "plumes" in between. The merits of this basic model for the study of the details of complex urban diffusion processes are obvious, and I trust that its implications and desirable refinements will be competently discussed by other participants at this Symposium.

Let me contrast the vector model with a "scalar model" (Figure 2-2) in which the volume of "city-air" is somewhat crudely defined. Pollutant emission is attributed to a quasi-uniform area source at the lower boundary. The major flushing agency is horizontal air motion, additionally supported by vertical eddy flux at the level h^* that tops the volume. If no other city is immediately upstream, the wind enters the volume relatively clean but leaves it loaded with emission products. The level h^* may coincide with an inversion of temperature, in which case vertical exchange through this level will be of minor importance. Such scalar or "box-models" of urban diffusion have been mentioned occasionally in the literature. They cannot be used for the study of spatial detail, but produce interesting, specific results, if emphasis is placed on time-series (either short- or long-range trends). Moreover, the box-models permit discussion of similarities between air diffusion and other natural processes such as the loading of a watershed by precipitation, discharge into river channels, and losses by evapotranspiration. It is not my

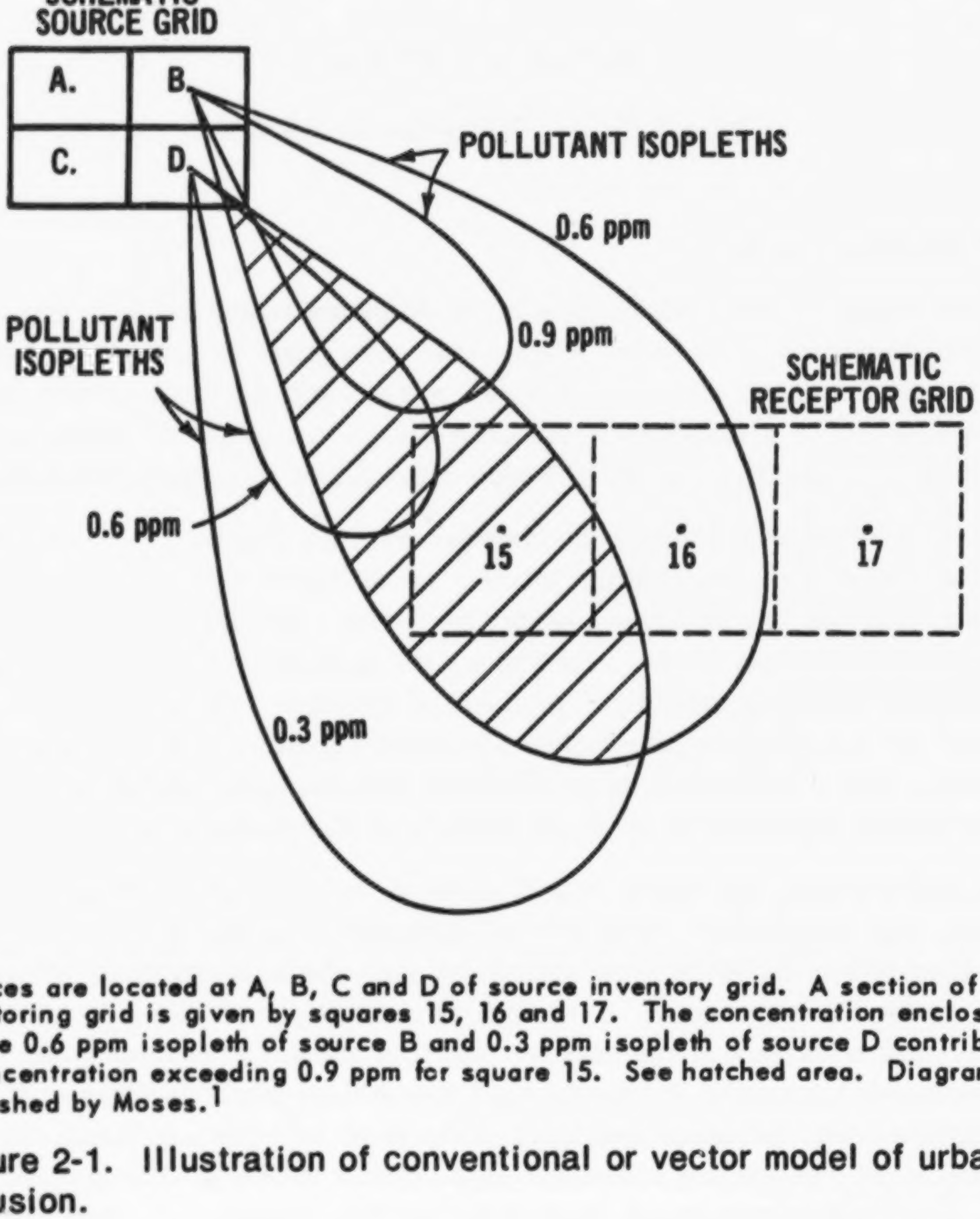
SCHEMATIC SOURCE GRID
A.
B.
C.
D.
POLLUTANT ISOPLETHS
0.6 ppm
0.9 ppm
POLLUTANT ISOPLETHS
SCHEMATIC RECEPTOR GRID
0.6 ppm
15
16
17
0.3 ppm

Sources are located at A, B, C and D of source inventory grid. A section of the monitoring grid is given by squares 15, 16 and 17. The concentration enclosed by the 0.6 ppm isopleth of source B and 0.3 ppm isopleth of source D contribute a concentration exceeding 0.9 ppm for square 15. See hatched area. Diagram as published by Moses.[1]

Figure 2-1. Illustration of conventional or vector model of urban diffusion.

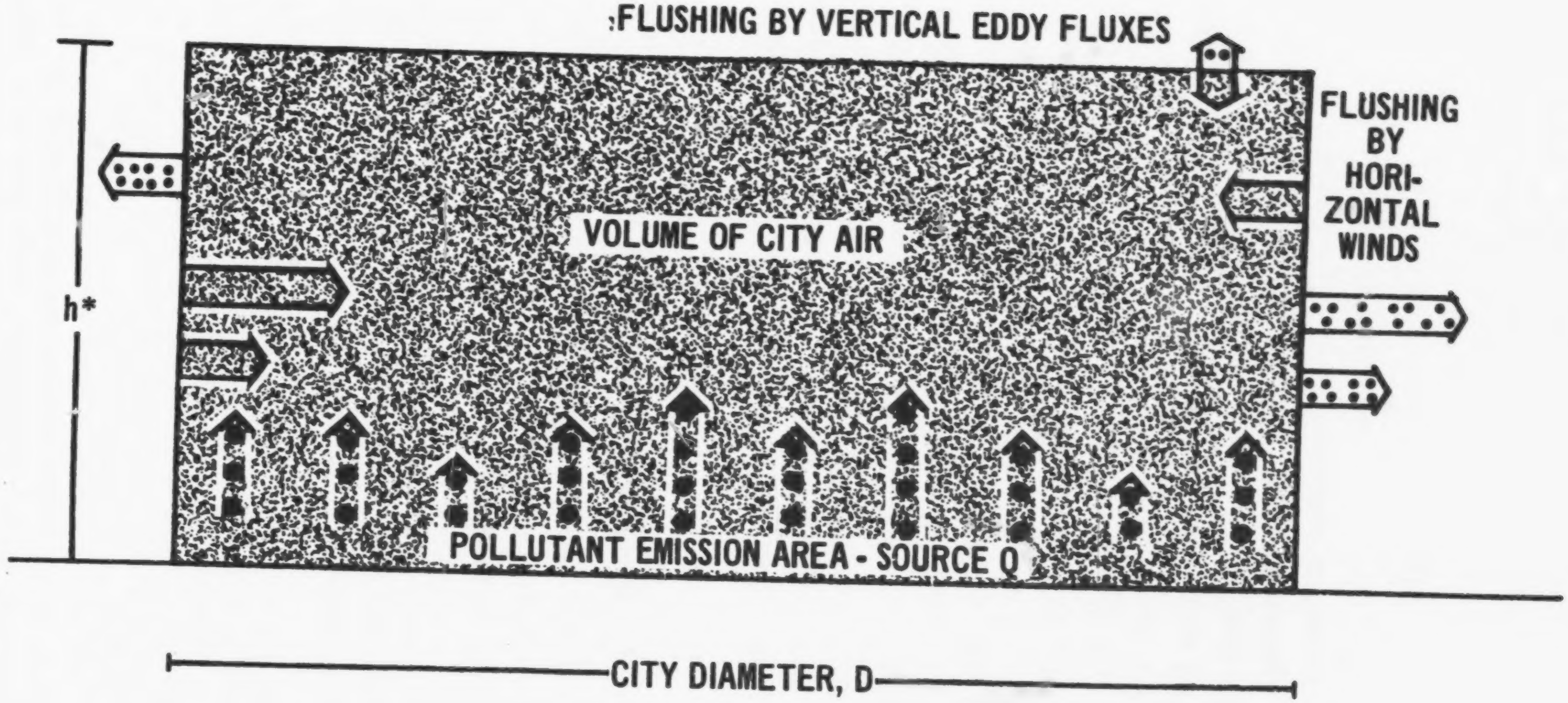
FLUSHING BY VERTICAL EDDY FLUXES
FLUSHING BY HORI-ZONTAL WINDS
VOLUME OF CITY AIR
h*
POLLUTANT EMISSION AREA - SOURCE Q
CITY DIAMETER, D

Figure 2-2. Schematic illustration of box or scalar model of urban diffusion.

intention, however, to discuss the descriptive concept of an "air shed."[2] I prefer instead to consider a basic similarity between air pollution dispersal and the hydrologic cycle that permits me to utilize a theoretical solution of the water balance equation recently described by Lettau.[3]

Parameter Considerations

Before moving to that point, let me insert a general statement: The entity of transport and flux processes must be taken into account in fluid dynamics problems. Thus, in atmospheric boundary layer studies we should not restrict our consideration to transport of mass (either intentionally or inadvertently loaded on the moving fluid) but should investigate concurrent generation and dissipation of both momentum and energy. The scalar model (Figure 2-2) has the advantage over the more specialized vector model of Figure 2-1, that it can, without alteration, express a city area as a *heat source* (essentially due to the combustion of fuels), as well as a *momentum sink* or *negative momentum source* (due to the efficiency of buildings as aerodynamic roughness elements). A coherent consideration of the transport and flux of mass, momentum and energy in any atmospheric boundary layer is also a logical starting point for the discussion of mechanical and thermodynamic feedback since the horizontal dimensions involved in urban boundary layer structure are comparable to meso-meteorological and synoptic-scale atmospheric processes.

Aerosol Effects on Sunlight Absorption—Example

Let me begin discussion of the combined aspects of long-term trends and feedback on meteorological phenomenon, by considering the attenuation of sunlight by pollutants in the volume of city air.

McCormick and Ludwig[4] have recently discussed climatic modification by atmospheric aerosol. Let me illustrate my approach with Figures 2-3 through 2-5,* taken from a recent publication by K. and H. Lettau.[5] A common

---

*On some graphs the word "climatonomy" will appear. This word is also found in the title of the references by Lettau[3] and K. and H. Lettau.[5] It is a new term that we use at the University of Wisconsin to indicate a systems approach to problems of climate. *System* in engineering problems is conventionally used to encompass the following components: (1) a process, (2) an input to the process, or a forcing function, (3) an output from the process, or a response function, (4) feedback, and (5) control of inputs, or management of the system. Typical of climatonomy is the use of a mathematical-physical model of a specific atmospheric process, such as the response of a climatic element to a defined forcing function, which may be an insolation cycle or another defined input like pollutant emission. The climatonomic approach considers physically significant parameterization of the problem so that, even though control or management may not be possible, one could reasonably and realistically answer such questions as what response can be predicted if, for reasons beyond control, the intensity of the forcing function, and/or the value of a response-controlling parameter, would be halfed, doubled, or increased by any specified multiplication factor. A characteristic result of a climatonomic case study is documented on Figures 2-4 and 2-5.

scheme appears on all three graphs. It is intended to bring out the contrast in attenuation of insolation by typical aerosol between a big city [represented by Kew (London), England] and that of an extremely dry desert [represented by the Pampa de la Joya, Peru]. We selected these data from the published literature because the measurements include not only direct sunlight or "beam radiation" but also scattered or diffuse light. Note that external conditions (sun's elevation angle, optical air mass, etc.) happen to be such that the attenuation of beam radiation was nearly the same at both stations.

In Figures 2-3 to 2-5 the upper horizontal line represents the atmosphere–space border, across which solar rays enter the atmosphere and reflected light ("earth-shine") returns to space. The lower horizontal line represents the earth–air boundary, at which the attenuated solar beam and the diffuse light scattered down from the sky arrive. The dashed arrows show the sunlight that is reflected by the ground and attenuated in the air before entering space; part is scattered back down and part is absorbed. Numbers along, and at the tips of the arrows show fractions of scattering and absorption as decimal fractions of the unit incident-extra-atmospheric irradiation. These are always separated into downward and upward components. Numbers above and below the braces indicate combined radiation intensities as decimal fractions of the unit solar radiation budget.

Figure 2-3 shows that beam attenuation was nearly identical in both cases with reductions from 100% to 61.8% in Kew, and to 61.9% in La Joya. The city air absorbs 22.5 percent and scatters 15.7 percent (5.2% outwards and 10.5% downwards), or about 2/3 of the absorption. The desert air on the other hand absorbs 14.3 percent and scatters 7.9% + 15.9% = 23.8%, about 5/3 of the absorption. Figures 2-4 and 2-5 suggest that the assumed aerosol increase, first by an arbitrary factor of two and then of five, leads to extinction of direct sunlight in both locations. This means that the sun, although visible in the sky, will not throw a shadow. Obviously, the "gloom at noon" under the opaque smog of the city where only 26.9 percent of the incoming energy reaches the ground will be more frightening than under the strongly-scattering, mineral-particle-containing desert dust where 55.6 percent of the energy reaches the ground. If an aerosol increase by a factor of five is possible, what can be done to control the increase once the factors are known? Let us discuss it first with the aid of the box (scalar) model of community air pollution.

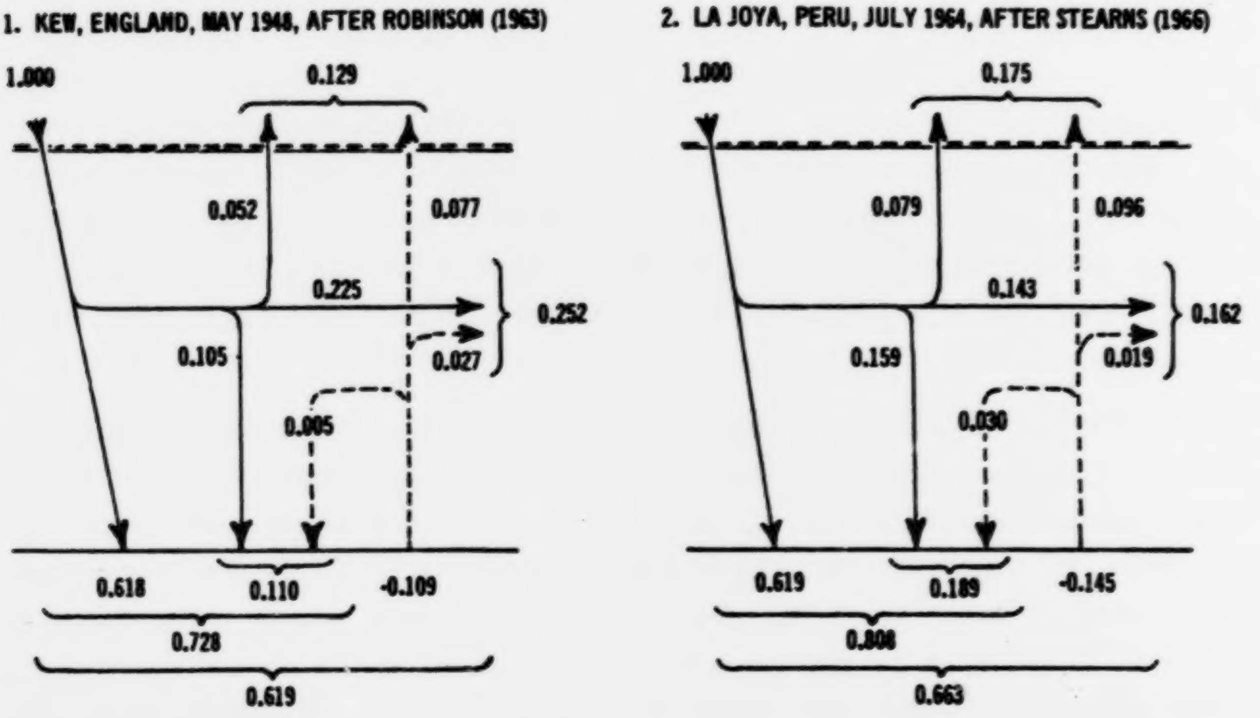

1. KEW, ENGLAND, MAY 1948, AFTER ROBINSON (1963)

2. LA JOYA, PERU, JULY 1964, AFTER STEARNS (1966)

1.000
0.129
0.052
0.077
0.225
0.252
0.105
0.027
0.005
0.618
0.110
-0.109
0.728
0.619
1.000
0.175
0.079
0.096
0.143
0.162
0.159
0.019
0.030
0.619
0.189
-0.145
0.808
0.663

Figure 2-3. Shortwave radiation budget—air over city versus air over desert.

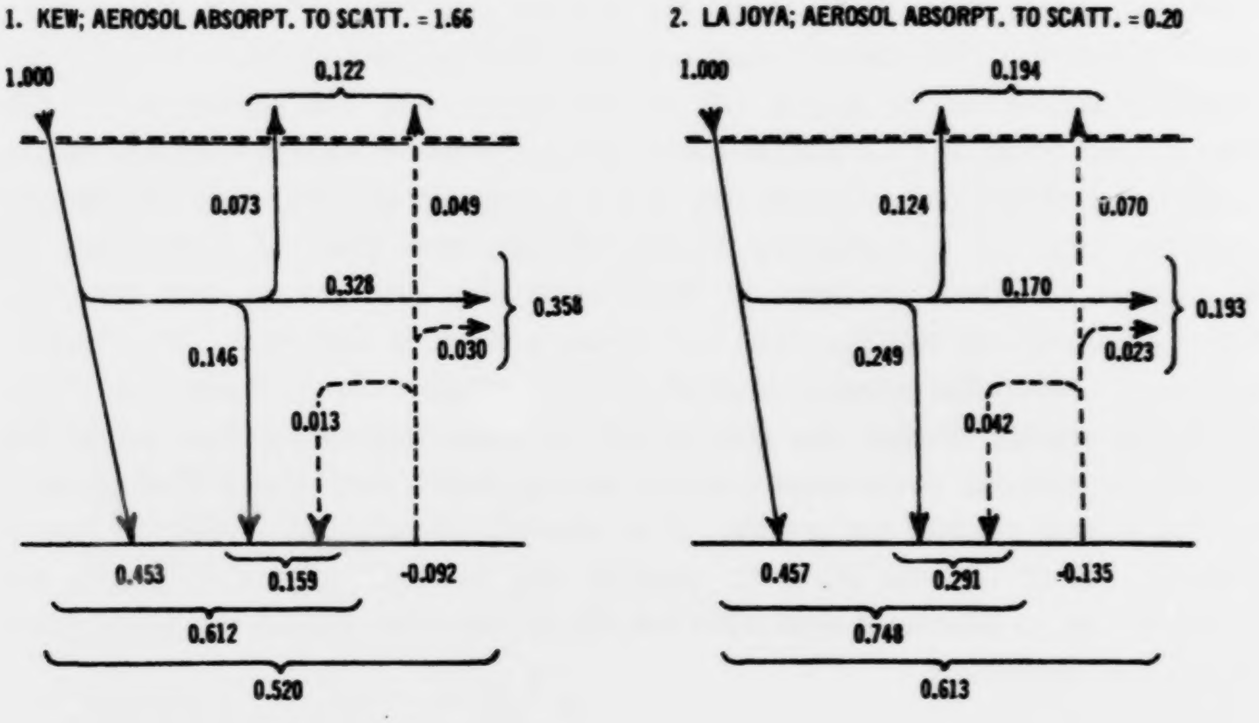

1. KEW; AEROSOL ABSORPT. TO SCATT. = 1.66

2. LA JOYA; AEROSOL ABSORPT. TO SCATT. = 0.20

1.000
0.122
0.073
0.049
0.328
0.358
0.146
0.030
0.013
0.453
0.159
-0.092
0.612
0.520
1.000
0.194
0.124
0.070
0.170
0.193
0.249
0.023
0.042
0.457
0.291
-0.135
0.748
0.613

Figure 2-4. Shortwave radiation budgets for city versus desert after aerosol increase by factor of 2. Other conditions same as in Figure 2-3. (Note: no change in ratio of scattering to absorption efficiency)

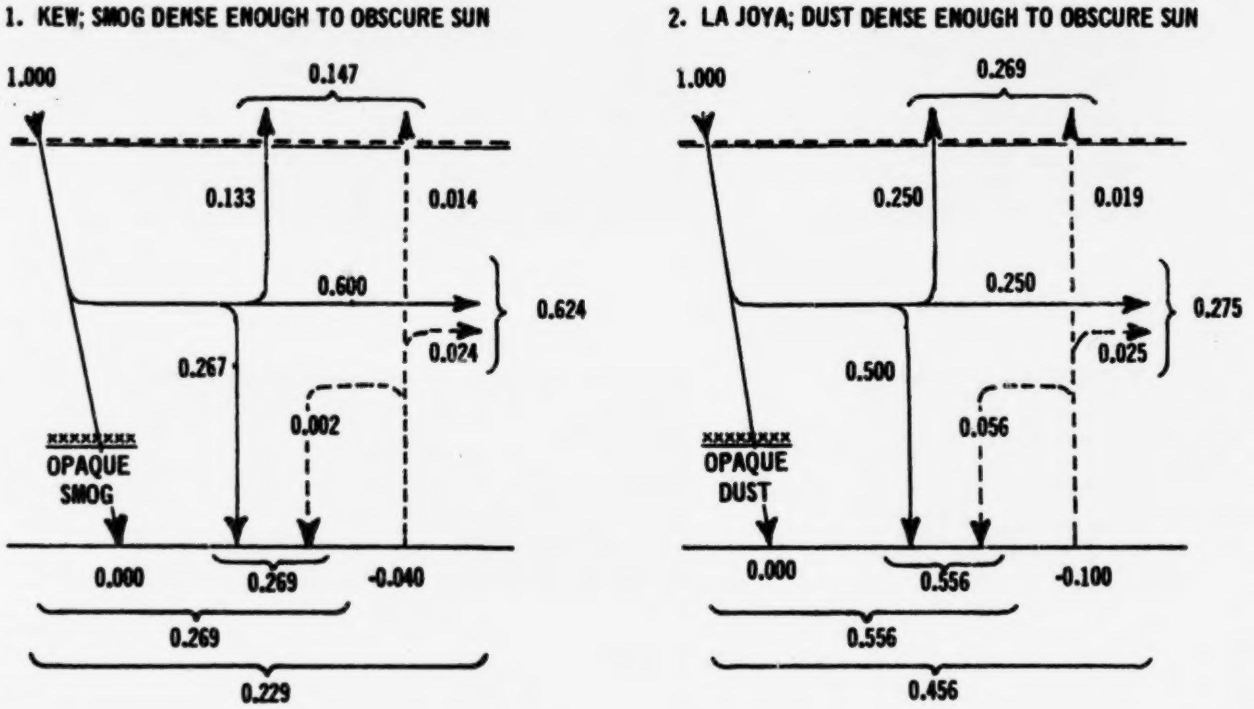
1. KEW; SMOG DENSE ENOUGH TO OBSCURE SUN
1.000
0.147
0.133
0.014
0.600
0.624
0.024
0.267
0.002
OPAQUE SMOG
0.000
0.269
-0.040
0.269
0.229
2. LA JOYA; DUST DENSE ENOUGH TO OBSCURE SUN
1.000
0.269
0.250
0.019
0.250
0.275
0.025
0.500
0.056
OPAQUE DUST
0.000
0.556
-0.100
0.556
0.456

Figure 2-5. Shortwave radiation budget– city versus desert – after aerosol increase by factor of 5.

BOX MODEL OF URBAN AIR DIFFUSIONS

Qualitative answers can be readily provided by a schematic "budget box" such as the one illustrated in Figure 2-6. It is assumed that the source strength of pollutant release per unit area of the lower boundary is the same for two cities of different size; and two different flushing rates are applied to both cities. These rates could correspond to two weather situations, one with relatively strong versus one with relatively weak winds. The particle loading of a comparable unit volume of air is illustrated in Figure 2-6 by the number and arrangements of "dots" carried by the outgoing air current, which in each case equals the number of "dots" released by the area source into the volume of city air. Obviously, a small city with a weak flushing rate would be no worse off than a big city with a good flushing rate. For example, an innocent activity like the burning of leaves could be well tolerated in a small city, but could generate intolerable smog conditions once the city became large.

Quantitative answers require consideration of the basic fluid dynamics equations. Let

s = specific admixture to air, (g meter^{-3})

$\underrightarrow{V} = \underrightarrow{i}\,u + \underrightarrow{j}\,v + \underrightarrow{k}\,w$ (meter sec^{-1})

S = strength of internal source, or sink if negative, of considered admixture (sec^{-1} meter^{-3})

ν = molecular diffusion coefficient (meter^{2} sec^{-1})

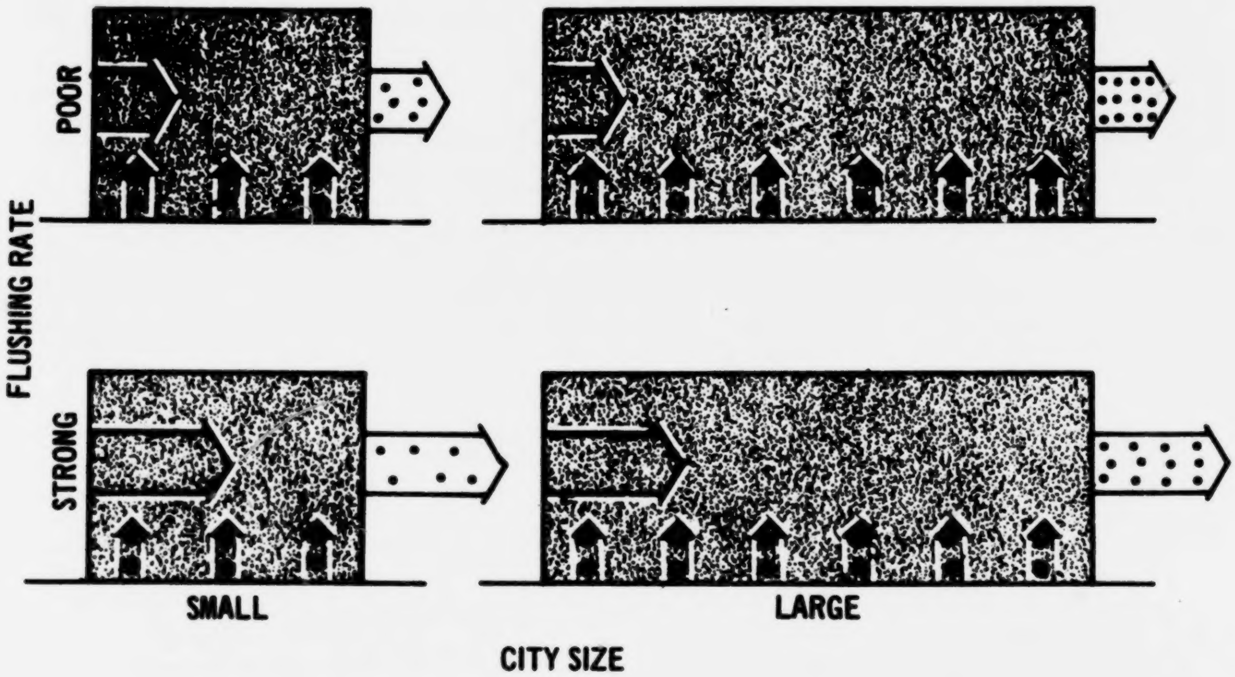

Figure 2-6. Schematic illustration of effects of city diameter and atmospheric flushing rate on pollutant concentration in box model of urban diffusion; assumes uniform area source of pollutant and removal from city volume by horizontal air motion only. Dots (.) indicate output of pollutant sources to city air volume. Arrows indicate ingoing (shaded) and outgoing (white) volumes of air per unit time. Forcing function, Q.

The principle of conservation yields

$$\frac{\delta s}{\delta t} + \nabla\cdot\underset{\rightarrow}{V}s - \nu\nabla^2 s = S \tag{1}$$

Eddy fluctuations are removed from the instantaneous values by time averaging and by introducing $s - s' = \bar{s}$, $S - S' = \bar{S}$, and $\underset{\rightarrow}{V} - \underset{\rightarrow}{V}' = \underset{\rightarrow}{\bar{V}}$, whereupon the primitive Equation (1) transforms into

$$\frac{\delta s}{\delta t} + \nabla\cdot\underset{\rightarrow}{\bar{V}}\,\bar{s} + \nabla\cdot\overline{\underset{\rightarrow}{V}'s'} - \nu\nabla^2\bar{s} = \bar{S} \tag{2}$$

It appears legitimate to neglect molecular diffusion, the eddy fluxes in the horizontal direction, and the transport by mean vertical motion, in comparison with vertical eddy flux and the transport divergence by mean horizontal wind components. This amounts to saying that

$$[(\bar{w}\,\bar{s})_z + (\overline{u's'})_x + (\overline{v's'})_y - \nu\nabla^2\,\bar{s}] \ll [\bar{u}\,\bar{s})_x + (\bar{v}\,\bar{s})_y + (\overline{w's'})_z] \tag{3}$$

where subscripts denote partial derivatives with respect to the three independent spatial variables (x,y,z).

From Equations (2) and (3), the simplified version of the primitive equation becomes

$$\frac{\delta s}{\delta t} + (\overline{u}\ \overline{s})_x + (\overline{v}\ \overline{s})_y = \overline{S} - (\overline{w's'})_z \tag{4}$$

It is characteristic for the box model of urban diffusion that we are primarily interested in representative area averages over city diameter D (m) and thickness h^* (m) of the boundary layer (Figure 2-2). Let such an average of any function, ϕ or representative function value, $\overline{\phi}$ be denoted by the following symbol:

$$[\overline{\phi}] = \frac{1}{h^* D} \int_{h^*}\int_{D} \overline{\phi}\ dx\ dz \tag{5}$$

The area source is represented by the boundary value $(\overline{w' s'})_0$ that is the vertical eddy flux of pollutant at height, z = 0. Actually existing dependencies on the cross-wind coordinate, y could be readily incorporated in the defining Equation (5) but may be suppressed for the purpose of this basic discussion.

In air pollution climatonomy, the forcing function is the effective strength of the area source, Q (per meter^2, per unit time), a function only of time, t,

$$Q(t) = [(\overline{w's'})_0] + [h^*\overline{S}] \tag{6a}$$

that is, the effective release qualified by effective internal sources. The response function is the bulk value of pollutant concentration in the volume of city air, q (m^{-3}), also a function only of time, where

$$q(t) = [\overline{s}] \tag{6b}$$

With the aid of q and D, the controlling process of horizontal advection is expressed by a bulk value of wind speed, U^* (m-sec^{-1})

$$U^*(t) = \frac{D}{q}\ [\ (\overline{u}\ \overline{s})_x + (\overline{v}\ \overline{s})_y\ ] \tag{6c}$$

The characteristic frequency, f^*, sec^{-1}, which I propose to call the "flushing frequency" of the volume of city air, is another controlling parameter. It is defined with the aid of the advection parameter U^* and eddy flux value $(\overline{w' s'})^*$ at $z = h^*$,

$$f^* = \frac{U^*}{D} + \frac{1}{h^* g}\ [(\overline{w's'})^*] \tag{6d}$$

Horizontal advection will significantly control the flushing frequency, especially when the level h^* coincides with a "lid" such as an inversion layer. The transformation of Equation (4) with the aid of Equations (5) through (6d), yields the equation governing the box model of urban diffusision,

$$\frac{\delta q}{\delta t} = \frac{Q}{h^*} - qf^* \tag{7}$$

Which is the equivalent of the governing equation of evapotranspiration climatonomy, see Lettau.[3] For further transformation let us introduce the reduced source strength or quasi-equilibrium value of pollutant concentration, q^* (m^{-3}):

$$q^* = \frac{Q}{h^*f^*} \tag{8a}$$

and a dimensionless time (t') which serves as the new independent variable,

$$t' = \int f^* \, dt \text{ ; or,} \qquad dt' = f^* \, dt \tag{8b}$$

In its final form the characteristic equation of the box model, or the governing equation of air pollution climatonomy, may be written as an ordinary differential equation,

$$\frac{dq}{dt'} = q^* - q \tag{9a}$$

which is solved by

$$q = e^{-t'} \left[q_0 + \int_0^{t'} e^{t'} \, q^* \, dt' \right] \tag{9b}$$

where q_0 is the initial value of concentration at time $t = 0$. Representative values of a parameter having the physical units of seconds per meter were estimated for a variety of cities by Holzworth,[7] and I suggest that for practical applications, Holzworth's *theoretical relative pollutant concentration* can be identified with $1/h^*f^*$ in Equation (8a).

Prediction of Pollutant Trends by Box Model

It is evident that Equation (9a) and its solution, Equation (9b), correspond to an initial-value problem only if q^* is a quasi-constant. In reality, even for time-independent source strength, Q, the value q^* will vary considerably because, according to Equation (8a), it is controlled by the atmospheric flushing frequency, which changes with the weather. An example of practical numerical application of the theory is illustrated in Figure 2-7.

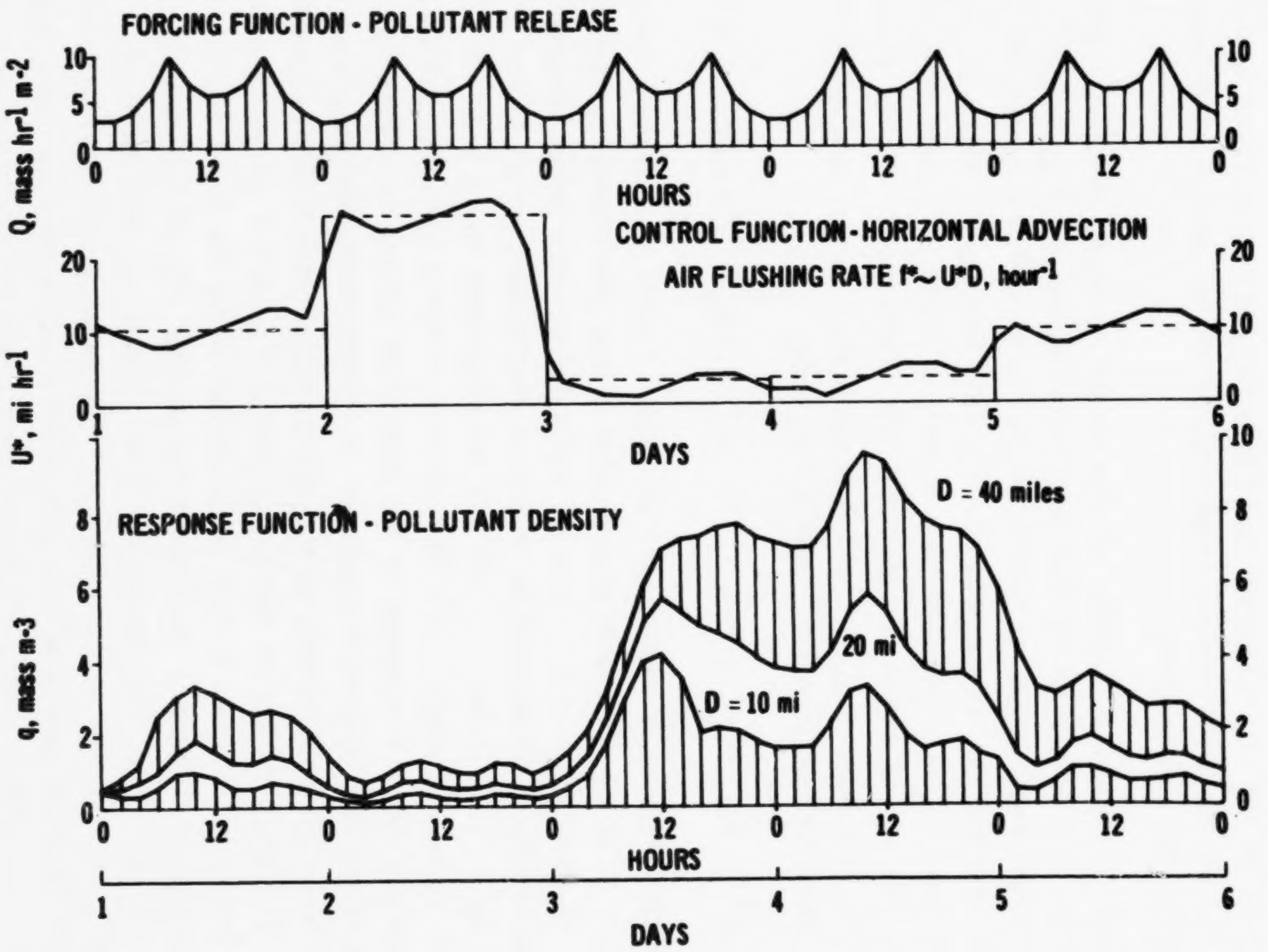

Figure 2-7. Calculated trends of pollutant concentration in response to indicated forcing function for day-to-day variation of atmospheric flushing parameters. Calculation by box-model for three different city diameters to demonstrate adverse effects of urban sprawl.

Over a period of 5 days, the area source is assumed to have the same daily average rate on which is superimposed a semi-diurnal variation with peaks at the hours of 8 am and 6 pm. While the first and fifth day have normal wind speed conditions, the second day is stormy and the third and fourth days, relatively calm. The bulk value U^* according to Equation (6c) is depicted in the middle part of Figure 2-7, showing slight diurnal variation with one peak per day induced by the normal insolation cycle. To bring out the effect of f^*-dependency on the city diameter—see Equation (6d)—three D-values were employed, 10 mi for a moderately large city, 20 mi for one of intermediate size, and 40 mi for a metropolis.

For practical numerical evaluation of the model, a fixed time-interval Δt equal to 2 hr, was employed for the calculation shown on Figure 2-7. For any period beginning at time t_i and ending at time $t_i + \Delta t$, representative values were assumed for source strength, Q_i, (the forcing function) and for atmospheric parameters. Representative values q_i^* and f_i^* were thus obtained with the aid of Equations (6c) and 6d). Knowing q_i at time t_i, the concentration, Δt later is $q_i + 1$ and was calculated numerically using the following version of Equation (9b), with $f_i^* \Delta t = \Delta t_i^!$:

$$q_{i+I} = e^{-\Delta t_i^!} \left[q_i + q_i^* (e^{\Delta t_i^!} - 1) \right] = q_i^* + (q_i - q_i^*)\, e^{-\Delta t_i^!} \qquad (10)$$

The numerical calculation may begin at time t_0 with an arbitrary initial concentration value q_0. The only prerequisite is that the chosen q_0 has the same order of magnitude as a typical q^* value for the city under consideration. For example, all three q-series shown in the lower part of Figure 2-7 begin with $q_0 = 1$ (in relative units) and are continued for a total of 120 hours, which means 60 steps in Δt. We see that within a few time steps the three q-functions align themselves to the individual forcing functions qualified by the respective flushing frequencies. A characteristic tendency toward lagging and smoothing-out details of the forcing function is evident as a city gets larger. The three curves on the lower part of Figure 2-7 are self-explanatory. The important feature is that, other factors being the same, the larger city must suffer considerably more than the smaller city during periods of nearly stagnant air. This follows as the direct result of reduction of the flushing rate in proportion to city diameter. The buildup of pollutant levels during a calm weather spell in a large city is more severe, and last for longer periods than in a smaller city. This quantitative result of numerical calculation supports the qualitative statements made previously in connection with the discussion of Figure 2-6.

While the box model excludes the possibility of investigating spatial detail of pollutant distribution, the emphasis on temporal variations is applicable to a number of important problems. Before we begin to talk about long-range trends, let us discuss another application of the box model to relatively

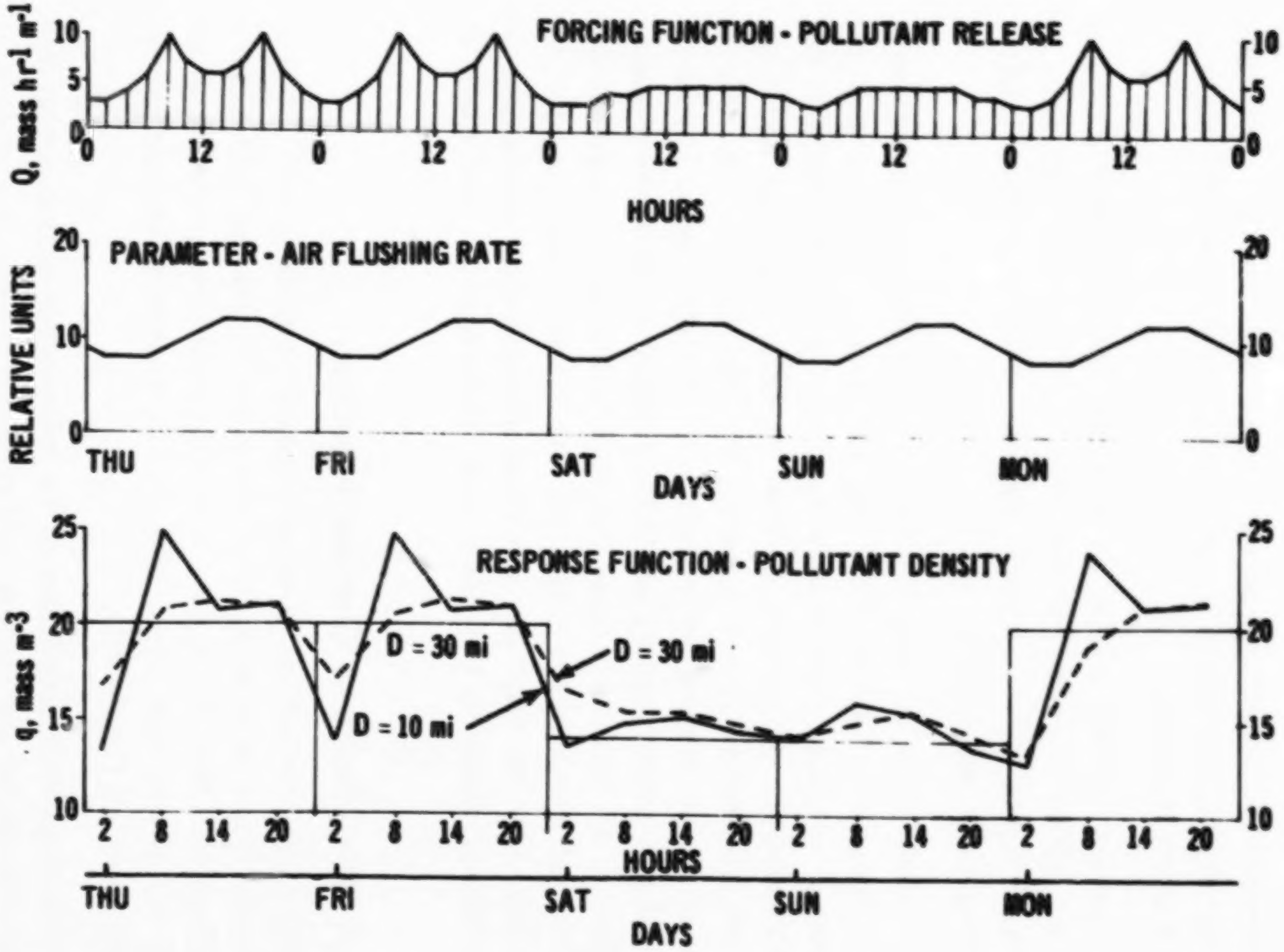

Figure 2-8. Trends of pollutant concentration in response to week-end lull of forcing function, calculated for constant diurnal cycle of atmospheric flushing parameter. Response function illustrated for city diameters of 10 miles and 30 miles, but normalized (to equal daily mean value) to bring out smoothing effect of larger city.

short-range fluctuations. Specifically, we refer to a time-variation on the forcing function caused by the weekday versus weekend cycle. While on Figure 2-7 the forcing function remained the same from day-to-day, Figure 2-8 schematically depicts a weekend decrease of emission. Two cities of different D-values were assumed, and the response functions normalized to bring out the damping and lagging predicted for the larger metropolitan area.

Direct measurements documenting diurnal peaks and weekend lulls that compare with the theoretical results shown on Figures 2-7 and 2-8 have been reported for a number of cities.

Examples of observed weekly cycles in a variety of pollutants including carbon monoxide, sulfur dioxide, smoke, and oxidants are discussed by McCormick and Xintaras;[6] W. Johnson;[7] Schuck, Pitts, and Wan;[8] Harris, Huffman, and Weiland;[9] and others.

Obviously, any application of the results of air pollution climatonomy, represented by Equations (9b) or (10), requires information not only on the input normally available from source inventory of urban emitters, but also on the atmospheric parameters defined in Equations (6c) and (6d). Applicability will be limited if, for instance, the parameter h^*, the mixing depth, is unsatisfactorily known. In principle h^* for downwind change in surface roughness and energy supply could be determined from the dynamic and thermal aspects of boundary layer development given the state of the lower atmosphere at the upwind edges. At the present time, however, it appears more practical to rely on statistical-climatological evaluation of meteorological measurements in the urban area. Reference is again made to Holzworth.[10]

Application of Box Model to Thermal Pollution

Equations (7) and (9a) permit an evidently steady state if $q = q_*$. This is used to predict the order of magnitude of the effect of thermal pollution in the air of a metropolis. New York City is a self-explanatory example of an urban complex for which heat input and pertinent atmospheric parameter values have been reported (Table 2-1).

It follows that the reported heating rate of 39 calories per second per square meter, or about 0.2 langley per minute, will raise the average temperature of the volume of city air approximately 2° C above its surroundings. Such a temperature-volume average suggests that the excess may reach 4° to 5° C at the center of the city and roof-top or stack levels. According to Bornstein,[11] this value is not uncommonly encountered in temperate zone cities such as New York.

It is evident that fuel combustion represents only one among several causes of the urban heat island. Atmospheric feedback, from city structures and air

Table 2-1 **EXAMPLE OF AIR POLLUTION CLIMATONOMY – LEVEL OF THERMAL POLLUTION IN NEW YORK CITY, CALCULATED FROM INPUT AND PARAMETER VALUES**

Element	Symbols	Numerical values	References
Area source — fuel combustion in winter	Q, $Q/c_p\rho$	39 cal m^{-2} sec^{-1} 0.13° C m sec^{-1}	Bornstein[11] Holzworth[10]
Parameter value	$1/h^*f^*$	16 sec m^{-1}	Holzworth[10]
Predicted excess of air temperature (quasi-equilibrium)	$Q/c_p\rho\ h^*f^*$	2.1° C	Climatonomy Equation (7) for $\frac{\partial p}{\partial t} = 0$

pollution, to dynamics of the lower atmosphere also involves both insolation and terrestial or long-wave radiation, and the soil moisture budget. Petersen[12] gives more detailed documentation.

To the best of my knowledge there have been no previous attempts to use the box model of urban diffusion for the calculation of thermal pollution levels. The application documented in Table 2-1 is, however, a logical step and it conforms with the philosophy outlined in my introductory remarks regarding the desirability of a simultaneous treatment of transfer of masses, momentum, and energy in boundary layer problems.

AERODYNAMIC ROUGHNESS AND MOMENTUM DRAIN IN URBAN AREAS

Having shown examples of the application of the box-model to diffusion of mass and thermal energy, we can now apply it to the drain of momentum encountered by the wind in its passage over a city.

First, it will be necessary to determine the representative aerodynamic roughness length, z_Q (cm), of the urban area. I propose to use a formula that has been derived from a series of out-of-doors micrometeorological experiments done over a period of years at the University of Wisconsin.

In late winter, hundreds of commercial bushel baskets were distributed over a section of level, almost undisturbed ice on Lake Mendota. Changes in the vertical wind profile as a function of the roughness modification upwind of an anemometer mast were analysed. The z_0 value of the undisturbed ice (about 0.01 cm) was increased systematically and in a controlled fashion to nearly 10 cm. It is established[13] that the z_0 value can be predicted using similarity concepts if we know the effective height H (cm), of the roughness elements; their silhouette area seen by the wind, a (m^2) and their lot area, A (m^2). Lot area refers to the total area of the test field divided by the number of elements.

$$z_0 = H\ a\ /\ 2A \qquad (11)$$

The factor 1/2 approximates the average drag coefficient of the roughness elements. A set of urban background data for use in Equation (11) is summarized in Table 2-2. The values are arbitrary within an order of magnitude. More specific information will be required for actual case studies of specified urban boundary layers. The same applies to the data in Table 2-3, where the estimated z_0 values for three building types were considered in a pilot study intended to show how the characteristic wind speed U can be determined for a specific city type, knowing only the overall atmospheric dynamics represented by the intensity of the horizontal pressure gradient in the lower troposphere. U can be predicted and, in turn, used to obtain the velocity, U^*, in Equation (6c).

Table 2-2 AERODYNAMIC ROUGHNESS LENGTH CALCULATED FROM EQUATION (11) FOR ESTIMATES OF BUILDING CHARACTERISTICS IN AN URBAN AREA

Building type (schematic)	Low	Medium	High-rise
Building height (approximate)	4 m	20 m	100 m
Assumed lot area	2000 m^2	8000 m^2	20000 m^2
Assumed silhouette area	50 m^2	560 m^2	4000 m^2
Calculated z_0	5 cm	70 cm	1000 cm

Table 2-3. APPLICATION OF LOGARITHMIC LAW TO WINDSPEED CALCULATION[a]

z_0	G (m/sec)	$\log_{10}(G/z_0 f)$	C	U (m/sec)
5	5	6.00	0.0378	3.3
70	5	4.85	0.0475	2.9
1000	5	3.70	0.0590	1.9
5	20	6.60	0.0342	12.8
70	20	5.46	0.0420	10.5
1000	20	4.30	0.0538	6.8

[a] Windspeed U calculated from Equation (12) at level of 150 meters for given surface roughness (z_0), given geostrophic speed (G) and subsequent geostrophic drag coefficient (C); derived from universal relationship between C and scaling factor for atmospheric boundary layers, $Ro_0 = G/z_0 f$

Ro_0 = surface Rossby number

f = Coriolis parameter = 1.0×10^{-4} sec^{-1} for these calculations assuming 43° geographic latitude.

To follow the procedure, take the calculated or estimated geostrophic speed G (cm sec^{-1}) as the ambient flow. Geostrophic speed is independent of roughness. Then, the surface Rossby number, $Ro_0 = G/z_0f$, where f = Coriolis parameter (sec^{-1}) can be calculated for a given z_0. Lettau[14] was the first to demonstrate that this Ro_0 serves as a scaling factor for atmospheric boundary layer structure and that it plays a role equivalent to the role of the Reynolds number that is used in engineering flow problems to determine the friction factor. The factor C, named the "geostrophic drag coefficient,"[14, 15] was shown to be a unique valued function of Ro_0 for thermally neutral states of the lower troposphere. If height z(cm or m) is restricted to the lowest part of the boundary layer, a first approximation value for U(z) in the model is provided by the logarithmic law, which can be written as

$$U(z) = 5.5\ C\ G\ \log_{10}\ (1 + z/z_0) \tag{12}$$

Application of Equation (12) is determined by the Karman constant and the natural-to-common logarithm conversion factor. Note that z_0-effects appear both directly, under the logarithm, and indirectly, through its Ro_0 dependency in the coefficient, C.

Tables 2-4 and 2-5 are self explanatory. Although the calculated values of the parameter $1/h^*f^*$ are comparable with actual conditions,[10] it must be remembered that h^* in Table 2-4 was arbitrarily kept constant at 300 m. Nevertheless contribution of the three essential factors (1) lowering of overall wind speed, (2) increase of city diameter, and (3) change from low- to high-rise buildings, can equivalently increase the net pollutant concentration. The last two effects favoring the increase of relative pollutant concentration (or the value of $1/h^*f^*$) could be of interest to the city planner.

Table 2-5 presents a result of air pollution climatonomy, comparable with the example shown in Table 2-1. The box model of urban diffusion applied to momentum predicts that for the conditions of a big metropolis such as New York City the average wind speed could be 2 m sec^{-1} lower than in a comparable situation over open country. The "negative area source," or momentum drain due to the increase of surface roughness, is estimated to equal a ground drag difference of 1.5 dynes cm^{-2}, based on geostrophic drag coefficients and the relationship defining surface stress τ_0 as $\rho C^2\ G^2$, where ρ indicates air density. Obviously, if the number of high-rise buildings in a central city is increased and the lot area is not enlarged, the resulting z_0 increase will favor stagnant air and the likelihood of pollution episodes. That effect is additive to the city-diameter effect. (Figure 2-7).

Table 2-4. ESTIMATE OF BOX-MODEL PARAMETER $1/h^*f^*$ FOR TWO DISTINCT CLASSES OF AMBIENT (GEOSTROPHIC) SPEED AND THREE CITY SIZES WITH TWO BUILDING TYPES[a]

Geostrophic speed, m/sec	City diameter, km	Building type[b]	$1/h^*f^*$,[c] sec/m^{-1}
20	4	Low	1
20	4	High-rise	2
5	4	Low	4
5	4	High-rise	7
20	20	Low	5
20	20	High-rise	10
5	20	Low	20
5	20	High-rise	35
20	80	Low	21
20	80	High-rise	39
5	80	Low	80
5	80	High-rise	140

[a] Compare Tables 2-2 and 2-3.
[b] See Table 2-2.
[c] For $h^* = 300$ meters.

Table 2-5. EXAMPLE OF AIR POLLUTION CLIMATONOMY: LOSS OF AIRFLOW MOMENTUM OVER AN URBAN AREA[a]

Element	Symbols	Numerical value	References
Momentum area sink (by aerodynamic roughness)	ΔT_0 $\Delta T_0 \rho$	1.5 dynes cm^{-2} 0.13 m^2 sec^{-2}	Geostrophic drag coefficient
Parameter value	$1/h^*f^*$	16 sec m^{-1}	Holzworth[10]
Predicted speed deficit Steady-state	$\Delta T_0 / \rho h^* f^*$	2.0 m sec^{-1}	Climatonomy Equation (7)

[a] Assuming an ambient (geostrophic) speed of 10 m/sec, an Aerodynamic Surface Roughness z_0 of 100 cm (hence, C = 0.050) for the City, and 5 cm (hence, C = 0.035) for the Upwind Region, and a Parameter Value of $1/h^*f^* = 16$ sec/m (Momentum Drain Conditions in New York City[1]

WIND PROFILE OVER CITIES

Boundary layer concepts lend themselves readily to application in urban diffusion problems. To emphasize this, let me use the results of one of the bushel basket experiments performed on the ice of Lake Mendota (Figures 2-9 and 2-10). The experiment was designed to study both control of surface roughness (Rossby number) and effect of thermal stratification (Richardson number). A total of 420 bushel baskets were used, half of them painted white, the other half, black. A lot area of about 2 m^2 was selected in a layout of two adjacent fields, 21 m cross wind, and 20 m downwind. The albedo values measured were 0.15 for the black and 0.65 for the white obstacles. The albedo of the aged snow on the ice averaged about 0.52. In the March sunshine, the effective heating of the field with the black obstacles was estimated at 0.07 langley min^{-1}, and that of the field with the white baskets at 0.03 langley min^{-1}, giving relatively differential heating rate of 0.04 langley min^{-1}.

Figure 2-9 illustrates the analysis of wind profile observations at a variety of x-positions for the anemometer mast, in the form of velocity defects (ΔV) and vertical motion computed for two-dimensional mean flow with the aid of the continuity equation. The velocity defects and updrafts are more pronounced for the black than for the white field. Temperature measurements suggested that the difference in Richardson numbers between black and white fields varied from about –0.005 to +0.005. For cases of relatively strong changes in vertical shear, however, it is questionable whether the Richardson number retains its significance as a scaling parameter.

Figure 2-10 shows the momentum balance for adjacent "budget boxes" in the x-z plane between the surface and 1.6 m. All values are in dynes cm^{-2}, double arrows refer to transport by mean (organized) velocity components ($\bar{u}$ and $\bar{w}$), thin arrows show the eddy flux, $\rho\overline{(u' w')}$, in the vertical direction at z=0 and z=1.6 m. The black field drains 2.9, and the white field 2.3 dynes cm^{-2}, and the loss due to transport to higher layers amounts to 3.0 and 1.8 dynes cm^{-2}, respectively. These values indicate an increase in the mixing depth due to Richardson number effects, similar to the dynamic roughness effect in boundary layer development over cities in Equation (11). Further experiments of this type are desirable.

Although the horizontal scale of our out-of-doors or free air experiments is significantly larger than the scale of wind tunnel studies, the similarity to the prototype of boundary layer structure over urban areas is still incomplete because on the larger, real scale the effect of Coriolis forces appears, causing directional shear of horizontal air motion. The two dimensionality of actual wind profiles over cities is not accounted for by the power-law $V \sim z^{a}$, frequently suggested for transport of material in the lower troposphere in urban pollution studies; reference is made to Davenport[17] and Turner.[18] In

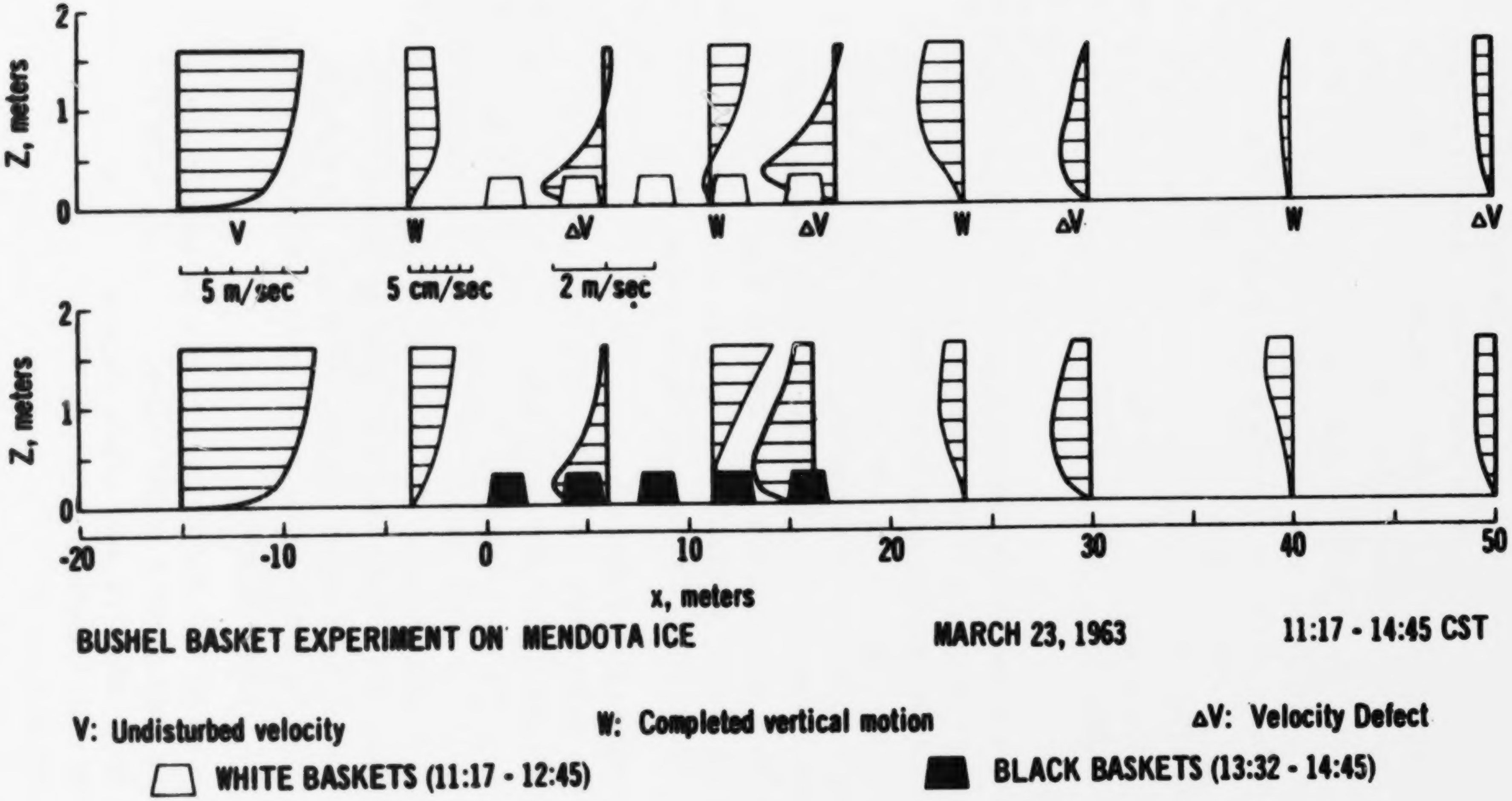

Figure 2-9. Analyzed results of micrometeorological experiment by Stearns and Lettau on March 23, 1963, using fields of bushel baskets on ice of Lake Mendota. Mimicks conditions found in boundary layer development over city. Undisturbed wind profile, extreme left. Vertical profiles of velocity defects and calculated vertical motion plotted for different mast positions at indicated downwind distances. Note stronger momentum drain and deeper mixing layer over black obstacles illustrating possible Richardson number effect.

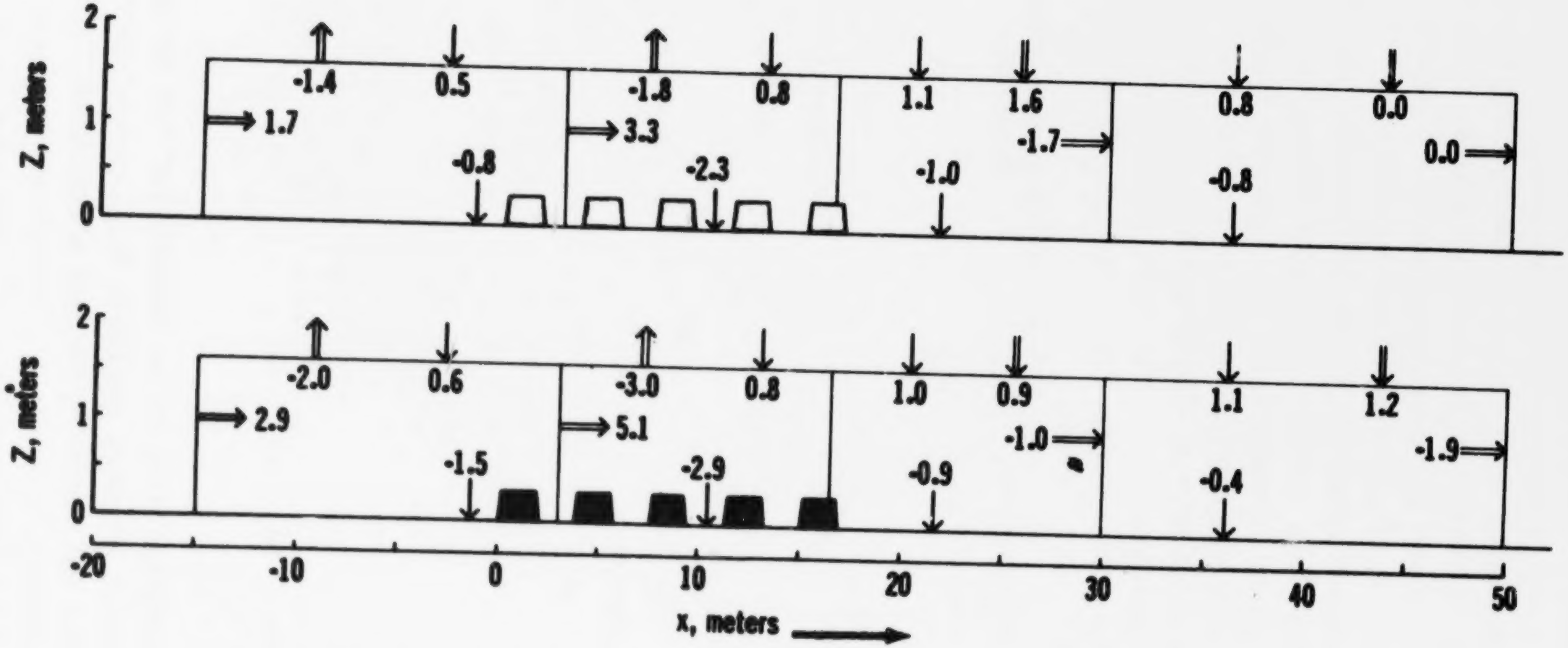
Z, meters
2
1
0
-1.4
0.5
1.7
-0.8
-1.8
0.8
3.3
-2.3
1.1
1.6
-1.0
-1.7
0.8
0.0
-0.8
0.0
Z, meters
-2.0
0.6
2.9
-1.5
-3.0
0.8
5.1
-2.9
1.0
0.9
-0.9
-1.0
1.1
1.2
-0.4
-1.9
-20
-10
0
10
20
30
40
50
x, meters

BUSHEL BASKET EXPERIMENT ON MENDOTA ICE MARCH 23, 1963 11:17 - 14:45 CST

Figure 2-10. Budget boxes showing horizontal momentum balance for experiment illustrated in Figure 2-9. Double arrows represent budget contributions due to mean components $\bar{u}$ and $\overline{w}$; single arrows, contributions due to eddy flux in vertical direction, including surface stress.

addition to the disregard for directional shear, the power law has two other disadvantages: (1) at low elevation the logarithmic law (which alone expresses the surface roughness effect rationally) is not approached as an asymptotic case, and (2) at high elevation, there is no asymptotic approach to the gradient or high geostrophic wind. Clearly, these two shortcomings mean that the power law is merely an interpolation formula, with difficulties expressing upper and lower boundary conditions. More realistic models of wind profile structure in atmospheric boundary layers are available in the literature. Let me restrict discussion to one of my earlier contributions to this problem. It concerns a universal wind spiral theory of the barotropic (thermally neutral) lower atmosphere.[13] The tabulated functions for the wind and stress components that this model generates are universally applicable to a wide range of external conditions. In order to verify a wind or stress spiral in the atmospheric boundary layer for a special case, the only scaling factor needed is the surface Rossby number. Figure 2-11 illustrates

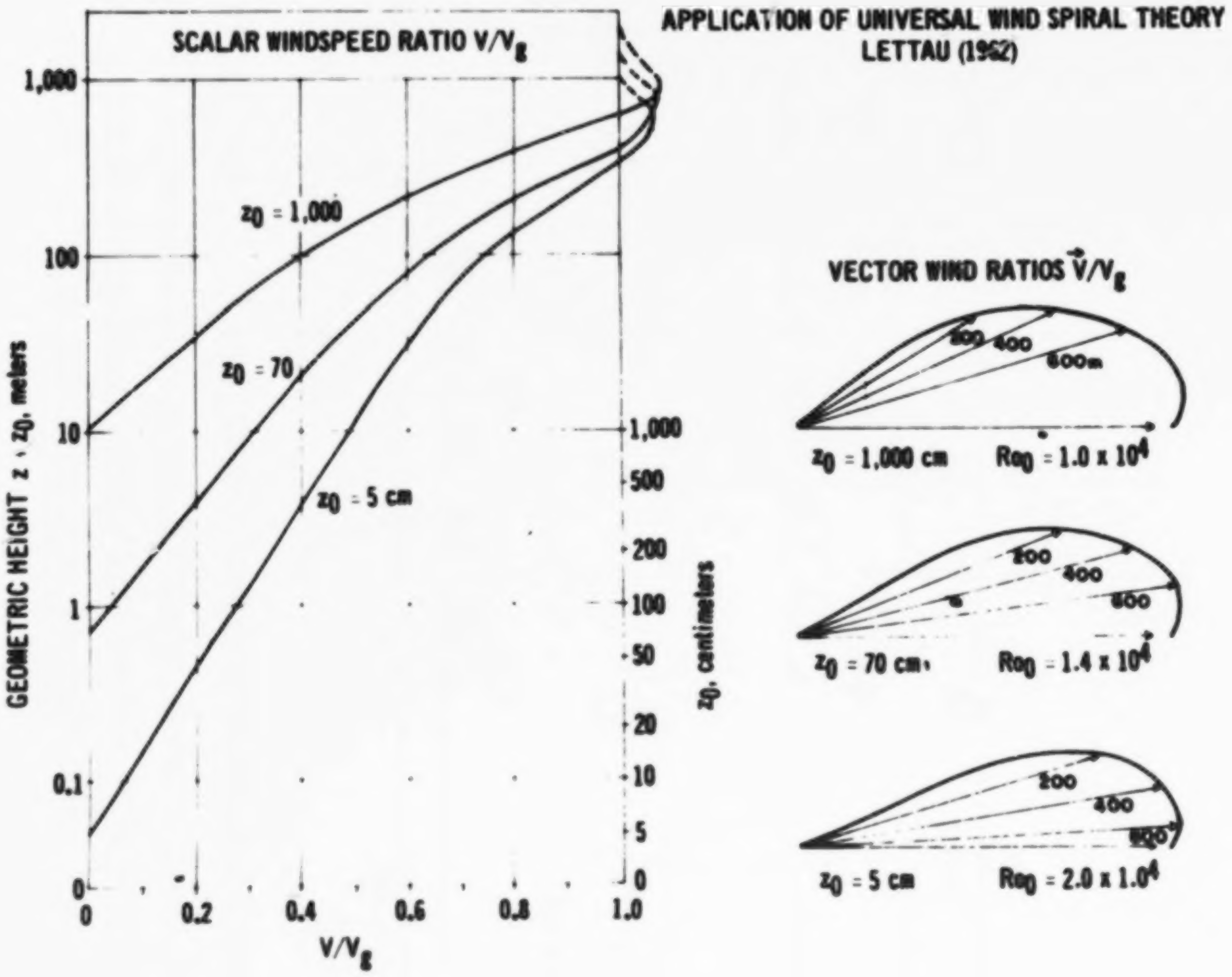

Figure 2-11. Universal Wind Spiral Theory verified for three values of surface roughness (Rossby numbers, Ro$_0$)) characteristic of urban areas. Calculated for thermally neutral atmosphere. Normalized to geostrophic speed (Vg). Symbols: z$_0$, aerodynamic roughness length, (meters); f, Coriolis factor (1.0 x 10^{-4} meters sec^{-1} for 43° surface latitude); Ro$_0$, Vg/z$_0$f.

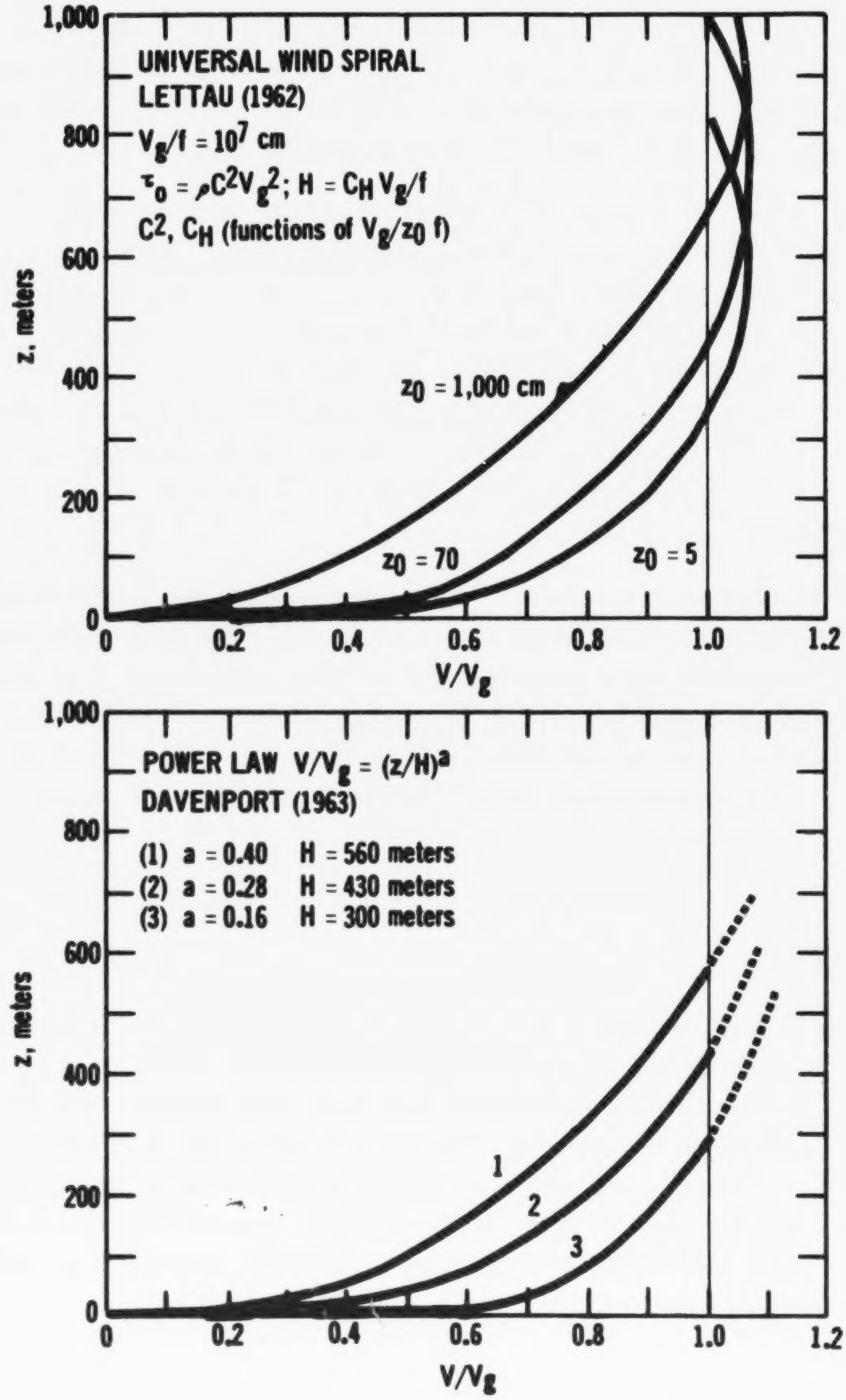

Figure 2-12. Comparison between Universal Wind Spiral Theory and Power Law treatment of vertical profiles of normalized horizontal wind speed (V/V_g). Symbols: V_g = geostrophic speed; f = Coriolis factor of 1.0 x 10^{-4} meters $\sec^{-1}$; τ = surface stress: ρ = air density; C = geostrophic drag coefficient; C_H = height coefficient; H = effective height of roughness elements (centimeters); z = geometric height; a = silhouette area seen by the wind (meters^2).

verification for three different Rossby numbers that correspond to the urban z_0-values shown in Tables 2-2, 2-3, and 2-4, a geostrophic speed of 10 m sec^{-1}, (denoted by the symbol V_g in Figures 2-11 and 2-12, and a Coriolis parameter $f = 1.0 \times 10^{-4}$ sec^{-1} (for 43° geographic latitude).

The two parts of Figure 2-11 illustrate scalar and vector wind ratios, normalized relative to geostrophic speed. For scalar wind speed, plotted linearly against a geometric scale in height, straight sections at small height, indicate that the logarithmic law is an asymptotic case. The scalar and vector graphs also document an asymptotic approach to the gradient wind at high elevations. There are reports in the literature of wind direction changes of the order of 10 degrees, at heights of about 60 m, between upwind and downwind towers. For reference see Graham's[19] analysis of data from Fort Wayne, Indiana.

Figure 2-12 compares the power law[17] profile with the scalar wind profile derived from the Universal Wind Spiral solution.[15] The latter provides all the necessary numerical scale factors, including the geostrophic drag coefficient C, and the height coefficient C_H, as unique-valued functions of the surface Rossby number. The power law is deficient in this respect and its application, with the assumptions listed on the lower part of Figure 2-12, is arbitrary or empirical.

SUMMARY

I hope to have convinced some of you that fluid-dynamical boundary-layer concepts are promising physical and meteorological bases for mathematical models of urban diffusion processes; and that mass, momentum, and energy transfers and transports can be effectively handled by a systems approach with: defined forcing functions, parameterization of response functions, and feedback and control functions. Much detailed research still has to be done, especially with regard to the combined feedback processes of turbulence generation by surface roughness and heating over urban areas.

REFERENCES

1. Moses, H. Mathematical Urban Air Pollution Models. National Center for Air Pollution Control, Chicago Dept. of Air Pollution Control, Argonne National Laboratory. Argonne, Ill. ANL/ES-RPY-001. April 1969. 69 p.
2. Lieber, H. Controlling Metropolitan Pollution Through Regional Airsheds: Administrative Requirements and Political Problems. J. Air Pollution Control Assoc. *18:*86-93, February 1968.
3. Lettau, H. Evapotranspiration Climatonomy. 1. A New Approach to Numerical Prediction of Monthly Evapotranspiration Runoff and Soil Moisture Storage. Mon. Weather Rev. 97:691-699, October 1969.
4. McCormick, R. A. and J. H. Ludwig. Climate Modification by Atmospheric Aerosols. Science. *156*(3780):1358-1359, June 9, 1967.
5. Lettau, H. and K. Lettau. Shortwave Radiation Climatonomy. Tellus. *21*:208-222, February 1969.
6. McCormick, R. A. and C. Xintaras. Variation of Carbon Monoxide Concentration as Related to Sampling Internal, Traffic and Meteorological Factors. J. Appl. Meteorol. *1*(2):237-243, June 1962.
7. Johnson, W. This Symposium, Chapter 5.
8. Schuck, E. A., J. N. Pitts, Jr., and J. K. S. Wan. Relationships Between Certain Meteorological Factors and Photochemical Smog. Int. J. Air Water Pollution. *10:*689-711, October 1966.
9. Harris, D. N., J. R. Huffman, and J. H. Weiland. Another Look at New York City's Air Pollution Problem. J. Air Pollution Control Assoc. *18*:406-410, June 1968.
10. Holzworth, G. C. Mixing Depths, Wind Speeds and Air Pollution Potential for Selected Locations in the United States. J. Appl. Meteorol. *6*(6):1039-1044, December 1967.
11. Bornstein, R. D. Observations of the Urban Heat Island Effect in New York City. J. Appl. Meteorol. *7*(4):575-582, August 1968.
12. Petersen, J. T. The Climate of Cities (A Survey of Recent Literature). National Air Pollution Control Administration. Raleigh, N. C. Publication Number AP-59. 1969. 48 p.
13. Lettau, H. Note on Aerodynamic Roughness-Parameter Estimation on the Basis of Roughness Element Description. J. Appl. Meteorol. *8*:828-832, November 1969.
14. Lettau, H. H. Wind Profile, Surface Stress and Geostrophic Drag Coefficients in the Atmospheric Surface Layer. In: Advances in Geophysics, Landsberg, H. E. and J. Van Mieghem (eds.) Vol. 6 New York, Academic Press, 1959. p. 241-257.
15. Lettau, H. H. Theoretical Wind Spirals in the Boundary Layer of a Barotropic Atmosphere. Beitr. Phys. Atmos. *35*(3/4):195-212, 1962.
16. Lettau, H. H. Problems of Micrometeorological Measurements (On Degree of Control in Out-of-Doors Experiments). In: The Collection and Processing of Field Data; A CSIRO Symposium, Bradley, E. F. and O. T. Denmead (eds.). New York, Interscience Publishers, 1967. p. 3-40.
17. Davenport, A. G. The Relationship of Wind Structure to Wind Loading. In: Proceedings of International Conference on Wind Effects on Buildings and Structures. National Physical Laboratory, Teddington, England, June 26-28, 1963. London, H. M. Stationery Office, 1965.
18. Turner, D. B. Workbook of Atmospheric Dispersion Estimates. National Air Pollution Control Administration. Cincinnati, Ohio. PHS Publication Number 999-AP-26. Revised 1969. 84 p.
19. Graham, I. R. An Analysis of Turbulence Statistics at Fort Wayne, Indiana. J. Appl. Meteorol. *7*(1):90-93, February 1968.

APPENDIX – GLOSSARY OF SYMBOLS

a	silhouette area of roughness element
A	lot area of roughness element
C	geostrophic drag coefficient
C_H	height coefficient
D	city diameter
f	Coriolis parameter
f^*	flushing frequency of volume of city air
G	ambient air flow, gradient wind, or geostrophic wind
h^*	upper boundary, or thickness, of volume of city air
H	effective height of roughness elements
q	average pollutant concentration for box model
q^*	quasi-equilibrium value of average pollutant concentration for box model
q_0	initial value of q at $t = 0$
$q(t)$	response function, of air pollution climatonomy
Q	area source of pollutant emission
$Q(t)$	forcing function of air pollution climatonomy
s	specific admixture to air
S	strength of internal source (sink, if negative) of considered admixture
t	time
t'	dimensionless time
Δt	time interval
U^*	bulk value of windspeed
$\underrightarrow{V}$	velocity vector $= \underrightarrow{i}\,u + \underrightarrow{i}\,v + \underrightarrow{k}\,w$
V_g	geostrophic windspeed
$\overline{(w' s')}$	vertical eddy flux of admixture
x	downwind coordinate
y	crosswind coordinate
z	height
z_0	aerodynamic roughness length of urban area
ν	molecular diffusion coefficient
ρ	air density
ϕ	function
$\overline{\phi}$	average of function

ABSTRACT

The method currently in practical use in the United Kingdom Meteorological Office for predicting levels of air pollution from source strengths and meteorological data is reviewed briefly. A study of 6-hour average SO_2 *concentrations in the town of Reading, recently published by the British Petroleum Research Centre, shows that, while the overall average may be predicted reasonably well by the foregoing method, the individual predicted values have large deviations from those observed.*

Some aspects of the theoretical and empirical basis for the estimation of the diffusive spread of material are considered—particularly the applicability of the gradient-transfer approach and the indications of Lagrangian similarity arguments regarding the effects of surface roughness and thermal stratification.

The vertical spread for neutral flow over a roughness typical of urban areas predicted on Lagrangian similarity is found to be compatible with that recently estimated from tracer experiments in St. Louis, Missouri, for evening, when neutral thermal stratification was indicated by temperature observations in the city. It has to be admitted, however, that the actual flow conditions were most unlikely to have been in equilibrium with the urban terrain over the whole depth of spread of the tracer. Furthermore, there is some indication of substantially greater spread during the day even when similar (neutral) stratification prevailed in the city; this feature remains to be explained.

Elementary aspects of the influence of the urban heat island in augmenting vertical spread are considered. Examination of the St. Louis data reveals some evidence to support the expected augmentation, but there is no obvious support for the notion that vertical spread into an initially stable atmosphere is controlled solely by the urban heat input as in Summer's model.[1]

Finally, brief consideration is given to the prospects of and requirements for improvement in the systems for predicting air pollution.

AUTHOR

Frank Pasquill took an Honours degree in physics at the University of Durham in 1935 and was awarded the D.Sc. in 1950. He joined the United Kingdom Meteorological Office in 1937 and since 1954 has held a special appointment for individual research. He is also head of the Meteorological Office's recently formed Boundary Layer Research Branch. Throughout his career he has been concerned with aspects of diffusion and turbulent transfer in the atmosphere. He is author of the book Atmospheric Diffusion.

3. PREDICTION OF DIFFUSION OVER AN URBAN AREA – CURRENT PRACTICE AND FUTURE PROSPECTS

FRANK PASQUILL

Meteorological Office, Bracknell, England

INTRODUCTION

There are three basic components in the development of any system of estimating the concentration of air pollution solely from a knowledge of the sources and of the meteorological conditions. The first is a theory within which the relations between the spread of the material and the properties of the airflow are at least implicit, if not entirely explicit. Secondly, for operational use, this theory must then be expressed in a suitable form (so-called diffusion formula or dispersion formula) giving the concentration of pollutant in terms of the source-strength and meteorological parameters. Finally, there is the requirement for observations of the levels of air pollution produced by known sources, against which the theoretical system can be tested and from which generalizations and predictions may then be made. It hardly needs to be said that the effective union of these components has proved to be a slow and complicated process, in which considerable care is still needed to distinguish the essential features and to avoid unrewarding expenditure of research effort.

The first purpose of the present paper is to note the stage reached in the United Kingdom in the provision and testing of prediction systems in practice. Although it is evident that for urban situations there are complexities that seem intractable to precise theoretical analysis, it is nevertheless important to extract as much guidance as possible from basic ideas about the diffusive action of idealized airflow. Only by such a process can we derive the greatest benefit from such practical experience as is now available, and hence make the most sensible appraisal of the further work required. Accordingly, the second purpose of the paper is to recall the basic concepts and to note some ideas and results that seem likely to be particularly relevant to future development. From this point, attention is turned specifically to the factors determining the average rate of vertical spread in urban airflow and then, briefly, to the prospects of achieving significant improvements in the ability to predict the distribution of air pollution from specified sources.

CURRENT PROGRAM IN UNITED KINGDOM

In the Meteorological Office of the United Kingdom, the *practical* estimation of pollutant concentrations from specified sources currently follows lines that were formulated some 10 years ago, largely under the stimulus of the accident at the Windscale Works of the Atomic Energy Authority. Although this system does not contain any specific application to urban conditions, it is nevertheless relevant to our present considerations in two respects. It has been widely used as a basis for examination and comparison of many measurements, including some of air pollution in urban conditions. Also, it is now in the process of a revision that has a bearing on the extension to urban conditions.

The details of the current system are set out and discussed in two articles[2,3] and here it is proposed to do little more than emphasize a few crucial features:

1. The original aim was to provide a practical system with which, as far as possible, crosswind and vertical spread of material could be estimated from data on the corresponding fluctuations of the wind.
2. For the case of short-range vertical spread from a ground level source, and, in general, when data on wind fluctuation were not available, broad estimates of spread were provided for categories of atmospheric stability specified in terms of surface wind speed and state of sky.
3. The broad estimates for short-range spread, < 1 kilometer (km), refer to level, unobstructed terrain with rather small aerodynamic roughness, z_0 about 3 centimeters (cm). (Standard notation is followed—see end of paper for list.)
4. The broad estimates for longer range, partially based on experimental data, automatically include some influence of the minor topographical and urban features present in the area of Central Southern England.
5. No means of quantitatively allowing for either major topographical features or urban influences were provided, though some qualitative appreciation of the effect of topography was briefly attempted in the latter of the two publications.
6. As far as the magnitude of spread was concerned, no distinction was drawn between surface and elevated sources.

In operational use, the system has been limited and inadequate in a number of respects; so far, no attempts have been made to allow for these inadequacies beyond the expression of rather broad qualifications and speculations.

Experimental and observational work on the distribution of air pollutants is carried out in the United Kingdom by the Warren Spring Laboratories, the Central Electricity Research Laboratories, and the British Petroleum Research Centre. It appears, however, that the only study published so far on the use of diffusion formulas in prescribing *urban* air pollution is the one carried out by the last-named organization in the town of Reading. That study included extensive measurements of the sulphur dioxide concentration distribution and detailed estimation of the source inventory over a 15-month period during 1964 and 1965. Aspects of the study have been discussed in papers by Marsh and Foster[4]; Marsh, Bishop, and Foster[5]; and Marsh and Withers.[6] The last of these publications compares the observations with estimates derived from the source inventory and meteorological data, using a number of methods, including those used in the Meteorological Office and referred to above.

The pollution data consisted of sulphur dioxide concentrations averaged over 6-hour sampling periods, for 40 sites in and around the town. Continuous records were available for wind direction, wind speed, air temperature, humidity, and the intensities of the vertical and lateral components of turbulence. The wind speed and turbulence measurements were made at a height of 14 meters (m) in a relatively open space, 100 m or more from buildings, about 10 m high, and about 700 m from the taller buildings in the center of the town. For the source distribution, three categories of fuel-burning installations were considered—domestic heating, industrial and commercial installations for space-heating, and processing plants. Domestic (space-heating) sources were divided into 251 housing areas with a diameter of roughly 400 m, and the strength of source in each area was based on official estimates of the average fuel consumption in private houses. Installations burning more than 10 tons of fuel per year were considered individually.

For evaluation of the diffusion formulas, Marsh and Withers[6] defined 67 area sources that were treated as individual sources if their centers were farther than 1000 m from the sampling site, and 7 major sources, that were treated as individual sources regardless of distance. If the center of an area was less than 1000 m from the sampling site, the individual housing areas or installations were also treated as individual sources. In some of the calculations, the housing areas and source areas were treated as equivalent line sources. For the domestic sources, a standard height of 15 m was adopted, but for individual sources the effective heights were estimated from the chimney height and the plume rise calculated from the CONCAWE empirical formula.[7]

Marsh and Withers[7] give an extensive series of comparisons of observed and calculated concentrations from which we shall reproduce only a selection that most directly reflects on the present point of interest. The calculated concentrations were obtained in three ways:

1. Using the familiar Gaussian form for the distribution from a point source with the standard deviations (of particle displacement) σ_y and σ_z obtained from wind fluctuation data.

2. As in (1.) but with σ_y and σ_z obtained from the broad estimates of spread.
3. From a regression of the *observed* values against a parameter involving the air temperature (as representing the variation of effective overall source strength) and the reciprocal of the wind speed.

The selection of comparisons, in which the observed concentrations have been corrected for 'background' concentration using measurements made upwind of the town, is given in Table 3.1

In Marsh and Withers' analysis, attention is focused primarily on the root-mean-square (r.m.s.) differences between the observed and calculated 6-hour average concentrations. In Table 3-1, these r.m.s. differences are always large and are of similar magnitude to the corresponding overall mean of the observed concentrations. Furthermore, the r.m.s. differences expressed relative to the observed mean are lowest for the regression method and highest for the broad estimates of spread. On this basis, Marsh and Withers conclude that diffusion formulas do not provide a satisfactory basis for calculating the pollution in a town and that a regression equation directly representing observations is to be preferred.

Table 3-1. COMPARISON OF OBSERVED AND CALCULATED SO_2 CALCULATIONS AT SIX SELECTED SITES IN READING, ENGLAND[6]

	Method of calculation	Mean of 6-hour concentration, $\mu g\ m^{-3}$		r.m.s.difference between calculated and observed C	r.m.s. obs. C
		Obs. $\bar{C}$	Calc. $\bar{C}$		
All periods[a]	a. Wind fluctuation	68	38	84	1.2
	b. Broad estimates of spread (stability categories)	68	88	132	1.94
	c. Regression on temperature and wind	68	–	68	1.0
119 selected periods[b]	a. Wind fluctuation	66	53	63	0.95
	b. Regression on temperature and wind	66	–	57	0.86

[a] Methods a. and b. follow Pasquill[2]

[b] Steady wind direction and speed (6 a.m. to 12 noon and 12 noon to 6 p.m. only) for which most confident estimates of emission were made.

It is not entirely surprising, however, to find that the 'regression method', which uses the actual observations, provides the least scatter between observed and calculated values. On the other hand, it is encouraging, that the 'wind fluctuation' method provides independent estimates with individual departures that are not very much larger than those of the regression method. Also, the fact that the least agreement in the individual 6-hour values is provided by the broad estimates of spread is not surprising, since the latter refer to aerodynamically smoother terrain and, as will be seen later, the rougher nature of the terrain is reflected in the wind fluctuation measurements. Finally, Marsh and Withers are inclined to attach little significance to the overall mean concentration. In view of the very wide range of the component values, it is particularly interesting that the observed and calculated mean values are as close as they are, and that their agreement is even closer when occasions are selected for greater reliability in wind and emission estimates. Before discounting the agreement on the score of the discrepancies in individual values, it would seem desirable to examine in more detail the significance of, and possible reason for, such discrepancies. (This point will be referred to again in the final discussion.)

BASIC CONCEPTS IN THEORETICAL ESTIMATION OF DIFFUSION

The theoretical treatment of diffusion in a turbulent fluid has developed along three main lines.

1. The *gradient-transfer relation,* in which the eddy transfer of material across a plane is represented as a product of the gradient of material (normal to the plane) and an eddy diffusivity, K.
2. *Statistical theory,* involving statistical descriptions and laws for the velocities and trajectories of typical particles in the fluid.
3. Dimensional analysis and *similarity theory.*

Discussion will be confined to some specific features that seem to have particular relevance to future development of methods for estimating urban air pollution.

Applicability of Various Approaches

The fundamental validity of the gradient-transfer approach has always been regarded as a matter of debate, and it is important to make clear the circumstances in which it is most acceptable. Any qualitative basis for the method, as is involved in the classical 'mixing length' theory or in direct analogy with kenetic theory of molecular motion, inevitably implies the notion that the physical scale and effective range of action of the turbulent elements be small compared with the domain over which the diffusible material is spread. Obviously, this condition may be expected to be approached as the spread of the material increases with time or distance of travel from the source.

Consistent with this *physical* idea is the formal result from statistical theory that, in the limit of *long time*, T, the spread of particles in homogeneous turbulence is proportional to $T^{1/2}$, as in the Fickian (constant K) solutions of diffusion.

Recognition of the existence of the foregoing parabolic law is confused by two practical features of atmospheric flow. The first is the width of the spectrum of eddy motion, which is such that diffusive spread over dimensions larger than *all* effective eddies may not be achieved in practice. The second is the lack of homogeneity in the atmosphere regarding such properties as mean wind speed and direction, and the intensity and scale of turbulence. No demonstration has yet appeared for the existence of the parabolic relation in horizontal spread. There is, however, evidence in Hogstrom's[8] experimental study using an elevated source, of a close approach to this relation for *vertical* spread in stable conditions. This seems entirely consistent with the idea that, in such conditions, the vertical scale of the eddies will be significantly limited. It is not unreasonable to expect this limitation in vertical scale to be effective irrespective of stability, provided the cloud or plume of material is not clear of the ground (i.e., as from an elevated source). In other words, *vertical* diffusion from a source that is effectively at ground level may reasonably be expected to be in accordance with the gradient-transfer theory, without necessarily leading to the parabolic law, since the effective K must then be expected to be a function of height. On the other hand, it is evident that the early stages of spread in the horizontal, or in the vertical, when the source is elevated, cannot generally be attributed to a constant diffusivity or to a function only of position in the flow. In these cases, the statistical theory appears to be a preferable alternative.

The Lagrangian similarity theory was originally put forward as a means of predicting the variation of a continuous point-source concentration with distance downwind. Since *crosswind* diffusion is implicity involved, there is some controversy regarding the fundamental validity of the approach, but this qualification does not apply to *vertical* spread. In any case, there is a basic restriction of the height range over which the horizontal shearing stress is effectively constant.

General Explicit Form for K

Well-known forms for K have been specified for two limiting conditions, i.e., for the constant-stress layer, when, for vertical momentum transfer

$$K = ku_* x / \phi \left(\frac{z}{T}\right) \qquad (1)$$

$$= ku_* z, \text{ at small } \left(\frac{z}{T}\right) \qquad (2)$$

and for particle spread in the limit of long time in homogeneous turbulence

$$K = \sigma_w^2 \, t_L \tag{3}$$

Invoking dimensionally acceptable and empirically determined relations between the variables σ_w, u_*, t_L, t_E, λ_m, and z, Equations (2) and (3) may be reduced to a common form

$$K = \frac{1}{10} \sigma_w \lambda_m \tag{4}$$

where λ_m is the equivalent wavelength for peak nS(n) in the spectrum of the vertical component.

Invoking a further relation between σ_w, λ_m, and ϵ (see Pasquill[9]), this may be further transformed to

$$K = \frac{1}{15} \epsilon^{1/3} \lambda_m{}^{4/3} \tag{5}$$

Note that equations (4) and (5) allow K to vary with height in an arbitrary way, according to the variation with height of the properties σ_w, ϵ, and λ_m, and prescribe the magnitude of K in terms of any two of these three quantities. The expressions for K are suggested as plausible universal forms, to be used irrespective of height and stability in the atmosphere, in future studies of the vertical spread at medium- and long-range from a surface source.

Estimation of the quantities λ_m, σ_w, and ϵ requires special turbulence measurements, either for direct use or for the specification of climatological values for subsequent use. Recent studies such as those of Busch and Panofsky[10], Pasquill[9], and Readings and Rayment[11] are relevant in the 'climatological' respect. The first of these provides information on σ_w and λ_m in the lowest hundred meters or so of the atmosphere, and the second and third are first steps towards a more comprehensive specification of σ_w and ϵ over the first kilometer.

Effect of Aerodynamic Roughness and Thermal Stratification on Vertical Spread

Examination of the effect of aerodynamic roughness and thermal stratification on vertical spread can be considered in terms of the gradient-transfer method, in so far as the effective K is appropriately specified. The forms of K suggested above do, in fact, reflect the roughness and stratification directly, in the case of Equations (1) and (2), and indirectly, through σ_w, λ_m, and ϵ, in Equations (3) and (4). Such forms may, therefore, be useful in making theoretical estimates, subject to the basic acceptability of the method. For those circumstances in which the gradient-transfer method is inapplicable, and in which the statistical theory is more appropriate (notably the calculation of crosswind spread or of vertical spread at relatively short range from an elevated source), the effects of roughness and stratification are reflected in the magnitudes of σ_w and t_L. Even for the case of vertical spread from a ground level source at relatively short range, however, the gradient-transfer method is complicated by the logarithmic form of wind profile applicable in neutral conditions; the Lagrangian similarity theory now seems to provide an approach that is neater analytically and more satisfying physically.

For neutral flow, the Lagrangian similarity theory provides the following relation between the mean height reached by successively released particles ($\bar{Z}$) and the mean horizontal distance that they have travelled in a given time, ($\bar{X}$).

$$\bar{X} = \frac{\bar{Z}}{kb} \quad [\ln \frac{c\bar{Z}}{z_o} \; -1 \; + \frac{z_o}{\bar{Z}} \; (1 - \ln c)\,] \qquad (6)$$

It has been argued that the dimensionless constant b is identical with von Karman's constant, k, and there is some observational evidence for this.[12] On the other hand, the constant c has not yet been well-determined. This constant is, in fact, the ratio of the mean horizontal velocity of the particles to the mean fluid velocity at the height $\bar{Z}$, and in the earlier forms of the treatment was assumed to be unity. Since it seems likely to be between ½ and 1 [a recent theoretical estimate by Chatwin[13] gives 0.56], the remaining uncertainty in its precise value is not particularly important. Given the constants b and c, and a specification of the characteristic aerodynamic roughness through z_0, Equation (6) can provide the magnitude of vertical spread as a function of distance.

In the testing and practical use of Equation (6), there are two other complications not yet mentioned, which, fortunately, seem unlikely to be of major importance in terms of the expected accuracies: 1.) Most published results on vertical spread have been expressed in the form of r.m.s. spread, σ_z or of 'height of cloud', conventionally defined as the height at which the concentration or dosage is one-tenth of the gound-level value. Conversion from $\bar{Z}$ to one or the other of these more useful forms requires the *shape* of the vertical distribution to be specified. In practice it is customary to assume the simple Gaussian form. While there is no obvious reason to prefer any other form in the case of crosswind spread from a point source or vertical spread from an elevated source, there is some doubt about its suitability in the case of vertical spread from a ground-level source. On theoretical grounds, the exponent s in the exponential form, $\exp(-\,bz^s)$, seems likely to be somewhat less than the Gaussian value of 2.0; and experimentally determined values lie in the range 1.1 to 1.5.[14, 15]

Measurements of vertical spread of air and the associated concentration of material from a continuous source refer to particles that have all travelled to a specified position at a distance x downwind from the source. On the other hand, in the foregoing theoretical result, the vertical spread is related to the mean of all distances travelled by all particles in a particular but otherwise unspecified time. In practice, the assumption is made, so far without any formal or observational demonstration, that the two specifications of vertical spread are identical when $x = \overline{X}$.

Finally, it should be noted that although Equation (6) has a fairly convincing theoretical background, it has so far been tested in a limited way, only for diffusion over surfaces with very small z_0 (1 cm to 3 cm).

Turning to the effect of thermal stratification, it may be noted that an extension of the Lagrangian similarity theory to stratified conditions has been developed and, to some extent, tested.[16] Here again, there are controversial features, with specific respect to the *vertical* spread.[12] Nevertheless, the notion that the effect of stability on properties of vertical spread is somehow characterised by the Monin-Obukhov length-scale has considerable appeal, and could be used as the stability parameter in correlating measurements of vertical spread. The writer has recently been reviewing this possibility in relation to the prairie grass measurements at O'Neill, Nebraska, in 1956, also with the objective of assigning values of L to the qualitative stability categories referred to earlier in this paper. A reasonably close correlation between σ_z and Panofsky's $L' \left(= \frac{K_h}{K_m} L\right)$ has already been demonstrated[12] (Figure 3-1), but L' (as distinct from L) has the complication of being a function of height even in the constant-stress layer. A completely satisfactory assessment of the values of L, to be associated with the prairie grass data, has not yet been achieved. At present, the most reasonable assessment is based on assuming $Ri = \frac{z}{L}$ as a working approximation in unstable conditions. This suggests that the minimum value of $|L|$ in the particular prairie grass data summarized by the writer[2] was between 3 and 4, and that the values of $|L|$ to be associated with stability categories A, B, and C are roughly 1, 3, and 10.

ESTIMATE OF EFFECT OF URBAN ROUGHNESS

Although the concept that the enhanced roughness in an urban area would cause an increase in vertical spread, as compared with open and relatively smooth country, seems to have been accepted, no theoretical estimate of the magnitude of the effect has yet been offered. For relatively short distance of travel, we can easily make such an estimate from the Lagrangian similarity treatment for neutral conditions. In Equation (6), $b = k = 0.4$; if c is 0.6, it then remains to specify the roughness length, z_0, for an urban area.

Davenport[17] quotes a value of 3 m for z_0, derived from wind profile observations by Jensen, in the center of Copenhagen, and by Shiotani and

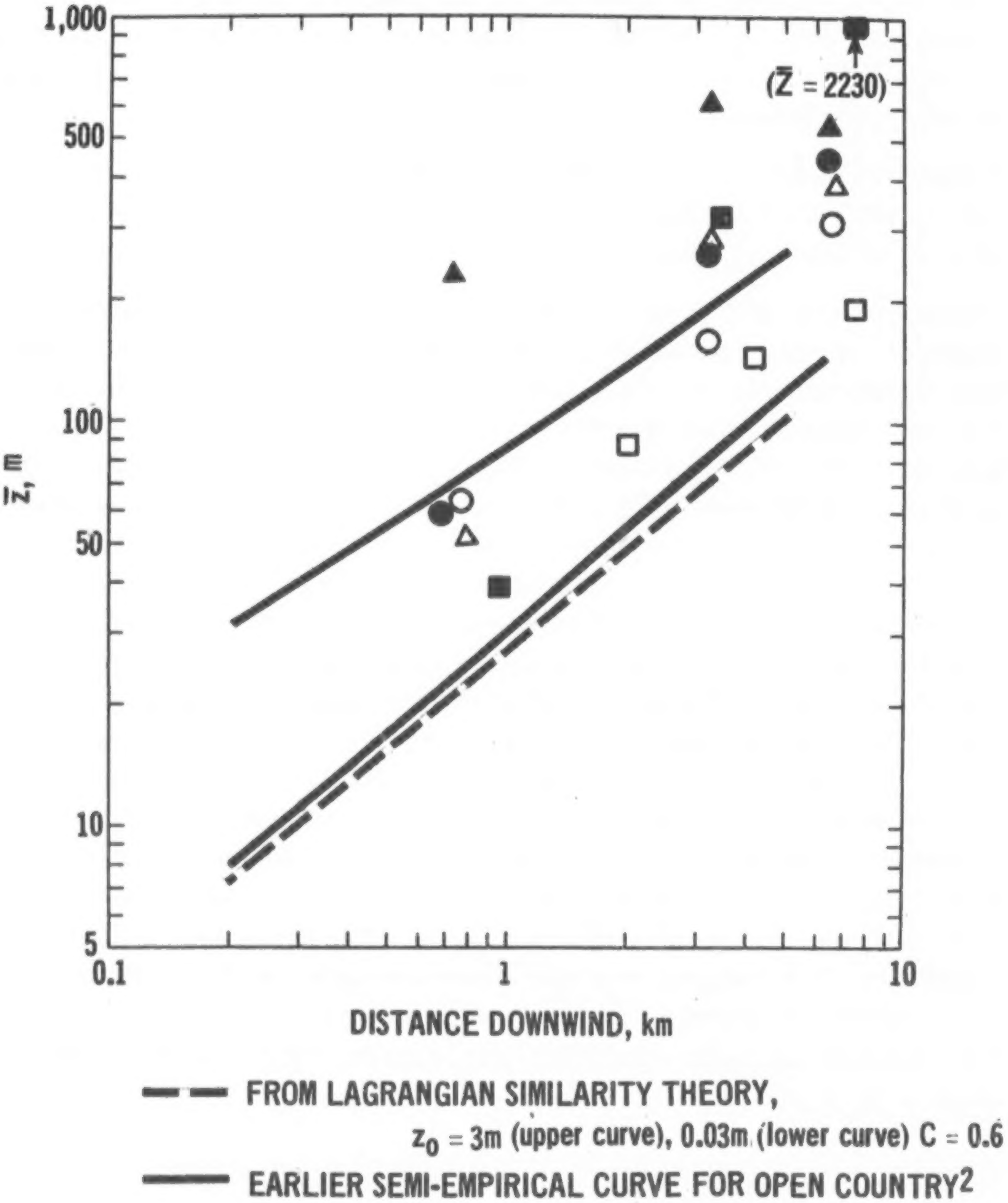

Points from St. Louis dispersion study experiments No. 16 (●), 24 (■), 35 (▲), 37 (○), 42 (□), 43 (△). Open points for daytime, solid for evening experiments.

Figure 3-1. Vertical spread Z as a function of distance from a source near ground level.

Yamamoto, in the suburbs of Tokyo. In a later paper on the wind profile and spectrum of wind speed in London, Ontario, Davenport[18] gives a further estimate of 2.3 m. An independent rough indication is provided by Marsh's [19] measurements of turbulence in the rather open site near the centre of Reading. These give $\sigma_w/\overline{u} = 0.17$ at a height of 14 m in neutral conditions. Adopting the value 1.25, which now seems to be well established for the ratio σ_w/u_*, and substituting in the usual form $k\overline{u}/u_* = \ln(z/z_o)$ for the wind profile, we obtain $z_0 = 0.7$m. This may be an overestimate since no allowance has been made for a zero-plane displacement in the wind profile. There is, however, probably another underestimation arising from the fact that σ_w was measured over an area more open, and hence, smoother than the town in general. On the whole, it would appear that values in the range 1 to 3 m may be taken as typical for modern urban complexes.

Equation (6) has accordingly been evaluated for distances in the range 0.2 to 5 km, using $z_0 = 3$ m and, for comparison with relatively smooth open country, = 0.03 m. The results are shown graphically in Figure 3-1. Note that the difference of 100-fold in roughness length brings an increase in vertical spread that ranges from 4-fold at the shortest distances to just over 2-fold at 5 km. The growth of vertical spread with distance may be approximated by a simple power law $\overline{Z} \propto \overline{X}^p$; the curve can be fitted at the greater distances with p equal to 0.85 for $z_o = 0.03$ m and 0.72 for $z_o = 3$ m. For comparison, the corresponding section of the semi-empirical curve for vertical spread in neutral conditions in open country[2] has been reproduced in Figure 3-1, after converting from a 'height of cloud' to $\overline{Z}$, assuming a vertical distribution of the form exp $(-b\overline{z}^{1.5})$. As already pointed out, this empirical curve corresponds to a z_0 of about 0.03 m, and is remarkably consistent with the Lagrangian similarity prediction. This latter agreement is not entirely new, having already been demonstrated for a distance of 100 m,[12] but here is additionally verified over the considerable range of distance up to 5 km. In view of the magnitude of vertical spread at the extreme distance, however, implying diffusion over some hundred of meters, i.e., outside the likely depth of the constant-stress region, the extension of the range of agreement may be rather fortuitous.

No useful *direct* measurements are yet available for vertical spread over an urban area, but indirect estimates have recently been published by McElroy and Pooler[20] on the basis of a tracer study in St. Louis, Mo. The St. Louis 'dispersion study' was carried out from 1963 to 1965, using a point source of fluorescent particles (zinc cadmium sulphide) near ground level. In each of about 40 experiments, the source was maintained for about 1 hour, and measurements of total dosage at the surface were obtained on three nearly circular arcs at distances between about 1 and 10 km. (A few vertical distribution measurements were made from a tethered balloon but, evidently, these did not provide any definitive information.)

By an application of mass conservation, McElroy and Pooler derive values of equivalent σ_z from the observed surface distribution of dosage and the amount of tracer emitted. In certain stages of their calculation, a Gaussian distribution in the vertical is assumed and, in adjusting the values for comparison with the $\overline{Z}$ of Figure 3-1, a correction has been included on the assumption that the vertical distribution was actually of the form exp ($-bz^{1.5}$). Actually, the effects of transforming from σ_z to $\overline{Z}$ and of correcting for the shape of the vertical distribution are both small and largely compensatory, and the net adjustment is less than 10 percent; so that, for practical purposes, the magnitudes adopted for $\overline{Z}$ are essentially those given for σ_z in Table 2 of McElroy and Pooler. The data for effectively neutral conditions, in which the bulk Richardson Number, Ri_B, was within the range ±0.01, i.e., those of experiments 16, 24, 35, 37, 42, and 43 are plotted on Figure 3.1. Note that the data from the four 'evening' experiments are all above the $z_o = 0.03$ m curve, and their average trend is obviously more in accordance with, though slightly lower than, the curve for $z_o = 3$ m. Closer examination of the variation with z_o suggests that the best fit to the evening data would occur with a z_o of about 1 m. In considering this result, it must be remembered that the theoretical treatment assumes horizontal uniformity and that the flow over the city is in equilibrium with the surface characteristics, at least over the height range encompassed by the vertical spread of the tracer. The values of $\overline{Z}/x$ range from about 0.06 at 1 km to about 0.04 at 5 km from the source. The corresponding ratio of $\overline{Z}$ to the upwind extent of flow over urban terrain is presumably smaller (since the source was not located at the upwind edge of the city) but it seems unlikely that it could be less than say, 0.03, at the longer sampling distance. Since the currently suggested ratio of the height of the new equilibrium layer to the fetch over a new terrain is $\leqslant 0.01$, the vertical distributions of the tracer cannot be assumed to have been entirely within the equilibrium layer.

Also, most of the estimates of vertical spread from the two 'daytime' experiments are substantially larger than those from 'evening' experiments. In considering this difference, it is to be noted that McElroy and Pooler used rather different procedures in deriving their σ_z. They assumed a Gaussian distribution from the start, with a wind constant with height for 'daytime' experiments. For the evening experiments, the wind was assumed to have a simple power law variation with height and an equivalent 'height' of cloud, h, was evaluated on the assumption that concentration was constant up to h and then fell to zero. The height, h, was converted to an 'equivalent Gaussian' σ_z by writing

$$h \, x_0 \, \overline{u}_e = \frac{\pi}{2} \, \sigma_z \, x_0 \, \overline{u}_d \qquad (7)$$

and assuming that the effective mean wind speeds, u_e and u_d, were the same. Since u_d is strictly a mean of the wind distribution over the real height of the cloud weighted according to the concentration, it follows that, if the cloud distribution did extend above h (as it would in a Gaussian distribution), $\bar{u}_d > \bar{u}_e$, and the σ_z derived from h would be an overestimate, suggesting that the discrepancy between the 'evening' and 'daytime' results could be a consequence of the difference in analytical procedure.

The tentative conclusion is that, in evening conditions with neutral thermal stratification within the city, the enhancement of the average vertical spread by urban roughness is consistent with similarity theory. In practice, this vertical spread is about two to four times that normally ascribed to neutral conditions over level, unobstructed, open country. In daytime conditions, however, which are apparently identical as regards thermal stratification in the city, the vertical spread implied by surface concentration downwind of a source appears to be substantially greater than can be accounted for by roughness. The reason for this discrepancy is not yet evident.

EFFECT OF URBAN HEATING

There is abundant evidence that the temperature regimen within an urban area is measurably different from that in open country. Mid-urban air temperatures are known to reach values higher than those in surrounding rural districts, by amounts ranging from a few tenths to several degrees Centigrade, the maximum effect (in UK cities) being found on calm clear nights in summer. There are probably two important contributions in the production of this *heat island.* The first is concerned with the natural heat transfers; the balancing of the net supply or loss by radiation must be provided predominantly by ground conduction and turbulent transfer in the air; whereas in vegetated areas, the loss of heat by evaporation is an important and, at times, controlling contribution. As a consequence, *surface* temperatures may reach appreciably higher values in towns and cities than in country districts. Cities also have a second 'man-made' supply of heat that will contribute to enhance urban temperatures.

It is to be expected that the urban heat island will affect both the horizontal airflow pattern and the vertical mixing over a city, especially when the airflow is naturally weak. This, in turn, may affect the distribution of pollution. Summers[1] has proposed a model of urban air pollution based on the concept that, with a stable incident airstream, the effective depth of mixing over a city is essentially determined by the heat released in the city from domestic heating and industrial operations.

In the first instance, it is useful to note the magnitudes of heat transfer that are likely to be involved. Summers estimates that, over the densely built-up area of Montreal, the heat output from space-heating and industrial activities is, on the average, about 4 × 10^{-3} cal cm^{-2} sec^{-1} and points out that in winter this amounts to an appreciable fraction (about one-fourth) of the heat received from the sun. In open country, even with strong insolation, the rate of transfer of heat from the surface by turbulent and convective transfer is probably not much larger than the urban heating rate quoted by Summers—for example, measurements of turbulent heat flux by Swinbank[21] range up to about 8 x 10^{-3} cal cm^{-2} sec^{-1}. On the other hand, on clear nights the turbulent transfer of heat to the surface is probably only about 10^{-3} cal cm^{-2} sec^{-1}.

It is probably a reasonable assumption that, in the absence of unnatural heat supplies, the turbulent transfer of heat over a city would be larger than over open country by day, and of similar or smaller magnitude by night. The net effect of also including a fraction (say half) of the unnatural output of heat might, therefore, range from a modest increase in the (upward) turbulent heat flux, H, during the day and a marked decrease, or even reversal, of the (downward) heat flux at night. A first-order estimate may then be attempted by regarding the effect on the rate of vertical spread as characterised by the length-scale, L, which is proportional to u_*^3/H. From the trend of the prairie grass data on short-range vertical spread (see Figure 1 of Pasquill[12]), it seems that a substantial reduction or reversal of the downward H (hence of 1/L) at night is likely to be more effective in proportionately increasing vertical spread than a corresponding increase of the upward H during the day.

The St. Louis data on vertical spread have been classified by McElroy and Pooler[20] in terms of qualitative stability categories equivalent to those defined by the writer,[2] as well as in terms of Richardson number and wind gustiness. The former classification provides an opportunity to examine the effect of urban heating in the following way.

Figure 3-2 (reproduced from McElroy and Pooler's[20] Figure 10) shows the mean curves of σ_z against distance, for the various stability classes. Here, classification D, for example, is not representative of effectively neutral conditions; rather it represents the net effect of an incident neutral atmosphere plus any effect of urban heating. Plotted on the same diagram are two mean curves for $Ri_B = \pm 0.01$, one reproduced from McElroy and Pooler's Figure 2, the other based on evening data only. If the latter curves are taken to represent neutral conditions *in the urban airflow,* then their departures from the McElroy and Pooler curves represent the net effect of natural atmospheric thermal stratification and urban heating. For comparison, we may use the 'open-country' curves of the writer's[2] Figure 2, here referring the curves to the D(1) curve as one truly representative of naturally neutral conditions.

Table 3-2 has been constructed from Figure 3-2 and the corresponding

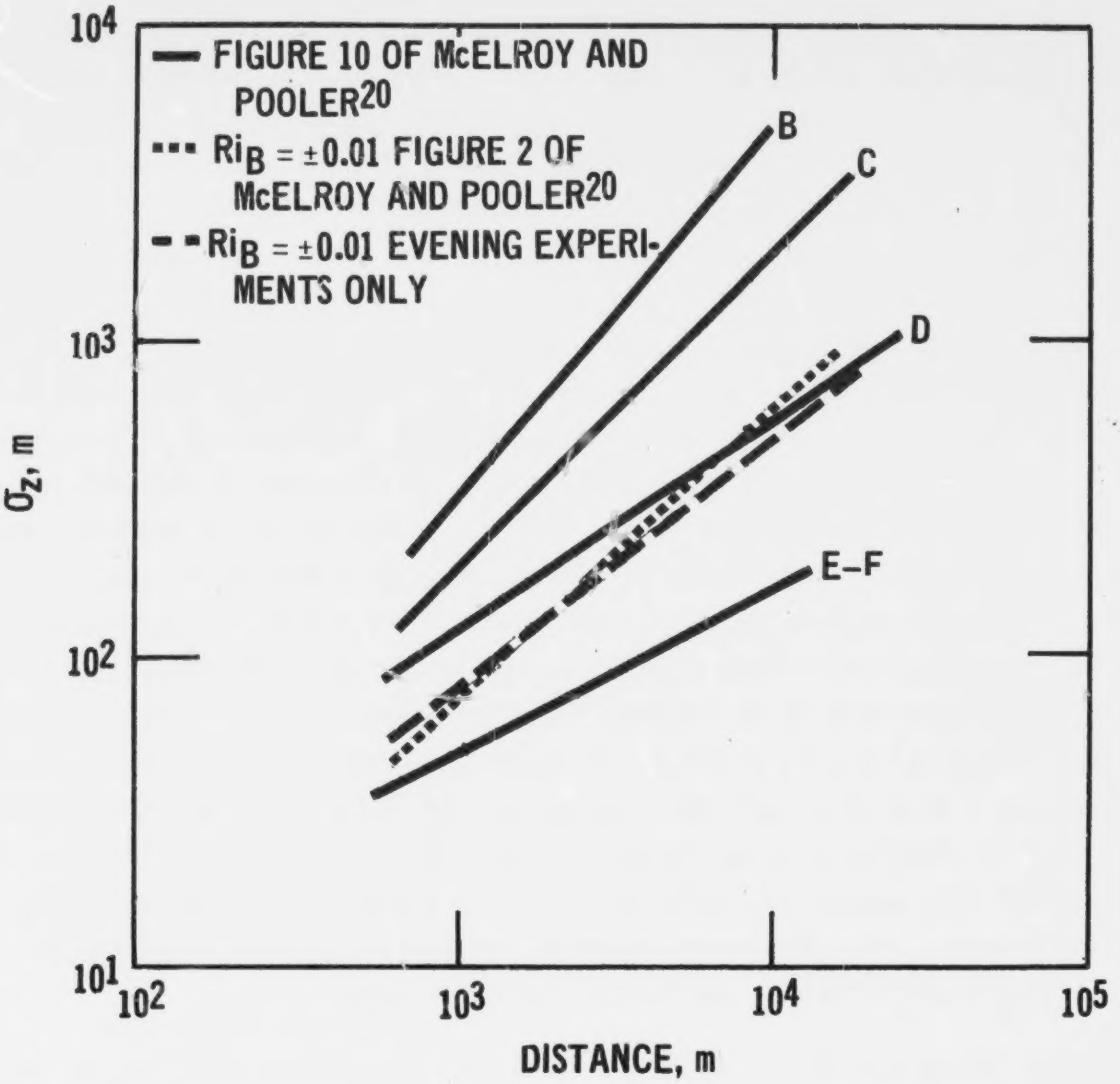

Figure 3-2. Vertical spread from ground-level source in St. Louis, Missouri.

Table 3-2. RATIO OF σ_z TO ITS VALUE IN EFFECTIVELY NEUTRAL CONDITIONS, FOR OPEN COUNTRY STABILITY CATEGORIES B TO F

Vertical distance, km	Location	Ratio of σ_z to value in effectively neutral conditions for stability categories,			
		B	C	D	E – F
1	St. Louis[a]	4.5	2.7	1.7	0.7
	St. Louis[b]	4.0	2.4	1.5	0.6
	Open country	3.2	1.9	1.0	0.5
10	St. Louis[a]	9	3.4	1.0	0.3
	St. Louis[b]	11	4.1	1.2	0.4
	Open country	6	2.4	1.0	0.3

[a] Using McElroy and Pooler's curve for Ri_B ± 0.01 in their Figure 2.

[b] Using data for Ri_B ± 0.01 in evening conditions only.

curves for open country to display the apparent effect of natural stability in the two cases at distances of 1 and 10 km. The figures in the table are the ratios of σ_z to its value in effectively neutral conditions. A modification of the effect of natural stability by urban heating should result in larger ratios over a city than over open country. For the shorter distance, this effect is evident consistently at all stabilities, but, for the longer distance, it is more obvious in the B and C than in the D and E-F categories. Thus, the speculation above that the effect of urban heating might be expected to be more obvious in naturally stable than in unstable conditions does not seem to be supported by the figures, which, in fact, imply a difference at the larger distance and no obvious difference at the shorter distance. Related to this, is the fact that in Figure 3-2 the slopes of the E-F and D curves are apparently quite different from the slopes of the curves for effectively neutral conditions within the city. A possible implication is that the artificial sources of heat act in two ways. Those producing heat at low level may lead to enhanced mixing at low level (hence, at short distances from the source of material), whereas those effective in heating relatively high layers (elevated sources and rising plumes) may reinforce the stability that is ultimately restrictive as regards vertical spread to greater heights (i.e., at longer distances from the source of material). Such a restriction would not apply to material released with the heat; however this type of release presumably was not the case in the tracer experiments under consideration.

As regards categories E-F and D, the temperature gradient data for St. Louis (obtained from 40- and 150-m levels on a 'downtown' television tower and represented in Ri_B) provide additional evidence. Of the five E-F cases, three have specified values of Ri_B, which are + 0.14, – 0.03, and + 0.12. From these there is no strong indication of a general elimination of the stable classification, consistent with the indication in Table 3-2 that at the longer distance the influence of urban heating had not brought the vertical spread in E-F conditions near the magnitude expected in effectively neutral conditions. On the other hand, for those occasions when a D classification is indicated consistently at all three of the meteorological sites employed (McElroy and Pooler's Table 3,[20] the values for Ri_B are in the range –0.05 to 0, i.e., no positive values, suggesting conversion to somewhat *unstable* thermal stratification in the urban airflow, which is generally consistent with Table 3-2.

It would be unwise to attach too much significance to these results alone, bearing in mind the considerable scatter in the data that lead to the curves on Figure 3-2, and the qualitative nature of the stability classification. In particular, there is some doubt about the precise comparability of the present urban and open country curves when so classified.

At this point, some comment on Summers' model[1] for vertical spread in the flow over an urban area of an initially stable atmosphere seems desirable. The essential principle of this model is that any heat released into the atmosphere from domestic and industrial processes is instantaneously mixed in the vertical, generating a growing layer with a dry adiabatic temperature lapse rate (or constant potential temperature) extending from the ground. This layer is identified with the mixing layer for pollutants, and the corresponding assumption of uniformity of concentration with height provides an easily deducible relation between rate of emission of pollutant, wind speed, and distance alongwind.

Initially Summers adopts linear profiles of temperature and wind, but for much of the ultimate analysis he eliminates the wind variation. The analysis can easily be generalized, using power law forms for the height-dependence of temperature and wind and also for the variation of heat input with downwind distance, x, from the upwind edge of the city. Taking for the potential temperature distribution

$$\begin{aligned} \theta(z) &= az^p \text{ at } x < 0 \\ &= ah^p \text{ at } x > 0,\ 0 < z < h \\ &= az^p \text{ at } x > 0,\ \quad z \geqslant h \end{aligned} \tag{8}$$

for the wind distribution

$$u = bz^\alpha = \frac{u_1}{z_1^\alpha} z^\alpha \tag{9}$$

uniform in the horizontal both upwind of and directly on the urban area, and for the surface heat input from urban processes

$$q(x) = cx^\gamma \text{ per unit area and unit time} \tag{10}$$

conservation of heat requires

$$h \propto u_1^{-\frac{1}{1+\alpha+\rho}} \quad x^{\frac{1+\gamma}{1+\alpha+\rho}} \tag{11}$$

Simplification to the case of $p = 1$, $\alpha = \gamma = 0$ gives

$$h \propto u_1^{-1/2} \quad x^{1/2} \tag{12}$$

as obtained by Summers, while more realistic values, say 0.3 for α and p, give a result that is only slightly different

$$\text{i.e. } h \propto u_1^{-0.6} \quad x^{0.6} \tag{13}$$

As a matter of practical interest, three examples of stable temperature and wind profiles observed near midnight at Cardington, England, have been analysed, by numerical integration, to get the heat required to convert to uniform potential temperature over various depths. The results are displayed in Figure 3-3. Of particular interest is the fact that over a considerable range there is, on the average, a fairly close fit to a relation

$$h \propto \left[\int_0^x q(x)dx \right]^{1/2} \tag{14}$$

which for uniform heat input implies $h \propto x^{1/2}$, as predicted by the simple model.

The heat input required to produce a value of h similar to the vertical spread of tracer material observed in St. Louis has been considered nominally for these cases where conditions of stability prevail (E-F). If we take the total vertical spread of the tracer cloud to be, say $2\sigma_z$, this gives, according to Figure 10 of McElroy and Pooler[20], a value of about 350 m at 10 km downwind from the source. Assuming uniform heat input, Figure 3-3 indicates that such a value for h at 10 km would require 7.4 x 10^{-3} cal cm^{-2} sec^{-1}, not unlike, though somewhat larger than, the figure of 4 x 10^{-3} estimated by Summers[1] for Montreal. Moreover, the temperature data already discussed for St. Louis imply that mixing to the stage of uniform potential temperature did not extend over the full depth of the tracer-cloud. In other words, the extent of vertical mixing is not determined solely by the urban heat input as implied in Summers' model but, as implied by the analysis of urban roughness, is probably controlled to a large extent by the surface roughness of the area.

CONCLUSIONS AND FUTURE PROSPECTS

In order to predict levels of air pollution in any condition of terrain, one must distinguish between two main classes of meteorological conditions—those in which the airflow is relatively well defined, with geostrophic wind speeds, say > 5 m sec^{-1} and those in which the wind is calm or very light and the general pattern of flow is not under any large-scale control. For the second class, the foregoing treatments are almost certainly inappropriate and a special approach recognizing the local and individual character of the flow pattern would appear necessary. For the first class, however, the preceding discussion suggests that the 'idealized' (open-country) treatment may be extended to urban situations to give at least a crude specification of the effect of increased roughness and, to some extent, the effect of urban heating on the general rate of vertical diffusion and the consequent average level of concentration from an array of sources. There are, of course, still many deficiencies in the system and it would be unrealistic to expect further improvements to appear rapidly.

Current and foreseeable investigations of the turbulent properties and

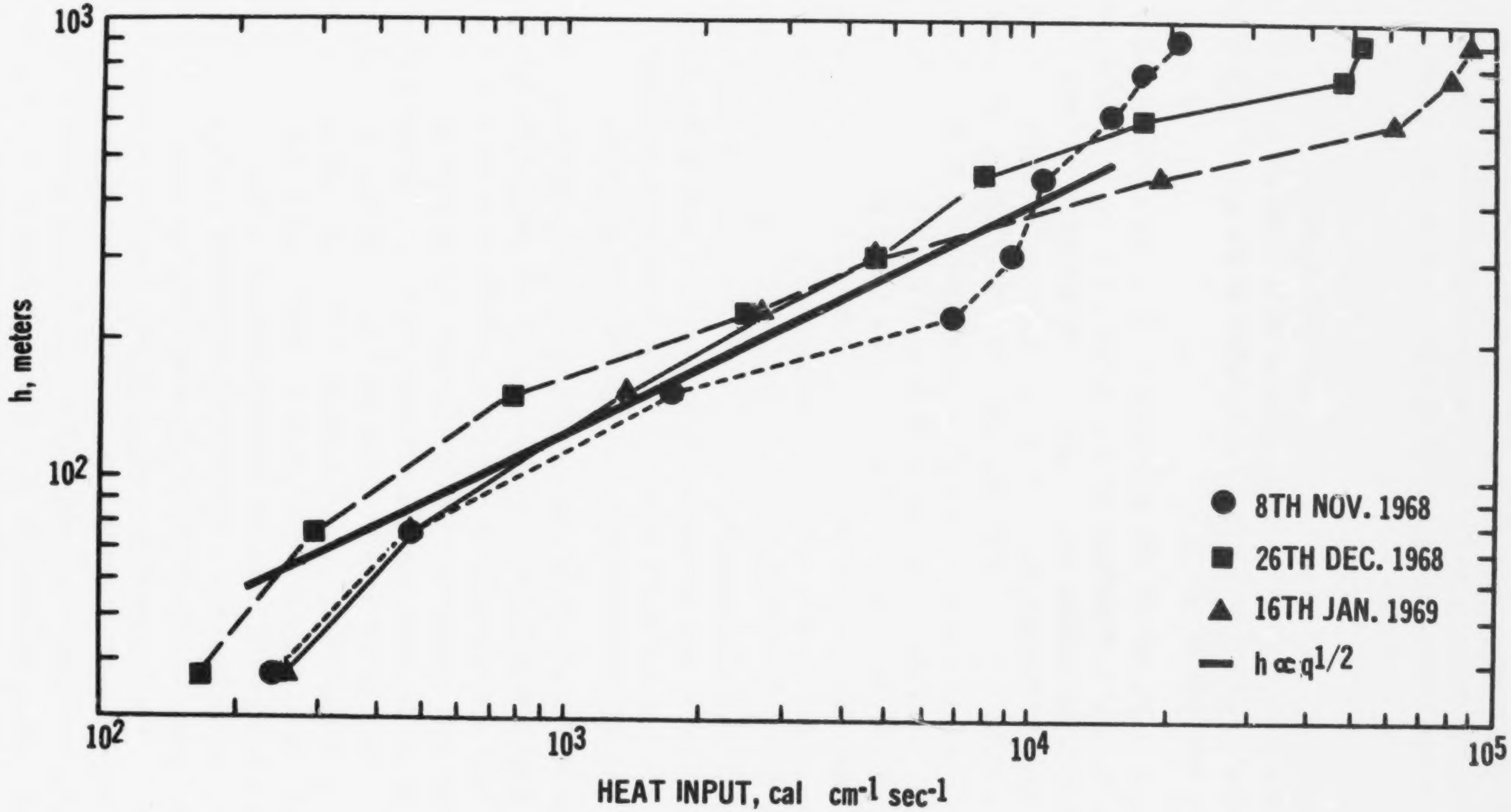

Figure 3-3. Heat input required to adjust 2300 temperature profile (Cardington-England) to uniform potential temperature $\theta(h)$ through layer 0-h.

diffusive action in the upper parts of the planetary boundary layer seem likely to be quite relevant to the matter of vertical diffusion at medium range over an urban area. With increasing height in the boundary layer, it seems clear that the character of the turbulent motion will have progressively greater dependence on buoyancy effects and progressively less dependence on the aerodynamic character of the surface. The latter feature is, to some extent, reflected in the theoretical results discussed earlier, in which the proportionate effect of a change of roughness on $\overline{Z}$ decreases with distance of travel. When vertical spread is large, whether as a result of instability or of long-distance travel, observations of turbulence at the greater heights will be particularly meaningful.

The continuous evolution of the boundary layer in response to changing surface roughness and surface heating is a matter attracting increasing attention in meteorological studies. Such studies should bring further insight both into the process of modification of an airstream as it leaves rural surroundings and flows over an urban area and into the analogy of the modification of an initially stable airflow by an urban heat input with the temporal modification of the nocturnal boundary layer by the sun's heat early in the morning. Except for complications that may arise from the particular variations of the heat input in time or space, and from the effects of wind shear in the advective case, we may take $\frac{\partial}{\partial t}$ as equivalent to $u\frac{\partial}{\partial x}$. Reference to existing information on the diurnal development of the vertical temperature profile may well be rewarding, but it is also evident that special observations on these evolutionary aspects are desirable. Examples that spring to mind immediately are the post-dawn evolution of the turbulence profile and the formation of an evening 'heat plume' over a large urban complex.

It may appear that much could also be done directly to improve our knowledge of the turbulent and diffusive structure over an urban area. Amid the complexities that are inevitably present, the problem is to isolate the controlling features and subject them to theoretical analysis and critical observation. For certain purposes, tracer experiments have an immediate appeal in that they provide a direct answer to the ultimate questions, but they may involve expensive repetitions unless supported and generalized by a rational theoretical approach. Thus it would seem no more than common sense to ensure, by examinations of the kind described previously, that the maximum information is extracted from a preliminary experiment, such as that conducted in St. Louis, before planning and embarking on repetitions or extensions. One of the outstanding prerequisites for the theoretical specification of the rate of vertical mixing is the provision of characteristic profiles of the intensity and scale of turbulence. For the effective vertical diffusivity, we recall that such a specification is provided by data on any two of the quantities σ_w, ϵ, and λ_m, and it would clearly be a step of major importance to extend to the higher parts of the boundary layer the generalizations that are now available for these same quantities in the lower layers. The experimental program now evolving at the Cardington station of the Meteorological Office is expected to provide such data, ultimately. It will be characteristic of open country with variable but relatively minor roughness from both natural and urban features. It would, of course, be valuable if at least some of the simpler observations were to be carried out over rougher terrain and specifically over a major urban complex. Measurements of the relatively high-frequency contribution to the intensity of turbulence, from which to derive estimates of ϵ, seem particularly worthy of consideration.

In the meantime, the attention of the Meteorological Office is focused on the exercise of making the most realistic estimates of the K profile, commensurate with the limited theoretical understanding and observational data currently available on the effects of natural thermal stratification and roughness. The intention is then to examine the consistency of these profiles with the independent data available on the vertical spread of windborne material over medium (10 km) and long distances (100 km). This exercise is an essential part of the previously mentioned revision and extension of the practical system for estimating pollutant concentration, and will be reported in detail elsewhere.

Most of this discussion has been concerned with the general rate of vertical mixing in the atmosphere and as such is meaningful only in relation to spatial integrals of pollutant concentration. As regards the detail of the variation of concentration in space and time, it is obvious, even from a consideration of relatively ideal conditions of diffusion, that there are additional limitations to be faced. From general estimates such as those provided by the writer,[2] it is easily demonstrated that the estimated concentration arising from a point source, at a given position relative to the source, may change by several-fold as a consequence of a 5- to 10-degree change in the assumed wind direction, especially in neutral and stable conditions. It would obviously be unrealistic to expect any better precision in specifying the effective wind direction from the observations available in an urban experiment such as that reported by Marsh and Withers.[6] From this uncertainty alone, it should not be surprising that the individual 6-hour dosages in that experiment deviated widely from the corresponding calculated values. Discrepancies introduced in this way and from other uncertainties, notably those in the magnitude of the spread and in the strengths of the sources, can be reasonably expected to contain a large random element. It would be of interest to examine whether there is, nevertheless, some measure of agreement in the statistical distributions of pollutant concentration as measured and as calculated (i.e., the frequency of occurrence of various levels of concentration in space or time). It may be significant in this connection that in Marsh and Withers' analysis[6] (Table 3-1) the r.m.s. differences between calculated and observed values are not greatly in excess of the r.m.s.

variations of the observations themselves (as represented in the simple regression analysis). A more direct examination of the compatibility of the distributions would be desirable, however, and if successful, would be an encouraging pointer to the prospects of predicting more than the average level of pollutant concentration.

ADDENDUM

Since this paper was completed, Mr. Marsh has followed up the suggestion made in the last paragraph and has derived frequency distributions of observed and calculated 6-hour concentrations for three of the sites in the Reading experiment. I am grateful to Mr. Marsh for his permission to reproduce the combined data here, in the form of a plot on a log-normal scales (Figure 3-4).

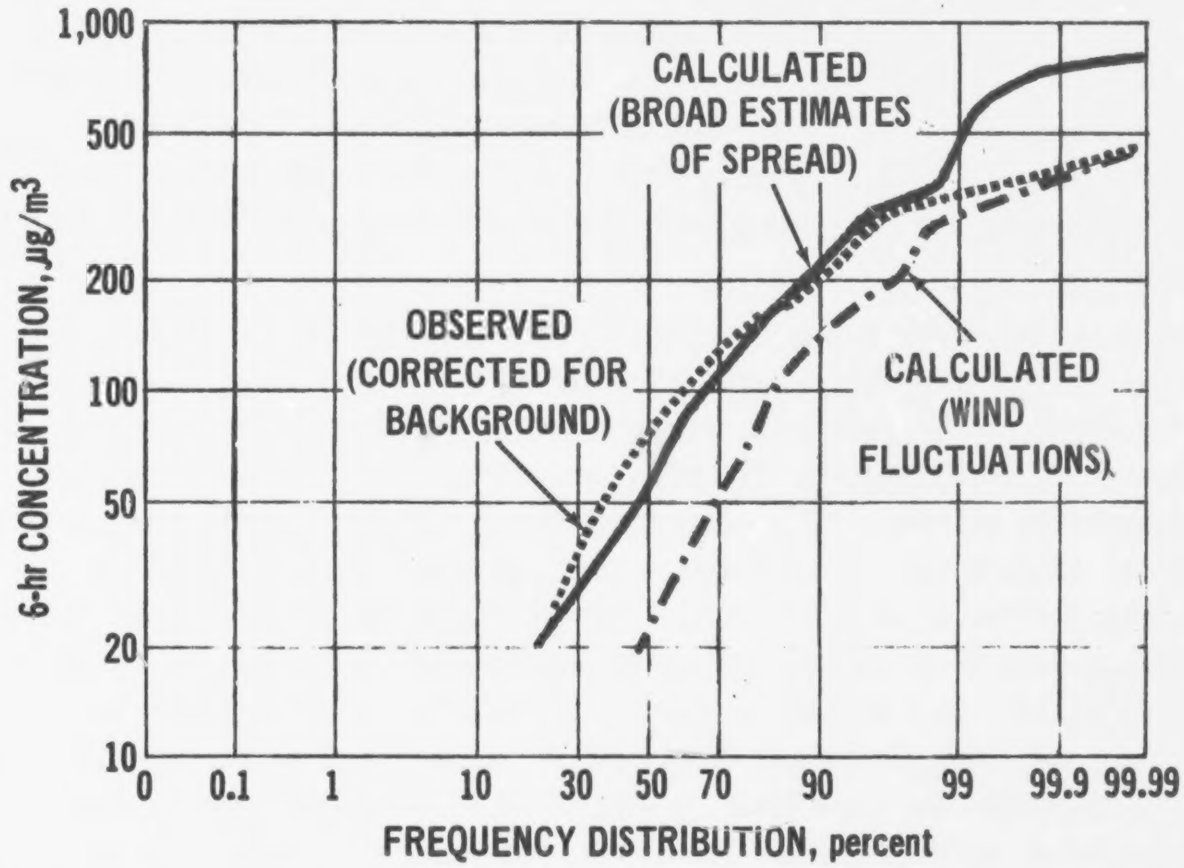

Figure 3-4. Marsh's reanalysis of Marsh and Wither's data.[6] Reading sites 1, 5, and 11; all periods.

The observed and calculated distributions are roughly in agreement and conform fairly well to a log-normal shape over a considerable range. The fact that, over most of the range, the broad estimates of spread provide better agreement must be fortuitous. Furthermore — and probably most important — it appears that the calculated distribution provided a statistical estimate of the incidence of the highest concentrations (say the concentration exceeded on a few percent of occasions), which would be satisfactory for many practical purposes. Obviously, a great deal of further work and discussion are required on this point, and the matter is, of course, taken further in Dr. Fortak's paper. It seems to me, however, that there is already some reason to anticipate that a useful statistical prediction of the probability distribution of pollutant concentration in an urban area is realizable in practice.

REFERENCES

1. Summers, P. W. An Urban Heat Island Model; Its Role in Air Pollution Problems with Applications to Montreal (abstract only). In: Proceedings 1st Canadian Conference Micrometeorology. 1967. 435 p.
2. Pasquill, F. The Estimation of the Dispersion of Windborne Material. Meteorol. Mag. *90*(1063):33-49, February 1961.
3. Pasquill, F. Meteorological Aspects of the Spread of Windborne Contaminants. In: Seminar on the Protection of the Public in the Event of Radiation Accidents, Geneva, November 18-22, 1963. Geneva, World Health Organization, 1965. p. 43-53.
4. Marsh, K. J. and M. D. Foster. An Experimental Study of the Dispersion of the Emissions from Chimneys. In Reading — I. The Study of Long-Term Average Concentrations of Sulphur Dioxide. Atmos. Environ. *1*(5):527-550, September 1967.
5. Marsh, K. J., K. A. Bishop and M. D. Foster. An Experimental Study of the Dispersion of Emissions from Chimneys. In Reading — II. A Description of the Instruments Used. Atmos. Environ. *1*(5):551-559, September 1967.
6. Marsh, K. J. and V. R. Withers. An Experimental Study of the Dispersion of the Emissions from Chimneys. In Reading — III. The Investigation of Dispersion Calculations. Atmos. Environ. *3*(3):281-302, May 1969.
7. The Calculation of Atmospheric Dispersion from a Stack. Stichting CONCAWE. The Hague, Netherlads. August 1966. 57 p.
8. Hogstrom, U. An Experimental Study on Atmospheric Diffusion. Tellus. *16* (2):205-251, May 1964.
9. Pasquill, F. The Vertical Component of Turbulence at Heights up to 1200 Metres. Atmos. Environ. *1*(4):441-450, July 1967.
10. Busch, N. E. and H. A. Panofsky. Recent Spectra of Atmospheric Turbulence. Quart. J. Roy. Meteorol. Soc. *94*(400):132-148, April 1968.
11. Readings, C. J. and D. R. Rayment. The High-Frequency Fluctuation of the Wind in the First Kilometre of the Atmosphere (in press). Radio Science. 1969.
12. Pasquill, F. Lagrangian Similarity and Vertical Diffusion from a Source at Ground Level. Quart J. Roy Meteorol. Soc. *92*(392):185-195, April 1966.
13. Chatwin, P. C. Dispersion of a Puff of Passive Contaminant in the Constant Stress Region. Quart. J. Roy. Meteorol. *94*(401):350-360, July 1968.
14. Pasquill, F. Atmospheric Diffusion. London, D. Van Nostrand Co., Ltd., 1962. 297 p.
15. Elliott, W. P. The Vertical Diffusion of Gas from a Continuous Source. Int. J. Air Water Pollution. *4*(1/2):33-46, June 1961.
16. Gifford, F. A. Diffusion in the Diabetic Surface Layer. J. Geophys. Research. *67*(8):3207-3212, July 1962.
17. Davenport, A. G. The Spectrum of Horizontal Gustiness Near the Ground in High Winds. Quart. J. R. Meteor. Soc. 87: 194. 1961.
18. Davenport, A. G. Instrumentation and Measurements of Wind Speed Spectra in a City. Proceedings of the First Canadian Conference on Micro-meteorology. Part III. Department of Transport. Toronto, Canada. 1967. 361 p.
19. Marsh, K. J. Measurements of Air Turbulence in Reading and Their Relation to Turner's Stability Categories (in press). 1969.
20. McElroy, J. L. and F. Pooler, Jr. St. Louis Dispersion Study, Volume II - Analysis. National Air Pollution Control Administration. Arlington, Va. Publication Number AP-53. December 1968. 51 p.
21. Swinbank, W. C. The Exponential Wind Profile. Quart J. Roy. Meteorol. Soc. *90*(384):119-135, April 1964.

ACKNOWLEDGMENT

This paper is published with the permission of the Director-General of the United Kingdom Meteorological Office.

APPENDIX – GLOSSARY OF SYMBOLS

b, c	dimensionless constants in the Lagrangian similarity treatment.
k	von Karman's constant (0.4).
H	vertical eddy flux of heat.
K	eddy diffusivity; subscripts M and H refer to momentum and heat, respectively.
L	Monin-Obukhov length scale, $-\dfrac{\rho Cp\ T\ u^3}{kgH}$
q	rate of heat input from urban processes.
Ri	Richardson number; subscript B denotes 'bulk' form using temperature difference over specified height interval.
S(n)	spectral density of wind component variance at frequency n.
t_L, t_E	Lagrangian and Eulerian integral time scales.
T	time of travel from source; absolute temperature.
$\overline{u}$	mean wind speed in x (alongwind) direction.
u_*	friction velocity.
$\overline{X}$	mean distance of travel of particles in a given time.
$\overline{Z}$	mean displacement of particles in vertical (z) direction.
z_0	roughness parameter in wind profile.
ϵ	rate of dissipation of turbulent kinetic energy per unit mass.
λ_m	equivalent wavelength ($= \overline{u}/n_m$) at which nS(n) is maximum.
ρ	air density.
σ	standard deviation; subscript w refers to vertical component of wind; y and z, to particle spread in respective directions.
ϕ	Monin-Obukhov universal function.
x	distance downwind
θ	potential temperature.

ABSTRACT

The basic structure of many current urban pollution models is examined from the point of view of underlying assumptions and physical basis. Initial attempts to extend steady-state models to variable conditions and long-term predictions are indicated, with a brief discussion of stochastic simulation of the concentration patterns and average seasonal and annual distributions. In view of the complexity of most computer-oriented models, a sensitivity analysis is recommended to identify the input parameters that most critically affect the concentration predictions.

AUTHOR

KENNETH L. CALDER obtained honors degrees in physics and mathematics at the University of London before joining the British Meteorological Office at its Porton Research Establishment in 1936. He left Proton in 1949 to accept an appointment with the U. S. Army Chemical Corps as Chief of the Meteorology Research Division at Fort Detrick. In 1968 Mr. Calder transferred to the Air Resources Laboratory of NOAA where he currently serves as Chief Scientist to the Division of Meteorology of the National Air Pollution Control Administration.

4. SOME MISCELLANEOUS ASPECTS OF CURRENT URBAN POLLUTION MODELS

KENNETH L. CALDER

*Air Pollution Control Office, NOAA**

INTRODUCTION

The last decade has witnessed an unprecedented interest and concern with the development of mathematical-physical models for predicting air pollution concentrations in an urban environment. It is not surprising that, in most of these efforts, we see the underlying influence of the pioneering thoughts of Francois Frenkiel on the subject, and it is fitting that he can be with us at this symposium. The ever increasing current interest in urban pollution modeling derives, of course, from its obvious potential value in nearly all practical problems involving quantitative consideration of air quality relative to the sources of pollution. These include air pollution abatement strategies, the forecasting of the occurrence of undesirable levels of urban pollution, and problems of urban planning for the future. Each one of these topics constitutes a large well-recognized area of study that is being vigorously investigated by many groups, although these matters lie outside the scope of the present symposium.

As a newcomer to the field of urban pollution modeling who was attempting, with no little trepidation, to select an appropriate topic for a paper to be presented before experts, I was primarily influenced by two considerations. First, was the knowledge that the fundamental physical and meteorological aspects of the subject would certainly be covered at the symposium in an authoritative fashion by Drs. Lettau and Pasquill. Second, was the fact that several quite comprehensive general papers and bibliographies on urban diffusion modeling have recently been written. Here it will suffice to mention the article by Wanta in Stern's book[1] and two comprehensive review articles prepared this year by Turner[2] and Moses.[3] With these recent articles, still another review seemed out of place for this meeting. Under these circumstances, it seemed more worthwhile to mention miscellaneous questions that come to mind in reading accounts of some of the currently available models—and, more particularly, those developed in the past few years by members of a U. S. air pollution meteorological team under the direction of Mr. R. A. McCormick. The somewhat fragmentary observations contained in this paper are made at a time when a rapidly expanding effort in modeling gives optimism for expecting a second generation of improved models to become available in the near future. While it is appreciated that the present paper raises a lot more questions than it answers, it is certainly not done with the feeling that the problem is so hopelessly complicated as to defy useful analysis. Instead, it is believed that an explicit recognition of some of the difficulties will lead to more mature appreciation of the limitations of modeling techniques among those who may be wanting to apply them. This recognition of the difficulties is also a prerequisite to the development of improved urban pollution models.

---

*National Oceanic and Atmospheric Administration, U. S. Department of Commerce.

A MULTIPLE-SOURCE URBAN POLLUTION MODEL

In the following discussion, we shall be concerned almost exclusively with modeling the effects of a chemically stable gaseous pollutant that is released from a stationary source in a city. Sulphur dioxide that results from the combustion of sulphur-containing fossil fuels in domestic, commercial, and industrial operations is normally regarded as the classical example. We shall also restrict attention to physically based models of the pollution distribution. These are explicitly constrained by the law of the conservation of matter, in contrast to empirical models that are based on statistical correlations established between observed concentrations of pollutant and simultaneously observed meteorological parameters, and that do not involve considerations of material balance.

Steady-State Equation

The starting point of the majority of urban pollution models is the postulation of a quasi-steady state. Thus, in spite of the obvious long-period variability of diffusion and meteorological conditions over an urban area, it is assumed that this variability can be treated as though it resulted from a sequence of different steady-state situations. The sequence interval may be some relatively short-term period—perhaps only of the order of an hour. During each "steady-state period," it is further assumed that a unique horizontal mean wind direction can be defined for the entire urban area, and that if this is used to define the x-axis of a rectangular coordinate system, with y-axis also horizontal, and z-axis vertical, then the mean concentration at a receptor location at ground level (x, y, 0) resulting from an elevated continuous point source (O, O, z_0), release of pollutant, of constant strength Q, per unit time has the function form Q R (x, y; z_0).

For a "given" meteorological situation, R denotes a fixed, i.e., nonstochastic, function, independent of the location of the origin of the coordinate system, i.e., is the same irrespective of the horizontal location of the source. Furthermore, R does not depend on the horizontal mean wind direction that defines the orientation of the coordinate system relative to the urban area. The assumption that the form of R is independent of the source location, is tantamount to the more formal statement that the concentration distribution function is invariant under arbitrary horizontal translations of the source-receptor pair. This might conceivably be a reasonable approximation over a very extensive area of uniform, level, open countryside. Considering, however, the edge effects that inevitably are associated with the relatively small, finite size of all cities, and the rather obvious horizontally inhomogeneous nature of the buildings and their distribution, the above assumption can only be a very crude approximation for an urban diffusion environment. The same comment would seem to apply with equal force to the assumption that the form of R is unaffected by the direction of the airflow over the city.

The specific functional form of $R(x, y; z_0)$ that is used in the so-called Gaussian plume dispersion models is, for $x \geqslant o$,

$$R(x,y;z_0) = \frac{\exp\left[-\frac{1}{2}\left\{\frac{y^2}{\sigma_y{}^2(x,S)} + \frac{z_0^2}{\sigma_z{}^2(x,S)}\right\}\right]}{\pi\ U\ \sigma_y(x,S)\ \sigma_z(x,S)} \qquad (1)$$

with $R \equiv 0$ for $x < 0$, i.e., no upwind travel of material,

U = a representative, constant, and spatially uniform, wind speed;

S = atmospheric stability category first introduced by Pasquill.[4] Here $S = 1$ may denote extremely unstablity and $S = 6$, extreme stablity, and

$\sigma_y(x,S), \sigma_z(x,S)$ = horizontal and vertical diffusion functions—the horizontal and vertical standard deviations of the Gaussian concentration distribution at distance x from the source. These diffusion functions are normally assumed to be parameterized by the stability category and are assumed independent of release height.[5]

In addition, in some models, a crude attempt may be made to allow for the known fact that diffusion in the vertical direction is frequently limited, such as when the pollutant is trapped between the ground surface and a stable layer aloft. When this occurs, a uniform vertical distribution of concentration would be expected throughout the effective mixing layer for sufficiently large values of x. One simple method of approximately allowing for this was suggested by Pasquill.[6] If the mixing layer is of height L, then Equation (1) is used for downwind distances, x, such that $\sigma_z(x,S) \leqslant \frac{1}{2}L$. When $\sigma_z(x,S) = L$, the resulting concentration becomes approximately uniform with height and of a magnitude appropriate to $\sigma_z = L$. At greater distances than this, the ground-level concentration is no longer reduced by vertical diffusion and the equation can continue to be used with $\sigma_z = L = \text{constant}$ and with the appropriate value of $\sigma_y\ (x, S)$.

In the original diffusion prediction scheme based on the atmospheric stability categories suggested by Pasquill,[4,6] the diffusion functions $\sigma_y(x,S)$ and $\sigma_z(x,S)$ were tentatively established from limited experimental data on diffusion over open level country. There was thus no allowance for the possible disturbing effects of buildings and topography. With some minor modifications, Turner[5] has utilized these functions in an urban diffusion model and has indicated both a working scheme for objective determination of the stability category and a crude qualitative method of adjusting the values to allow for urban conditions. More recently, the results of *ad hoc* experimental diffusion studies made with tracer material in metropolitan St. Louis, Missouri, have been reported by McElroy and Pooler,[7] and McElroy.[8] These studies have shown that, for low-level point sources, the crosswind diffusion in cities, although initially greater than in open country, soon converges to the latter value. Significantly greater vertical diffusion occurs in the city than in open country; and it is most pronounced under stable meteorological conditions. As is to be expected, however, many quantitative aspects of the urban point-source diffusion problem remain to be resolved, although it is encouraging that these recent urban experiments have generally confirmed the appropriateness of at least some aspects of the simple Gaussian model.

Area Source Application

With all the provisions mentioned in the preceding discussion, it is now only a small step to a formal mathematical formulation of a multiple-source urban pollution model. For any "steady-state period," choose the x-axis of the rectangular coordinate system along the horizontal mean wind direction for the urban area. Furthermore, let the urban pollution emission be regarded as a steady, horizontally distributed, area source such that $Q(x_o, y_o, z_o)\, dx_o\, dy_o$ is the total amount of pollutant emitted per unit time at an "effective" height, z_o from a horizontal element of area $dx_o\, dy_o$ surrounding the point (x_o, y_o). It is implied here that the function $Q(x_o, y_o, z_o)$ can be specified on the basis of appropriate emission inventory techniques for the entire urban area, and will have the value of zero outside this area. Then, assuming that at any ground-level receptor location (x, y), the total pollutant concentration is a simple additive function of the concentration contributions from all the individual elements of area, it is evident that

$$\chi(x,y) = \int_{-\infty}^{\infty} \int_{-\infty}^{\infty} Q(x_o,y_o,z_o)\, R(x-x_o, y-y_o; z_o)\, dx_o dy_o \qquad (2)$$

The area source concept has been justified as an appropriate idealization in urban diffusion modeling when there are too many sources (e.g., from domestic heating units) to be considered individually. It has sometimes been used, however, (e.g., Turner[5]) even when larger commercial and industrial sources are included in the emission inventory. For the primary purpose of reducing the computational effort, a single effective height of emission is sometimes selected, also. More realistically, large pollution emitters, like power plants with tall stacks, are treated as individual elevated point sources, and the effective height is calculated from the actual height plus the plume rise associated with upward momentum of discharge and thermal buoyancy effects. Consideration of plume rise is a somewhat controversial topic and far from straightforward, although it becomes an important element in realistic pollution models. A comprehensive and, hopefully, definitive, critical review of the subject has recently been prepared by Briggs.[9] [We note that the point source situation may be regarded as covered by Equation (2) by the formal device of the Dirac delta function. Thus, for a continuous point source at height z_0, of strength, q, per unit time, and with horizontal coordinates (a,b), we have $Q\ (x_0, y_0, z_0) = q\ \delta(x_0 - a)\ \delta\ (y_0 - b)$ so that Equation (2) gives $\chi = q\ R(x-a, y-b; z_0)$.

The integral of Equation (2) has to be evaluated by numerical methods, of course, once the source function $Q\ (x_0, y_0, z_0)$ and the diffusion function $R\ (x - x_0, y - y_0; z_0)$ have been specified. The calculations that are involved are normally so extensive that they necessitate use of a high-speed computer. Various and somewhat arbitrary devices have been used in the past for the approximate numerical integration, with no proper study of the errors incurred. For example, Pooler,[10] in developing a multiple-source SO_2-prediction model, used a source inventory for Nashville, Tennessee, based on 1-mile-square area sources; then replaced each square (with a single exception) with a point source at its center. Again, Turner[5] assumed that 1-mile-square area sources could be approximated by appropriate Gaussian-distributed, line sources oriented crosswind and passing through the center of each area. These approximations appear to be very crude and consideration of more sophisticated integration techniques should be worthwhile in the future.

It is, perhaps, obvious that an urban pollution model of the type we are considering, which requires as a quantitative input, a source-strength function, $Q\ (x_0, y_0, z_0)$, cannot yield concentration predictions that are more accurate than the pollutant source inventory itself. Unfortunately, the latter may be quite crude and is frequently based on indirect reasoning. The accuracy may also be expected to diminish rapidly as the time period over which the emissions are averaged becomes shorter. Sulphur dioxide, produced by the burning of coal and oil for space heating, for example, requires indirect estimation (see, e.g., Turner[11]) of diurnal and day-to-day variations of fuel comsumption. The estimations are made by using such empirical concepts as "heating-degree-days" (the depression of a suitably defined daily temperature below some limit like 65° F). While an annual emission inventory derived from the total annual consumption where fuel has a known sulphur content may be quite accurate, large errors can be expected in daily and hourly inventories. These are probably unavoidable due primarily to the fact that, in general, no adequate records of fuel consumption with fine enough resolution in time and space are available. This fact, itself, could impose an intrinsic limitation on the accuracy of urban pollution models as applied to short-period predictions.

EXTENSION OF MODEL TO VARIABLE CONDITIONS AND LONG TIME PERIODS

The basic model of the preceding discussion relates to meteorological and emission conditions that can be regarded as steady-state and that have prevailed for a sufficiently long period of time to permit full development of the concentration fields associated with the individual sources. In considering extension of the model to variable conditions, we will assume that the steady-state assumption is normally an adequate working approximation for time periods of the order of an hour, and that the general nonsteady-state or variable situation can be resolved into a succession of steady-states of this duration. In general, both the pollutant source distribution and the meteorological conditions must be regarded as varying between consecutive periods.

Quasi-Steady-State Applications

Since the x-axis for Equation (2) is determined by the mean urban wind direction, while the source distribution is specified in a coordinate system that is fixed relative to the city, and is also desirable for the concentration distribution, it will be necessary in utilizing Equation (2) to use the standard formulas for rotation of coordinate axes. In addition to the mean urban wind direction, the change in meteorological conditions occurring between consecutive 1-hour periods should reflect changes of the mean wind speed, U, the stability category, S, and the height, L, of the mixing layer, because these all will affect the concentration function $R(x, y; z_0)$. It is then evident that by repeated applications of Equation (2), each with an appropriate set of hourly parameter values, and an emission distribution estimate; we can simulate the pollutant concentration changes occurring at any receptor location over any specified period of time.

Precisely one such urban pollution model was developed by Turner[5] for the sulphur dioxide pollution in Nashville, Tennesee. This analysis was based on an emission inventory prepared for mile-square areas forming a rectangular array 17 by 16 miles. Source strengths and meteorological parameters were then estimated by 2-hour periods (instead of the 1-hour period above). The mean wind direction, to 16 compass points, and wind speed, to 0.1 meters per second (m sec^{-1}), were estimated from instrumental records at several wind stations in the area. The corresponding 2-hour stability category, S, was obtained by using an objective technique proposed by Turner (in this model, no allowance was made for a finite mixing height, i.e., $L = \infty$). In terms of these inputs to the model, 2-hour SO_2 concentration values were first estimated at a number of receptor locations at 1-mile intervals. From the 2-hour values, average 24-hour concentrations were then obtained. Comparison of the calculated 24-hour concentration values with those obtained by actual chemical sampling during a number of test periods occurring throughout a 1-year period showed quite reasonable agreement. In fact, Turner showed that even for 2-hour periods the calculated values were in fair agreement with corresponding observed values.

It is evident that, in principle, the above approach could be used to provide elaborate information on the characteristics of the concentration distribution in terms of forecast or observed meteorological and emission variations. If frequency statistics are available for the relevant meteorological parameters, then a probabilistic model is possible and the actual frequency distribution of the pollution concentration at a receptor can be estimated. (It should be noted that this is strictly true only if temporal variations of the source strength function, i.e., $Q(x_0, y_0, z_0)$, of Equation (2), are disregarded. Otherwise, it would be necessary to know the joint frequency function for Q and the meteorological parameters.)

Thus, after calculating the concentration values for all possible combinations of the three meteorological parameters: wind direction, wind speed, and stability category, and for simplicity assuming $L = \infty$, i.e., diffusion is unlimited in the vertical direction, we can get the frequency of occurrence of a particular concentration value from the sum of the joint frequencies of all the combinations of meteorological parameters that give rise to this concentration value. If hourly observations of wind direction are rounded off to the nearest 10 degrees, and there are, say, ten classifications of wind speed, then with only five possible stability categories, we obtain 36 x 10 x 5 = 1800 possible combinations; hence, 1800 meteorological situations for which the integral of Equation (2) has to be evaluated numerically for each receptor location of interest.

Since each of the meteorological "parameters" in reality has a continuous distribution, this use of only a finite number of combinations will, of course, mean that the real ensemble of diffusion situations is only being approximated in the mathematical simulation. Such extensive computation can quickly involve prohibitive time, even with present high-speed computers. Nevertheless, extensive calculations designed to characterize the concentration frequency distribution relating specifically to ground level SO_2 for the urban area of Bremen, Germany, have already been reported by

Professor Heinz Fortak.[12] We shall probably hear the latest news of this pioneering effort later at this symposium. It might be noted that the same approach could be used to provide probabilistic information on the two-dimentional concentration distribution, where the joint frequency distribution for concentrations at two or more receptor locations could be determined by the same enumerative procedure.

On the basis of extensive air pollutant concentration data for several pollutants and several U. S. cities, Larsen[13] has been able to show that the empirical frequency distribution of concentrations is closely approximated by the logarithmic-normal distribution. With the possibility discussed above for stochastic simulation, it would be of considerable interest to see whether the log-normal distribution can be generated by appropriate mathematical simulation.

A less ambitious objective than the determination of a concentration frequency distribution is that of determining just the long-term average value over some specified period—usually a month, season, or year. Although this can obviously be obtained in calculations of the type just considered, much simplification is possible when interest is restricted to average values. This simplification is achieved by a change in the order of integration and summation. In the previous consideration of an aggregate of 1800 possible meteorological situations corresponding to wind directions θ_i $(i = 1,2,3,\ldots 36)$, wind speeds, U_j $(j = 1,2,3,\ldots 10)$, and stability categories $S_k (k = 1,2,3\ldots 5)$, let $f(i, j, k)$ denote the corresponding joint frequency function. Also let $C(i, j, k)$ now denote the concentration for a particular meteorological situation as given by the integral of Equation (2) for a given receptor location. Then the long-term average concentration, say $\overline{C}$, is evidently given by the triple sum

$$\overline{C} = \sum_i \sum_j \sum_k C(i,j,k)\, f(i,j,k) \tag{3}$$

and would involve 1800 numerical evaluations of the integral. (Providing the source-strength function and the meteorological conditions are independent, the average concentration is calculated from an average value of source strength.) Consider now an elementary source of unit area at (x_0, y_0), that for a particular meteorological situation (i, j, k) produces a concentration $G(x_0, y_0; i, j, k)$ at some given receptor location. Then, for this source, the average concentration, say $\overline{G}(x_0, y_0)$, at the receptor will be given by

$$\overline{G}(x_0,y_0) = \sum_i \sum_j \sum_k G(x_0,y_0;i,j,k)\, f(i,j,k) \tag{4}$$

Evidently

$$\overline{C} = \int_{-\infty}^{\infty} \int_{-\infty}^{\infty} \overline{G}(x_0,y_0)\, dx_0 dy_0 \tag{5}$$

so that $\overline{C}$ is now expressed as a single integral that would have to be evaluated numerically. Although the sum in Equation (4) apparently involves

1800 terms, considerable simplification arises from the physically obvious fact that, for a given source-receptor pair, it is only a limited range of wind directions that really contributes to the concentration at the receptor. For example, Meade and Pasquill,[14] in their paper analyzing the average distribution of SO_2 pollution around Staythorpe power station in England, have shown that, with the assumption of a Gaussian type concentration distribution given by Equation (1), the average concentration at a receptor, produced by a fixed-point source and corresponding to all possible wind directions, can be approximated by a simple analytic formula. This actually involves only the wind direction frequency for the single wind sector (10 degrees in our example) that contains the source-receptor direction. In this case, the sum in Equation (4) would reduce to a double sum extending over all combinations of wind speed and stability category and would involve only 10 x 5 = 50 terms.

Multiple-source urban pollution models that essentially utilize this simplification and provide estimates of long-term average concentrations have been proposed by Pooler[10] and, more recently, Martin and Tikvart.[15] The Pooler model mentioned previously for the average monthly SO_2 concentrations at Nashville, Tennessee, is an example for which sampling data from an extensive air pollution study were available. Pooler disregarded atmospheric stability changes and, in effect, considered only a single stability category. The meteorological frequency function only involved consideration of wind direction and wind speed and was obtained from monthly summaries of hourly observations at the airport. In addition, the Pooler model assumed no limitation of vertical diffusion, i.e., the mixing height, $L = \infty$. The source inventory was based on 1-mile-square areas; then, for each receptor location in the numerical integration over the entire urban area, each square (with a single exceptional case) was replaced by a point source at its center. A reasonably close agreement was obtained between calculated and observed patterns of average monthly SO_2 concentrations.

The model proposed by Martin and Tikvart[15] differs only in its details and actually incorporates the simple Meade-Pasquill averaging formula. The meteorological frequency function involved the additional variable of stability category, S, and was thus established in terms of an array of 480 possible meteorological combinations from the long-term records of hourly meteorological observations that are normally available from Weather Bureau stations. A difficulty arising here is that the long-term records refer to airport locations and not to the nearby urban area that is of primary interest. In addition, a finite mixing height, L, was assumed, and a crude procedure proposed in an attempt to reflect the functions major diurnal changes. The calculations for both the above models become so extensive that they require the use of a high-speed computer. This is so in spite of the drastic mathematical approximations that have been adopted in order to simplify numerical evaluation of the surface integrals involved.

Instantaneous Gaussian Puffs Approach

The preceding models are all based on the postulated equivalence of the general long-term variable situation to a sequence of different quasi-steady states. This assumption allows model development in terms of the relatively simple steady-state concentration formula of Equation (1). To more accurately portray the general nonsteady-state situation, it will be necessary to regard the pollution emission from any point source as resulting in a series of "instantaneous puffs" that may follow different trajectories and have different rates of diffusion. Such a basis for a more general type of urban diffusion model in cases where meteorological conditions could not be regarded as constant and uniform for the whole urban area was explicitly indicated by Frenkiel[16] in his now classic paper. Such a modeling procedure implies the ability to specify separately the trajectory in space of every puff center and the puff concentration distribution at any time relative to the puff center. A sophisticated urban pollution model of this character, based on the assumption of a three-dimensional Gaussian distribution of concentration in the individual instantaneous puffs, was recently proposed by the late Professor Ben Davidson[17] and his associates at New York University. The Gaussian puff approach has also been applied by Start and Markee[18] to the calculation of average concentrations resulting from a prolonged point-source release of pollution in a valley where the winds underwent a marked diurnal cycling. Start and Markee also indicated the potential application of their model to urban air pollution problems. A further detailed application of the Gaussian puff concept to urban pollution modeling has been made recently at the Argonne National Laboratory under a contract supported by the National Air Pollution Control Administration, and a paper on this work is to be presented at this symposium. Models that utilize the Gaussian instantaneous puff rather than the steady-state Gaussian plume distribution of the continuous point source obviously possess greater flexibility and may well mark the advent of the second generation of urban air pollution models. Increased flexibility is, of course, only bought at the price of the very sophisticated knowledge required to predict, for an urban environment, both the trajectories in space and the diffusive spreading of the individual puffs. In principle, the important meteorological situation corresponding to the "calm" wind condition, which approximates the situation frequently encountered in episodes of high urban air pollution, could be discussed in terms of the Gaussian puff-type model. This is not possible in terms of the Gaussian plume of Equation (1), for which wind speed $U = 0$ represents a degenerate case.

SOME MISCELLANEOUS QUESTIONS

Prediction Limitations

The preceding discussion may have pointed to some of the difficulties of urban pollution modeling. In the past, most theoretical attempts to model the diffusive conditions in an urban environment have been based simply on a judicious adjustment—guided perhaps by a few *ad hoc* tracer experiments—of our knowledge of what happens in the much simpler situation over open, level country. Nevertheless, a reasonable agreement has been obtained between the predicted and observed concentration values in a number of different comparisons. In view of the somewhat tenuous nature of the physical basis of these models, however, it should be emphasized that they need to be applied with proper caution and, where possible, only by professional meteorologists fully conversant with the practical aspects of urban atmospheric diffusion. In a slightly different connection, this point has been emphasized by Scorer[19], who says: "There are NO universal formulae which can be used to describe what will happen to pollution emitted into the air, and this needs to be said because formulae have been so misused in the past by people who have been secretly frightened of realities and have dispensed according to the prescription of the most fashionable wizard. Responsibilities cannot be so easily shed. Pollution problems are certainly local, almost personal." It seems, however, to be a point worth reemphasizing, particularly in view of the current urgent demands for urban models to provide a quantitative basis for a variety of critical management decisions relating to urban air quality. It seems likely that any major improvement beyond the present somewhat empirical approach to urban diffusion modeling will require a much improved understanding of the dynamics and thermal structure of the continuously developing urban boundary layer. Detailed observational studies of the structure of the urban boundary layer of the type described recently by Clarke and McElroy[20] may provide the basis for such understanding. In any case, it should be evident that present models are based on some ideal assumptions and that considerable departures from the model predictions can be anticipated in the presence of any special local phenomena such as lake breezes and mountain-valley effects.

Parametric Sensitivity Analysis

In spite of the conceptual simplicity of the urban pollution models that have been discussed, the superposition of the effects produced by a large number of pollutant souces and their evaluation for complex sequences of meteorological conditions involves such large computational effort that, in most cases, it can only be handled with a high-speed computer. Under these circumstances, the more general features of the models may be obscured by the massive details of particular applications. At the present time, there appears to be a real need to study the sensitivity of the concentration predictions to variations in inputs to the models. In some cases, large variations in input may have little effect on output. With others, the reverse may be true. It, therefore, appears desirable to conduct a sensitivity analysis for some of the current models in order to identify the sensitive parameters and the conditions under which they are sensitive.

Two typical questions that come to mind, on which a sensitivity analysis would throw some light, relate to the degree of accuracy and detail that is necessary for an urban pollutant emission inventory, and the accuracy required to specify the concentration field corresponding to a single source. *Ad hoc* tracer diffusion experiments in cities, of the type described by McElroy and Pooler,[7] are difficult and expensive to perform. Since they must, to some extent, reflect localized conditions, they may not add significantly to the predictive accuracy of the model in general urban situations after a certain stage of specification is reached.

The sensitivity analysis is also valuable from a rather different point of view. Because it is not very difficult to identify a large number of the possible sources of error and unrealistic simplifications in existing models, in a qualitative way, there is a temptation to make rather arbitrary and simple adjustment for these in order to improve the agreement between computed and observed concentrations. This can be a dangerous procedure because, until a good understanding of the response of the model to its many inputs exists, there can be no guarantee that the adjustments necessarily reflect a real expression of improved physical understanding. Thus the apparently improved agreement could be fortuitous. In the above sense, some recently proposed models may already be over-complicated. We mention here the recent notable revelation by Dr. Frank Gifford of NOAA Atmospheric Turbulence and Diffusion Laboratory at Oak Ridge, that, at least for the calculation of isopleths of annual-average air quality in terms of a typical urban source inventory, the calculations can be organized and simplified to such an extent that they can be carried out quickly and easily by hand.

Of those models for which accounts have appeared in the open literature, the only other one specifically developed in a simple enough form to permit calculation from a source inventory without the aid of an electric computer, is that of Clarke.[21] At a time when computer-based models can be expected to proliferate rapidly, Dr. Gifford's recent success can serve as a reminder that simple models should not be overlooked since they might still be of great value.

REFERENCES

1. Stern, A. C. (ed.), Air Pollution. Vol. 1, 2d ed. New York, Academic Press, 1968. 694 p.
2. Turner, D. B. Workbook of Atmospheric Dispersion Estimates—Past, Present, and Future. Presented at meeting of Mid-Atlantic State Section of the Air Pollution Control Association. Philadelphia, APCA 9946. June 1969. 17 p.
3. Moses, H. Mathematical Urban Air Pollution Models. National Center for Air Pollution Control, Chicago Dept. of Air Pollution, Argonne National Laboratory. Argonne, Ill. ANL/ES-RPY-001. April 1969. 69 p.
4. Pasquill, F. The Estimation of the Dispersion of Windborne Material Meteorol. Mag. *90*(1063):33-49 February 1961.
5. Turner, D. B. A Diffusion Model for an Urban Area. J. Appl. Meteorol. *3*(1):83-91, February 1964.
6. Pasquill, F. Atmospheric Diffusion. London, D. Van Nostrand Co. Ltd., 1962. 297 p.
7. McElroy, J. L. and F. Pooler, Jr. St. Louis Dispersion Study, Volume II — Analysis. National Air Pollution Control Administration. Arlington, Va. Publication Number AP-53. December 1968. 51 p.
8. McElroy, J. L. A Comparative Study of Urban Rural Dispersion. J. Appl. Meteorol. *8*(1):19-31, February 1969.
9. Briggs, G. A. Plume Rise: A Critical Survey. Air Resources Atmospheric Turbulence and Diffusion Laboratory, Oak Ridge, Tenn. U. S. Atomic Energy Commission, Division of Technical Information. USAEC Critical Review Series. Publication Number TID-25075. 1969. 81 p.
10. Pooler, F., Jr. A Prediction Model of Mean Urban Pollution for Use with Standard Wind Rose. Int. J. Air Water Pollution. *4*(3/4):199-211, September 1961.
11. Turner, D. B. The Diurnal and Day-to-Day Variations of Fuel Usage for Space Heating in St. Louis, Missouri. Atmos. Environ. *2*:339-351, July 1968.
12. Fortak, H. G. Rechnerische Ermittlung der SO_2 — Grundbelastlung aus Emissionsdaten — Anwendung auf die Verhaltnisse des Stadtgebietes von Bremen. Institute for Theoretical Meteorology, The Free University of Berlin. 1966.
13. Larsen, R. I. A New Mathematical Model of Air Pollutant Concentration Averaging Time and Frequency. J. Air Pollution Control Assoc. *19*:24-30, January 1969.
14. Meade, P. J. and F. Pasquill. Study of Average Distribution of Pollution Around Staythorpe. Int. J. Air Pollution. *1*(1-2):60-70, October 1958.
15. Martin, D. O. and J. A. Tikvart. A General Atmospheric Diffusion Model for Estimating the Effects of One or More Sources. Presented at 61st Annual Meeting of the Air Pollution Control Association. APCA-68-148. St. Paul. June 1968. 15 p.
16. Frenkiel, F. N. Atmospheric Pollution and Zoning in an Urban Area. Sci. Monthly. *82:*194-203, April 1956.
17. Davidson, B. A Summary of the New York Urban Air Pollution Dynamics Research Program. J. Air Pollution Control Assoc. *17*:154-158, March 1967.
18. Start, G. E. and E. H. Markee, Jr. Relative Dose Factors from Long-Period Point Source Emissions of Atmospheric Pollutants. In: Proceedings of the USAEC Meteorological Information Meeting, Chalk River Nuclear Laboratories, September 11-14, 1967, Mawson, C. A. (ed.). Atomic Energy of Canada, Ltd. Chalk River, Ontario. Report Number AECL-2787. 1967. p. 59-76.
19. Scorer, R. S. Air Pollution. New York, Pergamon Press, Inc. 1968. 151 p.
20. Clarke, J. F. and J. L. McElroy. Experimental Studies of the Nocturnal Urban Boundary Layer. In: Proceedings of WMO Symposium on Urban Climates and Building Climatology, Brussels, Belgium, October 15-25, 1968.
21. Clarke, J. F. A Simple Diffusion Model for Calculating Point Concentrations from Multiple Sources. J. Air Pollution Control Assoc. *14:*347-352, September 1964.

5. A PRACTICAL MODEL FOR CARBON MONOXIDE

ABSTRACT

This paper reports our progress in the development of essentially two different types of diffusion models for carbon monoxide (CO): (1) a "synoptic" model, which calculates hour-to-hour concentrations, for vertification studies and possible operational use, and (2) a "climatological" model, which calculates arithmetic mean concentrations and frequencies of extreme concentrations, for planning use. The design of these two models, as well as the results of limited evaluation trials of an early version of the synoptic model are described.

The synoptic model design is based upon a modification of Clark's[1] *receptor-oriented model, and emphasizes practicality, generality and completeness. The present version of the model includes provision for handling extra-urban as well as intra-urban sources. In addition, a "street submodel" is being developed. Based largely upon experimental work, it converts the intra-urban background to street-level concentrations. When incorporated, this should substantially improve the agreement between calculated and observed values at the Continuous Air Monitoring Projects (CAMP) Stations.*

The climatological model is similar in basic form to the synoptic model but uses the joint frequency function for all combinations of specified classes of the input parameters, derived from a large body of hourly meteorological data. The arithmetic mean concentration thus obtained is then used in statistical relationships, derived by Larsen[2] *from carbon monoxide (CO) concentration data, to calculate the magnitude of high-percentile and maximum concentrations for any averaging time. Alternately, such calculations can be performed directly using the predicted concentration joint frequency function.*

Implementation of the model required the development of an objective technique for converting traffic data to a time- and space-dependent CO emission inventory, as well as methods for estimation of the meteorological variables appropriate to the urban area from routinely available (airport) weather data. The accuracy of these methods effectively establishes an upper limit to the model prediction accuracy.

Sample computed area-wide concentration patterns and time-varying point concentrations for St. Louis and Washington, D.C., are presented. As expected, the preliminary calculated concentrations are, for the most part, lower than those observed at the CAMP Stations, reflecting the need for incorporation of the street submodel into the program. The need for better treatment of light-wind conditions is also indicated by these evaluation trials; possible improvements are discussed.

AUTHORS

WARREN B. JOHNSON, JR., Manager of Environmental Meteorology Program, at SRI received a B.S. degree in electrical engineering from Texas A&M in 1957 and M.S. and Ph.D. degrees in meteorology from the University of Wisconsin in 1962 and 1965. At the University of Wisconsin, under Professor H. H. Lettau and subsequently at ESSA's Atmospheric Turbulence and Diffusion Laboratory in Oak Ridge, Tennessee, Dr. Johnson studied atmospheric boundary layer problems. At SRI, he has been developing lidar (laser radar) techniques for studying the behavior of pollutants in the atmosphere.

FRANCIS L. LUDWIG, Meteorologist, Environmental Research Department, at SRI received B.A. and M.A. degrees in meteorology from UCLA in 1957 and 1958, respectively. While at UCLA he participated in studies of Los Angeles air pollution problems. Since coming to SRI in 1959, Mr. Ludwig's interest has centered on atmospheric aerosols and urban meteorology.

ALBERT E. MOON, Senior Operations Analyst, Management Systems Division, at SRI received B.S. and M.S. degrees from the University of Texas in 1951 and 1952. He worked on the design of electrical and electronic control systems. He received a degree of Master of Business Administration from the Harvard Graduate School of Business Administration, in 1964 shortly before joining Stanford Research Institute. Since that time, he has evaluated public and private investments, including benefit-cost of mass transit systems in Los Angeles and San Mateo County, California.

5. DEVELOPMENT OF A PRACTICAL, MULTIPURPOSE URBAN DIFFUSION MODEL FOR CARBON MONOXIDE

WARREN B. JOHNSON, F. L. LUDWIG, AND ALBERT E. MOON
STANFORD RESEARCH INSTITUTE

INTRODUCTION

Scope and Objectives

There is a need for an objective, practical method of simulating the current and future impact of motor vehicles upon air pollution in urban communities. Such a technique could be used to assess the characteristics of current concentration patterns of primary vehicular pollutants in cities, as well as to predict the effects of exhaust emission controls and expressway routings upon future concentration distributions. We are currently engaged in the development of a simulation model of this nature, and this paper reviews our progress midway through the first year's effort. In this task, we have been aided considerably by previous urban diffusion modeling studies, which have been aptly reviewed and summarized by Wanta,[3] Stern,[4] Moses,[5] and Neiburger.[6] An investigation of carbon monoxide (CO) diffusion in Washington, D.C., by Ott *et al.*[7] could be considered a prototype for our study.

For simplicity, this initial modeling effort is restricted to CO, since (1) the gas is relatively inert in the atmosphere with no known significant natural sources or sinks in urban areas,[†] (2) motor vehicles are known to furnish large percentages of the CO in urban air (discussed in a subsequent section of this paper), and (3) CO is believed to be an important pollutant in terms of health effects. Later, it is planned to extend the model developed for CO to photoreactive, automobile-generated pollutants.

---

[*] Research sponsored by the Coordinating Research Council and the National Air Pollution Control Administration (Division of Meteorology).

[†] Evidence is mounting, however, that such sources and sinks may be found in the biosphere (Swinnerton,[8] Went,[9] and Robinson and Robbins.[10]).

Our goal is to develop a versatile model that can predict both urban background and street-level CO concentrations at any point within a city. Calculations of the following types are required:

1. Hourly concentrations as a function of time, for verification, use, and possible operational applications (with the "synoptic" model).
2. Long-term average concentrations and statistical predictions of high (and maximum) concentrations for planning purposes (with the "climatological" model).

We are aiming to complete a practical model that is convenient to use, economical to run, generally applicable to most cities, and, of course, accurate. To achieve the latter, we are attempting to develop capabilities for assessing concentration contributions resulting from diffusion on various scales, including the treatment of:

1. Extra-urban transport and diffusion, mainly from upwind cities.
2. General intra-urban diffusion from arterial and feeder streets.
3. Local (microscale) diffusion within streets.

Fundamental Concepts and Assumptions

Our basic approach has been to develop individual components of the model, and then to arrange these components into submodels, which can be appropriately combined to suit particular needs. This procedure affords maximum flexibility.

Other key elements in our rationale have been to

1. Bring the best features of previous efforts together into a single model.
2. Maintain simplicity until additional complexity is shown to be clearly required to achieve greater accuracy, and is justified by the accuracy of model inputs.
3. Strike an appropriate balance between the complexity of the model and the computing costs (program running time).

Input data requirements for the model include two major types, traffic and meteorological. For the synoptic model, it is necessary to assume that diurnally adjusted, average daily traffic data (which are all that are available on a network basis) are compatible with hour-to-hour (synoptic) meteorological data.

EMISSION INVENTORY DESIGN

Introduction

Estimates of vehicular emission of carbon monoxide range from 98 percent of the total for the Washington, D.C., area[11] and 91 percent in Los Angeles,[12] to 75 percent in the San Francisco Bay region.[13] (The latter estimate is for automobiles only.) Hence, the principal effort thus far (discussed in detail below) has been to model the mobile sources. Significant fixed sources, such as airports, will later be included in the emission inventory.

The inventory of motor-vehicle CO emissions is represented as a primary network of the major arterial streets and freeway links, plus a secondary background of emission from vehicles on the many local streets that are not included in the primary network.

Two kinds of data are used for the emissions inventory, (1) historical data, to re-create past conditions for comparison with recorded concentration measurements for model verification; and (2) forecast data, to estimate future concentrations.

Calculation of Primary Traffic Network Emissions Using Historical Data

Figure 5-1 illustrates the primary network used in the Washington, D.C., area.* The amount of travel on the major network is in excess of 90 percent of the total travel in the metropolitan area. Emission from each straight segment, or link, of the network is determined from the emission per vehicle-mile and the number of vehicle-miles traveled on the link.

CO emission, e (grams per vehicle-mile), is determined from the equation

$$e = c/S^{\beta} \qquad (1)$$

where S is the average speed over the link, in miles per hour (mi hr^{-1}), and c and β are constants. For vehicles in use before exhaust control systems were used, $c = 10^3$ and $\beta = 0.8$, as determined by Rose *et al.*[14] from observations on vehicles in several locations. For conditions where a majority of vehicles have exhaust-control devices, alternative values will be used for the coefficients.

To define the network and compute the emissions, the following input data are needed:

- Network description
- Node coordinates
- Link distances
- Link volumes
- Link speeds

Historical data for the network description, the node coordinates, and the link distances are obtained from highway and street maps. The network is described by assigning numbers to the intersections, or nodes, of the network and by identifying the pairs of nodes that are connected by links. The coordinates of the nodes establish the locations of the traffic links in the network. Link distances are measured along the links, rather than as the shortest distance between the nodes, although the assignment of the emissions assumes that the link is a straight line between the nodes.

---

*Computer-generated displays of this nature are very useful for examining the accuracy of the coding of the traffic links.

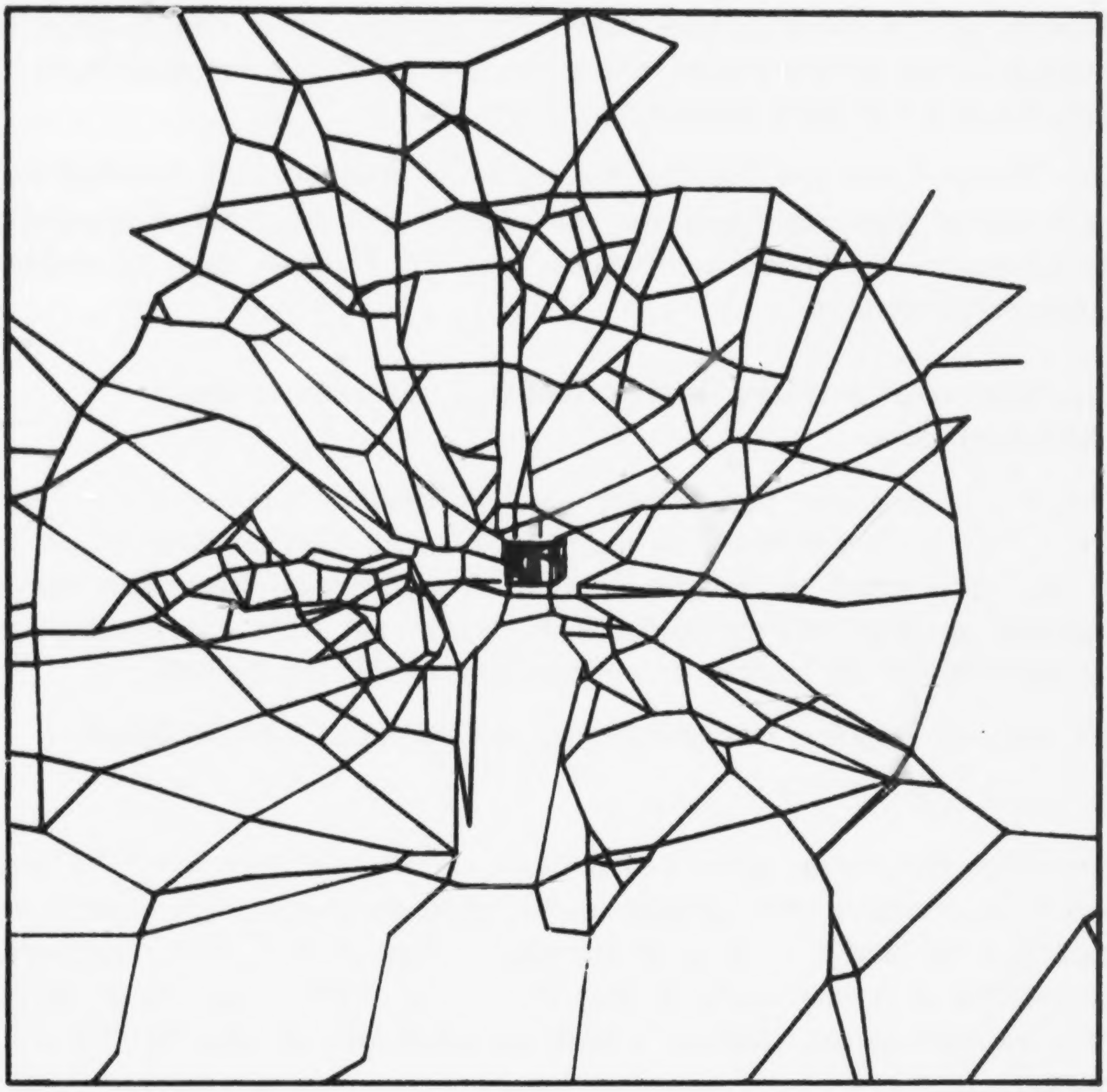

TA-7874-18s

Figure 5-1. Computer-generated display of traffic links in 24-by 24 mile central portion of primary network for Washington, D. C.

Historical link-volume data are obtained from traffic departments in the cities, towns, and counties of the region being studied. These agencies sample traffic volumes by means of portable counting units and a few fixed installations. The frequency of their observations may vary from almost continuously to as infrequently as once in two or three years. Because traffic varies according to seasonal, weekly, and daily cycles, an observation of volume for one day must be adjusted for the weekly and seasonal fluctuations. The resultant corrected value is recorded as the average daily traffic (ADT) for that location.

For use in the synoptic model, the emissions must be expressed in hourly averages, so the average daily traffic must be allocated among the hours of the day. Allocation can be accomplished using data on the hourly distribution of trips, which are compiled by the traffic study agencies of many areas. A typical diurnal pattern of trips is shown in Figure 5-2. There are, however, limitations to the accuracy of the assumption that the traffic on each link is distributed like the hourly trip pattern. We know that trips taken during the morning and evening peak hours are longer than those taken during other times of the day, and that the pattern of use of different kinds of streets in different parts of the city is different, as shown by the comparison of hourly volume on a freeway and a downtown arterial in the St. Louis area, shown in Figure 5-3. Accordingly, we are planning to use all data available to develop different hourly volume patterns for each facility type.

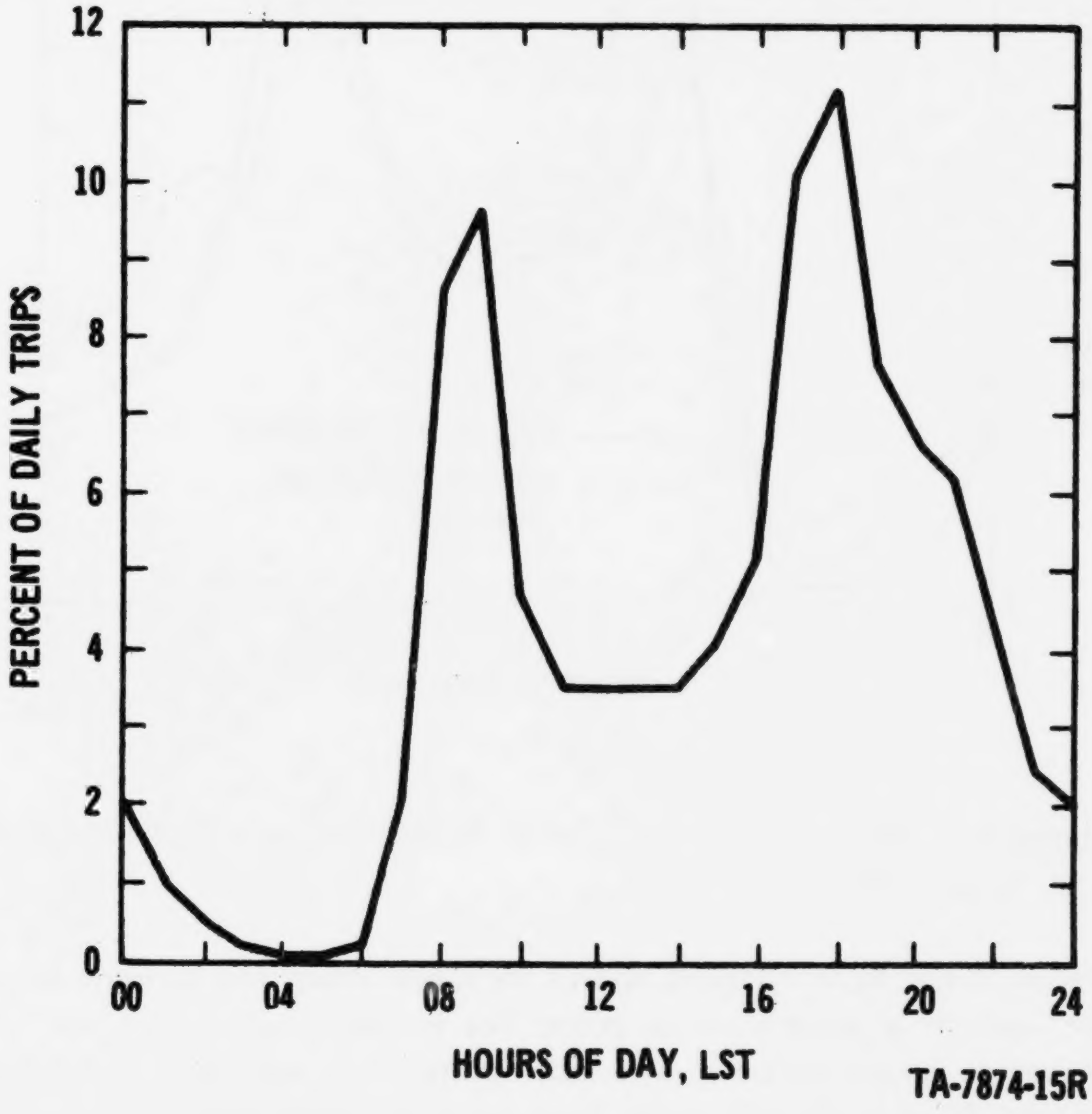

Figure 5-2. Hourly distribution of trips in Washington, D. C.[16]

Associated with the computation of hourly traffic volume from average daily traffic is a feature of the model that accounts for the fact that emissions at

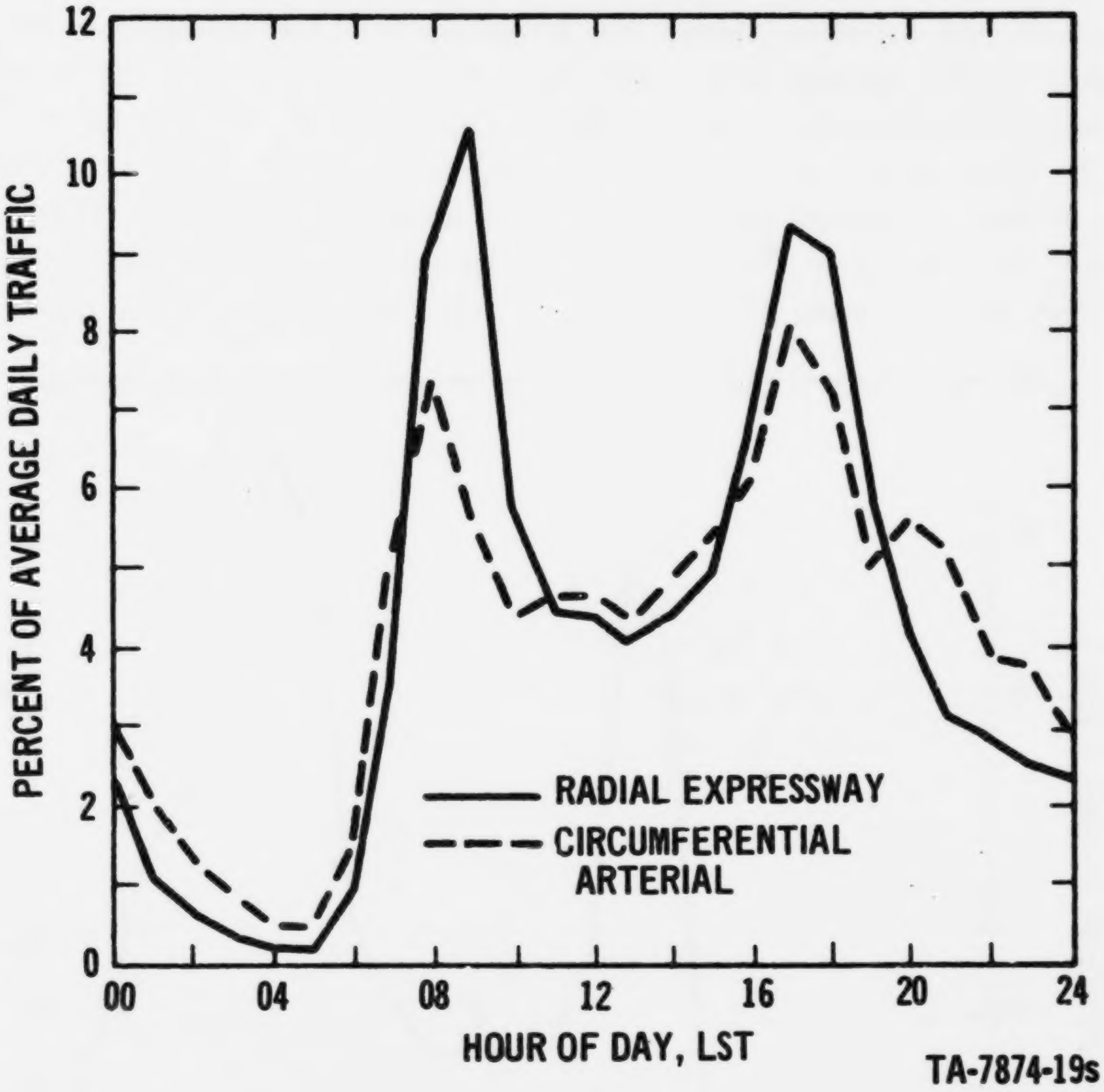

Figure 5-3. Hourly distribution of traffic for two facility types in St. Louis.[50]

different times from different source locations affect the concentration at a given time at a given receptor point. For example, with a 2-m sec^{-1} wind, the average concentration at a receptor point from, say, 0800 to 0900 Local Standard Time (LST) will result from emissions generated in the hour from 0700 to 0800 at a location 7.2 km upwind, and from 0600 to 0700 at a location 14.4 km upwind, and so on. A computational loop in the model uses wind speed to determine the displacement in time needed for each emission computation.

Link speeds for historical data are determined by using averages for peak and off-peak travel hours on the various kinds of route facilities in the area. Data for the average speeds are obtained from the traffic survey. Speeds used in the Washington, D.C. area were based upon the study by W. Smith and Assoc.[16] shown in Table 5-1.

Accuracy of the historical data is limited by the frequency with which it is recorded and by the accuracy of the factors used to correct it to average daily traffic. However, since locations with heaviest traffic are generally

Table 5-1. AVERAGE SPEEDS FOR WASHINGTON, D.C., HIGHWAY FACILITIES ($mi\ hr^{-1}$)

Facility type	Peak traffic hours (0700 to 0900, 1600 to 1800)	Off-peak traffic hours (0000 to 0700, 0900 to 1500, 1800 to 0000)
Suburban freeway	42	48
Downtown freeway	33	39
Suburban arterial	30	36
Downtown arterial	24	30
Local or feeder street	10	12

monitored most often, greatest confidence can be placed in data with highest volumes. In addition, very few data are available for Saturdays and Sundays, since traffic planners are concerned with recording peak demands, and peak demands on streets usually occur on weekdays. This lack of data impedes efforts to run weekly cycles, however, because peak traffic usually occurs on weekdays, peak pollution concentrations from motor-vehicle emissions also usually occur on weekdays.

Calculation of Secondary Traffic Emissions Using Historical Data

The number of vehicle-miles traveled on streets not represented by the primary network is computed from an estimate of the total vehicle-miles traveled in the area and the total vehicle-miles on the links of the primary network. The local street mileage is distributed over the study area by estimating the relative density of local streets as opposed to parks, open spaces, and primary streets, for each 4-square-mile area in a 2-mile by 2-mile grid covering the area. The average emission from the local street travel in each square is then assumed to emanate uniformly from that square. Although the emission per mile is high because of low speeds, the overall contribution is small because of the small fraction of the total area travel that is carried out on these local streets.

Calculation of Future Emissions Using Forecast Traffic Data

Most urban areas in the United States have completed or are conducting an area-wide transportation study to determine traffic demands and transportation facility needs for a specific future. Such studies are required for participation in Federal highway programs. Two important outgrowths of these studies are: (1) a design for a future traffic network for the area and (2) a forecast of the traffic volumes on the links of the network. The procedure for conducting these investigations has been highly developed and partially standardized. We are designing the emission inventory components of the model so that the magnetic tape form of network description, link volume, and link speed data, of widely used traffic-planning computer programs can serve as input for the diffusion model. In most cases, the only manual step required will be the measurement and coding of node coordinates for the network.

Accuracy of the forecast data is difficult to establish. One study that sought to appraise the accuracy of earlier forecasts was unsuccessful in finding a case where the planning recommendations had been followed closely enough to make the actual situation equivalent to the conditions that were forecast.[16] Checks made to establish the adequacy of calibration of the forecasting models are usually considered successful if the forecast for present conditions gives link volumes in wide corridors within 10 to 20 percent of counted volumes. Variations between the volumes on individual streets within the corridor may be much wider since the models do not distinguish between parallel routes as readily as do drivers.

INTRA-URBAN TRANSPORT AND DIFFUSION SUBMODEL

Spatial Partitioning of Emissions

Our diffusion model is a modified form of the receptor-oriented model developed by Clarke.[1] As shown in Figure 5-4, we use logarithmic spacing of the area segment boundaries to permit more precise location assignment for

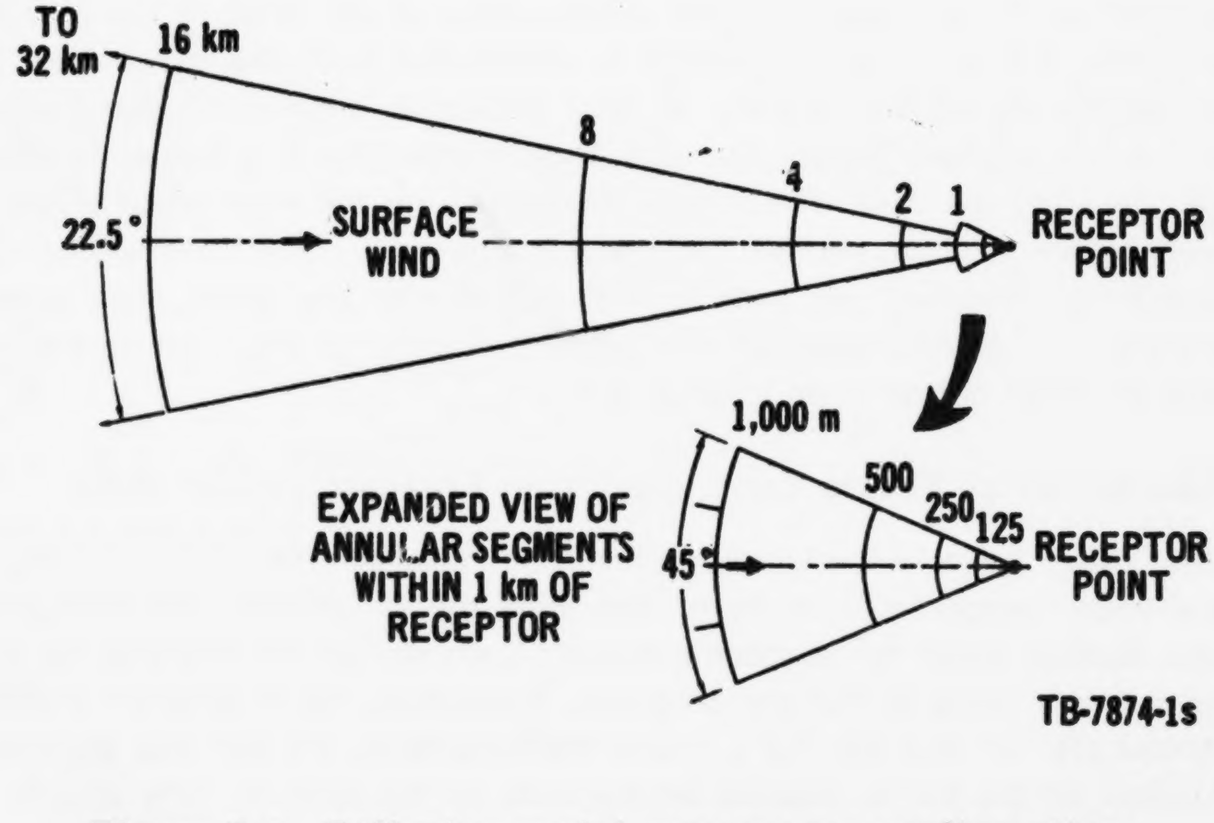

Figure 5-4. Diffusion model area-source configuration.

emissions near the receptor and to tend to equalize the contributions from each segment to the concentration at the receptor point. The closest segment extends from the receptor to 125 meters, roughly comparable to the size of a city block, while the farthest segment extends to 32 kilometers, approximately the diameter of a large city.

The 22.5° sector width is convenient and fits reasonably well the angular plume widths (between ±2σ points), predicted by Gifford's[17] model, for slightly unstable conditions. The sector width is expanded to 45° within the closest 1 kilometer to allow for the large initial lateral dispersion observed during the St. Louis tracer studies.[18,19]

Emissions from the line sources (links) in the traffic network are assigned to one of the nine area-segments as shown by Figure 5-5. To simplify these computations, the segment boundaries are taken as straight-line fits to the curved boundaries illustrated in Figure 5-4. The computations transform the rectangular node coordinates into polar coordinates originating at the receptor points and then determine whether all or part of a link falls within a given segment. The link is assumed to be a straight line connecting the nodes. Where part of the link is within a segment, an equivalent fraction of the link emission is included in the computation. The total emission within

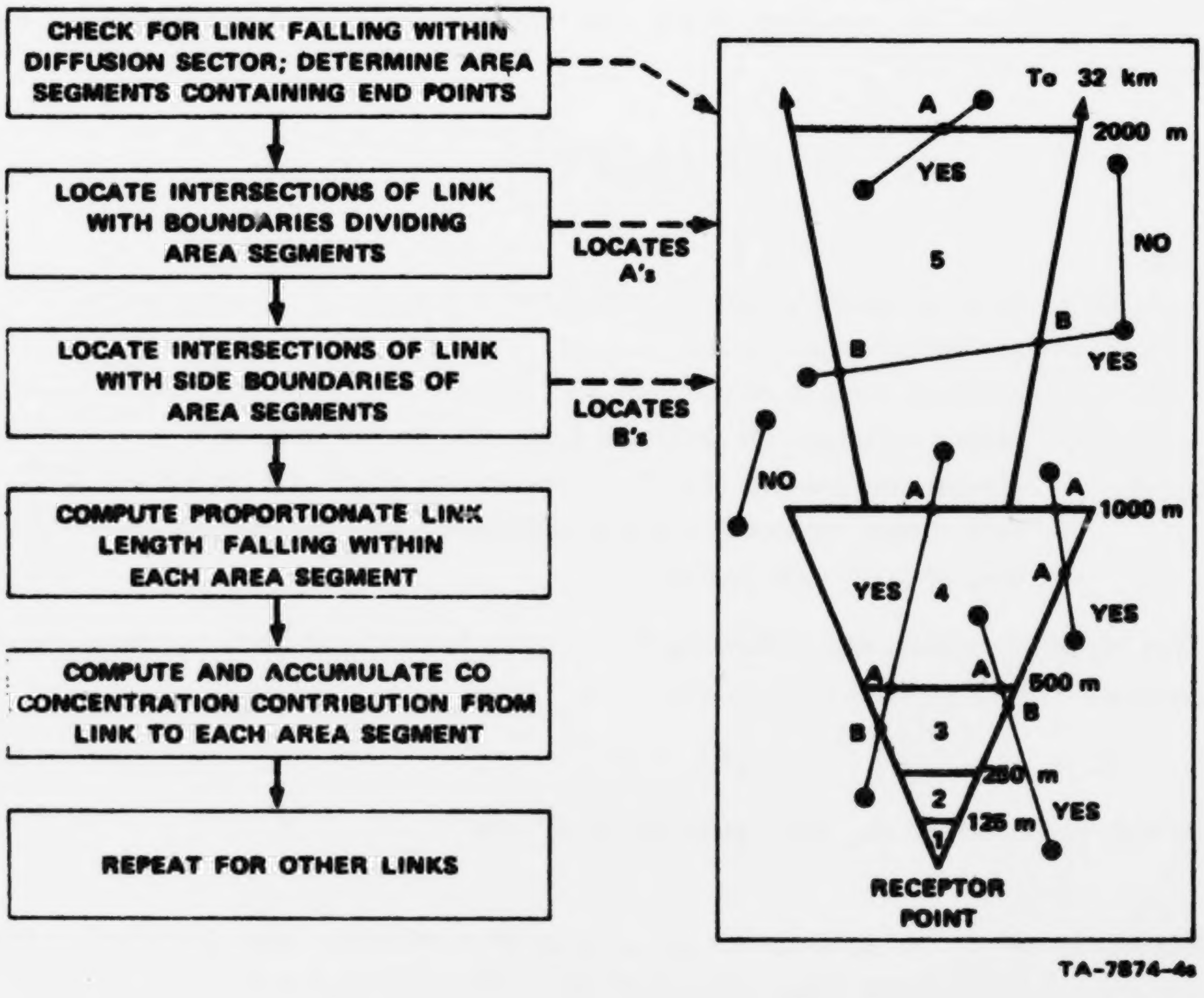
CHECK FOR LINK FALLING WITHIN DIFFUSION SECTOR; DETERMINE AREA SEGMENTS CONTAINING END POINTS
LOCATE INTERSECTIONS OF LINK WITH BOUNDARIES DIVIDING AREA SEGMENTS
LOCATES A's
LOCATE INTERSECTIONS OF LINK WITH SIDE BOUNDARIES OF AREA SEGMENTS
LOCATES B's
COMPUTE PROPORTIONATE LINK LENGTH FALLING WITHIN EACH AREA SEGMENT
COMPUTE AND ACCUMULATE CO CONCENTRATION CONTRIBUTION FROM LINK TO EACH AREA SEGMENT
REPEAT FOR OTHER LINKS
To 32 km
A
2000 m
YES
NO
5
B
B
YES
NO
A
A
1000 m
YES
4
A
YES
A
A
500 m
B
B
3
250 m
2
125 m
YES
1
RECEPTOR POINT

TA-7874-4s

Figure 5-5. Schematic of traffic link assignment subroutine.

each segment is assumed to be uniformly distributed and consists of the total emission from all the links and parts of links that lie within that segment, plus the secondary traffic emission in the segment.

As previously discussed in this paper, the secondary traffic emission is described in a 2-mile-square grid system. The values at the centers of the squares represent the average emissions over the squares. The secondary emission assigned to each segment in the diffusion model is computed by locating the center of the area segment, then interpolating among the four adjacent secondary emission grid centers. The value thus determined at the center of the segment is assumed to prevail over the entire segment.

The contributions of each area segment to the concentration at the receptor point are computed separately and then totaled. The calculation of pollutant concentrations from each of these individual segments is based on a combination of two simple mathematical models, the Gaussian and the "box." A similar approach has been employed by Miller and Holzworth.[20]

Basic Gaussian Model

Gifford[17] has developed a generalized diffusion model to describe the plume from a continuous ground-level point source, assuming perfect reflection at the ground. In its simplest form, for the ground-level concentration, the equation is

$$C = \frac{Q}{\pi \sigma_y \sigma_z u} \exp \left(-y^2/2\sigma_y^2\right) \tag{2}$$

where

C = ground-level concentration (g m^{-3})

Q = source strength (g sec^{-1})

u = average wind speed (m sec^{-1})

y = lateral (crosswind) distance from the plume axis (m)

σ_y, σ_z, = lateral and vertical standard deviations of plume concentration (m); these parameters are functions of source-receptor distance and atmospheric stability.

This equation takes the following basic form for ground-level concentrations emitted from a ground-level line source:

$$C = Q_L \left(\frac{2}{\pi}\right)^{1/2} (u\sigma_z)^{-1} \tag{3}$$

In this formulation Q_L has the units g m^{-1} sec^{-1}

Estimates of σ_z as a function of atmospheric stability and pollutant travel distance or time have been proposed by Gifford[17] and Smith and Singer,[21] and urban observations of this type have been reported by Pooler[18] and

McElroy.[19] At present, we are using Gifford's* values, but the model is flexible and can use any set of functions that can be reasonably approximated, over the intervals between segment boundaries, with expressions of the form:

$$\sigma_z = a_{ij}\, r^{b_{ij}} \tag{4}$$

Where r is the travel distance, the subscript i refers to annular segments upwind of the receptor point (see Figure 5-4), and j refers to the stability classes. The σ_z functions are, thus approximated by a series of power functions, each appropriate to some upwind distance interval and stability class. This allows us to select different representations for different distances, if we choose. Short ranges, in particular, may require special treatment to account for the initial rapid mechanical mixing found in urban areas.[18, 19] We are testing two ways of handling this initial dispersion: (1) adding 25 meters to σ_z over all distances, as suggested by Pooler[18] and by McElroy;[19] and (2) using a value of σ_z throughout the closest segment corresponding to Gifford's values at a distance of 125 meters.

Substituting Equation (4) into the line-source equation and integrating with respect to r from $r = r_i$ to $r = r_{i+1}$ gives the contribution for stability class j from the *i*th segment area source Q_A:

$$\left(\frac{C}{Q_A}\right)_{ij} = \frac{0.8}{u\ a_{ij}} (1-b_{ij})^{-1} \left(r_{i+1}^{1-b_{ij}} - r_i^{1-b_{ij}}\right) \qquad b_{ij} \neq 1$$

$$= \frac{0.8}{u\ a_{ij}} 1n\left(\frac{r_{i+1}}{r_i}\right) \qquad b_{ij} = 1 \tag{5}$$

where r_i and r_{i+1} are, respectively, the distance to the downwind and upwind boundaries of the *i*th segment. In this expression Q_A has the units (g m^{-2} sec^{-1}). This basic Gaussian model applies when there is no effective limitation to vertical mixing or when the cloud has not spread sufficiently to be affected by such a limitation.

Transition from Gaussian to Box Model

When the layer into which the pollutants are being dispersed is restricted, they will tend to become uniformly mixed at a sufficient distance from the source. Under these conditions, the box model is used. The concentration arising from the uniform area source in the *i*th annular segment is

$$\left(\frac{C}{Q_A}\right)_i = -\frac{r_{i+1} - r_i}{uh} \tag{6}$$

where h is the depth of the layer into which the pollutants are mixed.

---

*Gifford's work is a modification of that by F. Pasquill (unpublished) and Meade[22] The Gifford-Pasquill curves are based upon data from open country, and probably underestimate the diffusion in urban areas. We are examining possible improvements on this point.

We have chosen to change from the Gaussian model to the box model at that point where the two equations (in their respective line source formulations) give equal concentration values. The distance to that point, r_T, is given by:

$$r_T = \left(0.8h/a_{ij}\right)^{1/b_{ij}} \tag{7}$$

The part of the annular segment inside r_T is treated according to the Gaussian model, and the part that is outside, according to the box model. For this application r_T is substituted for r_{i+1} in the Gaussian equation and for r_i in the box equation.

Determination of Model Inputs

The model requires meteorological inputs of mixing depth, stability, and wind speed and direction. At present, the model uses winds observed at the nearest airport. Central urban daytime wind speeds above the buildings are known to be on the order of 30 to 40 percent less than airport speeds, and a correction for this effect is planned, but not yet incorporated into the computations.

The case of calm winds cannot be handled by the model without some adjustment. At present, the model assumes that a wind that is reported as calm has a speed of 2.0 m sec^{-1} and that its direction is the same as the most recently measured direction. Other approaches to this problem are possible, but they require special models to be developed for the calm-wind case, as will be discussed later.

The stability and the mixing depth are not directly measured quantities and require estimation methods. We are using Turner's[23] criteria for determining stability from routinely available data. This procedure estimates the stability class on the basis of cloud cover, ceiling height, wind speed, and solar elevation. The stability class is used to select the Gifford-Pasquill σ_z function. Following Turner, we are using five stability classes ranging from "very unstable" (Class 1) to "slightly stable" (Class 5), eliminating the "stable" and "very stable" classes. These conditions are known to occur very seldom over cities because of the heat-island effect. Mixing depth over the urban area is determined for nighttime cases from Summers'[24] simple model of the urban heat island and from an empirical relationship involving heat island intensity, city population, and low-level rural (airport) lapse rate, as discussed in detail in Appendix A.

Afternoon mixing depth is determined from the height of intersection of the morning sounding and the dry adiabat passing through the maximum temperature for the day. Other daytime values are interpolated on the basis of the observed hourly temperatures (see Appendix). The model currently uses a uniform mixing depth throughout the area.

Model Limitations and Prospective Refinements

The simple model that has been outlined here has a number of limitations. Refinements are possible, but one must first determine whether such refinements are warranted in view of the limitations of the available meteorological and traffic data in terms of accuracy and representativeness. In addition, the increased prediction accuracy must be worth any additional computing costs. We are currently considering several potential model refinements in this context.

Suitability of Input Parameters

The model currently takes the airport wind speed to apply over the entire urban area. We plan to adjust this value to give a more realistic wind speed over the city. Graham[25] found an urban/rural average wind speed ratio for Ft. Wayne of 0.67 at 15 meters height and 0.64 at 60 meters. In Nashville, Schnelle *et al.*[26] found the roof-level wind speed, U_r, to be related to the airport wind speed, U_a, as

$$\overline{U}_r = 0.33\ \overline{U}_a + 1.0\ \text{m sec}^{-1}$$

where the overbars refer to daily averages. Graham's observations also show the wind direction over the city to be backed by 10° to 15° from that at the outskirts, which could also warrant a correction to the airport data. These results are mostly for daytime conditions. At night the wind speed over the city may be higher than that at the airport.

Incorporation of nonuniform meteorological parameters over the city would be more complex. Spatial variations in nocturnal mixing depth have been observed by Clarke[27] in Cincinnati, and Bornstein[28] in New York, and modeled in limited fashion by Summers[24] and Leahey.[29] The desirability of inclusion of such effects is under study. Efforts are also being made to improve the form of the traffic data to include (1) diurnal volume patterns for each road type, and (2) weekend data.

Nonsteady Conditions

The steady-state nature of the model is a more important limitation. The reasonably uniform spatial distribution of the traffic network, however, helps to offset this situation. Wind direction changes from hour to hour are included simply by switching to a new diffusion sector in the model, which serves reasonably well for strong winds on the order of 30 km hr^{-1}, or 8 m s^{-1} (the diffusion sector extends to 32 km). A special feature of the model accounts for the finite travel time of emissions under light wind conditions (see page 5-2), but no provision is made for directional changes in trajectories, as observed by Angell *et al.*[30] and Hass *et al.*[31] from tetroon flights. We are considering a modification that would calculate the contribution of each previous hour's emission to the concentration at the receptor for a given hour, and would accommodate wind directional changes by relocating the apparent receptor point and diffusion sector with respect to the traffic network.

The Stagnation Case

The most important pollution situation, the stagnation with very light winds, is virtually impossible to treat with our present model. The nocturnal urban circulation for this case has been reasonably well documented[32, 33] and takes the form of a convective cell driven by the urban heat island. One approach that we are considering for night hours involves treatment of the circulation as that of a height-limited, ground-based "thermal" or vortex ring, symmetrically oriented over the urban area. The wind field would be taken as convergent toward the center of the city. Allowing for recirculation, a time-dependent concentration distribution would be calculated by means of a cylindrical version of the box model (which might be called a "pan" model). A critical parameter would be the entrainment rate for clean air at the top and circumference of the "pan," which might be estimated on the basis of convection theory.[34, 35] A more realistic treatment would allow superposition of this circulation upon a weak gradient flow, giving the buoyant heat plume observed by Clarke.[27]

DIFFUSION SUBMODELS FOR OTHER SCALES

Microscale (Street) Diffusion

Because of the finite spacing of sources within a city, area source simulation such as is used in the intra-urban model is best applied at scales above a certain lower limit. This minimum spatial scale can be considered to be on the order of a city block, hence the choice of 125 m as the finest resolution in the intra-urban model. For shorter source-receptor distances, an alternative technique is needed.

Additional complications arise because, contrary to the usual situation in nonurban diffusion studies, the scale of the largest urban roughness elements (buildings, etc.) is very large compared to the local scales of emission and reception. This means that the aerodynamic effects of structures become important.

Models that do not include the effects of microscale diffusion will normally undercalculate concentrations in comparison with those measured at CAMP Stations, which are usually located near streets. For example, the model used by Ott *et al.*[7] gave average concentrations that amounted to 36 percent of the CAMP average.

A "street submodel" that can be used to calculate curbside CO concentrations is currently under development. The effort thus far has been based largely upon the extensive measurements of Georgii[36] in Frankfurt/Main, Germany, although the work of McCormick and Xintaras,[37] Schnelle *et al.*,[26] and Rouse[38] have also been considered.

Georgii's experiment involved extensive measurements of CO concentrations and wind speeds at different levels above three different streets in built-up areas, along with occasional traffic counts. One major finding was that the CO concentrations on the leeward sides of buildings were considerably higher than those on the windward sides, implying a helical cross-street circulation component in the opposite direction from the roof-level wind. In addition, the averaged data showed that (1) the vertical concentration profiles on either side of the street assume an exponential form, (2) the mode of air circulation above the street apparently changes when the roof top wind speed exceeds about 2 m sec^{-1}, and (3) the concentrations are exponentially related to traffic density. Examination of the measurements reported by Schnelle *et al.*[26] also indicates general agreement with (1) and (2) above; their data are insufficient for verifying (3).

Georgii's observations show that the roof-level concentrations differ only slightly from windward to leeward sides of the street-side buildings. It is reasonable to assume that the urban background concentrations calculated by the intra-urban model are approximately equivalent to roof-level concentrations. The effect of the street is to increase incoming roof-level concentrations by a factor that depends upon the receptor location relative to the wind direction, the height above the street, the wind speed at average roof level, and the traffic density.

Georgii's averaged data for a traffic density of 1400 vehicles per hour (the mean traffic density during his experiment) are well approximated by the empirical relationships

$$\frac{C_W}{C_r} = \exp\left[(0.55)\quad(1 - z/z_r)\right]$$

$$\frac{C_L}{C_r} = \exp\left[(0.87 + 0.098\,u_r)\ (1 - z/z_r)\right], \qquad (8)$$

where C_W and C_L are concentrations on the windward and leeward sides of the street-side buildings,

C_r = rooftop concentration (g m^{-3})
u_r = rooftop wind speed (m sec^{-1})
z_r = average rooftop height (m), and
z = receptor height (m).

The windward concentration ratio (C_W/C_r) turns out to be approximately independent of wind speed. This is apparently because the wind effect at this more exposed location is mostly absorbed by changes in C_r. On the leeward side, the concentration ratio increases with increasing wind speed, reflecting the relatively greater effect of sheltering at street level as the wind increases.

Although changes in traffic density, thus emission rate, in the adjacent street are not reflected directly in these equations, some justification for their application exists if it is assumed that the local traffic at a given time is always proportional to that in the city as a whole. For this case, the traffic changes will be reflected in the rooftop concentration, C_r, calculated by the intra-urban model, and hence, in C_W and C_L.

An additional problem in applying the above empirical results is that of defining leeward and windward cases on the basis of receptor location, street orientation, and wind direction. The problem is compounded further when the receptor is located at the corner of a street intersection, as is frequently the case with CAMP stations. In addition, in the vicinity of many intersections are buildings with widely varying heights, as well as open spaces such as parking lots. These complications make it difficult to apply the empirical relationships on a general basis. Additional work is necessary before treatment of microscale effects is incorporated into the model.

Macroscale (Extra-urban) Diffusion

In addition to considering sources in the immediate urban area, the model also takes into account the background pollution that is transported from one urban area to another. We have accepted, *a priori,* that the treatment of extra-urban transport can and should be considerably more gross than the treatment of nearby sources.

The first problem to be faced in the development of an extra-urban diffusion model is that there is no convenient way of knowing the upwind trajectory of the air arriving at a city. We can either determine the trajectory from past and present meteorological data or we can assume that the air has come from somewhere within a very large upwind segment. The latter approach seems more practical, particularly if we ever hope to apply the model to climatological data. Even the synoptic problem of trajectory determination by objective means seems too complicated to be warranted.

We apply the box model to a quadrant centered on the upwind direction and extending from 32 to 1000 km upwind of the receptor. The source strength is assumed to be constant in time and space throughout the sector, and is estimated from yearly fuel consumption[39] for those states and Canadian provinces whose centers fall within the sector. To determine the total emission rate within the area, we use the total amount of motor vehicle fuel consumed and the conversion factor: 1 gallon of fuel yields 1.32×10^3 grams of carbon monoxide. If the yearly (3.15×10^7 sec) consumption of fuel within the quadrant extending to 1000 kilometers is given by F, then the average CO emission rate Q in the area (7.86×10^{11} m^2) is given by:

$$Q = 5.32 \times 10^{-17} F \quad (g\ m^{-2}\ sec^{-1}). \tag{9}$$

The model input includes a table of 16 values of F, one for each of the wind directions used. This table is changed for each city. According to the box model, the concentration C from some upwind segment is

$$C = \frac{\left(Q\,(r_2 - r_1)\right)}{uh} \tag{10}$$

where r_2 and r_1 are the distances to the outer and inner segment boundaries (in this case 10^6 and 32×10^3 m), u is the wind speed, and h is the depth of the layer through which the material is mixed. Substituting Q from Equation (9) and the values of r_1 and r_2 gives the following equation for concentration from extra-urban sources, C_e:

$$C_e = \frac{5.15 \times 10^{-11} F}{uh} \tag{11}$$

The afternoon mixing depth, calculated in the intra-urban diffusion model, is used in Equation (11) because the pollutants are likely to have traveled for long enough periods that they will have had time to be mixed through the depth of the afternoon layer. We are aware that the local mixing depth will not necessarily be appropriate to the region upwind of the city, but more detailed treatment of this problem does not seem to be warranted. To approximate the normal vertical wind shear in the lower atmosphere, we have taken the average transport wind velocity through the depth of the mixing layer to be 1.5 times the maximum airport winds for the day.

In addition to the material generated within the segment extending to 1000 km, the general "worldwide" background is included. Robinson and Robbins[10] have estimated this to be about 0.2 part per million (ppm) (about 2.4×10^{-4} g m^{-3}) at sea level in the mid-latitudes of the northern hemisphere. This value is added to that calculated from Equation (11) to give the total extra-urban concentration, which generally amounts to a few tenths ppm. This extra-urban contribution is, in turn, added to the concentrations from urban sources calculated for each point in the city. The extra-urban contribution is calculated once for each 24-hour period, and that value is applied from one midnight to the next.

SYNTHESIS OF BASIC MODEL TYPES

The previous sections have described the individual portions or components of the diffusion model. Here we discuss the organization of these components into models capable of furnishing the desired outputs.

Synoptic Model

The synoptic model is designed to take the data for some hour, calculate and display point concentrations or concentration isopleths within the city for that hour, and then proceed to the next hour. This is repeated until the time period of interest has been covered on an hour-by-hour basis. The temporal changes of concentration for a selected location can be compared with the measured values during the same period.

The organization of the model is shown in Figure 5-6. In this flow chart it is assumed that the traffic data for the city are already stored and that the inputs consist of the meteorological parameters and those parameters necessary for the application of the stability and mixing depth subroutines (see Appendix A). The calculations start with determination of the afternoon (maximum) and night (minimum) mixing depths from the appropriate sounding. Then the meteorological parameters for the starting hour are read and the stability class determined. Mixing depths are calculated by different methods according to whether it is day or night. Concentrations are calculated and then the next hour's data are read.

The diurnal variation of mixing depth estimated by the model is schematically illustrated in Figure 5-7. A constant, the night (minimum) mixing depth, is assigned to the hours from midnight until the first hour after sunrise. This value is based on the morning temperature sounding. The day values are interpolated between the night (minimum) and afternoon (maximum) values on the basis of surface temperature (see Appendix A). The mixing depth from sunset to midnight is interpolated by time between the sunset and the new night (minimum) value based on the next morning's temperature sounding. This process makes the transition to the night mixing depth somewhat smoother.

The meteorological data used with this model consist of hourly surface observations and 1200 Greenwich Mean Time (GMT) (early morning) upper-air soundings, both on punched cards in edited form.

The traffic data are stored in the computer in the form described in an earlier section. Each traffic link is identified by the location of its endpoints. Data regarding length, daily traffic volume, and type (arterial, freeway, etc.) are associated with each link. This information, when combined with hour of the day, receptor location, wind direction, etc., is converted by the emission model to appropriate source strengths.

Sample results of calculations with the synoptic model are presented later in this paper.

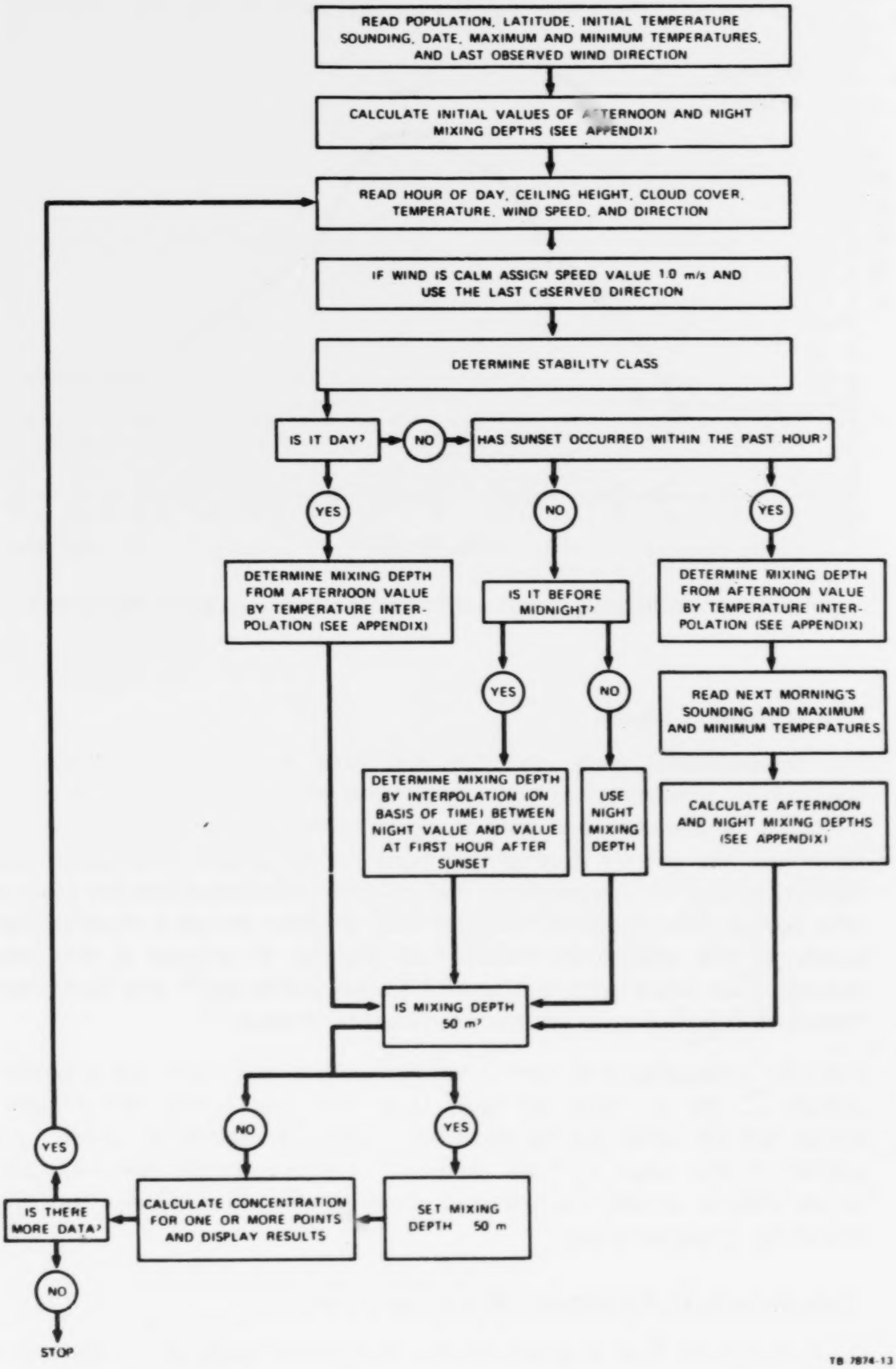
READ POPULATION, LATITUDE, INITIAL TEMPERATURE SOUNDING, DATE, MAXIMUM AND MINIMUM TEMPERATURES, AND LAST OBSERVED WIND DIRECTION
CALCULATE INITIAL VALUES OF AFTERNOON AND NIGHT MIXING DEPTHS (SEE APPENDIX)
READ HOUR OF DAY, CEILING HEIGHT, CLOUD COVER, TEMPERATURE, WIND SPEED, AND DIRECTION
IF WIND IS CALM ASSIGN SPEED VALUE 1.0 m/s AND USE THE LAST OBSERVED DIRECTION
DETERMINE STABILITY CLASS
IS IT DAY?
NO
HAS SUNSET OCCURRED WITHIN THE PAST HOUR?
YES
NO
YES
DETERMINE MIXING DEPTH FROM AFTERNOON VALUE BY TEMPERATURE INTERPOLATION (SEE APPENDIX)
IS IT BEFORE MIDNIGHT?
DETERMINE MIXING DEPTH FROM AFTERNOON VALUE BY TEMPERATURE INTERPOLATION (SEE APPENDIX)
YES
NO
READ NEXT MORNING'S SOUNDING AND MAXIMUM AND MINIMUM TEMPERATURES
DETERMINE MIXING DEPTH BY INTERPOLATION (ON BASIS OF TIME) BETWEEN NIGHT VALUE AND VALUE AT FIRST HOUR AFTER SUNSET
USE NIGHT MIXING DEPTH
CALCULATE AFTERNOON AND NIGHT MIXING DEPTHS (SEE APPENDIX)
IS MIXING DEPTH 50 m?
NO
YES
YES
IS THERE MORE DATA?
CALCULATE CONCENTRATION FOR ONE OR MORE POINTS AND DISPLAY RESULTS
SET MIXING DEPTH 50 m
NO
STOP
TB 7874-13

Figure 5-6. Flow chart of synoptic model calculations.

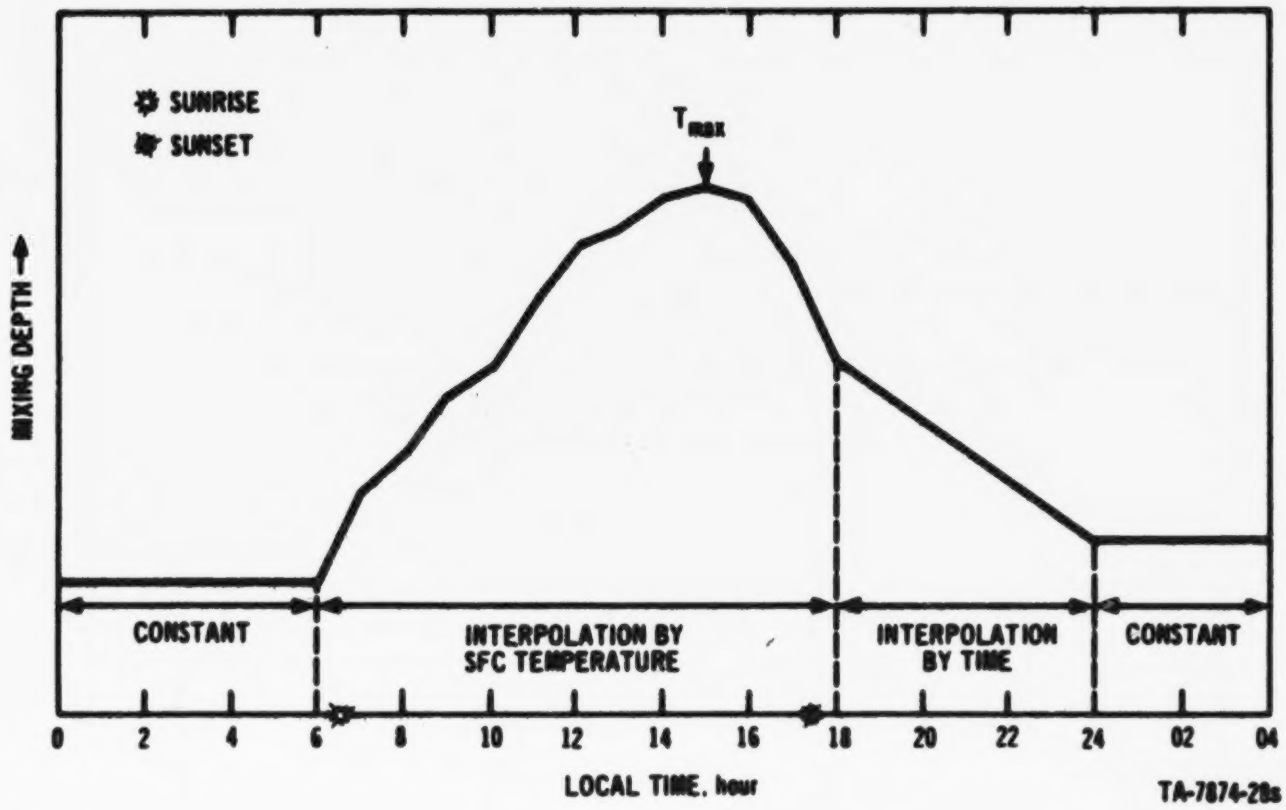

Figure 5-7. Modeled diurnal variation of mixing depth (schematic).

Climatological Model

Our computational work, thus far, has been limited to calculations of hour-to-hour concentrations with the synoptic model, based on hourly meteorological observations and average daily traffic data adjusted for diurnal conditions. We also are developing a capability to calculate average concentrations, as well as high-percentile and maximum concentrations over various time periods. That capability requires what we have termed a climatological model. In this section we discuss how we plan to proceed in this task, drawing upon recent work by Larsen,[2] Larsen and Burke,[40] and Martin and Tikvart.[41] A similar approach has been used by Frankel.[42]

Basically, a two-step procedure is involved: (1) an arithmetic mean concentration ($\overline{C}$), for a 1-hour averaging time is calculated from the diffusion model, and (2) either the statistical relationships developed by Larsen[40] are applied to this value to yield estimates of high-percentile and maximum concentrations, or else the predicted concentration-joint-frequency function is used for direct estimate.

Calculation of Arithmetic Mean Concentrations

Computation of $\overline{C}$ at a point requires a different treatment of the input data, as suggested by Martin and Tikvart.[41] This computation requires a large body of hourly meteorological data, preferably for a period of at least a year. The discrete joint probability density function $f(x_1, x_2, \ldots x_k)$ is tabulated* for all combinations of classes of hourly values of the model input parameters x_1 to x_k. By definition,

$$\sum_{n_1} \sum_{n_2} \ldots \sum_{n_k} f(x_1, x_2, \ldots x_k) = 1 \tag{12}$$

where the n's denote the number of class intervals for each parameter.

The judgment as to the number of classes to be established for each parameter must be based on a compromise between expected accuracy and required computing time. The latter can become critical when the diffusion model, $C(x_1, x_2, \ldots x_k)$, is used to compute $\overline{C}$ at several hundred receptor points, where the calculations at each point take the form

$$\overline{C} = \sum_{n_1} \sum_{n_2} \ldots \sum_{n_k} f(x_1, \ldots x_k) \quad C(x_1, x_2, \ldots x_k) \tag{13}$$

Here the concentration computed for each combination of parameter classes is weighted by the probability of occurrence of that combination, and all such fractions are summed to give the average (arithmetic mean). The quantity (N) of individual concentration computations for each point is determined by the size of the k-dimensional joint-density-function array:

$$N = n_1 \times n_2 \times \ldots \times n_k$$

Obviously the number of parameters, as well as the number of classes, affects the computing cost.

For our study, the traffic input is currently identified uniquely by the time of day, since available detailed data are only sufficient to establish the diurnal cycle. As indicated by Figures 5-2 and 5-3, the source emissions can be adequately represented by five time classes, two during peak and three during off-peak traffic periods: 0000 to 0600, 0700 to 0900, 1000 to 1500, 1600 to 1800, and 1900 to 2300 LST. Wind speed is divided into 6 categories, wind direction into 16, and stability into 5. At times it may be feasible to reduce the number of classes for wind direction to 8.

The remaining parameter, mixing depth h, is the most difficult to obtain, since its determination requires a morning temperature sounding (see Appendix A). Frankel[42] handled this problem by adjusting Holzworth's[15, 43, 44] climatological mixing-depth values on the basis of the stability class, effectively eliminating mixing depth as a separate parameter in the joint probability function. This seems to be a logical, if rather inexact approach. Deletion of the requirement for temperature soundings has a considerable computational advantage. To simplify his model, Pooler[45] also used the principle of minimizing the number of variables, by eliminating stability and taking the vertical diffusion parameter to be a function only of wind speed.

---

*Special computations and tabulations of this nature are available from the National Climatic Center, Asheville, N. C.

We are currently searching for a relationship between mixing depth and other meteorological parameters. Since obtaining this relationship on the basis of physical reasoning alone does not appear promising, we plan to analyze 4 months (1 month per season) of surface and radiosonde data for both Washington, D.C., and St. Louis. The mixing-depth values computed by the method developed for the synoptic model (see Appendix A) will then be stratified by time classes and correlated with the other meteorological parameters, particularly stability. If the correlations are significant, the result should be a general empirical expression for mixing depth for each time class. If not, we will resort to the best alternative, adjustment of climatological values.

If the planned number of classes and parameters are feasible, we will end up with the following computation:

$$\overline{C} = \sum_{i=1}^{5} \sum_{j=1}^{5} \sum_{k=1}^{6} \sum_{m=1}^{16} f(t_i, S_j, U_k, \theta_m)\; C(t_i, S_j, U_k, \theta_m). \quad (14)$$

This amounts to (5 x 5 x 6 x 16) = 2400 concentration calculations for each point. Since the diffusion model orientation is constant, for each point, the traffic links need only be scanned once, saving computer time.

Calculation of High-Percentile and Maximum Concentrations

The arithmetic mean concentrations ($\overline{C}$) for a 1-hour averaging time, obtained by the method just described, can be used to calculate estimates of high-percentile and maximum concentrations by means of Larsen's[2] statistical model.* Larsen analyzed 3 years of concentration data for seven pollutants from CAMP stations in six cities, and found that

1. Concentrations are approximately log-normally distributed for all pollutants, in all cities, and for all averaging times.
2. The median concentration (50 percentile) is proportional to a power of the averaging time.

These conclusions were derived mainly from the concentration data from the important region above the median concentration.

Larsen discussed certain significant applications of these general findings. Since arithmetic mean concentrations, $\overline{C}$, for all averaging times are equal, and since the concentration distribution is log-normal, the geometric mean concentration $\overline{C}_g$, for any averaging time t can be calculated from:

$$(\overline{C}_g)_t = \overline{C}/(S_g)_t^{\,0.5\ \ln(S_g)_t}. \quad (15)$$

---

*Such calculations could also be performed directly using the predicted concentration joint frequency function, if the latter were based upon a sufficiently large body of Meteorological data.

$\overline{C}$ is available from the diffusion model calculations, and $(S_g)_t$, the standard geometric deviation for a given averaging time, may be obtained for CAMP station measurements of carbon monoxide from the tabulations by Larsen and Burke.[40]*

The concentration $(C_p)_t$ associated with any percentile p, of the frequency distribution, for any averaging time t, may be calculated from

$$(C_p)_t = (\overline{C}_g)_t \ (S_g)_t^q \qquad (16)$$

where the number of standard deviations, q, is found from tables of the standardized cumulative normal distribution, where:

$$p/100 = \frac{1}{\sqrt{2\pi}} \int_{-\infty}^{q} e^{-x^2/2} \, dx \qquad (17)$$

The maximum concentration during a 1-year period for an averaging time to t hours is designated by $(C_{max})_t$; it is given by

$$(C_{max})_t = (\overline{C}_g)_{1\text{-hr}} \ (S_g)_{1\text{-hr}}^{3.81} \ t^m \qquad (18)$$

where values of m as a function of S_g are those tabulated by Larsen.[2]

Using these relationships and the arithmetic mean concentrations furnished by the diffusion model, we can calculate, for any averaging time, (1) the concentration expected for any percentile and (2) the maximum concentration expected once a year. It is also straightforward to generalize (2) above to the calculation of maximum concentrations expected once during any given period.

PRELIMINARY RESULTS TO DATE

Status

At the present time the basic designs for both the synoptic model and the climatological model are fairly complete. The synoptic model, less the street and extra-urban submodels, is programmed and running. Traffic data for Washington, D.C., and St. Louis have been coded, and data for three other cities are in the process of reduction. We are currently evaluating the model output in terms of its sensitivity to parametric changes and its response to design refinements. Sample results of some of these trial computations with the synoptic model are presented here, to furnish an idea of its eventual capabilities. The other models and submodels and necessary input data are in the preparation stages.

---

*The values of $(S_g)_{1\text{-hr}}$ for CO measured at the CAMP Stations in eight cities range from 1.44 to 1.95, with a mean of 1.63. Application of the model to non-CAMP cities will require an estimate of S_g or its calculation using CO data. The probable factors having the greatest effect upon S_g are (1) the receptor siting, and (2) variability of the meteorological parameters. Consideration of these factors could allow estimation of S_g for any city, based upon those calculated for the CAMP cities.

Analysis and Display Techniques

To facilitate model development, we are taking advantage of modern computer techniques, particularly objective contour analysis and graphical display. In this work we are using special subroutines called CONTOOR and GRAPH 4* with the CDC 6400 computer and the CDC 280 cathode-ray tube (CRT) peripheral display system. The CONTOOR subroutine furnishes objective isolines describing the CO concentration distribution over an urban area on the basis of a grid of point values calculated according to the diffusion model. The GRAPH 4/280 combination permits such contour analyses (or the results of any other calculations – see Figure 5-1, page 5-4) to be displayed on the CRT and photographed. This facility significantly expedites the trial and evaluation procedure.

A sample product of these techniques is given in Figure 5-8. Here the

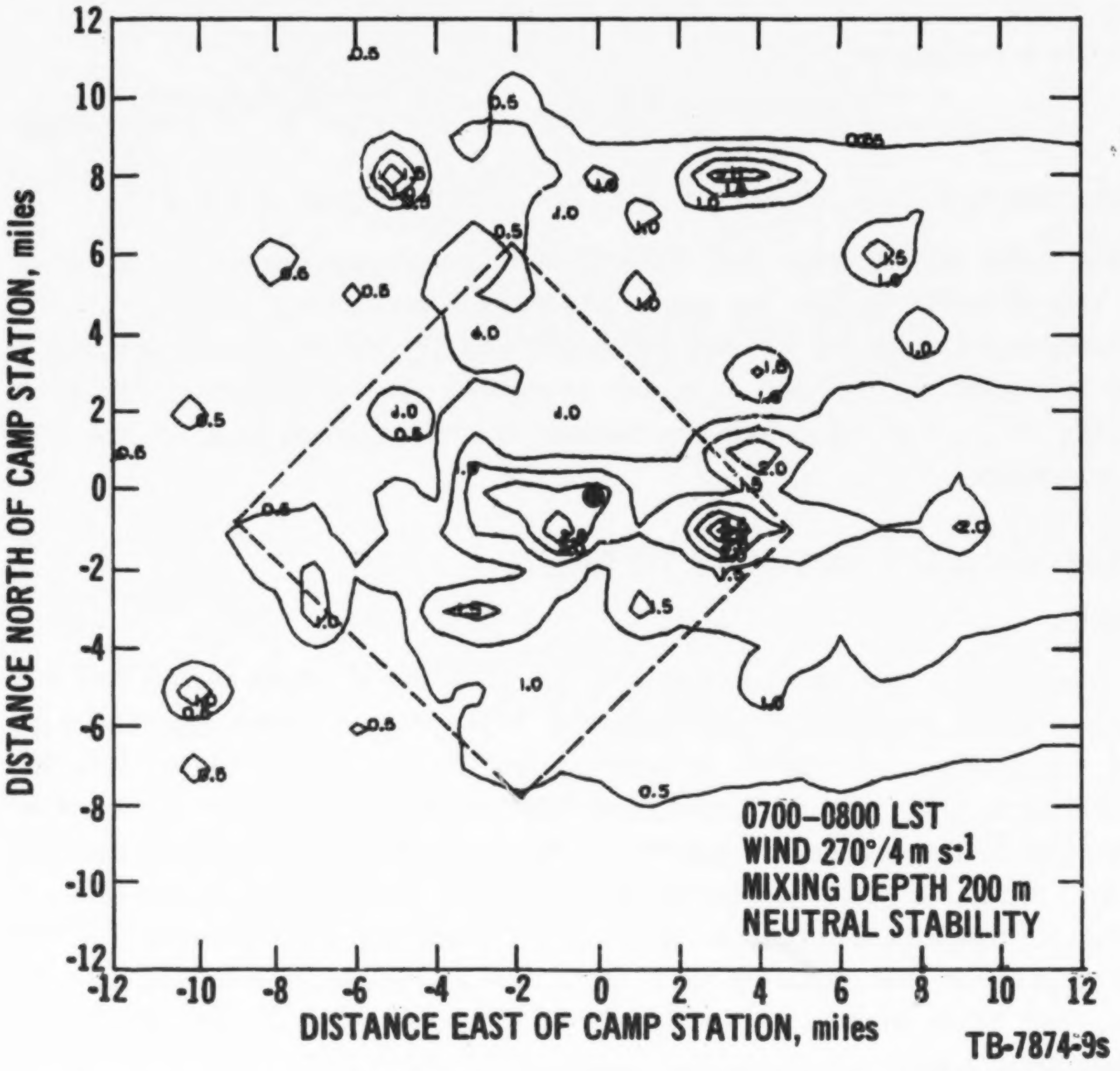
DISTANCE NORTH OF CAMP STATION, miles
12
10
8
6
4
2
0
-2
-4
-6
-8
-10
-12
-12
-10
-8
-6
-4
-2
0
2
4
6
8
10
12
DISTANCE EAST OF CAMP STATION, miles
0700–0800 LST
WIND 270°/4 m s-1
MIXING DEPTH 200 m
NEUTRAL STABILITY
TB-7874-9s

Figure 5-8. Calculated intra-urban concentration distribution of carbon monoxide (ppm) over Washington, D. C. -- computer generated contour analysis and display.

---

*These subroutines were developed by S. Briggs and B. Sifford of Stanford Research Institute, respectively.

GRAPH 4/280 display of the CONTOOR objective analysis is superimposed upon the primary traffic network for Washington, D.C. Good correspondence between the CO concentrations and road density is evident. The analysis was based upon concentrations over a 25 x 25 section grid of 625 points, as calculated by an early version of the diffusion model from simulated meteorological data. The objective contouring compares well with a manual analysis of the identical data, presented in Figure 5-9. Differences between the two patterns were traced to plotting and drawing errors by the analyst. The smoother hand analysis may look better, but the objective analysis is substantially faster, cheaper,* and more accurate.

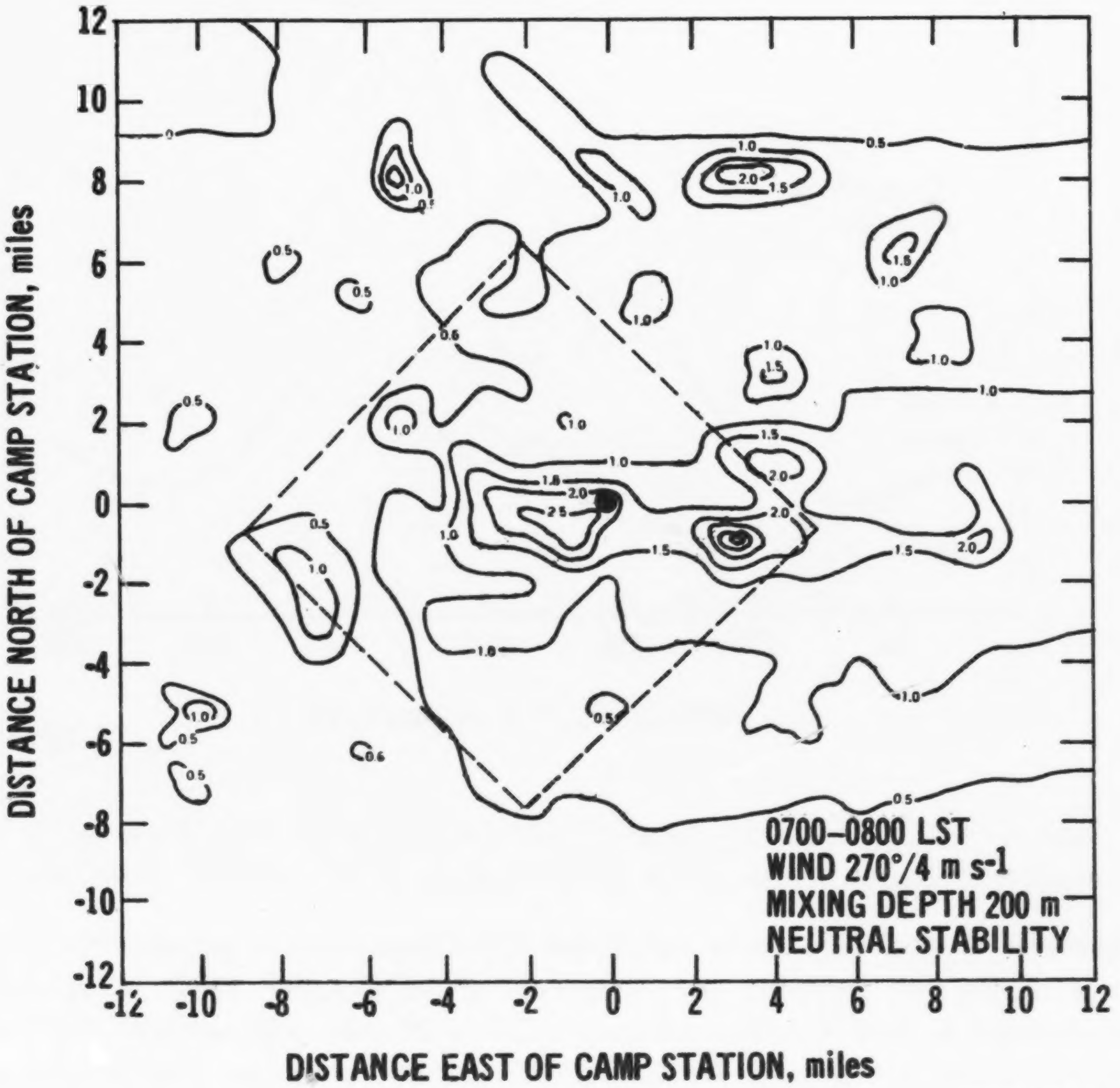
DISTANCE NORTH OF CAMP STATION, miles
12
10
8
6
4
2
0
-2
-4
-6
-8
-10
-12
-12
-10
-8
-6
-4
-2
0
2
4
6
8
10
12
DISTANCE EAST OF CAMP STATION, miles
0700–0800 LST
WIND 270°/4 m s-1
MIXING DEPTH 200 m
NEUTRAL STABILITY
0.5
1.0
1.5
2.0
2.5

TB-7874-8s

Figure 5-9. Same as Figure 5-8, but hand contoured.

---

*Computer costs for the diffusion calculations in Figure 10 were about $20. The objective was an additional $5.

Model Sensitivity and Evaluation Trials

Figure 5-10 illustrates the type of tests of model sensitivity to parameter changes that are in progress. (This and all subsequent graphs were also produced by the GRAPH 4/280 system.) Tests of this nature are helpful in the refinement of the model design. The figure shows that the highest concentrations at the Washington CAMP station should occur for west winds, all other parameters being equal.

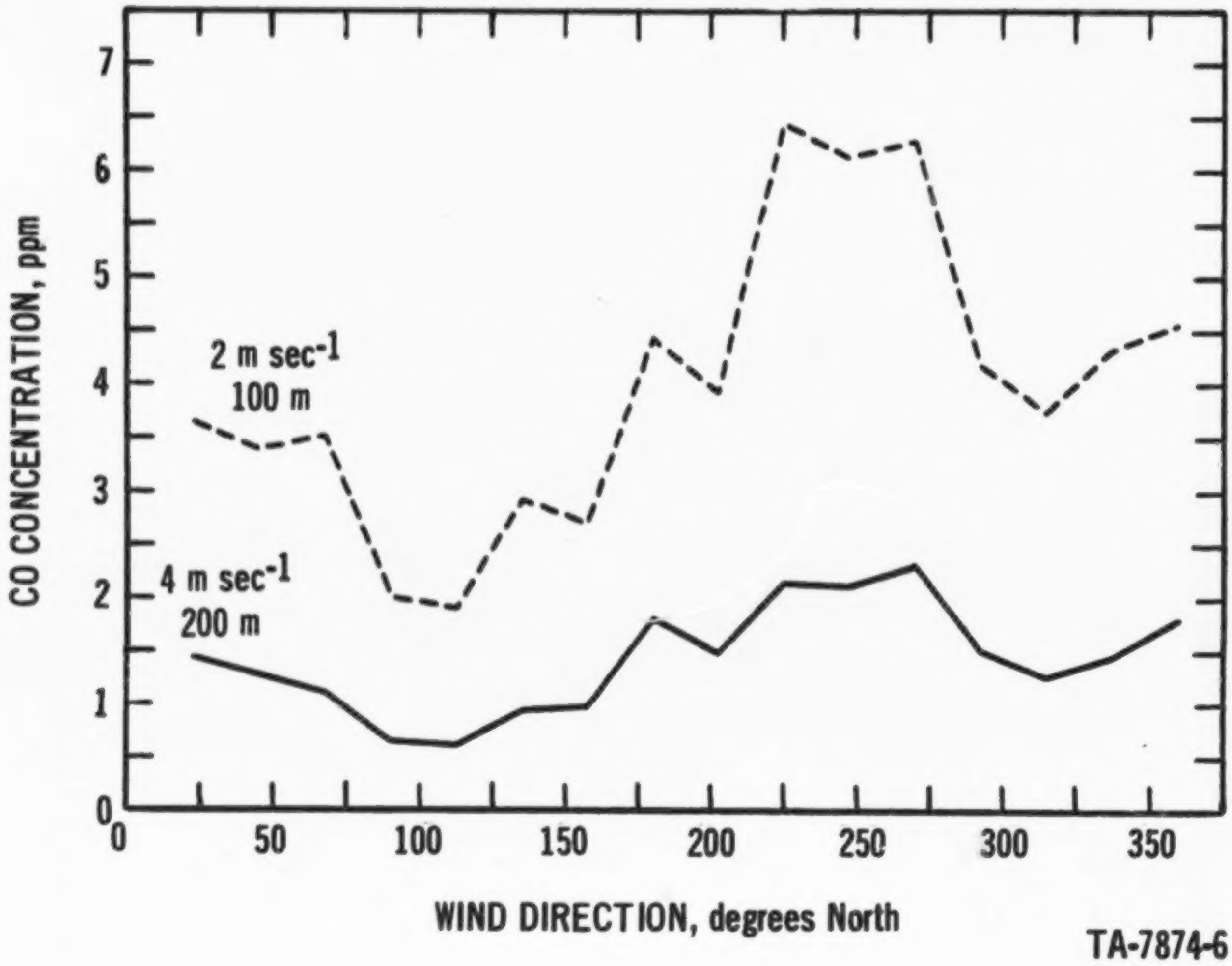

Figure 5-10. Effect of dilution factor and wind direction upon computed concentrations at Washington, D. C. CAMP station.

Figures 5-11 and 5-12 show calculated CO concentration patterns for St. Louis during the morning and afternoon of 16 October 1964, using real meteorological data. Calculations over a 24- x 24-mile grid centered on the CAMP station are shown. At the CAMP station, observed concentrations were 19 and 5 ppm for 0700 to 0800 LST and 1500 to 1600 LST. These are substantially larger than the values calculated at the center of the grids, (approximately 6 and 3 ppm for morning and afternoon). This is as it should be, since these calculations are for the intra-urban component (roof-level concentrations) only.

The typical drop in concentrations from early morning to mid-afternoon is apparent. It is also of interest to note the reasonably high concentrations in

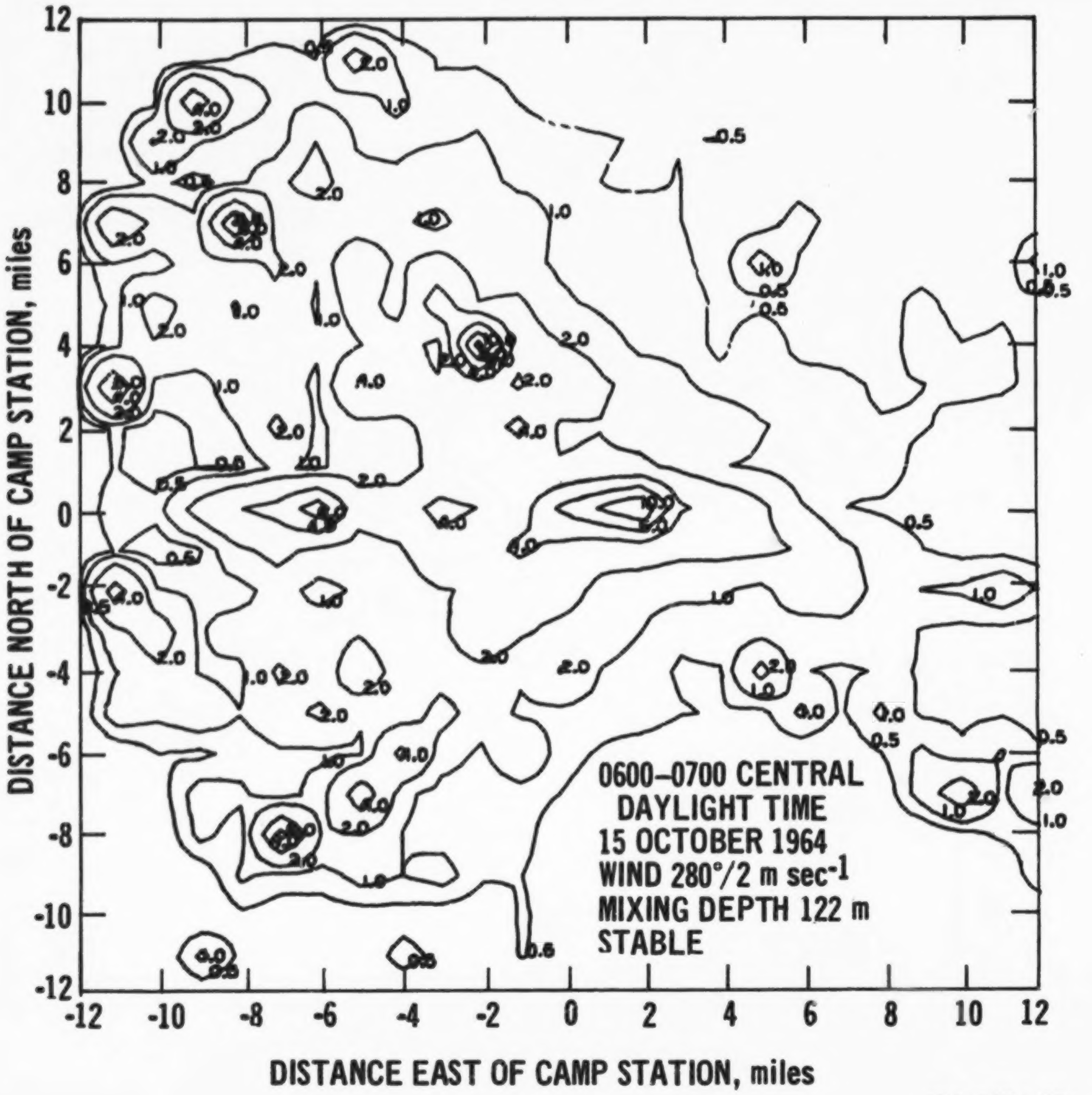
12
10
8
6
4
2
0
-2
-4
-6
-8
-10
-12
DISTANCE NORTH OF CAMP STATION, miles
-12
-10
-8
-6
-4
-2
0
2
4
6
8
10
12
DISTANCE EAST OF CAMP STATION, miles
0600–0700 CENTRAL
DAYLIGHT TIME
15 OCTOBER 1964
WIND 280°/2 m sec-1
MIXING DEPTH 122 m
STABLE

TA-7874-25s

Figure 5-11. Calculated intra-urban CO concentration distribution (ppm) for St. Louis area during early morning.

the morning near the junctions of freeways on the western side of St. Louis.

The same data as Figure 5-12 were used earlier in an attempt to furnish an idea of the capability of the basic intra-urban model to compute detailed concentration patterns over small areas. Those results are given in Figure 5-13, where the horizontal scale has been decreased by a factor of ten, and the box size is now only 2.4 x 2.4 miles, still centered on the CAMP station. The concentration pattern shows a large spatial variability that is related to the distribution of downtown streets represented by the underlay.

The results of trials using the synoptic model to calculate hourly concentrations continuously for a week are presented in Figures 5-14 and 5-15. To provide a true test of the model's capabilities, weeks with a variety of

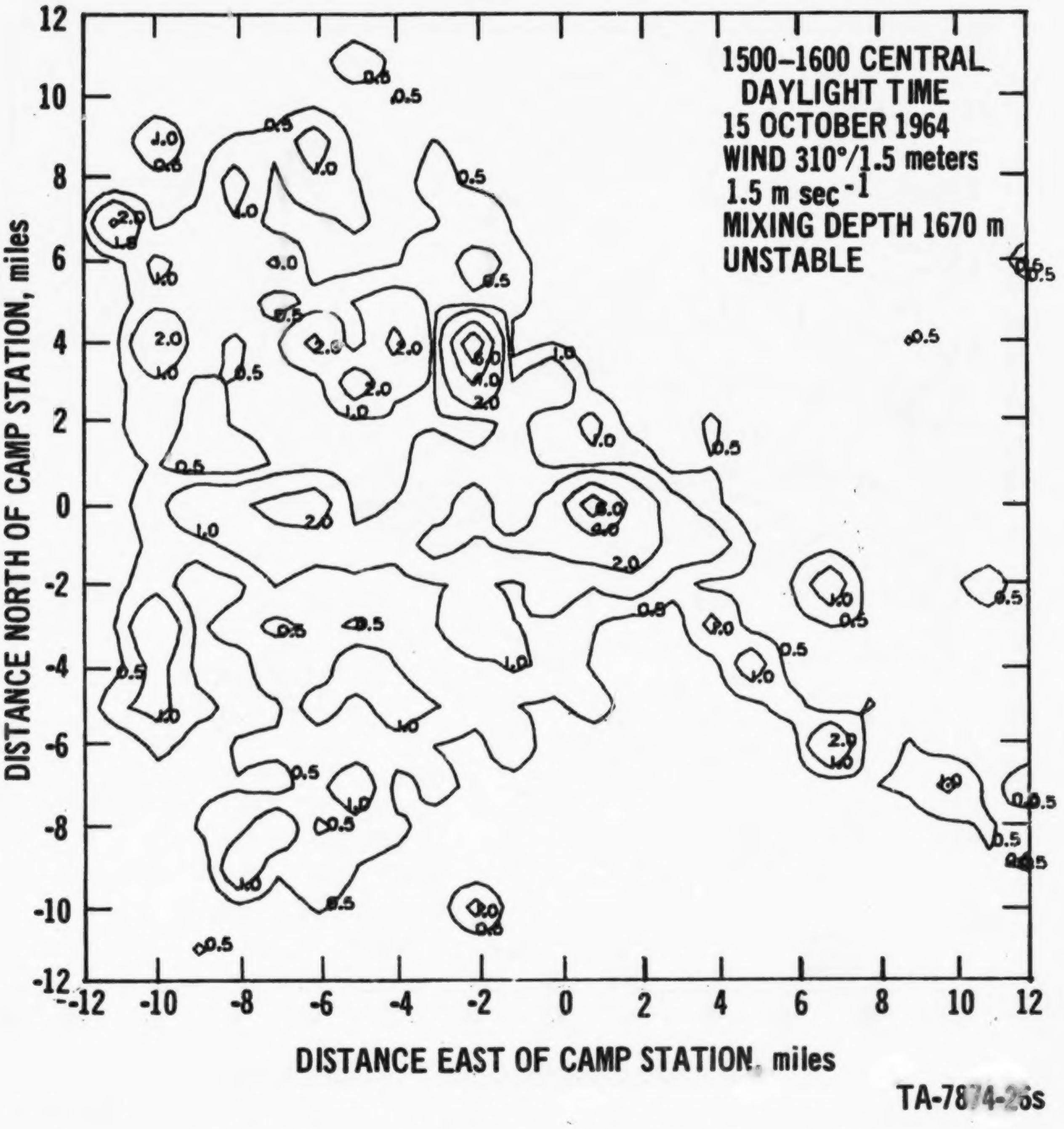

1500–1600 CENTRAL DAYLIGHT TIME
15 OCTOBER 1964
WIND 310°/1.5 meters
1.5 m sec^{-1}
MIXING DEPTH 1670 m
UNSTABLE
DISTANCE NORTH OF CAMP STATION, miles
DISTANCE EAST OF CAMP STATION, miles
12
10
8
6
4
2
0
-2
-4
-6
-8
-10
-12
0.5
1.0
2.0
TA-7874-26s

Figure 5-12. Same as Figure 5-11, but for late afternoon.

observed concentrations were selected. To account for a suspected instrumental zero-calibration problem, the observations, indicated by the dashed curves in the figures, have all been adjusted downward by 1 ppm. In an attempt to more accurately treat the effects of nearby sources, the closest diffusion area segment was divided into two sections for these calculations. One segment extends from the receptor to 62.5 m in range, and the other extends from 62.5 out to 125 m.

The CO observations during the January period (Figure 5-14) were anomalously high, and the model generally gives underestimates for this week. A variety of weather conditions prevailed; cold fronts passed St. Louis on the evenings of 17, 19, and 23 January. The poorest performance of the model occurs on 19, 21, and 22 January, when the wind was generally southerly.

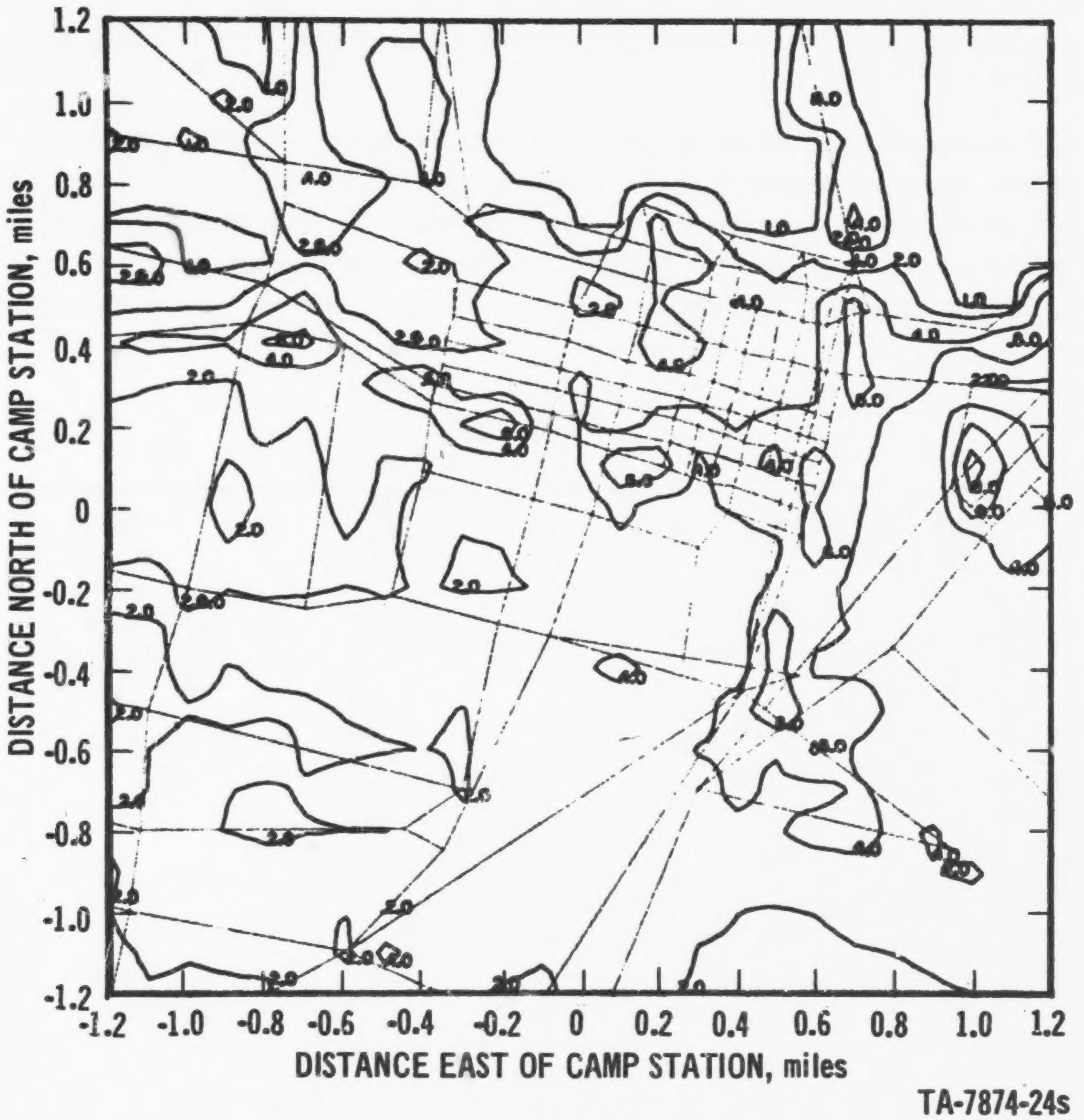
DISTANCE NORTH OF CAMP STATION, miles
1.2
1.0
0.8
0.6
0.4
0.2
0
-0.2
-0.4
-0.6
-0.8
-1.0
-1.2
-1.2
-1.0
-0.8
-0.6
-0.4
-0.2
0
0.2
0.4
0.6
0.8
1.0
1.2
DISTANCE EAST OF CAMP STATION, miles
TA-7874-24s

Figure 5-13. Same as Figure 5-12, but scale reduced by a factor of ten to give detailed CO concentration pattern in central portion of St. Louis business district.

This suggests that the high observed concentrations are caused by the nearby sources on the adjacent streets, since the St. Louis CAMP station is located on the northwest corner of an intersection.

Weather conditions during the October period were not so variable, and more typical CO concentrations were observed. In contrast to the January period, the predicted concentrations are mostly too high. The poorest agreement occurs when the reported airport winds are very light or calm. For these cases, the model uses a wind speed of 2 m sec^{-1} and the wind direction last observed. It is probable that much of the prediction error is due to this uncertainty in wind direction, part of the general difficulty encountered in applying airport observations to urban areas. Better results might be achieved for very light-wind conditions if a symmetrically convergent urban circulation, driven by the heat island effect, were included in the model.

No agreement was expected between the calculated and observed weekend values, since no weekend traffic distribution has yet been incorporated into the model. It is interesting, however, to note the low concentrations observed on Sundays, and the late peak in the observed concentration at about 1100 on Saturday, 23 January (Figure 5-14), probably due to shopping traffic.

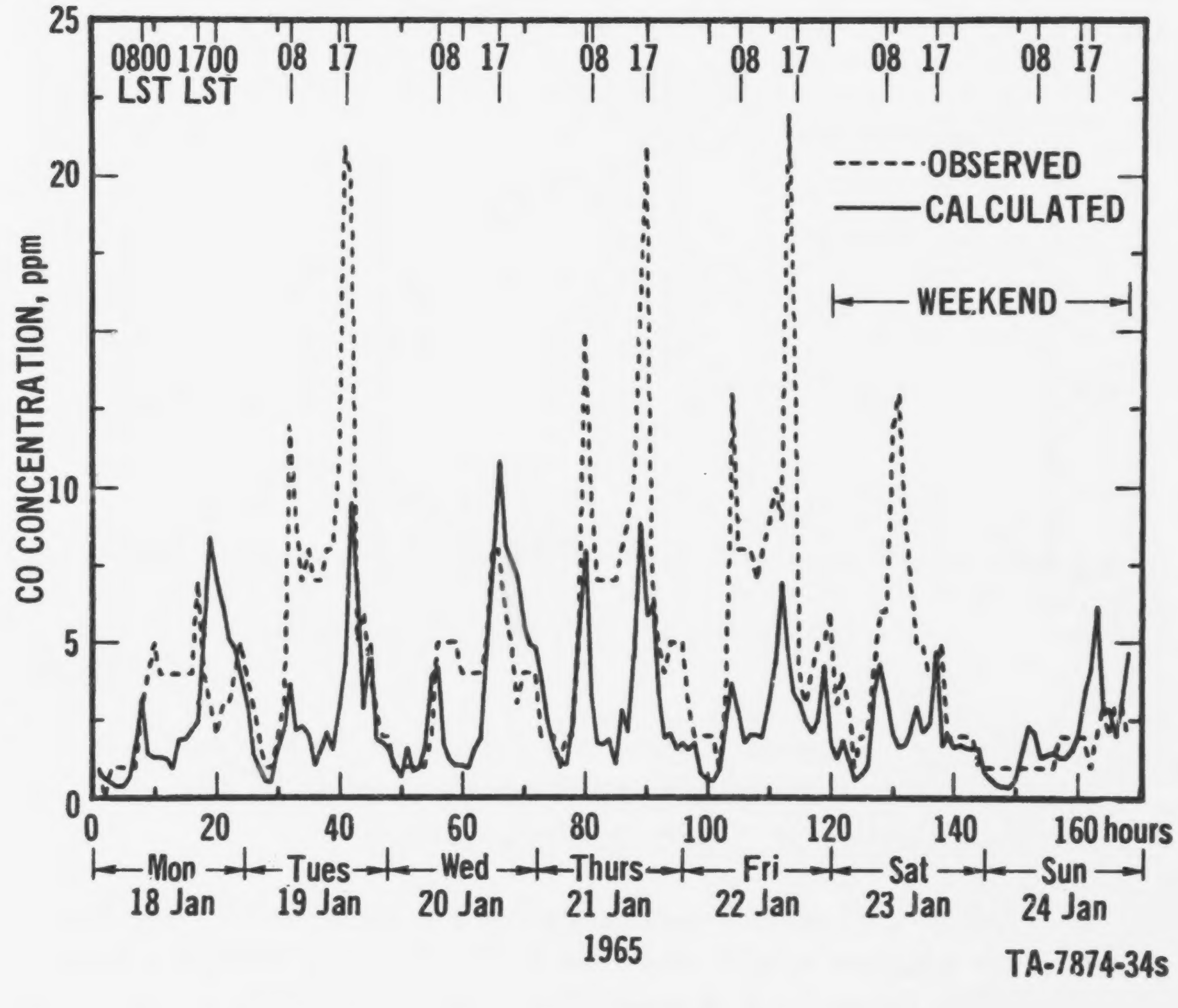

Figure 5-14. Hourly predicted and observed CO concentrations at St. Louis CAMP station for period 18-24 January 1965.

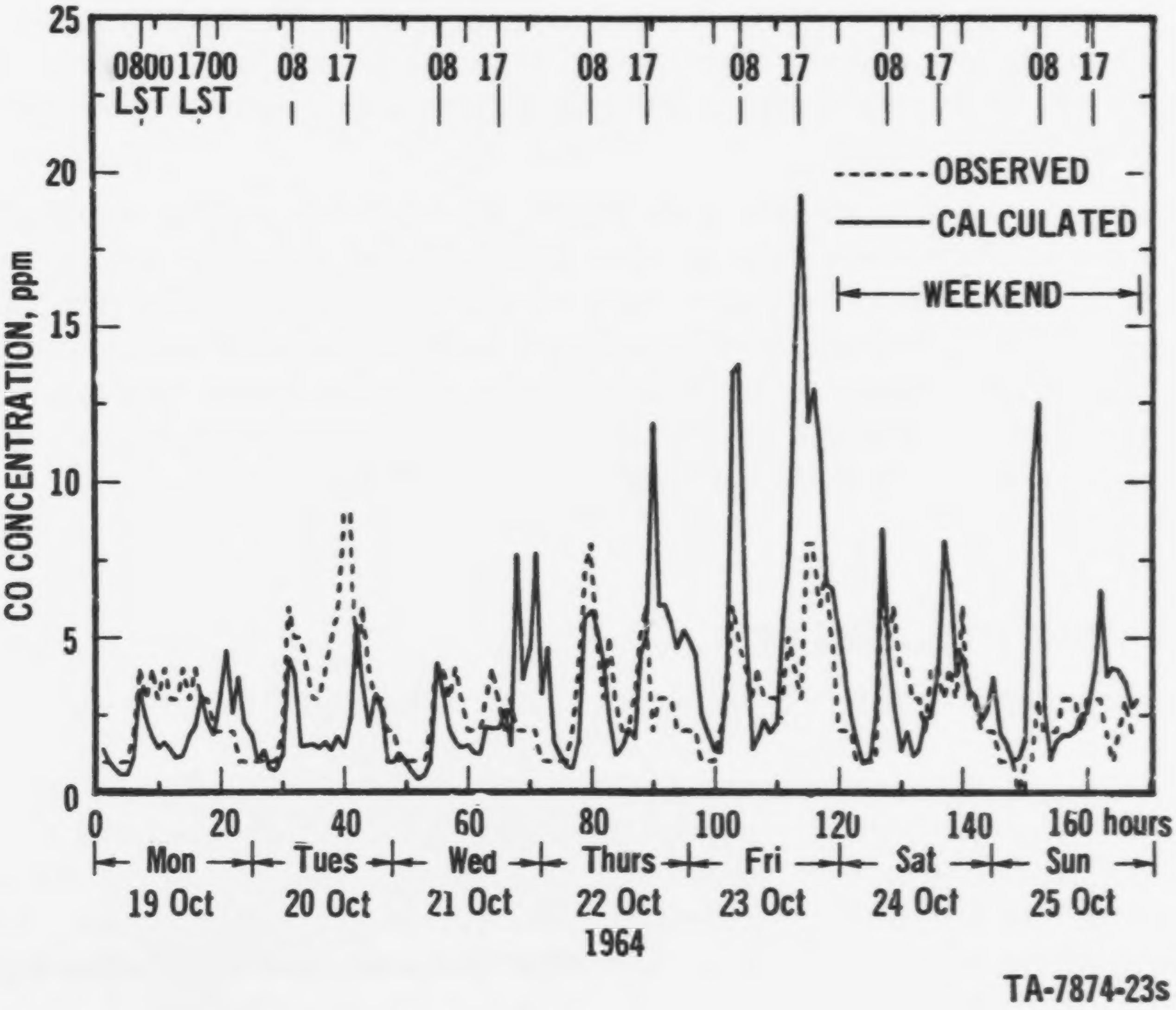

Figure 5-15. Same as Figure 5-14, but for period 19-25 October 1964.

SUMMARY AND CONCLUSIONS

The model design described here is believed to be a realistic and practical approach toward developing capabilities for accurate and economical calculation of: (1) hour-to-hour CO concentrations, using synoptic weather data, and (2) average, high-percentile, and maximum concentrations, using climatological weather data and forecast traffic data. The simplified model design makes full use of several previous modeling efforts, with the incorporation of necessary and appropriate modifications. Unique features of this model include (1) an objective treatment of the traffic data to give a time- and space-dependent emission inventory, (2) a technique for estimating hourly values of mixing depth, and (3) a method (under development) for calculating street-level concentrations. So far we have not used adjustable "calibration" constants in the model.

Final evaluation of the model must be deferred until all the sub-models, and any necessary refinements are incorporated. To date the preliminary evaluation trials have been instructive in showing model performance. Two expected results are already apparent: (1) agreement with observed (CAMP) values depends critically upon proper treatment of microscale effects, and (2) the steady-state model in its present form gives poor results for light-wind conditions.

Since the model is designed to be general, only routinely available input data are used. This means reliance upon airport weather data and rather gross traffic data, placing an upper limit on the accuracy obtainable with the model. The substantial effort expended in the development of techniques, to estimate the required model input variables, using such largely inappropriate input data, underscores the need for additional, routine, pollution-oriented, meteorological and traffic measurements within cities.

ACKNOWLEDGMENT

This research was jointly sponsored by the Coordinating Research Council under Contract No. CAPA 3-68 (1-68) and by the National Air Pollution Control Administration under Contract No. CPA 22-69-64. We are grateful for the assistance of the following individuals at Stanford Research Institute: Mrs. Shirley Reid, who secured and supervised the reduction of the traffic data; Robert Mancuso and Hisao Shigeishi, who programmed the model and carried out the computer trials; and Elmer Robinson, who aided in planning the model development.

We also thank the members of the CRC-APRAC Urban Diffusion Project Group for their guidance and suggestions, and for supplying useful technical information.

APPENDIX
DETERMINATION OF MIXING DEPTHS FOR USE WITH SYNOPTIC MODEL

F. L. Ludwig

Initial attempts to estimate mixing depths for the synoptic model from surface observations only, were unsuccessful. The method finally chosen for estimating daytime mixing depths follows the commonly accepted approach[20] and requires knowledge of the early morning temperature sounding. The maximum afternoon mixing depth (h_{max}) is calculated as the height at which the dry, adiabatic lapse rate from the maximum surface temperature (T_{max}) intersects the morning sounding. The calculations of mixing depth are made in pressure coordinates, and then converted to heights with the hydrostatic equation and the gas law.

For nighttime hours, a minimum mixing depth (h_n) is estimated as follows. For daylight hours other than the time of maximum temperature, the mixing depth h_d is obtained by linear interpolation between h_{max} and h_n, according to the temperature T:

$$h_d = \left(\frac{T-T_{min}}{T_{max}-T_{min}}\right)\left(h_{max}-h_n\right) + h_n \qquad \text{(A-1)}$$

The estimation of nighttime mixing depth over the city is based on Summers'[24] model of the urban heat island and Ludwig's[48,49] empirical relationship between rural lapse rates and the intensity of urban heat islands. If we assume T to be a linear function of the log of pressure (very nearly the same as Summers' assumption of T as a linear function of height), then the temperature, T_h, at some height, h, outside the city is given by:

$$T_h = T_0 + \frac{dT}{d\ln p}\Delta \ln p \approx T_0 + \bar{p}\,\frac{dT}{dp}\ln\left(\frac{p_h}{p_0}\right) \qquad \text{(A-2)}$$

where T_0 and p_0 are the rural surface temperature and pressure, respectively, p_h is the pressure at h, and $\bar{p}$ is the average of p_0 and p_h.

If air moving into a city is heated from below to the extent that complete mixing takes place through a depth h, then the temperature at height h will remain T_h and the lapse rate below h will become adiabatic. The dry, adiabatic lapse rate γ_d (in pressure coordinates) is given by

$$\gamma_d = \frac{TR}{pc_p} = 0.287 \frac{T}{p} \approx 0.287 \frac{\overline{T}}{\overline{p}} \qquad \text{(A-3)}$$

where R and c_p are the gas constant and specific heat at constant pressure for dry air, T and p are absolute temperature and pressure, and $\overline{T}$ and $\overline{p}$ are the respective average values within the layer from the surface to height, h. For the urban situation, Equation (A-2) becomes

$$T_h = T_u + \overline{p}\ \gamma_d \ \ln\left(\frac{p_h}{p_o}\right) \qquad \text{(A-4)}$$

where T_u is the surface air temperature in the center of the urban area.

Subtracting Equation (A-4) from Equation (A-2) gives:

$$T_u - T_o = \overline{p} \left[\ln\left(\frac{p_h}{p_o}\right)\right]\left(\frac{dT}{dp} - \gamma_d\right) \qquad \text{(A-5)}$$

Substituting Equation (A-3) into Equation (A-5) gives:

$$T_u - T_o = \left[\ln\left(\frac{p_h}{p_o}\right)\right]\left(\overline{p}\frac{dT}{dp} - 0.287\ \overline{T}\right) \qquad \text{(A-6)}$$

Ludwig[48] has shown that $(T_u - T_o)$ can be approximated within about 2° C by the following equation:

$$T_u - T_o = p^{1/4}\left(0.0633 - 0.298 \frac{dT}{dp}\right) \qquad \text{(A-7)}$$

where P is the population of the urban area and dT/dp is expressed in °C per millibar. The equation is based on 85 sets of data from 18 different cities.

Substituting Equation (A-7) into Equation (A-6) gives:

$$\ln\left(\frac{p_h}{p_o}\right) = P^{1/4} \frac{\left(0.0633 - 0.298 \frac{dT}{dp}\right)}{\left(\overline{p}\cdot\frac{dT}{dp} - 0.287\ \overline{T}\right)} \qquad \text{(A-8)}$$

The value of dT/dp is determined on the basis of the lowest portion of the morning sounding between the surface and the first reported level above the surface; $\overline{p}$ and $\overline{T}$ are the averages of the pressures and temperatures at these points.

To convert $\ln\left(\frac{p_h}{p_o}\right)$ to mixing depth, we can use the thickness equation.

If temperature is assumed equal to $\overline{T}$ throughout the layer then:

$$h = -\ln\left(\frac{p_h}{p_o}\right) \frac{R\overline{T}}{g} = -29.3\ \overline{T}\ \ln\left(\frac{p_n}{p_o}\right) \tag{A-9}$$

and Equation (A-8) becomes

$$h_n = -\frac{29.3\ \overline{T}\ P^{1/4}\left(0.0633 - 0.298\ \frac{dT}{dp}\right)}{\left(\overline{p}\ \frac{dT}{dp} - 0.287\ \overline{T}\right)} \tag{A-10}$$

In applying the preceding equations to the calculation of mixing depth for the diffusion model, we use Equation (A-1) for the first hour after sunset. Between this hour and midnight, the mixing depth is interpolated by time between the values given by Equations A-1 and A-10. The latter is the nighttime minimum mixing depth, h_n, which is assumed to apply for all other night hours. The values of the parameters in Equation (A-10) are determined from the sounding for the next morning.

The assumption of a constant urban mixing depth throughout the early morning hours is based on observations presented by Ludwig and Kealoha[49] for Dallas, and Ft. Worth, Texas. These observations show that the urban heat island develops rather quickly in the evening. If the urban heat island and the urban mixing layer are related, as suggested by Summers' model, then the mixing depth should reach its nighttime value by the middle of the night similar to the heat-island intensity.

To take care of those instances when the calculated mixing depth is unreasonably high or low, we assigned limiting values of 4000 m maximum or 50 m minimum.

REFERENCES

1. Clarke, J. F. A Simple Diffusion Model for Calculating Point Concentrations from Multiple Sources. J. Air Pollution Control Assoc. *14*:347-352, September 1964.
2. Larsen, R. I. A New Mathematical Model of Air Pollutant Concentration, Averaging Time and Frequency. J. Air Pollution Control Assoc. *1*:24-30, January 1969.
3. Wanta, R. C. Meteorology and Air Pollution. In: Air Pollution, Stern, A. C. (ed.):, Vol. 1, 2d ed. New York, Academic Press, 1968. p. 187-226.
4. Stern, A. C. The Systems Approach to Air Pollution Control. North Carolina University, Dept. of Environ. Science and Engineering. Chapel Hill. Publication Number 216. 1969. 51 p.
5. Moses, H. Mathematical Urban Air Pollution Models. National Center for Air Pollution Control, Chicago Dept. of Air Pollution Control Argonne National Laboratory. Argonne, Ill. ANL/ES-RPY-001. April 1969. 69 p.
6. Neiburger, M. Diffusion Models of Urban Air Pollution. In: Proceedings of WMO Symposium on Urban Climates and Building Climatology, Brussels, Belgium, October 15-25, 1968. to be published by World Meteorological Organization. Geneva, Switzerland. In press. 17 p.
7. Ott, W., J. F. Clarke, and G. Ozolins, Calculating Future Carbon Monoxide Emissions and Concentrations from Urban Traffic Data. National Center for Air Pollution Control. Cincinnati, Ohio. PHS Publication Number 999-AP-41. June 1967. 40 p.
8. Swinnerton, J. W., V. J. Linnenbom, and C. H. Cheek. Distribution of Methane and Carbon Monoxide Between the Atmosphere and Natural Waters. Environ. Sci. Technol. *3*:836-838, September 1969.
9. Went, F. W. On the Nature of Aitken Condensation Nuclei. Tellus. *18*(2-3): 549-556, 1966.
10. Robinson, E. and R. C. Robbins. Sources, Abundance and Fate of Gaseous Atmospheric Pollutants. Stanford Research Institute. Menlo Park, Calif. Final Report, SRI Project PR-6755. 1968. 123 p.
11. Washington, D. C., Cincinnati, Ohio., Metropolitan Area Air Pollution Abatement Activity. National Center for Air Pollution Control. 1967. 46 p.
12. Chass, R. L. *et al.* Total Air Pollution Emissions in Los Angeles County. J. Air Pollution Control Assoc. *10*(5):351-366, October 1960.
13. Report for Consultation on the San Francisco Bay Area Air Quality Control Region. National Air Pollution Control Administration. 1968.
14. Rose, A. H. *et al.* Comparison of Auto Exhaust Emissions from Two Major Cities. J. Air Pollution Control Assoc. *15*:362-366, August 1965.
15. Holzworth, G. C. Estimates of Mean Maximum Mixing Depths in the Contiguous United States. Mon. Weather Rev. *92*:235-242, May 1964.
16. Smith, Wilbur and Associates. Transportation Survey—National Capital Region. Prepared for National Capital Planning Commission. New Haven, Conn. 1958. 125 p.
17. Gifford, F. A., Jr. Use of Routine Meteorological Observations for Estimating Atmospheric Dispersion. Nucl. Safety. *2*:47-51, June 1961.
18. Pooler, F., Jr. A Tracer Study of Dispersion Over a City. J. Air Pollution Control Assoc. *16*:677-681, December 1966.
19. McElroy, E J. L. A Comparative Study of Urban and Rural Dispersion. J. Appl. Meteorol. *8*(1):19-31, February 1969.
20. Miller, M. E. and G. C. Holzworth. An Atmospheric Diffusion Model for Metropolitan Areas. J. Air Pollution Control Assoc. *17*:46-50, January 1967.
21. Smith, M. E. and I. A. Singer. An Improved Method of Estimating Concentrations and Related Phenomena from a Point Source Emission. J. Appl. Meteorol. *5*(5): 631-639, October 1966.

22. Meade, P. J. Meteorological Aspects of the Peaceful Uses of Atomic Energy. Part 1. Meteorological Aspects of the Safety and Location of Reactor Plants. World Meteorological Organization. Geneva, Switzerland. Publication Number 97 TP41. Technical Note Number 33. 1960. 33 p.

23. Turner, D. B. A Discussion Model for an Urban Area. J. Appl. Meteorol. *3*(1): 83-91, February 1964.

24. Summers, P. W. The Seasonal, Weekly, and Daily Cycles of Atmospheric Smoke Content in Central Montreal. J. Air Pollution Control Assoc. *16*:432-438, August 1966.

25. Graham, I. R. An Analysis of Turbulence Statistics at Fort Wayne, Indiana, J. Appl. Meteorol. *7*(1):90-93, February 1968.

26. Schnelle, K. B., F. G. Ziegler, and P. A. Krenkel. A Study of the Vertical Distribution of Carbon Monoxide and Temperature Above an Urban Intersection (APCA Paper No. 69-152). 1969. 65 p.

27. Clarke, J. F. Nocturnal Urban Boundary Layer Over Cincinnati, Ohio. Mon. Weather Rev. *97*(8):582-589, August, 1969.

28. Bornstein, R. D. Observations of the Urban Heat Island Effect in New York City. J. Appl. Meteorol. *7*(4):575-582, August 1968.

29. Leahey, D. M. A Model for Predicting the Variation of Pollution Within the Urban Heat Island (APCA Paper No. 69-107). 1969. 45 p.

30. Angell, J. K. *et al.* Tetroon Trajectories in an Urban Atmosphere. J. Appl. Meteorol. *5*(5):565-572, October 1966.

31. Hass, W. A. *et al.* Analysis of Low-level, Constant Volume (Tetroon) Flights Over New York City. Quart. J. Roy. Meteorol. Soc. *93*(398):483-493, October 1967.

32. Pooler, F., Jr. Airflow Over a City in Terrain of Moderate Relief. J. Appl. Meteorol. *2*(4):446-456, August 1963.

33. Hilst, G. R. and N. E. Bowne. A Study of the Diffusion of Aerosols Released from Aerial Line Sources Upwind of an Urban Complex. Travelers Research Center, Inc. Hartford, Conn. Final Report. Vol. I. Contract DA 42-007-AMC-37(R). 1966. 241 p.

34. Turner, J. S. The Motion of Buoyant Elements in Turbulent Surroundings. J. Fluid Mech. *16*:1-16, May 1963.

35. Lilly, D. K. Models of Cloud-topped Mixed Layers Under a Strong Inversion. Quart J. Roy. Meteorol. Soc. 94(401):292-309, July 1968.

36. Georgii, H. W., E. Busch, and E. Weber. Investigation of the Temporal and Spatial Distribution of the Emission Concentration of Carbon Monoxide in Frankfurt/Main. Frankfurt/Main University, Institute for Meteorology and Geophysics. Report Number 11; Translation Number 0477, NAPCA. 1967. 66 p.

37. McCormick, R. A. and C. Xintaras. Variation of Carbon Monoxide Concentrations as Related to Sampling Interval, Traffic, and Meteorological Factors. J. Appl. Meteorol. *1*(2):237-243, June 1962.

38. Rouse, H. Air Tunnel Studies of Diffusion in Urban Areas. Meteorol. Monogr. *1*(4):39-41, November 1951.

39. Highway Statistics for 1966. Bureau of Public Roads. Washington, D. C. 1968. 186 p.

40. Larsen, R. I. and H. W. Burke. Ambient Carbon Monoxide Exposures. Presented at 62d Annual Meeting of the Air Pollution Control Association. New York. (NAPCA) June 22-26, 1969. 38 p.

41. Martin, D. O. and J. A. Tikvart. A General Atmospheric Diffusion Model for Estimating the Effects on Air Quality of One or More Sources. Presented at 61st Annual Meeting of the Air Pollution Control Association, for NAPCA, St. Paul. June 1968. 18 p.

42. Frankel, M. L. Regional Air Pollution Analysis—Phase I. TRW Systems Group. Redondo Beach, Calif. Status Report. Sales Number 11 130 000, 1965. 467 p.

43. Holzworth, G. C. Mixing Depths, Wind Speeds and Air Pollution Potential for Selected Locations in the United States. J. Appl. Meteorol. *6*(6):1039-1044, December 1967.

44. Holzworth, G. C. Large-scale Weather Influence on Community Air Pollution Potential in the United States. J. Air Pollution Control Assoc. *19*:248-254. April 1969.

45. Huber, M. J., H. B. Boutwell, and D. K. Witheford. Comparative Analysis of Traffic Assignment Techniques with Actual Highway Use. Highway Research Board. Washington, D. C. National Cooperative Highway Research Program Report 58. 1968. 85 p.

46. Miller, M. E. Forecasting Afternoon Mixing Depths and Transport Wind Speeds. Mon. Weather Rev. *95*:35-44, January 1967.

47. Ludwig, F. L. Urban Air Temperatures and Their Relation to Extra-urban Meteorological Measurements. Presented at Meeting of the American Society of Heating, Refrigerating, and Ventilating Engineers for Stanford Research Institute. San Francisco. January 1970.

48. Ludwig, F. L. Urban Temperature Fields. In: Proceedings of WMO Symposium on Urban Climates and Building Climatology, Brussels, Belgium, October 15-25, 1968. To be published by World Meteorological Organization, Geneva, Switzerland. In press. 23 p.

49. Ludwig, F. L. and J. H. S. Kealoha. Urban Climatological Studies. Stanford Research Institute. Menlo Park, Calif. Final Report. Contract OCD-DAHC-20-67-C-0136. (Work Unit 1235A). March 1968. 191 p.

50. Gilman and Co. St. Louis Metropolitan Area Traffic Study. Prepared for City and County of St. Louis. New York. 1959. 154 p.

6. AN URBAN DISPERSION MODEL

ABSTRACT

A computerized, multiple-source, atmospheric dispersion model designed for operational use in air resource management has been formulated and programmed for the IBM 360-75 system. This "integrated puff" model provides a more realistic physical simulation of the processes of smoke plume dispersion than has hitherto been employed, since it provides for simulation of near-zero wind speed conditions, models three-dimensional wind vector variation and atmospheric diffusion, including upwind-downwind diffusion, and permits variation of stability and mixing layer depth with time.

This paper describes the development and preliminary validation testing of the model with data from a 3-year, computerized inventory of sulfur dioxide air quality data recorded by the receptors of the Chicago, Illinois, telemetered air monitoring system.

A detailed, 2-year inventory of Chicago coal and oil burning SO_2 *emission sources was acquired, data storage formats were designed, and computer algorithms were developed to generate hourly average estimates of emissions from major utility, industrial, residential, commercial, and institutional sources. Small emitters were aggregated into square-mile area sources.*

The model consists of a series of algorithms assembled around a kernel that represents the transport and diffusion of pollutant species from point and area sources according to a Gaussian distribution in three dimensions. This kernel, which represents a three-dimensional puff of smoke, is integrated according to a time-series of piecewise constant wind vectors and piecewise constant atmospheric stability parameters to simulate the transient behavior of a continuous smoke plume. Smoke plume rise and downwash phenomena are simulated.

The model is incorporated in a master air pollution data management system, which is employed to store, retrieve, process, analyze, and display emission, meteorology, and air quality data. This system is used to study micrometeorological dispersion, to form and input data arrays, and to validate its own theoretical predictions against recorded air quality data.

At present, the model is in the early stages of validation and has been tested against 1 month of hourly-average SO_2 *data from five Chicago air quality monitoring stations. A statistical sample of approximately 2300 data points is presently available. The ratio of standard deviation* to mean values for all hourly SO_2 predictions is 0.93. For 6-hour average predictions, this ratio is 0.64 and for 24-hour average predictions it drops to 0.43. Over 66% of the 24-hour average SO_2 predictions are within ±0.05 part per million (ppm) of observed values and approximately 90% are within ±0.1 ppm of actual dosages.

Hourly time series plots of observed and actual SO_2 concentrations indicate that the model is sufficiently accurate to test selective hypotheses about the model itself and to evaluate urban air resource management strategies.

AUTHORS

JOHN J. ROBERTS, the lead engineer for the development of computerized mathematical models of atmospheric diffusion processes for the Chicago Air Pollution Systems Analysis Program. CAPSAP is an interdisciplinary, environmental science research and development program supported by the Department of Health, Education and Welfare, the Atomic Energy Commission and the City of Chicago. It is directed towards the development of physical and economic mathematical models for use in air resource management planning and air pollution systems analysis. Dr. Roberts is a major participant in the Argonne study of the design and implementation of episodal and long-range emission control programs. He recently organized a program of research to develop numerical models of hydrothermal plumes from power plants and has also been associated with the Argonne-U.S. Navy magnetohydrodynamic research program.

Dr. Roberts received a B.E.E. from Rensselaer Polytechnic Institute in 1958 and then spent four years teaching in the U.S. Navy Nuclear Power program. He received a Ph.D. in nuclear engineering at the University of California, Berkeley, in 1966.

EDWARD J. CROKE is the director of the CAPSAP. Prior to joining Argonne National Laboratory in 1963, as a systems analyst for the NASA refractory metal nuclear rocket program, he was with the James Forrestal Research Center at Princeton, and was later propulsion systems project officer for the Agena Satellite program of the Air Force Systems Command.

He holds a B.S.E. in physics from the University of Illinois and an M.S.E. from Princeton in 1960. He has subsequently pursued postgraduate studies in geophysical sciences, operations research, systems analysis and management sciences at the University of Chicago and Northwestern University.

ALAN S. KENNEDY received an M.S. in mathematics at Washington University in 1962. He joined the Applied Mathematics Division of Argonne National Laboratory in 1963 and has continued his studies toward a Ph.D. in operations research at Northwestern University.

From his study of data management problems associated with an operational air pollution control department, he developed a system of storage, retrieval, and analysis of air quality, meteorological, and emission data for CAPSAP.

6. AN URBAN ATMOSPHERIC DISPERSION MODEL

JOHN J. ROBERTS, EDWARD S. CROKE
and ALLEN S. KENNEDY

Argonne National Laboratory

INTRODUCTION

A computerized, multiple-source, atmospheric dispersion model has been formulated and programmed for the IBM 360-75 system. This "integrated puff" model provides a more realistic physical simulation of the processes of smoke plume dispersion than has hitherto been employed, since it provides for simulation of near-zero wind speed conditions, models three-dimensional wind vector variation and atmospheric diffusion, including upwind-downwind diffusion, and permits variation of stability and mixing layer depth with time.

A source-oriented model is essential for the development of optimal incident control strategies and long range abatement plans. For example, a preliminary version of the integrated puff model was programmed and subsequently employed to develop a prototype optimal control model for an urban power plant network.[1] That prototype model will be used in combination with Chicago's emission inventory data as the primary analytical tool in the performance of a series of air pollution system-analysis studies including:

1. Cost-effectiveness analysis of alternative control strategies for specific source-aggregates such as power plants, the food processing industry, the steel industry, asphalt batching, etc.
2. Development of rapid-response, automated optimal incident control strategies for the urban power plant network, optimal gas allocation to dual fuel sources, process emission control, etc, based on operations research techniques.
3. Development of long-range air pollution abatement plans oriented around the computer simulation of the city, with projections of its population, fuel use, production and transportation network growth

---

*Work jointly sponsored by the National Air Pollution Control Administration, the Atomic Energy Commission, and the Chicago Department of Air Pollution Control.

patterns, so that emission control legislation, zoning ordinances, etc., can be tested on a simulation of Chicago urban area of the future, and cost-effectiveness studies can be performed to evaluate the economic impact of pollution abatement measures.

The model described in this paper has several aspects in common with earlier efforts[2, 3, 4] (e.g. Koogler, 1967; Turner, 1964; Clarke, 1964):

1. An emission inventory is developed; large emitters are considered as point-sources and smaller residential commercial and industrial emitters homogenized as area-sources on a standard grid.
2. A mathematical algorithm (typically based on the representation of turbulent diffusion by a Gaussian distribution) is used to describe the advection and diffusion of plumes from each of the sources or source areas.
3. Contributions from individual plumes are summed and sometimes integrated over time to give pollution doses at arbitrary locations.
4. The model is validated by statistical comparison with field measurements taken by an array of monitors.
5. While the results of the validation study may indicate a refinement of certain physical assumptions (such as the plume rise formulation) or inclusion of additional sources (such as distant power plants), no further improvement by linear regression or similar curve fitting techniques is permitted; that is, the model is not tuned to a particular receptor or city. This last point is particularly important if the model is to be used in the development of incident control strategies and long-range urban planning.

The essence of an air pollution dispersion model as a collection of algorithms, a set of assumptions and subsequent calculations for every stage of the analysis, from the compilation of the emission inventory to the validation of the results, is discussed briefly in the following sections.

DEVELOPMENT OF AN EMISSION INVENTORY

A major task element of the Chicago Air Pollution Systems Analysis program was the development of an inventory of hourly average emissions for the power plants and industrial, residential, commercial, and institutional SO_2 sources that are the primary contributors to Chicago's sulfur oxide air pollution problem.

Figure 6-1 shows the location and distribution of the largest individual coal and oil burning sources of sulfur oxides, while Figure 6-2 shows the source density of residential emitters. They were too numerous to inventory individually. Figure 6-3 depicts, by source category, the distribution and magnitude of Chicago's SO_2 emitters.

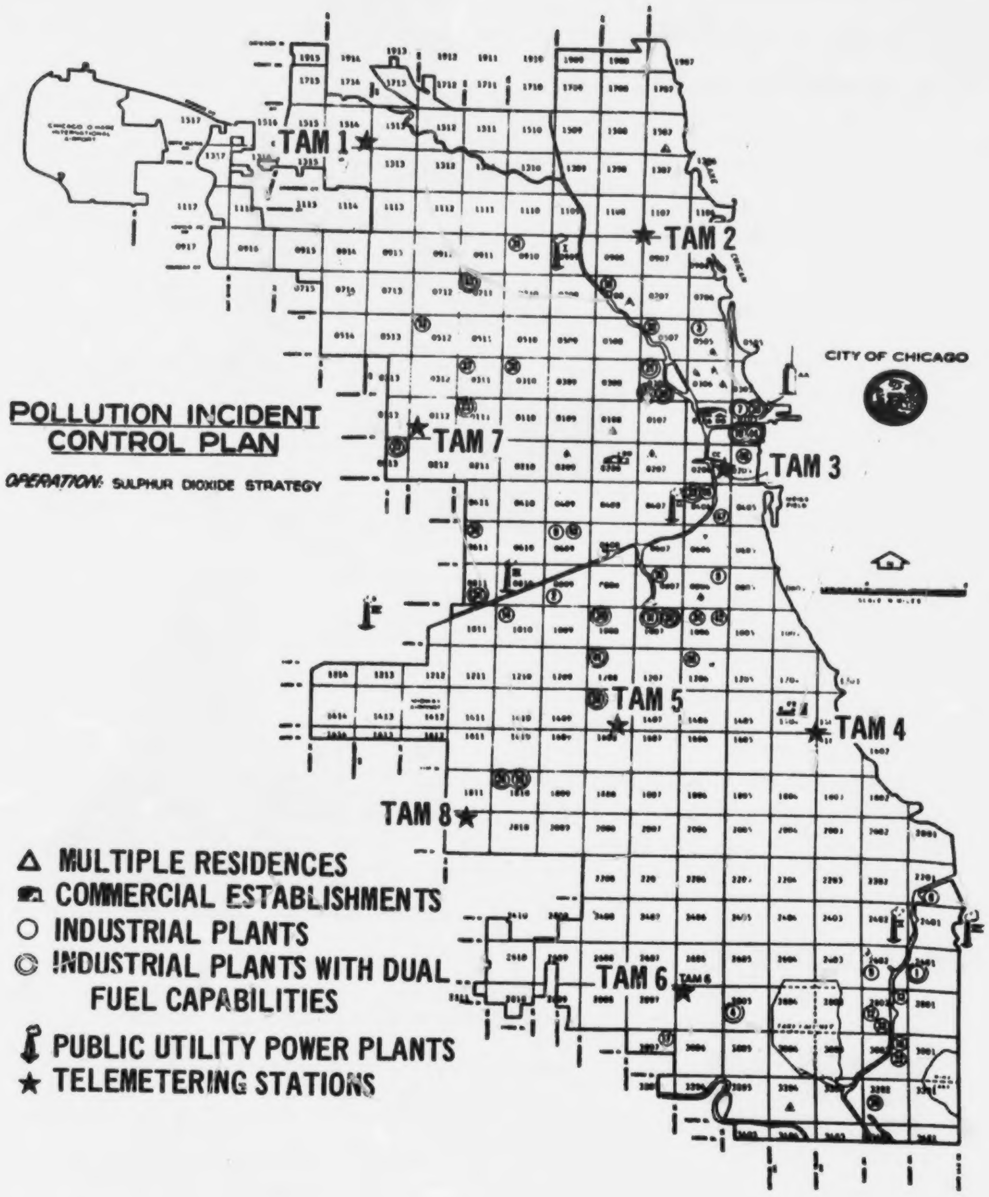
POLLUTION INCIDENT CONTROL PLAN
OPERATION: SULPHUR DIOXIDE STRATEGY
CITY OF CHICAGO
TAM 1
TAM 2
TAM 3
TAM 4
TAM 5
TAM 6
TAM 7
TAM 8
△ MULTIPLE RESIDENCES
COMMERCIAL ESTABLISHMENTS
○ INDUSTRIAL PLANTS
© INDUSTRIAL PLANTS WITH DUAL FUEL CAPABILITIES
PUBLIC UTILITY POWER PLANTS
★ TELEMETERING STATIONS

Figure 6-1. Map of major Chicago sources and TAM stations.

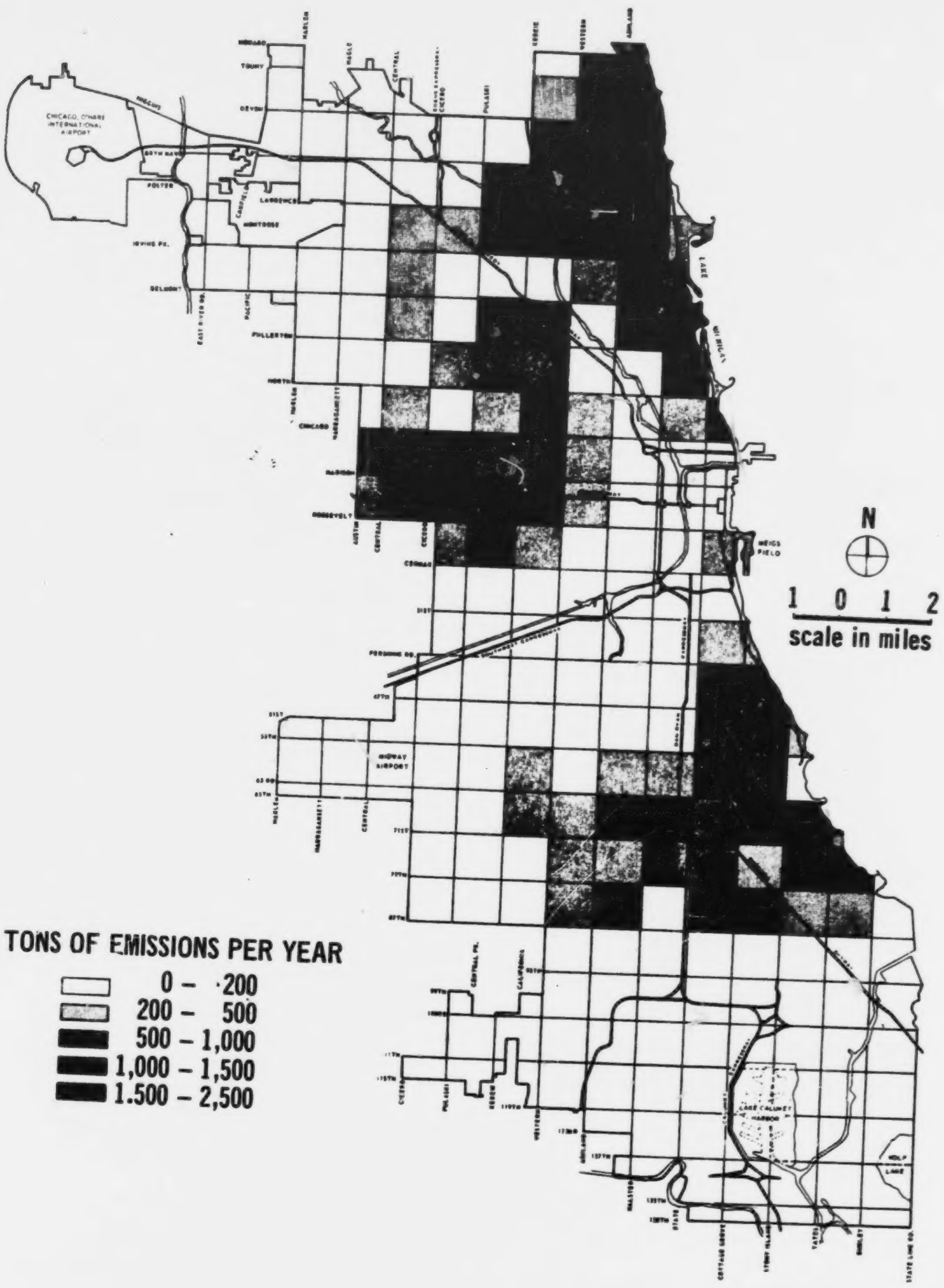
TONS OF EMISSIONS PER YEAR
0 - 200
200 - 500
500 - 1,000
1,000 - 1,500
1.500 - 2,500
N
1 0 1 2
scale in miles
CHICAGO O'HARE INTERNATIONAL AIRPORT
MIDWAY AIRPORT
MEIGS FIELD
LAKE MICHIGAN
LAKE CALUMET HARBOR
WOLF LAKE

Figure 6-2. Sulfur dioxide from residential space heating, 1968.

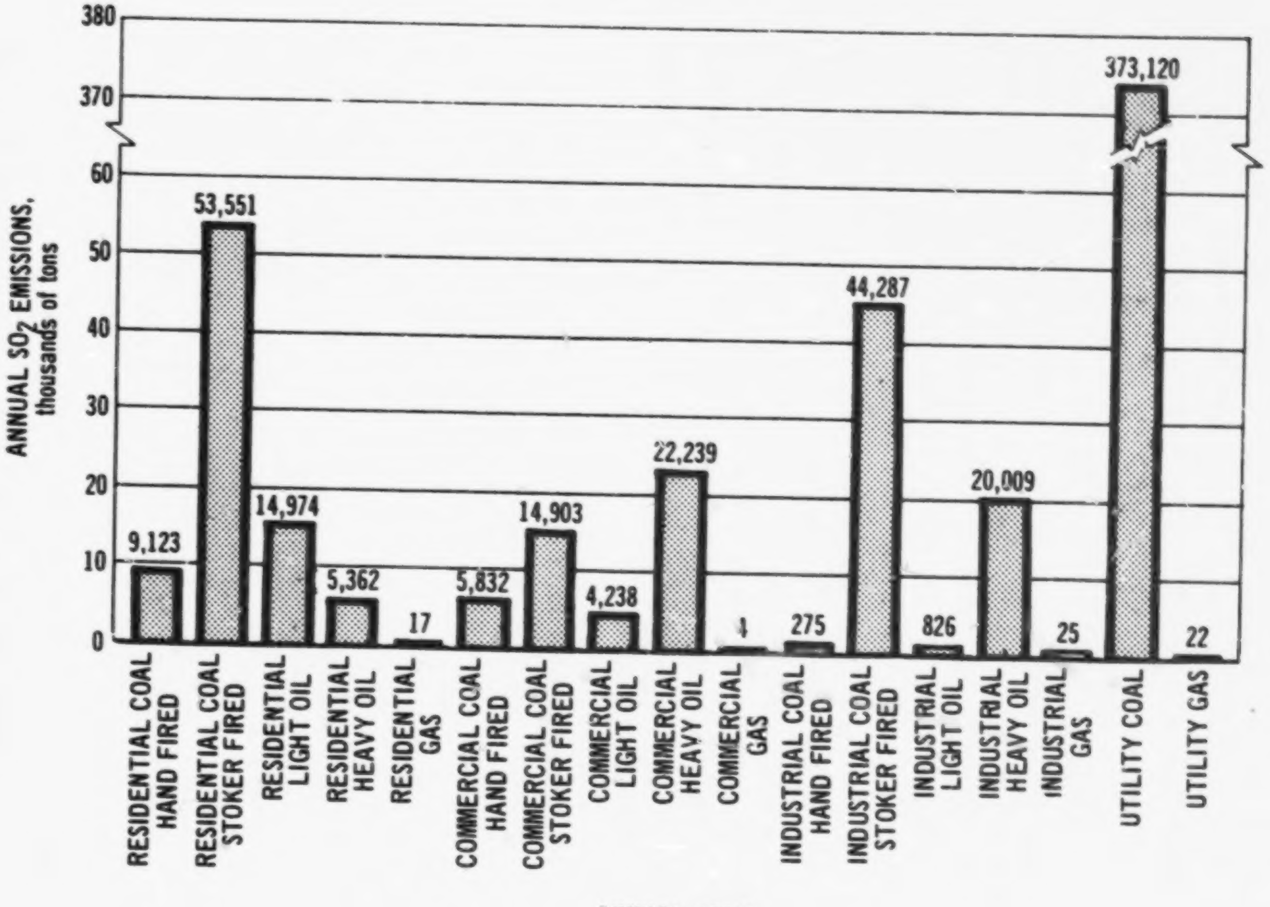

Figure 6-3. Distribution of sulfur dioxide sources.

The Chicago Air Quality Monitoring System

Chicago operates a network of eight telemetered air monitoring (TAM) stations that continuously and automatically record 5-minute, average SO_2 concentrations at 15-minute intervals throughout the day. The data recorded by these stations during 1966 and 1967 are typical of a city that is characterized by a highly unhomogeneous SO_2 source distribution and density. Table 6-1 provides a summary of the air quality situation of Chicago as recorded by the network of TAM stations.

Since the source density, type, and distribution in the immediate vicinity of a receptor may, under certain meteorological conditions, dominate the ambient air quality recorded, it is of value to examine the record of the eight TAM stations from the standpoint of their proximity to Chicago's SO_2 sources. This exercise is particularly useful, since it provides an indication of what types of sources are likely to have the predominant effect on the recorded air quality, and therefore serves as an indicator of the level of effort that should be expended to develop a detailed emission inventory. Moreover, an understanding of the distribution of sources relative to each of the monitoring stations that provide the data required to validate the Chicago atmospheric diffusion model explains certain of the results predicted by the model. Table 6-1 shows the distribution of 1-hour SO_2 dosages recorded at the eight TAM stations.

Table 6-1. TOTAL NUMBER OF RECORDED 1-HOUR SO_2 DOSAGES (1966-67)

TAM station	Total dosage, ppm			
	0.2	0.3	0.4	0.5
1	182	59	18	5
2	618	203	70	30
3	3210	1838	975	483
4	1990	966	491	268
5	525	207	84	45
6	364	169	94	65
7	934	332	122	35
8	206	51	15	6

TAM Station 1

TAM station 1 is located near the northwestern limits of Chicago in an area characterized by residential neighborhoods of relatively recent construction, and a limited amount of light industrial development. Heating plants in this sector of the city are predominantly natural-gas fired and relatively little coal or oil is consumed by industrial or commercial sources. TAM 1 is thus sited in a relatively clean section of the city, insofar as sulfur oxide emissions are concerned. This conclusion is borne out by the fact that recorded high ambient SO_2 concentrations at TAM 1 are at least one order of magnitude less frequent than at monitoring stations located nearer to the urban core area.

TAM Station 2

Station 2, located in the northeast sector of the city approximately 1.5 miles from the lakeshore, is in a mixed industrial-residential area that contains a large concentration of high-rise gas-fired residential structures. The prevailing southwesterly wind flow tends to transport SO_2 from the central utility-industrial cluster into this area, but average dosages tend to be relatively low because of the comparatively large transport distances involved. This is evidenced by the relatively high ratio of low to high concentrations recorded at TAM 2 compared to TAM 3 or TAM 4 where localized coal and oil burning sources are more significant. The nearest major SO_2 source to TAM 2 is a moderate sized coal fired power plant located approximately 1.5 miles southwest.

TAM Station 3

This receptor is centrally located atop a large office building in the Chicago loop business district. It is not only surrounded by a cluster of large commercial and institutional space-heating sources, but it is also situated directly northeast of a major concentration of industrial plants and a line formed by the three largest power plants within the city limits. Since the prevailing wind flow is southwesterly, a high incident frequency due to this industrial-utility concentration and to local space heating effects is to be expected at TAM 3. As indicated in Table 6-1 this station is, in fact, located in the most polluted sector of the city.

TAM Station 4

TAM 4 is located in the south-central Hyde Park area of Chicago within 1 mile of Lake Michigan. The immediate area is characterized by a row of highrise apartments sited along the lakefront, a large concentration of old coal- or oil-fired low-rise, six-flat apartment buildings and a single major source – the University of Chicago steam plant. TAM 4 is approximately 5 miles southeast of Chicago's central industrial-utility complex. As indicated in Table 6-1, the frequency of high, recorded SO_2 concentrations at TAM 4 is second only to that of TAM 3. Statistical analysis of TAM 4 air quality data has indicated that the air quality in this area is very strongly correlated with ambient temperature – a finding that indicates the Hyde Park area is largely self-polluted by local, residential space-heating sources.

TAM Station 5

TAM 5 is situated approximately 6 miles inland in the south central sector of the city. It is approximately 3 miles south of the central industrial-utility complex, atop a school building in a neighborhood of low-rise apartments and single family dwellings. Residential buildings in the TAM 5 area are somewhat newer than in TAM 4, and gas tends to predominate over coal and oil for space-heating purposes. TAM 5 is nearer to the central industrial-utility cluster than any of the other monitoring stations; however, only a few large sources are located southwest of the site. This fact, combined with the relatively low level of residential emissions in its immediate vicinity, results in comparatively modest number of high SO_2 concentrations recorded there.

TAM Station 6

Station 6, in the extreme southeast of the city, is sited in a residential area located approximately 5 miles west of a second large concentration of Chicago industrial and power plants. Immediately adjacent to the Chicago source-cluster is the Gary-Hammond industrial complex. Since the receptor is also located within one mile of the southwest city limits of Chicago, it is exposed to emissions from two areas for which an emission inventory is not, at present, available. According to the data presented in Table 6-1, TAM 6 is located in one of the less polluted areas of the city. This conclusion is consistent with the fact that the metropolitan region southwest of the city is relatively free of large SO_2 sources, and that east winds, which would bring in SO_2 from the south Chicago-Gary-Hammond area, are comparatively infrequent in the midwest Great Lakes region.

TAM Station 7

TAM 7 is sited atop a school building within 0.5 mile of the western city limits and almost 7 miles directly west of the central business district. The immediate neighborhood is predominantly residential, although a few large industrial plants are located within 2 miles of the receptor in the northeast and southwest directions. The station is approximately 6 miles northwest of the central industrial-utility cluster.

A detailed emission inventory for the regions immediately west and south of this receptor is not yet available, since these areas lie outside the Chicago city limits. It is known, however, that the area west of TAM 7 is a mixed residential, light-industrial sector in which gas heating predominates, while the highly industrialized city of Cicero, Illinois, lies immediately south of TAM 7, within 2 miles of the receptor.

Although the relative scarcity of southeasterly winds minimizes the influence of the central Chicago source-cluster on TAM 7, the area experiences significant SO_2 concentrations with moderately high frequency, making it the third or fourth most frequently polluted site.

TAM Station 8

Like the TAM 6 receptor, TAM 8 is located in a residential neighborhood near one of the southwestern extremities of Chicago's irregular western border. Two relatively large industrial plants lie within 1 mile northeast of the site; however, the area itself is relatively free of significant SO_2 sources. Since the western city limits are within 0.5 mile and the southern city limits are within 1 mile, emission data for virtually the entire southwestern quadrant, relative to TAM 8, are not available.

As indicated in Table 6-1 the TAM 8 receptor is sited in one of the least polluted areas of the city.

Power Plants

Electric power for the Northern Illinois region is provided by a network of 15 power generating stations, of which six are located in the Chicago metropolitan area. These six coal-fired plants, shown in Figure 6-1 account for approximately 65% of the sulfur oxides released into the Chicago atmosphere. Table 6-2 indicates the relative contribution of each plant in terms of its annual fuel consumption.

Table 6-2. RELATIVE CONTRIBUTION[a] OF NORTHERN ILLINOIS POWER PLANTS TO CHICAGO SO_2 CONCENTRATION

Plant designation	SO_2	
	Amount, tons yr^{-1}	% of Chicago total
Crawford	107,954	18,97
Ridgeland	100,540	17.67
Fisk	73,438	12.90
State Line	70,606	12.42
Northwest	10,566	1.86
Calumet	10,016	1,76
Total	373,120	65.58

[a] In terms of annual fuel consumption

Of these installations, four: the Fisk, Crawford, Ridgeland, and State Line plants are capable of partial or total conversion from coal to natural gas during periods when the latter fuel is available at "dump" or "interruptible" rates.

Because of the extremely large emission rates associated with the urban power plants and because of their complex, but relatively consistent diurnal emission cycle, the acquisition of the most accurate body of emission data available constituted a high-priority task in the emission inventory. Fortunately, the Chicago utility maintains excellent records of plant operation. These were provided for the period January 1966 through December 1967. The data array required was:

1. Hourly power generation, in megawatts (Mw), for each generator unit of each power plant, including an indication of whether the power was generated with coal or gas.
2. Monthly coal and natural gas consumption rates for each boiler-generator combination.
3. Monthly average coal-sulfur-content analyses for each plant.
4. A set of boiler-turbine-generator efficiency curves for each generator unit. These presented efficiency vs. power output for each unit.
5. A set of stack temperature vs. output curves for each plant.
6. A physical description of each plant layout, including the relationship between boilers, turbines, generators, and stacks, stack heights, etc.

The above information was combined in a computer algorithm for calculation of the hourly fuel consumption and SO_2 emission rates for each stack of each plant of the system. Details of the computational procedure are provided in the program progress reports.[5]

The resultant body of power plant emission data was stored in the master data file of the Air Pollution Information and Computation System (APICS) from which it could be retrieved and automatically input to the dispersion model. The details of the APICS system are described by Kennedy and Anderson,[6] and in the program progress reports.[5, 7]

Industrial Sources

There are over 2500 relatively large coal and oil burning industrial plants in the City of Chicago, which are responsible for approximately 10 percent of the average annual sulfur oxides emitted within the city limits. The 100 largest plants account for over 83 percent of the total industrial emissions, and the largest 50, for over 64 percent.

The inventory of industrial emissions was derived from four sources:

1. *Department of Air Pollution Control Survey.* A Comprehensive annual average inventory compiled in 1963 by the Chicago Department of Air Pollution Control was computer processed to establish industrial SO_2 emissions on a square-mile basis. Within any given square-mile sector, industrial emissions were assumed to be uniformly distributed.
2. *Argonne National Laboratory Field Survey.* Detailed fuel consumption and physical and operating cycle data for the 50 largest SO_2 sources

were obtained through a field survey system designed by Argonne and implemented by Laboratory and city engineers. This involved a program of site visitations and personal or telephone interviews with plant personnel.

3. *Natural Gas Utility Records.* The 1966-67 natural gas consumption and fuel costs records for all dual fuel plants among the 50 largest SO_2 sources were obtained from the local, natural gas supply utility.
4. *Fuel Supply Records.* The Midwest Coal Producer's Institute, an organization of wholesale coal suppliers, provided records of the average annual coal consumption by major industrial sources during 1966-67.

Industrial sources that were not sufficiently large to be included among the largest 50 emitters were aggregated into uniformly distributed square-mile area-sources. All plants in this category were assumed to have a stack-height of 150 feet.

Industrial Source Simulation Programs

The 50 largest sources of SO_2 were treated as individual point sources. A detailed analysis of the diurnal, weekly, and seasonal operating pattern of each of these plants, in combination with fuel consumption records, gas-use patterns, and such characteristics as process-vs. space-heating fuel-use practices was incorporated into an industrial-plant-emission-simulation computer algorithm (PLANTSIM) to generate an operating-shift-oriented emission estimate for each plant.

The data file for large industrial sources is designed to include enough information about each plant to characterize its "expected" emission pattern by operating-shift for each day throughout the year. For this purpose "shifts" are defined as follows:

Shift 1:	12 midnight to 8 am	(0000) to (0800)
Shift 2:	8 am to 4 pm	(0800) to (1600)
Shift 3:	4 pm to 12 midnight	(1600) to (2400)

Up to three daily emission patterns may be assigned to each plant. These are as follows:

1. W — weekday or normal operation.
2. S — Saturday.
3. H — Sunday or special holidays.

Finally, a monthly weighting is provided to allow for variation due to seasonal patterns, etc. Each plant requires two computer cards; (1) a source identification card, and (2) a source emission card. An example of each is shown in Figures 6-4 and 6-5 respectively. A description of each item on the cards is provided in Table 6-3 and Table 6-4.

SOURCE NO.	NAME (125 CHARACTERS MAX INCL. BLANKS)	TYPE	GRID	COORDINATES		STACK DATA								WORK SCHEDULE						
						1		2		3		4								
				x	y	HGT.	%	HGT.	%	HGT	%	HGT.	%	M	T	W	T	F	S	S
1 3	5 29	31 34	36 39	41 45	46 50	52 54	55 56	57 59	60 61	62 64	65 66	67 69	70 71	73	74	75	76	77	78	79
2	CAMPBELL SOUP 2550 WEST 35 STREET	2032	0000	8.2	-3.5	175	25	175	25	250	50			W	W	W	W	W	S	H

Figure 6-4. Sample of source identification card.

SOURCE NO.	MAXIMUM SPACE HTG. LOAD (THERM/hr)	MAXIMUM PROCESS LOAD (THERM/hr)	MONTHLY FUEL USE WEIGHTING (% OF MAXIMUM PROCESS)												SHIFT FUEL WEIGHTING (% OF MONTHLY PROCESS)									% SULPHUR COAL	AVG. % COAL	% SULPHUR OIL	AVG. % OIL	% GAS SP. HTG	% GAS PROCESS	AVG. TEMP. GAS (°F)	GAS PRICE (¢/THERM)
															W			S			H										
			J	F	M	A	M	J	J	A	S	O	N	D	1	2	3	1	2	3	1	2	3								
1 3	5 9	11 15	17	18	19	20	21	22	23	24	25	26	27	28	30 31	32 33	34 35	36 37	38 39	40 41	42 43	44 45	46 47	49 51	53 55	57 59	61 63	65 67	68 70	72 73	75 79
2	500	5000	6	6	6	5	5	4	2	4	6	7	6	6	70	99	99	70	20	20	30	30	30	2.8	100			100	100	40	0.042

Figure 6-5. Sample of source emission card.

Table 6-3. SOURCE I.D. CARD

No.	Item	Description
1	Source no.	Plant sequence number
2	Name	Plant name (not to exceed 25 characters including blanks), address included if sufficient space available
3	Type	Standard industrial code
4	Grid	City of Chicago square-mile number
5	Coordinates	x- and y-coordinates relative to standard City of Chicago-coordinate-system
6	Stack data	Four stacks maximum (1, 2, 3, 4) HGT – Stack height, (feet) % – The percent of total emission emitted from each stack
7	Work schedule	Each day of week assigned one of the following: W – Weekday S – Saturday H – Sunday or holiday

Table 6-4. SOURCE EMISSION CARD

No.	Item	Description
1	Source no.	Plant sequence number
2	Max space htg load	Maxium hourly thermal requirements for space-heating
3	Max process load	Maximum hourly requirements for process
4	Monthly fuel use weighting	Achieves monthly variation in process fuel use. Each month assigned weight (0, 1,...,9) ≡ average percent (0%, 10%, ...,90%) of maximum process fuel used during month
5	Shift-fuel-use weighting	Within each day pattern (W, S, H), weight (0%, ...99%) assigned to each shift, ≡ average percent of current monthly process fuel used during shift
6	% Sulfur-coal	Average percent of sulfur in coal
7	Avg % coal	Average percent of thermal load due to coal (0 implies coal not used)
8	% Sulfur oil	Average percent sulfur in oil
9	Avg % oil	Average percent of thermal load due to oil (0 implies oil not used)
10	% Gas SP HTG	Percent of space heating thermal requirements that can be supplied by gas
11	% Gas process	Percent of process thermal requirements that can be supplied by gas
12	Avg gas temp	Average ambient temperature (°F) at which dual fuel plant receives gas on "interruptible" supply contract
13	Gas price	Gas rate (cents per therm) for dual fuel plants

The PLANTSIM code is completely general. Large, individual space-heating sources or major institutional sources such as coal-fired water-pumping stations can be treated in exactly the same manner as industrial plants. In the case of heating plants, the process-load portion of the operating cycle input is zeroed and emissions are calculated solely on the basis of temperature. A special-purpose plant such as a pumping station may be treated as an industrial plant that consumes fuel according to a characteristic processing cycle. Individual power plants that have a repeatable diurnal operating cycle may also be simulated by PLANTSIM; however, power plants that are a part of a regional power grid may not have a consistent and repeatable emission pattern, since such plants are likely to engage in power-load transfer among plants — on at least a seasonal, if not a weekly or diurnal basis.

All sources treated in PLANTSIM are assigned individual physical stack heights based on the field survey data.

PLANTSIM Computations

When the temperature, T, is between -10°F and 55°F, a linear relationship for the space-heating thermal load L^S is assumed. This is expressed as follows:

$$L^S = L^S_{MAX} \frac{[55 - T]}{65} \qquad (-10 \leqslant T \leqslant 55) \tag{1}$$

Then the total thermal load is

$$L = L^S + L^P , \tag{2}$$

where L^P, the process load, is determined from the appropriate month, day, and shift factors. The amount of load due to coal, L^C, and due to oil, L^0, is then determined, and the SO_2 emission due to each source is calculated as follows:

1. $$C(\text{tons/hour}) = \frac{L^C(TH^{*}\,hr^{-1}) \times 10^5\,(Btu\ \ TH^{-1})}{12000\,(Btu\ lb^{-1}) \times 2000\,(lb.ton^{-1})}$$

$$SO_2^C\ (TH\ hr^{-1}) = C(tons\ hr^{-1}) \times 3.68 \times S^C(\%)$$

2. $$0(kgal/hr) = \frac{L^0(TH) \times 10^5\ (Btu\ TH^{-1})}{18000\,(Btu\ lb^{-1}) \times 8000\,(lb\ \ kgal^{-1})}$$

$$SO_2^0\ (TH\ hr^{-1}) = 0(kgal\ hr^{-1}) \times 157.0 \times S^0(\%)$$

Thus, the total SO_2 emission is

$$SO_2 = SO_2^C + SO_2^0 \tag{3}$$

---

*Therms

When the ambient temperature is such that a dual fuel interruptible plant is likely to be receiving natural gas, the amount of SO_2 produced is correspondingly reduced.

In order to facilitate data storage according to a uniform and consistent format, each plant is assumed to have four stacks. For plants having less than four stacks, zeros are filled-in for non-existent stacks. The following parameters are associated with each stack:

1. SO_2 emission in pounds per hour
2. Heat emission in therms per hour.

These parameters are determined by weighting the total SO_2 and heat emissions for the plant by the percentage emitted from each stack. The heat emission, H, is assumed to be 15 percent of the thermal input.

Example

Consider the example of the Campbell Soup Company shown in Figures 6-4 and 6-5 and assume that emission data are required for the following set of conditions:

January
temperature 30°F
weekday pattern
first shift

Then,

$$L^S = 500\left(\frac{55 - 30}{65}\right) = 200 \text{ TH hr}^{-1}$$

$$L^P = (.70)(.60)5000 = 2100 \text{ TH hr}^{-1}$$

$$L = 2300 \text{ TH hr}^{-1}$$

$$L^C = 2300 \text{ TH hr}^{-1}$$

$$L^O = 0$$

$$C = \frac{2300 \times 10^5}{12000 \times 2000} \cong 10 \text{ tons hr}^{-1}$$

$$SO_2 = 10 \times 36.8 \times 2.8 = 1000 \text{ lb hr}^{-1}$$

$$H = (.15)2300 = 345 \text{ TH hr}^{-1}$$

For Stack 1

$$SO_2^{(1)} = (.25)1000 = 250 \text{ lb hr}^{-1}$$

$$H^{(1)} = (.25)345 = 85 \text{ TH hr}^{-1}$$

For Stack 2

$$SO_2^{(2)} = (.25)1000 = 250 \text{ lb hr}^{-1}$$

$$H^{(2)} = (.25)345 = 85 \text{ TH hr}^{-1}$$

For Stack 3

$$SO_2^{(3)} = (.50)1000 = 500 \text{ lb hr}^{-1}$$

$$H^{(3)} = (.25)345 = 170 \text{ TH hr}^{-1}$$

For Stack 4

$$SO_2^{(4)} = 0$$

$$H^{(4)} = 0$$

Residential Space-Heating Sources

Residential space-heating sources account for approximately 15 percent of the annual total emissions for the city. The inventory of coal- and oil-fired residential space-heating sources was derived primarily from data supplied by the market research organization of the local natural gas supply utility. This information was in the form of a city-wide, field-sampling survey of space-heating sources categorized by fuel use and by the number of dwelling units per building surveyed. For the purposes of the emission inventory, the survey data was aggregated into two groups – moderate sized residential structures of 19 dwelling units or less and large apartment complexes of 20 or more dwelling units.

Since residential sources are generally too numerous to treat individually, the two building size categories described above were treated as uniformly distributed square-mile area sources. The source density per square mile for each category was assigned on the basis of the natural gas utility market research data.

The operating cycle of the moderate sized heating plants was based on a 55°F degree-day proration of a seasonal average fuel consumption modified by an empirical function[5] that represents the daily cycle of automatic stoking during waking periods followed by a hold-fire and cool-down during sleeping periods. This cycle was simulated by a "Janitor Function" that maintains heating sources on an automatic stoking cycle between 6 AM and 11 PM on days having a minimum night ambient temperature in excess of 5°F. For nights with a minimum temperature below 5°F, the automatic stoking period was assumed to begin at 3 AM. This pattern was derived through an interview survey of building superintendents and heating plant operators. A hot water heating baseload equal to 10 percent of the daily heating fuel use was assumed for all residential buildings in this category. Hourly-average emissions were assumed to be distributed uniformly throughout the automatic stoking period and were assumed to be constant during the hold-fire period. All moderate-size residences were assigned a uniform physical stack height of 50 ft.

Large residential buildings were considered to operate on an automatic stoking cycle at all times. Fuel use and SO_2 emissions were based on a 55°F degree-day proration and a hot water heating baseload equal to 10 percent of the daily heating-fuel use was assumed. All buildings in this size category were assumed to have a 200 ft physical stack height – an assumption based on a sensitivity analysis of the effect of stack height on the ground level air quality, and on surveys of actual building sizes.

The hourly-average emissions for large size residential buildings were assumed to be distributed uniformly throughout the stoking period.

Commercial and Institutional Sources

Commercial and institutional sources account for about 8 percent of the total emissions in Chicago. Fuel use and SO_2 emission data for large commercial and institutional sources such as office buildings, water-pumping stations, educational institutions, etc., were derived from a computer analysis of a comprehensive inventory developed in 1963 by the Chicago Department of Air Pollution Control, combined with the results of a field survey of major sources conducted in 1968 by Argonne National Laboratory and the Department of Air Pollution Control.

With a few notable exceptions, the commercial and institutional sources are too small and numerous to treat individually. They are therefore aggregated as area sources, uniformly distributed throughout each square mile of the city. The square-mile source-density is based on the 1963 inventory.

Virtually all sources in this category burn fuel primarily for space and hot water heating and operate on an automatic stoking cycle. Emissions from these sources were therefore calculated in exactly the same way as in the case of the large residential sources.

Certain commercial and institutional plants are sufficiently large to warrant inclusion as individual point sources. Among these are the five Chicago pumping stations and a number of space-heating plants that are associated with extremely large buildings. An operational analysis of the pumping stations was conducted in order to define their diurnal emission cycle. They were then treated in essentially the same manner as the large industrial plants. Individual large commercial heating plants were treated in a manner similar to the large residential structures. The validity of the latter assumption was established through a detailed survey of the operating cycles of most of these sources, which included, among others, the large University of Chicago heating plant, the Union Station, the Chicago Merchandise Mart, and the Chicago Housing Authority complexes.

METEOROLOGICAL AND AIR-QUALITY DATA

Chicago's TAM Networks

In January 1966, the Chicago Department of Air Pollution Control (DAPC) began recording wind speed and direction and sulfur dioxide levels at eight telemetered air monitoring (TAM) stations (starred locations on the map, Figure 6-1). These continuous measurements are integrated over 5-minute periods; 15-minute averages are then telemetered to the DAPC office where they are recorded. Tape records of these 15-minute observations have been reduced to hourly averages. Thus, although the accuracy of data from some of the aerovane sites is limited by 15- to 30-foot masts and/or close proximity to taller buildings or smoke stacks, the procedure for developing hourly averages is excellent. This is in contrast to special airport data where the aerovane sites are excellent, but only brief hourly observations are recorded.

In the dispersion model, the wind speed and wind direction from the TAM aerovane nearest to the dose-point is used to determine the trajectory of all plumes sensed at that point. This temporary assumption will eventually be eliminated by using all eight stations to develop a wind field for the city. In contrast to single city-wide values of wind speed and direction from the nearest airport, the data from a local aerovane is sensitive to special circulation patterns such as lake breezes.

Airport Data

Tapes containing hourly standard weather data from Midway Airport and Glenview Airport (15 mi north of Chicago) have been obtained from the National Climatic Center.

Argonne Meteorological Data

The observing station at Argonne National Laboratory (25 mi southwest of Chicago) was specifically designed to measure parameters controlling diffusion: atmospheric stability, wind speed and direction at five levels up to 150 ft., net and solar radiation, etc. The hourly averages stored there on magnetic tape, are the only stability records available in the Chicago area. Unfortunately, the data are for a shallow layer taken in an open, grass covered field. Transformations relating these data to the urban environment are currently underway.

Upper-Air Data

Radiosonde observations from the U.S. Weather Bureau RAWIN station at Peoria, Illinois (140 mi southwest of Chicago) and Green Bay, Wisconsin (180 mi north of Chicago) have been obtained from the National Climatic Center. These data have been extrapolated to estimate the height of the mixing layer in Chacago (see below).

Atmospheric Stability

Turbulent diffusion of pollutant species is represented in the model by a Gaussian puff kernel with dispersion coefficients $\sigma_{x_i}(T)$, $\sigma_{y_i}(T)$, $\sigma_{z_i}(T)$; where T is the travel time and i, the atmospheric stability index. The classification system proposed by Turner[3] has been employed using weather data from Midway Airport.

Height of Mixing Layer

The mixing layer defines a zone within which pollutants can be diluted. The height of this layer is probably the most critical parameter in determining ground level SO_2 concentrations resulting from emissions from tall stacks. With a high lid ($>$ 2000 ft) plumes from power plants tend to travel far and disperse widely before touching ground. With a sharp temperature inversion beneath the physical stack-height, plumes will travel in stable air, which greatly inhibits vertical diffusion, and touch ground far from the local urban area. High ground-level concentrations occur in the intermediate range of mixing-layer heights where the plumes are trapped beneath the lid and disperse rapidly to the ground in unstable air. Figures 6-6 and 6-7 show vertical profiles of temperature and sulfur dioxide measured by an instrumented helicopter at a point 4 miles downwind of a major industrial area in Chicago. The sharp inversion at 2300 ft (700 m) has clearly defined a vertical mixing zone within which SO_2 levels are nearly uniform.

Except for the low level rural temperature profiles measured at Argonne, no vertical soundings are available for the Chicago area during the period from January 1966, when the TAM network became operational, to January 1969. This is the period during which meteorological air quality and emission data have been accumulated at Argonne. It was therefore necessary to design a scheme for estimating the height of the mixing layer from historical weather data. (In July, 1969 the Weather Bureau in the Chicago Air Quality Control Region began a program of daily balloon soundings at 0600 and 1200 from Midway Airport. This data will be available for future validation studies of the dispersion model and will also be used to validate the objective mixing-layer height estimate described in this section.)

The computerized objective mixing-layer depth estimates are based on an interpolation scheme between two rawinsonde stations, Green Bay, Wisconsin, and Peoria, Illinois. The soundings are usually taken at 0600 and 1800

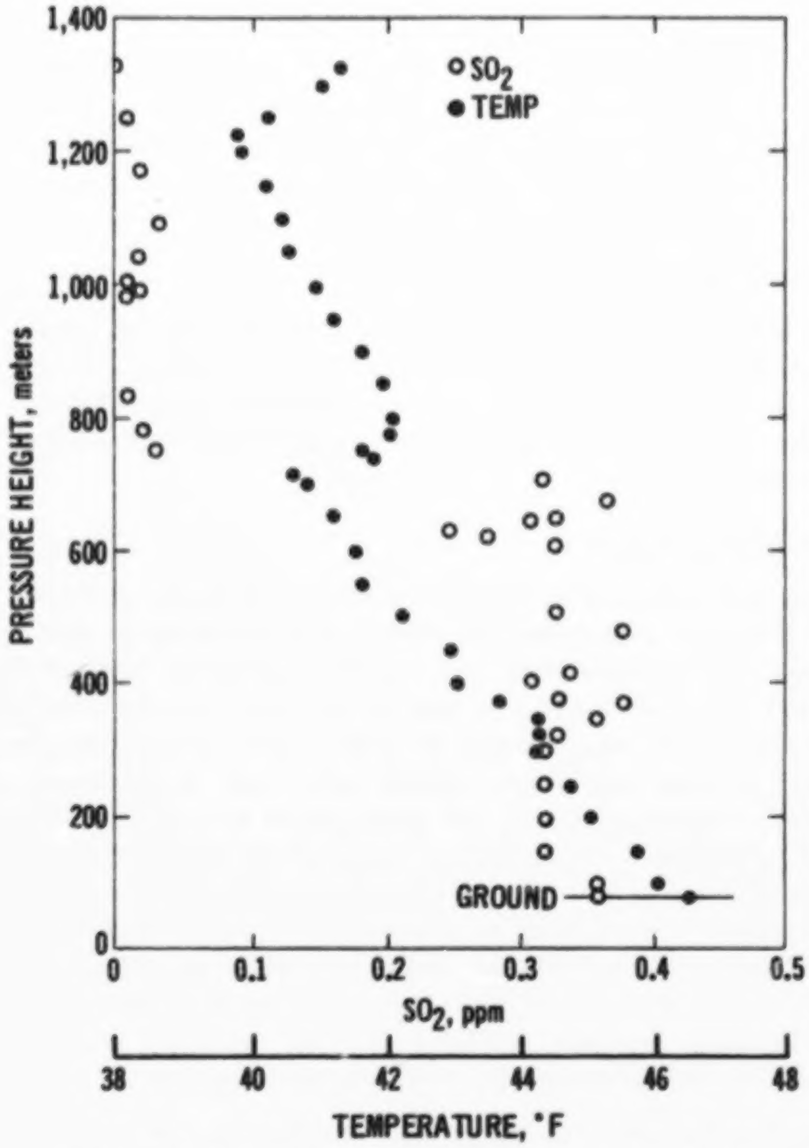

Figures 6-6 and 6-7 (superimposed) Vertical profile of SO_2 concentrations and temperature in Hinsdale, Illinois, April 11, 1969 at 10:20 am. (D. Nelson, Argonne National Laboratory).

Central Standard Time (CST). The mandatory and significant levels for each station are merged to form a single pressure-temperature array for each sounding. The Chicago rural (Argonne) temperature profile is formed either by "shifting" one of the two to the Argonne surface temperature or by interpolation between the Peoria and Green Bay soundings. If only one station is in the same air mass as Chicago, the sounding from that station is transposed, without changing its shape, to the Argonne surface temperature at sounding time. If both Peoria and Green Bay are in the same air mass as Chicago (as determined by inspection of the daily weather map), then a linear interpolation is performed. This procedure forms a pressure-temperature array for the 0600 and 1800 rural profiles.

The next step is to compute the hourly rural profiles using temporal weighting. The profile for any hour is a linear interpolation in time between the bracketing 0600 and 1800 rural soundings.

The hourly urban mixing depth and mixing depth indices are now computed. The height of the mixing layer is defined by the intersection of a dry adiabat from the *urban* surface temperature with the constructed Argonne *rural* temperature profile. In the Chicago case mixing-layer heights calculated by this objective procedure are compared with more subjective estimates provided by a local meteorological consulting firm. While actual magnitudes differed, there was a good agreement in terms of diurnal trends. Calculated values agreed very closely with data from two helicopter soundings but, in both cases, the inversions were above 2000 ft and therefore not in the critical range where plume trapping could occur.

TRANSPORT OF AIRBORNE POLLUTANTS

Pollution concentrations from a given source are evaluated in this model by forming a convolution sum of two time-series: (1) piecewise (hourly) constant stack emissions, and (2) a discrete transfer function based on the mathematical representation of an integrated puff. The latter is found by integration of a Gaussian kernel representing advection according to a time series of piecewise constant wind vectors and three-dimensional dispersion according to a time series of piecewise constant classes of atmospheric stability. (For example, results indicate that one of the more important types of short-term pollution incidents, the morning fumigation, which is characterized by low winds (up to 6 mph) and by a sharp transition from stable stratification to strong vertical mixing, is simulated successfully.) Details of the development of the kernel and limitations on its range of applicability are discussed in the following sections.

Dispersion Kernel

For a steady mean wind, U, in the downwind x-direction, with y and z representing unbounded crosswind and vertical dimensions, a normal distribution yields the following Green's Function:

$$\frac{\chi(t,t')}{Q(t')} = \frac{\exp -\left\{ \frac{[x - U(t-t')]^2}{2\sigma_x^2} + \frac{y^2}{2\sigma_y^2} + \frac{z^2}{2\sigma_z^2} \right\}}{(2\pi)^{3/2}\ \sigma_x(t-t')\ \sigma_y(t-t')\ \sigma_z(t-t')} \tag{4}$$

where $\chi(t,t')$ is the concentration at time, t due to an instantaneous release, Q, at time t' and position $(0,0,0)^{8,9}$. The dispersion coefficients σ_x, σ_y, σ_z, are assumed to be functions only of the delay time $T = t - t'$ and the atmospheric stability class[3]

Assume Q(t) a piecewise constant over a fundamental time interval, Δ (e.g., Δ = 1 hour); then, for the special case of a steady wind in the x-direction, the concentration $\chi(x,y,z,m)$ at time $t = m\Delta$ can be found by a convolution of the piecewise constant emissions with a series of integrals (the discrete transfer function) evaluated over m periods of duration Δ:

$$\chi(x,y,z,m) = \sum_{n=1}^{m} Q_{m-n+1} \int_{(n-1)\Delta}^{n\Delta} \frac{\exp-\left[\dfrac{(x-uT)^2}{2\sigma_x^{\,2}} + \dfrac{y^2}{2\sigma_y^{\,2}} + \dfrac{z^2}{2\sigma_z^{\,2}}\right]}{(2\pi)^{3/2}\ \sigma_x(T)\ \sigma_y(T)\ \sigma_z(T)}\, dT \quad (5)$$

$$= \sum_{n=1}^{m} Q_{m-n+1}\ G_n$$

This is represented schematically in Figure 6-8 by the buildup of SO_2 due to three (m = 3) consecutive 2-hour (Δ = 2) piecewise constant emissions.

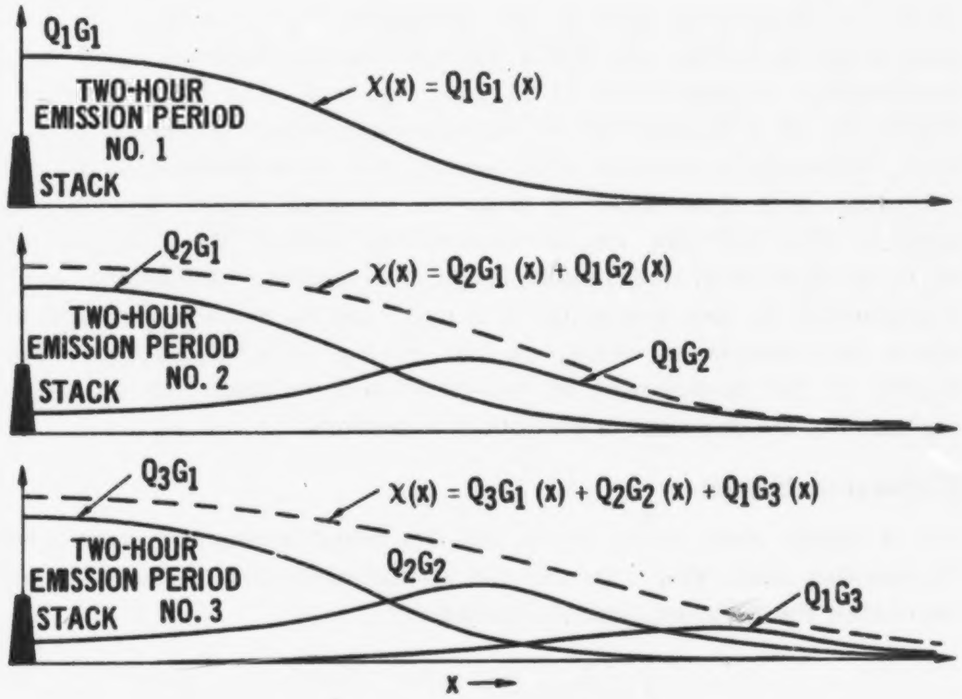

Q_1G_1
TWO-HOUR EMISSION PERIOD NO. 1
STACK
$\chi(x) = Q_1G_1(x)$
Q_2G_1
$\chi(x) = Q_2G_1(x) + Q_1G_2(x)$
TWO-HOUR EMISSION PERIOD NO. 2
STACK
Q_1G_2
Q_3G_1
$\chi(x) = Q_3G_1(x) + Q_2G_2(x) + Q_1G_3(x)$
TWO-HOUR EMISSION PERIOD NO. 3
STACK
Q_2G_2
Q_1G_3
x →

Figure 6-8. Buildup of SO_2 as superposition of consecutive 2-hour releases for case of steady wind in x-direction.

Equation (5), the contribution from an individual source to the concentration at time $m\Delta$, must then be summed over all sources.

Equation (5) can be generalized to account for variation (piecewise constant) in wind direction, wind speed, and atmospheric stability:

$$G_{m,n} = \int_{(n-1)\Delta}^{n\Delta} dT \; \frac{\exp - \left\{ \dfrac{\left[x - \Delta \sum\limits_{j=m-n+2}^{m} u_j - u_{m-n+1} (T - \Delta(n-1))\right]^2}{2\sigma_h^2(T)} + \dfrac{\left[y - \Delta \sum\limits_{j=m-n+2}^{m} v_j - v_{m-n+1} (T - \Delta(n-1))\right]^2}{2\sigma_h^2(T)} + \dfrac{z^2}{2\sigma_z^2(T)} \right\}}{(2\pi)^{3/2} \sigma_h^2(T) \, \sigma_z(T)} \qquad (6)$$

where variations in wind velocity are represented by the piecewise constant series $[u_j]_1^m$ and $[v_j]_1^m$. Note that this result is contingent upon the assumption of $\sigma_x = \sigma_y = \sigma_h$, a horizontal dispersion coefficient. There are valid arguments (to be reviewed in a later section) why this assumption is questionable, except perhaps, for very low wind speeds. From a computational standpoint, the puff appears circular if $\sigma_x = \sigma_y$, and consequently, since its x,y shape is independent of wind direction, the generalization of the kernel to accommodate variations in wind direction is greatly simplified. The propagation of a circular puff for varying wind speed and direction is easily visualized by the schematic of Figure 6-9.

In simulating lake breezes and unusual urban circulations, continuity in the wind field and conservation of the mass of pollutant require introduction of a vertical velocity component. This component as well as the horizontal quantities u and v will be hightly dependent upon space and time variations. Equation (6) considers only time dependence of the wind, although one can use different sequences $[u_j]_1^m$ and $[v_j]_1^m$ depending upon the location of the dose point. Using the lake breeze and, in particular, a dose point near the confluence, as an example, we must allow for two converging streams and a vertical motion which is highly space dependent. The algorithms presented in this paper are not yet expressed in a manner sufficiently general to handle this space dependence. However, it seems relatively straightforward to approximate a three-dimensional velocity field with the three components u(x,y,t), v(x,v,t) and w(x,y,t) and restate the basic algorithm.

Variable Atmospheric Stability

Postulating variations of σ with a travel time T and requiring continuity of σ at each time step,[3] we might describe a three step process by the paths shown in Figure 6-10.

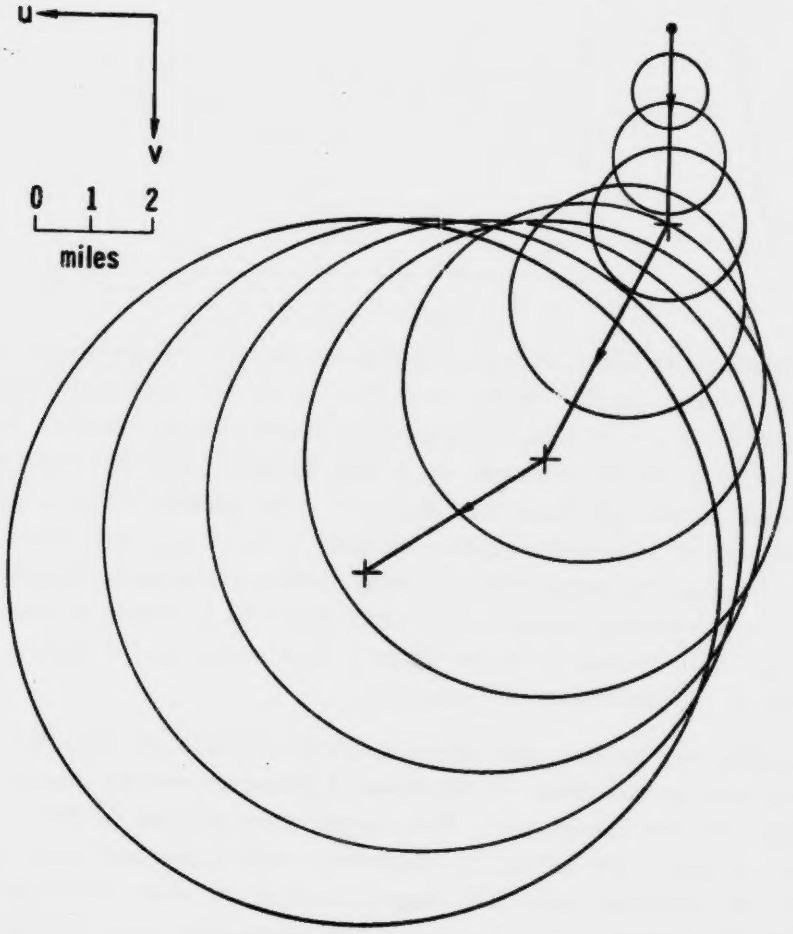

Figure 6-9. Three-hour propagation of circular puff from an instantaneous release. Assumption: $\sigma_X = \sigma_Y$ horizontal dispersion coefficient.

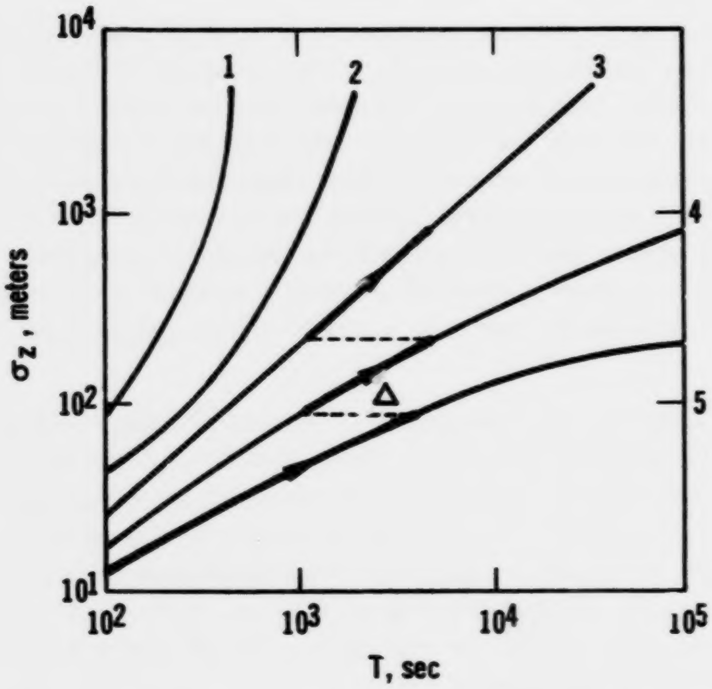

Figure 6-10. Three-step variations in atmospheric stability class, exact method (500 sec, σ continuous).

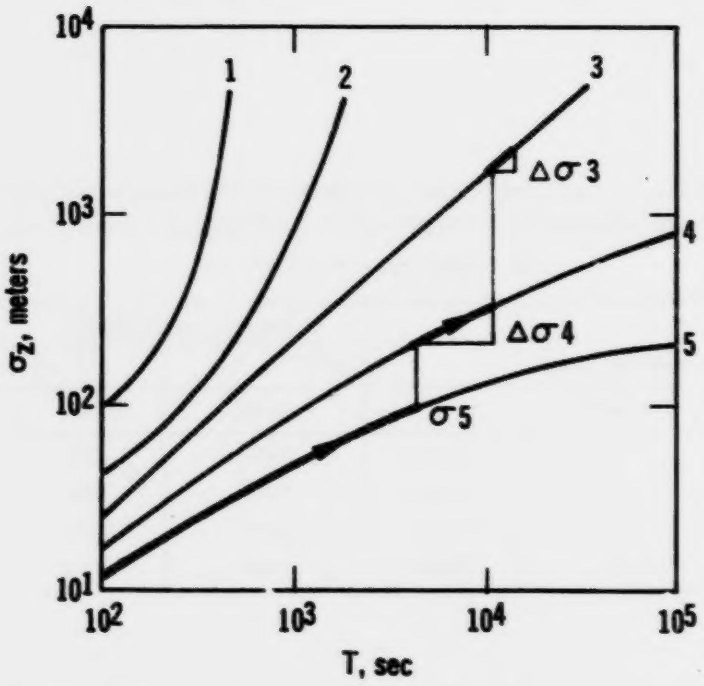

Figure 6-11. Three-step variations in atmospheric stability class by approximate method (Δ = 500 sec, T continuous, $\sigma = \sigma_5 + \Delta\sigma_4 + \Delta\sigma_3$).

Associated with each puff are functions of time, $\sigma_h(t)$ and $\sigma_z(t)$, that could, in principle, be calculated according to the procedure of Figure 6-10. This procedure requires calculation of a psuedo-time for travel within each new stability class. Although the stability class does not change every hour, a computer program based on hourly steps must provide a general algorithm for handling this situation. Unfortunately, the process in Figure 6-10 appears devoid of any simple algorithm suitable for economic programming on the computer. The problem is that the dispersion coefficient σ should be kept continuous in spite of the fact that we are forced to employ a set of discrete functions.

An approximation to the "continuous σ" scheme of Figure 6-10 is proposed in Figure 6-11 for which the time of flight is continuous and the value of $\sigma(t)$ is determined by adding *changes* in σ. A comparatively simple algorithm can be written to implement the procedure shown in Figure 6-11. The two procedures are compared in Table 6-5 where a tolerable error is incurred by the "approximate" method of Figure 6-11 as opposed to the "exact" method of Figure 6-10. For this comparison, we allowed a single change in stability class at the beginning of period 2.

Table 6-5. EXACT METHOD[a] VERSUS APPROXIMATE METHOD[b] FOR DETERMINING ATMOSPHERIC DISPERSION COEFFICIENT

(Δ = 5000 sec; σ At 10,000 sec)

Atmospheric stability class[c]		Dispersion coefficients			
		σ_y(m)[d]		σ_z(m)	
Period 1	Period 2	Exact	Approx.	Exact	Approx.
4	5	2000	1900	200	230
5	4	1900	1700	200	220
3	5	2400	2500	1000	1100
5	3	2500	2100	1100	1120

[a] Figure 6-10

[b] Figure 6-11

[c] Piecewise constants (see section—Transport of Airborne Pollutants)

[d] "m" indicates number of discrete transfer functions (periods) to which σ is applied (see section—Dispersion Kernal)

Dispersion Cofficients

The integrated puff model is similar to earlier dispersion models in that a Gaussian distribution with appropriate dispersion parameters is the fundamental assumption. Although the puff model is closer to physical reality, it is still dependent and quite sensitive to these dispersion coefficients.

There are a number of sets of functions for σ_y and σ_z with either downwind distance or time-of-flight as the independent variable, and, for the most part, resultant curves are in mutual agreement. Some modifications (for example, by Turner[10] in the St. Louis study) have been made to account for greater instability over a city, since most curves are based on experiments over level rural terrain. Recent field experiments in St. Louis by McElroy and Pooler[11] support these modifications; although their estimates of the coefficient of vertical diffusion may be excessive if applied to smoke plumes, because their data was obtained by tracer releases at ground level.

The choice of the function σ_x (j,t) required for the integrated puff model is a serious consideration. Data from field experiments on instantaneous and steady releases[12, 11] have been processed to yield dispersion coefficients which fit the plume model, where concentration:

$$\chi = \frac{Q \exp - \left\{ \frac{y^2}{2\sigma_y{}^2} + \frac{z^2}{2\sigma_z{}^2} \right\}}{2\pi \ \sigma_y \ \sigma_z \ U} \tag{7}$$

Extensive horizional measurements were employed to determine σ_y statistically; and σ_z by inferrence. Clearly the introduction of an additional dispresion coefficient σ_x with a corresponding change in the basic equation will alter the analysis of the experiments and thus the conclusions regarding the magitude of dispersion coefficients.

Another concern is the assumption $\sigma_x = \sigma_y$ which results in the advecting/diffusing circular puff discussed and shown in Figure 6-9. Although not strictly correct, it is convenient to consider σ_x as the superposition of two components: (1) horizontal turbulence due to eddies of a scale smaller than the puff size, and (2) upwind/downwind elongation due to vertical shear. Thus, while the assumption $\sigma_x = \sigma_y$ may be reasonable for unstable and neutral conditions of atmospheric stability, it may be inappropriate in situations where the effect of wind shear is magnified by the existence of a stable atmosphere that inhibits vertical mixing.[13, 14] However in these cases, smoke plumes from major emitters will probably not touch ground within the urban area.

The dispersion coefficients used to obtain the results presented here obey the sets of functions

$$\sigma_{y,i}(t), \sigma_{z,i}(t); \qquad i = 1,5$$

from the equation proposed by Turner[10] for use in his St. Louis model (Figures 6-12 and 6-13 for i = 1 to 7). Furthermore, it is assumed that $\sigma_x = \sigma_y$.

Plume vs. Puff Calculations

Equation (5) which, for constant Q, expresses the steady-state concentration according to the integrated puff formulation; will in general not agree with the plume model equation (7) evaluated at $\overline{T} = x/u$. However, on the centerline (y = 0, z = 0) the two equations yield almost identical results for $u \geqslant 1$ mph.

The linear plots of σ_z (T) and σ_y (T) in Figures 6-14 and 6-15 indicate that for the first few hours of travel time, the dispersion coefficients in Figures

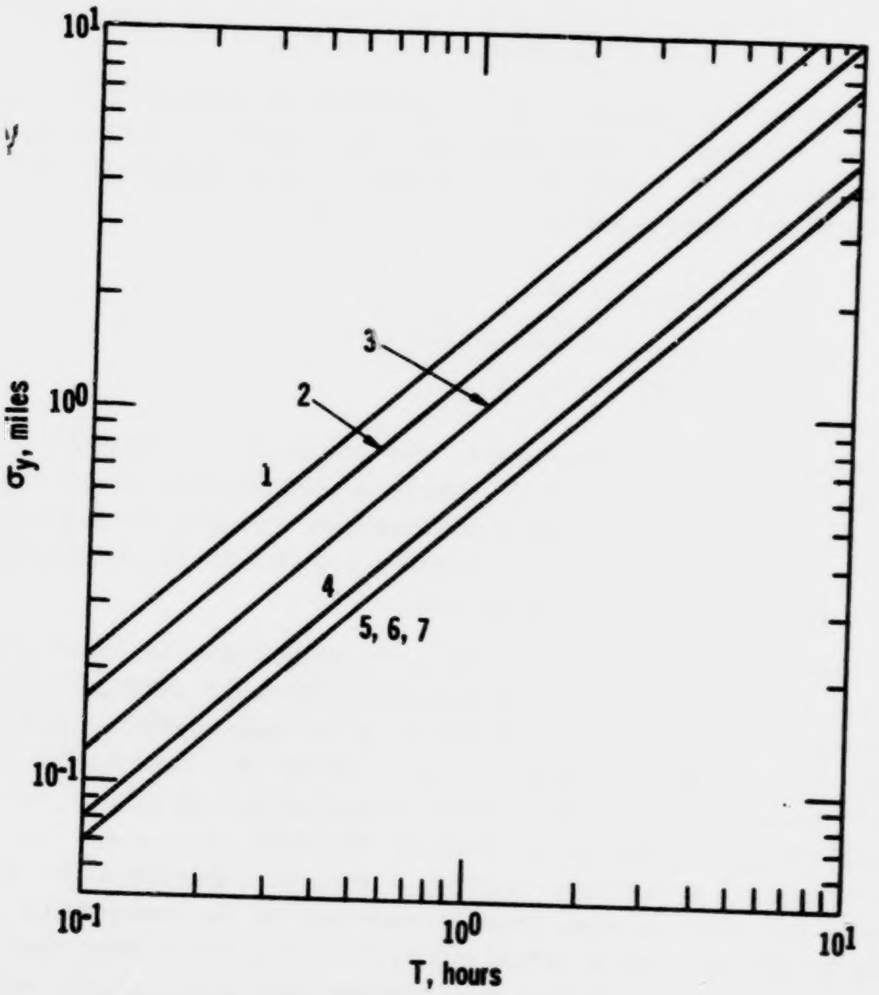

Figure 6-12. Sets of lateral dispersion coefficients, $\sigma_{y,i}(t)$, for atmospheric stability classes i = 1 to 7; used in St. Louis model by Turner.[10]

6-12 and 6-13 can be approximated by the linear relations: $\sigma_x = \sigma_y = \alpha T$; $\sigma_z = \gamma T$. Substitutions of these functions into Equation (4) for $y = z = 0$ yields the following:

$$\chi_{\mathbb{C}} = Q \int_0^\infty dT \; \frac{\exp - \left\{ \dfrac{(x - UT)^2}{2\, \sigma_z^2(T)} \right\}}{(2\pi)^{3/2} \quad \sigma_x(T)\sigma_y(T)\,\sigma_z(T)}$$

$$= \frac{Q}{2\pi\, (\alpha\bar{T})(\gamma\bar{T})\, U} \left\{ \frac{e^{-r^2}}{2\sqrt{\pi}\, r} + \frac{\operatorname{erf}(r)}{2} + \frac{1}{2} \right\} \qquad (8)$$

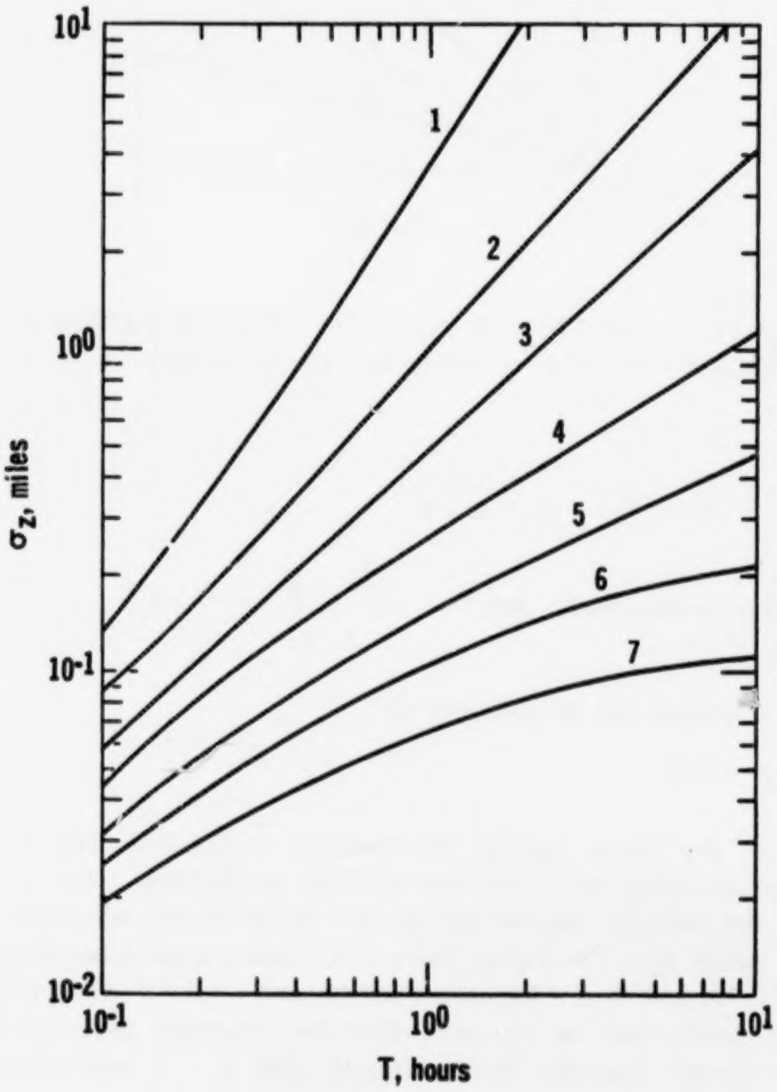

Figure 6-13. Sets of vertical dispersion coefficients $Q_{x,\,i}(t)$, for atmospheric stability classes $i = 1$ to 7; used in St. Louis model by Turner.[10] T = plume travel time.

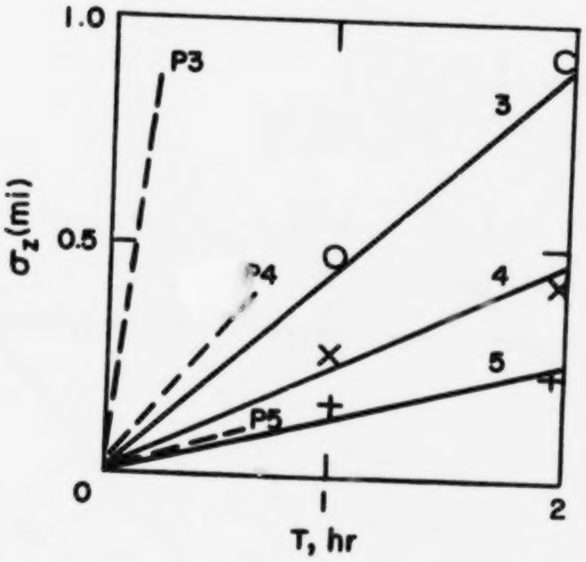

Figure 6-14. Linear plot of $\sigma_z(T)$ for stability classes 3, 4, and 5. Plots labeled "P" are recent data from St. Louis.[11]

where $\overline{T} = \frac{x}{u}$, $r = \frac{u}{\sqrt{2a}}$

and (the error function) $\operatorname{erf}(r) = \frac{2}{\sqrt{\pi}} \int_0^r e^{-t^2}\, dt$

Thus the integral can be evaluated as:

$$\chi_{\text{℄}} = P\,F \qquad (9)$$

where P, the factor outside the brackets in Equation (8) is the plume equation evaluated at $\overline{T}$, the time of flight to the dose point x. The terms within the bracket, represented by the factor F, are tabulated below for several values of r. For a given value of r, there is a corresponding value of a, (Figure 6-15) and thus u for each stability class i = 3,4,5. According to Table 6-6 for steady state on the centerline, the integrated puff calculation is 3 percent greater than the plume formula when u = 1 mph under unstable atmospheric conditions.

Table 6-6 also indicates that the ratio of puff to plume results becomes infinite as u → 0. As the wind speed approaches zero, the plume equation

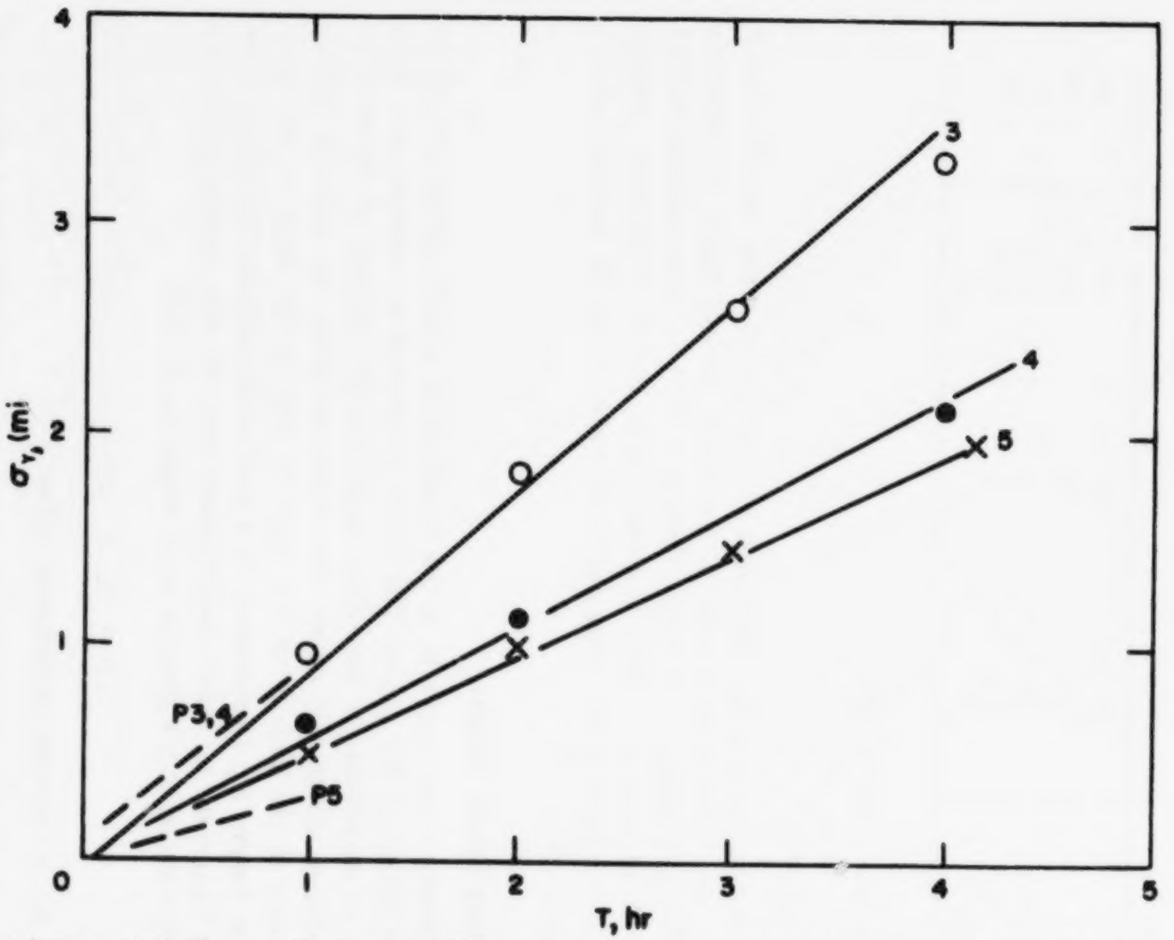

Figure 6-15. Linear plot of σy (T) for stability classes 3, 4, and 5. Plots labeled ''P'' are recent data from St. Louis.[11]

Table 6-6. CALCULATED VALUES OF CENTERLINE[a] PLUME[b] – PUFF CONVERSION FACTOR, F,[c] FOR SELECTED VALUES OF r IN STABILITY CLASSES 3, 4, 5[d] DURING FIRST FEW HOURS OF TRAVEL TIME

$r = u/\sqrt{2}\,a$	Stability class horizontal wind speeds, mph			F
	u_3	u_4	u_5	
10	12	8	7	1.00
1	1.2	0.8	0.7	1.03
0.7	0.8	0.5	0.4	1.10
0.5	0.6	0.4	0.3	1.22
0	0	0	0	∞

[a] $y = z = 0$

[b] Plume Equation (4) evaluated at $T = \frac{x}{u}$

[c] Equation (9) $\chi_{℄} = PF$

[d] See Figure 6-15

with dispersion coefficients expressed as functions of travel time $\overline{T} \approx (x/u)$ goes to zero. This is in contrast to the plume formula based on dispersion coefficients as functions of travel distance x. This function becomes infinite as u → 0. In contrast to these two versions of the plume equation, concentrations estimated by the integrated puff model in Eq. (5) approach an x^{-2} distribution as u → 0.

Effective Stack Height

The effective stack height H, is the height above ground which best defines the centerline of the plume. The plume is assumed to originate as a point source at an altitude H feet above ground at the location of the stack. If aerodynamic downwash causes the plume to break up and mix rapidly downward in the vicinity of the stack, H may be set equal to the actual physical height, H_s. Observations of a local utility indicate this phenomenon occurs frequently for wind speeds greater than 15 mph. Otherwise a plume rise ΔH is added to the physical stack height H_s, so that:

$$H = H_s + \Delta H \qquad (10)$$

where ΔH is estimated as described below:

Smoke plume rise calculations in this model are based on a plume rise formula derived from observations at TVA stations and other power plants[15]. (The momentum term in the original formulation is omitted in the following equation since its contribution is generally negligible compared to thermal buoyancy.)

$$\Delta H = \frac{KQ_s^{1/2}}{U} \qquad (11)$$

where ΔH = plume rise (ft)
Q_s = heat emission rate from stack (Btu hr^{-1})
U = wind speed (mph) at the height of the stack
K = 0.870 (unstable–Class 3), 0.354 (neutral–Class 4), 0.222 (stable–Class 5)

Values of the heat emission rate may be approximated by a fixed percentage of the total heat rate (heating value of the fuel times the fuel rate). The percentage depends on the type and efficiency of the burning and heat exchange equipment but may be categorized as follows:

Power plant – 12%
Large industrial, commercial – 20%
Small industrial, commercial and residential – 35%

The mean wind at the physical stack height, H_s should never be used in the plume rise Equation (11). In evaluating the dispersion kernel (Equation 6), wind at the effective stack height H, corresponding to the plume centerline, is used. In each case, the desired value for the wind speed will be usually greater than that measured at a local airport or TAM station (typically at 30 ft to 100 ft above the ground). Equation (12) provides a correction term for altitudes up to 1000 ft. The exponent P is dependent on the stability class, as shown in Table 6-7.

$$U \text{ (at height } z_2) = U \text{ (at height } z_1)(z_2/z_1)^P \qquad (12)$$

Table 6-7. EXPONENT FOR WIND PROFILE LAW[16]

Stability Class	P
stable (5)	0.5
neutral (4)	0.2
unstable (3)	0.2

The experimental data in the reference cited, indicated a slightly more uniform vertical wind speed profile for unstable than for neutral conditions, but the model is not sensitive to this distinction.

Four restrictions placed on the use of Equation (11) are listed in Table 6-8.

Table 6-8. RESTRICTIONS ON PLUME RISE FORMULA (Equation 11)

Mixing-layer height H_m	Low wind speeds U	Stability class and Coefficient K
a. Effective stack height H, cannot be greater than mixing-layer height, H_m, if stack is beneath mixing layer; i.e. $H \leq H_m$ if $H_s < H_m$ b. If $H_s > H_m$, assume $H_m = \infty$ with plume rise and dispersion according to stable atmospheric conditions	If U estimated to be < 4 mph, value 4mph used in Equation (11)	If the physical stack height, $H_s \geq 200$ feet, K = 0.354 (neutral used even though the stability index indicates unstable conditions.

The restrictions on mixing-layer height in Table 6-8 are based on the assumption of an impenetrable atmospheric layer (lid) at height H_m. The effluent from a stack which emits its plume just beneath the lid will probably penetrate into the stable layer rather than obey the assumption of perfect reflection at the lid. Unfortunately, there do not appear to be any data that describe this situation.

The restriction in Table 6-8 limiting the minimum wind speed to be used in Equation (11) reflects the fact that the equation is an empirical one in which the parameters n and m in an equation of the form $\Delta H = K\ Q_s^n\ U^m$ were found by multiple linear regression. A comparison of Equation (11) with TVA data[17] indicates good agreement down to wind speeds of about 6 mph. Below this, the (l/u) factor in the equation causes an over-estimation of the plume rise. An arbitrary restriction has been made, therefore, on a minimum value of U in Equation (11).

The restriction on stability class and coefficient K, occurs because, for plume rise calculations, the vertical variation of temperature at heights greater than 200 feet is best characterized by a neutral lapse rate, even though unstable conditions may exist in the first few hundred feet above ground.

A single value of plume rise is also ascribed to each of the three classes of area-sources (previously discussed) whenever the wind is less than a critical wind speed. With winds less than 6 mph, low-rise residential buildings are assumed to have an effective stack height of 100 feet; high-rise residential and commercial buildings, 300 feet; and industrial area-sources, 300 feet. The model proves to be insensitive to these assumptions as long as the initial value of σ_z (σ_{zo}) is greater than or equal to 100 feet.

Finite Geometry

The fundamental puff kernel has been defined for z from $(-\infty, +\infty)$ with z=0 on the plume axis. If we assume perfect reflection at the ground, the concentration C, at time m, at a receptor position (x,y,z), due to a single source at position (x',y',z',) is:

$$C = \chi(x-x', y-y', z-z', m) + \chi(x-x', y-y', z+z', m) \qquad (13)$$

where the coordinates have been stated relative to the ground and Equation (6) determines χ.

An objective calculational procedure was developed to estimate the height of the mixing layer that is assumed to define an impenetrable barrier for vertical dispersion. In earlier work, the distribution under the lid had been calculated by a single plume until vertical diffusion implied the pollutant had reached the lid, at which time abrupt transition to the equation for uniform vertical mixing was made.

In order to avoid this abrupt transition and simultaneously, to allow for time-dependent (piecewise, constant, hourly) values of H_m multiple reflections between ground and the inversion are represented by pairs of image sources. For example, the first image source above the lid is the reflection about H_m of the actual source; the second image source above the lid is the reflection about H_m of the first below-ground image (Figure 6-16). Depending upon the lid height and the time of travel, up to five pairs of images may be required to adequately represent a condition of uniform vertical mixing in an urban area.

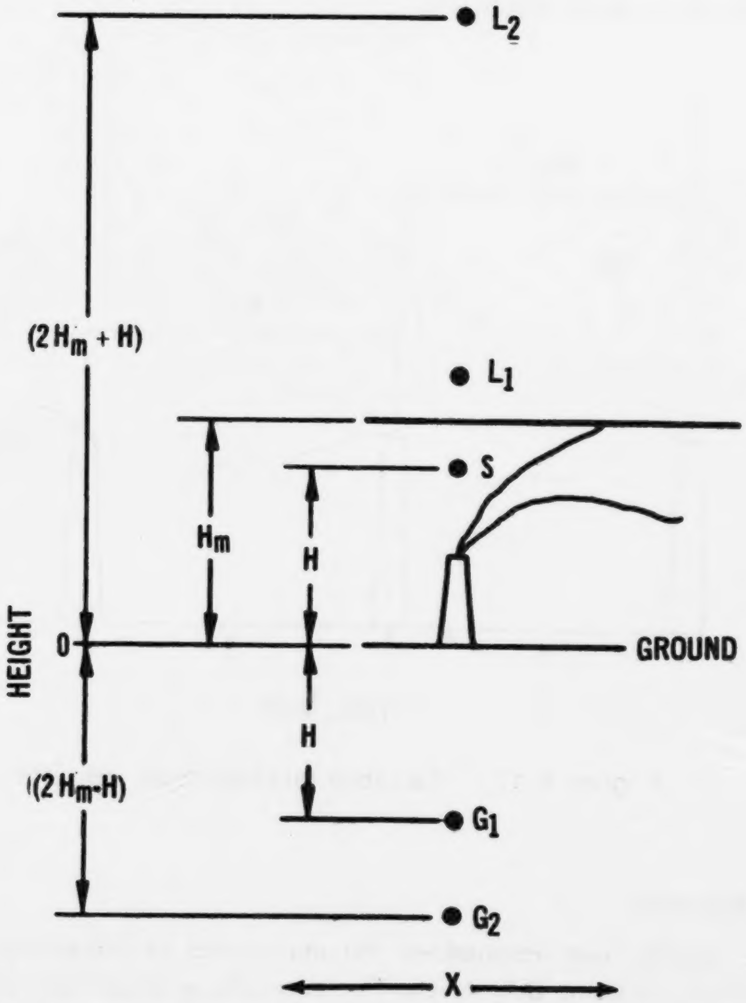

Figure 6-16. Multiple reflections of pollutant between stable layer and ground, represented mathematically by two sets of image sources. Image G_1 reflected above lid at L_2. Image L_1 reflected below ground at G_2. S = first image source, reflection of actual source.

Since the lid height may vary during the lifetime of each 1-hour puff, algorithms have been formulated to allow for specification of a different effective lid height for each hour m, look-back time n (Equation (5), and source J. For example, in Figure 6-17 the height of the mixing layer is steadily decreasing during the three 1-hour periods. Calculations of concentrations due to stack emissions during the first hour (m=1) would be based on lid height H_{m_1} for m=1, n=1, and the lid height H_{m_2} for m=2, n=1 and 2. Concentrations due to stack emissions during the second hour (m=2) would be based on lid height H_{m_2} for m=2, n=1, and on H_{m_3} for m=3, n=2. Concentrations due to stack emissions during the third hour (m=3) would be based on an infinite lid with diffusion coefficients corresponding to stable atmospheric conditions.

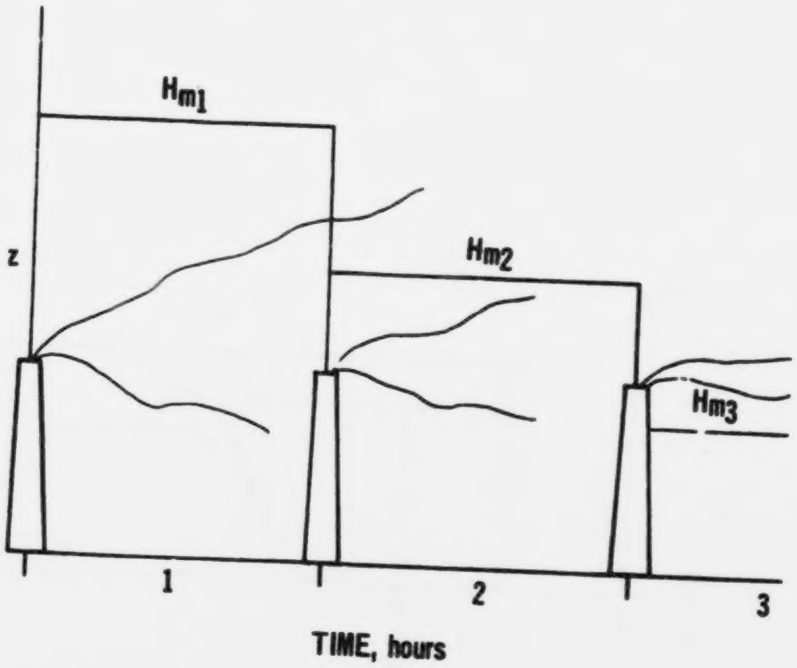

Figure 6-17. Variable mixing-layer heights.

Area Sources

Earlier studies have emphasized the importance of residential coal use in determining ambient SO_2 levels. For example, at Hyde Park (TAM-4) SO_2 levels of 0.2 to 0.3 ppm for southwest winds 6 to 9 mph can be attributed almost entirely to space-heating by coal-fired boilers in three-story buildings.[19]

The realistic modeling of residential zones characterized by multiple-sources too numerous to represent by individual plumes is therefore critical to the success of a source-oriented dispersion model for Chicago. For the Chicago grid system these so-called area-sources can be visualized in one of two modes:

1. For winds less than a critical speed the individual emissions resemble plumes. For three-story buildings, visual observations indicate that a representative plume rise for wind speeds less than 6 mph is about equal to the building height, i.e., approximately 50 feet.
2. Above the critical wind speed, mechanical turbulence, primarily downwash, destroys the plume slightly above the rooftop level.

Similar arguments apply to high-rise, commercial, and industrial area-sources previously described. In the first case, we might approximate the area-source as a uniform horizontal sheet of small thickness Δz located at $z = 100$ feet.

In the second mode, it is reasonable to assume uniform mixing over the volume of the building.

The integrated puff model is ideally suited to the task of synthesizing these source configurations. In contrast to the plume equation, limited to crosswind and vertical coordinates, thereby representing a two-dimensional front, the puff incorporates the downwind coordinate and thus represents a three-dimensional cloud of pollutant.

The area source is approximated by a psuedo point source. This is similar to algorithms employed in plume models; but as mentioned above, the more sophisticated puff kernel results in a volumetric source rather than a two-dimensional wave front. In addition to giving a more realistic description of downwind dispersion, the puff model can, therefore, directly evaluate the effect of the area-source upon the area itself.

The volumetric source is synthesized by specifying three initial dispersion coefficients: σ_{x0}. σ_{y0} and σ_{z0}. These are then associated with times t_x, t_y, and t_z which are the solutions to:

$$\sigma_{x0} = \sigma_x(i,t_x), \ \sigma_{y0} = \sigma_y(i,t_y), \ \sigma_{z0} = \sigma_z(i,t_z) \qquad (14)$$

where $\sigma(i,t)$ is the family of functions describing the dispersion coefficients at time, t, for stability class, i. A virtual source is thus defined at upwind distances $\delta_x = ut_x$ and $\delta_y = vt_y$ from the center of the area (see Figure 6-18).

The choices of σ_{x0}, σ_{y0} and σ_{z0} as well as the effective source height, z, depend upon the representative building height for each square mile and the mode of initial transport: plume or downwash. The transport equation (Equation 6) is then modified with $x - \delta_x$ replacing x, $y - \delta_y$ replacing y, and $T + t_x$, $T + t_y$, $T + t_z$ replacing T in the appropriate locations.

For a square-area source of side length, n the value of σ_{y0} is defined by

$$\sigma_{y0} = n/2.4 \qquad (15)$$

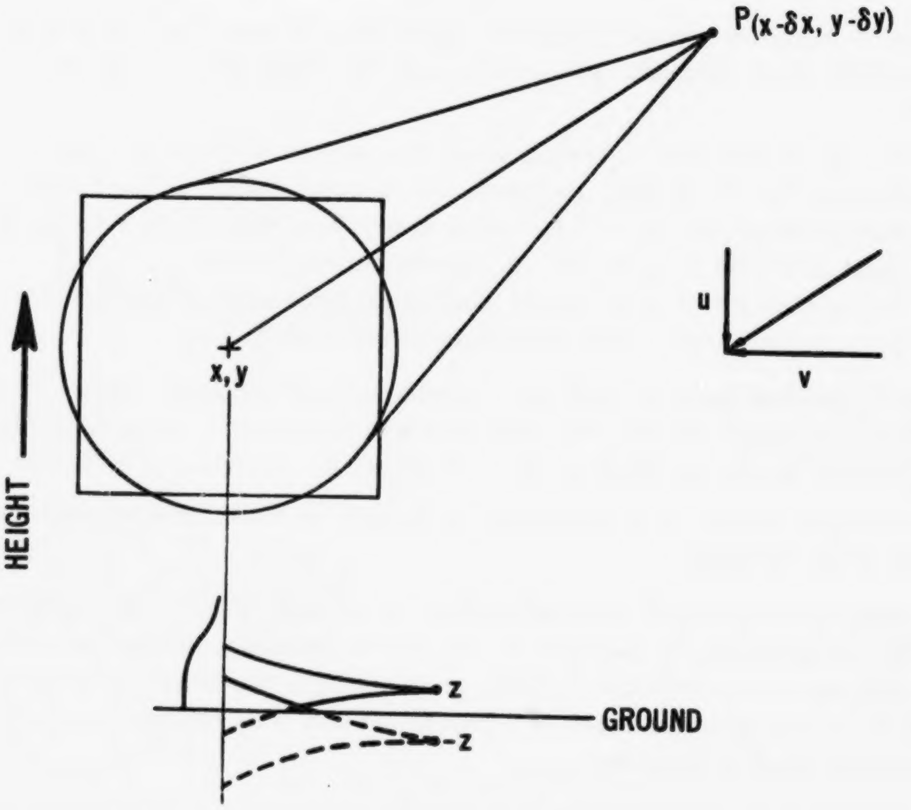

Figure 6-18. Volumetric synthesis P, of area source of buildings of height z, at upwind distances of δx and δy; from center of area source (x, y).

This insures that the concentration will be independent of position along a line on the downwind side of a row of identical area sources (Figure 6-19).

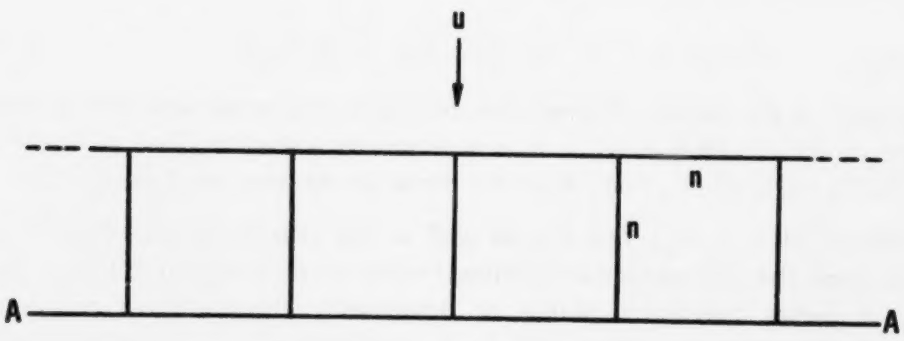

Figure 6-19. Choice of $\sigma_{y0} = n/2.4$, insures uniform concentrations along line A-A for row of identical area sources.

AN INTEGRATED SYSTEM FOR AIR RESOURCE DATA MANAGEMENT AND DISPERSION MODEL DEVELOPMENT

The preceding sections of this paper have described the array of emission inventory, meteorology and air quality data that was acquired and processed in order to test and validate the diffusion model. This computerized file containing nearly 3 years of hourly-average data for a wide variety of parameters, represented a singularly valuable resource, but at the same time, it presented a formidable problem in data management. The development of the "integrated puff" model required that this data file be exploited in two ways:

1. Analysis of statistically significant subsets of this array of data could be expected to yield information concerning the relative significance of many of the parameters and phenomena that were modeled. Moreover, the insights into the micrometeorological characteristics of the Chicago metropolitan area obtained through analysis of this data should serve as a guide to the interpretation and evaluation of the output of the model.
2. Time series arrays of emission-inventory data, and raw and processed meteorology data were required as inputs to the puff model, while a corresponding array of measured sulfur oxide concentrations had to be merged and compared with puff model output in order to analyze and validate its theoretical predictions against real-world data. The latter represented a major and laborious task if it was done manually.

An automatic data management system was clearly required in order to achieve these objectives. This need was met by the development of a master Air Pollution Information and Computation System (APICS) designed to automate the entire process of data storage, retrieval, manipulation, analysis, and display, associated with the dispersion model development effort.

The APICS system consists of the IBM PL-1 data storage and retrieval code nested in a series of operational subroutines and computational codes tailored to the analysis of air pollution data. With this system, the data stored in the master file can be partitioned in any way desired. Any combination, array or subset of emission, meteorology and/or air quality data can be formed and retrieved. The selected data array can be accessed through a FORTRAN subroutine which allows the user to manipulate the array in any desired way. For example, the analyst may form a new data array which consists of products of components of the original array raised to some power, etc. Standard subroutines for computing atmospheric stability, smoke plume rise, etc., are included as options in this system.

The array of data in the master file may be analyzed with a multivariate linear regression analysis code or a discriminant analysis code, both part of the system and the results may be displayed as tables, histograms or CALCOMP plots.

The air pollution data management system described above provides a uniquely powerful tool for the development and testing of the dispersion model. The emission simulation model previously described and the dispersion model algorithms previously described have been incorporated into the APICS system, so that the testing and validation process, conducted with a 3-year computerized inventory of hourly-average meteorology and sulfur dioxide air quality data, is totally automated. Meteorology and emission data from the master data file are input to the dispersion model, and sulfur dioxide concentrations are calculated; these results are compared with the corresponding measured air quality data and displayed in a single operation within the Argonne, IBM 360-75 computer. The sensitivity of the model to variations of critical meteorological parameters and the effects of modifications in the structure of the model itself can be tested. When the dispersion model development effort is completed in the early part of 1970, a manual of operations for the APICS system as well as for the dispersion model itself will be prepared for general use.

RESULTS, CONCLUSIONS, and PROJECTIONS

TAM Stations

The month of January, 1967 was chosen for an initial comparison of the model with recorded sulfur dioxide data. Five TAM stations were selected representing a wide range of geographical and emission features (Figure 6-1).

TAM 1, situated in a low-density residential area in the northwest corner of the city, sees little SO_2 unless southeasterly winds carry plumes from the power plants and other industries 11 miles away.

Prevailing southwest winds are responsible for high concentrations occasionally observed at TAM 2. This station is also influenced by the high-rise concentration along the lakeshore during northeasterly winds, especially during lake breeze conditions.

TAM 3 generally records the highest sulfur dioxide levels in the city. It is situated in the midst of coal-burning commercial buildings (for example, Union Station, several blocks to the west emitted 8×10^6 pounds of SO_2 per year until it recently shifted to gas). Furthermore, southwest winds, sweeping up the "industrial corridor," along which three power plants and major industries are located, cause extremely high pollution concentrations downtown, especially when vertical ventilation is limited by an inversion. Peak hourly averages greater than 1 ppm have been recorded.

TAM 4 is situated along the lake at the edge of over 20 square miles of coal-burning three-story residences. Studies of the frequency of air pollution incidents in Chicago from January 1966 to December 1967 indicate that this station has the highest number of midwinter short-term air pollution incidents (6 hrs to 24 hrs duration). For example, in January 1966 and January 1967, TAM 4 had a total of thirty 6-hour periods for which SO_2 levels exceeded 0.4 ppm. The corresponding figures for TAMS 1,2, and 3 are 0,1 and 8. Furthermore, plumes from the industrial corridor 7 miles northwest are often sensed at TAM 4.

TAM 5 is similar to TAM 1 except that northerly winds are responsible for occasionally high SO_2 levels. Other TAM stations (6 through 8) were not included in this initial validation effort because they are situated on the borders of the city, and no inventory has yet been assembled for the areas of Cook County immediately outside the city limits or for the Gary-Hammond, Indiana, industrial zone.

Ninety-seven station-days (2328 hourly values) were studied for the month of January 1967 at TAM stations 1 through 5. A station malfunction on any particular day eliminated that station from the data set for that day. Malfunctions, either due to sensor or transmission difficulties, were automatically logged on the original Chicago air quality tapes.

Computer Requirements

The model has been programmed for the IBM -360 computer. Since each hourly time step for each source and each receptor involves a numerical integration, some effort has been expended to:

1. Limit the number of integrations by employing a preliminary test to estimate whether or not a particular plume is likely to contribute to a given dose point (for example, there is no reason to evaluate the contribution from a stack located 5 miles downwind of the receptor).
2. Approximate integrals, where possible, by the mean value theorem.
3. Lump distant area sources together.

As presently constructed, the model run with hourly time steps requires between 0.5 and 0.75 minute of computer time per station-day. Thus the run for five TAM stations for the 97 station-days in the month of January 1967 required less than 2 hours. Recent analytical work (see Plume vs. Puff Calculations page 6-28) indicates that dispersion coefficients can be approximated by the linear relationships $\sigma_y = \alpha T$, $\sigma_z = \gamma T$ where α and γ are constants. Under these circumstances, the integral (Equation 6) can be evaluated in closed form. It is anticipated that run time with this modification will be approximately equal to that required for a standard plume model.

Statistical Results

There are numerous statistical tests that have been applied to source-oriented, pollution-dispersion models. The importance attached to any particular test clearly depends upon the intended use of the model.[20] One of the more standard presentations involves evaluating the percentage of calculated values within a given tolerance of the corresponding observed values. This is equivalent to a scattergram, but less dazzling and more easily interpreted.

Table 6-9 lists these percentages for each TAM station and for the citywide collection. Hourly data and 2-hour, 6-hour, and 24-hour averages are evaluated in terms of five criteria.

Table 6-9. STATISTICAL EVALUATION OF INTEGRATED PUFF MODEL DATA: PERCENTAGE OF CALCULATED POLLUTANT CONCENTRATIONS WITHIN DESIGNATED TOLERANCE LIMITS OF SAMPLE DATA[a]

Item	Hour avg.	TAM stations					
		1	2	3	4	5	1-5
Mean (μ_{obs}) $\frac{(\mu_{obs}-\mu_{calc})}{\mu_{obs}} \times 100\%$		0.06 ppm – 10%	0.12 ppm + 16%	0.33 ppm + 14%	0.15 ppm – 3%	0.06 ppm – 9%	0.14 ppm + 7.4%
Std. dev. (obs-calc)	1	0.09 ppm	0.10 ppm	0.20 ppm	0.13 ppm	0.10 ppm	0.13 ppm
Std. dev/mean		1.7	0.88	0.62	0.84	1.6	0.93
% < 0.025 ppm	1	58%	37%	12%	26%	45%	35%
% < 0.05 ppm	1	69%	63%	23%	53%	71%	57%
% < 0.1 ppm	1	84%	81%	47%	79%	89%	77%
No. data points	1	288	576	432	408	624	2328
Std. dev. (obs-calc)	2	0.08	0.09	0.18	0.11	0.09	0.12
Std. dev/mean	2	1.3	0.78	0.56	0.77	1.5	0.83
% < 0.025 ppm	2	58%	40%	15%	29%	45%	37%
% < 0.05	2	70%	66%	27%	52%	70%	58%
% < 0.1 ppm	2	83%	83%	49%	81%	88%	78%
No. data points	2	144	288	216	204	312	1164
Std. dev (obs-calc)	6	0.07	0.08	0.14	0.08	0.07	0.09
Std. dev/mean	6	1.1	.65	0.42	0.58	1.2	0.64
% < 0.025 ppm	6	56%	36%	10%	32%	46%	36%
% < 0.05 ppm	6	67%	66%	29%	54%	72%	59%
% < 0.1 ppm	6	90%	88%	56%	85%	91%	83%
No. data points	6	48	96	72	68	104	388
Std. dev (obs-calc)	24	0.04 ppm	0.05 ppm	0.10 ppm	0.07 ppm	0.04 ppm	0.06 ppm
Std. dev/mean	24	0.71	0.44	0.30	0.45	0.70	0.43
% < 0.025 ppm	24	25%	46%	17%	59%	58%	43%
% < 0.05 ppm	24	75%	62%	39%	77%	77%	66%
% < 0.1 ppm	24	100%	96%	67%	88%	96%	90%
No. data points	24	12	24	28	17	26	97

[a] Chicago, January, 1967

Monthly and daily predictions are in excellent agreement with observed values. Marsh and Withers[21] indicate that, for their Reading, England, model as well as for others in the literature, the ratios of the standard deviations (observed-calculated) to the observed means are all higher than 1.1. From Table 6-9 the corresponding value for 24-hour averages is 0.43. It is 0.64 for 6-hour averages and 0.93 for 1-hour averages.

Results for individual TAM stations vary, depending primarily upon the monthly mean. For example, almost all values for TAMS 1 and 5 fall within ±0.1 ppm since the means are only 0.06. For the same reason, however, the ratios $(\sigma_{obs-calc})/\ \mu_{obs}$ are high for these stations.

Figure 6-20 (a and b) shows daily averages at TAMS 1 to 5 for January 1967. Six-hour averages are presented in Table 6-9 because 6 hours is the minimum practical time step for the implementation of incident control strategies.[22] On a citywide basis 59 percent of the calculated 6-hour values are within ±0.05 ppm and 83 percent within ±0.1ppm. The results for 6-hour averages are also presented in Figure 6-21. Assuming the solid lines delineate a region of successful predictions, then 59 percent of the calculations are "correct", the skill score (based on chance) is 0.42; the model explained 52 percent of the variants in the observed data set. For 24-hour averages this statistic is 74 percent.

Tables 6-10 and 6-11 illustrate the use of the model in evaluating the frequency of short-term air pollution incidents. The contingency tables are based on the following air pollution "war game" rules:

1. A threshold SO_2 level is defined for a given averaging period.
2. If the model predicts that this level will be exceeded, then action is taken.
3. If action is taken and the observed average is greater than the threshold *less* a tolerance (here .025 ppm), then incident is said to have actually occurred.
4. If no action is taken and the observed average is less than the threshold *plus* a slight tolerance (here 0.025 ppm), then an incident is said not to have occurred.

When compared to chance, the model is significant at better than the 99.9% confidence level and the skill scores for this air pollution war game range from 0.64 to 0.80. Skill scores are defined by the ratio $(V-V^1)/(T-V^1)$ where V is the number of correct estimates (here yes*yes + no*no cases), T the total number of cases, and V^1 the value of V expected by some means other than the model under evaluation. (For example, instead of chance, a simpler plume model might be used.) It is worth noting, also, that in terms of incident control policies; taking serious actions, such as temporarily curtailing industrial production is costly. Air pollution cost-benefit studies conducted at Argonne show that as much as $10 million per day can be

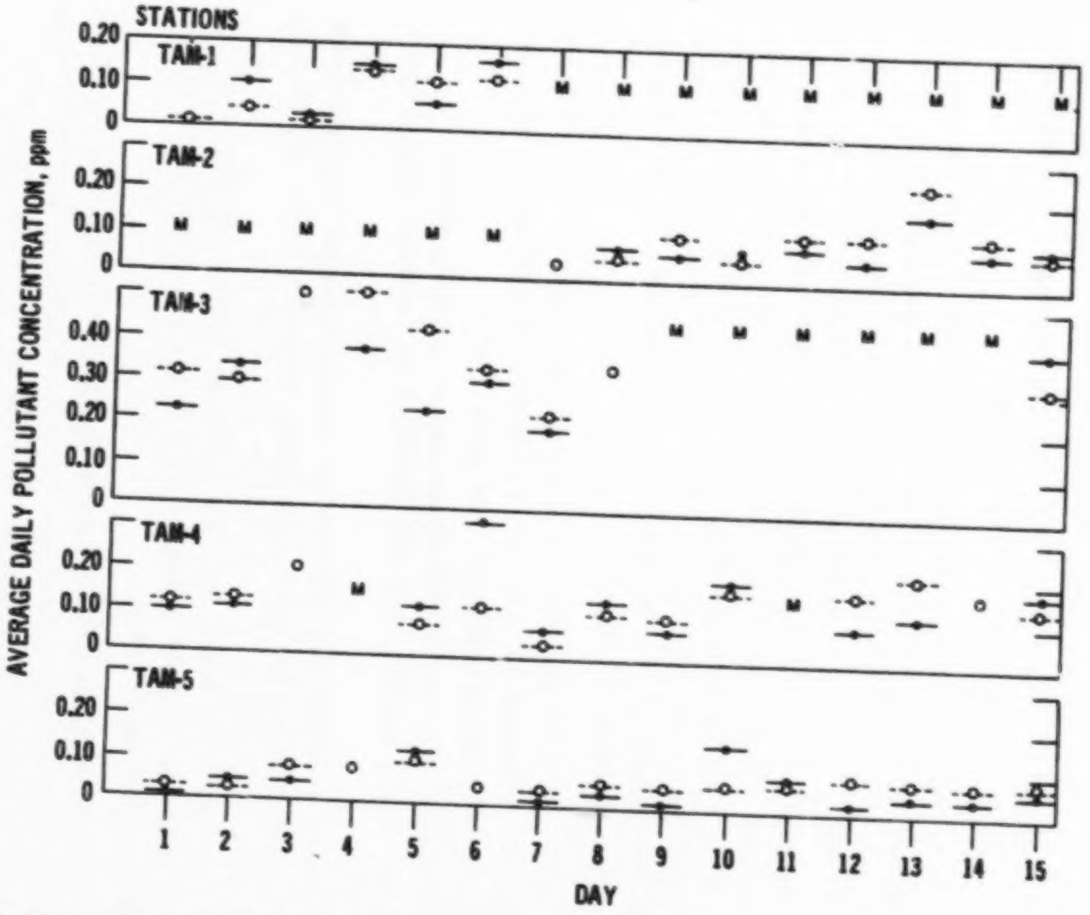

Figure 6-20a. Daily pollutant concentration averages, Chicago, January 1 to 15, 1967. "M", missing data.

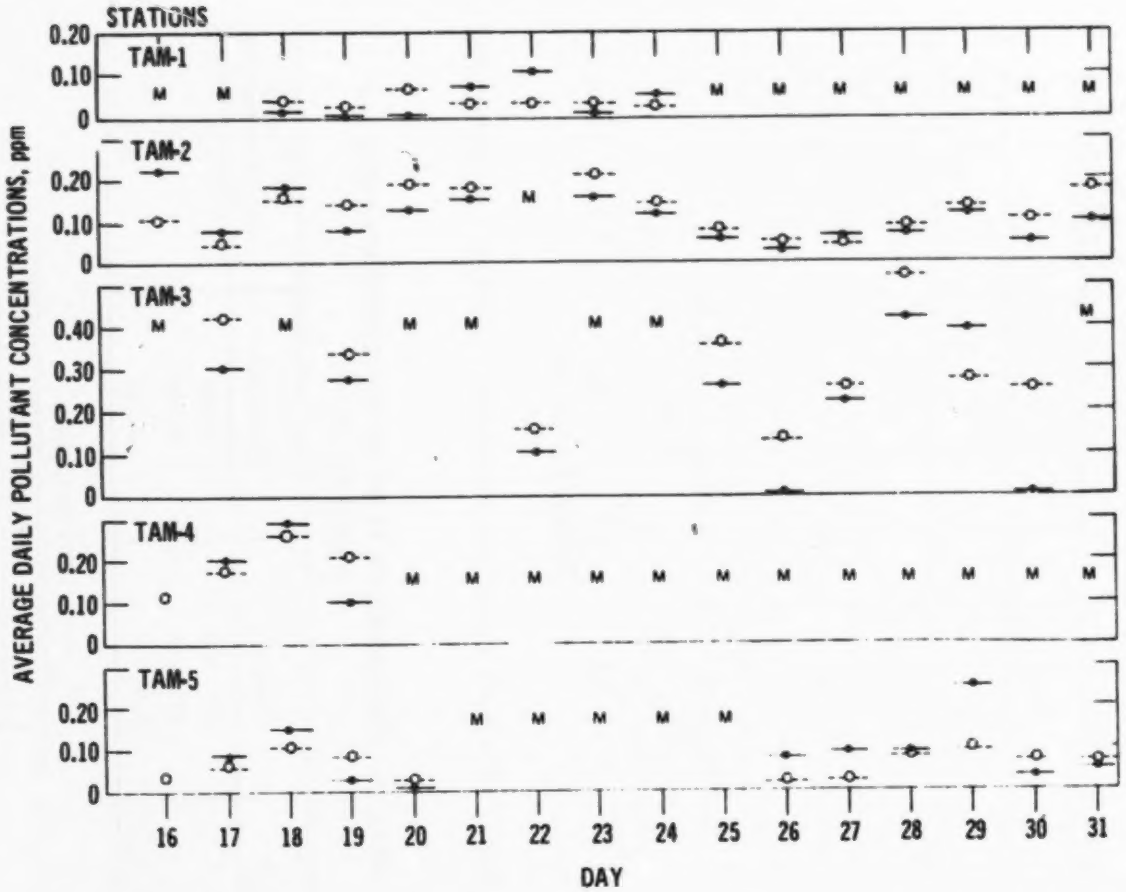

Figure 6-20b. Daily pollutant concentration averages, Chicago, January 16 to 31, 1967. "M", missing data.

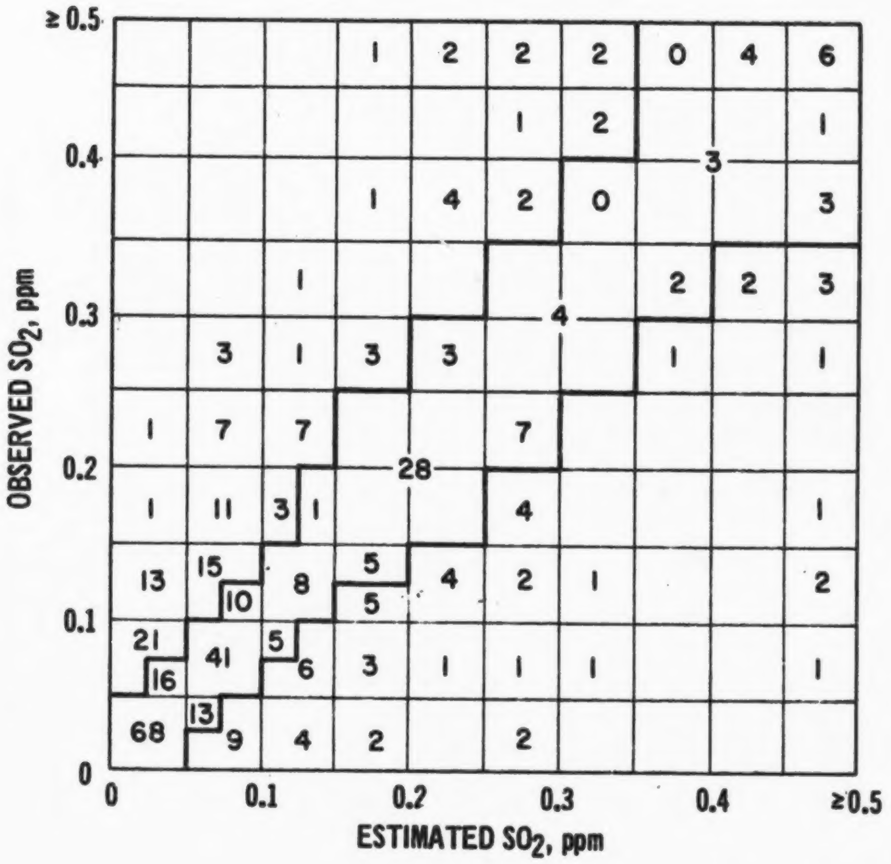

Figure 6-21. Six-hour pollutant averages, Chicago, January 1967.

Table 6-10. FREQUENCY OF 24-HR INCIDENTS FOR STATIONS 1–5 JANUARY 1967

Symbol	Threshold	Tolerance	Skill score (Based on chance)
x	0.1 ppm	0.025	0.76
y	0.2 ppm	0.025	0.73
z	0.3 ppm	0.025	0.75

CONTINGENCY

		Predict	
		Yes	No
Occur	Yes	x 44 y 17 z 9	x 9 y 6 z 1
	No	x 3 y 3 z 3	x 41 y 71 z 84

Table 6-11. FREQUENCY OF 6-HR INCIDENTS FOR STATIONS 1–5 JANUARY 1967

Symbol	Threshold	Tolerance	Skill score (Based on chance)
x	0.1 ppm	0.025	0.76
y	0.2 ppm	0.025	0.64
z	0.3 ppm	0.025	0.80

CONTINGENCY

		Predict	
		Yes	No
Occur	Yes	x 145 y 62 z 32	x 32 y 28 z 10
	No	x 14 y 20 z 6	x 197 y 278 z 340

involved in lost wages and production for a city such as Chicago. Thus, in practice, the tolerance used above would have to be enlarged sufficiently to insure that the model scores significantly better than shown in Tables 6-9 and 6-10

Hourly Time Series

Figure 6-22 is a sample of strip charts for January 1967 showing hourly wind speed, wind direction, temperature (all measured at Midway Airport), atmospheric stability class, and the mixing height as estimated by the objective method previously described. Figure 6-23 is a sample of strip charts also for January 1967 showing smoothed hourly values of observed (solid lines) and estimated (dotted lines) sulfur dioxide for TAMS 1–5. For readability, the hourly values have been smoothed by the formula: $X(n) = 1/4(X(n-1) + 2X(n) + X(n+1)$ where n is the hour number. They are then approximately equivalent to 2-hour averages. Missing data is denoted by an "M".

This appears to be the first paper which presents time series such as these. They clearly show that the model, which, statistically, looks very promising, has its exceptionally good and equally disappointing moments. The model as presently constructed has a number of strong points: among them a dispersion kernel that can respond in a physically realistic way to transients in wind direction, wind speed, source strength, and mixing-layer height, and which synthesizes area sources exceptionally well; and industrial inventory that estimates seasonal and daily shift patterns, based on an emission inventory procedure geared to a boiler-room superintendent; an objective, mixing-layer height-estimation technique, which, although suffering from the

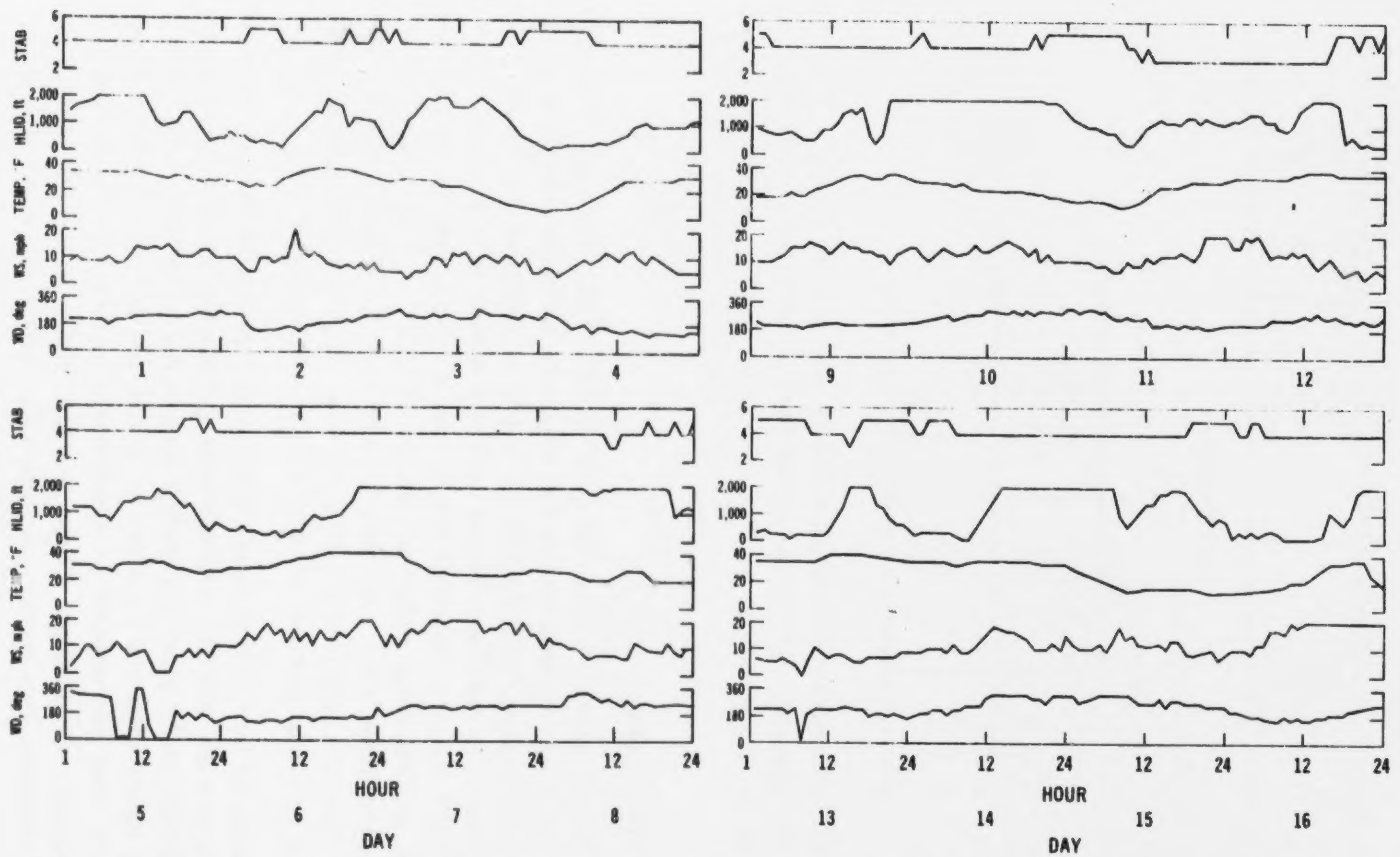

Figure 6-22. Stripchart of hourly values of (top to bottom ordinates) atmospheric stability classification, estimated mixing-layer height, temperature at Midway airport, and wind speed and direction, January 1 to 16, 1967.

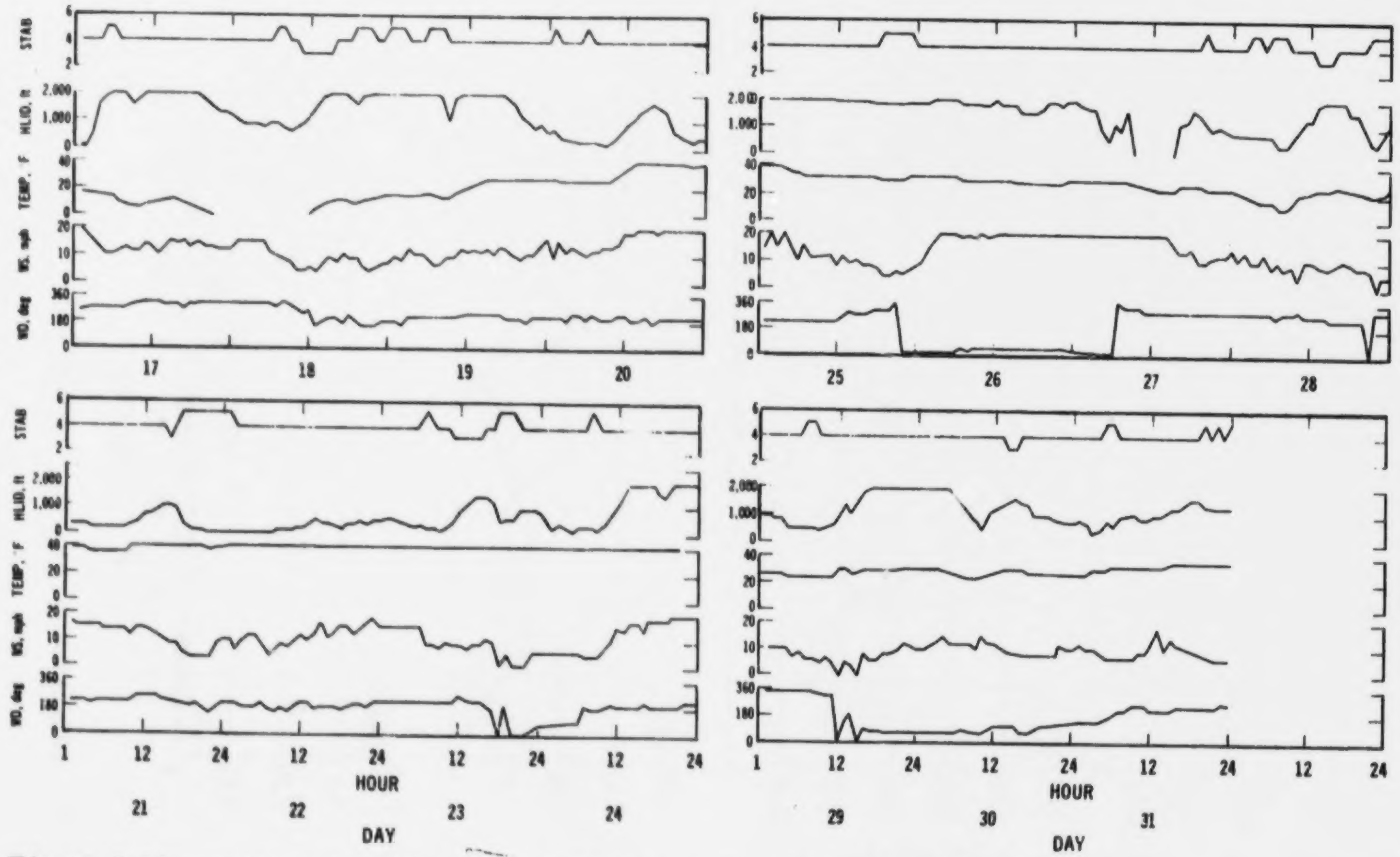

Figure 6-22 (continued). Stripchart of hourly values of (top to bottom ordinates) atmospheric stability classification, estimated mixing-layer height, temperature at Midway airport, and wind speed and direction, January 17 to 31, 1967.

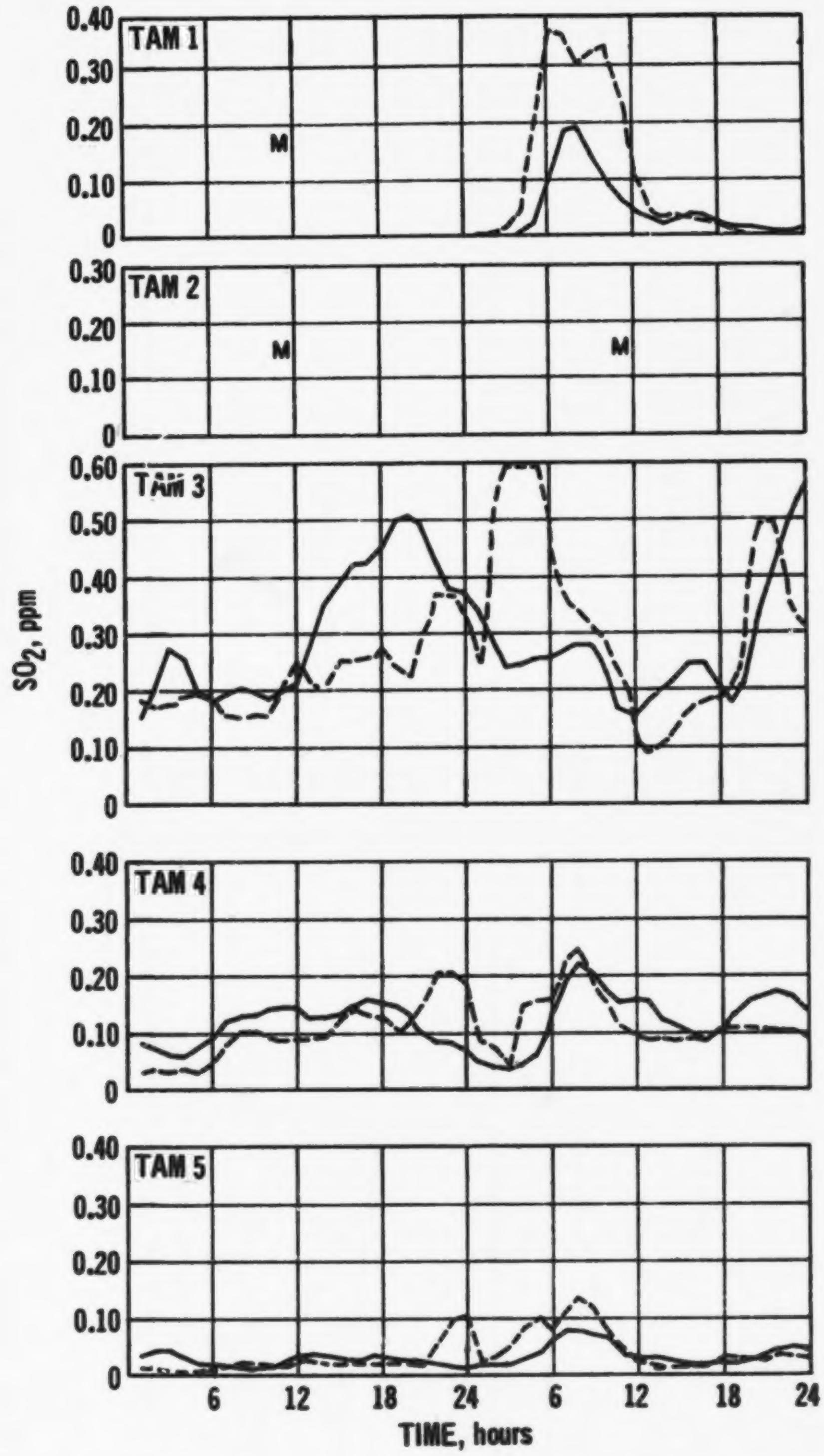

——— observed, - - - - - estimated M-missing data.

Figure 6-23. Sample of smoothed hourly values of SO_2 concentrations at TAM stations 1 to 5, January 1 and 2, 1967.

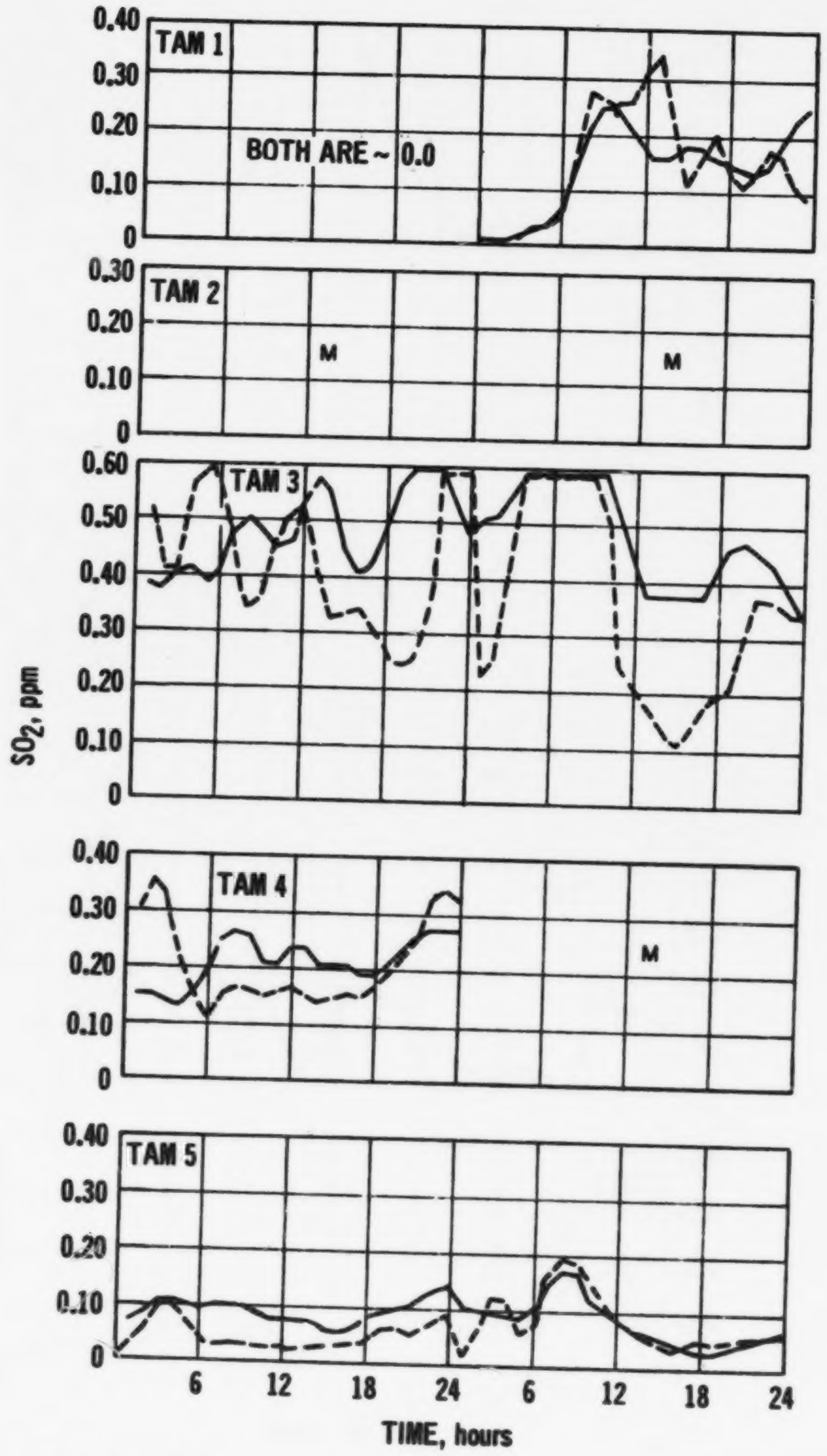

——— observed, - - - - estimated M-missing data.

Figure 6-23 (continued). Sample of smoothed hourly values of SO_2 concentrations at TAM stations 1 to 5, January 3 and 4, 1967.

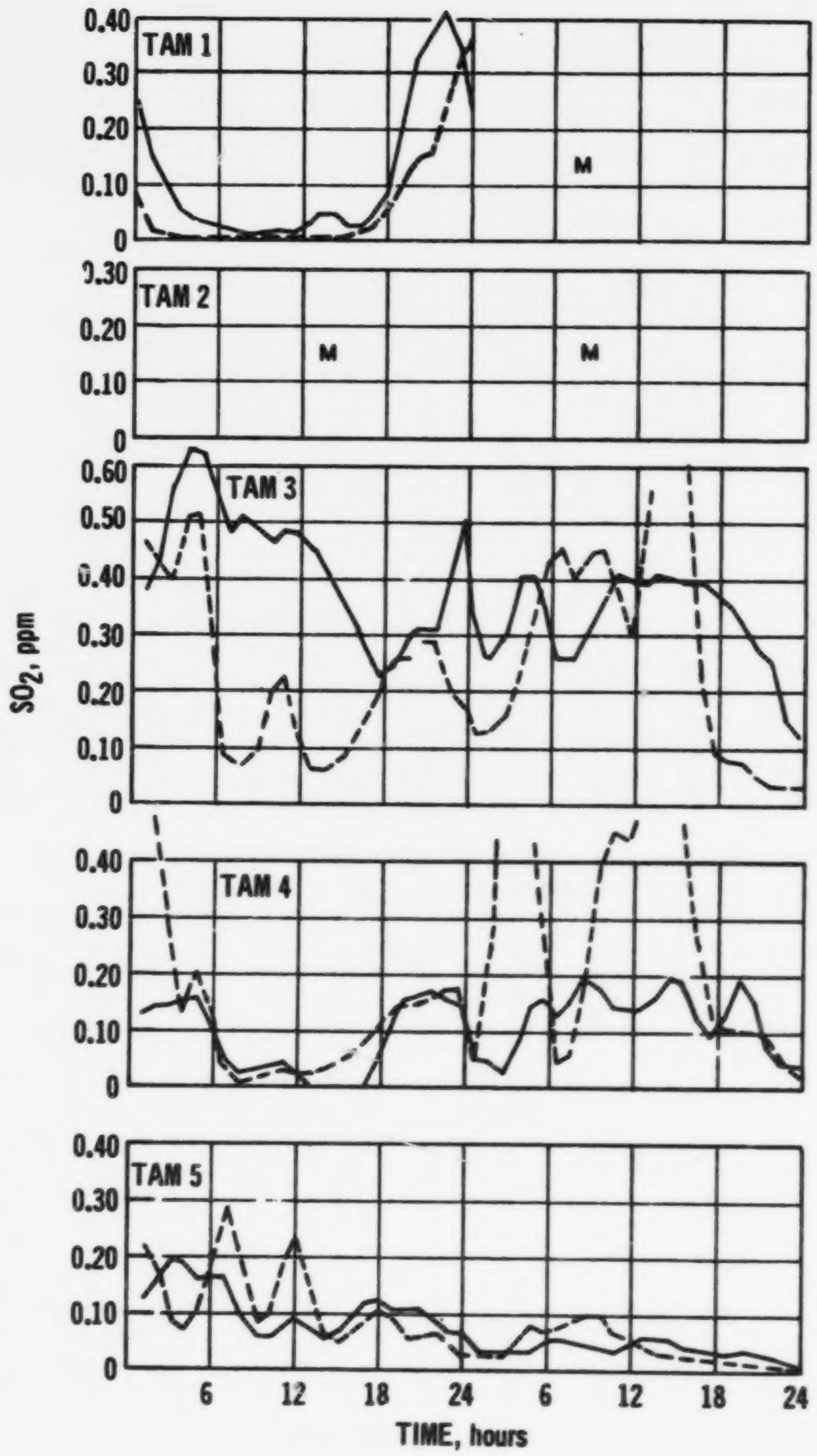

——— observed, - - - - estimated. M-missing.

Figure 6-23 (continued). Sample of smoothed hourly values of SO_2 concentrations at TAM stations 1 to 5, January 5 and 6, 1967.

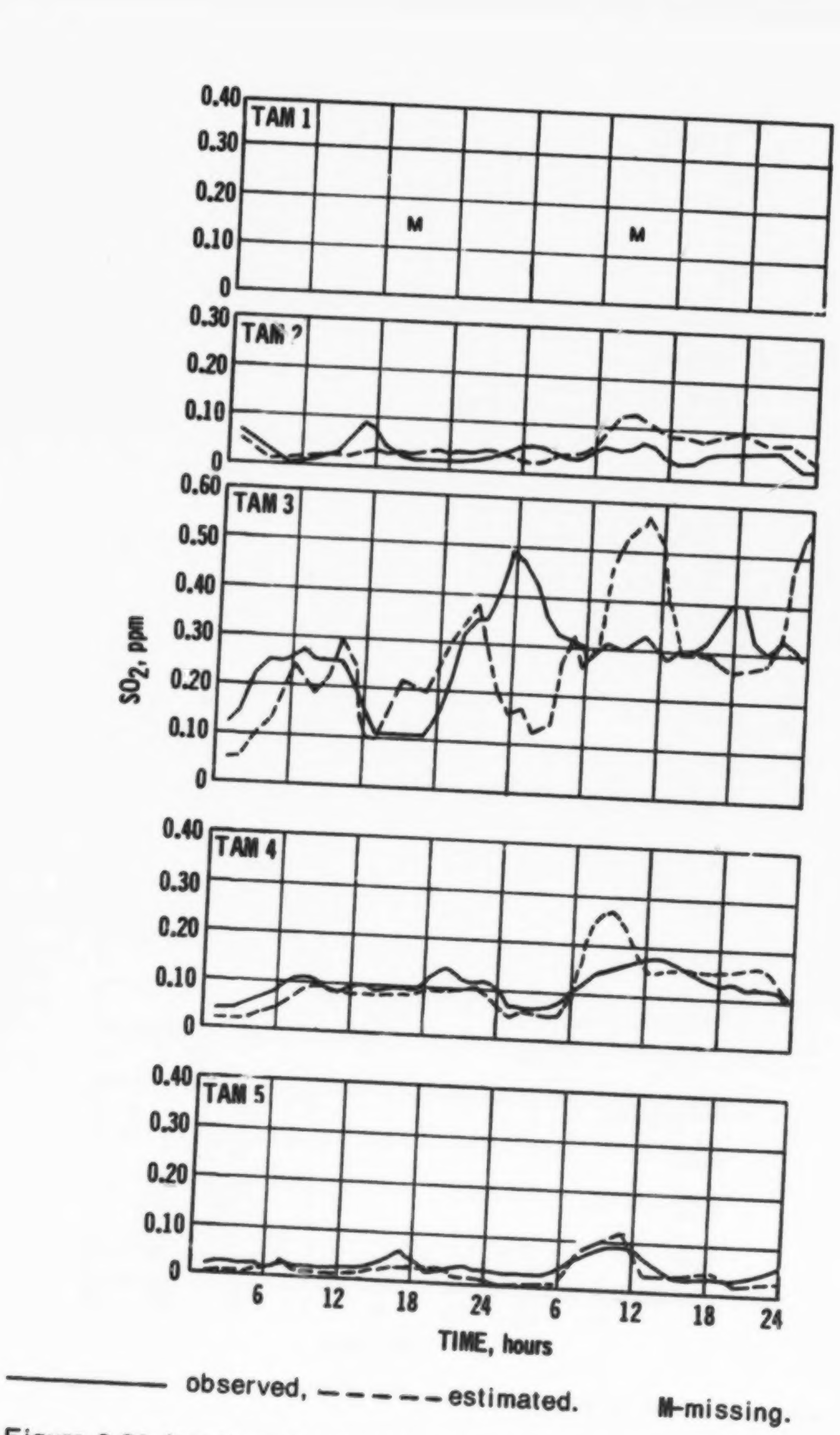

Figure 6-23 (continued). Sample of smoothed hourly values of SO_2 concentrations at TAM stations 1 to 5, January 7 and 8, 1967.

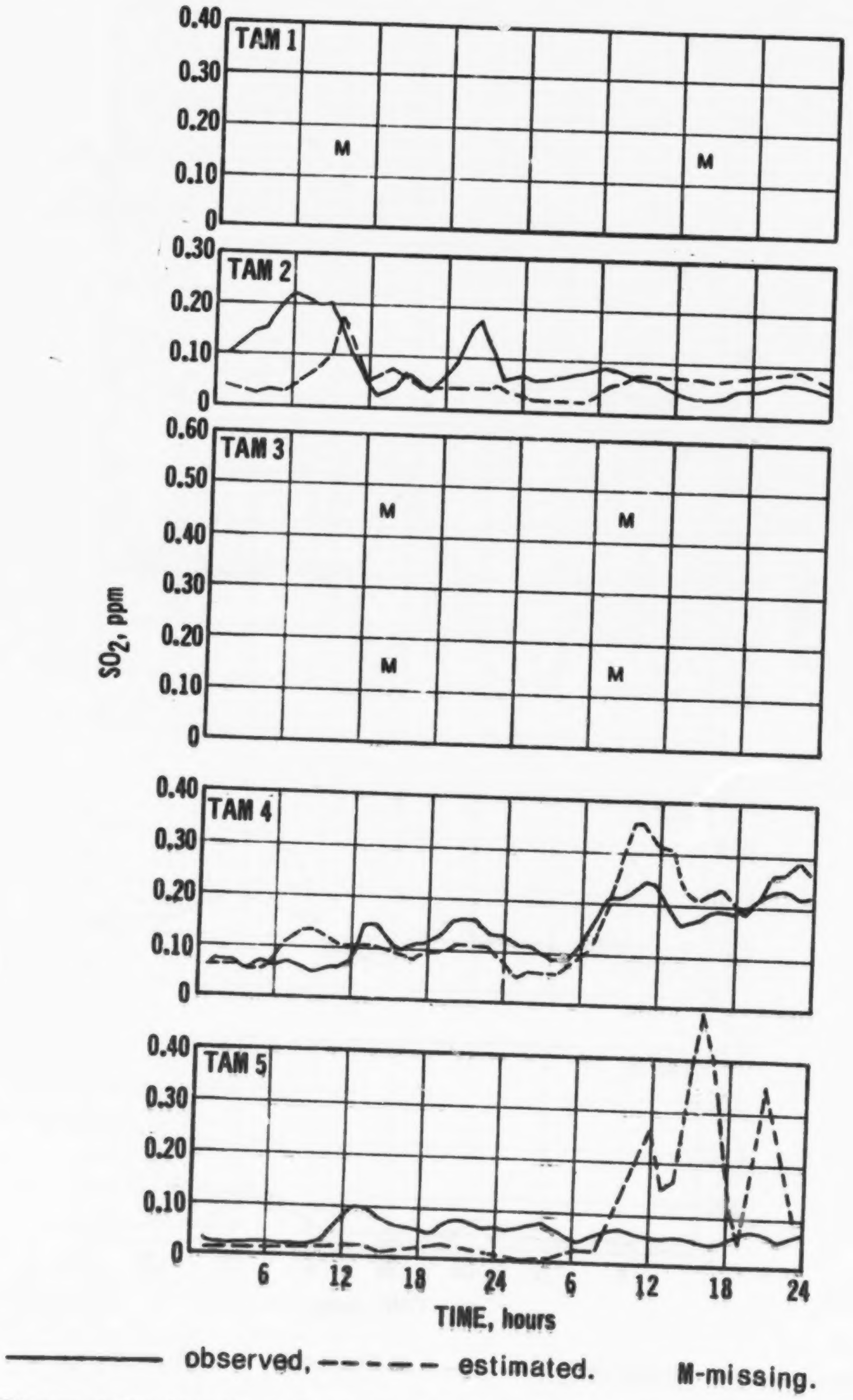

Figure 6-23 (continued). Sample of smoothed hourly values of SO_2 concentrations at TAM stations 1 to 5, January 9 and 10, 1967.

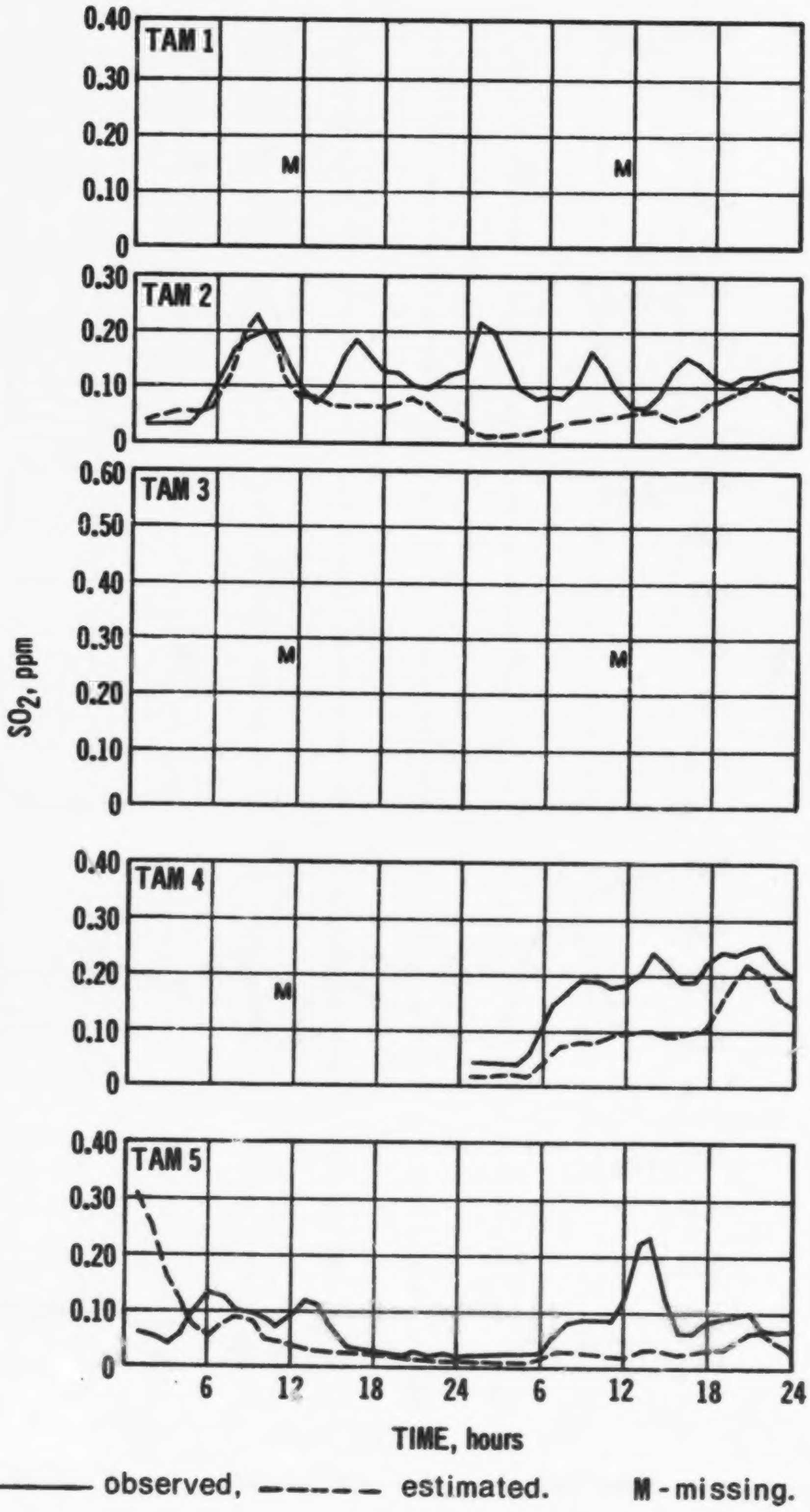

Figure 6-23 (continued). Sample of smoothed hourly values of SO_2 concentrations at TAM stations 1 to 5, January 11 and 12, 1967.

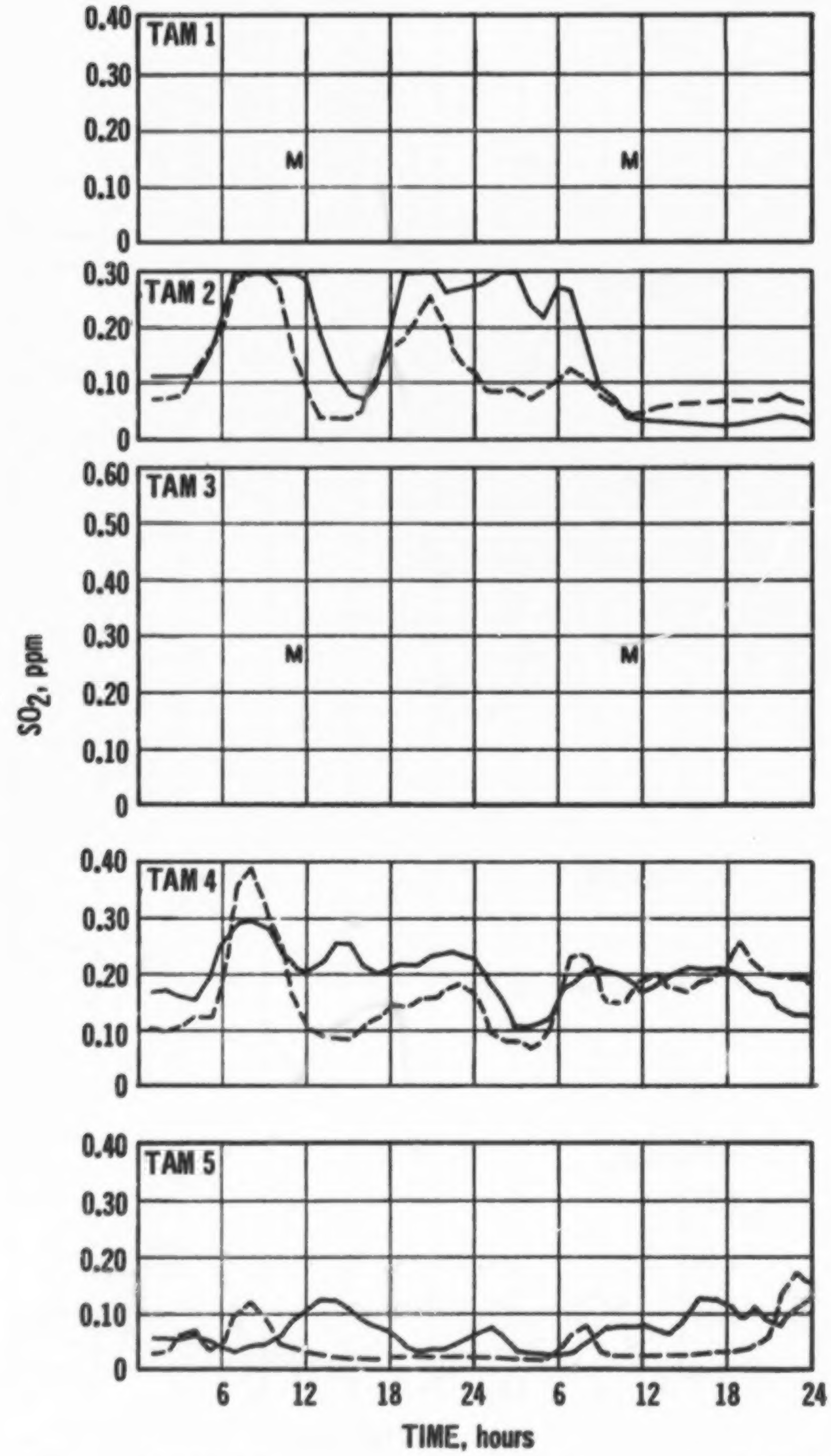

——— observed, – – – – estimated. M - missing.

Figure 6-23 (continued). Sample of smoothed hourly values of SO_2 concentrations at TAM stations 1 to 5, January 13 and 14, 1967.

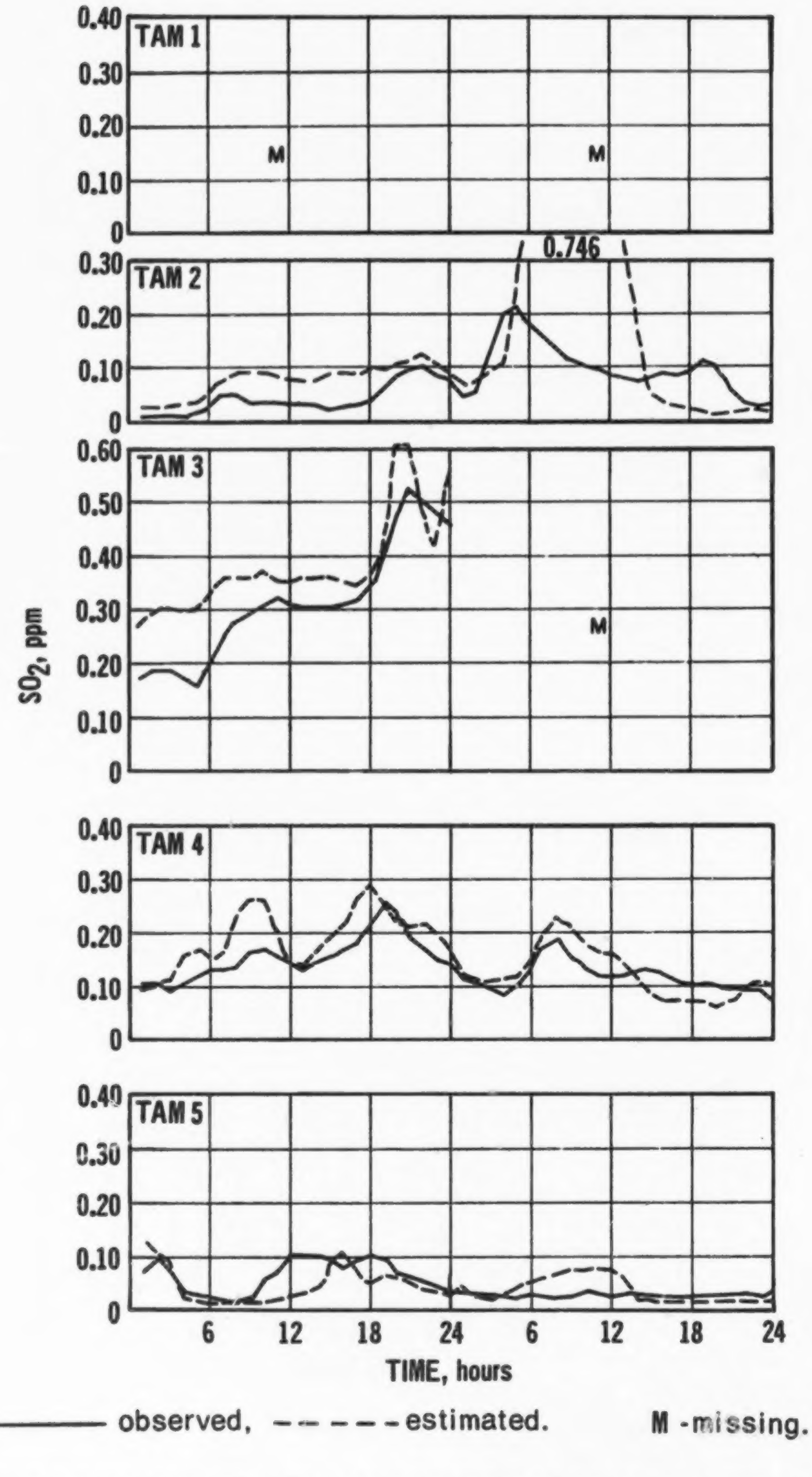

Figure 6-23 (continued). Sample of smoothed hourly values of SO$_2$ concentrations at TAM stations 1 to 5, January 15 and 16, 1967.

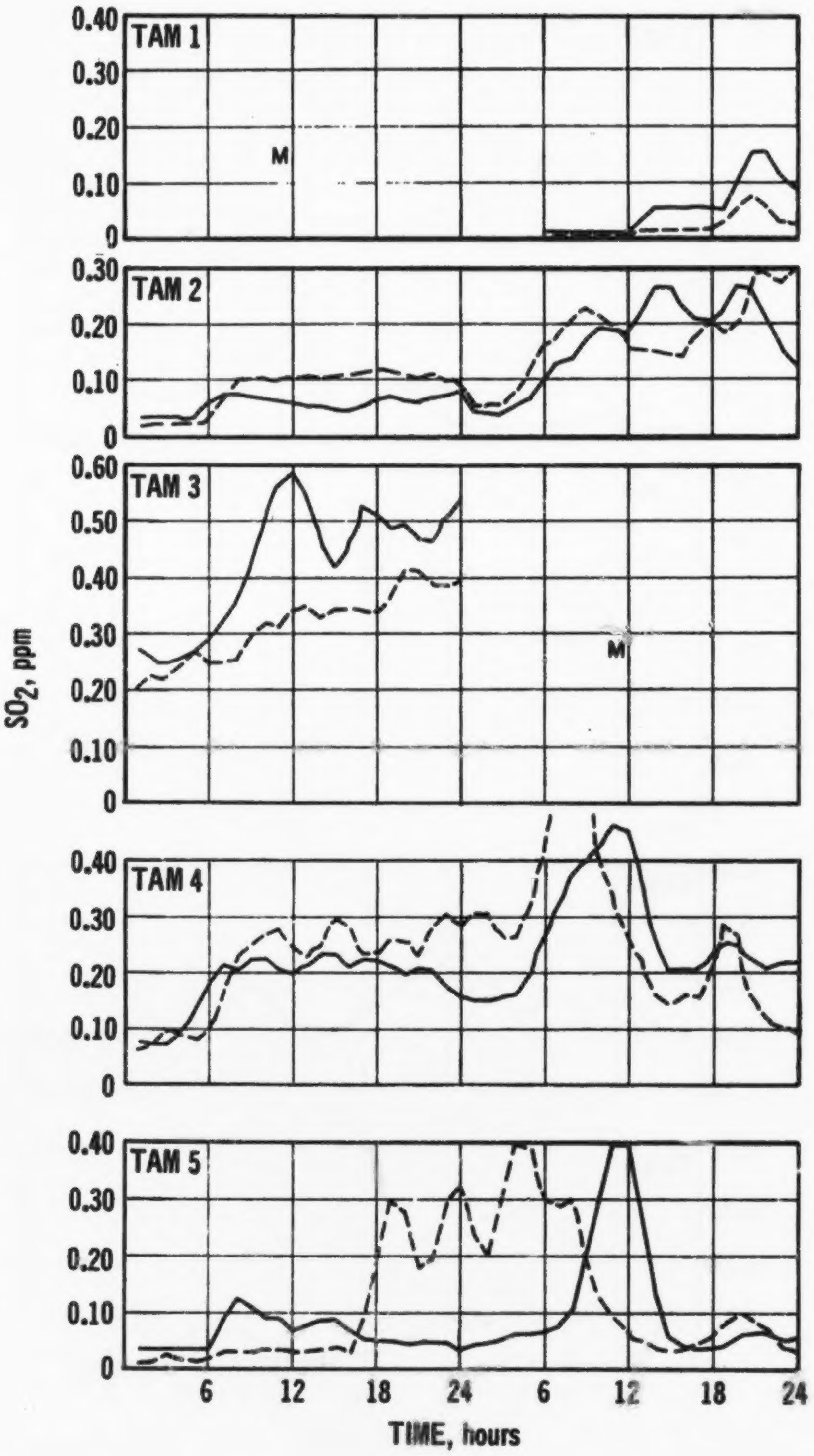

observed, - - - - - estimated. M - missing.

Figure 6-23 (continued). Sample of smoothed hourly values of SO_2 concentrations at TAM stations 1 to 5, January 17 and 18, 1967.

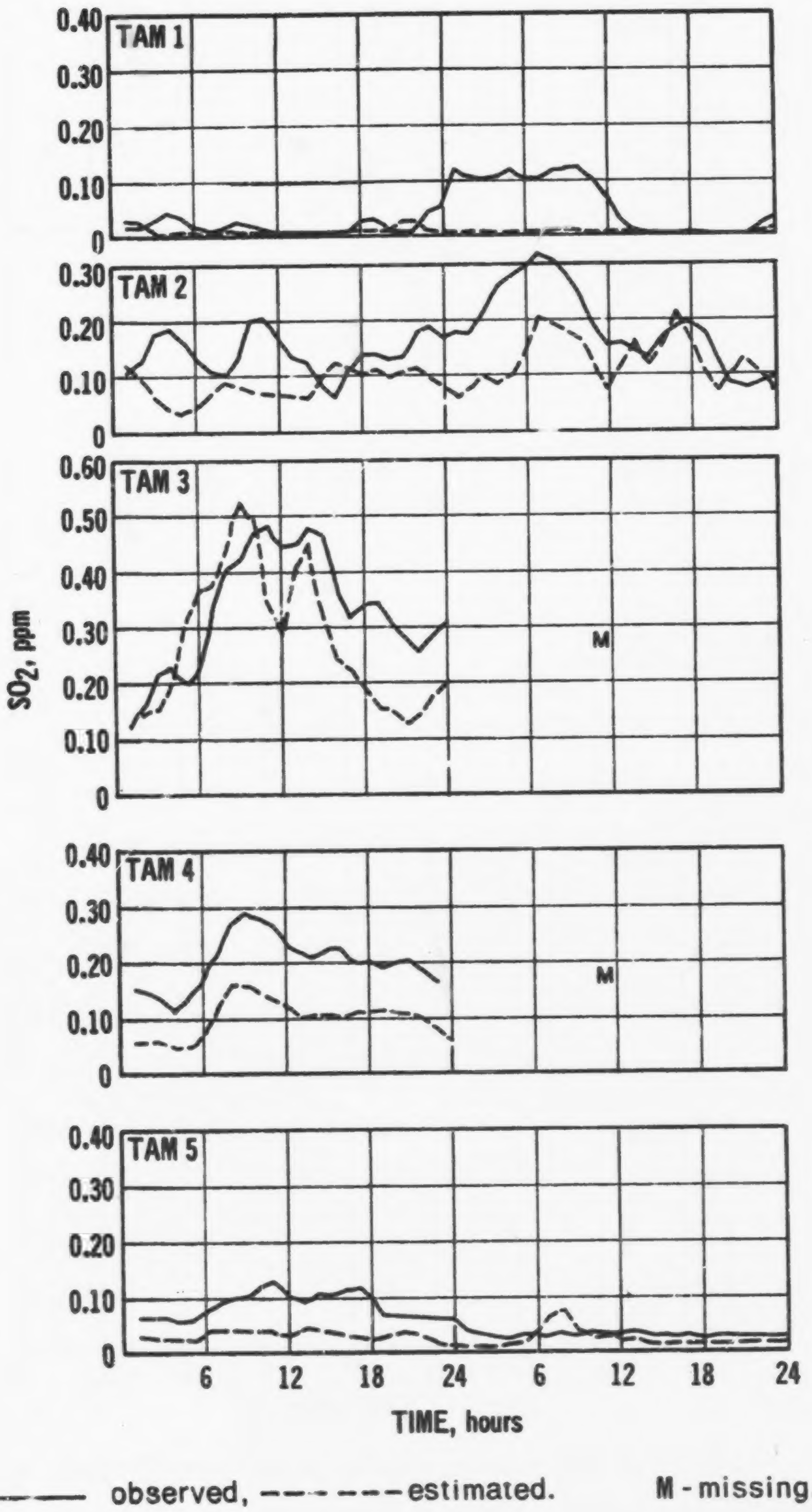

Figure 6-23 (continued). Sample of smoothed hourly values of SO$_2$ concentrations at TAM stations 1 to 5, January 19 and 20, 1967.

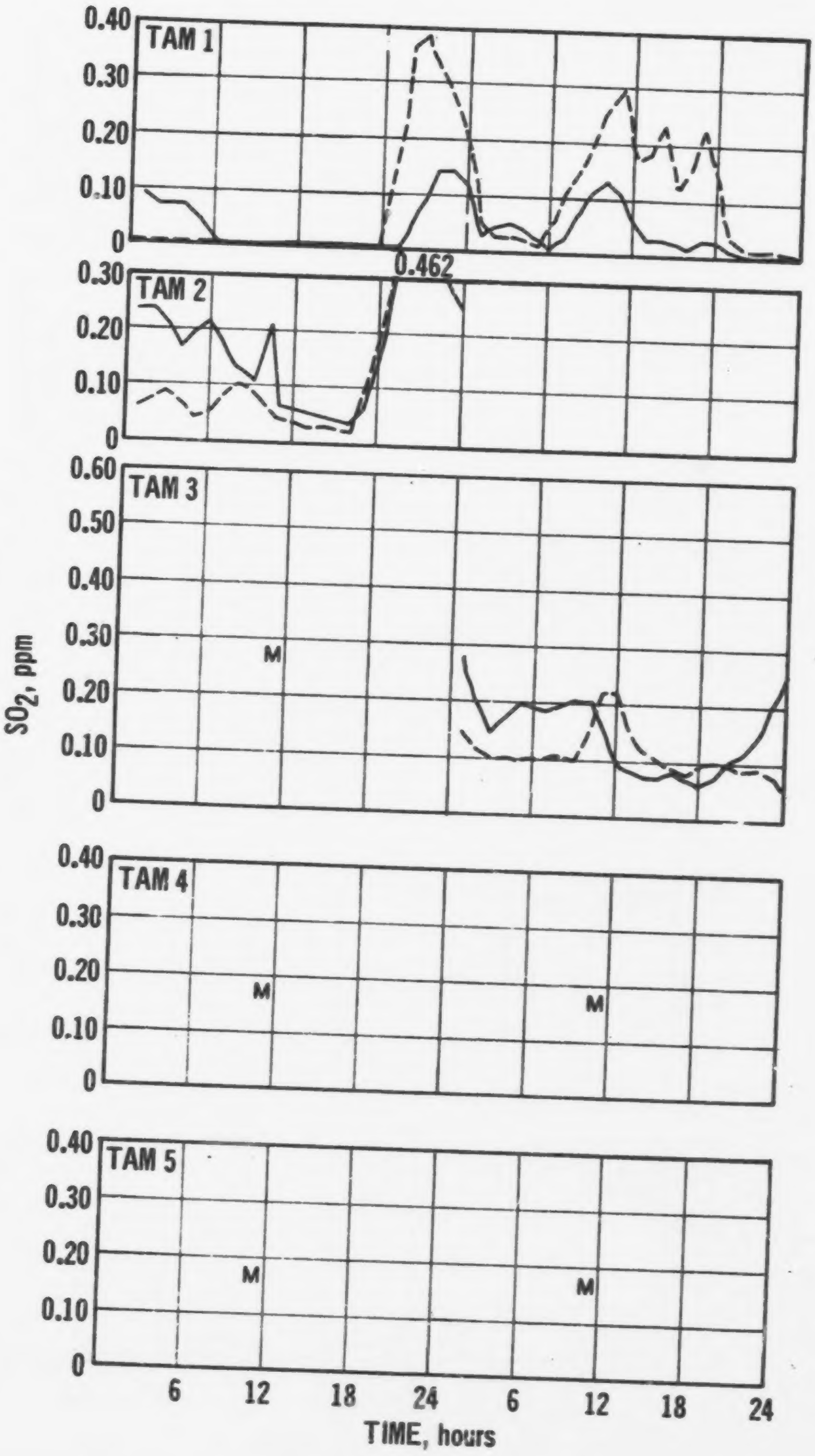

———— observed, – – – – – estimated. M - missing.

Figure 6-23 (continued). Sample of smoothed hourly values of SO_2 concentrations at TAM stations 1 to 5, January 21 and 22, 1967.

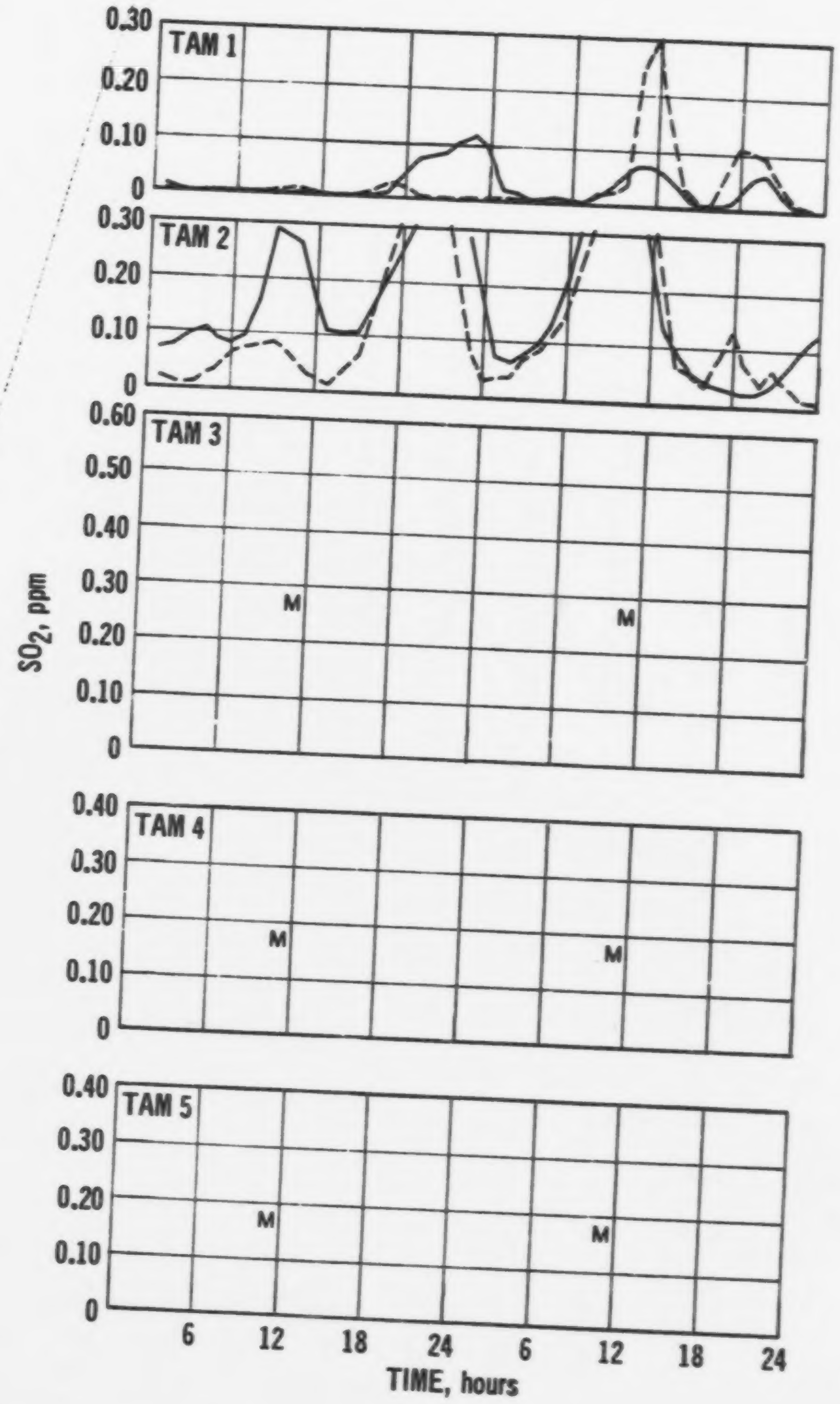

————observed, – – – – –estimated. M - missing.

Figure 6-23 (continued). Sample of smoothed hourly values of SO_2 concentrations at TAM stations 1 to 5, January 23 and 24, 1967.

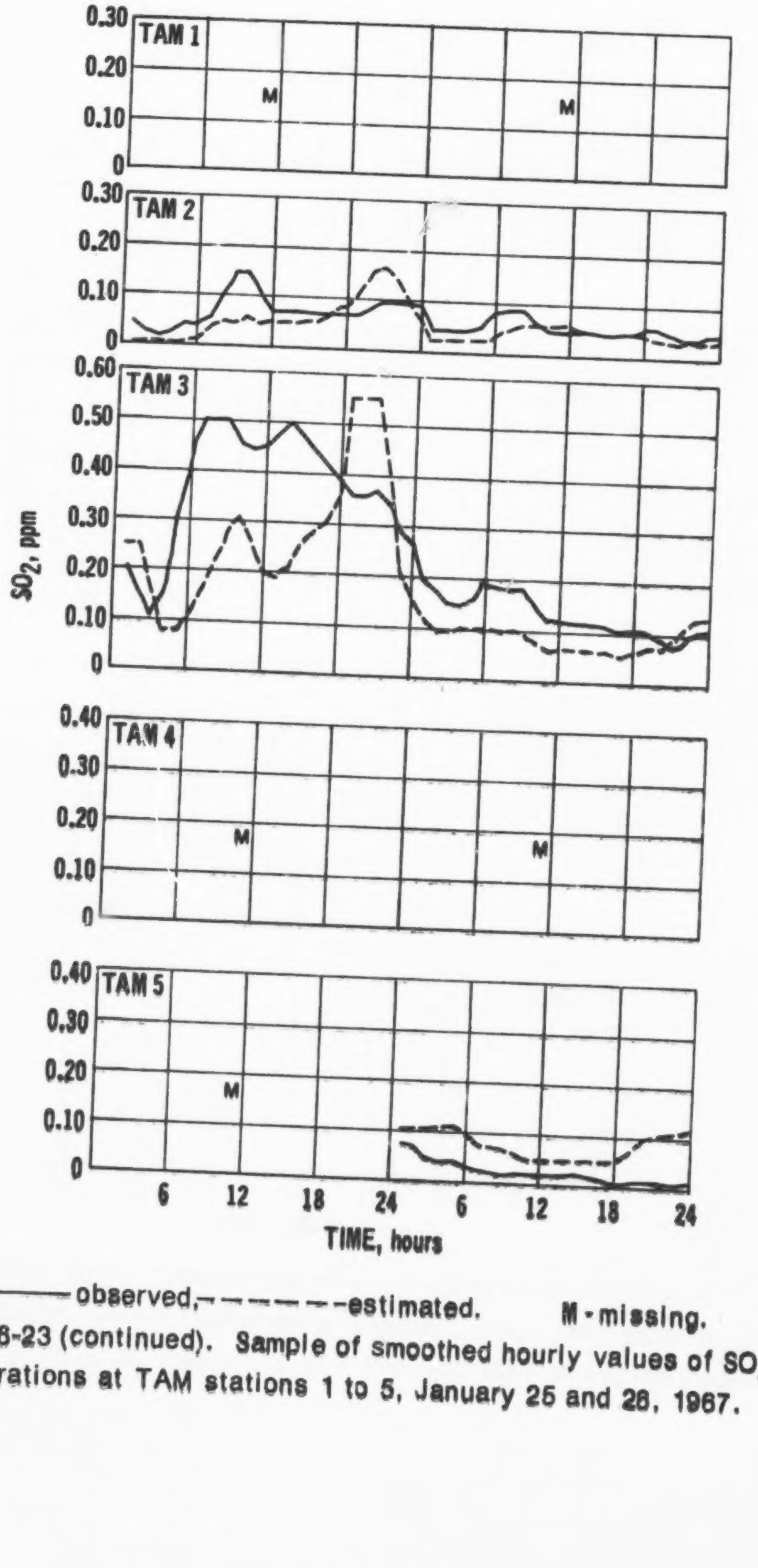

——————observed,– – – – – – –estimated. M - missing.

Figure 6-23 (continued). Sample of smoothed hourly values of SO_2 concentrations at TAM stations 1 to 5, January 25 and 26, 1967.

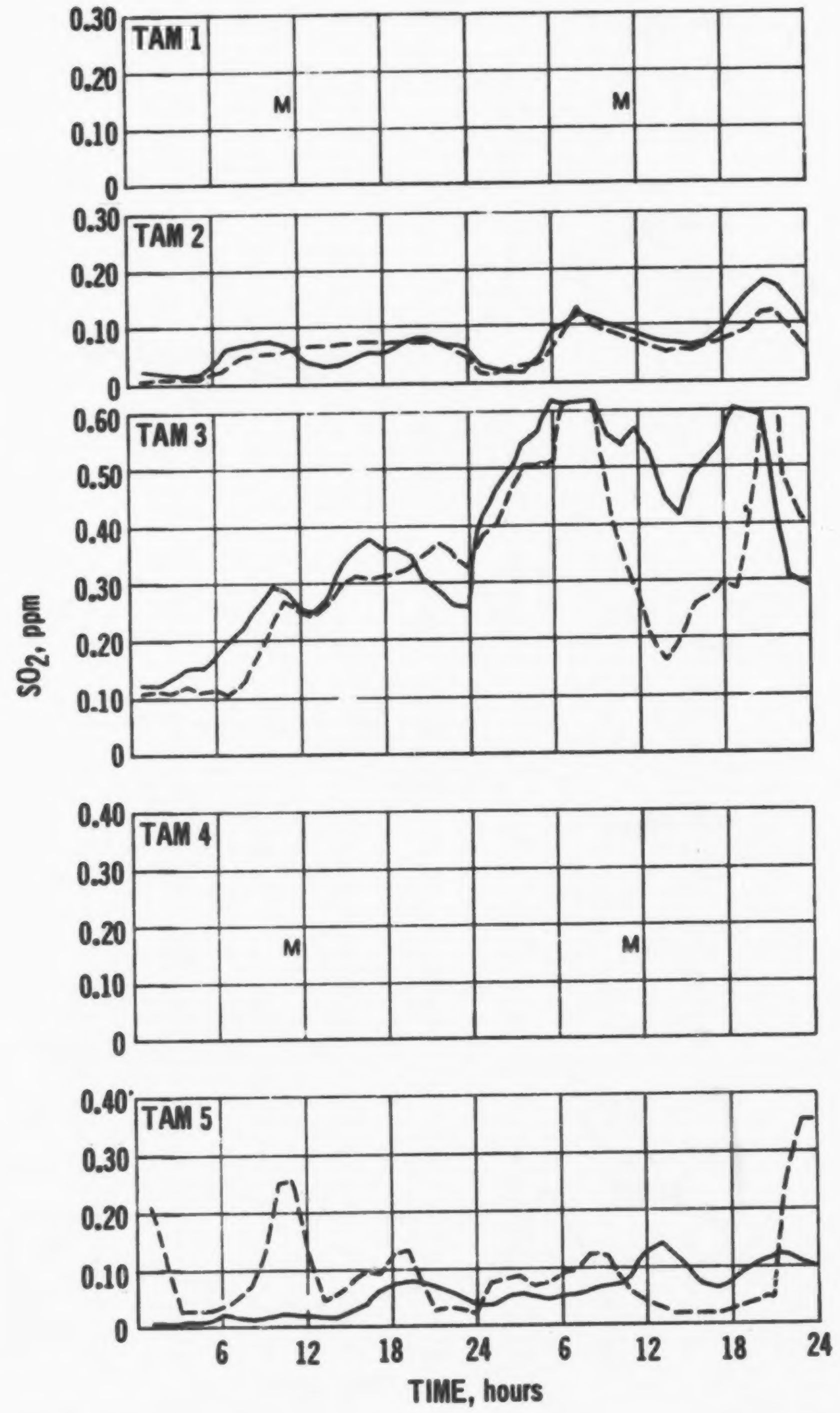

————observed,– – – – – –estimated. **M** - missing.

Figure 6-23 (continued). Sample of smoothed hourly values of SO_2 concentrations at TAM stations 1 to 5, January 27 and 28, 1967.

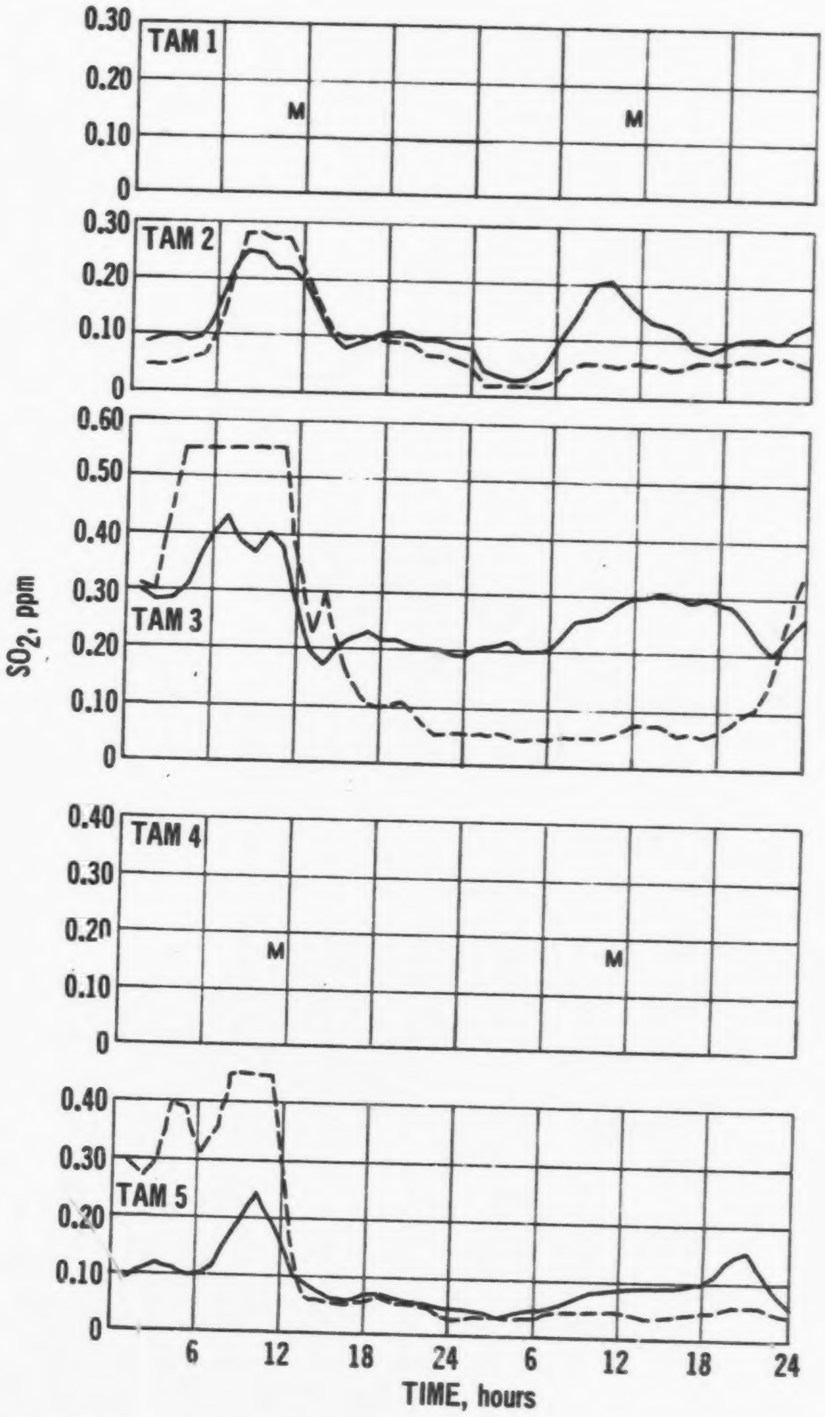

————observed, – – – – –estimated   M - missing.

Figure 6-23 (continued). Sample of smoothed hourly values of SO$_2$ concentrations at TAM stations 1 to 5, January 29 and 30, 1967.

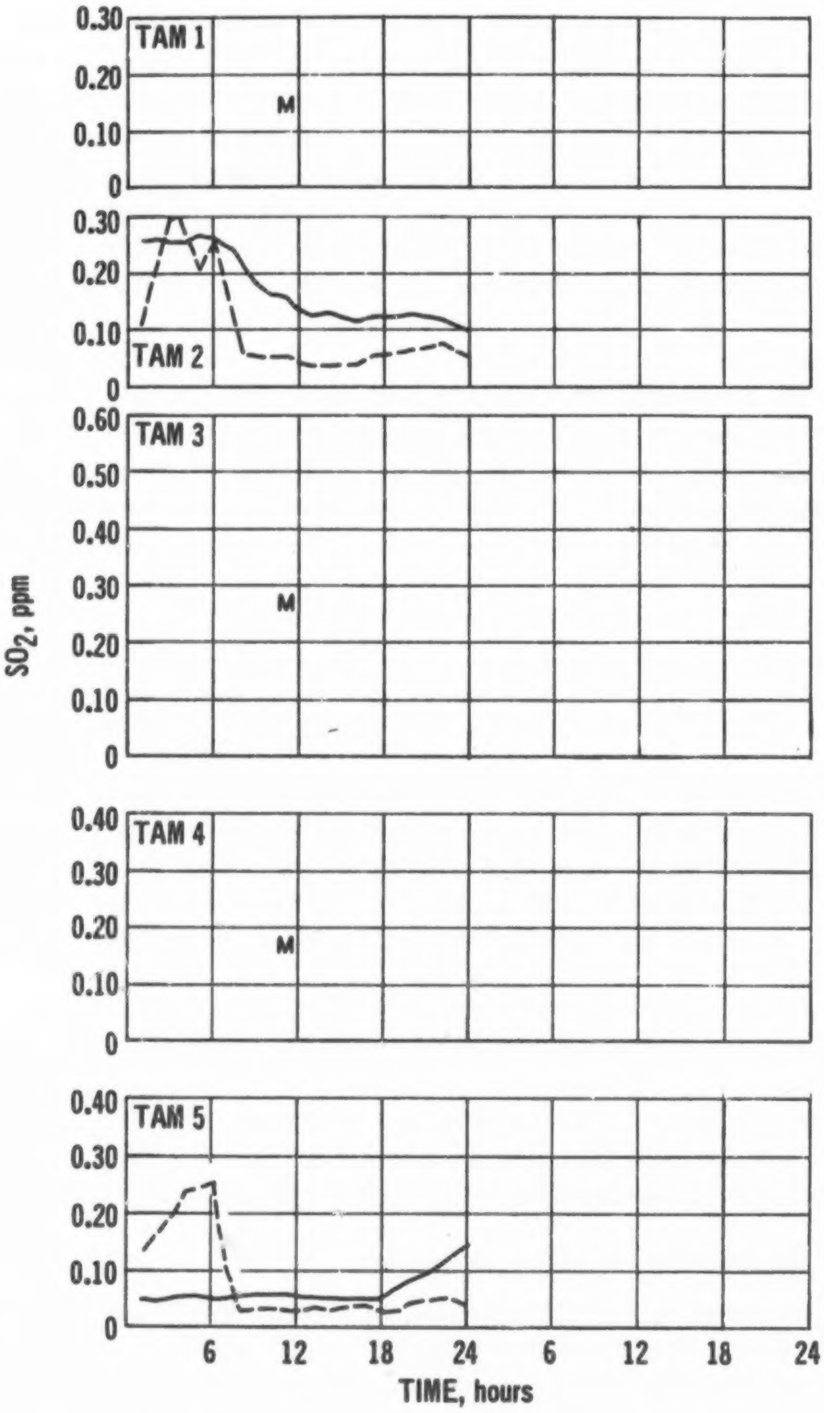

———— observed, – – – – – estimated. M - missing.

Figure 6-23 (continued). Sample of smoothed hourly values of SO$_2$ concentrations at TAM stations 1 to 5, January 31, 1967.

obvious problems of extrapolating vertical temperature profiles over distances greater than 100 miles, correlates well with subjective estimates of diurnal trends; and an overall system of data storage, retrieval, and analyses designed to meet the operational requirements of an urban air pollution control administration. Weak points are also evident; most significantly, a poor determination of the wind field, which should be improved by deriving an hourly wind map but which, in any event, is limited in Chicago by the accuracy of the TAM aerovanes. Under certain circumstances the model is also extremely sensitive to meteorological parameters—both observed and derived. (For example, when the height of the mixing-layer approaches the physical stack-height of a major power plant, the calculation of ground-level concentrations due to that plant may vary by a factor of 10 or more, depending upon whether the plume is assumed to travel above or to be trapped beneath the lid.) There are also further refinements that should be made in the model: major point sources and area sources outside the city limits must be included in the emission inventory; the local effect of the topography of city center on the mixing-layer height and the effective atmospheric stability should be included; plume rise formulations might be modified to synthesize a gradually ascending plume; the run-time can be greatly reduced if the equations can be integrated analytically.

The sample strip charts give clear evidence of many of these items. The results, magnitudes, and trends appear to be sufficiently consistent to test selected hypotheses, about both the model and the air pollution meteorology of the urban area. The following is a list of topics for which the hourly time series of meteorological and air quality variables give evidence.

The Importance of Residential and Commercial Heating Sources and Low-Lying Industrial Sources

The importance of residential and commercial heating sources and low-lying industrial sources can be seen easily by an overall comparison of ambient SO_2 levels at the five stations with emission maps (Figures 6-1 and 6-2). The model predicts station means for January to within plus or minus 20 percent.

The Importance of Wind Direction

January 9 and 10 at TAM 4 are days of almost constant temperature (28°F), wind speed (15 mph), and mixing-layer height (2000 ft). Yet the SO_2 level rose steadily from below 0.1 ppm on January 9, to 0.2 on the 10th, as The wind swung from 220° (comparatively low residential emissions) to 270° (significantly higher residential emissions) to 300° (high residential emissions plus the distant industrial area). On the same two days, TAM 2 saw approximately the reverse trend of upwind source concentration. TAM 3, on January 27, responded to a gradual shift in wind direction from NE to NW.

Large Point Sources are Assumed to Touch Ground – But Do Not

The Crawford power plant (III in Figure 6-1), as opposed to others with different stack configurations, is regularly predicted to reach ground level whenever its plume centerline passes over TAM 5 (4 mi south), but it is consistently barely detected (for example, TAM 5, Jan. 5, 10, 27, 29).

Large Point Sources Trapped Beneath a Lid Cause Very High Concentrations Downwind

For example: TAM 1, Jan. 1, 4, 5
TAM 3, Jan. 15 (note dropping lid had little difference on TAM 2)
TAM 2, Jan. 21, 23

Periods of Very Low Winds

Winds of $\leqslant$ 5 mph occur on the following occasions:

Jan 3 (0300-0800) – 5 (1300-1600) – 13 (0600-0900)
18 (1000-1300) – 21 (2000-2200) – 23 (1800-2400)
24 (0000-0900) – 25 (1800-2400)

Almost uniformly, the model yields satisfactory predictions of trends and magnitudes of SO_2 levels during these critical periods of low winds and potentially high SO_2 levels.

Transition Hours–Sunrise and Sunset

From 0600 to 1000 and from 1500 to 1900 are diurnal periods of significant change in the dispersive capacity of the urban atmosphere. During these periods the model is influenced by changes in atmospheric stability and mixing-layer height. The model appears capable of simulating the corresponding diurnal trends in SO_2 level; although, occasionally the sensitivity of the relationship between assumed lid height and physical stack height of upwind point sources causes large discrepancies between predicted and observed concentrations (example TAM 4, Jan. 6).

The Emission Inventory

This should be extended beyond the city limits. For example, TAM 5 is consistently under-predicted when winds are from the SW. The receptor is 4 mi from the Cicero residential/commercial area. Approximately 20 mi to the southwest is the Romeoville Power Plant which regularly emits more than 2 x 10^6 pounds SO_2 per hour. For a southwest wind at 10 mph, the plume concentration on the ground at TAM 5 is approximately 0.03 ppm with no lid present. Examples of under-predictions at TAM 5 during SW winds:

January 11, 12, 13 (midday) January 9, 19 (all day)

Abrupt Changes in Windspeed and Direction

On January 23 (1800), January 24 (0700), January 28 (2300), and January 29 (1300) abrupt changes in wind speed and direction were simulated with acceptable accuracy.

REFERENCES

1. Croke, K. and A. Kennedy. An Air Quality Control Program for Large Industrial Sources in the City of Chicago. Presented at 62d Annual Meeting of the Air Pollution Control Association. New York. June 22-26, 1969.
2. Koogler, J. B. *et al* A Multivariable Model for Atmospheric Dispersion Predictions. J. Air Pollution Control Assoc. *17*:211-214, April 1967.
3. Turner, D. B. A Diffusion Model for an Urban Area. J. Appl. Meteorol. 3(1):83-91, February 1964.
4. Clarke, J. F. A Simple Diffusion Model for Calculating Point Concentrations from Multiple Sources. J. Air Pollution Control Assoc. *14:*347-352, September 1964.
5. Croke, E. J. *et al.* Chicago Air Pollution System Model; Second Quarterly Progress Report. National Center for Air Pollution Control, Chicago Dept. of Air Pollution Control, Argonne National Laboratory. Argonne, Ill. ANL/ES-CC-002. May 1968. 160p.
6. Kennedy, A. and J. Anderson. A Computerized Information and Computation System for Environmental Studies. Presented at 62d Annual Meeting of the Air Pollution Control Association. New York. June 22-26, 1969.
7. Pasquill, F. The Estimation of Diffusion from Meteorological Data. In: Atmospheric Diffusion. London, D. Van Nostrand Co. Ltd., 1962. p. 179-204.
8. Slade, D. Estimates of Dispersion from Pollutant Releases of a Few Seconds to 8 Hours in Duration. Air Resources Laboratories. Washington, D. C. Technical Note 39-ARL-3. 1966.
9. Croke, E. J. *et al.* Chicago Air Pollution System Model; Fourth Quarterly Progress Report. National Center for Air Pollution Control, Chicago Dept. of Air Pollution Control, Argonne National Laboratory. Argonne, Ill. ANL/ES-CC-004. March 1969.
10. Private communication with D. B. Turner. Bureau of Criteria and Standards, National Air Pollution Control Administration. 1968.
11. McElroy J. L. and F. Pooler, Jr. St. Louis Dispersion Study, Vol.II Analysis. National Air Pollution Control Administration. Arlington, Va. Publication Number AP-53. December 1968. 61 p.
12. Cramer, H. E. *et al.* Meteorological Prediction Techniques and Data System. Geophysics Corporation of America. Bedford. Mass. GCA Technical Report Number 64-3-G. March 10, 1964. 252 p.
13. Bowden, K. F. Horizontal Mixing in the Sea Due to a Shearing Current. J. Fluid Mech. *21*:83-95. January 1965.
14. Cramer, H. E. and R. K. Dumbauld. Experimental Designs for Dosage Predictions in CB Field Tests. Geophysics Corporation of America. Bedford, Mass. GCA Technical Report Number 68-17-G. 1968
15. Carson, J. E. and H. Moses. The Validity of Currently Popular Plume Rise Formulas. In: Proceedings of the USAEC Meteorological Information Meeting, Chalk River Nuclear Laboratories, September 11-14, 1967. Mawson, C.A. (ed.). Atomic Energy of Canada, Ltd. Chalk River Ontario. Report Number AECL-2787. 1967 p. 1-20.
16. DeMarrais, G. A. Wind-speed Profile at Brookhaven National Laboratory. J. Meteorol. *16*(2):181-190, April 1959.
17. Carpenter, S. G. *et al.* Report on Full-Scale Study of Plume Rise at Large Electric Generating Stations. Presented at 60th Annual Meeting of the Air Pollution Control Association. Cleveland, June 11-16, 1967.
18. Turner, D. B. Workbook of Atmospheric Dispersion Estimates. National Center for Air Pollution Control. Cincinnati, Ohio. PHS Publication Number 999-AP-26. 1967. 84 p.
19. Croke, E. J. *et al.* Chicago Air Pollution System Model; Third Quarterly Progress Report. National Center for Air Pollution Control, Chicago Dept. of Air Pollution Control, Argonne National Laboratory. Argonne, Ill. ANL/ES-CC-003. October 1968. 254 p.

20. Moses, H. Mathematical Urban Air Pollution Models. National Center for Air Pollution Control, Chicago Dept. of Air Pollution Control, Argonne National Laboratory. Argonne, Ill. ANL/ES-RPY-001. April 1969. 69 p.
21. Marsh, K. J. and V. R. Withers. An Experimental Study of the Dispersion of the Emissions from Chimneys in Reading - III. The Investigation of Dispersion Calculations. Atmos. Environ. *3*(3):281-302, May 1969.
22. Croke, E. J. *et al.* Chicago Air Pollution System Model; First Quarterly Progress Report. National Center for Air Pollution Control, Chicago Dept. of Air Pollution Control, Argonne National Laboratory. Argonne, Ill. ANL/ES-CC-001. February 1968. 106 p.

ACKNOWLEDGMENT

The authors of this paper wish to acknowledge with gratitude the significant contributions of Messrs. J. Norcs and L. Conley of Argonne National Laboratory and Mr. J. Lin and the late Mr. R. Votruba of the Chicago Department of Air Pollution Control.

The advice and counsel of Mr. D. B. Turner of the National Air Pollution Control Administration, Mr. H. Moses of Argonne National Laboratory, and the late Dr. B. Davidson of New York University were also of great value to the atmospheric dispersion model development program.

APPENDIX – GLOSSARY OF SYMBOLS

C	concentration of pollutant at a receptor point
G_n	derivative of discrete transfer function representing value of curve at point of intersection, n
H	effective stack height (centerline of plume)
H_m	height of mixing layer, lid height
H_s	actual, physical height of stack
ΔH	plume rise height
i	atmospheric stability class
K	constant, conversion coefficient
L^P	process load
L^S	space-heating thermal load
m	number fundamental time intervals over which discrete transfer function is integrated
n	iteration integer; or "look back" time
P	exponent describing stability class
$Q(t)$	piecewise constant pollutant release function
r	dimensionless number used to simplify Equation (8)
T	delay time = (t - t')
$\overline{T}$	puff travel time
U	steady mean wind velocity
$[u_j]_1^m, [v_j]_1^m.$	constant series for variations in horizontal wind velocity
V	number of correct estimates
V'	value of V predicted from a different model
$\chi(t,t')$	concentration at time t, due to instantaneous release, Q at time t' and position (0,0,0)
x	horizontal wind distance, downwind
y	horizontal wind distance, crosswind
z	vertical wind distance
Δz	approximate, of area-source thickness

Z	effective source height
a	parameter used to define σ in terms of T, units: $\frac{\text{length}}{\text{time}}$
δ_x, δ_y	upwind distances
Δ	fundamental time increment
σ_h	horizontal dispersion coefficient
$\sigma_h(t)$	dispersion coefficient as function of time
σ_x	dispersion coefficient in x-direction

ABSTRACT

Analyses of tracer-dispersion data in Japan, especially those of vertical concentration profiles, indicate that the tracer-cloud height generally increases with the downwind distance. The increase is larger over an urban area than a rural area. When the tracer crosses over a hill, it rises remarkably. Over a complicated topography the rise of tracer-cloud is larger than over a flat terrain, a circumstance well reflected in the surface concentration pattern. When the tracer-cloud height varies greatly with the downwind distance, the surface concentration decreases uniformly downwind in spite of the elevated source.

AUTHOR

***SHIN'ICHI SAKURABA** is Chief of the Applied Meteorology Laboratory, Meteorological Research Institute, Tokyo. He is currently involved with tracer studies of medium range atmospheric dispersions in littoral, industrial areas of Japan, in connection with the nation's air pollution control program. In other meteorological work he has been concerned with atmospheric turbulence up to the 500-meter level and plume rise from a high stack*

7. SENSITIVITIES OF AIR QUALITY PREDICTION TO INPUT ERRORS AND UNCERTAINTIES

SHIN'ICHI SAKURABA*

Meteorological Research Institute, Tokyo

INTRODUCTION

In earlier dispersion-data analyses, the height of the tracer cloud was usually assumed to be constant; this frequently resulted in an over-estimate of the vertical dispersion parameter, especially over an urban area or a sloped terrain. When vertical concentration profile data are available at one or two points downwind, tracer-cloud height can be estimated from the surface-concentration analysis. Some dispersion data in Japan are analyzed along this line

RELEASE TIME AND SAMPLING TIME IN DETACHED PLUME EXPERIMENT

In field studies of atmospheric dispersion made in urban areas of Japan, the drum-impactor was used at two points downwind to measure the travel time of the tracer cloud, the time-concentration curve and eventually the total time, T_D, required for the passage of a detached tracer-plume. In these experiments the sampler, which measured the concentration, was actuated before the dispersing tracer arrived and was deactivated after the last of the tracer was assumed to have passed, so the real sampling time, T, of the sampler is usually equal to T_D. However T_D or T is not always equal to the release time, τ, of tracer.

Table 7-1 shows the result of experiments in 1968.

**In collaboration with M. Moriguchi and I. Yamazi*

Table 7-1. COMPARISON OF RELEASE TIME, τ, AND TOTAL TIME T_D OF DETACHED PLUME DISPERSION[a]

Location of experiment	Number of experiments	Frequency		
		$T_D = \tau$	$T_D > \tau$	$T_D < \tau$
Toyama	8	5	3	0
Wakayama	8	5	3	0
Oita	13	5	1	7
Total	29	15	7	7

[a] Japan, 1968.

Here τ was usually 30 min and $T_D = \tau$ shows the case for $|T_D - \tau|$ smaller than 5 min. It is noteworthy that the total frequency of $T_D > \tau$ is the same as that of $T_D < \tau$, though the total number of cases is small.

Figures 7-1 and 7-2 show the time-concentration curves at x = 2.5 km and x = 5.0 km respectively, x being the downwind distance. τ is 27.5 min and the source height, *h*, is 150 meters (m) The ordinate is 1-minute concentrations in relative units and the abscissa is time. The increase of T_D with the downwind distance is small. These cases are listed as $T_D = \tau$ in Table 7-1.

Figures 7-3 and 7-4 show the examples of $T_D > \tau$ when τ is 26 min and *h* = 200 m. In Figure 7-3 the concentration curve of surface-source tracer released simultaneously with the 200-meter source is also shown by black circle. In case of *h* = 200 m, T_D is 48 min at x = 1.5 km and 72 min at x = 5.0 km. The elongation of T_D with the downwind distance is remarkable, and in these cases it may happen that T_D exceeds the sampling time T. Figure 7-5 shows an example $T_D < \tau$ when τ = 30 min and *h* = 150 m.

Now it is important to investigate the mechanism of how the time width, T_D, of detached plume elongates or contracts with the downwind distance x, since the analysis of surface concentration data composing most of dispersion-experiment data depends exclusively on such mechanisms.

In case of Figures 7-3 and 7-4 half-hourly pilot balloon observations were made at the source x = 0 (P_1) and x = 3.8 km (P_2). The wind direction was due west and the pibal station, P_2, was east of the source. The two drum-impactor sites D_1, and D_2, were also east of the source as follows:

	P_1 (source)	D_1	P_2	D_2
x	0	1.5	3.8	5.0 km

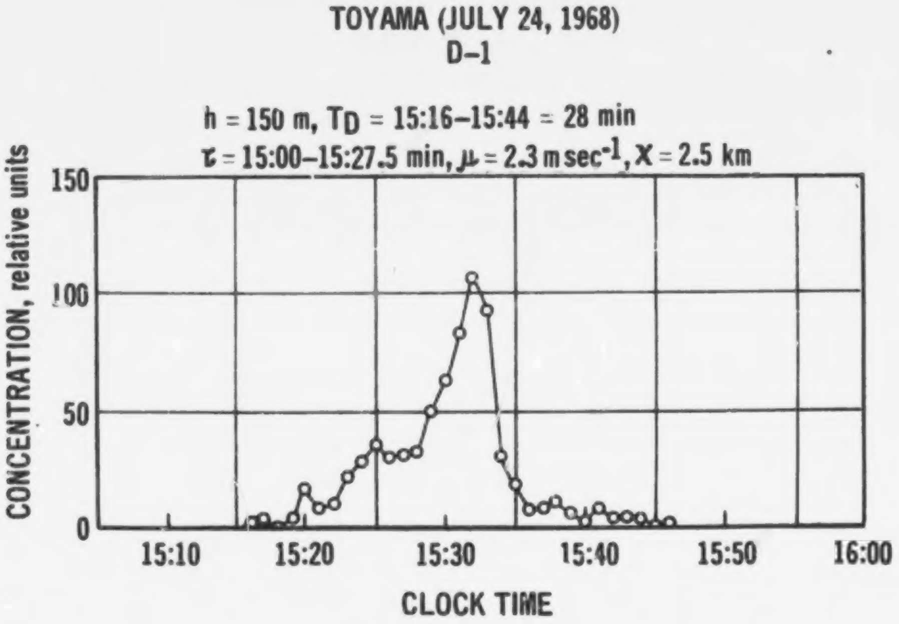

Figure 7-1. Time-concentration curve at $X = 2.5$ km. $T_D = \tau$

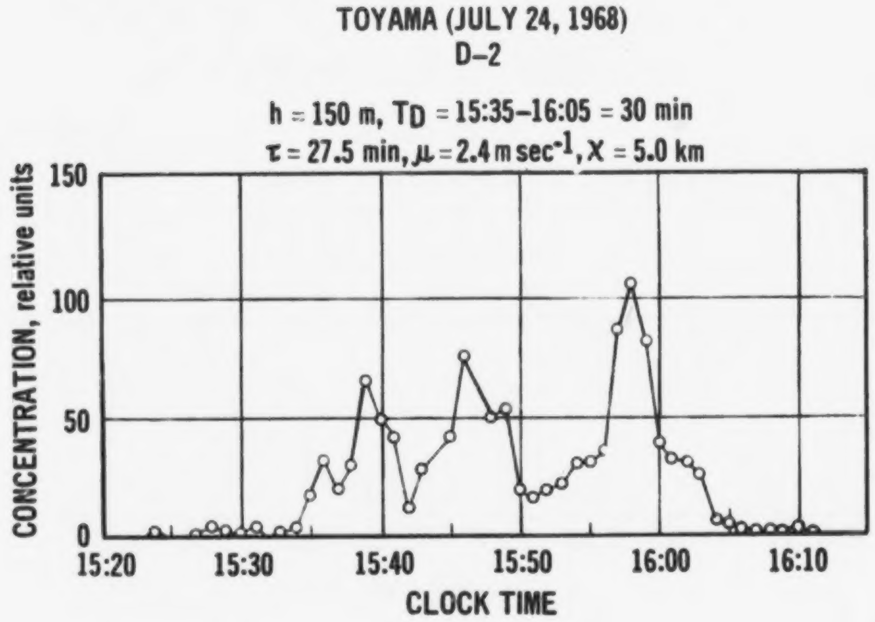

Figure 7-2. Same as figure 7-1 but for $X = 5.0$ km.

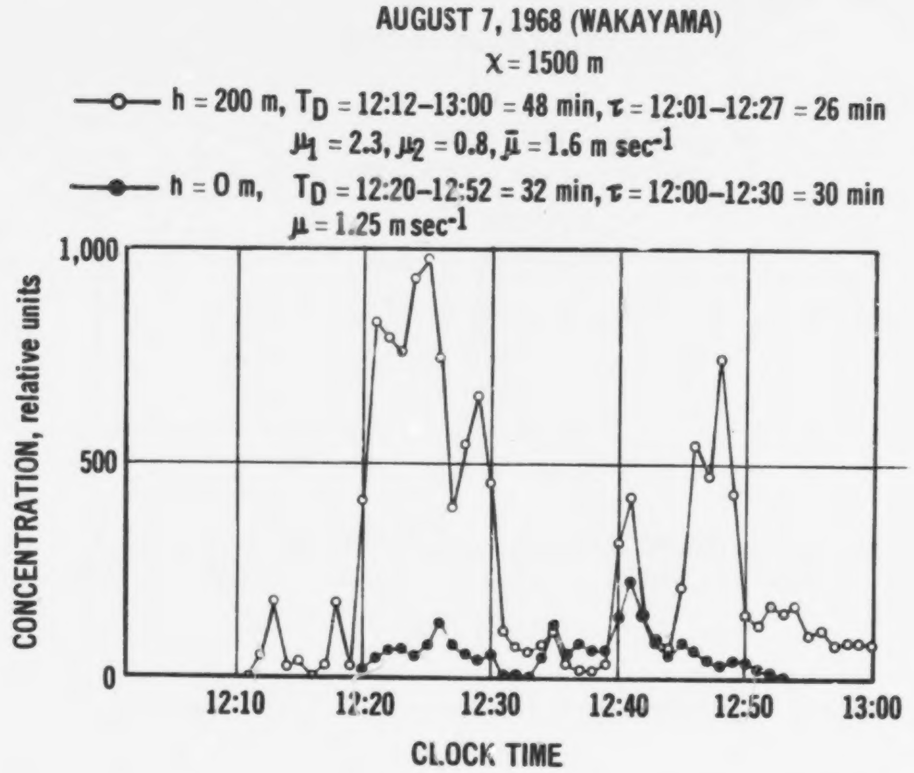

Figure 7-3. Time-concentration curve at X = 1.5 km. $T_D > \tau$

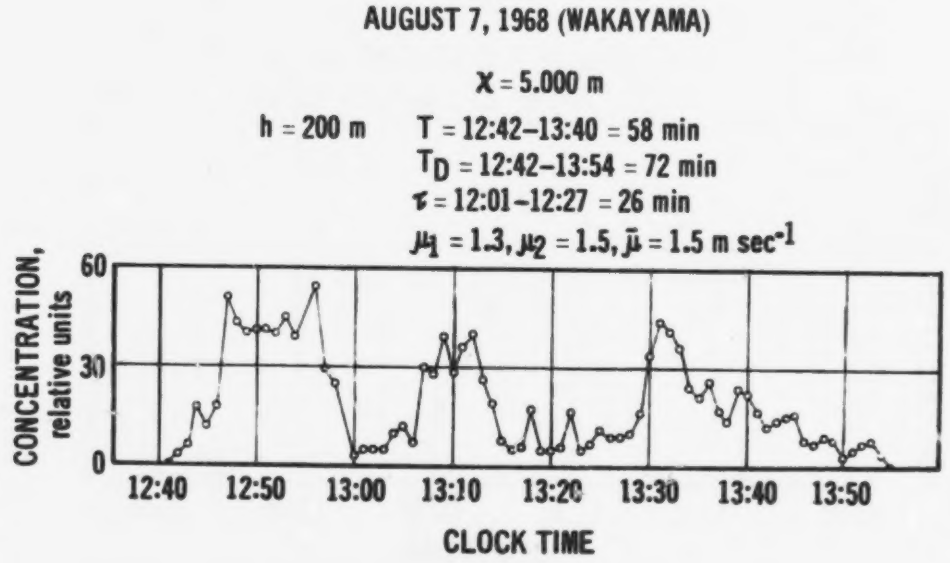

Figure 7-4. Same as Figure 7-3 but for X = 5.0 km.

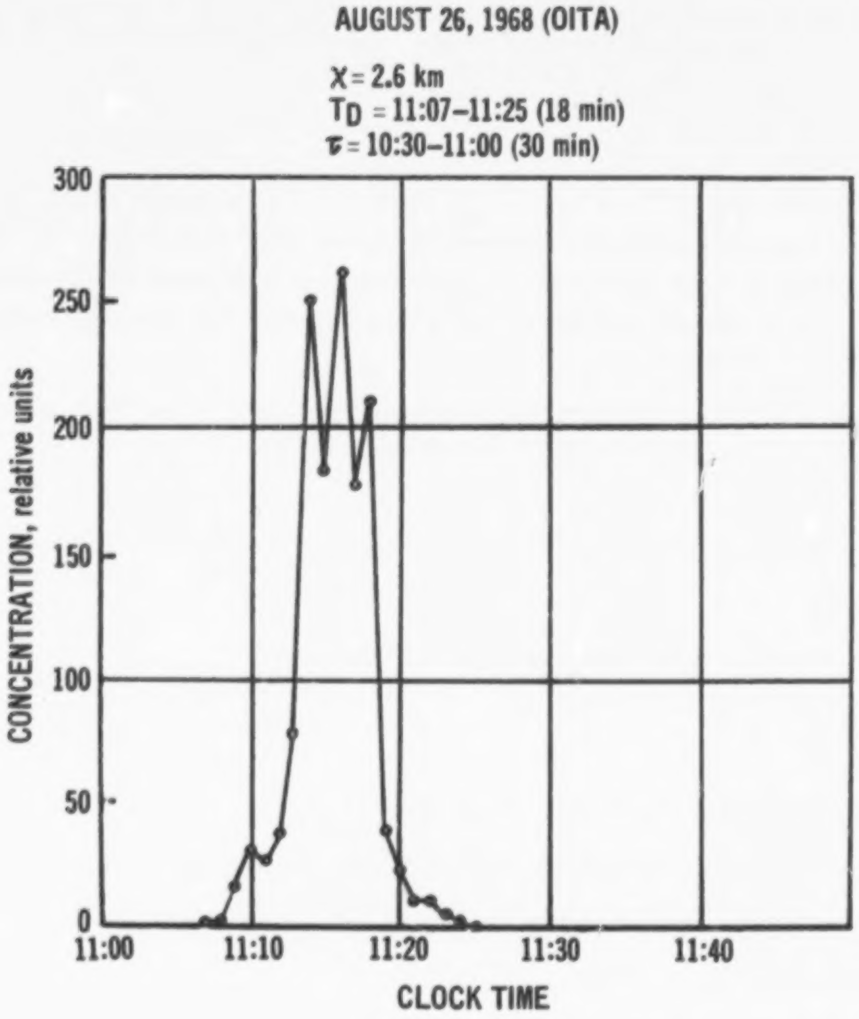

Figure 7-5. Time-concentration curve at $\chi = 2.6$ km. $T_D < t$.

The tracer was released at 12:01, ending at 12:27. The wind speeds at 200 m level at P_1 and P_2 are as follows:

P_1		P_2	
Time	Windspeed (m $\sec^{-1}$)	Time	Windspeed (m $\sec^{-1}$)
12:00	2.4	12:00	1.3
12:30	0.9	12:30	1.3
		13:00	1.3

According to the drum-impactor data, the transport speed of the tracer is:

Speed, m sec^{-1}	Part of tracer cloud	x, km
2.3	front	0 to 1.5
0.8	rear	
2.0	front	1.5 to 5.0
1.1	rear	

This, compared with pibal data, suggests that the elongation or contraction of T_D occurs by the windspeed difference between the front-part and the rear-part of tracer cloud.

Next we will try to compute T_D based on pibal data. If the front of tracer flows with the speed 2.4 m sec^{-1}, it will reach D_1 at

$$12{:}01 + 1500 \text{ m}/2.4 \text{ m sec}^{-1} = 12{:}11$$

and P_2 at

$$12{:}01 + 3800 \text{ m}/2.4 \text{ m sec}^{-1} = 12{:}27$$

The corresponding arrival time of the rear

$$12{:}27 + 1500 \text{ m}/0.9 \text{ m sec}^{-1} = 12.55 \qquad (D_1)$$

$$12{:}27 + 3800 \text{ m}/0.9 \text{ m sec}^{-1} = 13.37 \qquad (P_2)$$

The calculated T_D is, at D_1

$$12{:}11 - 12{:}55 = 44 \text{ min.}$$

While the observed T_D is

$$12{:}12 - 13{:}00 = 48 \text{ min.}$$

From P_2 on, the tracer speed is 1.3 m sec^{-1}, so the arrival time at D_2 is

$$12{:}27 + 1200 \text{ m}/1.3 \text{ m sec}^{-1} = 12{:}42 \qquad \text{(front)}$$

$$13{:}37 + 1200 \text{ m}/1.3 \text{ m sec}^{-1} = 13.52 \qquad \text{(rear)}$$

$$T_D = 70 \text{ min}$$

The observed T_D at D_2 is

$$12{:}42 - 13{:}54 = 72 \text{ min.}$$

The coincidence is good, supporting the view that the elongation or contraction of a detached plume is due to the windspeed difference at its front and rear. The sampling time T, by the way, and the estimated or observed T_D in this case are as follows:

x	0.6	1.5	3.0	5.0 km
T	33	48	57	58 min
T_D	33	[48]	68	[72] min

Here the numeral in brackets shows the observed value. Evidently samplers at 3 km and 5 km downwind were stopped before the tracer passed by.

AVERAGE CONCENTRATION AND DISPERSION EQUATION

The dispersion equation for a continuous point source is:

$$\frac{u}{Q}\ C(x, y, z) = f\ [\sigma_y(x),\ \sigma_z(x),\ h, y, z] \tag{1}$$

and the equation of mass continuity is

$$\iint u\ C\ dy\ dz = Q \tag{2}$$

The notations are customary ones. In dispersion-data analysis we must refer to Equation 1. Some kind of average concentration conforming to Equation 1 must then be introduced to compensate for having only the exposure data, especially when T_D is not equal to τ, or when T_D is not known.

Let C be the instantaneous concentration. The exposure, E, and the average concentration, $\overline{C}$ are

$$E = \int^{T_D} C\ dt \tag{3}$$

$$\overline{C}\ (T_D) = \frac{1}{T_D} \int^{T_D} C\ dt = E/T_D \tag{4}$$

where T_D was already defined in the previous section and t is time.

Case 1. $\tau_D = T$

This corresponds to the case when the sampler has captured all the tracer material passing by, which is usually the case with the dispersion experiment. Then, from the equation of mass continuity,

$$\int^{T} dt \iint u\,C\,dy\,dz \;=\; Q\tau \qquad (5)$$

$Q\tau$ shows the total mass of tracer released. Dividing by T,

$$\iint \overline{u\,C}\;\;dy\;dz \;=\; Q\,\tau/T \qquad (6)$$

where

$$\overline{u\,C} \;=\; \frac{1}{T}\int^{T} u\,C\,dt \;\approx\; \bar{u}\;\bar{C}\;(T)$$

$$\bar{C}\,(T) \;=\; \frac{1}{T}\int^{T} C\,dt$$

So Equation 6 becomes

$$\iint \bar{u}\;\bar{C}\;(T)\;dy\,dz \;=\; Q\,\tau/T \equiv Q' \qquad (7)$$

The dispersion equation corresponding to Equation 7 should be

$$\bar{u}\,\bar{C}\,(T)\,/\,Q' \equiv \bar{u}\,\bar{C}\;(T)\;\frac{T}{\tau} \;=\; f \qquad (8)$$

Equation 7 shows that the source intensity corresponding to the average concentration $\bar{C}(T)$ is not Q, but Q'. Q coincides with Q' only when $T = \tau$.

Equation 8 may be simplified, by introducing the concentration C, defined by

$$E = \int^{T} C\,dt = \int^{\tau} C'\,dt \qquad (9)$$

and the corresponding average concentration $\overline{C}\ (\tau)$:

$$\overline{C}\ (\tau) = \frac{1}{\tau}\int^{\tau} C'\ dt \qquad (10)$$

Namely Equation 8 becomes

$$\overline{u}\ \overline{C}\ (\tau)\ /\ Q = f \qquad (11)$$

Equation 11 does not contain T explicitly and is convenient for the concentration analysis.

Case 2. $T_D > T$

This is a rather rare case and sampling time does not cover the whole range of the time concentration curve. Such an example was already shown (Figure 7-4). The best estimate for the equation of mass continuity in this case, is

$$\int^{T} dt \iint u\,C\,dy\,dz = Q\tau \frac{T}{T_D} \qquad (12)$$

which yields:

$$\overline{u}\ \frac{T_D}{T}\ \overline{C}\ (\tau)\ /\ Q = f \qquad (13)$$

Equations 11 and 13 will be used later in the surface-concentration analysis.

Estimation of tracer-cloud height based on surface-concentration analysis

Since 1967 the vertical measurement of tracer material has been made at two points downwind, from which the center-line height, $\overline{z}$, of the tracer-cloud as well as the vertical dispersion parameter, σ_z, is derivable. Examination of 45 vertical concentration profiles, made it clear that $\overline{z}$ varies remarkably with the downwind distance, and in turn seriously affects the surface concentration pattern. In the sea breeze layer, in which most dispersion experiments were conducted, $\overline{z}$ generally increases with the downwind distance. The increase is larger over an urban area than a rural area, and over a sloped area than a flat area. Next we will examine the possibility of estimating, $\overline{z}$ from the surface concentration.

We will begin with the dispersion equation:

$$\frac{u}{Q} C\,(Cx, y, z) = f\,[\sigma_y(x),\ \sigma_z(x),\ \overline{z}(x),\ y,\ z] \qquad (14)$$

$\overline{z}$ is the center-line height of the tracer cloud or the gravity-center height of concentration and a function of downwind distance x.

C/Q is:

$$C/Q = \frac{T_D}{T}\ \overline{C}\,(\tau)\,/\,Q \qquad (15)$$

as proved in the previous section, and T_D/T is in most cases unity.

To determine $\overline{z}$ (x) from Equation 14, the transport speed u , the source intensity Q , the horizontal dispersion parameter σ_y and the vertical dispersion parameter σ_z must be known. The determination of σ_y is simple and needs no special comment; u may be accurately determined by the drum-impactor record. At one or two points downwind we have the concentration-profile data, or $\overline{z}$ and σ_z. Then Q is determined from the Equation 14, with the concentration data The constancy of Q may also be checked if the concentration-profile data are available at two points downwind. It was found that Q is almost constant down to at least 5 km, as far as the elevated-source dispersion is concerned.

Now, from Equation 14 ,

$$u\ Ca\,/\,Q = f\,[\sigma_y(x), \sigma_z(x),\ \overline{z}\,(x),\ 0,\ 0] \qquad (16)$$

$Ca \equiv C(x,0,0,)$ is the axial concentration at the surface. We already have $\overline{z}$ and σ_z at one or two points downwind. Then, from σ_z , the corresponding Pasquill stability could be determined. If the Pasquill stability thus determined is fairly constant over the downwind distance concerned, the estimation of $\overline{z}$ (x) from Equation 16 becomes possible. It was made clear from the measurement of σ_z at two points downwind that in the case of elevated sources the Pasquill stability can be regarded constant down to about 5 km distance, even over an urban area. It is important to note here that the Pasquill stability decided from the observed σ_z should be adopted.

In the following sections we will give some examples of $\overline{z}(x)$ over an urban area analyzed along the line stated in this section.

Yokohama experiment

Figure 7-6 is the sampling network of the Yokohama experiment. Two sources, 60 m and 113 m high, were placed at the Negishi industrial area, at the southern extremity of Yokohama City. From the 60-meter source to 1.6 km arc, the terrian is flat. Beyond the 1.6 kilometer arc, there is a tableland about 50 m high bounded by a cliff (see Figure 7-10). Beyond the 3.5 kilometer arc is the central part of Yokohama City. In the experiment of July 26, 1967, two fluorescent particle tracers were released from a 60-meter source and 113-meter source simultaneously. The tracer drifted in the southerly wind; hit the tableland; crossed over it; and flowed over the congested area of Yokohama City.

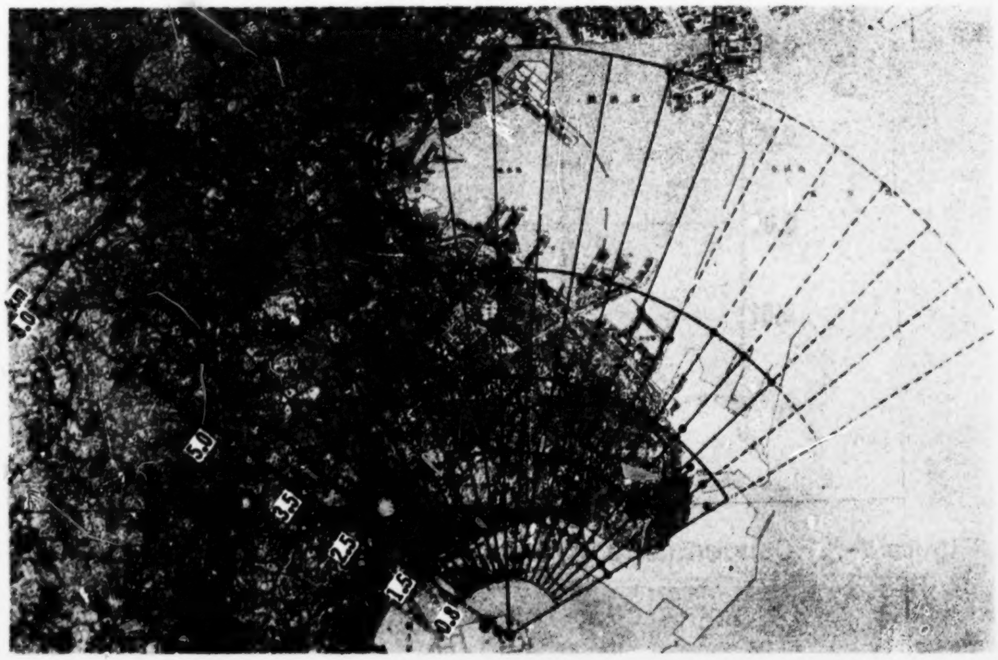

Figure 7-6. Network of Yokohama experiment.

The concentration-profile sounding was made at two sites, one at x = 2.3 km on the tableland and the other at x = 4.8 km near the coast of Yokohama Port, the downwind distance x being measured from the 60-meter source. Figure 7-7 shows the concentration-profile at x = 2.3 km The analysis is usually made, assuming the Gaussian distribution of concentration in the vertical. The profile in Figure 7-7 does not lend itself to such an analysis; however, it is certain that $\bar{z}$ is larger than 250 m, the highest level of sounding.

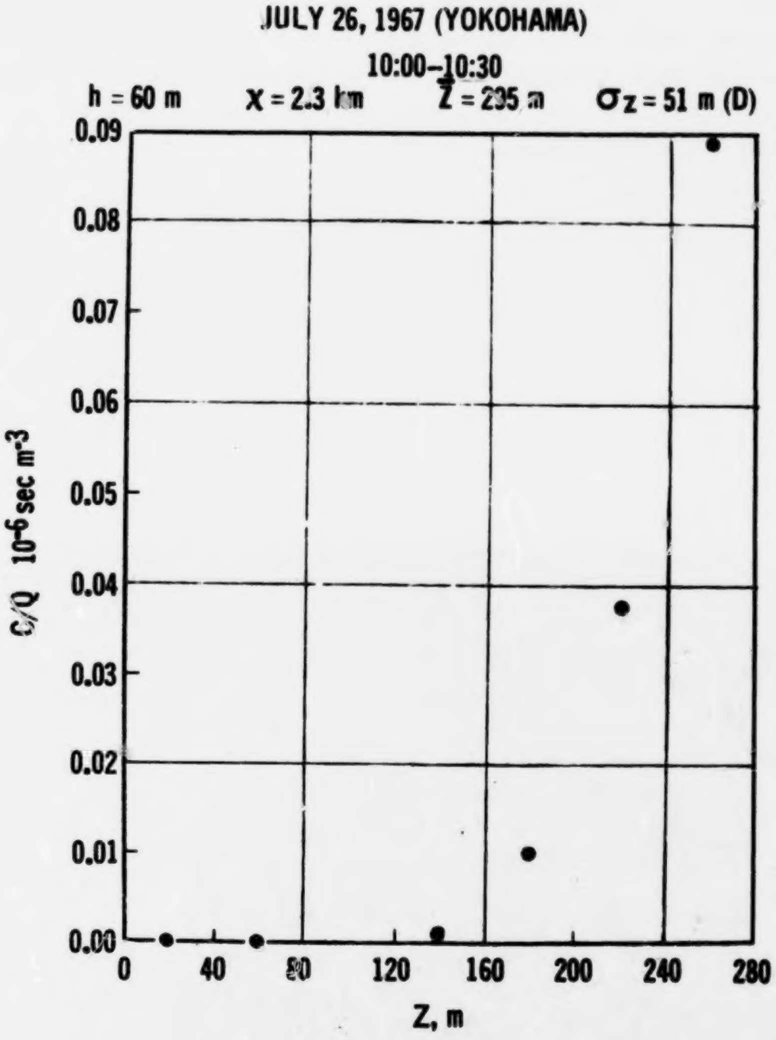

Figure 7-7. Concentration profile at X = 2.3 km. source height 60 meters.

Figure 7-8 shows two soundings: one is at x = 4.8 km from the 60-meter source and the other is at x = 3.7 km from the 113-meter source. In the former $\bar{z}$ is 170 m and σ_z is 56 m, the Pasquill stability, E; , while in the latter $\bar{z}$ is 175 m and σ_z is 54 m, the Pasquill stability, D to E. In the following the Pasquill stability E will be adopted to treat the dispersion from the meter 60-meter source.

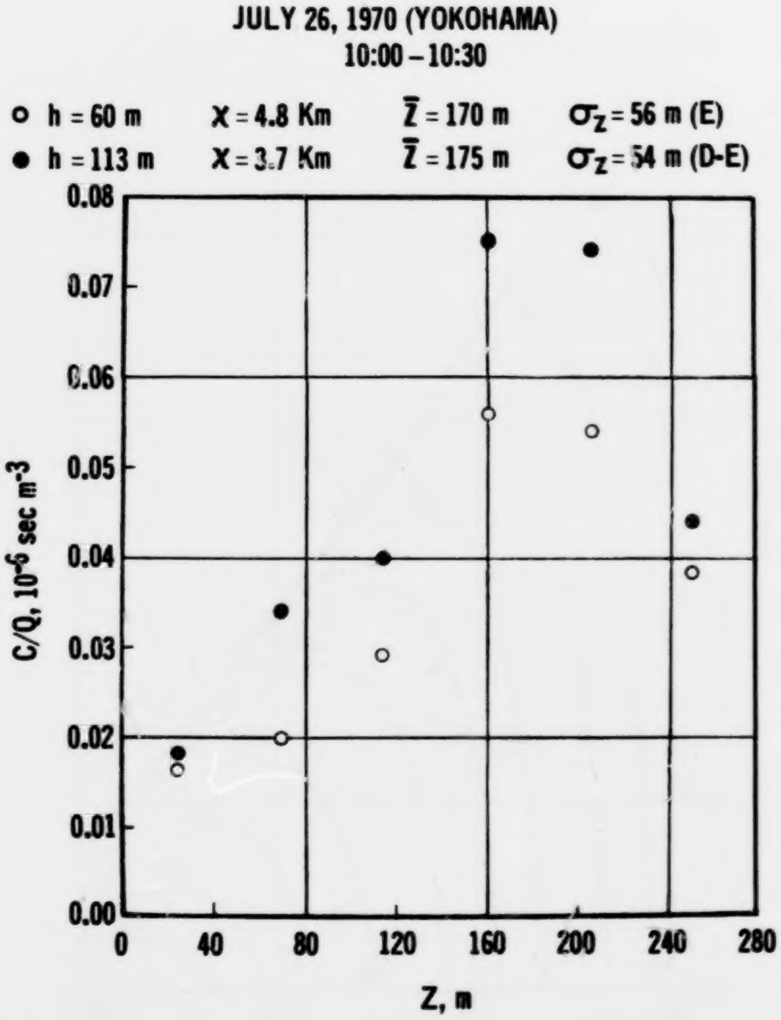

Figure 7-8. White circle same as Figure 7-7 but for $X = 4.8$ km, black circle, concentration profile at $X = 3.7$ km, source height, 113 meters.

Figure 7-9 shows the result of the surface concentration analysis made with the procedure stated in the previous section, The curve is the isoline of $\bar{z}$, in meters, when the Pasquill stability is E. The white circle shows only how the

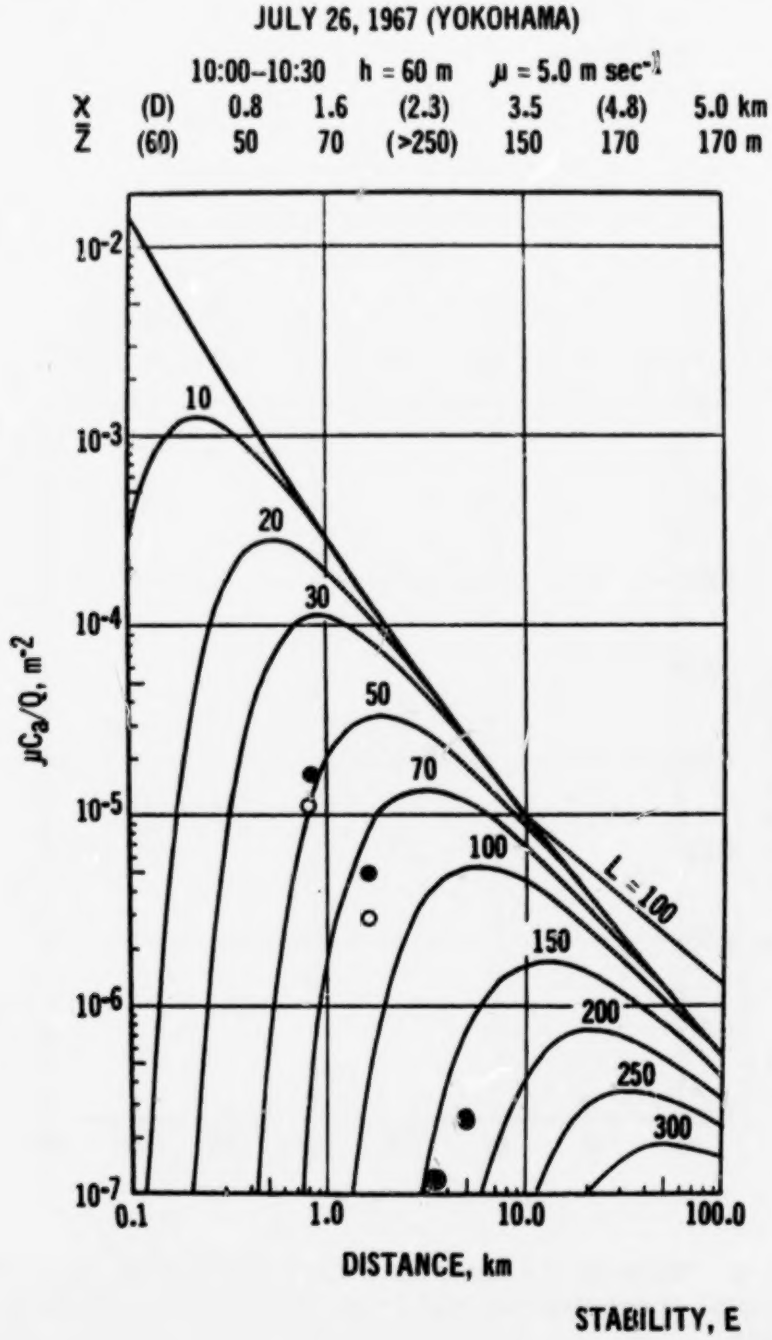

Figure 7-9. Surface axial concentration versus downwind distance curve, case of Pasquill stability E. Labelled numeral shows tracer-cloud height, meters.

normalized surface axial concentration varies with the downwind distance and has no connection with z. The black circle shows the surface concentration modified such that xy conforms to that in Pasquill stability E. This is because xy and xz are usually different in Pasquill stability. In the case in Figure 7-9, the Pasquill stability of xy is higher than E at x = 0.8 km and 1.6 km, while at x = 3.5 km and 5 km it is about the same; $\bar{z}$ can be read from the black circles in Figure 9.

The result, depicted together with the topography in Figure 7-10 is summarized as follows:

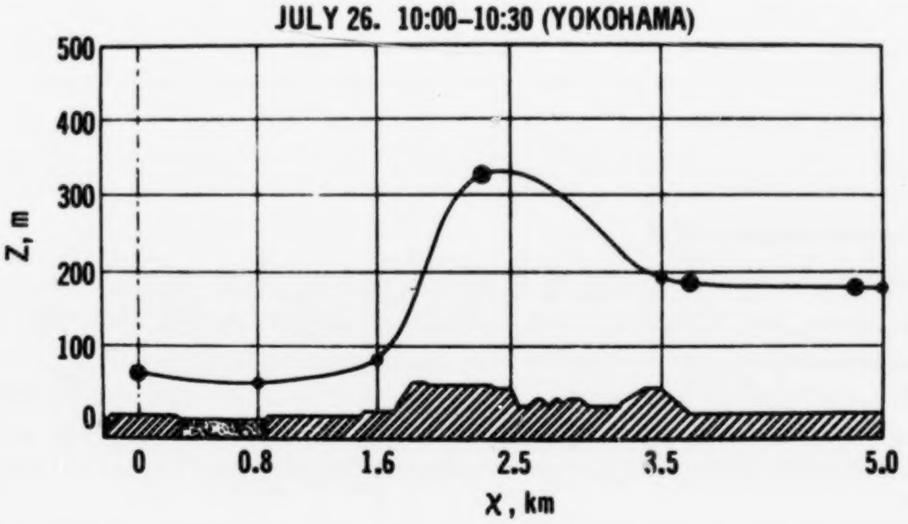

Figure 7-10. Tracer-cloud height variation with downwind distance and topography in Yokohama experiment.

x	(0)	0.8	1.6	(2.3)	3.5	(4.8)	5.0 m
$\bar{z}$	(60)	50	70	(>250)	150	(170)	170 m

Here $\bar{z}$ is estimated from the surface concentration, except for the bracketed numbers which are the results of direct analysis of concentration profiles or the source height.

An 0.8-km arc runs along a pier. The tracer released from the 60-meter height flowed north, descended a little over a small canal ahead of the 0.8-km arc, and began to rise, passing over the industrial plant area between the 0.8-km and 1.6-km arcs. Crossing the tableland beyond the 1.6-km arc it rose remarkably, then descended over the congested area. The difference of $\bar{z}$ between x = 0 and x = 5 km is 110 m. Because of such large variations of $\bar{z}$, the surface concentration decreases rather uniformly with the downwind distance and does not have the value, characteristic of an elevated source.

Mizushima experiment

Mizushima is an industrial area facing the Seto Inland Sea, and Figure 7-11 shows one example of the analysis in the Mizushima experiment. The Pasquill stability is D, which is due to the concentration profile sounding at x = 5.2 km; and the source height is 90 m.

x	(0)	1.0	2.0	3.0	5.0	(5.2) km
$\bar{z}$	(90)	65	120	170	130	(130) m

The 1.0-km arc runs along a pier and there is a small canal ahead of this arc, similar to the situation in the Yokohama experiment. The tracer flowing north descended over the canal and began to rise significantly over the congested plant area between x = 1.0 km and x = 3.0 km. Beyond the 3.0 km arc there follows the flat, rural area with scattered small towns. There the tracer descends

Toyama experiment

The experiment was conducted at the western suburb of Toyama City, facing the Japan Sea, a flat rural area extending to 5.0 km arc. The 150-meter source was sited near the coast and the tracer flowed inland (Figure 7-12). The tracer flowed horizontalily down to the 5.0 km arc and rose at the 8.0 km arc where there are hills. The Pasquill stability was D. The surface concentration curve is typical of the elevated source, since $\bar{z}$ does not vary.

Kainan City experiment

Kainan, south of Wakayama City, is situated in a narrow valley surrounded north and south by mountains about 150 to 400 m high and extends east-west. The west end of the city is open to the sea. The 200-meter and surface-sources were placed at the mouth of the valley. The tracer flowed in over Kainan City with the west wind.

Figure 7-13 shows the concentration profile at x = 550 m; for the source height of 200 m; $\bar{z}$ 154 m; and σ_z was 33 m; the Pasquill stability was C. Figure 7-14 is the same profile, but for x = 1.5 km. Here the ordinate is the ratio of the source to surface concentration and the abscissa is $z / \bar{z}$, parameter ξ being $\sigma_z / \bar{z}$. Figure 7-14 shows that $\bar{z}$ is 200 m and σ_z is 126 m, when the Pasquill stability is B-C. Two kinds of Pasquill stability were used, B-C and C. In the other runs of the experiment the Pasquill stability was all B-C, so in this case the same stability was also adopted.

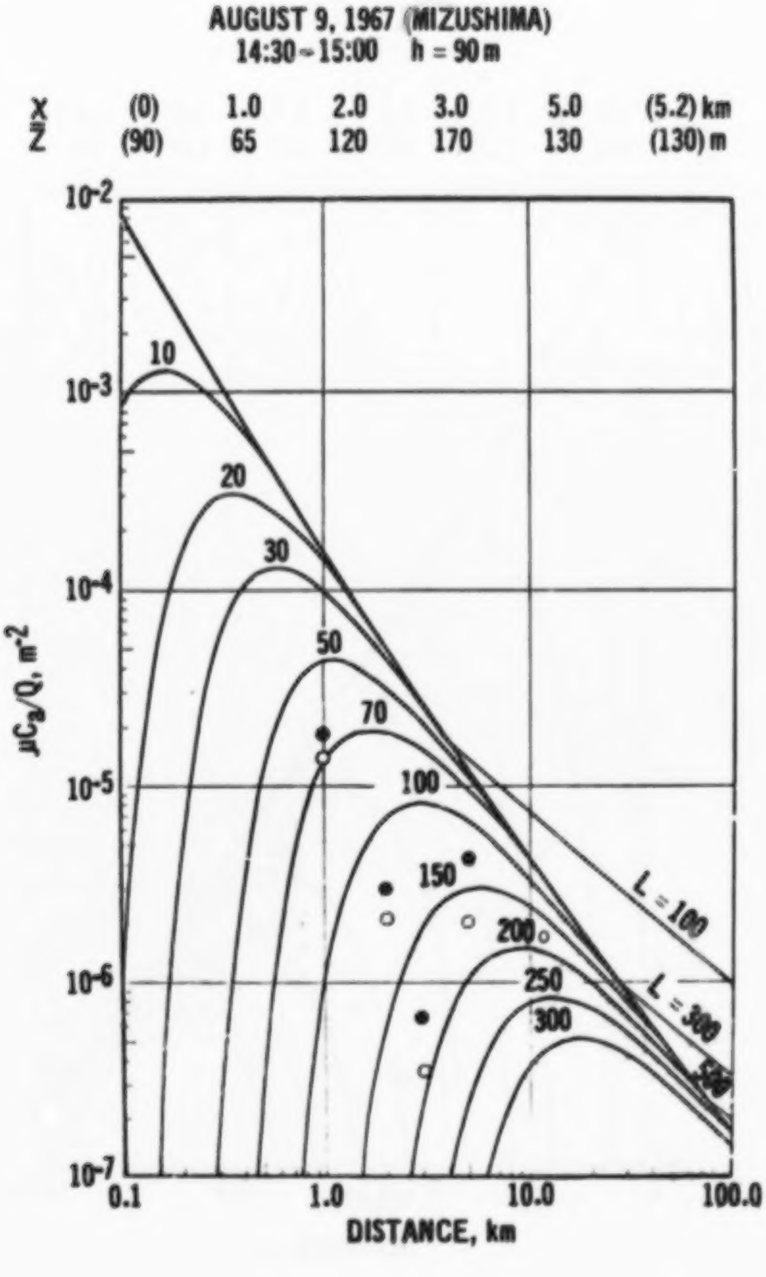

Figure 7-11. Same as Figure 7-9 but for Pasquill stability D, Mizushima experiment.

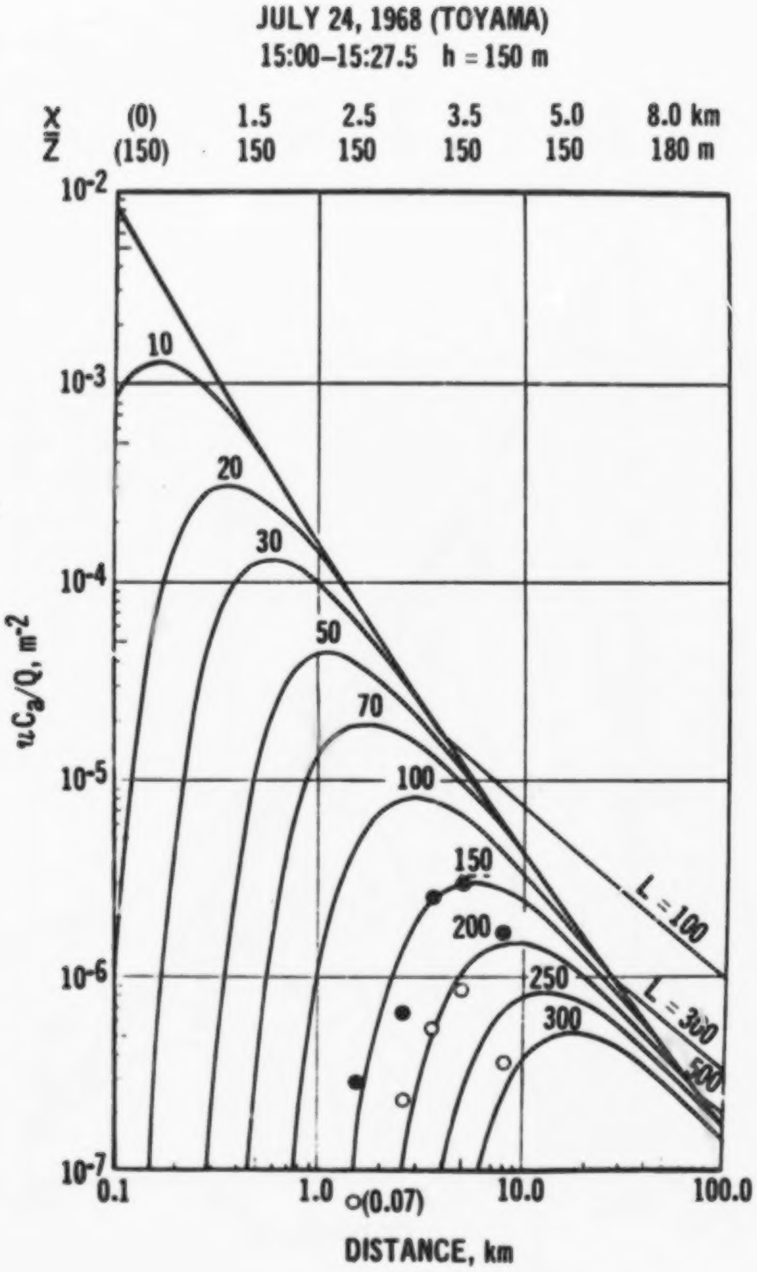

Figure 7-12. Same as Figure 7-11 but for Toyama experiment.

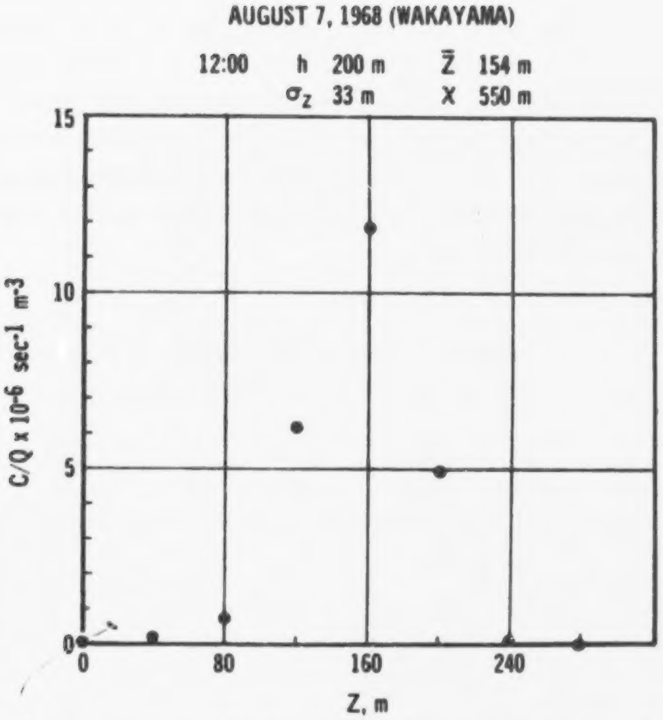

Figure 7-13. Concentration profile at $X = 550$ meters, source height 200 meters. Pasquill stability C.

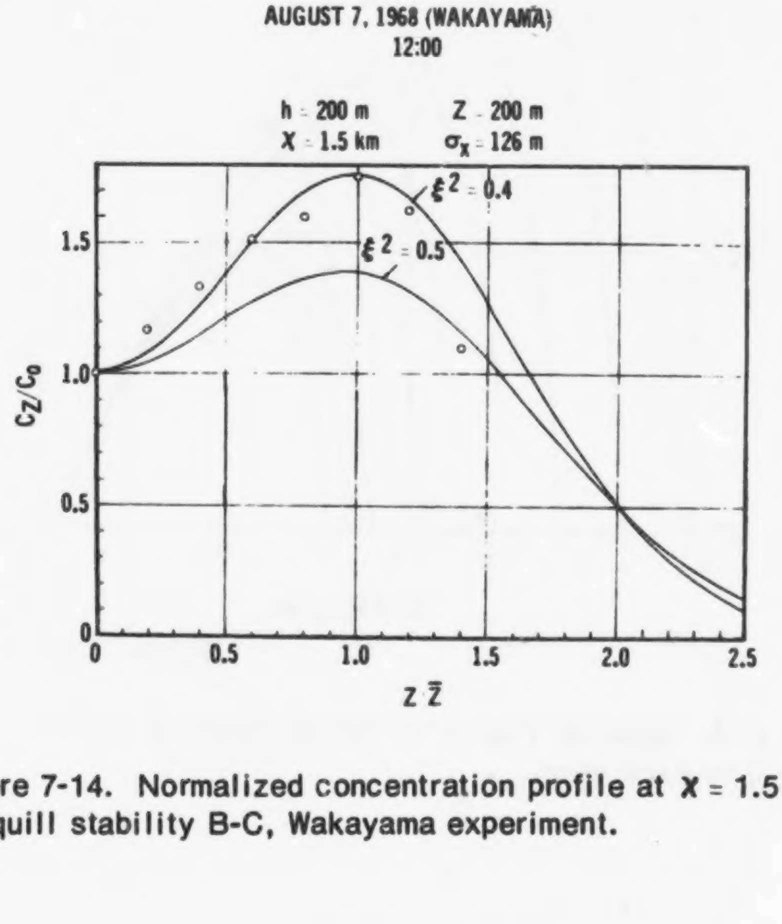

Figure 7-14. Normalized concentration profile at $X = 1.5$ km, Pasquill stability B-C, Wakayama experiment.

Figure 7-15 is the final result of the analysis. The tracer descends about 50 m at the 0.6-km arc, resumes its initial height at the 1.5-km arc and then begins to rise remarkably. At about 150 m east of the source there is a building about 50 m high, which seems to have affected the lowering of tracer to the 0.6-km arc. This is reflected in the concentration profile from the surface-source released simultaneously with 200-m source (Figure 7-16) $\bar{z}$ being 130 m at x = 1.6 km.

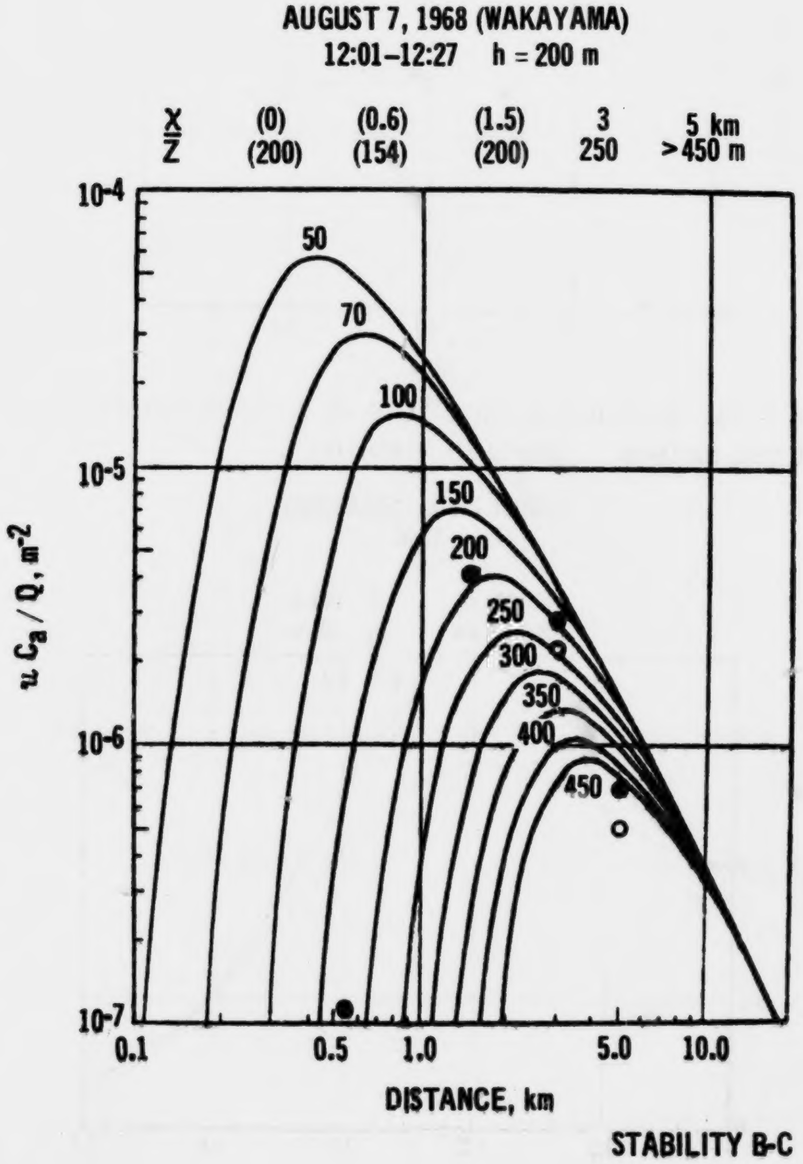

Figure 7-15. Same as Figure 7-9 but for Pasquill stability B-C, Kainan City experiment.

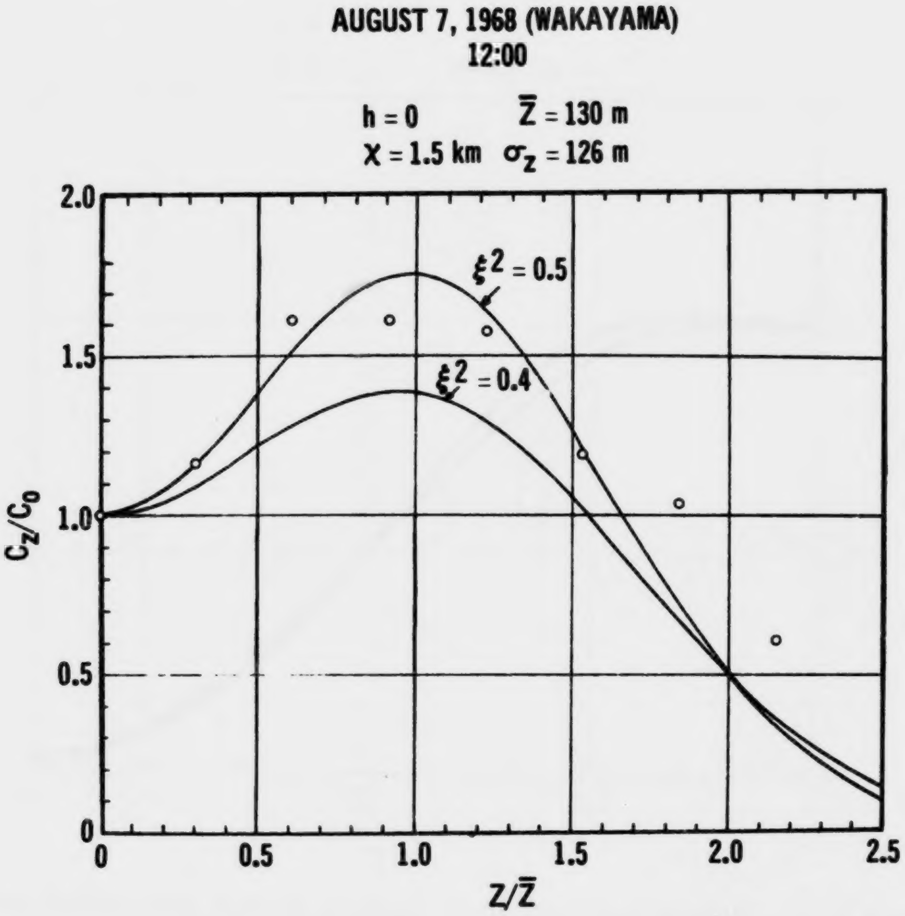

Figure 7-16. Normalized profile of surface-source concentration at X = 1.5 km, Wakayama experiment.

The weather conditions such as stability and wind speed or profile were almost the same as the case in Figure 7-12. The big difference is in the terrain. The Pasquill stability is certainly much affected by the topography.

Oita experiment

There are many examples to show that the tracer-cloud released from the surface-source rises more or less over an urban area. One example is picked out here from the Oita experiment.

The surface source was near the coast and the tracer flowed over Oita City. The concentration profile at x = 2.6 km is shown in Figure 7-17; $\bar{z}$ is 65 m and the Pasquill stability is D. Figure 7-18 is the result of the analysis:

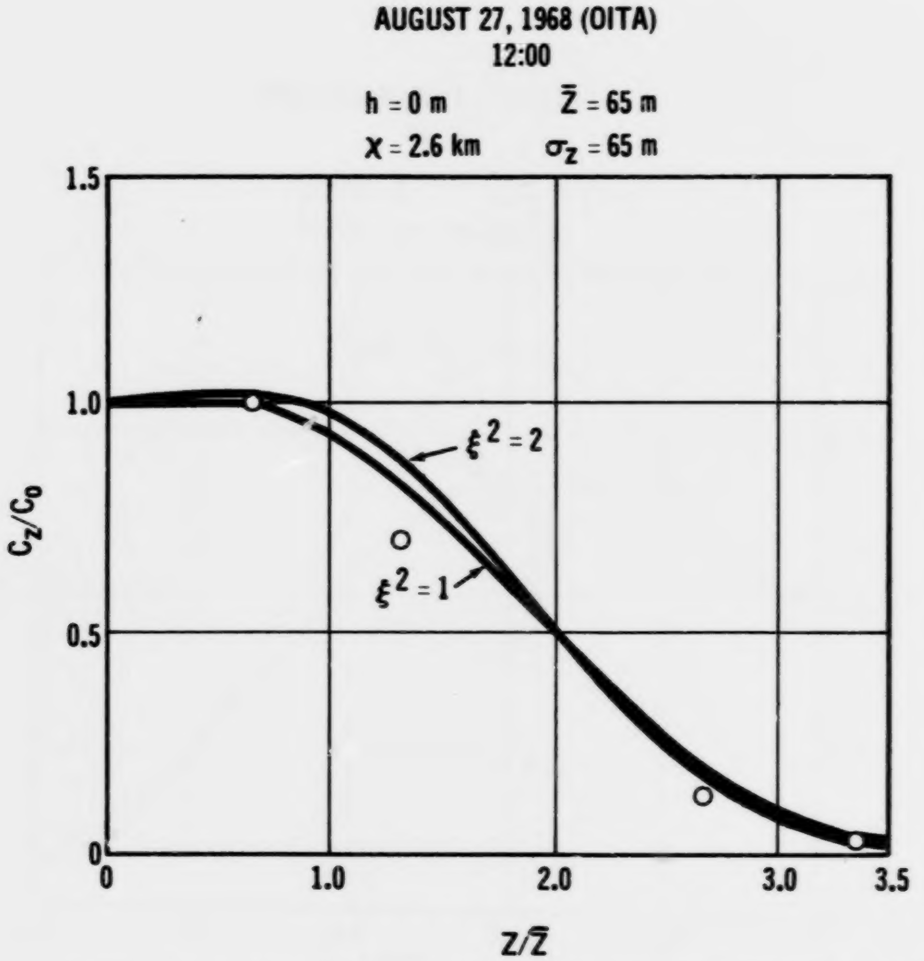

Figure 7-17. Normalized profile of surface source concentration at X = 2.6 km, $\xi = \sigma_Z/\bar{Z}$ Pasquill stability D.

x	(0)	0.6	1.5	(2.6)	3.0	5.0 km
$\bar{z}$	(0)	45	65	(65)	80	140 m

The increase of $\bar{z}$ with the downwind distance is conspicuous.

CONCLUSION

Examining dispersion-experiment data in Japan, we found that the height of the tracer cloud generally increases with the downwind distance. The height increase is larger over an urban area than over a rural area. Therefore, the earlier analysis, assuming constant height for the tracer clouds, tends to overestimate σ_z, especially over an urban area. The height variation also affects the surface concentration. When the tracer crosses over a hill, its rise is remarkable. In general, the tracer rise is larger over a complicated topography. Over a flat terrain the rise is small.

The source heights of our experiments were 0 to 200 m. The present conclusion is valid in this source-height range

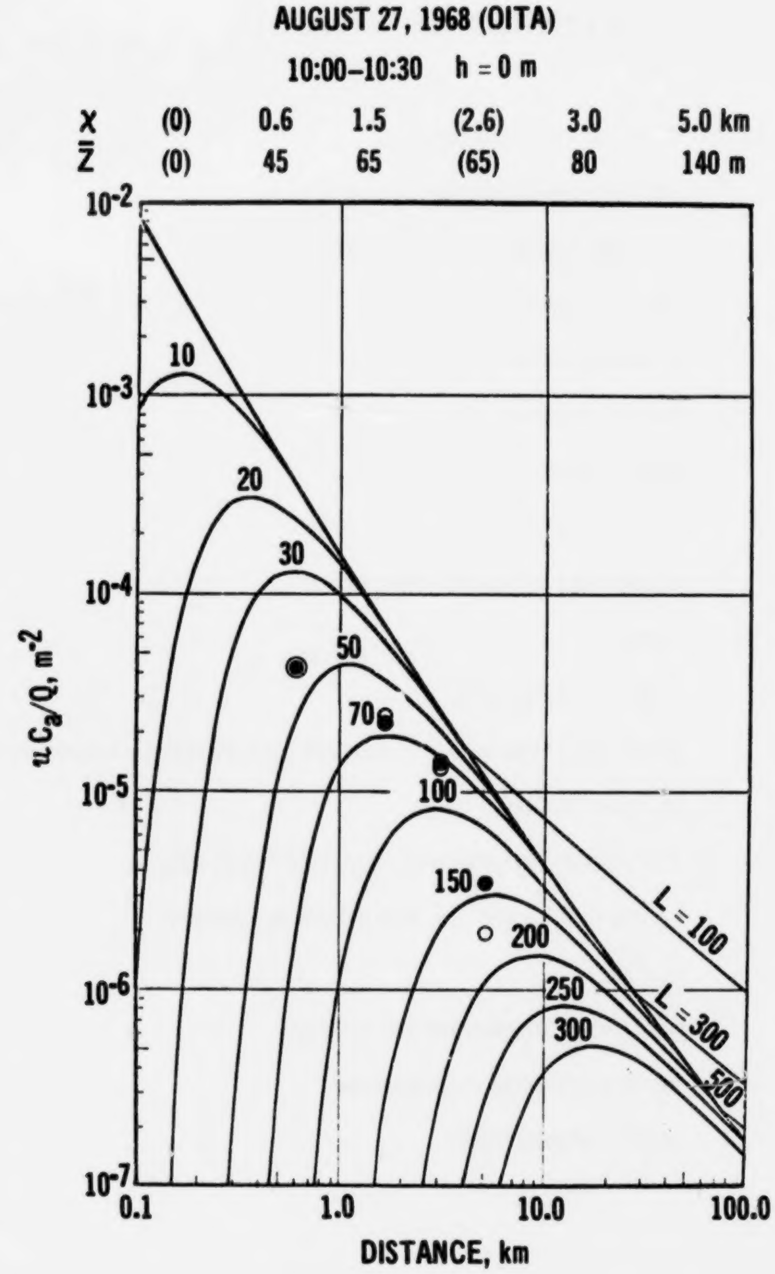

Figure 7-18. Surface axial concentration versus downwind distance curve, Pasquill stability D.

APPENDIX – GLOSSARY OF SYMBOLS

A, B, C, D, E	Pasquill stability ratings
C	instantaneous tracer concentration
$\overline{C}$	average tracer concentration
D_1, D_2	drum-impactor sites
E	exposure time
H	source height
P_i	pibal station, i
Q	source intensity
Q_T	total mass of tracer released
t	time
T	real sampling time
T_D	total time required for passage of a detached tracer plume
u	transport speed
x	horizontal (downwind) distance from source
$\overline{z}$	centerline height, or gravity-center height
ξ	$\sigma_z/\overline{z}$
σ_y	horizontal dispersion parameter
σ_z	vertical dispersion parameter
τ	tracer release time

ABSTRACT

With the advent of computer-oriented simulation models of the physical and chemical system that produces varying levels of air quality, it is both possible and desirable to assess the model's sensitivities to errors and uncertainties in the input variables. From such analyses, it is possible to derive more explicitly the levels of accuracy that must be observed in the specification of the inputs for source strengths and distributions, wind velocity, horizontal and vertical diffusion rates, and pollutant chemical reactions or physical decay and loss rates, if the air quality predictions derived from these inputs are to remain within useful limits of accuracy and uncertainty.

For the present report, a single case study is utilized to test the sensitivity of the Travelers Research Corporation Regional Model to random and systematic errors in the source-strength input and to systematic errors in the remaining input variables. It has been found that random errors in the source strengths do not produce comparable errors in the air quality prediction. Beyond this, and in order of decreasing sensitivity, the TRC model has been found to be highly sensitive to systematic regional wind-direction errors and moderately sensitive to systematic errors in source-strength estimates, decay or loss rates, and vertical diffusion rates. The model is insensitive to errors in lateral diffusion rates, at least for the multiple-source distribution encountered in Connecticut. These sensitivites are quantified for the case studied.

The case used for the sensitivity analyses also provided an opportunity to determine the effect of changes in the input variables on the verification of the model, since observations of SO_2 were available from the verification program. Significant improvements in the TRC model verification, over that obtained from the original, independantly chosen, input variables, were found when either the source strengths or the decay or loss rates were adjusted appropriately. This result suggests the need for much better understanding of the decay and loss of airborne SO_2.

AUTHOR

DR. GLENN R. HILST, a native of Kansas, holds degrees from MIT and the University of Chicago. He has worked in association with the General Electric Company, Argonne National Laboratory, and The Travelers Research Center on various facets of air and water quality control and environmental safety. Dr. Hilst is presently editor of the Journal of Applied Meteorology.

8. ELEVATION OF TRACER CLOUD OVER AN URBAN AREA*

DR. GLENN R. HILST†

The Travelers Research Corporation

INTRODUCTION

The advantages of a capability to simulate the physical and chemical behavior of the air quality system are so obvious as to require no further emphasis here. The very existence of this Conference and the reports we have heard on the state-of-the-art for simulation modeling (within useful limits of accuracy) also speak to these advantages, even the *need* for an ability to evaluate alternative air quality control strategies *before* massive and costly programs are instituted. This is the ultimate utility of simulation modeling; happily, along the way, these modeling attempts also provide us with the possibility of unusually clear recognition of where our ignorance, errors, and uncertainties lie. It is on this facet of simulation modeling of air quality systems that I should like to focus.

In particular, our work at Travelers Research Corporation (TRC) now permits us to make a preliminary assessment of (1) just how faithfully the TRC Regional Model simulates the real-world air quality system in Connecticut and (2) the sensitivities of that model's air quality predictions to errors and uncertainties in the input parameters and variables. I shall discuss these two topics in reverse order.

At the outset, let me emphasize that these studies have utilized only the TRC Regional Model; therefore, the results are limited to that particular version. Since the basic methods employed by the model are quite conventional and common to most modeling efforts, it is reasonable to assume that the sensitivities found are appropriate to other models that also purport to predict air quality with a similar time and space resolution. I leave this extension to your own good judgment.

---

*The work reported here was supported as an in-house program development effort by TRC. The TRC Regional Model was developed under a grant from the Connecticut Research Commission, however, and the verification data used here were obtained under joint support from the Connecticut Research Commission and the National Air Pollution Control Administration.

†The very substantial assistance of Mr. Charles R. Case, Computer Operations, and the advice and counsel of Dr. G. D. Robinson, Mr. N. E. Bowne, and Dr. R. R. Hippler are gratefully acknowledged.

TRC REGIONAL MODEL

The model whose sensitivities and predictive capabilities are under study here has been reported on extensively over the past 2 years. Verification of the model was undertaken in a 1968-69 study that is the subject of a report by the TRC staff[4] and a preliminary paper by Bowne,[5] both of which are just now becoming available.

In brief, the TRC model is designed to predict ground-level concentrations of a semiconservative pollutant emitted from multiple sources within a region of the order of 5,000 square miles. The model is capable, in principle, of resolving those concentrations on an hour-by-hour basis, with a space resolution of 5,000 feet. Since the design of the model is quite general with regard to time and space resolution, the only real limitations on these features are (1) computer capacity and speed, (2) ignorance regarding the appropriate decay and loss of a pollutant over great distances of travel, and (3) a very large degree of uncertainty regarding the transport and dispersion processes over very short distances of travel. As presently configured, the model fits nicely into the IBM 360/40 and requires about 10 minutes of that computer's time to provide a 100-point prediction of any single air quality pattern.

The TRC model employs the conventional Gaussian diffusion representation of dilution of the pollutant (with a simple exponential decay) from each individual area or point source that could contribute to the concentration at the point (or small area) and time of interest. These sources are identified by computing the prior trajectory of the air resident over that point at the time of interest and by noting the lateral dispersion appropriate for the traverse from the source to the point of interest. Chronological variations in the wind field and atmospheric dispersion are accounted for by changing the input variables at 2-hour intervals.

The basic equation used is shown in Figure 8-1; the total concentration at (x, y, 0) is obtained by summing over all appropriate source locations (ξ,η,ζ). Except for the transporting wind velocity field, which defines $(x-\xi)$, $(y-\eta)$, and $(z-\zeta)$, all of the input variables for air quality prediction are explicit in this equation. They are as follows:

$Q(\xi,\eta,\zeta)$ = the source strength at $x = \xi$, $y = \eta$, $z = \zeta$.

$\bar{u}(\xi,\eta,\zeta)$ = the mean wind speed at the source during the time of emission (strictly, the *harmonic* mean).

u = the transporting wind speed that determines the time of flight from x to ξ, etc.

$$\chi(x,y,z \mid \xi,\eta,\zeta) = \frac{1}{\pi}\underbrace{\left[\frac{Q(\xi,\eta,\zeta)}{\overline{u}(\xi,\eta,\zeta)}\right]}_{A}\underbrace{\left[\exp - \frac{\lambda(x-\xi)}{u}\right]}_{B}\underbrace{\left[\frac{\exp\left[-\frac{1}{2}\left(\frac{y-\eta}{\sigma_y(x-\xi)}\right)^2\right]}{\sigma_y(x-\xi)}\right]}_{C}\underbrace{\left[\frac{\exp\left[-\frac{1}{2}\left(\frac{z-\zeta}{\sigma_z(x-\xi)}\right)^2\right]}{\sigma_z(x-\xi)}\right]}_{D}$$

Class of error and uncertainty	Terms of equation affected	Nature of error and uncertainty
Source strength	A	Both random and systematic likely
Decay or loss	B	Largely unknown - tends to be systematic
Dispersion	C, D	Tend to be systematic
Positional	A, B, C, D	Both random and systematic likely

Figure 8-1. Classification of input errors and uncertainties for model sensitivity tests.

λ = the decay or loss coefficient for the pollutant under consideration.

$\sigma_y(x-\xi)$ = the standard deviation of the cross-wind spread of the pollutant eminating from $\xi\,\eta\,\zeta$.

$\sigma_z(x-\xi)$. = the standard deviation of the vertical spread of the pollutant emanating from $\xi\,\eta\,\zeta$.

These are the input variables that we can manipulate in seeking concurrence between predicted and observed air quality levels and to which these predicted levels will be more or less sensitive. Our first study is an attempt to quantify these sensitivities via the model itself.

POTENTIAL ERRORS AND UNCERTAINTIES IN THE ESTIMATES OF INPUT VARIABLES

For a typical air quality pattern prediction, the TRC model requires approximately 200,000 input estimates. The probability of errors and uncertainties in these input estimates is very high. Figure 8-2 is a pictorial representation of the different mistakes that could be made for a *single* source situation and, as noted in the figure, there are eight distinct sources of input error and uncertainity. They are:

1. Misplacement of source with respect to geography and elevation.
2. Misestimation of source strength.
3. Misestimation of wind speed at source.
4. Miscalculation of trajectory of pollutant cloud or plume, due to erroneous or uncertain wind fields.
5. Misjudgment of vertical diffusion of cloud or plume, including erroneous distribution functions, as well as parametric errors.
6. Misjudgment of the lateral diffusion of cloud or plume, including erroneous distribution functions, as well as parametric errors.
7. Misestimation of decay or loss of pollutant.
8. Misplacement of receptor or monitor.

This appears to be an exhaustive list; at any rate, it is a sufficient one for our present purpose.

Figure 8-1 shows that, for sensitivity-analysis purposes, these eight sources of error and uncertainty may be grouped into four convenient classes:

1. Source strength estimates.
2. Pollutant decay or loss estimates.
3. Pollutant diffusion and distribution estimates.
4. Positional errors and uncertainties.

Of these, the first three are self-evident and essentially independent of one another. The fourth, however, in effect, affects all of the other estimates since, as shown in Figure 8-1, each of the terms in the diffusion equation

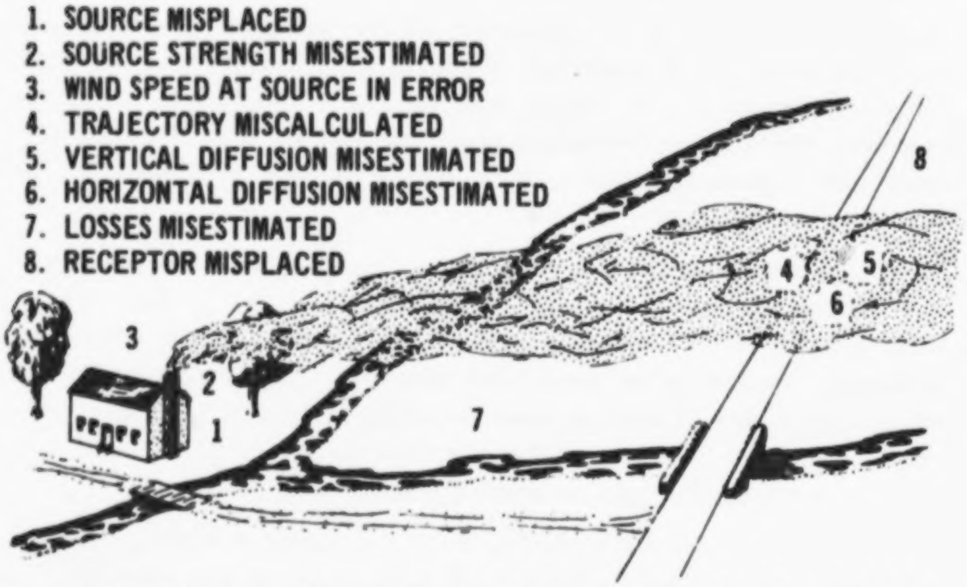
1. SOURCE MISPLACED
2. SOURCE STRENGTH MISESTIMATED
3. WIND SPEED AT SOURCE IN ERROR
4. TRAJECTORY MISCALCULATED
5. VERTICAL DIFFUSION MISESTIMATED
6. HORIZONTAL DIFFUSION MISESTIMATED
7. LOSSES MISESTIMATED
8. RECEPTOR MISPLACED
3
2
1
7
4
5
6
8

Figure 8-2. Sources of input errors and uncertainties in variables utilized in air quality simulation models.

upon which the model is based depends upon the *positions* of the source and the receptor. Errors and uncertainties in estimating the relative positions of the source and the receptor, and in estimating the time of flight and path between the two, *automatically* involve errors in the estimates of the source strength and the decay or loss and diffusion of the pollutant. For example, if the transporting wind direction is misestimated, the receptor "sees" the wrong sources, the time of flight is misjudged, and the diffusion is misestimated. The only time when no "error" is involved occurs when the sources and meteorological conditions are absolutely uniform over the region, a case of less than trivial interest.

The nature of likely errors and uncertainties in the input parameters is of considerable interest, particularly the distinction between *random* and *systematic* errors. In preparing source inventories, we fully expect a random component of error since we can seldom even measure the output of a given source precisely, and we know that most sources do not operate at a single, steady emission rate. On the other hand, we should also expect some systematic component of error, with a tendency for this component to be in the nature of an *underestimate*. This is because of the high probability that, amidst thousands and tens of thousands of sources, we will tend to overlook some entirely, but will not be inclined to compensate with imaginary sources.

On the other hand, quite irrespective of the reality of simple exponential decay or losses of the pollutant, the error in estimating this rate of loss is apt to be systematic in nature. For the more complicated photochemical reactions and product formation rates, for which I have not seen anything more than rudimentary simulation models, a mixture of random and systematic errors may appear.

For short times of flight and averaging, we would expect, from the nature of atmospheric diffusion, to see sizable random errors in the estimates of vertical and lateral diffusion rates. Over longer distances and times of averaging, however, when these local variabilities have been suitably smoothed, any error should tend to become systematic. Since the model requires at least 1-hour averages through these variations, our primary problem is probably with systematic over- or under-estimates of diffusion.

The positional errors are of two kinds: (1) geographic misplacement, which is largely a surveying problem (for fixed sources and receptors) and a fixed-point referencing problem (for mobile sources and receptors), and (2) advection or trajectory errors due to erroneous estimates of the wind field and location within the wind field. Suppression of the geographical error depends upon the precision one is willing to pay for in locating sources and receptors; these errors are probably random in nature. The trajectory errors, however, will depend upon the precision and spatial density of airflow measurements at various altitudes in the lower levels of the atmosphere. Although both random and systematic errors are probably present, the requirements for maintaining mass continuity for our representation of these flow fields operate strongly for systematic errors. The wind fields in adjacent grid cells are not independent of one another; an error in one estimate is reflected in neighboring estimates by this generally positive correlation, through the equation of continuity.

Finally, as is evident from the choice of words in the last few paragraphs, we recognize the conventional distinction between errors and uncertainties: errors can be identified and corrected whereas uncertainties cannot be corrected. Beyond this, the effects of these "mistakes" are indistinguishable for our present purposes, and we shall refer to them simply as "errors." The distinction between *random* and *systematic* errors is of much greater importance.

THE TESTS FOR SENSITIVITY

The objective of sensitivity tests is, of course, to measure the error in the predicted quantity, in this case, pollutant concentration, as a function of increasing errors in each of the input variables. The rate of change of the *predictand* error as a function of the rate of change of the *predictor* error is the measure of the sensitivity of the former to the latter. Since in air-quality pattern predictions (the regional problem) we are dealing with numerous predicted values that range through several orders of magnitude, it is convenient to measure the *relative* error rather than the absolute error in the air quality predictions.

Let

X_T = the "true" concentration of a pollutant at a given station,

X_E = the estimate of concentration after an input parameter error is introduced.

Then

$$\frac{X_T - X_E}{X_T} = \text{fractional error in } X \text{ produced by the input error.}$$

For N separate estimates, we have

$$\overline{\left(\frac{X_T - X_E}{X_T}\right)} = \frac{1}{N} \sum \frac{X_T - X_E}{X_T}\,, \tag{1}$$

and

$$(v')^2 = \frac{1}{N} \sum \overline{\left(\frac{X_T - X_E}{X_T}\right)}^2 - \left(\frac{X_T - X_E}{X_T}\right)^2, \tag{2}$$

where equations (1) and (2) specify the mean and variance of the fractional error distribution, respectively. We have chosen these distributions and their mean and variance (or the standard deviation, $\left[\overline{(v')^2}\right]^{1/2}$) as the measures of predictand errors. We should note that the value of $(X_T - X_E)/X_T$ must be less than or equal to one, since X_E cannot be less than zero. Assumptions with regard to the distribution functions for the fractional errors do not arise in the present analysis, but with this latter constraint, we expect these distributions to be skewed toward negative values of the fractional error of X.

The technique used for assessing the fractional error in X was simply: to run the model for a reasonable set of input parameters, solve for the concentration at 100 stations uniformly spaced over the Connecticut input parameters in a stepwise fashion. The mean and standard deviations of the fractional error in X were then constructed for each solution referenced on the original or "true" solution.

In order to assure a systematic and controlled variation of the input-parameter error (and, incidentally, to conserve computer time), the following error generator was employed:

Let

X_T = the original or "true" value of any input parameter;

X_E = the erroneous value of the input parameter.

Then take

$$X_E = X_T\ (1 \pm a + b), \tag{3}$$

where a is the fractional error in X due to random errors and b is the fractional error in X due to systematic errors. Then

$$\frac{X_T - X_E}{X_T} = -b \mp a \tag{4}$$

and $-b \mp a \leqslant 1$. In order to give a the character of a random variable, it was assigned the values $+|a|, o, -|a|$ with equal frequency and applied to the collection of input variables, such as the source strength Q, on a random basis. Likewise, a systematic error was generated by assigning a single value to b.

It follows directly from Equation (4) and the assignments of a that

$$\left(\overline{\frac{X_T - X_E}{X_T}}\right) = -b \tag{5}$$

and

$$\overline{(v'_x)^2} = \frac{2}{3}\ a^2, \tag{6}$$

i.e., the mean and variance of the fractional input errors are specified separately by a and b.

For the present sensitivity test, a random error analysis has been done only for the source strength field, Q. Analyses of systematic errors have been completed for all of the input parameters except windspeed. The measures used are shown in Figure 8-3.

RESULTS OF SENSITIVITY TESTS

The situation chosen for these sensitivity tests was based on a real-world case for which verification measurements of SO_2 levels over a 21-station network covering Connecticut were available. The exact period was from 0600 to 0800 on October 30, 1968. (A 2-hour average was used in the verification program in order to assure significant sampling of SO_2, hence this 2-hour test period, rather than 1-hour.) The weather prior to the morning of October 30th was mostly clear to partly cloudy, with NW winds at 4 to 6 meters per second (m sec^{-1}). Surface temperatures during the night were in the low 30's with some reports of frost.

Prediction error measure	Input error measure		
	Class	Random error	Systematic error
$\overline{\left(\frac{\chi_T - \chi_E}{\chi_T}\right)}$ and $\sqrt{\overline{\left(\frac{\chi_T - \chi_E}{\chi_T}\right)^2} - \overline{\left(\frac{\chi_T - \chi_E}{\chi_T}\right)}^{\,2}}$	Source strength	$\overline{\left(\frac{Q_T - Q_E}{Q_T}\right)^2}^{\,1/2}$	$\overline{\left(\frac{Q_T - Q_E}{Q_T}\right)}$
	Decay	—	$(\lambda_T - \lambda_E)$
	Dispersion	—	$\left(\frac{\sigma_T - \sigma_E}{\sigma_T}\right)$
	Positional	—	$(\theta_T - \theta_E)$

Figure 8-3. Measures of input and air quality prediction errors used in sensitivity analysis.

The source inventory for SO_2 emissions in Connecticut is shown in Figure 8-4A. A summary of this inventory shows the following frequency of emissions in pounds per day per square mile (lbs day^{-1} mi^{-2}).

$\frac{\text{Emission rate (Q)}}{\text{Source cell area}}$, lb day^{-1} mi^{-2}	Number of source cells per 25 x 10^6 ft
> 1000	27
100 – 1000	98
10 – 100	827
1 – 10	3,248
< 1	1,358

As is clear from the map and summary, the emissions of SO_2 over this region are far from uniform, but they do exhibit a pattern of rural land usage in the northwest and northeast sections (with some notable local anomalies) and an industrialized and urbanized belt from southwest to northeast through the central portion of the region. There is also a relatively strong source region extending northward along the Thames River in the southeast section of the region.

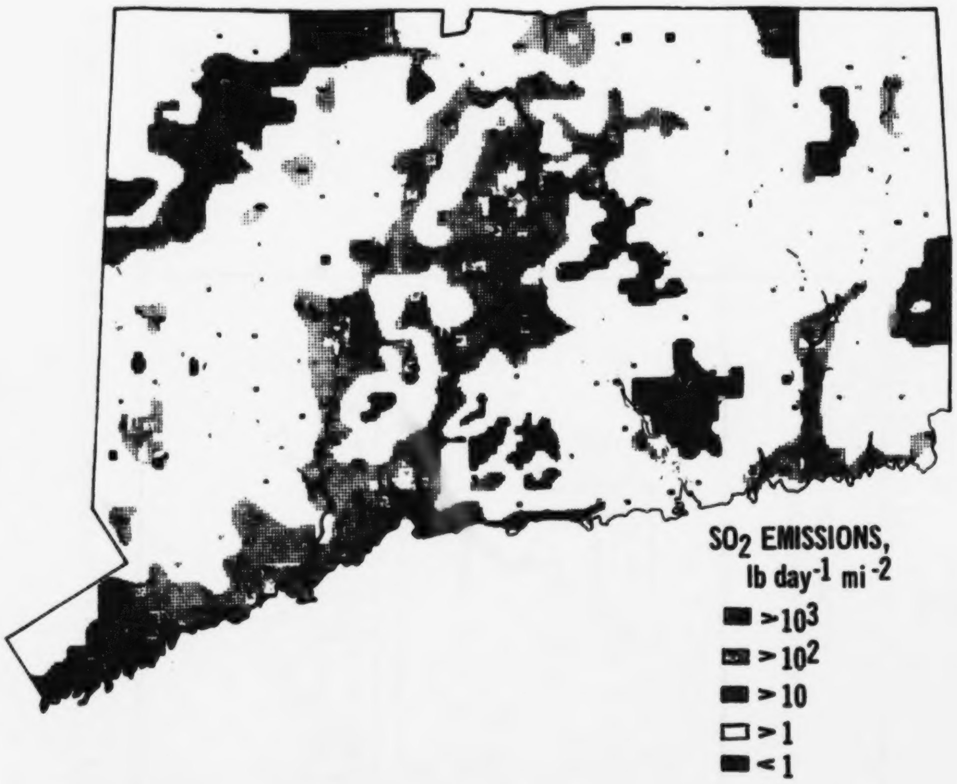

Figure 8-4A. Source inventory for SO_2 emissions in Connecticut used in TRC regional model.

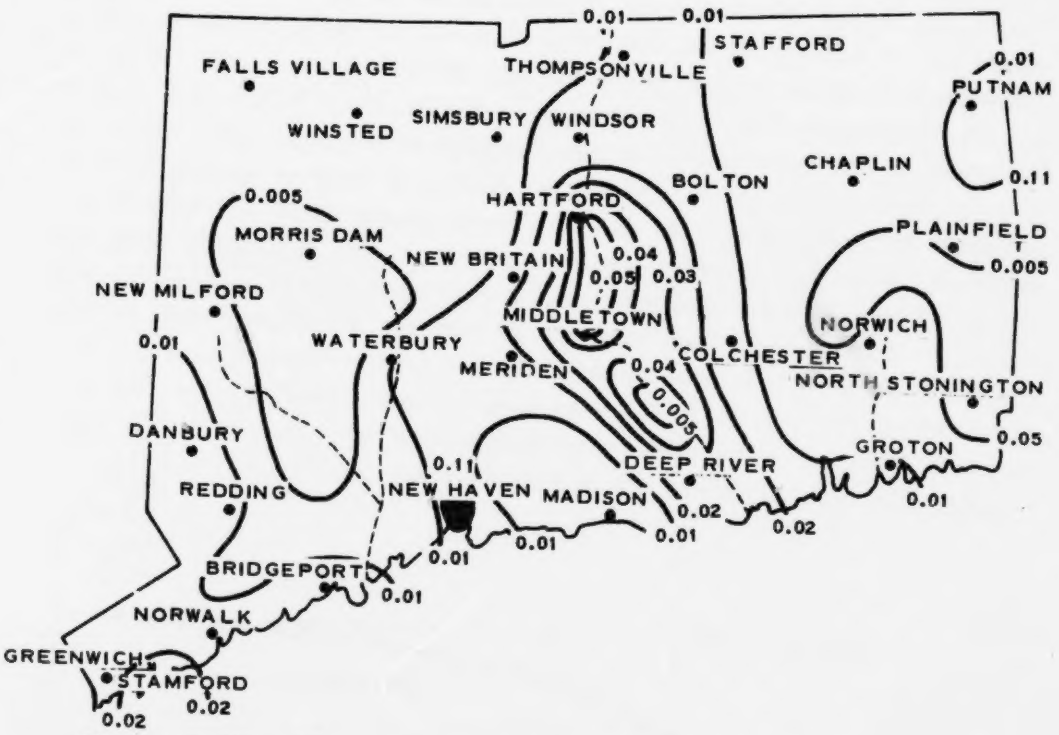
0.01
0.01
STAFFORD
FALLS VILLAGE
THOMPSONVILLE
0.01
PUTNAM
WINSTED
SIMSBURY
WINDSOR
CHAPLIN
0.11
BOLTON
HARTFORD
0.005
MORRIS DAM
PLAINFIELD
NEW BRITAIN
0.04
0.005
0.05
0.03
NEW MILFORD
MIDDLETOWN
NORWICH
0.01
WATERBURY
COLCHESTER
MERIDEN
0.04
NORTH STONINGTON
0.005
DANBURY
GROTON
0.05
DEEP RIVER
0.11
REDDING
NEW HAVEN
MADISON
0.01
0.02
0.01
0.02
0.01
BRIDGEPORT
0.01
0.01
NORWALK
GREENWICH
STAMFORD
0.02
0.02

Figure 8-4B. SO_2 concentrations predicted by TRC model for 0600–0800, October 30, 1968, from original, independently specified input variables.

Figure 8-4 B. shows the pattern of SO_2 concentrations predicted by the TRC model from the original choices of input parameters. (These choices are listed in Table 8-1.) The values of predicted SO_2 concentrations range from 0.003 ppm at North Stonington in the southeast corner of the region to 0.11 ppm at New Haven in the south-central part of the region. The pattern of concentrations shows the major axis of high concentrations extends from Hartford to the coast near Deep River; New Haven is something of a local anomaly.

Table 8-1. CHOICES OF INITIAL INPUT PARAMETERS FOR TRC REGIONAL MODEL USED TO ESTABLISH REFERENCE CONCENTRATIONS FOR SENSITIVITY TESTS

Input parameter	Value or method of choice
Source strength	Connecticut source inventory for SO_2, corrected for diurnal variations and degree days[a]
Wind field	320° at 6 m sec^{-1}
Decay coefficient	0.231, Half-life of 3 hr
Diffusion coefficients	Appropriate to a partly-cloudy night with moderate wind speeds[a]

[a] See Reference 3.

Figure 8-5 shows the frequency distribution of predicted values of SO_2 concentration occasioned by this original choice of input parameters. This distribution is quite typical, being strongly skewed toward large values of X_T. Note however that there are several values of $X_T < 0.005$ ppm. Since X_T enters in the denominator of our measures of the mean and variance of the fractional errors in X, these low values can lead to spuriously high values of these measures. This situation led to no particular difficulty in the sensitivity tests, but required special attention in the verification tests discussed in later sections. Examples of the distribution of $(X_T - X_E) / X_T$ are shown in Figure 8-6, where they are plotted for increasing values of the *random* error in the source strength. As can be seen from Figure 8-6, the distributions of $(X_T - X_E) / X_T$ are reasonably symmetrical near zero and are well behaved. (The frequency distributions of $(X_T - X_E) / X_T$ are tabulated for each sensitivity test in Appendix A.)

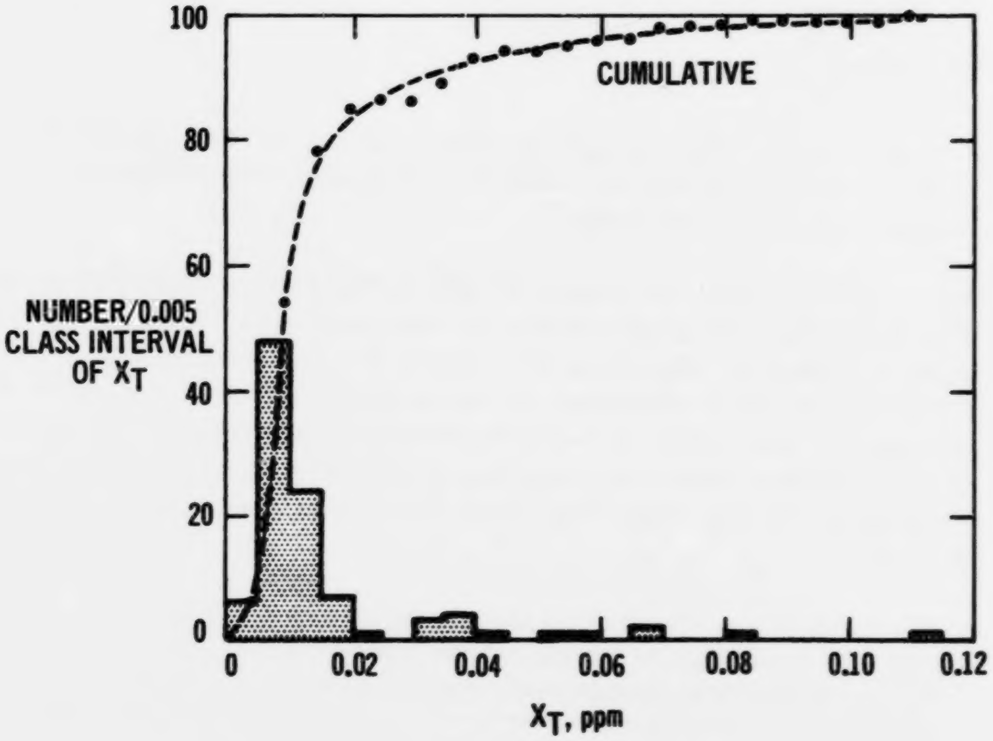

Figure 8-5. Frequency distribution of SO_2 concentrations predicted by TRC model for 0600–0800, October 30, 1968, from original, independently specified input variables.

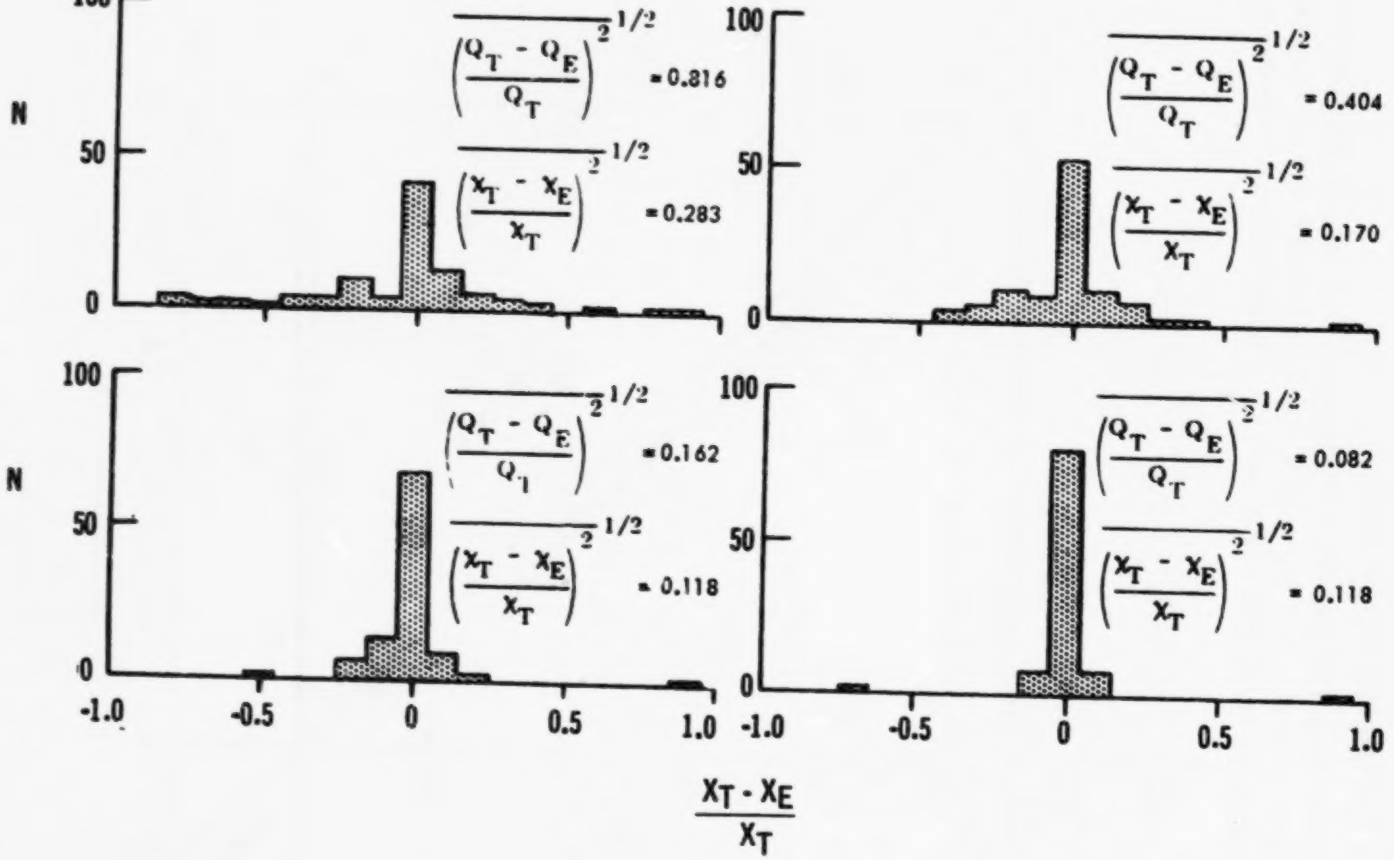

Figure 8-6. Frequency distributions of fractional error in concentration predictions, $(X_T - X_E)/X_T$, as random error of source strengths, $(Q_T - Q_E)/Q_T$, is increased.

Sensitivity to Random Errors in Q.

Since the model prescribes that the concentration X is directly proportional to the source strength Q, there must be a one-to-one correspondence between systematic errors in Q and errors in X. In terms of our measures of sensitivity,

$$\overline{[(X_T - X_E)/X_T]} = \overline{[(Q_T - Q_E)/Q_T]},$$

and

$$(v')^2 \equiv 0.$$

This result, which derives directly from the model, is shown in Figure 8-7.

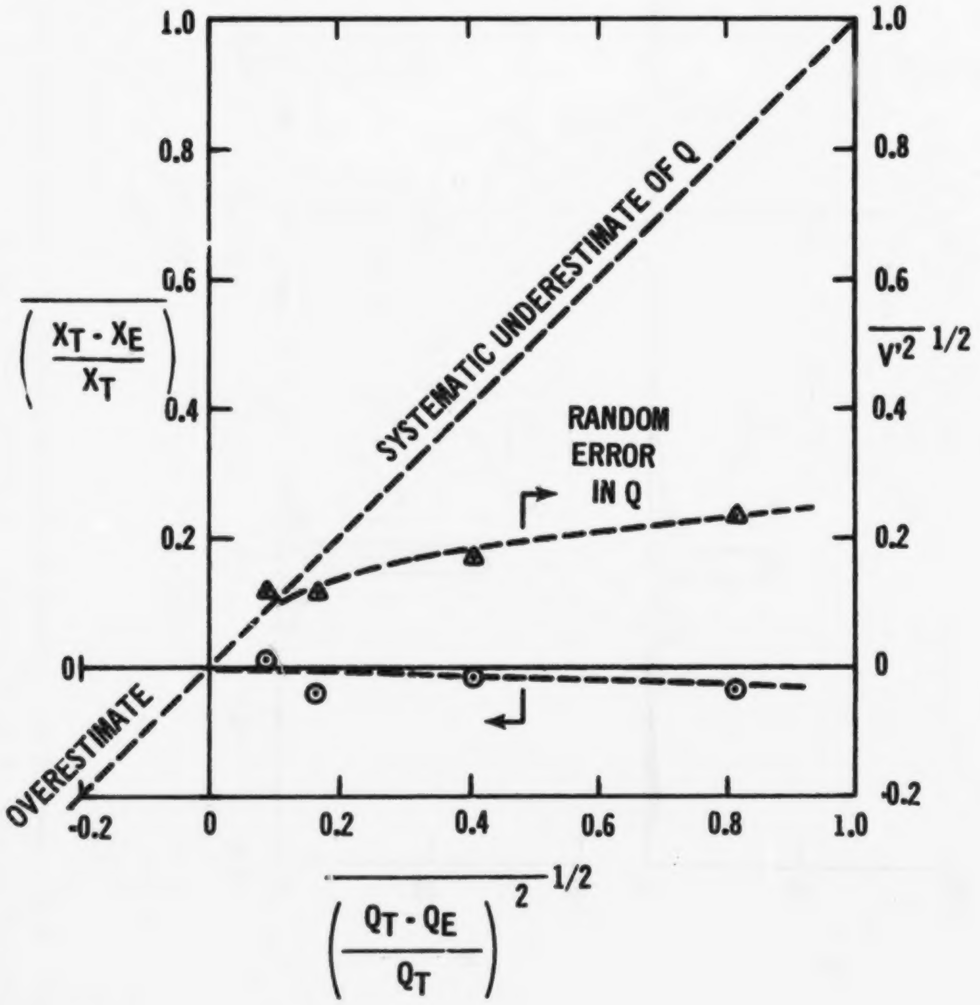

Figure 8-7. Mean and standard deviation of errors in concentration predictions as functions of a random and systematic errors in source-strength estimates.

Random errors in Q produce a different result, namely

$$\overline{[(X_T - X_E) / X_T]} = 0,$$

but $\overline{(v')^2}$

is non-zero, i.e., while no systematic error in the prediction of concentration is introduced by random errors in Q, the distribution of the fractional errors in N is broadened as the random errors in Q increase. The calculated values for this relationship are tabulated in Table 8-2 and plotted in Figure 8-7. (The distributions of $(X_T - X_E) / X_T$ are shown in Figure 8-6.)

Table 8-2. CALCULATED VALUES OF MEAN AND STANDARD DEVIATION OF $(X_T - X_E) / X_T$ AS FUNCTION OF THE RMS[a] ERROR IN Q (RANDOM) (LIMITS ASSESSED AT THE 95 PERCENT CONFIDENCE LEVEL)

$\overline{\left(\frac{Q_T - Q_E}{Q_T}\right)^2}^{1/2}$	$\overline{\frac{X_T - X_E}{X_T}}$	$\overline{(v')^2}^{1/2}$
0.082	0.001 ± 0.02	0.101 < 0.118 < 0.134
0.163	−0.004 ± 0.02	0.101 < 0.118 < 0.134
0.409	−0.016 ± 0.03	0.146 < 0.170 < 0.194
0.823	−0.033 ± 0.05	0.244 < 0.283 < 0.323

[a] Root mean square.

The most notable feature of this particular analysis is the relative insensitivity of the concentration predictions to large random errors in the specification of the source strengths, at least as compared with systematic errors in this term. Evidently, among multiple sources these random errors tend to cancel each other effectively. Assuming a Gaussian distribution of

$$(X_T - X_E) / X_T,$$

which appears reasonable in this case from Figure 8-6, the range of this fractional error in X increases only by a factor of 2 while the root mean square value of the error in Q increases by a factor of 8. (Extreme errors are listed in Appendix A.)

This is a result of no small consequence when we specify the accuracy required for source inventories. If this result is substantiated by more exhaustive sensitivity analyses of other source distributions, a very real trade-off between required accuracies in source inventories, which are difficult and expensive at best, and useful accuracies of concentration predictions can be proposed. Clearly, accuracy of concentration prediction cannot be the sole criterion for source inventory accuracy. The latter must also be used to determine abatement strategies, and the need for accuracy on this account may be overriding. But, with this provison it is clear that concentration predictions are much more vulnerable to *systematic* errors in the source specification than they are to *random* errors in this input variable.

Sensitivity to Systematic Errors in Decay Coefficient, λ.

Although the physical reality of a simple exponential decay of SO_2 with travel time has not been rigorously demonstrated, our experiences with the TRC model show that a distinct improvement in SO_2 concentration predictions is achieved with this corrective term. It is, therefore, at least of practical interest to determine the sensitivity of X to variations in this empirical input parameter. Our reference here is a half-life of 3 hours (λ = 0.231 hr^{-1}).

The effect of varying systematically the decay coefficient, λ , on the mean and standard deviation of $(X_T - X_E) / X_T$ is tabulated in Table 8-3 and shown graphically in Figure 8-8.

Table 8-3. CALCULATED VALUES OF MEAN AND STANDARD DEVIATION OF $(X_T - X_E) / X_T$ AS FUNCTION OF λ, DECAY COEFFICIENT OF SO_2 (LIMITS ASSESSED AT 95 PERCENT CONFIDENCE LEVEL)

λ, hr^{-1}	$\overline{\left(\frac{X_T - X_E}{X_T}\right)}$	$\overline{(v')^2}^{\,1/2}$
0.693 (HL[a]=1)	0.486 ± 0.04	$0.187 < 0.217 < 0.247$
0.462 (HL=1.5)	0.326 ± 0.03	$0.151 < 0.176 < 0.201$
0.231 (HL=3)	0	0
0.085 (HL=8)	−0.439 ± 0.08	$0.328 < 0.381 < 0.434$
0 (HL=∞)	−0.918 ± 0.17	$0.734 < 0.853 < 0.971$

[a] Half-life.

As should be expected, a systematic change or error in λ produces a systematic change in both the mean and variance of the fractional error in X . It is also clear, however, that these errors are more sensitive to an underestimate of λ , i.e., an overestimate of the half-life, than to an underestimate of the half-life. When referenced on a 3-hour half-life, which is an arbitrary choice, more rapid decay leads to only a moderate rate of increase in the mean and range of concentration prediction errors. Neglect of the decay term (λ = 0) produces the maximum mean and range of the fractional error in X, both of which tend to approach ±1.0.

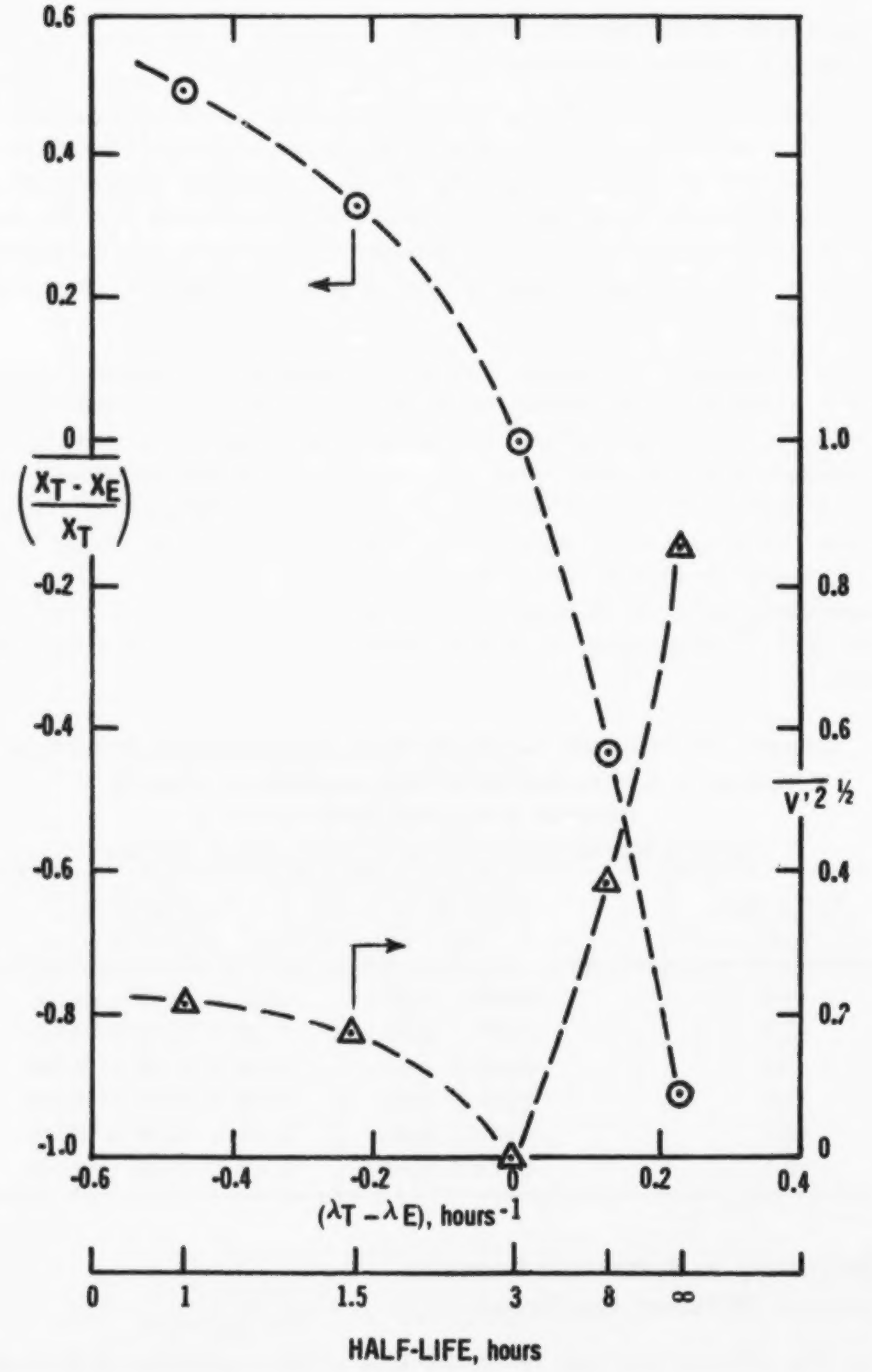

Figure 8-8. Mean and standard deviation of errors in concentraration predictions as functions of systematic errors in estimate of the half-life of pollutant.

Sensitivity to Systematic Errors in Lateral Diffusion Coefficient, σ_y .

As used in the TRC model, the lateral diffusion coefficient, σ_y , specifies the relative contributions of the sources arranged across the prior trajectory of the volume of air that is resident over the point at a time for which an air quality assessment is desired. In principle, this is no different from the more conventional practice of carrying a pollutant forward from each source point or area and speading it laterally according to the Gaussian distribution specified by σ_y.

More importantly, of course, the lateral spread of a pollutant emanating from multiple sources quickly mixes pollutant with pollutant and tends to produce a more or less uniform cross-wind concentration. It is not surprising, therefore, that we have found the model's predictions of ground level concentration to be quite insensitive to errors in the lateral diffusion coefficient. These errors are tabulated in Table 8-4 and shown graphically in Figure 8-9. As can be seen, the mean error in $(X_T - X_E) / X_T$ is not significantly different from zero and the spread of these errors, as measured by $\overline{(v')^2}^{1/2}$ comparable to those produced by a random error in Q (Figure 8-7).

Table 8-4. CALCULATED VALUES OF MEAN AND STANDARD DEVIATION OF $(X_T - X_E) / X_T$ AS FUNCTION OF SYSTEMATIC ERRORS IN LATERAL DIFFUSION COEFFICIENT σ_y (LIMITS ASSESSED AT 95 PERCENT CONFIDENCE LEVEL)

$\frac{\sigma_{yT} - \sigma_{yE}}{\sigma_{yT}}$	$\overline{\left(\frac{X_T - X_E}{X_T}\right)}$	$\overline{(v')^2}^{1/2}$
−0.2	−0.003 ± 0.02	0.105 < 0.122 < 0.139
+0.2	0.007 ± 0.03	0.130 < 0.151 < 0.172
−0.5	−0.018 ± 0.03	0.138 < 0.161 < 0.183
+0.5	0.012 ± 0.03	0.138 < 0.161 < 0.183
−0.7	−0.032 ± 0.04	0.170 < 0.197 < 0.224
+0.7	0.014 ± 0.03	0.141 < 0.164 < 0.187

Sensitivity to Systematic Errors in Vertical Diffusion Coefficient, σ_z

Vertical diffusion has been recognized as a critical component of air quality prediction for some time, principally through the employment of measures of the depth of the mixed layer.[6] The inherent sensitivity of concentration predictions to errors in σ_z derives directly from the basic diffusion equation (Figure 8-2), since, for ground level concentrations, $(z = 0)$,

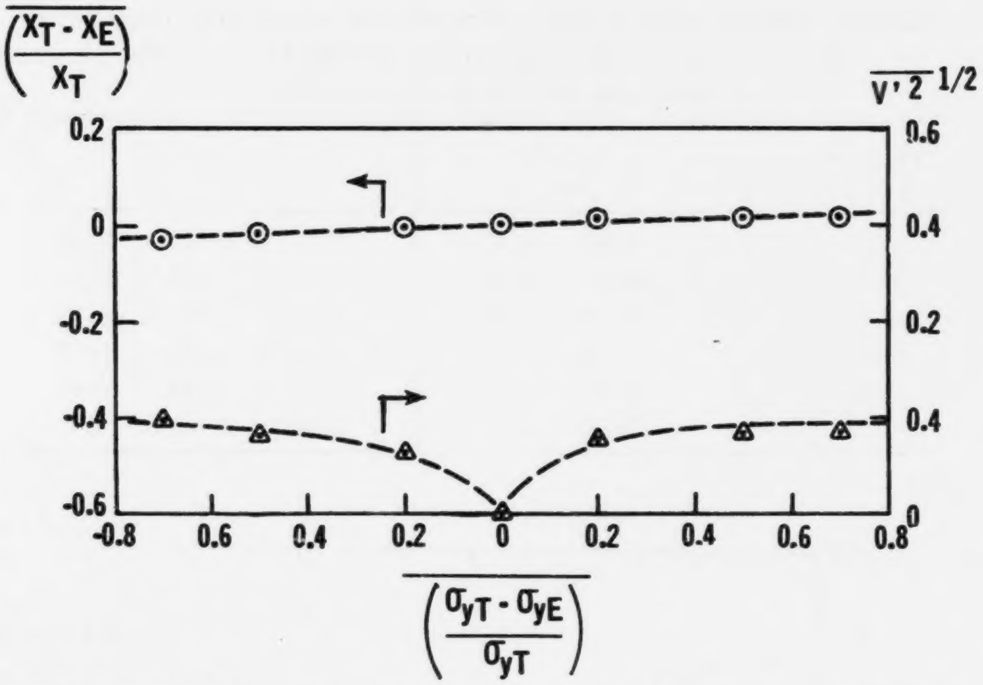

Figure 8-9. Mean and standard deviation of errors in concentration predictions as functions of systematic errors in estimate of lateral diffusion coefficients.

$$\frac{\delta X}{X} = \left(\frac{\zeta^2 - \sigma_z^2}{\sigma_z^{\,2}}\right) \frac{\delta \sigma_z}{\sigma_z} \tag{7}$$

is the fractional change in X as a function of the fractional change in σ_z. Equation (7) indicates that the fractional error in X will be large when σ_z is small relative to the source height, ζ, a situation that may extend to considerable distances when vertical mixing is slow (stable conditions).

The tests of sensitivity of $(X_T - X_E) / X_T$ to fractional changes in σ_z are tabulated in Table 8-5 and shown graphically in Figure 8-10. The extreme sensitivity of X to σ_z when σ_z is small $(\sigma_{zT} - \sigma_{zE} \rightarrow \sigma_{zT})$ is clearly evident from this figure. For substantial *overestimates* of σ_z $(\sigma_{zT} - \sigma_{zE} < 0)$, this sensitivity behaves very similar to errors in σ_y.*

---

*The avoidance of the sensitivity to small values of σ_y is, in part, due to the fact that area sources with a minimum dimension of 5,000 feet predominate in the model.

Table 8-5. CALCULATED VALUES OF MEAN AND STANDARD DEVIATION OF $(X_T - X_E) / X_T$ AS FUNCTION OF SYSTEMATIC ERRORS IN VERTICAL DIFFUSION COEFFICIENT, σ_z

$\frac{\sigma_{zT} - \sigma_{zE}}{\sigma_{zT}}$	$\overline{\left(\frac{X_T - X_E}{X_T}\right)}$	$\overline{(v')^2}^{\,1/2}$
−0.2	0.055 ± 0.03	$0.112 < 0.130 < 0.148$
+0.2	−0.071 ± 0.03	$0.143 < 0.164 < 0.187$
−0.5	0.120 ± 0.03	$0.133 < 0.155 < 0.177$
+0.5	−0.236 ± 0.05	$0.206 < 0.240 < 0.276$
−0.7	0.151 ± 0.03	$0.145 < 0.168 < 0.191$
+0.7	−0.429 ± 0.15	$0.669 < 0.776 < 0.885$

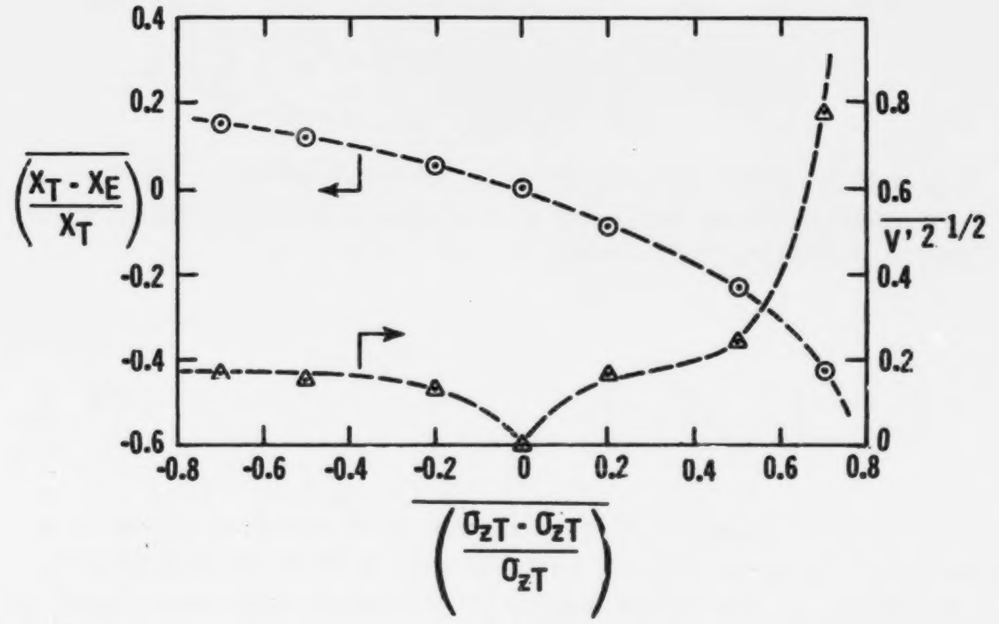

Figure 8-10. Mean and standard deviation of errors in concentration predictions as functions of systematic errors in estimate of vertical diffusion coefficients.

Sensitivity to Positional Errors Introduced by Systematic Errors in Wind Direction, Θ.

As noted previously, positonal errors, i.e., mislocation of the sources, receptors, and pollutant trajectories, automatically invoke errors in all of the input parameters. For the present study, a systematic error in the direction of the general wind field was utilized for the assessment of sensitivity to these compounded errors. Variations in windspeed were suppressed since, between the "stretching" effect at the source and the time-of-flight effect in the decay of the pollutant, errors in windspeed estimates tend to be compensatory. Rather, the wind direction field over the region was simply rotated the desired number of degrees from the originally chosen wind direction, 320°.

As might be expected, the errors produced by this input-error generation were rather spectacular. They are tabulated in Table 8-6 and shown graphically in Figure 8-11. (One completely erroneous station contributed so strongly to the variance of $(X_T - X_E) / X_T$ for $\Theta_T - \Theta_E = +20^\circ$ that this point has been deleted.)

Table 8-6. CALCULATED VALUES OF MEAN AND STANDARD DEVIATION OF $(X_T - X_E) / X_T$ AS FUNCTION OF SYSTEMATIC ERRORS IN WIND DIRECTION, Θ (LIMITS ASSESSED AT 95 PERCENT CONFIDENCE LEVEL)

$\Theta_T - \Theta_E$, degrees	$\overline{\left(\frac{X_T - X_E}{X_T}\right)}$	$\overline{(v')^2}^{\,1/2}$
+10	−0.134 ± 0.04	0.191 < 0.222 < 0.253
−10	−0.124 ± 0.04	0.193 < 0.218 < 0.248
+20	0.436 ± ?	–
−20	−0.232 ± 0.26	1.14 < 1.32 < 1.51
+40	−0.152 ± 0.22	0.930 < 1.08 < .123
−40	−0.524 ± 0.33	1.45 < 1.68 < 1.92

As can be seen from Figure 8-6, the mean fractional concentration errors are not spectacular, but the spread of these errors, as measured by $\overline{(v')^2}^{\,1/2}$, is. To relate this analysis to a practical situation, it is as though one had a single wind measurement at the center of the region and extrapolated this measurement, with its error, to the entire region. Much more sophisticated analyses are imaginable and should be pursued. But this analysis points clearly to the need for accurate representations of the regional wind field.

Summary of Sensitivity Tests

In order to compare and summarize these sensitivity test results, all of the systematic input errors have been standardized as a fraction of the original input value and the mean and standard deviation of $(X_T - X_E) / X_T$ have been plotted for each of these in Figure 8-12. (Errors in λ were normalized by 0.231, the value appropriate to a 3-hour half-life, and errors in Θ were normalized by dividing by 180°, the maximum error that could be encountered in this input parameter.)

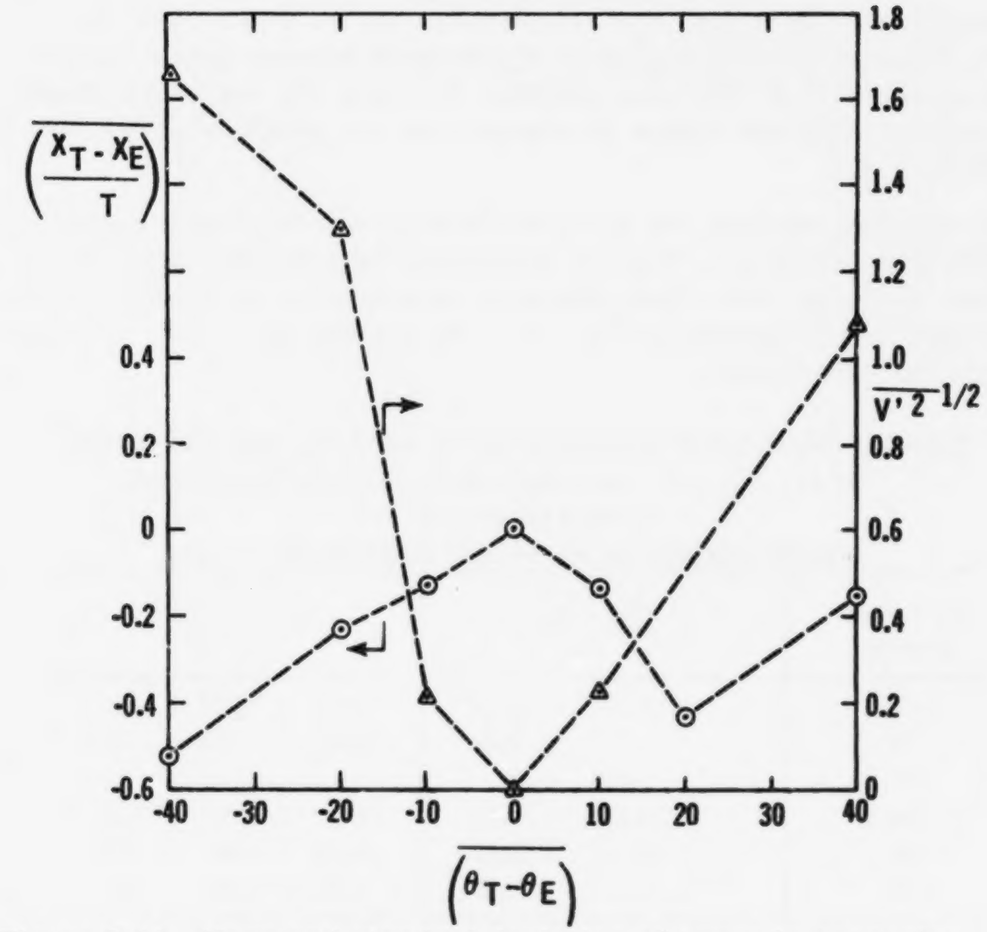

Figure 8-11. Mean and standard deviation of errors in concentration predictions as functions of systematic errors in estimate of regional wind direction.

In studying Figure 8-12, it is well to keep in mind that the reference values for the input parameters are arbitrarily chosen. These curves should not be constructed as a universal or general representation of error sensitivity. With this caveat, however, it is clear that the sensitivities of concentration prediction to systematic input errors in the expected range of ± 0.5 may be ranked as follows:

1. Wind field directional errors.
   Mean error ⩽ ± 50 percent; individual errors > 200 percent.
2. Source strength errors.
   Mean errors ⩽ ± 50 percent; individual errors ⩽ ± 50 percent.
3. Decay rate errors.
   Mean error ⩽ 40 percent; individual errors ⩽ ± 50 percent.
4. Vertical diffusion errors.
   Mean error ⩽ 25 percent; individual errors ⩽ ± 50 percent.

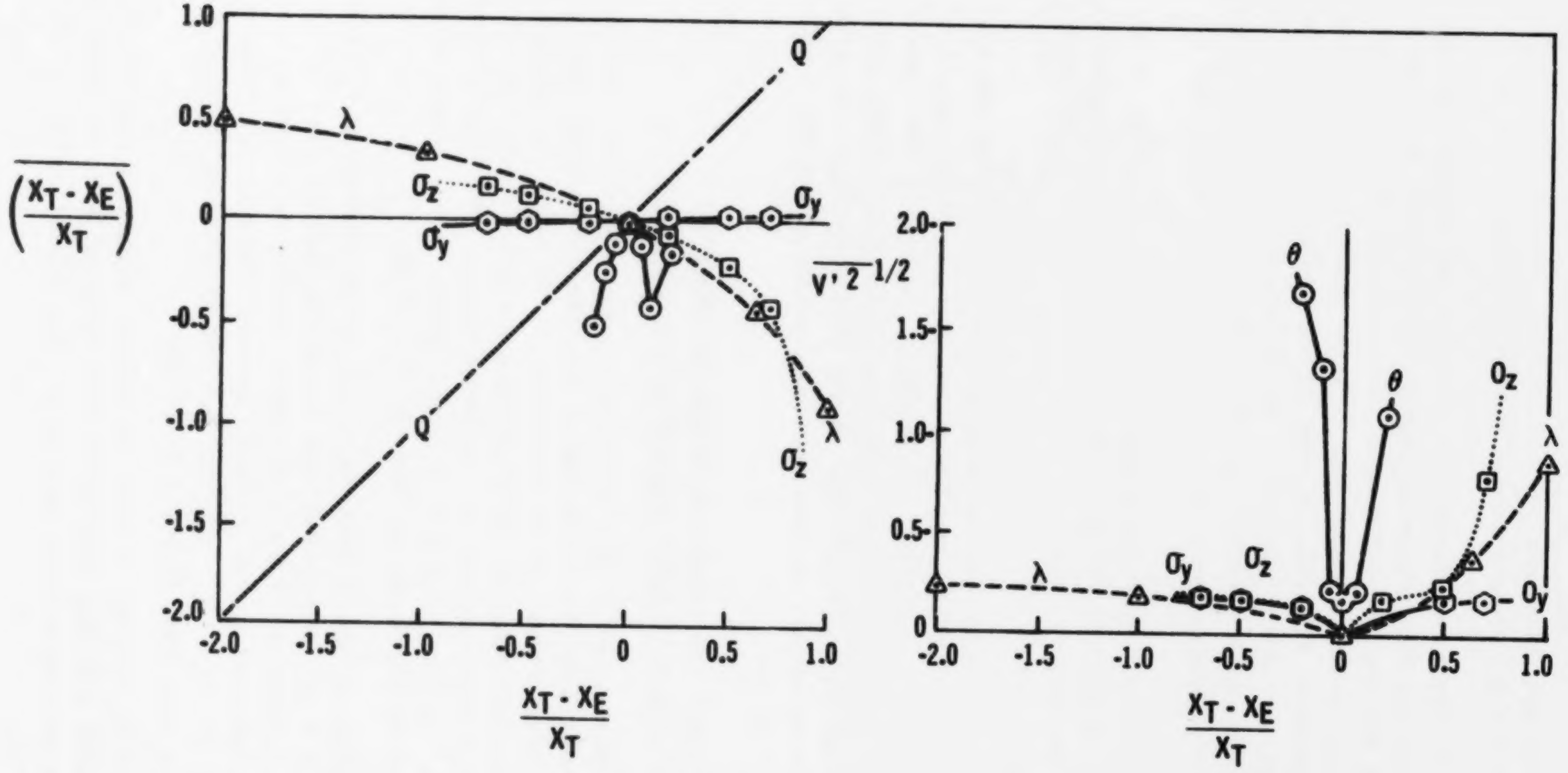

Figure 8-12. Comparative summary of mean and standard deviation of errors in concentration prediction as function of fractional systematic errors in each input variable. Sensitivity of model to errors is measured by slope of curves.

5. Horizontal diffusion errors.
   Mean error $\leqslant$ 5 percent; individual errors $<$ 40 percent.

The greatest sensitivites are found when errors become so large that input parameters approach their singular or limiting values (0 for σ_z, and ∞ for λ) but, assuming that prudence in the use of models will obviate this difficulty, by far the most serious expected error is found when the wind direction field is misestimated. Errors in the mean of the concentration prediction, averaged over the region, approach ± 25 to 50 percent, and errors in individual concentration predictions readily exceed 200 percent of the true value when wind direction errors reach and exceed 20°.

Surprisingly, air quality predictions showed no particular sensitivity to random source strength errors. As noted previously, however, this is probably a function of the density of the multiple sources and deserves more rigorous study from that point of view.

Finally, this whole study must be recognized as the case study that it is. Because of the obvious importance of a clear and quantitative measure of the accuracies and uncertainties of simulation predictions, this type of analysis should be extended and generalized far beyond this first effort. Insofar as these results pertain only to the TRC Regional Model, other models should be similarly exercised and examined for sensitivities to input errors and uncertainties.

A CASE STUDY OF SENSITIVITIES OF MODEL VERIFICATION TO INPUT PARAMETER VALUES

Since direct observations of SO_2 concentrations are available for 21 stations within Connecticut for the period used in the above sensitivity analyses, an unusually detailed analysis of the sensitivities of the model verification to changes in the input parameters arises as a welcome bonus in this study. This is, of course, a single case and must be treated as such. The results are well worth noting, however, (For a more general analysis of the verification of the TRC Regional Model, see the 1969 TRC Staff Report.[4])

For this analysis, we simply need redefine X_T as the *observed* value of SO_2 concentration at any given station and X_E as the predicted value for that station for any given set of input parameters, including the original set used as the base reference for the sensitivity analyses. The mean and standard deviation of $(X_T - X_E) / X_T$ constitute the test for goodness of fit or the verification of the model's predictive capabilities.

The values of X_T observed at the 21 verification stations and the fractional error associated with each observation when compared with the predicted values using the original input parameters (Table 8-1) are shown in Figure

8-13. As can be seen from that figure, the fractional errors in the verification of observed concentrations tend to cluster around zero, with the notable exceptions of two stations for which the observed concentrations are very low, 0.002 and 0.003 ppm (0.001 ppm is the threshhold level for the measurement system used to monitor SO_2). If these stations are eliminated, the mean value of $(X_T - X_E) / X_T$ is, in fact, zero, and there is a great temptation to do exactly that. The temptation has been resisted, however, primarily because there are several other observations of SO_2 in the < 0.005 ppm region that did not produce anomalous error values; one would be hard pressed to justify their retention if the two bad actors were eliminated on the grounds of unreliability of observation. Hence we retained all 21 stations.

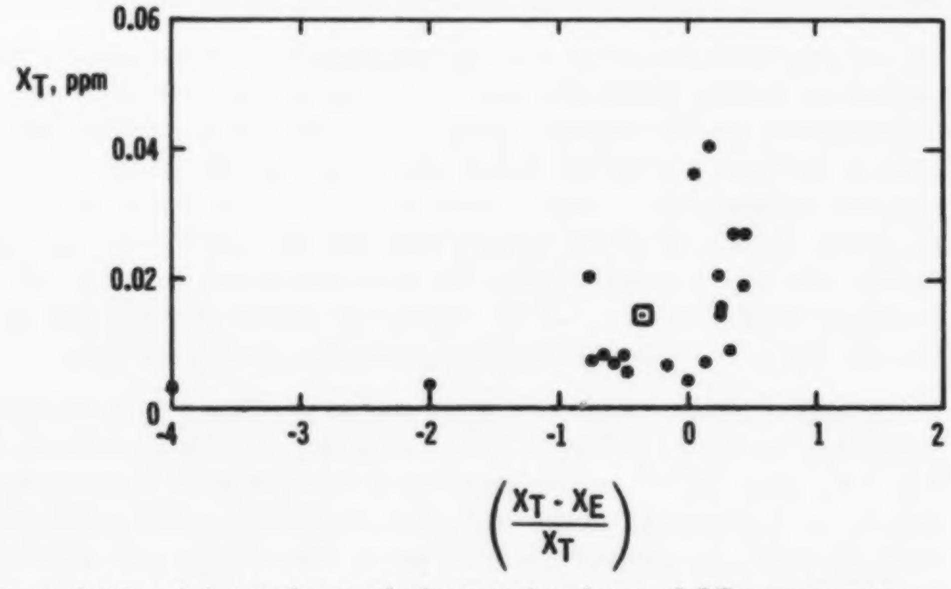

Figure 8-13. Joint values of observed values of SO_2 concentrations and fractional error in values predicted by TRC model, using original, independently specified values of input variables, for period 0600–0800, October 30, 1968.

Using the original input variables described in Table 8-1, the verification parameters for the observed *versus* predicted values of SO_2 were

$$\overline{\left(\frac{X_T - X_E}{X_T}\right)} = -0.642,$$

and

$$\overline{(v')^2}^{\,1/2} = 1.225$$

hardly an inspiring result. The question then asked was, "Could this verification be improved by varying input parameters for the model?" Normally, of course, input parameters must be chosen independently of the verification data, but the question is valid for analytical purposes.

Knowing the general behavior of the model and the results of the sensitivity analysis, we can immediately speculate that improved verification of the mean value of $(X_T - X_E) / X_T$ can be obtained in any or all of three ways: (1) reduce the source strengths uniformly by 40 percent (since in the mean, concentration predictions were overestimated by this amount), (2) increase the vertical diffusion rates by an amount that compensates the overestimate, and (3) decrease the half-life of SO_2, so as to compensate for the overestimate of X. In addition, we can test to see if systematic changes in either the wind direction or the horizontal diffusion rate reduce the verification errors.

We are also vitally concerned with the individual station verification (since it appears air quality assessment and control will be based on local values of concentration, not the regional average). It is imperative, therefore, that the *range* of verification errors be reduced also, a feature that is measured by the standard deviation of $(X_T - X_E) / X_T$, $\overline{(v')^2}^{1/2}$. It would be desirable, of course, to test all of the combinations and permutations of input parameters; and this is possible, given the time and resources to perform the necessary iterative solutions of the model. The present analysis does not go that far; rather, we have examined only one input variable at a time.

The effects of *random* variations in the source strengths on the verification parameters are shown in Figure 8-14. (Values and confidence limits of $(X_T - X_E) / X_T$ and $\overline{(v')^2}^{1/2}$ are tabulated for all input variables in Appendix B.) Clearly, no improvement in the verification is achieved by this manipulation; both the mean and standard deviation are at their minima with the original source inventory.

The effects of *systematic* variation of the source strengths are shown in Figure 8-15 and, as expected, a uniform reduction by 40 percent of all the source strengths reduces the mean error in X to very near zero, and the standard deviation of the fractional error in X is reduced to 0.75 from its original value of 1.225. This is a distinct improvement; in fact, it is the best result that could be obtained from single-input-variable manipulation. Examination of Figure 8-16, however, shows that an equivalent improvement could be obtained by reducing the estimated half-life of SO_2 from 3-hours to 1-hour. The mean error for this case is also near zero and the standard deviation is reduced to 0.860. Figure 8-17 shows that even a very substantial increase in the vertical diffusion coefficients produces only a slight improvement in the mean error of concentration prediction, and no improvement at all in the standard deviation of the fractional errors in X, as should have been expected from the sensitivity analysis.

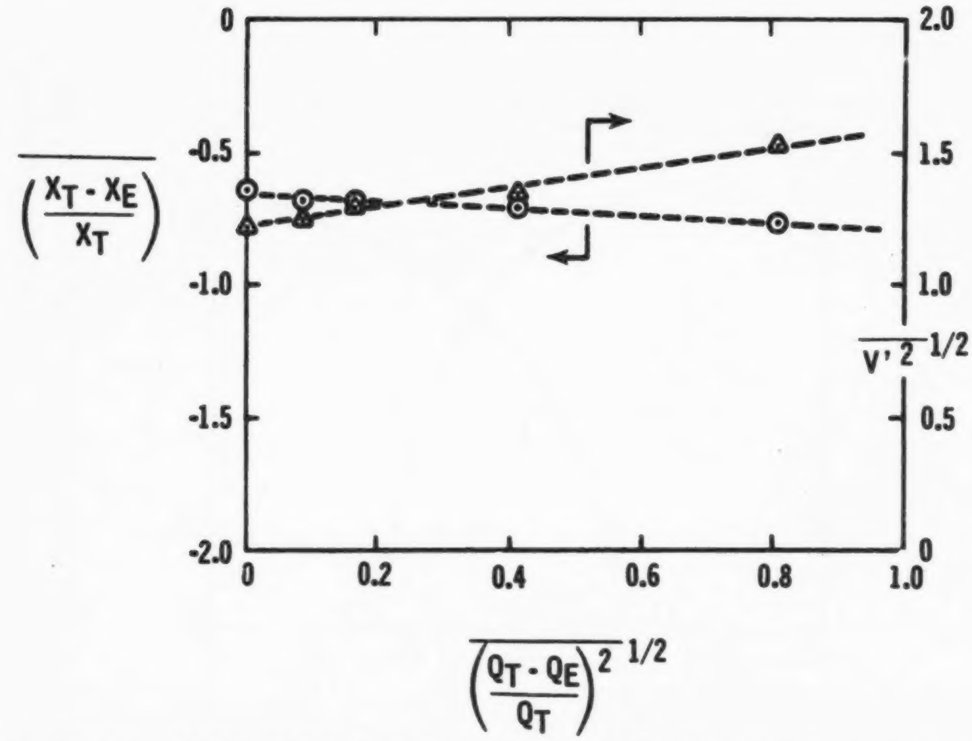

Figure 8-14. 0600–0800, October 30, 1968, verification scores for TRC model as a function of random errors in source strength specifications.

The effects of variations of the *horizontal diffusion coefficient* and of the *wind direction* are shown in Figures 8-18 and 8-19, respectively. Clearly, the TRC model could not be more indifferent to the choice of horizontal diffusion coefficients for this case. The model's sensitivity to the compounded errors introduced by changing the wind direction is reiterated in Figure 8-19, but the original choice of wind direction provides the best fit for this verification test.

To summarize this case study, Figure 8-20 shows the maximum improvements in the verification of the model that were achieved by varying, in turn, the vertical diffusion, the decay rate, and the source strengths. Of these, only the latter two provide a significant improvement in the verification scores. (See Appendix B for confidence limits on $(X_T - X_E) / X_T$ and $\overline{(v')^2}^{1/2}$ for these tests.)

No sweeping conclusions can be drawn from this single case study, but it seems unlikely that the source inventory for Connecticut is in error by a 40 percent overestimate. The other verification tests showed that mean concentrations were underestimated as frequently as they were overestimated using the same source of inventory. Rather, this partial result seems to emphasize the importance of better understanding of the decay and loss of SO_2.

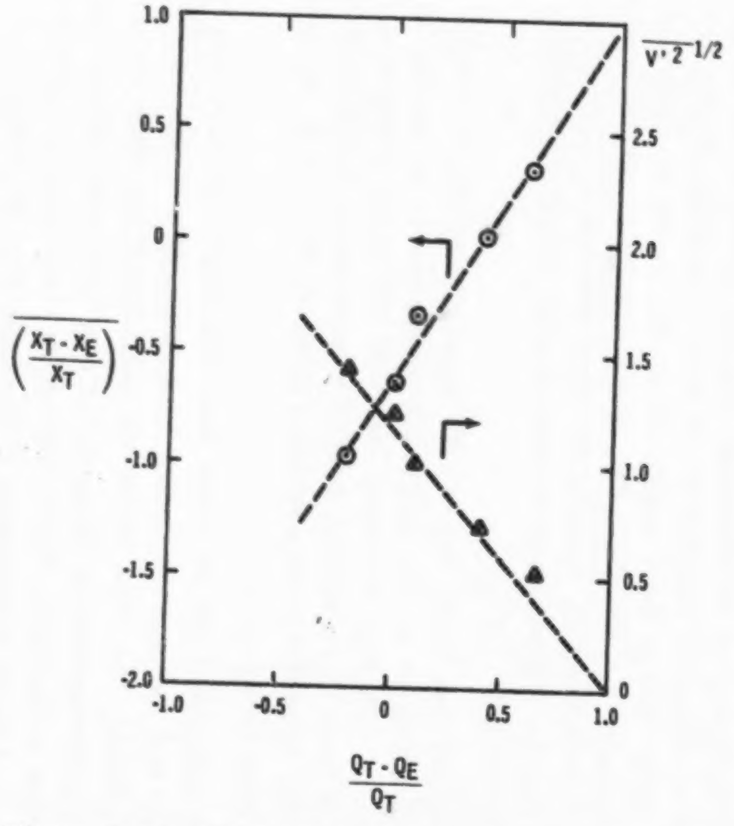

Figure 8-15. 0600–0800, October 30, 1968, verification scores for TRC model as a function of systematic changes in source strength specifications.

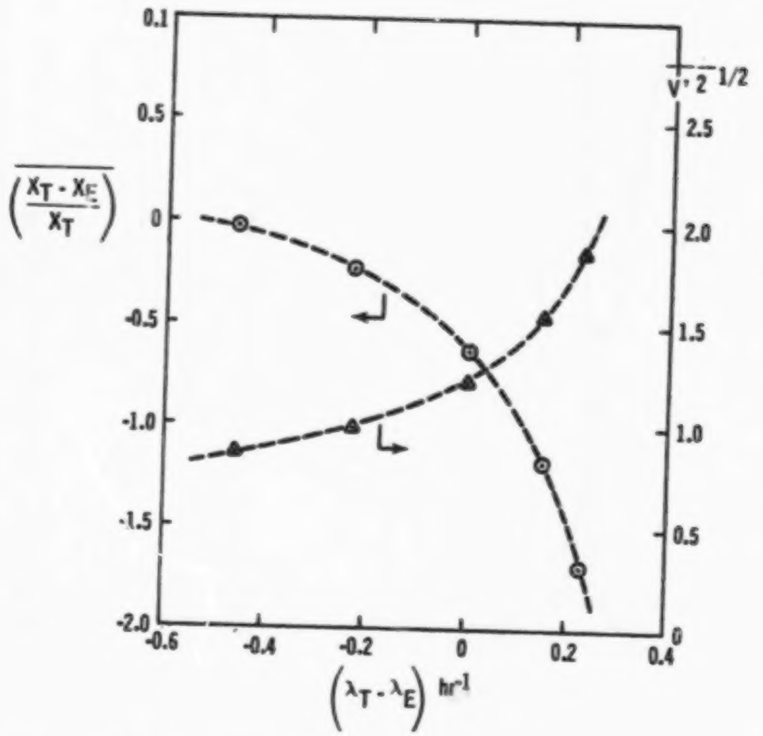

Figure 8-16. 0600–0800, October 30, 1968, verification scores for TRC model as a function of systematic changes in decay rate for SO_2.

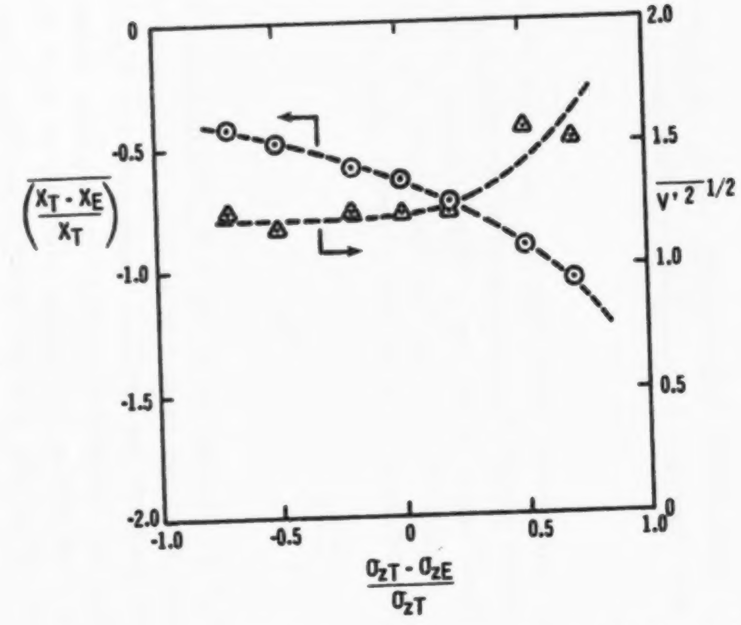

Figure 8-17. 0600–0800, October 30, 1968, verification scores for TRC model as a function of systematic changes in vertical diffusion coefficients.

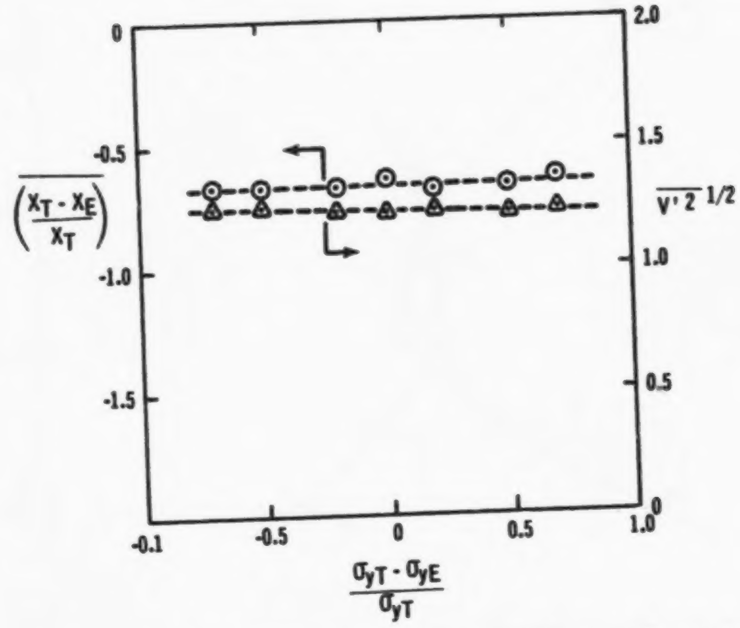

Figure 8-18. 0600–0800, October 30, 1968, verification scores for TRC model as a function of systematic changes in lateral diffusion coefficients.

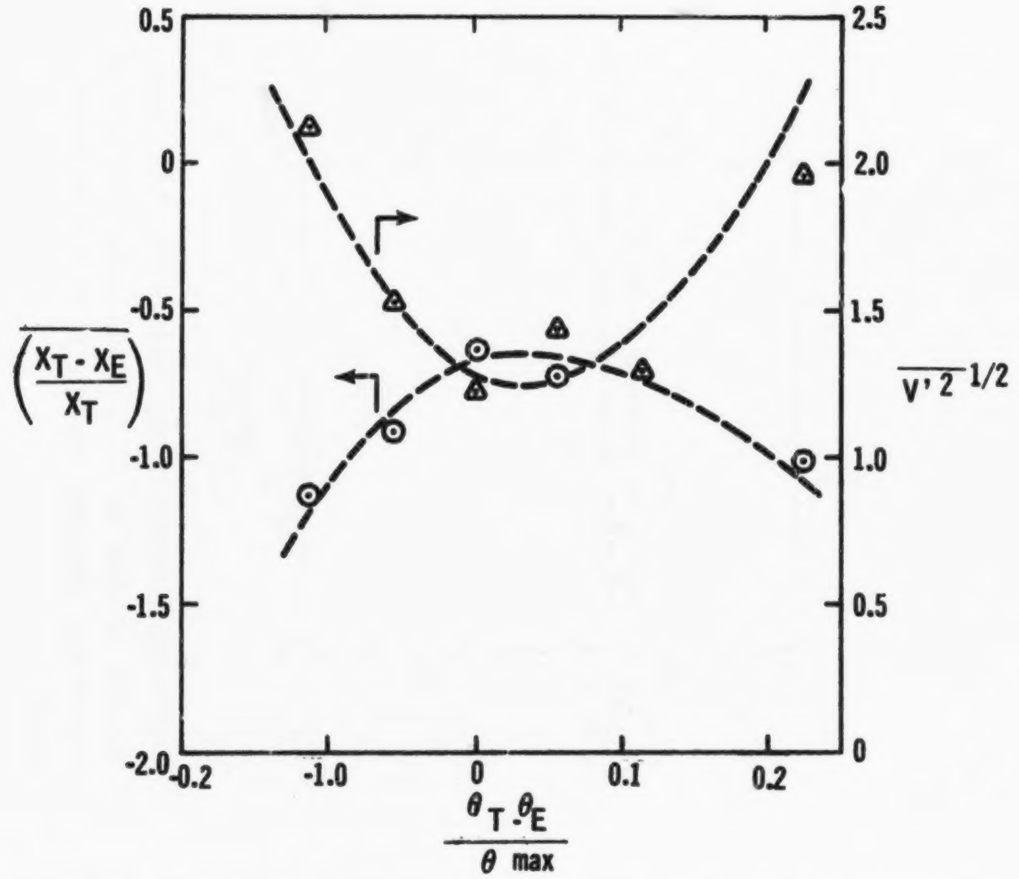

Figure 8-19. 0600–0800, October 30, 1968, verification scores for TRC model as a function of systematic changes in regional wind direction.

The empirical exponential decay and loss term used in the TRC model operates to reduce concentrations most at those stations that are relatively far removed from major source areas. The "effective" distance from each station to the contributory sources for that station, X_e, may be calculated from the model's estimates of X for two different values of λ ,

$$X_e = \frac{u}{\lambda_3 - \lambda_1} \ln \frac{X_{E3}}{X_{E1}} \qquad (7)$$

a parameter that is expected to change with wind direction. For the present case (NW winds), X_e ranges from 2 to 41 miles in Connecticut (Figure 8-21) and clearly portrays both the rural and urban areas and the presence of local sources in otherwise nonsource areas. For example, Danbury, Stamford, Bridgeport, and New Haven are subject primarily to local sources of SO_2 with NW winds, while the Hartford-Middletown-Deep River axis of SO_2

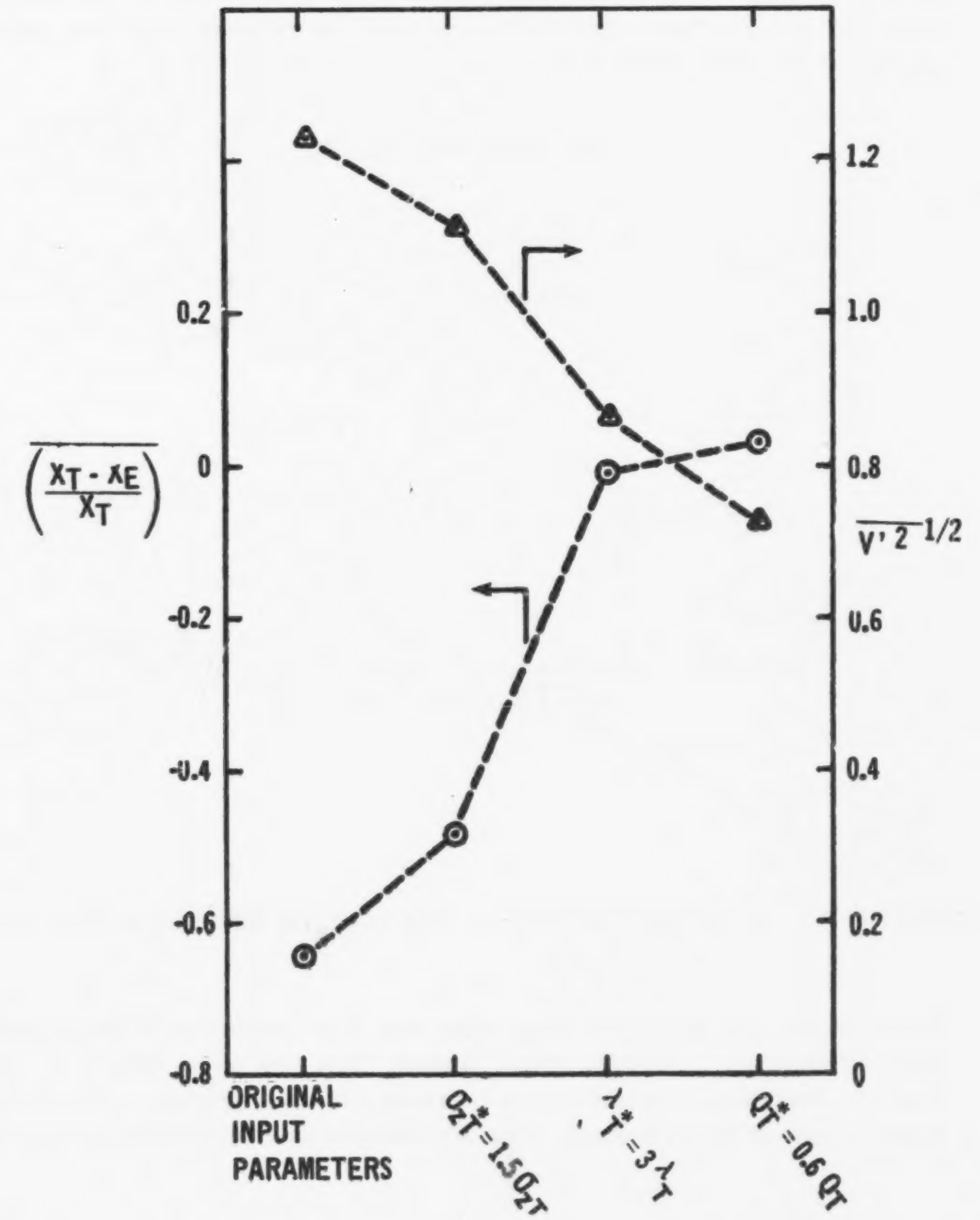

Figure 8-20. Summary of maximum improvements in verification of TRC model predictions of SO_2 concentrations for period 0600–0800, October 30, 1968, by independent manipulation of vertical diffusion, decay rate, and source strength field.

concentrations (Figure 8-5) represents the regional concentration of sources in the Hartford-Middletown area. Similarly, the Norwich-Groton area constitutes a regional source of SO_2. On the other hand, the New Milford-Morris Dam and the Colchester regions are obviously far removed from the major sources of SO_2 that affect them.

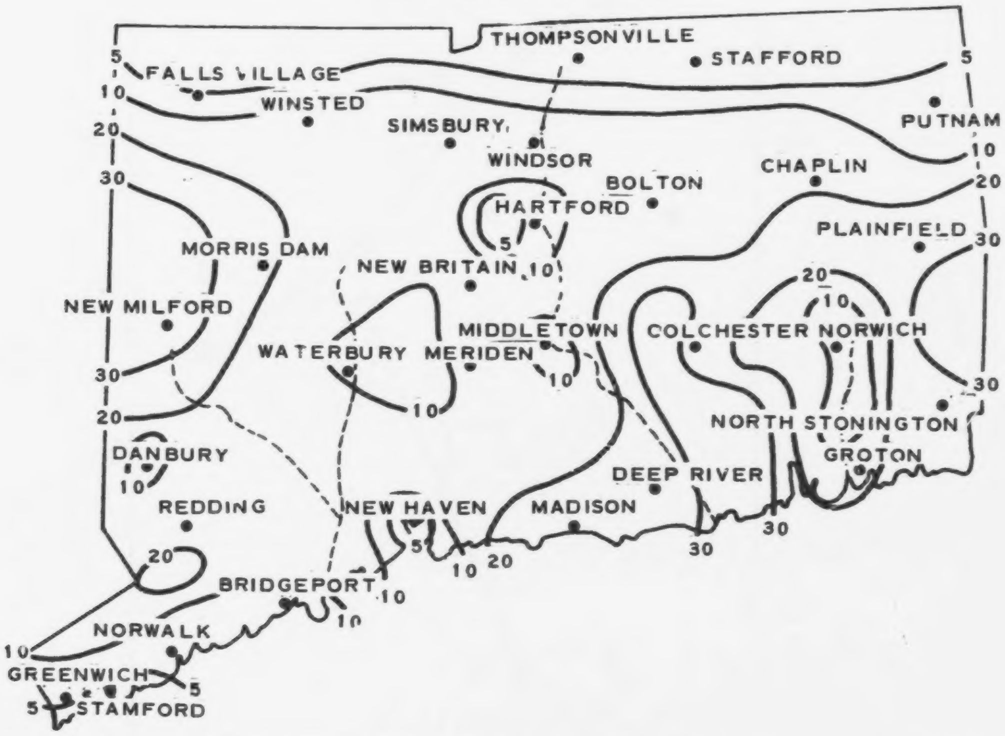

FIXED SAMPLING STATIONS

THOMPSONVILLE
STAFFORD
FALLS VILLAGE
WINSTED
SIMSBURY
WINDSOR
PUTNAM
BOLTON
CHAPLIN
HARTFORD
PLAINFIELD
MORRIS DAM
NEW BRITAIN
NEW MILFORD
MIDDLETOWN
COLCHESTER
NORWICH
WATERBURY
MERIDEN
NORTH STONINGTON
GROTON
DANBURY
DEEP RIVER
REDDING
NEW HAVEN
MADISON
BRIDGEPORT
NORWALK
GREENWICH
STAMFORD
5
10
20
30

Figure 8-21. Effective distance to SO_2 sources for case of NW winds.

These results are, of course, more suggestive than conclusive at the present level of analysis. If nothing else, however, they do point clearly to the powerful analytical capabilities of a reasonably faithful simulation model. As noted by one of my colleagues, these are indeed powerful, if expensive tools.

REFERENCES

1. Hilst, G. R. An Air Pollution Model of Connecticut. In: Proceedings the IBM Scientific Computing Symposium on Water and Air Resource Management. Yorktown Heights, N. Y. October 1967. IBM. Data Processing Division. White Plains. 1967. 251-274.
2. Bowne, N. E. Simulation Model for Air Pollution Over Connecticut. J. Air Pollution Control Assoc. *19*:570-574, August 1969.
3. Hilst, G. R. J. E. Yocom, and N. E. Bowne. The Development of a Simulation Model for Air Pollution over Connecticut, Vol. I. Travelers Research Center, Inc. Hartford, Conn. Final Report to the Connecticut Research Commission. TRC Report No. 7233-2798. 1967. 66p.
4. Hilst, G. R. Verification by Observation of the Application of An Air Pollution Model to the State of Connecticut (in press). Travelers Research Center, Inc. Hartford, Conn. Final Report to the Connecticut Research Commission. TRC Report No. 7242-365. September 1969.
5. Bowne, N. E. A Mathematical Model of Air Pollution in the State of Connecticut. Presented at 62d Annual Meeting of the Air Pollution Control Association. New York. June 22-26, 1969.
6. Holzworth, G. C. Estimates of Mean Maximum Mixing Depths in the Contiguous United States. Mon. Weather Rev.

APPENDIX A

Frequency distribution of errors in predicted concentration, $(X_T - X_E)/X_T$, for designated errors or values of variables. (100-station sensitivity tests.)

Range of $(X_T - X_E)/X_T$	Rms error in $(Q_T - Q_E)/Q_T$				Value of half-life, λ (hr^{-1})			
	0.082	0.163	0.409	0.823	0.693	0.462	0.085	0
0.860 to 0.959	1	1	1	1	1	1	1	1
0.760 to 0.859	0	0	0	1	11	0	0	0
0.660 to 0.759	0	0	0	0	17	2	0	0
0.560 to 0.659	0	0	0	1	11	8	0	0
0.460 to 0.559	0	0	0	0	15	13	0	0
0.360 to 0.459	0	0	1	3	14	18	0	0
0.260 to 0.359	0	0	1	4	11	20	0	0
0.160 to 0.259	0	2	6	5	10	20	0	0
0.060 to 0.159	8	9	10	13	10	13	0	0
0.040 to 0.059	81	68	53	42	0	5	4	4
−0.140 to −0.041	8	13	9	4	0	0	16	12
−0.240 to −0.141	1	6	10	10	0	0	15	4
−0.340 to −0.241	0	0	5	4	0	0	13	6
−0.440 to −0.341	0	0	4	4	0	0	8	11
−0.540 to −0.441	0	1	0	1	0	0	9	6
−0.640 to −0.541	0	0	0	2	0	0	10	7
−0.740 to −0.641	1	0	0	2	0	0	6	3
−0.840 to −0.741	0	0	0	3	0	0	4	5
−0.940 to −0.841	0	0	0	0	0	0	1	2
<−0.940	0	0	0	0	0	0	13	39
Avg of <−0.940	0	0	0	0	0	0	−1.181	−1.770
Largest (−) value	–	–	–	–	–	–	1.667	3.333
Avg of $(X_T - X_E)/X_T$	0.001	−0.004	−0.016	−0.033	0.486	0.326	−0.439	−0.918
Std. dev. of $(X_T - X_E)/X_T$	0.118	0.118	0.170	0.283	0.217	0.176	0.381	0.853

APPENDIX A (continued)

Range of $(X_T - X_E)/X_T$	Fractional error in σ_z, $(\sigma_{zT} - \sigma_{zE})/\sigma_{zT}$					
	0.2	+0.2	0.5	+0.5	0.7	+0.7
0.860 to 0.959	1	1	1	1	1	1
0.760 to 0.859	0	0	1	0	1	0
0.660 to 0.759	0	0	2	0	0	0
0.560 to 0.659	0	0	1	0	2	0
0.460 to 0.559	0	0	2	0	0	0
0.360 to 0.459	0	0	4	0	1	11
0.260 to 0.359	0	1	9	19	3	15
0.160 to 0.259	2	8	18	22	3	20
0.060 to 0.159	7	27	8	15	7	13
0.040 to 0.059	38	52	25	38	24	37
−0.140 to −0.041	21	4	6	3	4	2
−0.240 to −0.141	26	6	4	1	9	0
−0.340 to −0.241	3	0	8	1	1	1
−0.440 to −0.341	1	0	3	0	4	0
−0.540 to −0.441	0	1	0	0	1	0
−0.640 to −0.541	0	0	3	0	4	0
−0.740 to −0.641	0	0	0	0	4	0
−0.840 to −0.741	1	0	2	0	2	0
−0.940 to −0.841	0	0	0	0	3	0
<−0.940	0	0	3	0	26	0
Avg of <−0.940	0	0	−1.429	0	1.339	0
Largest (−) value	–	–	1.857	–	−2.333	–
Avg of $(X_T - X_E)/X_T$	−0.071	0.055	−0.236	0.120	−0.429	0.151
Std. dev. of $(X_T - X_E)/X_T$	0.164	0.130	0.240	0.155	0.776	0.168

APPENDIX A (continued)

Range of $(X_T - X_E)/X_T$	Fractional error in σ_y, $(\sigma_{yT} - \sigma_{yE})/\sigma_{yT}$					
	0.2	+0.2	0.5	+0.5	0.7	+0.7
0.860 to 0.959	1	1	1	1	1	1
0.760 to 0.859	0	0	0	0	0	0
0.660 to 0.759	0	0	0	0	0	0
0.560 to 0.659	0	0	0	0	0	0
0.460 to 0.559	0	0	1	0	1	0
0.360 to 0.459	1	0	1	0	1	0
0.260 to 0.359	0	0	0	0	0	0
0.160 to 0.259	2	1	3	2	4	2
0.060 to 0.159	8	6	8	9	8	12
0.040 to 0.059	82	83	78	75	77	65
−0.140 to −0.041	3	3	3	1	3	6
−0.240 to −0.141	1	4	3	6	3	7
−0.340 to −0.241	0	1	1	2	1	3
−0.440 to −0.341	1	0	0	0	0	1
−0.540 to −0.441	0	0	0	1	0	0
−0.640 to −0.541	0	0	0	3	0	1
−0.740 to −0.641	0	1	0	0	0	1
−0.840 to −0.741	0	0	0	0	0	0
−0.940 to −0.841	0	0	0	0	0	0
< −0.940	1	0	1	0	1	1
Avg of < −0.940	−1.000	0	−1.000	0	1.000	−1.239
Largest (−) value	1.000	—	1.000	—	1.000	1.239
Avg of $(X_T - X_E)/X_T$	0.007	0.003	0.012	0.018	0.014	0.032
Std. dev. of $(X_T - X_E)/X_T$	0.151	0.122	0.161	0.161	0.164	0.197

APPENDIX A (continued)

Range of $(X_T - X_E)/X_T$	Systematic error in wind direction, Θ, (°)					
	+10	-10	+20	-20	+40	-40
0.860 to 0.959	1	3	1	3	3	6
0.760 to 0.859	2	1	1	4	2	2
0.660 to 0.759	1	1	0	1	4	3
0.560 to 0.659	0	4	3	1	3	5
0.460 to 0.559	2	1	4	3	5	6
0.360 to 0.459	3	1	8	8	6	8
0.260 to 0.359	6	3	5	5	7	5
0.160 to 0.259	6	6	9	7	10	5
0.060 to 0.159	17	12	9	15	2	9
0.040 to 0.059	32	34	25	20	15	7
-0.140 to -0.041	2	6	4	1	9	1
-0.240 to -0.141	9	9	8	6	12	6
-0.340 to -0.241	5	5	4	4	3	5
-0.440 to -0.341	1	1	3	2	4	4
-0.540 to -0.441	0	1	2	1	0	2
-0.640 to -0.541	1	0	2	2	1	0
-0.740 to -0.641	0	2	0	3	0	1
-0.840 to -0.741	2	2	3	1	4	4
-0.940 to -0.841	4	0	0	0	0	2
<-0.940	6	8	9	10	10	19
Avg of <-0.940	-2.386	-2.030	-5.317	-3.422	-2.410	-3.340
Largest (-) value	4.000	3.615	28.000	7.667	8.500	7.600
Avg of $(X_T - X_E)/X_T$	-0.134	-0.124	-0.436	-0.232	-0.152	-0.524
Std. dev. of $(X_T - X_E)/X_T$	0.222	0.218	?	1.32	1.08	1.68

APPENDIX B

The mean and standard deviation of fractional error in verification of SO_2 predictions at 21 stations as function of indicated changes in input variables. (Confidence limits assessed at 95 percent level.)

Random Variation of Source Strengths, Q.

$\left(\frac{Q_T - Q_E}{Q_T}\right)^{2}{}^{1/2}$	$\overline{\left(\frac{X_T - X_E}{X_T}\right)}$	$\overline{v'^2}^{1/2}$
0	-0.642 ± 0.54	$0.848 < 1.225 < 1.60$
0.082	-0.673 ± 0.055	$0.865 < 1.25 < 1.64$
0.163	-0.690 ± 0.57	$0.903 < 1.30 < 1.70$
0.409	-0.701 ± 0.59	$0.937 < 1.35 < 1.77$
0.823	-0.753 ± 0.63	$1.07 < 1.54 < 2.02$

Systematic Variation of Source Strengths, Q.

$\left(\frac{Q_T - Q_E}{Q_T}\right)$	$\overline{\left(\frac{X_T - X_E}{X_T}\right)}$	$\overline{v'^2}^{1/2}$
-0.2	-0.961 ± 0.63	$1.00 < 1.44 < 1.90$
0	-0.642 ± 0.54	$0.848 < 1.225 < 1.60$
$+0.2$	-0.323 ± 0.44	$0.693 < 1.00 < 1.31$
$+0.4$	0.027 ± 0.32	$0.501 < 0.723 < 0.947$
$+0.6$	0.331 ± 0.22	$0.349 < 0.504 < 0.660$

Systematic Variation of the Decay Rate for SO_2, λ

$(\lambda_T - \lambda_E)$,* hr^{-1}	$\overline{\left(\frac{X_T - X_E}{X_T}\right)}$	$\overline{v'^2}^{1/2}$
-0.462	-0.013 ± 0.38	$0.595 < 0.860 < 1.13$
-0.231	-0.230 ± 0.43	$0.648 < 0.987 < 1.29$
0	-0.642 ± 0.54	$0.848 < 1.225 < 1.60$
0.146	-1.18 ± 0.68	$1.08 < 1.55 < 2.03$
0.231	-1.70 ± 0.82	$1,29 < 1.86 < 2.44$

*λ_T = 0.231 hr^{-1} (3-hr half-life)

APPENDIX B (continued)

Systematic Variation of Vertical Diffusion Coefficient, σ_z.

$\left(\frac{\sigma_{zT} - \sigma_{zE}}{\sigma_{zT}}\right)$	$\left(\frac{X_T - X_E}{X_T}\right)$	$\overline{v'^2}^{-1/2}$
0	−0.642 ± 0.54	0.848 < 1.225 < 1.60
−0.2	−0.596 ± 0.54	0.858 < 1.24 < 1.62
+0.2	−0.733 ± 0.54	0.851 < 1.23 < 1.61
−0.5	−0.483 ± 0.51	0.810 < 1.17 < 1.53
+0.5	−0.911 ± 0.69	1.09 < 1.57 < 2.06
−0.7	−0.428 ± 0.54	0.858 < 1.24 < 1.62
+0.7	−1.06 ± 0.67	1.06 < 1.52 < 1.99

Systematic Variation of Lateral Diffusion Coefficient, σ_y

$\left(\frac{\sigma_{yT} - \sigma_{yE}}{\sigma_{yT}}\right)$	$\left(\frac{X_T - X_E}{X_T}\right)$	$\overline{v'^2}^{-1/2}$
0	−0.642 ± 0.54	0.848 < 1.225 < 1.60
−0.2	−0.666 ± 0.54	0.858 < 1.24 < 1.62
+0.2	−0.678 ± 0.54	0.858 < 1.24 < 1.62
−0.5	−0.665 ± 0.55	0.865 < 1.25 < 1.64
+0.5	−0.657 ± 0.54	0.845 < 1.22 < 1.60
−0.7	−0.663 ± 0.55	0.865 < 1.25 < 1.64
+0.7	−0.644 ± 0.54	0.851 < 1.23 < 1.61

Systematic Variation of Regional Wind Direction, Θ.

$(\Theta_T - \Theta_E)$ (°)	$\left(\frac{X_T - X_E}{X_T}\right)$	$\overline{v'^2}^{-1/2}$
0	−0.642 ± 0.54	0.848 < 1.225 < 1.60
+10	−0.723 ± 0.63	1.00 < 1.44 < 1.88
−10	−0.905 ± 0.67	1.06 < 1.53 < 2.00
+20	−0.716 ± 0.57	0.903 < 1.30 < 1.70
−20	−1.14 ± 0.98	1.54 < 2.22 < 2.77
+40	−1.02 ± 0.86	1.36 < 1.96 < 2.56
−40	—	—

APPENDIX C – GLOSSARY OF SYMBOLS

a	fractional error in X due to random error
b	fractional error in X due to systematic error
Q	source strength field, emission rate
$Q(\xi,\eta\zeta)$	source strength at $x = \xi$, $y = \eta$, $z = \zeta$
u	transporting wind speed that determines time of flight from x to ξ, etc.
$(v')^2$	variance of fractional error distribution
$\overline{(v')^2}^{1/2}$	standard deviation of fractional error distribution
X	concentration
X_E	erroneous value of any input parameter
X_T	"true" value of any input parameter
λ	decay or loss coefficient for pollutant under consideration
$\sigma_y(x-\xi)$, $\sigma_z(x-\xi)$	standard deviation of crosswind and vertical spread respectively of pollutant from ξ, η, ζ
Θ	wind direction
σ_y, σ_z	lateral and vertical diffusion coefficients

9. TIME – SPACE MODEL FOR SO_2

ABSTRACT

A multiple-source diffusion model for the simulation and prediction of long-term (climatological) ground-level sulfur dioxide concentrations in urban areas is described. The computer input consists of data from an emission source inventory together with statistics on relevant diffusion parameters.

Because of the capacity of available computers, only a limited number of the largest emission sources (approximately 150) can be treated individually. Smaller industrial emission sources are treated as residential sources. These are represented by a large number of stacks (about 150) of the same dimensions, distributed over areas of 1 square kilometer, for which the mean area emissions have been estimated.

The meteorological input consists of data on wind direction, windspeed, and Pasquill-Turner stability classes.[1, 2] *These parameters are assumed to be spatially homogeneous throughout the metropolitan area. Low-level emissions (residential) are correlated with low-level windspeeds and Pasquill-Gifford diffusion parameters,*[1, 3] *whereas high-level emissions (industrial) are correlated with extrapolated windspeeds and Brookhaven diffusion parameters.*[4] *The program also uses corresponding statistics for urban boundary layer depths and values for parameters affecting absorption at the earth's surface.*

The diffusion model used is basically Gaussian. It is modified, however, such that turbulent diffusion is restricted exclusively to the depth of the urban boundary layer. This is true for all sources having effective emission heights less than the height of the upper limit of the boundary layer. The rate of decay of sulfur dioxide is taken into account, as well as the experimentally determined absorption at the earth's surface.

The model calculates fields of steady-state ground-level concentrations that correspond to a given spatial distribution of emission sources and to any possible combination of relevant meteorological diffusion parameters. Knowledge of frequency distributions of these meteorological diffusion parameters permits the derivation of frequency distributions of ground-level concentrations for any location within or outside of the metropolitan area. The computerized experiments simulate frequency distributions of ground-level concentrations for a great number of regularly arranged grid points (up to 2500 with a mesh size of 500 by 500 meters) and for a variety of time periods (months, heating *period, seasons, year, etc.). The frequency distributions are characterized by a limited number of parameters (mean, percentiles, etc.). Each parameter is plotted as a system of isograms on a map of the metropolitan area.*

Experiments to validate the model were conducted during the heating period in 1967-68 at four continuously monitoring stations that had been installed at special locations within the limits of the metropolitan area of Bremen. During the sampling period, the assumption of a sufficiently homogeneous wind field was validated by wind measurements at the same locations. The calculated frequency distributions of half-hourly mean values of concentrations generally agreed fairly well with those derived from observed values. Comparison, however, shows that the model does not simulate ground-level concentration fields in the vicinity of industrialized areas very well, because uncontrollable low-level emissions from industrial plants could not be taken into account in the diffusion model.

AUTHOR

HEINZ G. FORTAK is a professor of meteorology and Director of the Institute for Theoretical Meteorology at the Free University of Berlin. His scientific interests include: general hydrodynamics, turbulence, dynamic meteorology, and oceanography.

9. NUMERICAL SIMULATION OF TEMPORAL AND SPATIAL DISTRIBUTIONS OF URBAN AIR POLLUTION CONCENTRATION

HEINZ G. FORTAK

Institut fur Theoretische Meteorologie
der Freien Universitat Berlin

INTRODUCTION

Increasing industrialization in Germany during the 1950's led to great interest in the problem of ascertaining minimum stack heights essential to pollution control. In line, therefore, with its responsibilities in developing air pollution standards and criteria, the *Kommission Reinhaltung der Luft* [Air Pollution Control Commision] within the Association of German Engineers [*Verein Deutscher Ingenieure* (VDI)] established a research group on air pollution meteorology in 1958. The group was expected to develop the scientific basis for an approximate solution to the problem. The results of research during the first period, based mainly on the work of Sutton,[5] led to a simple nomogram for estimating minimum stack heights.[6, 7] The nomogram is widely used for legal and administrative purposes, although, among other shortcomings, very little is known about one of the most important input parameters of the model and therefore of the nomogram. This parameter (in German, *Immissions-Grundbelastung*) characterizes the temporal and spatial distributions (air loadings with time) of ground-level concentrations of pollutants in the area in which the newly built stack is located. In most cases the location is in an urban area already possessing a great number of emission sources. It is extremely difficult to define such a measure. A simple number constant in space and time, as proposed by the VDI,[7] will not suffice for urban areas. Instead, such a parameter is dependent on horizontal space coordinates and, ultimately, on time (e.g., season).

In view of the crucial dependence of minimum stack heights on this parameter, some means of predicting ground-level concentrations in urban areas must be found before the stack-height problem can be solved.

Based on the work of Frenkiel,[8] the multiple-source urban diffusion model being described in this paper was developed by the author in 1962. It was hoped that this model would be able to solve problems of the kind mentioned above. After financial support for programming and computing time became available, a number of simulation experiments were conducted from 1963 through 1965. A tentative report was published early in 1966.[9] During that time the first papers on urban air pollution modeling by Turner[2] and Clarke,[10] although they aimed at the solution of the real-time prediction problem, were of great help. Especially, the replacement of Pasquill's stability categories[1] by Turner's[2] proved to be quite useful.

The purpose of the diffusion model is perhaps understood best by a discussion of Figure 9-1, which shows the logical structure of some features of the urban air pollution problem. Assuming that sufficient input data are available, a mathematical multiple-source urban air pollution model should yield a set of output data such as that indicated in Figure 9-1.

The most important of these data certainly is a real time short-term prediction of concentrations for the entire urban area. Most authors in the field of urban air pollution modeling were interested primarily in that problem. Following Turner,[2] they applied the well known steady-state theory of transport and dilution to simulate and predict time series of concentrations. Quite recently, Marsh and Withers[11] demonstrated the inadequacy of such a procedure. The model of Davidson[12] that applies a non-steady-state theory should provide a means of solving the short-term prediction problem, as well as the problem of time series simulation, more successfully. If this turns out to be true, the very important feedback circuit, "warning system," can be closed; i.e., appropriate control measures can be applied to the source-emission input in order to reduce the predicted concentrations below a given limit.

The problem of minimum stack heights and, more generally, that of city planning is connected with the problem of simulation and prediction of long-term (climatological) ground-level concentration fields. Here, time series of concentrations are of minor interest; instead, statistics of observed or calculated concentration fields for given long periods of time are important.

There is no doubt that for a given location and a given period of time only the frequency distribution of ground-level concentrations forms the basis of what could be called "air pollution climatology." Generally, these frequency

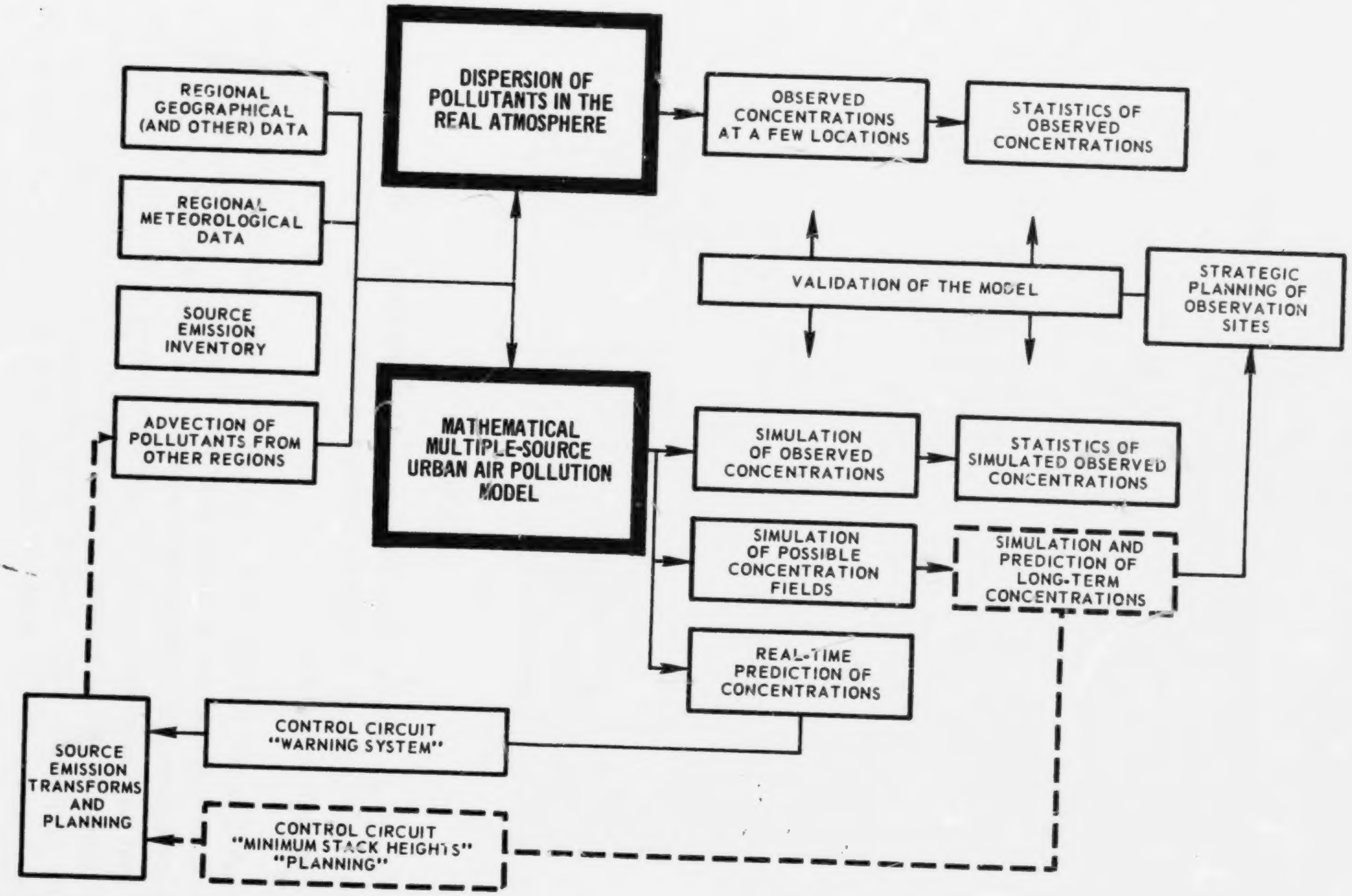

REGIONAL GEOGRAPHICAL (AND OTHER) DATA
REGIONAL METEOROLOGICAL DATA
SOURCE EMISSION INVENTORY
ADVECTION OF POLLUTANTS FROM OTHER REGIONS
DISPERSION OF POLLUTANTS IN THE REAL ATMOSPHERE
MATHEMATICAL MULTIPLE-SOURCE URBAN AIR POLLUTION MODEL
OBSERVED CONCENTRATIONS AT A FEW LOCATIONS
STATISTICS OF OBSERVED CONCENTRATIONS
VALIDATION OF THE MODEL
STRATEGIC PLANNING OF OBSERVATION SITES
SIMULATION OF OBSERVED CONCENTRATIONS
STATISTICS OF SIMULATED OBSERVED CONCENTRATIONS
SIMULATION OF POSSIBLE CONCENTRATION FIELDS
SIMULATION AND PREDICTION OF LONG-TERM CONCENTRATIONS
REAL-TIME PREDICTION OF CONCENTRATIONS
CONTROL CIRCUIT "WARNING SYSTEM"
SOURCE EMISSION TRANSFORMS AND PLANNING
CONTROL CIRCUIT "MINIMUM STACK HEIGHTS" "PLANNING"

Figure 9-1. Major elements of the urban air pollution problem connected with mathematical modelling.

distributions vary from location to location within the urban area and with time and season. Figure 9-2 shows a typical example of the frequency distribution in winter of measured half-hourly mean values of sulfur dioxide concentrations in Bremen.

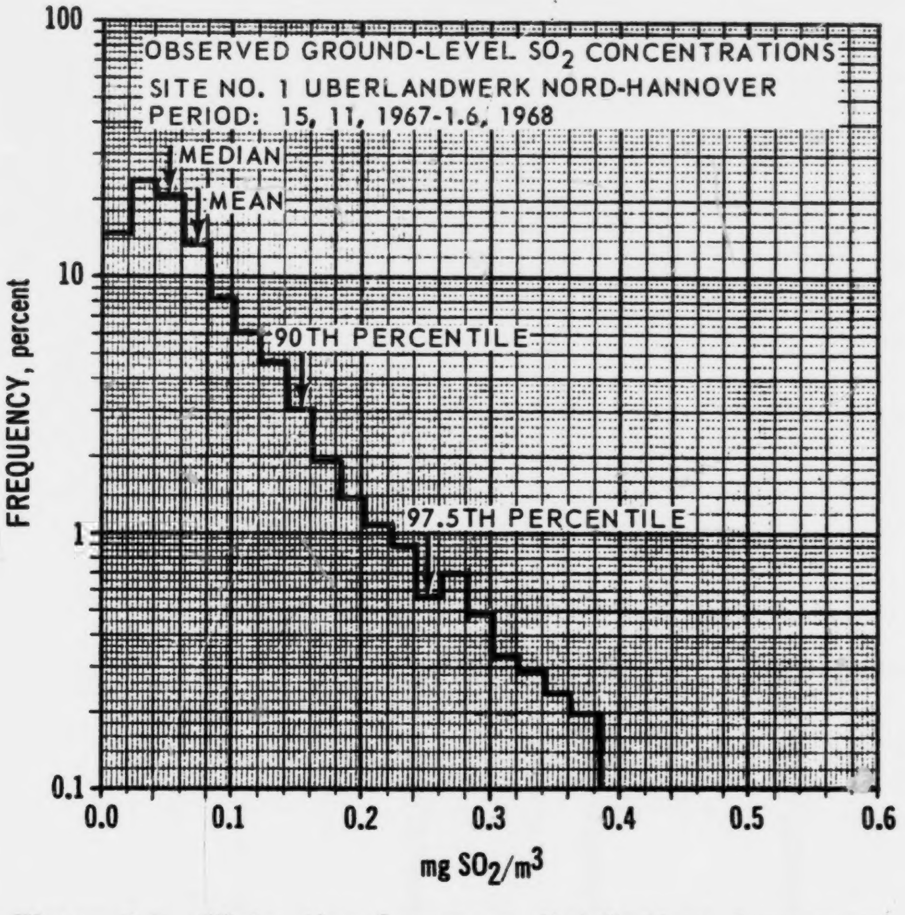

Figure 9-2. Winter time frequency distribution of measured half-hourly mean values of sulphur dioxide concentrations downtown Bremen.

Although it is not believed that a calculated steady-state field of concentration will fit observations at many locations within the urban area very well, it can be expected that statistical evaluation of a great number of such fields may lead to reasonable results in a climatological sense. This expectation forms the basis for this paper. If the expectation is justified, the feedback circuit, "minimum stack heights, city planning," can be closed and, in addition, means for the strategic planning of observation sites will then be available.

The following information is used in calculating pollutant concentrations: period of time (month, heating period, seasons, year, etc.) divided into equal intervals (for example, hours); data from source emission inventories; relevant meteorological parameters, etc. From these data the model then calculates possible steady-state ground-level concentrations for each interval of time and for a large number of grid points within the urban area. From the stored concentration data, the frequency distribution of concentrations is obtained for each grid point. If the frequency distribution is characterized by a set of parameters (mean percentiles, etc.), these parameters are plotted as a system of isograms on a map of the urban area. Such maps then may be used to define the *Immissions-Grundbelastung* (ground-level concentrations), to solve problems of city planning as well as problems of strategic planning observation sites.

From the very beginning the main concern of the investigation was to apply the model to a real situation and to validate the model by suitable measurements. For several reasons the city of Bremen was chosen for the first mathematical experiments. Local authorities of the city of Bremen were willing and able (in 1963) to collect information on source emissions, which led to a very complete source emission inventory. The location of the city, on flat terrain and only 40 miles from the North Sea, is favorable in many respects: the city is well ventilated throughout the year and, in addition, the relevant meteorological fields are approximately homogeneous horizontally. In addition, advection of pollutants from other regions can be neglected. The input data, therefore, were well defined and relatively simple and allowed the application of a simple model.

MATHEMATICAL MODEL

The steady-state theory of the transport and dilution of pollutants is based on a number of simplifying assumptions: the relevant meteorological fields are stationary and are horizontally homogeneous; dispersion is not limited in the vertical direction; mean windspeed exceeds a certain lower limit; and the earth's surface is flat and not absorbing. The well-known formula for the spatial distribution of a pollutant[1] then is:

$$\chi = \frac{Q}{U} \exp[\gamma\tau] \frac{\exp\left[-\frac{y^2}{2\sigma_y^2}\right]}{\sqrt{2\pi}\,\sigma_y} \left\{ \frac{\exp\left[\frac{(h-z)^2}{2\sigma_z^2}\right]}{\sqrt{2\pi}\,\sigma_z} + \frac{\exp\left[-\frac{(h+Z)^2}{2\sigma_z^2}\right]}{\sqrt{2\pi}\,\sigma_z} \right\} \qquad (1)$$

As usual, $h = h_s + \Delta h$ is effective stack height, $\tau = x/U$ is travel time, and $T = 1/\gamma$ is decay time.

Assuming that the plume standard deviations, σ_y and σ_z, are functions of travel time, τ, it can be shown that Equation (1) is a solution of the following[1 3] initial-value and boundary-value problem:

$$\frac{\partial\chi}{\partial\tau} = \frac{d}{d\tau}\left(\frac{\sigma_y^2}{2}\right)\frac{\partial^2\chi}{\partial y^2} + \frac{d}{d\tau}\left(\frac{\sigma_z^2}{2}\right)\frac{\partial^2\chi}{\partial Z^2} - \gamma\chi \qquad (2)$$

$$\tau \rightarrow 0 : \quad \chi \rightarrow \frac{Q}{U} \, \delta(y) \, \delta(h-Z) \tag{3}$$

$$Z = 0 : \frac{\partial \chi}{\partial Z} = 0 \tag{4}$$

$$Z \rightarrow \infty : \chi \rightarrow 0 \tag{5}$$

The initial condition, that is, Equation (3), expresses the fact that a point source of strength, Q, is located at the effective stack height h. The boundary conditions show that there is reflection of the pollutant at the earth's surface and further that dispersion is not limited in the vertical direction.

It may be noted that Equation (1) has the character of Green's function in the special boundary-value problem, Equations (2), (4), and (5). It seems legitimate, therefore, to apply Equation (2) to problems connected with boundary conditions different from those described by Equations (4) and (5) Two important assumptions are in question; that of a non-absorbing ground and that of unlimited vertical dispersion. Denoting by H the height of a ceiling restricting dispersion to a limited layer of the lower atmosphere (urban boundary layer), and denoting by $a(\tau, y)$ the absorption coefficient of the ground, the boundary conditions, Equations (4) and (5), can be replaced by:

$$Z = 0 : \frac{d}{d\tau} \left(\frac{\sigma_z^2}{2} \right) \frac{\partial \chi}{\partial Z} = a(\tau, y) \chi \tag{6}$$

$$Z = H : \quad \frac{\partial \chi}{\partial Z} = 0 \tag{7}$$

Even if absorption is not a function of location, only mathematical, rather than experimental, methods are suitable for solving Equation (2) together with Equations (3), (6), and (7).[14] In view of the uncertainties connected with absorption at the ground, and with the functional behavior of plume standard deviations for such cases, only experimental calculations were performed with boundary-condition Equation (6).

Important for practical applications, however, is the assumption that dispersion is confined only to the urban boundary layer; i.e., the utilization of boundary condition Equation (7) for the upper ceiling of the layer (Figure 9-3).

Standard methods[15-17] allow the derivation of a modified version of Equation (1) so that it now describes dispersion in a boundary layer of depth H:

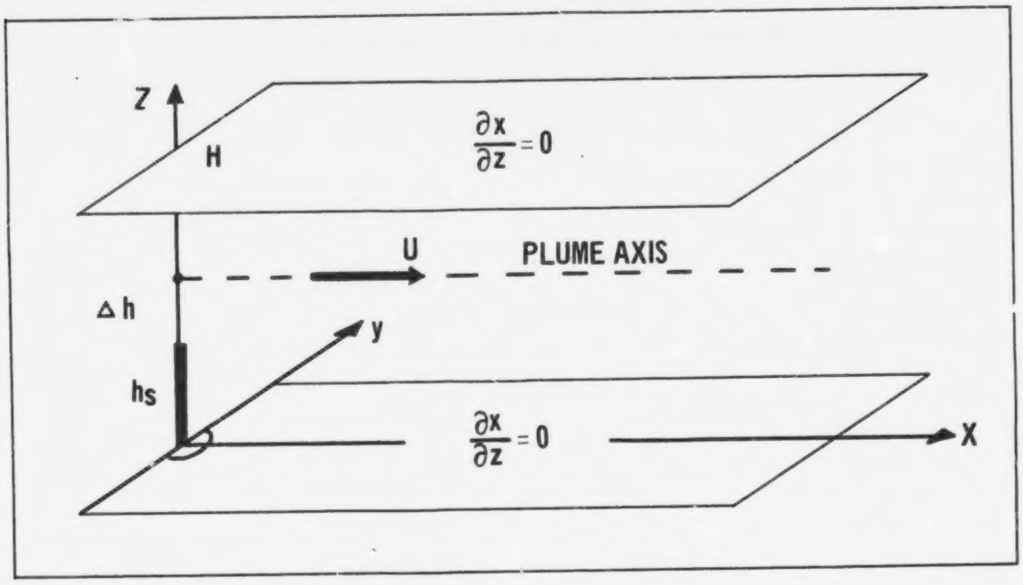
Z
H
$\frac{\partial x}{\partial z} = 0$
U
PLUME AXIS
Δh
y
hs
$\frac{\partial x}{\partial z} = 0$
X

Figure 9-3. Model assumptions.

$$\chi = \frac{Q}{2HU} \exp[-\gamma\tau] \frac{\left[\exp -\frac{y^2}{2\sigma_y^2}\right]}{\sqrt{2\pi}\ \sigma_y} \left\{ \Theta_3 \left(\frac{h-z}{2H} \ ; \ \frac{\sigma_z^{\ 2}}{2H^2} \right) + \Theta_3 \left(\frac{h+z}{2H} \ ; \ \frac{\sigma_z^{\ 2}}{2H^2} \right) \right\} \tag{8}$$

Here

$$\Theta_3(V,W) = \frac{1}{\sqrt{\pi W}} \sum_{\eta=-\infty}^{\infty} \exp\left[-\frac{(V+\eta)^2}{W}\right] \tag{9}$$

is a Jacobian theta-function.

It can be shown that Equation (8) differs only slightly from Equation (1) for H > 3h. If, however, the ceiling approaches the effective stack height, i.e., if H → h, then the ground-level concentration increases drastically.

So far only a single source has been considered. In an urban area, a large number of such sources exist. In reality, all of them are point sources as far as emissions are concerned. They may be divided into three groups. Group 1 consists of all industrial stacks, including those of power stations and gasworks; Group 2 consists of stacks of small industries, contributing, say, less than 0.02 percent each to the total output into the city; Group 3 consists of all domestic sources burning fuel for space heating.

Industrial emission sources of Group 1 are treated individually by applying Equation (8). Since they are irregularly distributed over the urban area, and since Equation (8) applies to a source-oriented coordinate system, the transformation of coordinates shown in Figure 9-4 is performed.

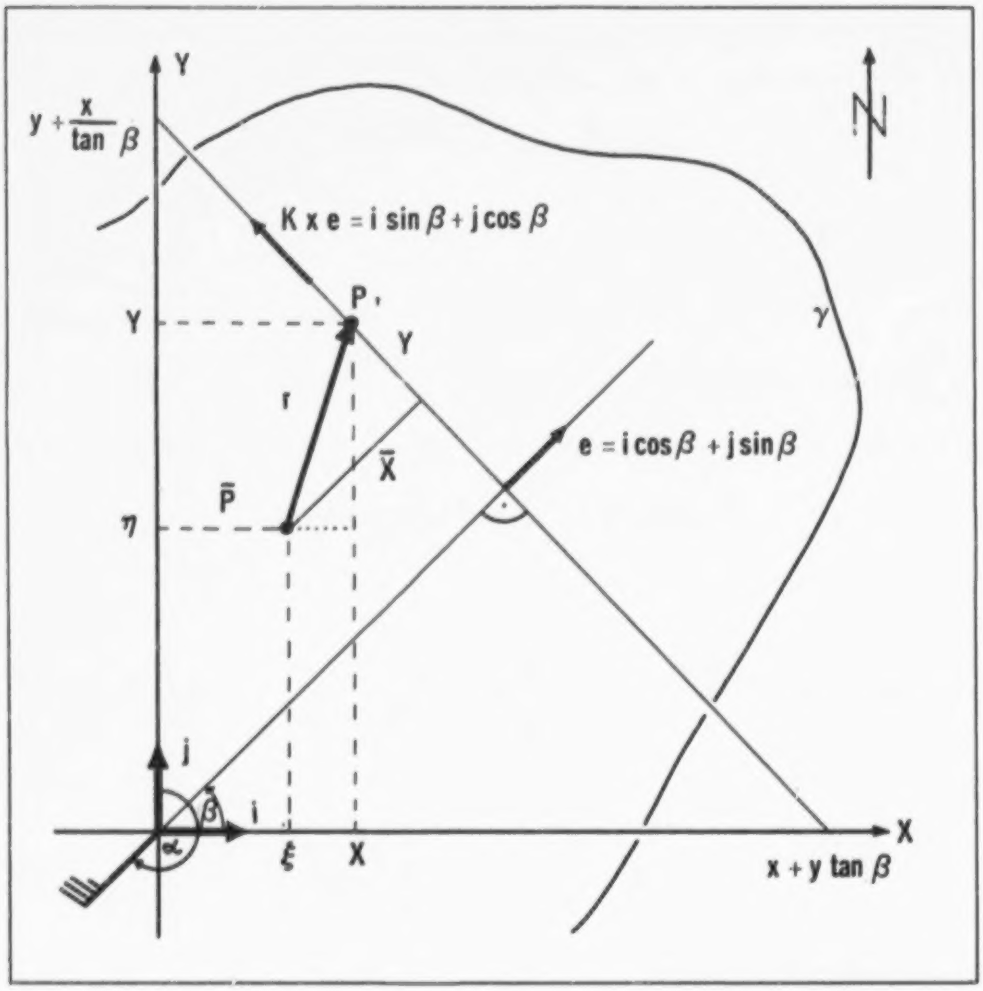
Y
$y + \frac{x}{\tan\beta}$
N
$K \times e = i\sin\beta + j\cos\beta$
P
Y
Y
γ
r
$\overline{X}$
$e = i\cos\beta + j\sin\beta$
$\overline{P}$
η
j
β
i
α
ξ
X
X
$x + y\tan\beta$

Figure 9-4. Transformation of coordinates from a source-oriented system to a geographically fixed system.

If a denotes wind direction ($\beta = 3\pi/2 - a$) , P(x,y) a receptor point, and (ξ_n, η_n) the location of a point source, then the individual source distance in wind direction, $\overline{X}_n$, and the individual crosswind distance, $\overline{Y}_n$, of the receptor point, p(x,y), are given by:

$$\overline{X}_n = e\cdot\gamma = (x-\xi_n)\cos\beta + (Y-\eta_n)\sin\beta \qquad (9)$$

$$\overline{Y}_n = k(e\cdot\gamma) = -(x-\xi_n)\sin\beta + (Y-\eta_n)\cos\beta$$

where

$$\gamma = i(x-\xi_n) + j(Y-\eta_n)$$

Now, source strength, wind speed, travel time, plume standard deviations, and effective stack height are dependent on $(\xi_n \eta_n)$ and $(\overline{X}_n, \overline{Y}_n)$, respectively. Individual source strength is denoted by $Q = Q(\xi_n,\eta_n) = Q_n$. Wind speed relevant for transport and dilution of pollutants originating from the source at (ξ_n,η_n) is given by $U = U(\xi_n,\eta_n)$. Travel time is indicated by $\tau_n = X_n/U_n$, plume standard deviations by $\sigma_y = \sigma_y(\tau_n) = \sigma_{y,n}$ and $\sigma_z = \sigma_z(\tau_n) = \sigma_{z,n}$, and local effective stack by $h = h(\xi_n,\eta_n) = h_{s,n} + \Delta h(\xi_n,\eta_n)$. Introducing these new parameters and coordinates into Equation (8), the ground-level concentration originating from emission source "n," i.e., $\chi_n(x,y,z)$, is obtained.

The concentration fields from all individual sources can be superimposed. Contributions to the concentration at receptor point, P, come from all upwind sources having coordinates, $\xi_n \leqslant x + y \tan\beta$, $\eta_n \leqslant y + x/\tan\beta$. . If N denotes the total number of upwind sources, the concentration P is given by:

$$\chi = \frac{1}{2H} \sum_{n=1}^{N} \frac{Q_n}{U_n} \exp[-\gamma\bar{\tau}n] \frac{\exp\left[-\frac{\overline{Y}_n^{\,2}}{2\sigma_{y,n}^2}\right]}{\sqrt{2\pi}\,\sigma_{y,n}} \left\{\Theta_3\left(\frac{h_n - Z}{2H};\frac{\sigma_{z,n}^2}{2H^2}\right) + \Theta_3\left(\frac{h_n + Z}{2H};\frac{\sigma_{z,n}^2}{2H^2}\right)\right\} \tag{10}$$

It is obvious that computing time goes up tremendously with an increasing number of individual sources. It is impossible, therefore, to treat all domestic sources of Group 3 individually. In this context one generally talks about area sources. The source strength, Q, is replaced by a local source strength density (source emission per unit area), $q(\xi,\eta)$. Local relevant mean wind speed, $U(\xi,\eta)$, as well as local plume rise, $\Delta h(\xi,\eta)$, are connected with the emission height $h_s(\xi,\eta)$ of the area source. The coordinates, $\overline{X}_n, \overline{Y}_n$, with respect to an individual source are replaced by $\overline{x}, \overline{y}$ which obey the same relations, in Equation (9), as $\overline{X}_n$ and $\overline{Y}_n$ do. If the sum in Equation (10) is replaced by an integral, the contribution of all upwind area sources to the concentration at receptor point, P, is given by:

$$\chi = \frac{1}{2H} \int\limits_{\xi \leqslant x + y\tan\beta} d\xi \int\limits_{\eta \leqslant y + x/\tan\beta} d\eta \; \frac{q(\xi,\eta)}{U(\xi,\eta)} \exp[-\gamma\bar{\tau}] \; \frac{\exp\left[-\frac{\bar{y}^2}{2\sigma_y^2(\bar{\tau})}\right]}{\sqrt{2\pi}\;\sigma_y(\bar{\tau})} \tag{11}$$

$$\left\{\Theta_3\left(\frac{h(\xi,\eta) - Z}{2H};\frac{\sigma_z^2(\bar{\tau})}{2H^2}\right) + \Theta_3\left(\frac{h(\xi,\eta) + Z}{2H};\frac{\sigma_z^2(\bar{\tau})}{2H^2}\right)\right\}$$

Superposition of concentrations, in Equations (10) and (11), gives the steady-state concentration field at any location in space, (X,Y,Z), if individual point sources as well as area sources act together in that urban area.

Apart from the fact that source emission data for area sources, i.e., $q(\xi,\eta)$ are not available, the analytical integration of Equation (11) cannot be performed. Numerical integration replaces the integral by a sum which represents the area source by a dense, regularly spaced system of point sources having source strength, $q(\xi_i,\eta_k)\Delta\xi\Delta\eta$. This, in fact, has been done in the model. The selection of the area element, $\Delta\xi\Delta\eta$, depends upon resolution and scale. In addition, the characteristics of dispersion as well as the conditions of emission (emission heights) are important. In order to find a satisfactory answer to that question, a number of mathematical experiments was performed. An area source, 500 m by 500 m was represented by a successively increasing number of point sources (Figure 9-5).

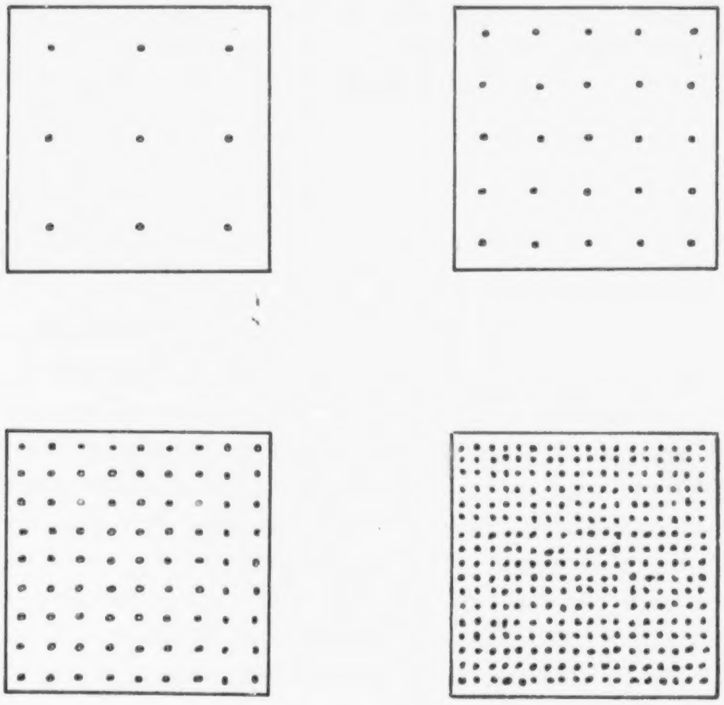

Figure 9-5. Simulation of an area source by the use of increasing number of point sources distributed regularly over an area 500 x 500 meters.

As Figures 9-6 and 9-7 show, an area size of $\Delta = \Delta\xi\Delta\eta = 56$ m x 56 m should be sufficient for the representation of an area source by a great number of point sources under the conditions indicated in Figures 9-6 and 9-7.

In order to get the same degree of approximation for a wide range of windspeeds and stability categories, the 500 m by 500 m area source must be represented by at least 100 individual sources ($\Delta = \Delta\xi\Delta\eta = 50$ m x 50

m) or better, by 144 individual sources ($\Delta = \Delta\xi\Delta\eta \approx$ 42 m x 42 m). This corresponds roughly to the mean distance between individual stacks from space heating units.

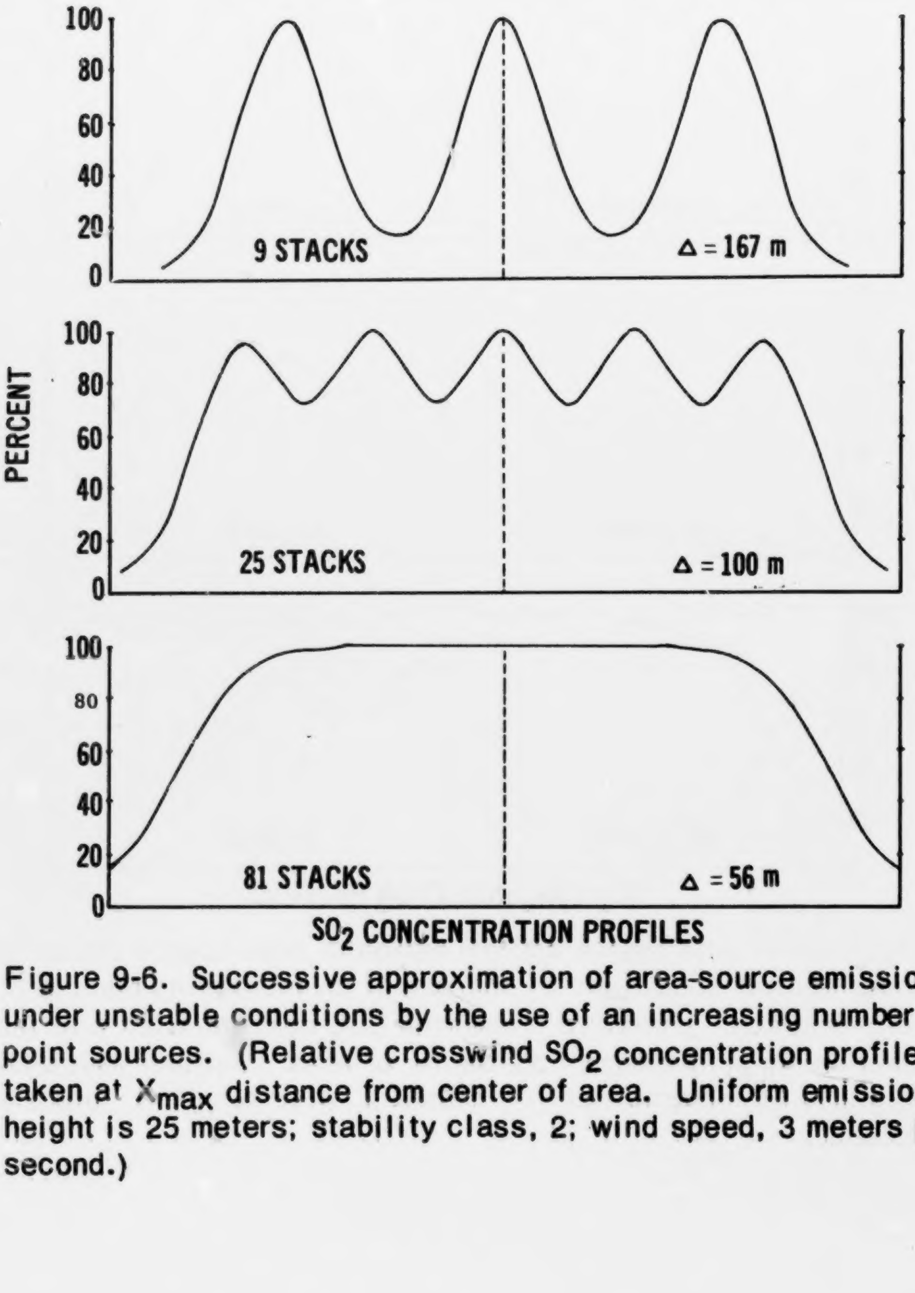

Figure 9-6. Successive approximation of area-source emissions under unstable conditions by the use of an increasing number of point sources. (Relative crosswind SO_2 concentration profiles taken at X_{max} distance from center of area. Uniform emission height is 25 meters; stability class, 2; wind speed, 3 meters per second.)

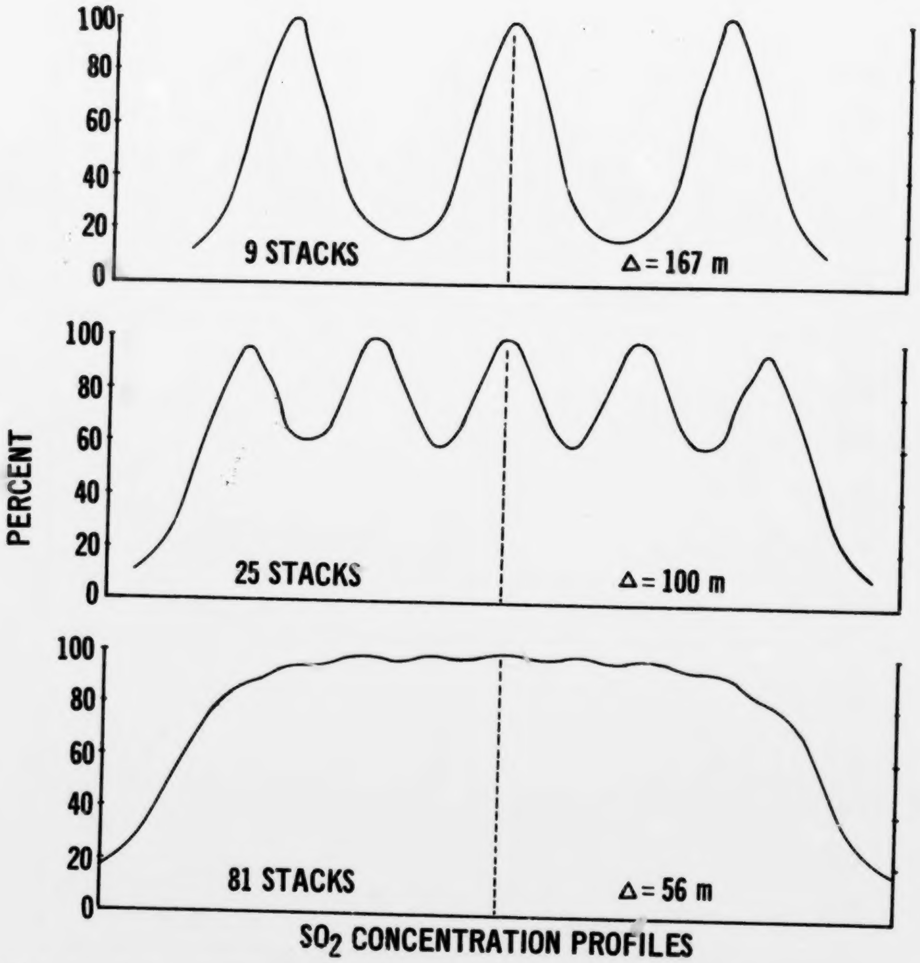

Figure 9-7. Successive approximation of area-source emissions under neutral conditions by the use of an increasing number of point sources. (Relative crosswind SO_2 concentration profiles taken at X_{max} distance from center of area. Uniform emission height is 25 meters; stability class, 2; wind speed, 3 meters per second.)

METEOROLOGICAL DATA INPUT

A set of meteorological data consists of windspeed, wind direction (both taken at anemometer level), and stability category. All three are hourly values taken at the Bremen airport. Observations of windspeed and wind direction at four sites in the city during winter (1967-68) validated the assumption that the airport observations are representative for the urban area of Bremen, at least during winter, which is the most important period with respect to air pollution in Bremen. Stability categories were computed using Turner's scheme.[2]

It was discovered during simulation experiments that 36 wind direction measurements (wind roses divided into 10-degree intervals) are necessary to provide reasonable ground-level concentration fields. Windspeed was divided into seven classes. Including five stability categories, a total number of 1260 combinations exist, of which, however, only about 600 are realized.

Frequency distributions of wind data were calculated for each stability category for a variety of periods (months of the year, seasons, years, and five to ten years). Figure 9-8 shows a typical example of a long-term distribution.

Data on plume standard deviations for urban areas were not available during the years of experimentation. Therefore, the well-known Pasquill-Gifford values[1, 3] were used for low emission heights (space heating), whereas the Brookhaven values [4, 18] were applied in a slightly modified version to high industrial stacks (Figures 9-9 and 9-10). The results of the St. Louis dispersion study indicate that utilization of those values given in Figures 9-9 and 9-10 inevitably lead to a systematic overestimation of ground-level concentrations.[19] This trend was, in fact, apparent when the results of calculations were compared with those obtained by observations.

Finally, the problem of mean windspeed, U, which is relevant for the transport and dilution of pollutants, was solved in the usual manner. Wind observations were extrapolated from anemometer level to physical stack height for each stack by means of a power-law-profile assumption. This extrapolation was assumed to be a function of stability and was made by the use of parameters taken from the literature (Figures 9-8, 9-9, and 9-10).

EMISSION SOURCE INVENTORY

All emission sources, as mentioned earlier, were classified in three groups. All individual stacks (Group 1) with emission rates greater than 1 kilogram

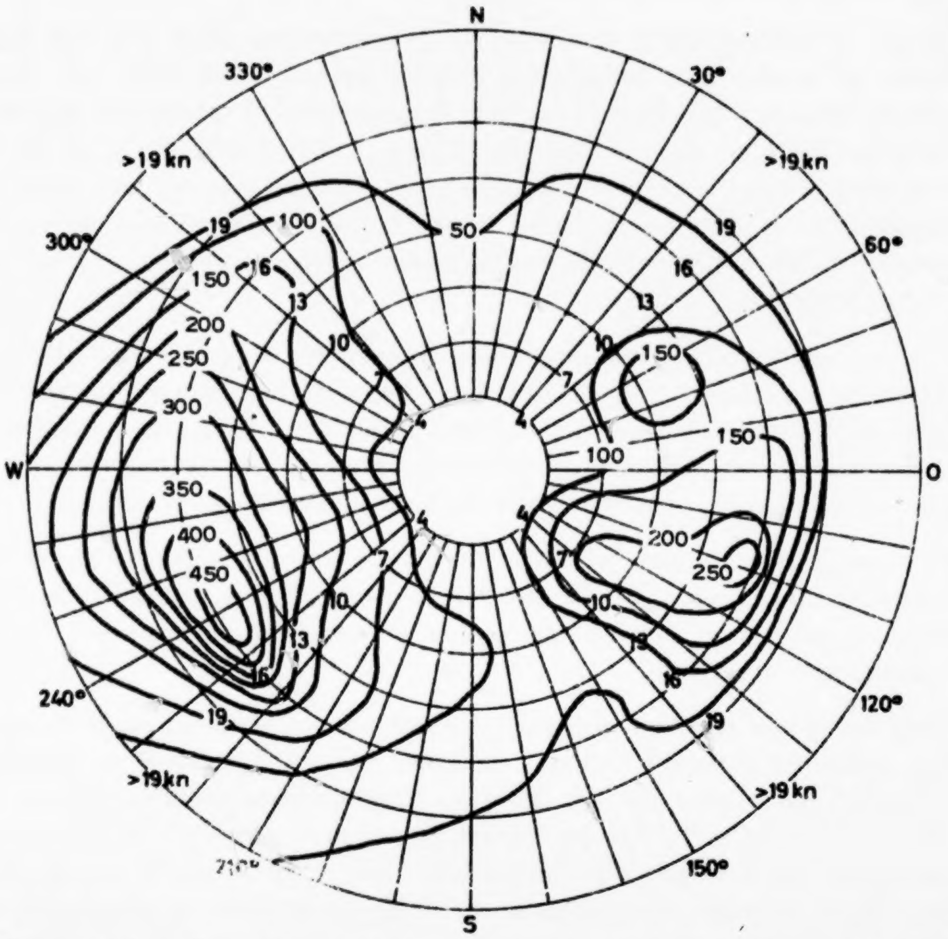

Figure 9-8. Frequency distribution of wind direction and windspeed for Bremen, 1954 to 1959. Stability class: 4 (neutral). Isopleth numbers represent hours per period.

sulfur dioxide (SO_2) per hour were treated individually. The record contained: geographical location, physical dimensions of the stack, output by volume, exit velocity, exit temperature, and, finally, emission data that included maximum emissions and mean winter and summer emissions. In addition, data were obtained whenever possible on daily variations in emissions and emissions during holidays.

Effective stack heights were calculated by applying Stumke's empirical formula,[20] similar to the well-known CONCAWE-formula, which is applicable to all types of stacks in Bremen.

Group 1 emission sources, consisting of 136 stacks, contributed 75 percent to the total emission rate in Bremen during winter 1965 (Table 9-1). Spatial distribution per square kilometer is given in Figure 9-11 for these sources.

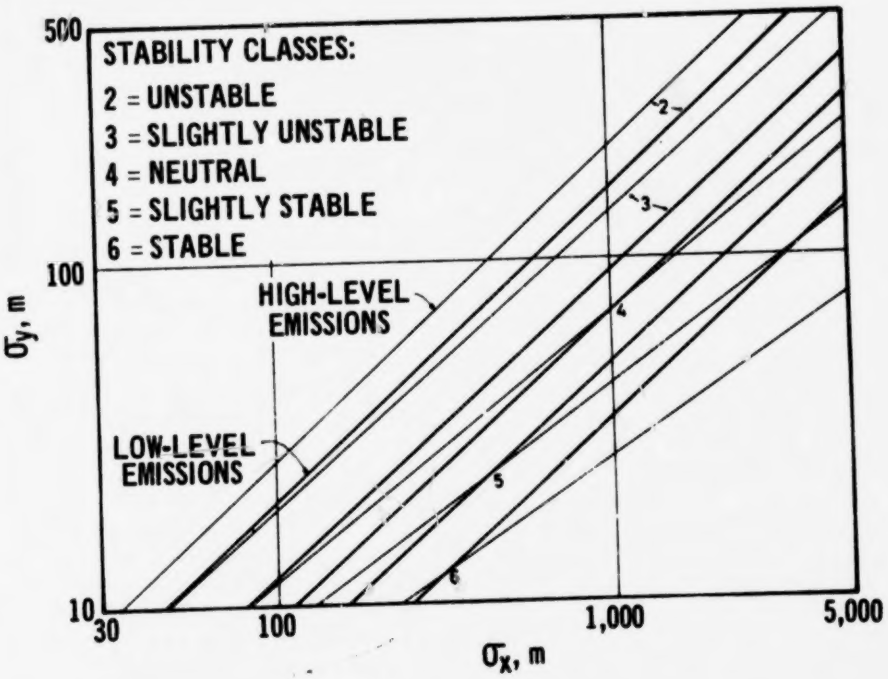

Figure 9-9. Crosswind-plume standard deviations.

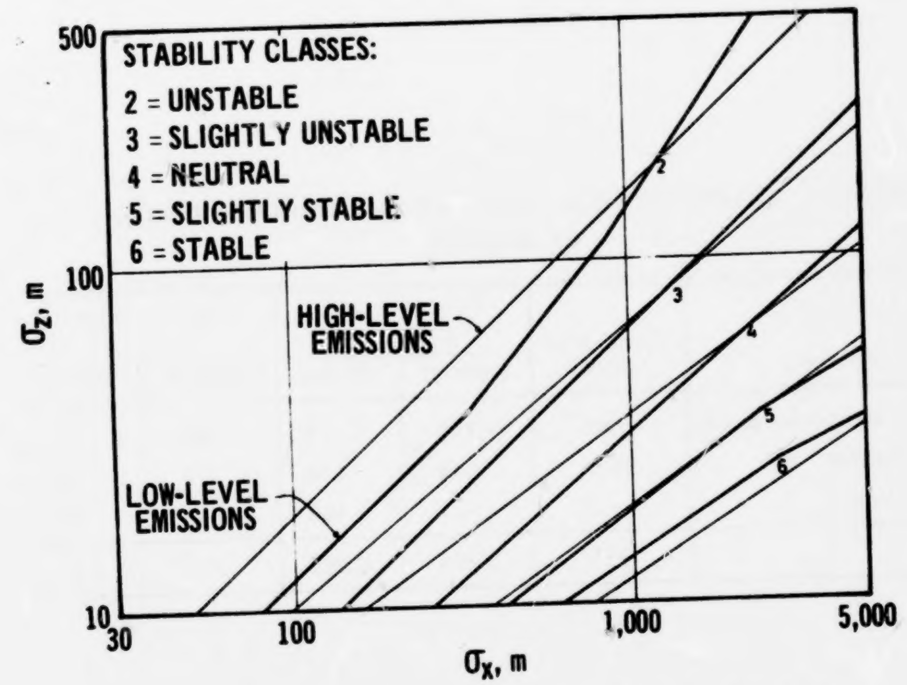

Figure 9-10. Vertical-plume standard deviations.

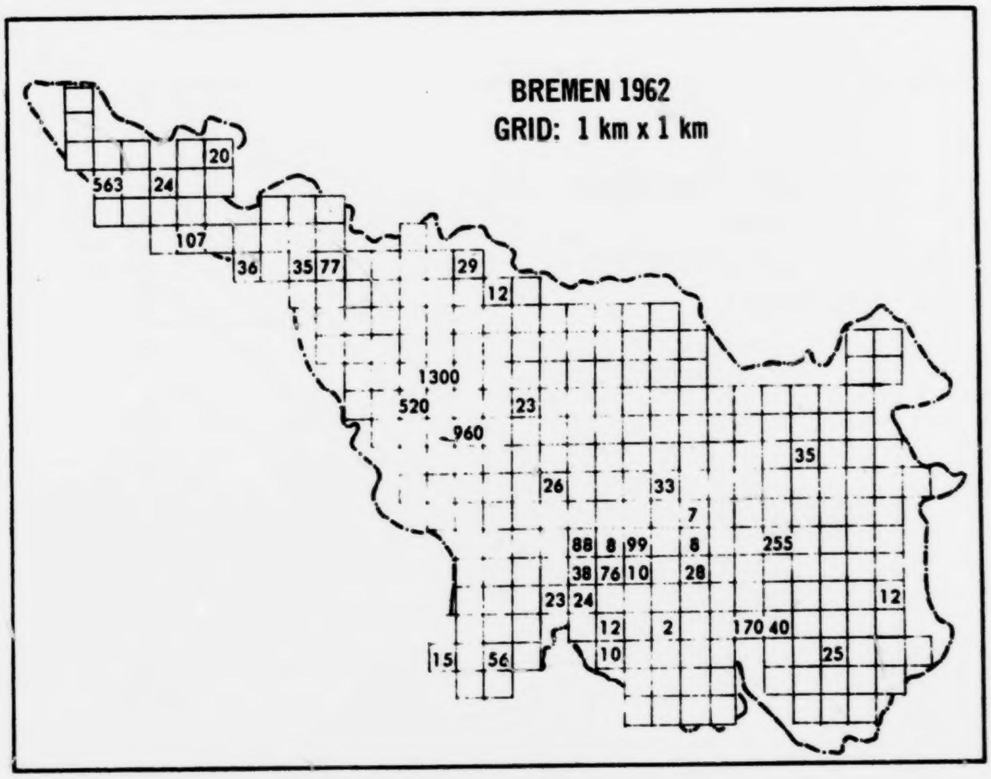
BREMEN 1962
GRID: 1 km x 1 km
20
563
24
107
36
35
77
29
12
1300
520
23
960
35
26
33
7
88
8
99
8
255
38
76
10
28
23
24
12
12
2
170
40
15
56
10
25

Figure 9-11. Spatial distribution of mean winter time industrial emissions.

Table 9-1. STATISTICS FROM 1965 EMISSION-SOURCE INVENTORY OF BREMEN

Source	Number of stacks	Total emissions, kg SO_2 hr^{-1}		Percent of total emissions	
		Summer	Winter	Summer	Winter
Industries and power plants	136	1,423	4,715	99	75
Small industries	425	46	116	1	2
Space heating	–	–	1,458	–	23
Total	561	3,469	6,289	100	100

A large number of individual stacks from small industries contributed less than 0.02 percent each to the total emission rate, i.e., less than 1 kilogram SO_2 per hour. They contributed only 1 to 2 percent altogether and, therefore, were not treated individually. Instead, the same technique was used as that applied to emissions from space heating (Figure 9-12).

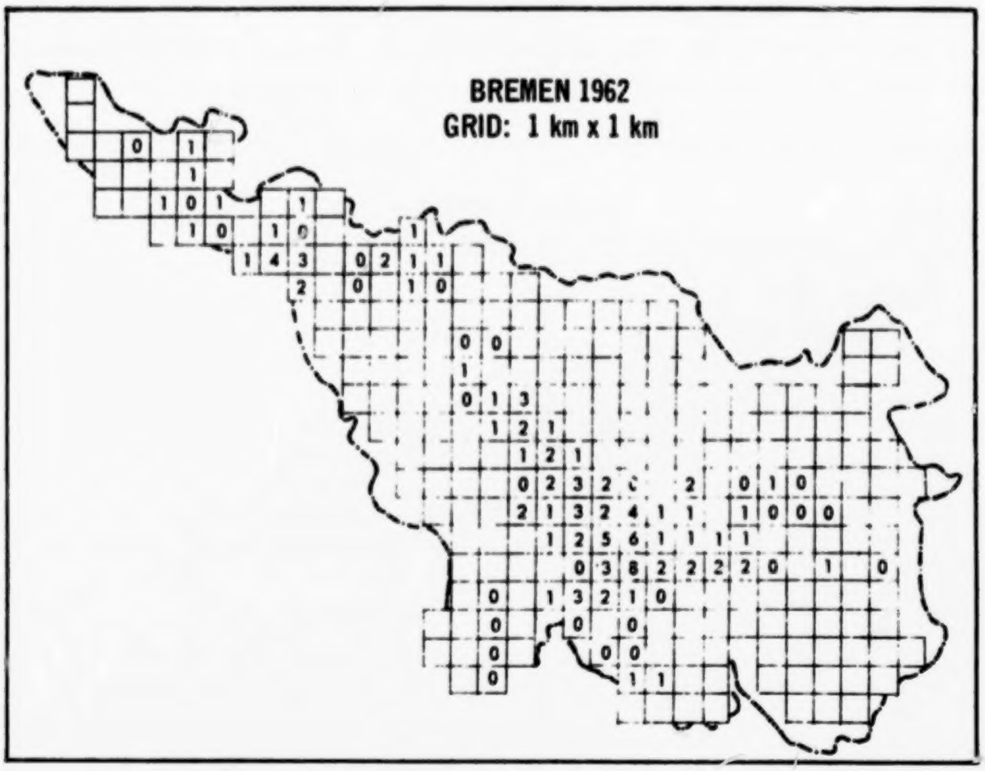

Figure 9-12. Spatial distribution of mean winter time industrial emissions from small industries.

Although it contributed less than 25 percent to the total emission rate, space heating is the dominant factor in air pollution in Bremen because of low emission heights.

Emissions from space heating were obtained in the following way. The spatial distribution of dwelling units in Bremen, which number about 200,000 was known very well. Further, the total amount of coal and fuel oil consumption during heating periods was known. From the sulfur content of the fuels, the total fuel consumption, and the total number of dwelling units, a mean emission rate of 8 grams SO_2 per hour per dwelling unit was obtained. This is the amount that would have been emitted daily during the heating period if the daily mean temperature had remained constant. In several experiments, a relationship between daily mean temperature and daily emission was used to make emissions from space heating a function of time.

A mean emission height of 25 meters was assumed for downtown emissions and 15 meters for suburban emissions. The corresponding effective stack heights were calculated by a simpler method than that used for tall stacks.

Emissions from space heating were treated as "area sources" as described earlier. A grid produced areas 500 m by 500 m. The number of dwelling units in each area was counted. Multiplying by 8 grams SO_2 per hour (or the corresponding, temperature-corrected value) gave the mean emission rate for that area (Figure 9-13). This amount was then divided by the number of individual stacks (from 81 to 144) representing the area source.

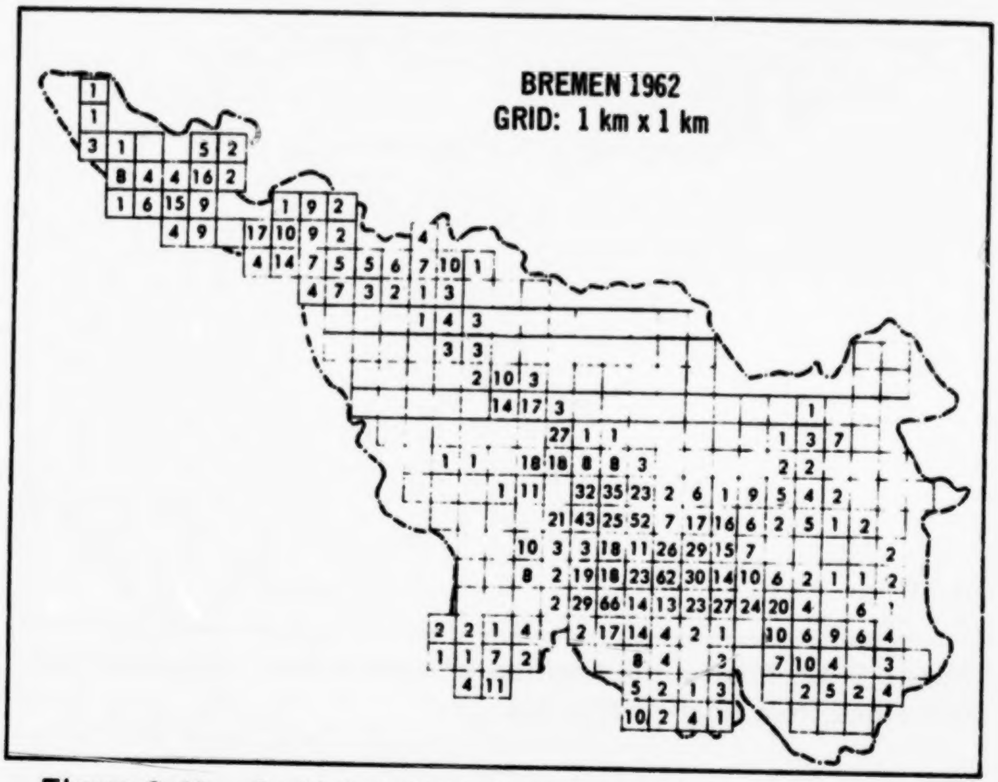

Figure 9-13. Spatial distribution of mean heating period industrial emissions from space heating, kg SO_2/km^2-hr.

The fact that area sources are represented by a large number of individual, equivalent stacks simplifies the calculations a great deal. The distribution of dwelling units in Bremen is such that only about 250 areas, 500 m by 500 m, are covered with dwellings. Since the density of these dwellings varies spatially, the emission rates of the 250 types of stacks, in general, differ from each other. Their physical dimensions and their plume rise values, however, are equal, or are grouped into only two categories (downtown and suburban). With the shift of calculated concentration fields from one point source location to the other within an area of 500 m by 500 m, the computing time is very much reduced.

RESULTS OF SIMULATION EXPERIMENTS

An inventory of all possible steady-state ground-level concentration fields forms the basis of simulation experiments. This inventory was obtained by calculating concentration fields for all possible combinations of meteorological parameters. It has already been noted that about 600 such combinations, representing given weather situations, can occur in Bremen. This number depends, of course, on the classification of windspeed and wind direction used. If one calculates the concentrations at the points of a grid (a grid distance of 500 meters) about 600 numbers have to be stored at each grid point. Since the computer program was written for a grid of 2500 points, a total number of 1.5 million numbers have to be stored. If the source inventory is assumed to be time-dependent (heating period, non-heating period, etc.), the number of concentration values to be stored increases considerably.

The use of concentration field inventory data together with frequency distributions of relevant meteorological parameters permits the derivation of frequency distributions of concentrations for each point on the grid. Other statistics, as well, can be obtained quite simply, such as SO_2 wind roses. Figures 9-14 to 9-17 demonstrate this clearly. Sulfur dioxide wind roses were calculated for the four sites where monitoring stations were later installed. These figures, together with Figures 9-11 to 9-13, show the possibility of identifying large emission sources by means of SO_2 wind roses. It may seem that this is by no means an easy task because emission sources with quite different emission heights work together with meteorological factors having complicated frequency distributions. It may be noted that the simulated SO_2 wind roses coincide considerably well in structure with those obtained by measurement.

Among the many experiments performed, the investigation of the influence of boundary layer thickness on ground-level concentration was the most interesting. The upper ceiling was lowered from 500 m to 25 m. In cases in which the ceiling reached the effective height of an individual stack, this effective height was reduced with the decreasing height of the ceiling until it reached two-thirds its original value. This stack was then thrown out of the inventory on the assumption that the plume would penetrate the ceiling Figures 9-18 and 9-19 show how the isogram patterns change and they also show the tremendously increased concentrations that result if the depth of the mixing layer is approximately equal to the effective height of space heating emissions. Figure 9-20 demonstrates this behavior for a specific location in downtown Bremen. It is obvious that this picture looks different for different locations. Only mathematical experimentation of the kind applied here can simulate the complicated behavior of ground-level concentrations.

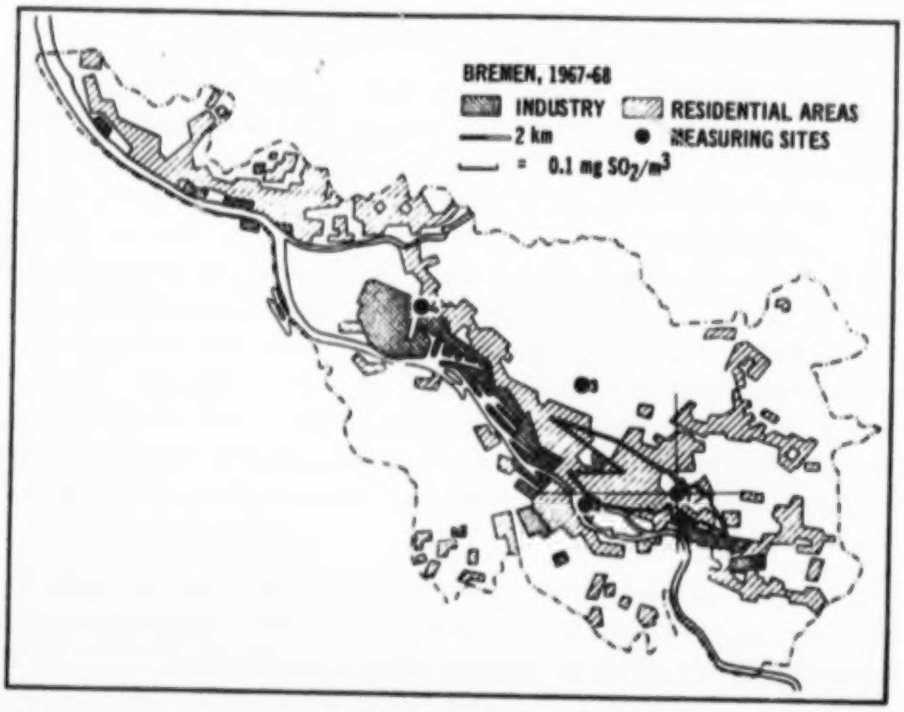
BREMEN, 1967-68
INDUSTRY
RESIDENTIAL AREAS
2 km
MEASURING SITES
= 0.1 mg SO_2/m^3

Figure 9-14. Calculated heating-period-SO_2-wind rose for Site 1 in downtown Bremen.

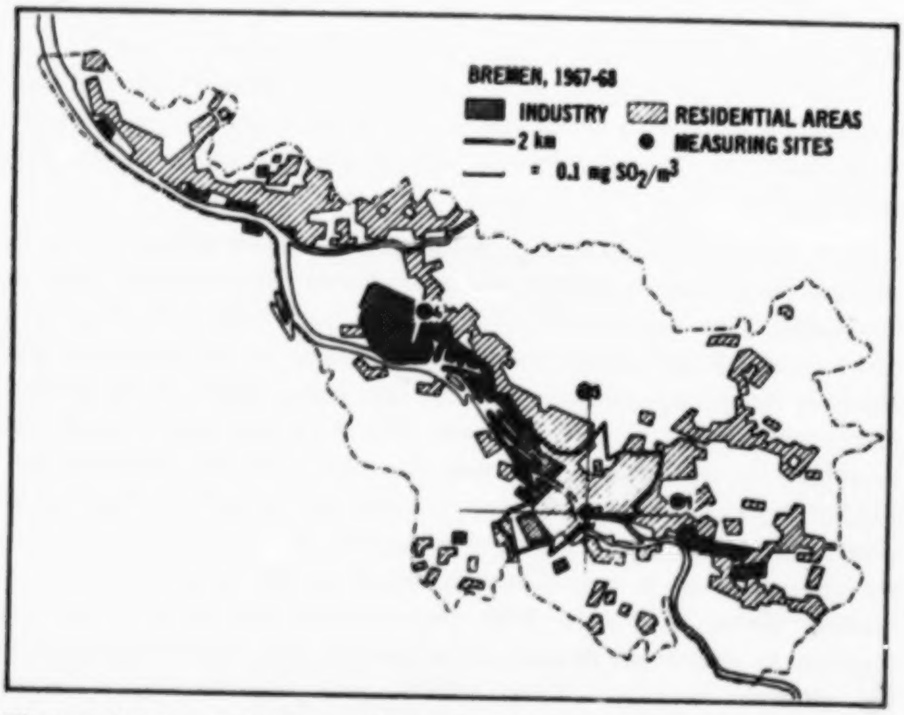
BREMEN, 1967-68
INDUSTRY
RESIDENTIAL AREAS
2 km
MEASURING SITES
= 0.1 mg SO_2/m^3

Figure 9-15. Calculated heating-period-SO_2 wind rose for Site 2 in downtown Bremen.

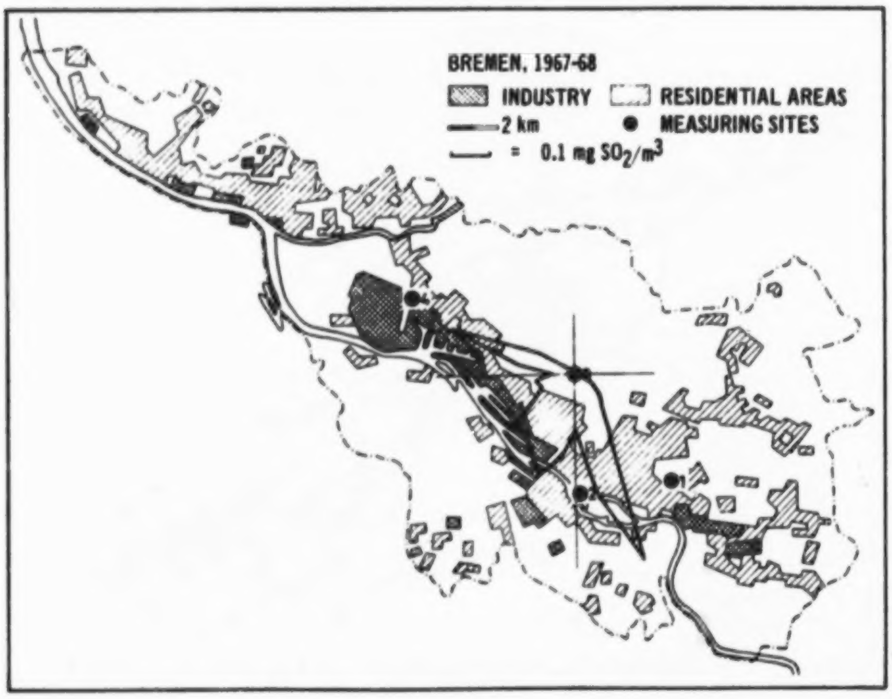
BREMEN, 1967-68
▨ INDUSTRY
▨ RESIDENTIAL AREAS
2 km
● MEASURING SITES
= 0.1 mg SO2/m3
1
2
3
4

Figure 9-16. Calculated heating-period-SO_2-wind rose for Site 3 on the outskirts of Bremen.

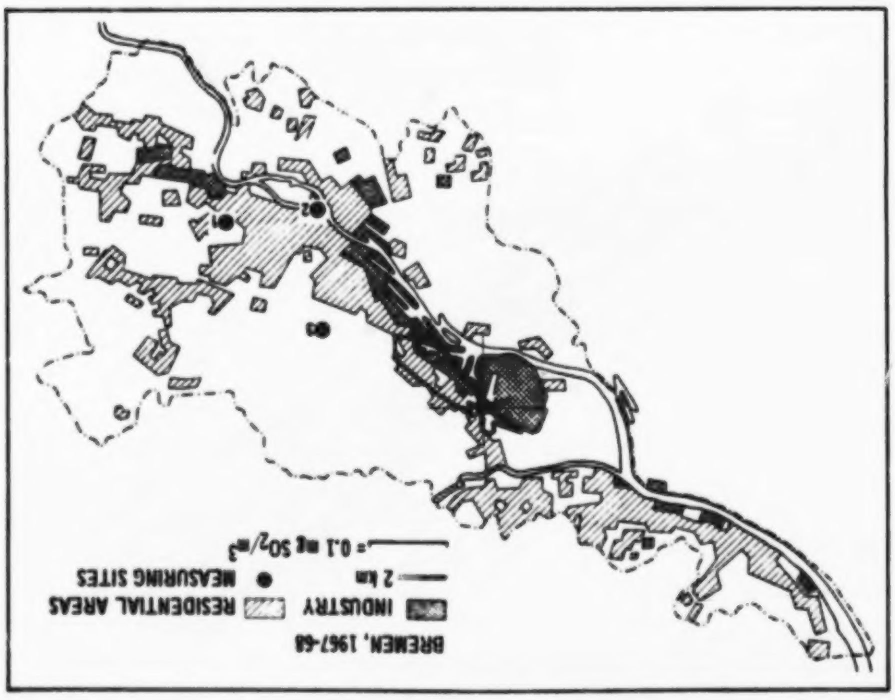
BREMEN, 1967-68
▨ INDUSTRY
▨ RESIDENTIAL AREAS
2 km
● MEASURING SITES
= 0.1 mg SO2/m3
1
2
3
4

Figure 9-17. Calculated heating-period-SO_2-wind rose for Site 4, in close proximity to an industralized area.

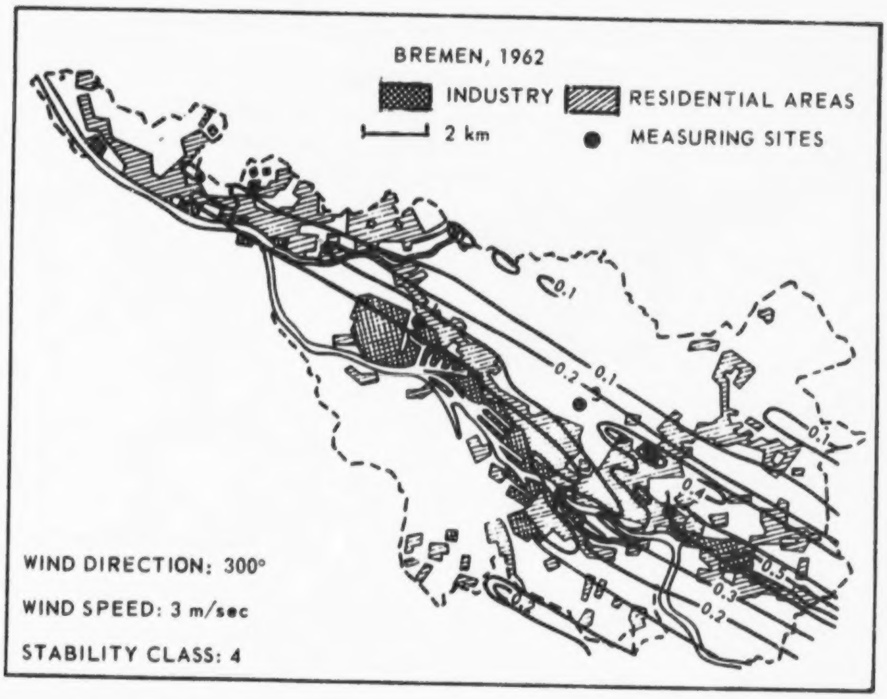
BREMEN, 1962
INDUSTRY
RESIDENTIAL AREAS
2 km
MEASURING SITES
0.1
0.2
0.1
0.1
0.4
0.5
0.3
0.2
WIND DIRECTION: 300°
WIND SPEED: 3 m/sec
STABILITY CLASS: 4

Figure 9-18. Calculated field of ground-level-SO_2 concentration in mg/m^3 for a special meteorological situation and a boundary layer thickness of 100 meters.

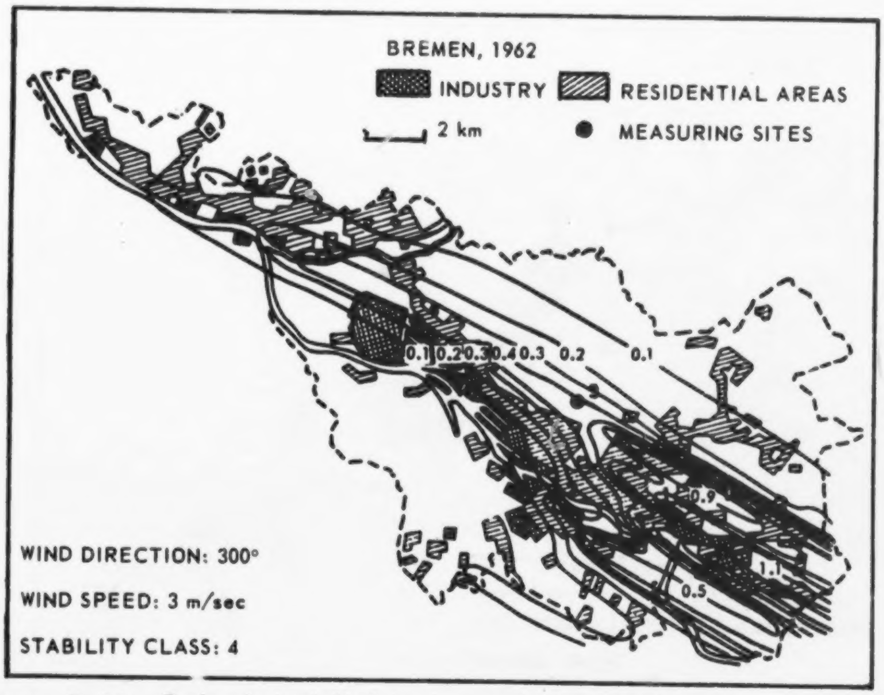
BREMEN, 1962
INDUSTRY
RESIDENTIAL AREAS
2 km
MEASURING SITES
0.1
0.2
0.3
0.4
0.3
0.2
0.1
0.9
1.1
0.5
WIND DIRECTION: 300°
WIND SPEED: 3 m/sec
STABILITY CLASS: 4

Figure 9-19. Calculated field of ground-level-SO_2 concentration in mg/m^3 for a special meteorological situation and a boundary layer thickness of 25 meters.

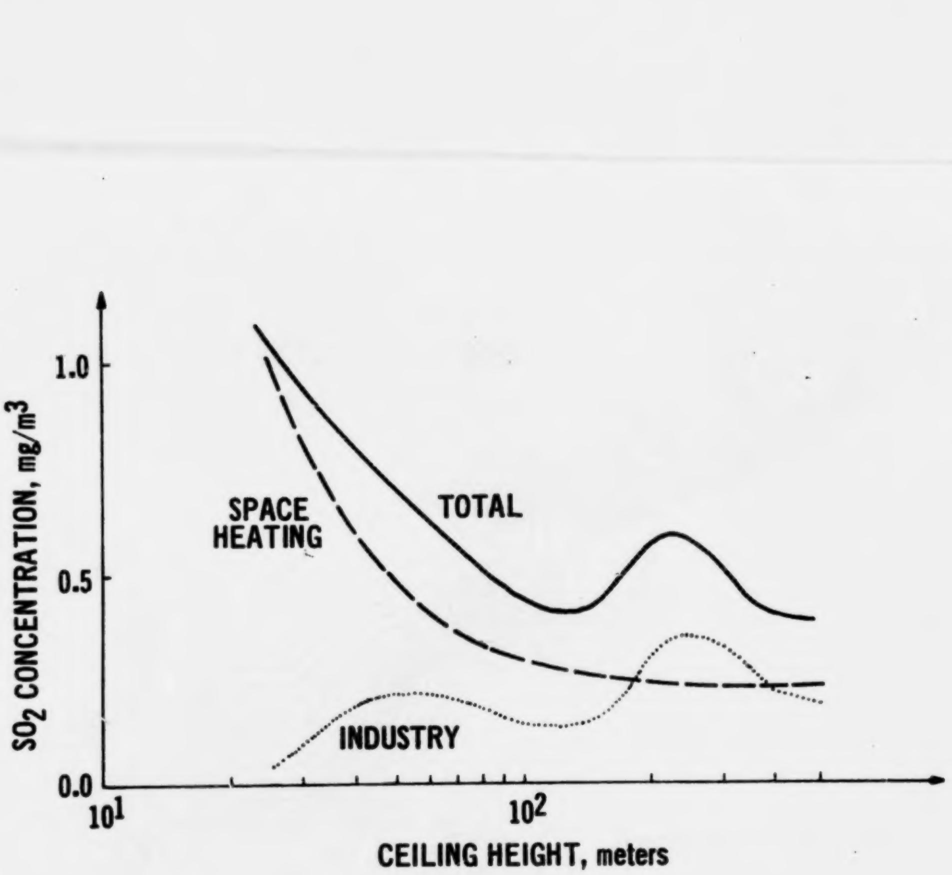

Figure 9-20. Variations in ground-level concentrations of SO_2 in downtown Bremen as a function of boundary layer thickness.

As mentioned in the introduction, frequency distributions of ground-level concentrations were of chief interest from the beginning of this investigation. The method for obtaining these for desired periods of time is straightforward. It must be stated, however, that the derived distributions are not complete because up to now no theory exists for explaining the dilution of pollutants under calm weather conditions. These cases, therefore, were excluded from the statistics as were cases with limited boundary layer depths. Neither source of error, however, plays an important role in Bremen. The frequency of calm conditions as well as the frequency of low-level inversions was small during all periods of time investigated.

Stored data on fields of steady-state concentrations (Figure 9-21) form the basis of statistics of this kind.

Steady-state concentration fields, together with frequency distributions of meteorological parameters, can be used to calculate frequency distributions of concentrations for each grid point. These distributions were characterized by a set of three parameters:

1. The percentage of time (in hours) for which ground-level concentrations exceeded a given value (0.1 milligram SO_2 per cubic meter). Figure 9-22 shows the pattern of this parameter for the heating period of 1962. As seen, only 20 percent of the period concentrations in downtown Bremen were below 0.1 milligram SO_2 per cubic meter.

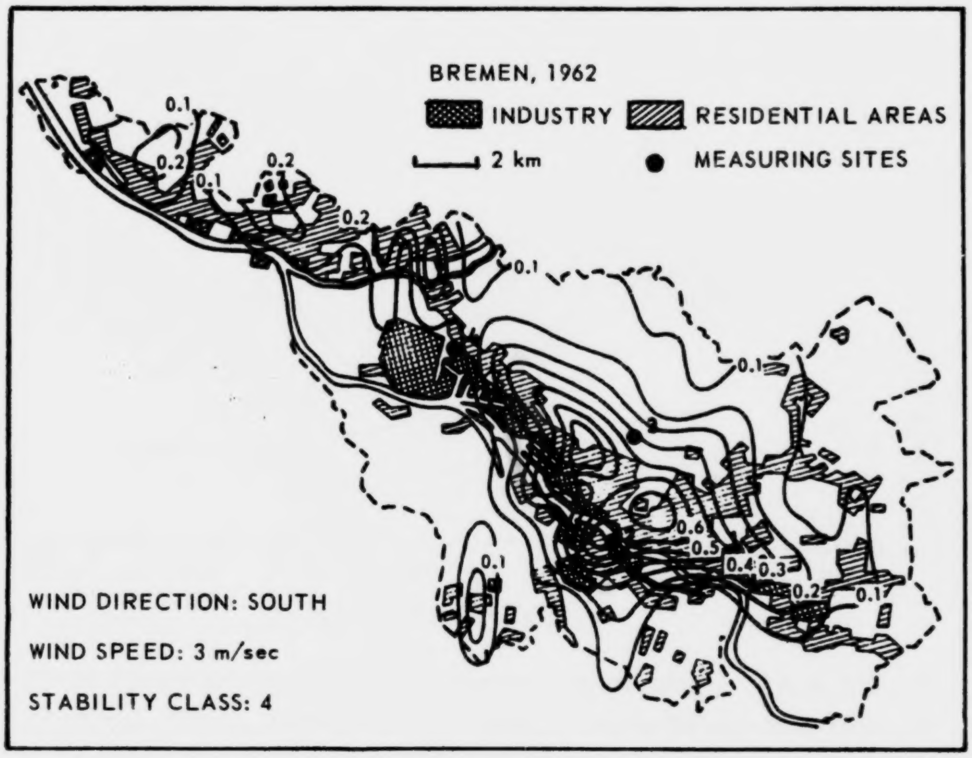
BREMEN, 1962
▨ INDUSTRY
▨ RESIDENTIAL AREAS
2 km
● MEASURING SITES
0.1
0.2
0.1
0.2
0.2
0.1
0.1
0.1
0.6
0.5
0.4
0.3
0.2
0.1
WIND DIRECTION: SOUTH
WIND SPEED: 3 m/sec
STABILITY CLASS: 4

Figure 9-21. Typical possible field of calculated steady-state ground-level SO_2 concentrations in mg/m^3.

2. The mean concentration for the period. Figure 9-23 shows the pattern of this parameter. Typically, the pattern of the mean concentration shows little structure and does not contain much information.
3. An upper percentile; for example, the 97.5th percentile. The numbers in Figure 9-24 indicate that for only 2.5 percent of the time (in hours) concentrations exceeded that value given by the respective number.

The following Figures, 9-25 thru 9-27 show the corresponding pattern for a nonheating period in which only industrial sources are contributing emissions.

It might be possible to define *Imissions-Grundbelastung* with the help of these maps of characteristic parameters. This investigation is one step forward in this direction.

VALIDATION OF THE MODEL

During the heating period of 1967-68, four monitoring stations were installed at specially chosen locations. The locations were planned as strategically as possible. First of all,.an attempt was made to place all stations on a mean concentration isogram (Figure 9-23). Second, an attempt was

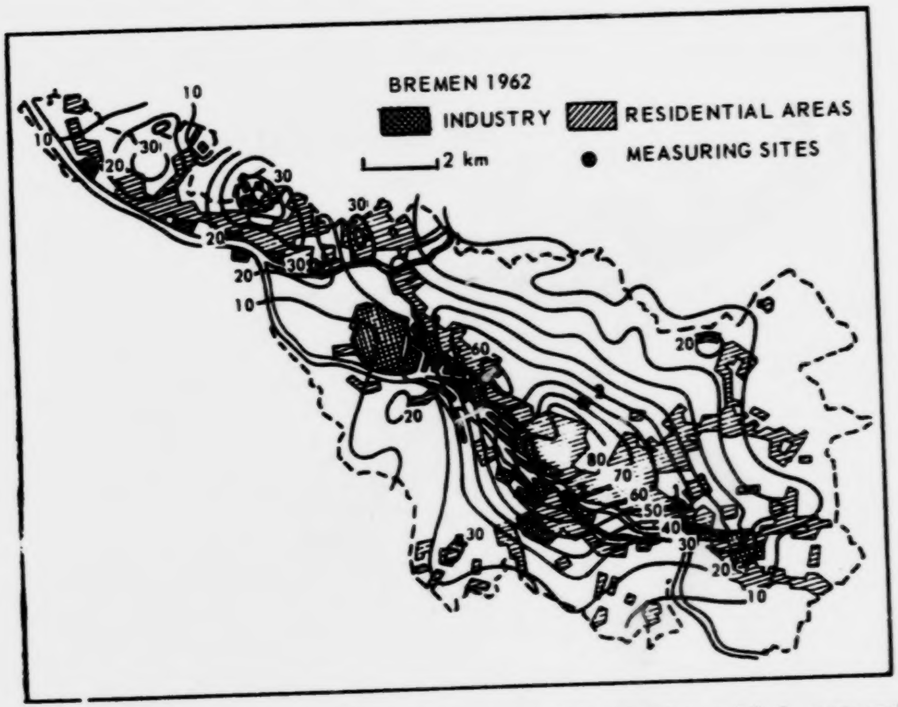
BREMEN 1962
INDUSTRY
RESIDENTIAL AREAS
2 km
MEASURING SITES
10
10
30
20
30
30
20
20
30
10
20
60
20
80
70
60
50
40
30
30
20
10

Figure 9-22. Percentage of cases (hours) for which ground-level concentrations exceeded 0.1 mg SO/m^3. Winter 1962.

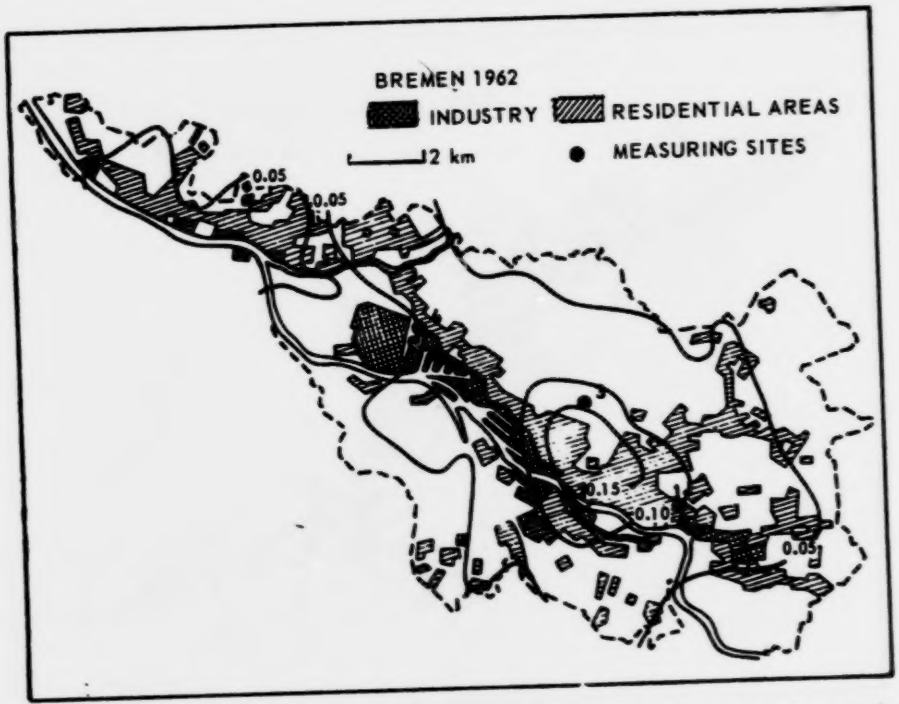
BREMEN 1962
INDUSTRY
RESIDENTIAL AREAS
2 km
MEASURING SITES
0.05
0.05
0.15
0.10
0.05

Figure 9-23. Mean ground-level-SO_2 concentration in mg/m^3.

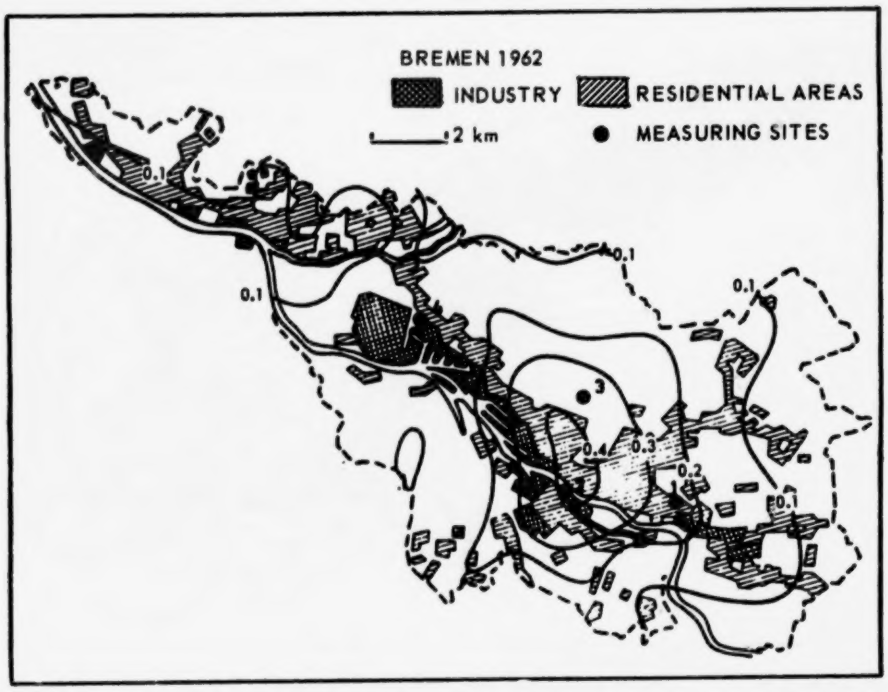
BREMEN 1962
INDUSTRY
RESIDENTIAL AREAS
2 km
MEASURING SITES
0.1
0.1
0.1
0.1
3
0.4
0.3
0.3
0.2
0.1

Figure 9-24. 97.5th percentile SO_2 concentrations in mg/m^3. Winter 1962.

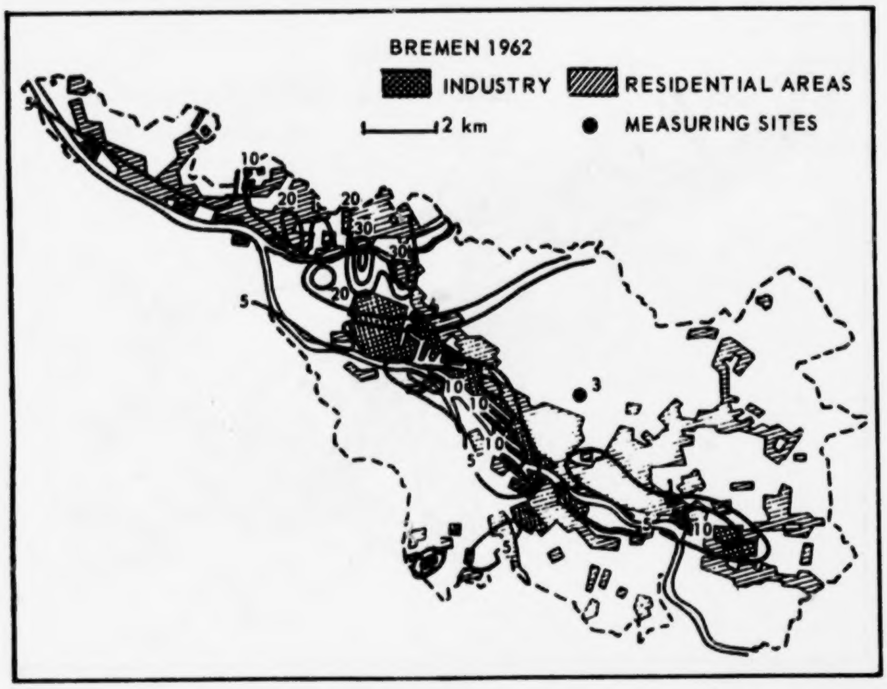
BREMEN 1962
INDUSTRY
RESIDENTIAL AREAS
2 km
MEASURING SITES
5
10
20
20
30
30
20
5
10
10
10
5
3
5
5
10

Figure 9-25. Percentage of cases (hours) for which ground-level concentration exceeded 0.1 mg SO_2/m^3. Summer 1962.

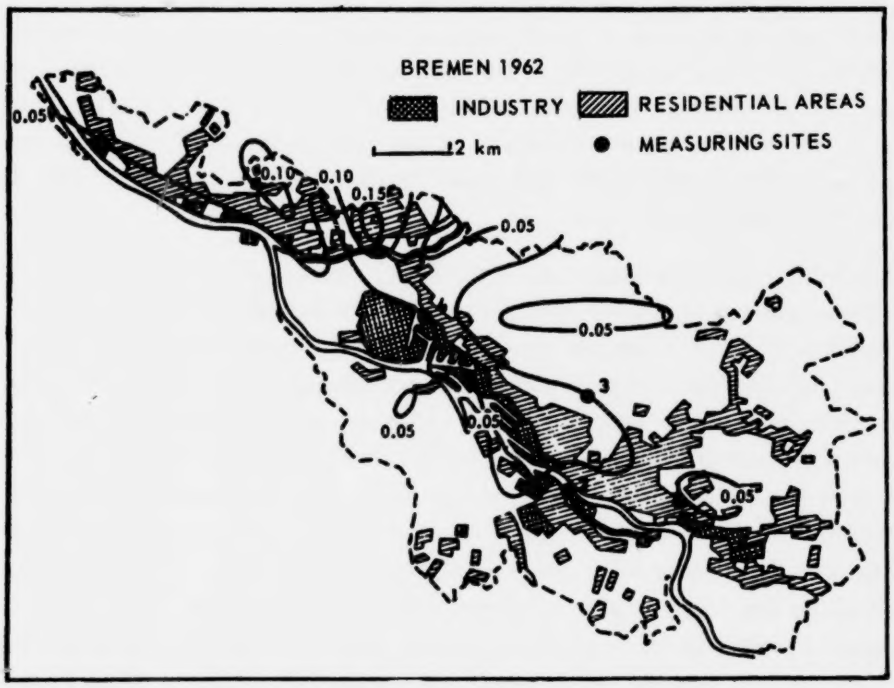
BREMEN 1962
INDUSTRY
RESIDENTIAL AREAS
2 km
MEASURING SITES
0.05
0.10
0.10
0.15
0.05
0.05
3
0.05
0.05
0.05

Figure 9-26. Mean ground-level-SO_2 concentration in mg/m^3. Summer 1962.

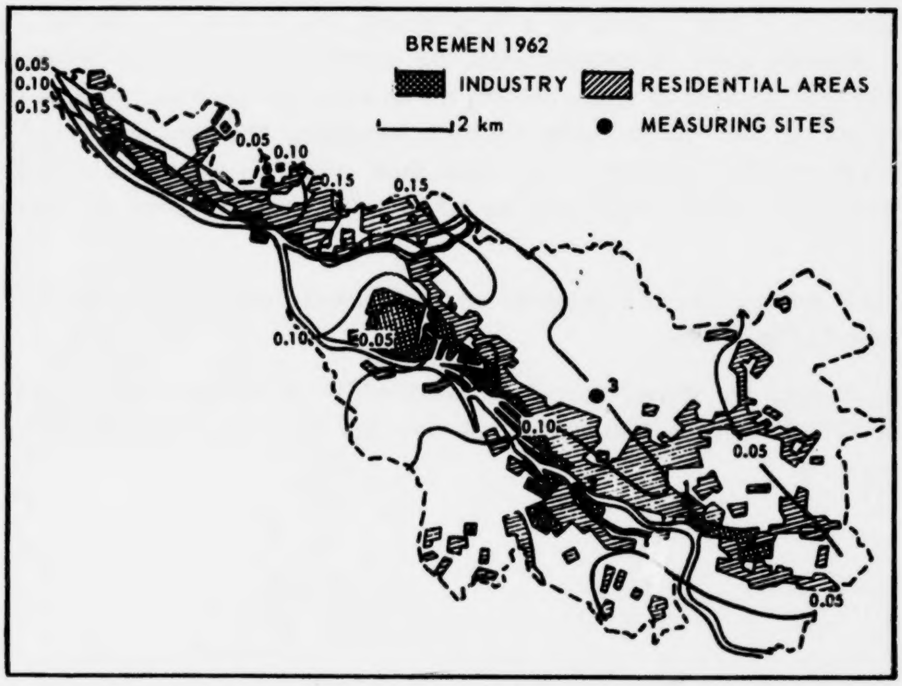
BREMEN 1962
INDUSTRY
RESIDENTIAL AREAS
2 km
MEASURING SITES
0.05
0.10
0.15
0.05
0.10
0.15
0.15
0.10
0.05
3
0.10
0.05
0.05

Figure 9-27. 97.5 percentile of ground-level-SO_2 concentrations in mg/m^3. Summer 1962.

made to locate stations in areas as diverse as possible. Station 1 was located in a "normal" downtown area, surrounded mainly by residences. Station 2 was located in the very center of the city on an island. It was surrounded, however, on all sides by the water of the river Weser and of the waterworks. Station 3 was located on the outskirts of the city, separated from downtown Bremen by a large park with tall trees. Station 4 was located in the near vicinity of a large plant.

The monitoring stations measured half-hourly values of SO_2 concentrations. From these values, frequency distributions were derived for every month of the period and for the period as a whole. At the same time, mathematical simulation of the same distributions was performed using the latest version of the emission source inventory and utilizing meteorological statistics for the sampling period. Figures 9-28 through 9-31 show comparisons of observed and calculated frequency distributions. The simulation of Station 1 (downtown "normal" area) is quite satisfactory, as indicated in Table 9-1. For Station 2 (waterworks on the Weser island), the model obviously overestimates the concentrations systematically (Figure 9-29). Overestimation may occur for one or both of two reasons: absorption at the water surfaces, or an insufficient spread as a result of improperly chosen urban plume standard deviations. The same holds for Station 3 (separated from downtown Bremen by a large park), where the filtering effect of the park was not taken into account.

At Station 4 (in the vicinity of a large plant), the reverse is observed. The model systematically underestimates the concentrations. Since emissions from low-level sources of space heating are small in the neighborhood of that station, low concentration values could be expected. The comparatively high concentrations that actually occur have their origin in uncontrollable low-level emissions, which could not be taken into account, from the nearby plant.

Table 9-2 summarizes the observed and calculated mean concentrations for each monitoring station.

Finally, it can be stated that it is worthwhile to invest more effort in diffusion modeling, for simulation may one day be a very important tool in city planning.

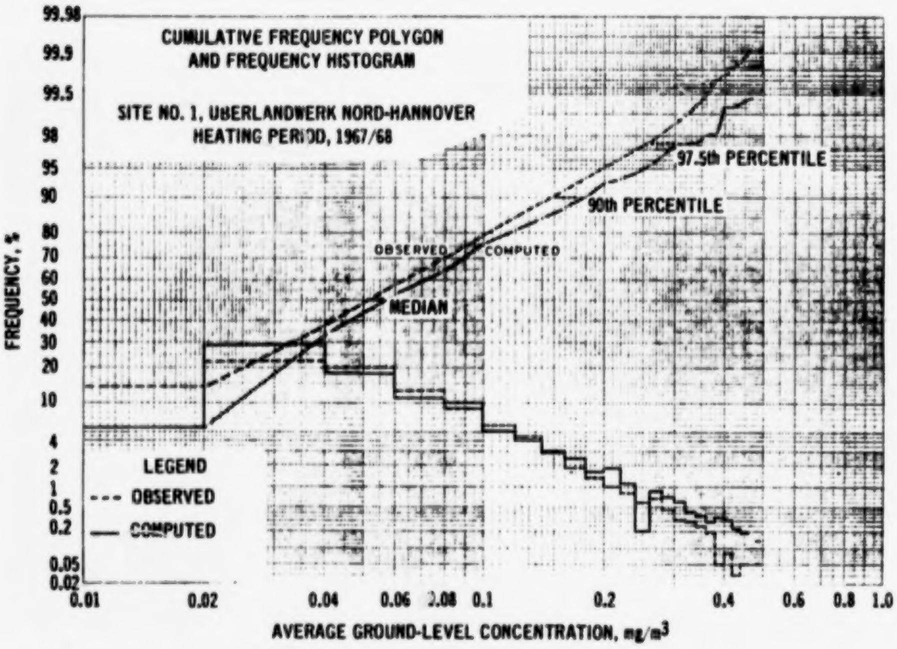

Figure 9-28. Comparison between observed and computed frequency distributions of ground-level concentrations in downtown Bremen.

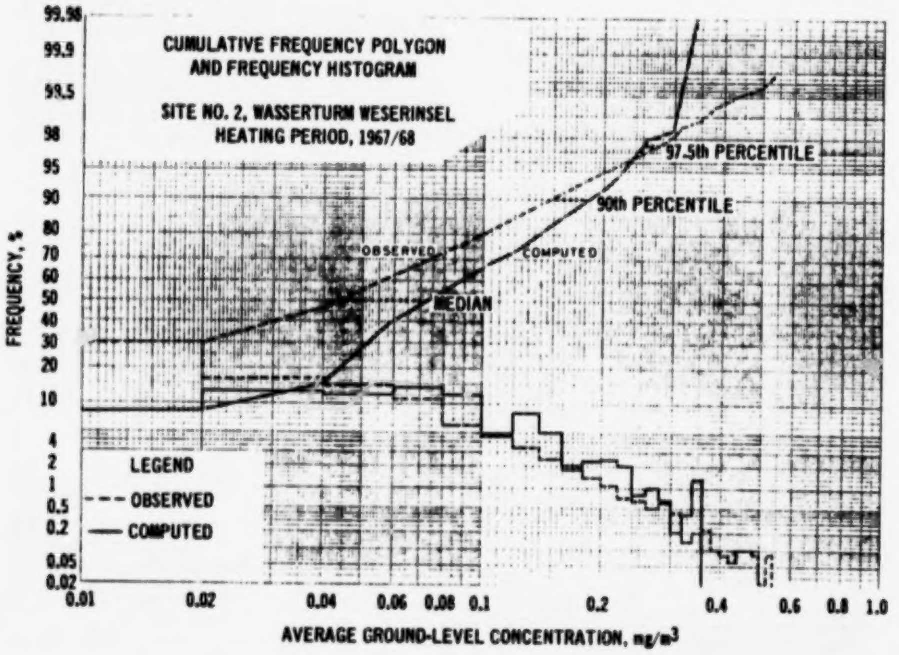

Figure 9-29. Comparison between observed and computed frequency distributions of ground-level concentrations in downtown Bremen.

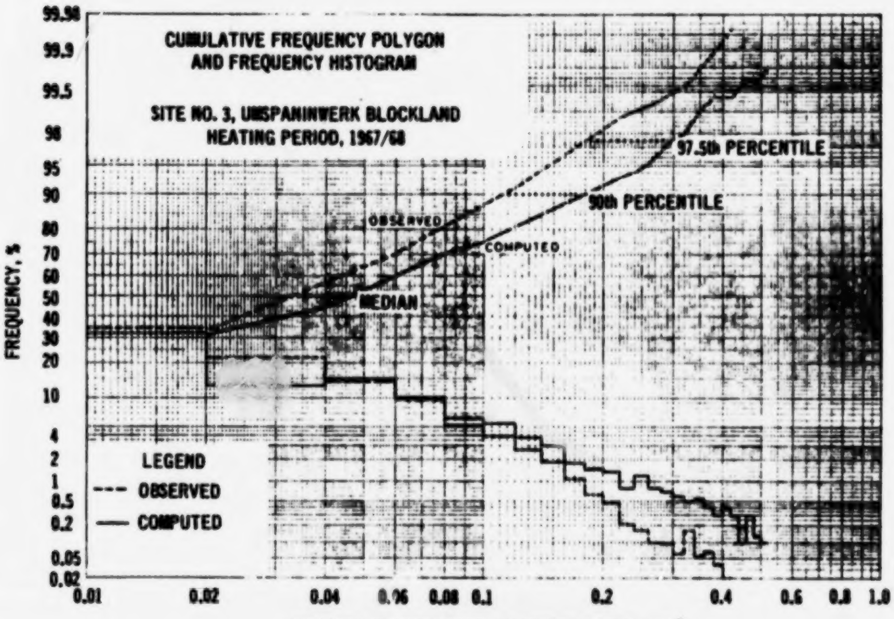

Figure 9-30. Comparison between observed and computed frequency distributions of ground-level concentrations on outskirts of Bremen.

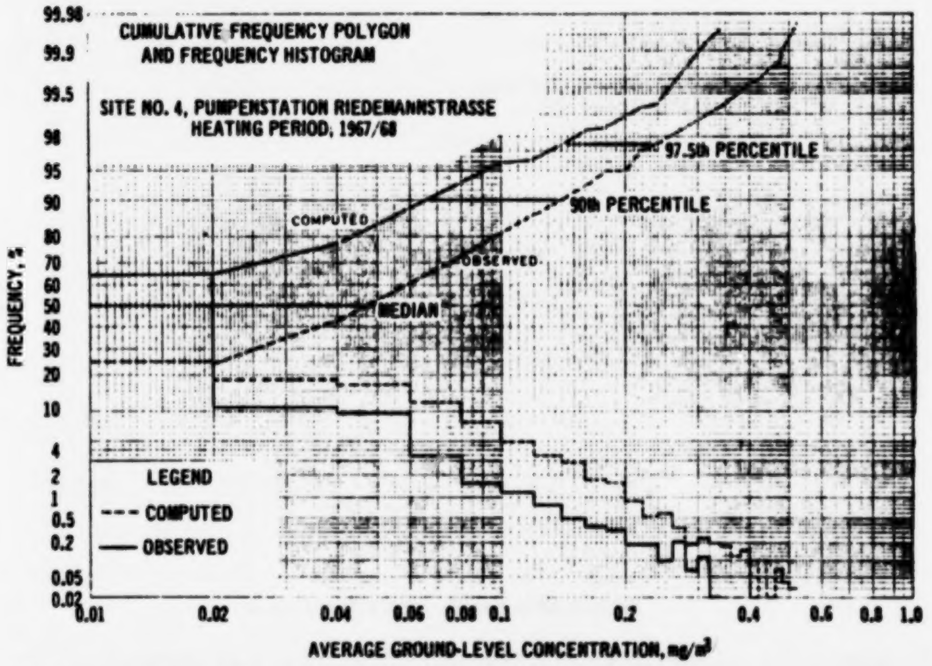

Figure 9-31. Comparison between observed and computed frequency distributions of ground-level concentrations in an industrial district.

Table 9-2. OBSERVED AND CALCULATED MEAN SO_2 CONCENTRATIONS IN BREMEN; HEATING PERIOD, 1967-1968

($mg\ m^{-3}$)

Site	1		2		3		4	
	Calc.	Obs.	Calc.	Obs.	Calc.	Obs.	Calc.	Obs.
November	0.14	0.11	0.15	0.10	0.14	0.08	0.05	0.10
December	0.10	0.08	0.12	0.08	0.10	0.06	0.03	0.07
January	0.10	0.10	0.12	0.13	0.09	0.08	0.04	0.08
February	0.09	0.08	0.12	0.08	0.07	0.06	0.04	0.08
March	0.08	0.07	0.10	0.04	0.07	0.05	0.04	0.07
April	0.09	0.07	0.11	0.05	0.06	0.05	0.05	0.07
May	0.05	0.06	0.07	0.03	0.04	0.03	0.03	0.05
Total	0.09	0.08	0.12	0.08	0.08	0.06	0.04	0.08

REFERENCES

1. Pasquill, Frank. Atmospheric Diffusion. London, D. Van Nostrand Co. Ltd., 1962. 297 p.
2. Turner, D. B. A Diffusion Model for an Urban Area. J. Appl. Meteorol. *3*(1):83-91, February 1964.
3. Gifford, F. A. The Problem of Forecasting Dispersion in the Lower Atmosphere. AEC Division of Technical Information Extension. Oak Ridge, Tenn. 1961.
4. Singer, I. A. and M. E. Smith. Atmospheric Dispersion at Brookhaven National Laboratory. Int. J. Air Water Pollution. *10*:125-135, February 1966.
5. Sutton, O. G. Micrometeorology; A Study of Physical Processes in the Lowest Layers of the Earth's Atmosphere. New York, McGraw-Hill, 1953. 333 p.
6. Verein Deutsche Ingenieure. VDI-Forschungsheft 483, Ausgabe B, Band 27, 1961.
7. *Ausbreitung luftremder Stoffe in der Atmosphare Zusammenhang zwischen Emission und Immission Schornsteinhohen in ebenem, unbebautem Gelande. Verein Deutscher Ingenieure, VDI-Kommission Reinhaltung der Luft.* Germany. VDI 2289. June 1963. 7p.
8. Frenkiel, F. N. Atmospheric Pollution in Growing Communities. In: Annual Report of the Board of Regents of the Smithsonian Institution, Publication 4272, 1956. Washington, D. C. Government Printing Office. 1957. p. 269-299.
9. Fortak, H. G. *Rechnerische Ermittlung der* SO_2 *– Grundbelastung aus Emissionsdaten – Anwendung auf die Verhaltnisse des Stadtgebietes von Bremen. Institute for Theoretical Meteorology,* The Free University of Berlin. 1966.
10. Clarke, J. F. A Simple Diffusion Model for Calculating Point Concentrations from Multiple Sources. J. Air Pollution Control Assoc. *14*347-352, September 1964.
11. Marsh, K. J. and V. R. Withers. An Experimental Study of the Dispersion of the Emissions from Chimneys in Reading -- III: The Investigation of Dispersion Calculations. Atmos. Environ. *3*(3):281-302, May 1969.
12. Davidson, B. A Summary of the New York Urban Air Pollution Dynamics Research Program. J. Air Pollution Control Assoc. *17*:154-158, March 1967.
13. Frenkiel, F. N. Turbulent Diffusion: Mean Concentration Distribution in a Flow Field of Homogeneous Turbulence. In: Advances in Applied Mechanics, von Mises, R. and T. von Karman (eds.), Vol. III. New York, Academic Press Inc., 1953. p. 61-107.
14. Fortak, H. G. *Einbeziehung der Sinkgeschwindigkeit und partiellen Absorption am Erdboden in die Ausbreitungsrechnung, speziell im Falle nicht-FICKscher Diffusion. Institute for Theoretical Meteorology,* The Free University of Berlin. 1964.
15. Fortak, H. *Zur allgemeinen Berechnung von Suspensionsverteilungen in turbulenten Stromungen. Gerlands Beitr.* Geophys. *66*(1):65-78, 1957.
16. Stumke, H. *Vorschlag einer empirischen Formel fur die Schornsteinuberhohung.* Staub (Dusseldorf). *23*:549-556. December 1963.
17. Fortak, H. G. *Ausbreitung von Staub und Gasen um eine kontinuierliche Punktquelle in einer bezuglich Windgeschwindigkeit und Austausch geschichteten Atmosphare. Verein Deutscher Ingenieur. VDI-Forschungsheft* 483. 1961.
18. Singer, I. A. and M. E. Smith. Relation of Gustiness to Other Meteorological Parameters. J. Meteorol. *10*(2):121-126, April 1963.
19. McElroy, J. L. and F. Pooler, Jr. St. Louis Dispersion Study, Vol. II – Analysis. National Air Pollution Control Administration. Arlington, Va. Publication Number AP-53. 51 p.
20. Fortak, Von Heinz. *Sinkstofftransport in Geraden Kanalen als Randwertproblem. Acta Hydrophysica.* *4*(1):26-48, 1957.

ACKNOWLEDGMENT

In the course of the research, a number of members of the *Institut fur Theoretische Meteorologie der Freien Universitat Berlin* contributed to this work, in many ways, mainly in programming and organizing. Especially, the author wishes to thank the following for the valuable cooperation, without which these experiments could not have been performed: R. Bleck, J. Schwirner, H. Buttner, H. Woick, and P. Lenschow.

APPENDIX – GLOSSARY OF SYMBOLS

$a(\tau,y)$	absorption coefficient of the ground
h	effective stack height
h_s	actual stack height
Δh	plume rise
H	height of dispersion ceiling
N	total number of upwind sources
$P(x,y)$	receptor point
$q(\xi,\eta)$	local source-strength density
Q	source strength
T	decay time, $1/\gamma$
U	wind speed
$(\overline{X}_n,\overline{Y}_n)$	source distance in downwind and crosswind directions, respectively
α,β	wind direction angle coefficients
Δ	source area
(ξ_n,η_n)	location of a point source
π	3.14
σ_y,σ_z	standard deviations of plume spread in y and z directions, respectively
γ	travel time
χ	concentration

ABSTRACT

A source-oriented three-dimensional model of diffusion and transport based upon the statistical concept of turbulent diffusion was developed for application to an urban area. A simple algorithm was found for computing the concentration field from time-dependent continuously emitting area sources of different scales. The model was applied to the New York City metropolitan region by introducing known specific meteorological conditions and the known pollutant (SO_2) source distribution as input data. The validity of the model has been verified in a preliminary manner. The results appear promising, giving concentration fields computed on spatial scales down to 0.2 mile.

AUTHORS

Until his death in 1968, BEN DAVIDSON was Professor of Meteorology at New York University, a consultant to both the U. S. Weather Bureau and Brookhaven National Laboratory, and chairman of the working group on sites for wind power installations of the World Meteorological Organization. He has also been on the University of Chicago Review Committee for the Radiological Physics Division of Argonne National Laboratory and on the Air Pollution Training Grants Committee. Most of his research was concerned with turbulence diffusion, local wind circulations, and urban air pollution models.

LIAU JANG SHIEH, a staff member of the Internationl Business Machines Corporation Palo Alto Scientific Center, received his Ph. D. in Meteorology at NYU in 1969 for work done with Dr. Davidson. He also holds an M.S. from NYU and a B.S. from National Taiwan University, Formosa.

JAMES P. FRIEND is the director of the U. S. Department of Health, Education, and Welfare Air Resources Engineering Training Program at NYU, where he is Associate Professor of Atmospheric Chemistry. He is a member of the ad hoc *committee for Air Pollution Manpower Affairs, NAPCA, and holds a S.B. in chemistry from Massachussetts Institute of Technology, and an M.S. and Ph. D. in chemistry from Columbia. His principal research is in the area of stratospheric aerosols and mathematical models of air pollution dynamics.*

10. A MODEL OF DIFFUSION IN URBAN ATMOSPHERES: SO_2 IN GREATER NEW YORK

**LIAU J. SHIEH, BEN DAVIDSON,
AND JAMES P. FRIEND**

New York University

INTRODUCTION

The essential components of a model of dispersion and transport of pollutants in an urban atmosphere are (1) distribution and strengths of sources of pollutant in space and time, (2) a set of meteorological conditions as functions of space and time, (3) a mathematical formula (algorithm) representing the physical concepts of dispersion and transport, and (4), in combination with the formula of (3), an expression for the removal (decay, settling, or absorption on surfaces) of the pollutant.

The model described below was developed in the Urban Air Pollution Dynamics Research Project at New York University. It was a task of the project, not only to develop the model, but to provide sufficient data so that the model could be tested. The pollutant chosen was sulfur dioxide (SO_2) and the urban region was a 50 by 50 mile square containing greater New York City. Commensurate with the requirements implied by the previous paragraph, the project provided a survey of SO_2 emissions throughout the area. Also, during specific test periods of 2 to 5 days duration, it provided wind, temperature, and SO_2 concentration measurements at several points within the area. Helicopter-borne instruments were used for vertical soundings of temperature and SO_2 concentrations.

The model of diffusion and transport in urban atmospheres was fashioned from the statistical theory of turbulent diffusion. In that theory, concentration profiles in diffusing plumes are represented as Gaussian distributions. An attempt was made to maintain generality within the Gaussian framework of the theory. The formulated theory was thus applicable in three dimensions to non-isotropic and time-dependent motions of the atmosphere. The model constructed on the basis of the theory was made to accept as data (1) any specified time and space distributions of area and point source strengths, (2) specified meteorological parameters (wind, temperature, thermal stability, diffusivity, and height of inversion layer) as functions of time and space, and (3) the (initial) field of pollutant concentrations over the region at any given time. The output of the model consists of fields of pollutant concentrations in three dimensions at 2-hour intervals after the initial time.

---

*Contribution No. 84, Geophysical Sciences Laboratory of the Department of Meteorology and Oceanography, New York University. This research was sponsored by the U. S. Department of Health, Education, and Welfare under Grant No. AP 00328-04.

DATA

As used here, the term "data" refers to quantities entered into the computational scheme as input.

A summary of the meteorological and SO_2 source and concentration data obtained in the Urban Dynamics project was given by Davidson[1] and will be given in complete detail by Davidson *et al.*[2]

Meteorology

Winds for the various trial periods were obtained from a fixed network of stations in the Greater New York region and from analyses of data obtained from pibal ascents at three or four fixed sites plus a reference ascent at JFK airport made on a continual basis throughout each trial period. Scudder[3] analyzed stream-line patterns derived from various wind data and noted characteristics ranging from essentially straight streamlines, through curved inflected ones, to sharp discontinuous ones. He also found high wave number patterns. These patterns generally depend upon the strength of the prevailing synoptic wind field, time of day, and insolation. Evidently the combined effects of land-sea, land-river, urban-rural, and other contrasting topographical features produce complicated mesoscale wind flow patterns.

In view of the observed complexity of flow over the New York City area it is clear that a realistic model of diffusion and transport must be capable of incorporating space- and time-dependent winds. Turbulent diffusion processes are treated in the model by the statistical theory of diffusion. Transport of the pollutants is based on the average trajectory of parcels according to the analyzed wind field. This trajectory method was studied and verified by Druyan.[4]

Bornstein[5] frequently found temperature inversions at elevations of 200 to 300 meters over the metropolitan area in nighttime and early morning hours, when the inversion was at ground level in rural areas. This is the heat island effect due to release of heat from urban surfaces. The air beneath the inversion generally exhibited vertical temperature gradients ranging from isothermal to adiabatic.

As Davidson[1] pointed out, "the diffusive consequences of the temperature structure over the urban area are enormous. One would expect good vertical diffusion below the elevated inversion, but virtually zero diffusion through the base of the inversion."

The model includes this thermal stratification effect by treating the observed elevated inversion layer as a physical barrier to diffusion of the pollutant. The height of the inversion at all points at all times is entered as data in the computational scheme. The meteorological network and the grid used in model computations are shown in Figure 10-1.

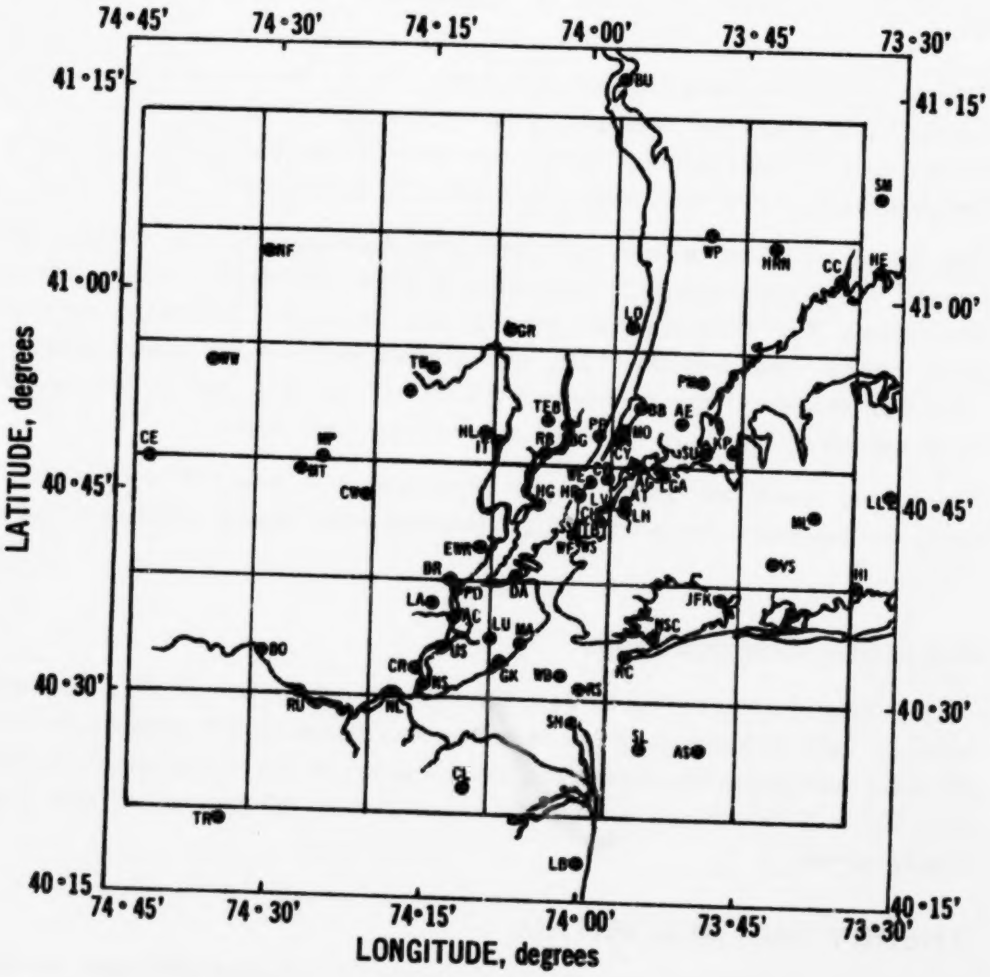
74°45'
74°30'
74°15'
74°00'
73°45'
73°30'
41°15'
41°00'
40°45'
40°30'
40°15'
LATITUDE, degrees
LONGITUDE, degrees
BU
SM
RF
WP
HRN
CC
NE
LD
GR
WW
TB
PR
TEB
BB
AE
CE
MP
NL
IT
RB
BG
PB
MO
CY
SU
KP
WT
CW
WE
HG
HB
LV
LGA
AT
LL
CH
LN
ML
WF
WS
EWR
VS
BR
PD
DA
HI
LA
AC
JFK
LU
MA
NSC
BO
US
CR
KS
GK
WB
RS
RC
RU
NL
SH
SL
AS
CL
TR
LB

Figure 10-1. Meteorological grid system and observational network.

SO_2 Emissions

A comprehensive source survey was conducted in the 50 by 50 mile-square region shown in Figure 10-1, and a portion of it is shown in Figure 10-2. Two types of sources were delineated: (1) area sources representing emissions from fuel combustion used for space heating and production of hot water and (2) continuous point sources representing industrial emissions from electrical power generating plants, large hospital heating plants, large industrial heating plants, and chemical plants.

Messrs. P. Halpern and L. Randall* have analyzed the diurnal and daily variations of SO_2 emission rate for area sources. Their findings have been directly incorporated into the model:

$$Q_{day} = 0.7 \frac{Q_{year}}{4871} DD + 0.3 \frac{Q_{year}}{365} \qquad (1)$$

where Q_{day} is the daily total output of SO_2, Q_{year} the annual total output, and DD is the number of degree days for the date of interest. The diurnal variation of the area-source strength was found to depend upon atmospheric temperature in the manner shown in Figures 10-3 and 10-4.

The survey of point sources was conducted by Messrs. Kaiser, Simon, and Ingram.* The most complete data were available for electric power generation plants. For other sources most of the important parameters such as stack height, heat emission rate, and diurnal variation of source strength were not available. Hence, assumed values of these are used in the model. Total output of SO_2 was, however, obtained for each source.

The model treats the point source emissions in a straightfoward manner using the equations for a continuous elevated point source emitting a Gaussian plume.

Initial SO_2 Concentrations

In all model computations to date the initial concentration of SO_2 has been taken as zero everywhere. Experience has shown that under steady wind and emission conditions the concentrations computed at the end of the first time step (Δt = 2 hours) are greater than or equal to 90 percent of the final steady values.

THEORY AND ALGORITHM

The model is based on the statistical theory of turbulent diffusion. In this theory it is hypothesized that the concentrations in a cloud of trace material (called pollutant in this paper) emitted from an instantaneous point source

---

*Members of the research staff, New York University.

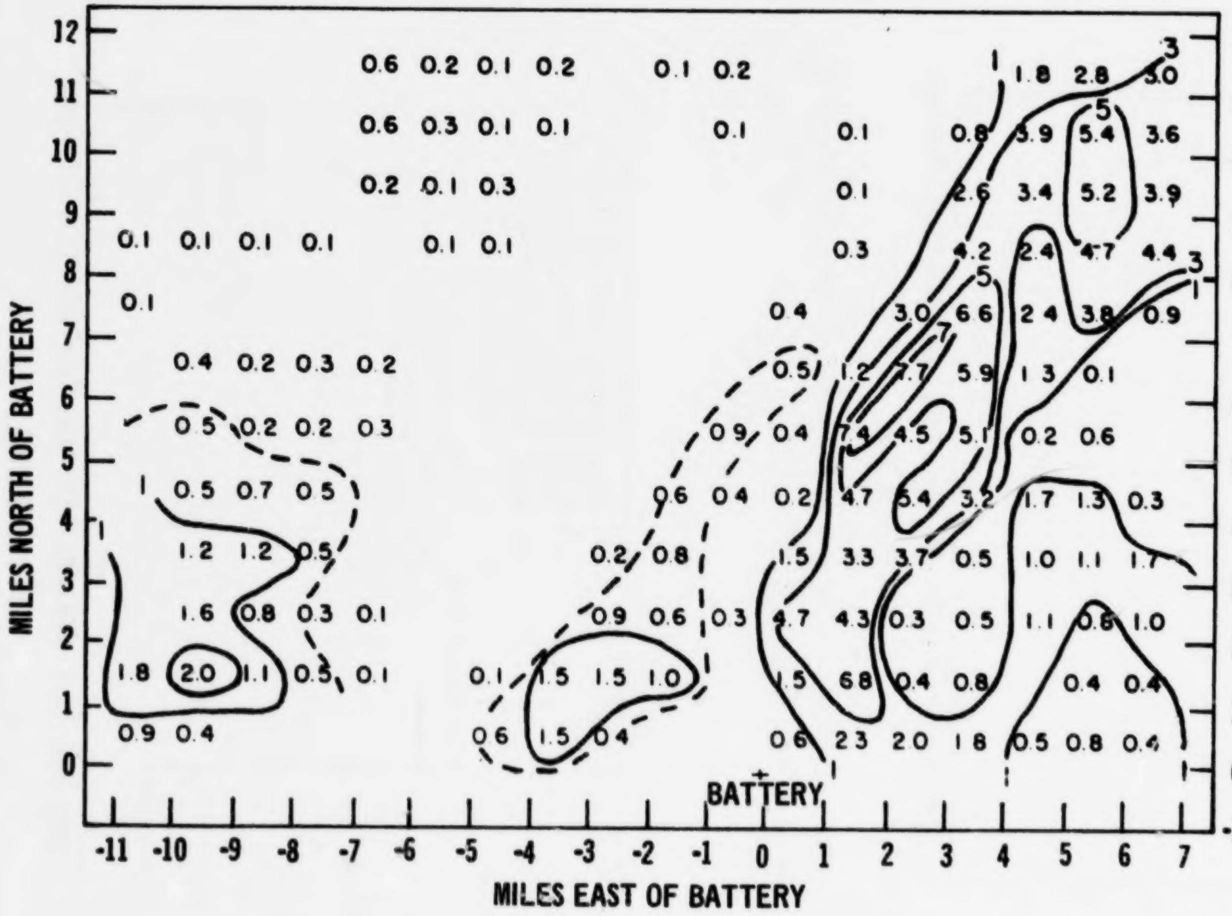
MILES NORTH OF BATTERY
MILES EAST OF BATTERY
BATTERY
-11 -10 -9 -8 -7 -6 -5 -4 -3 -2 -1 0 1 2 3 4 5 6 7
-1 0 1 2 3 4 5 6 7 8 9 10 11 12

Figure 10-2. SO$_2$ source inventory (tons mi^{-2} year^{-1}).

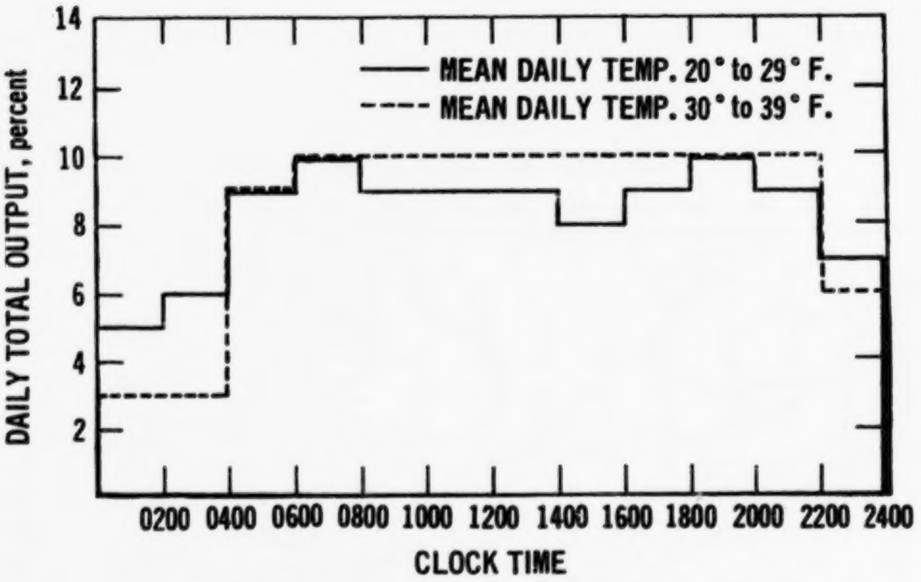

Figure 10-3. Diurnal variation of SO_2 output during days with mean temperature ranges of 20° to 29° F and 30° to 39° F.

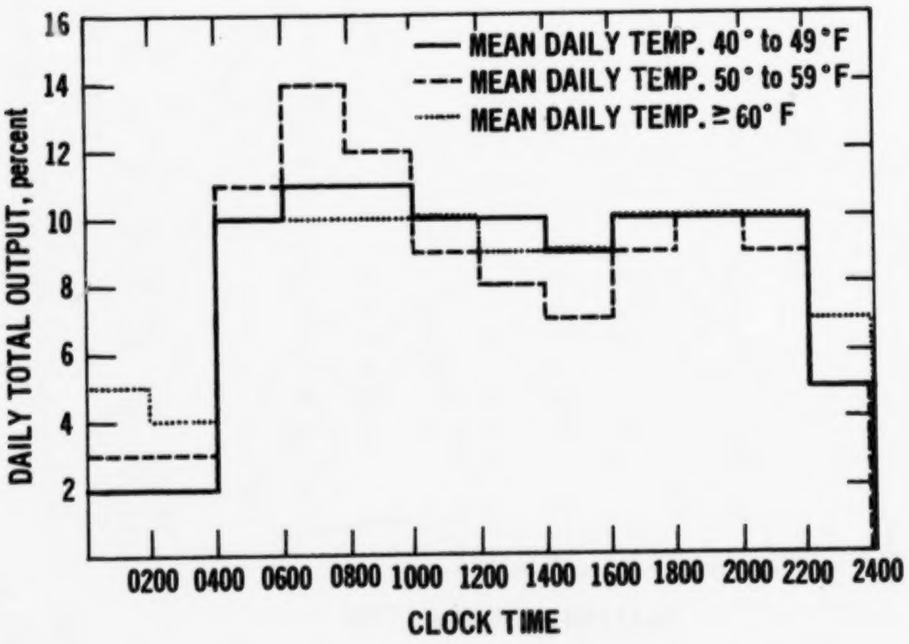

Figure 10-4. Diurnal variation of SO_2 output during days with mean temperature 40° to 49° F, and ≥ 60° F.

are given by a three-dimensional Gaussian distribution. Empirical data supporting the use of such an hypothesis were found by Sutton,[6] Frenkiel,[7] Ogura,[8] and others. Application of the theory to the atmosphere was studied by many investigators, e.g., Batchelor;[9, 10] Hay and Pasquill;[11] Cramer, Record, and Vaughn;[12] Barad and Haugen;[13] and Lin and Reid.[14]

Models of urban atmospheric diffusion using statistical diffusion theory have been formulated for several specific urban areas—in one case a whole state, Connecticut—under various simplifying assumptions concerning area-source representations, and temporal and spatial uniformity of meteorological conditions. The pertinent features of these models including the regions represented and the assumptions made were recently reviewed by Moses[15] and will not be further discussed here.

In addition to the diffusion mechanism, the transportation of pollutant is affected by large-scale flow, which is taken here as mean wind. It is assumed that, as the material is released from a point source, it is dispersed and the whole cloud is simultaneously transported along a trajectory given by the mean wind field.

With the above assumptions the equation for the concentration distribution in three dimensions in a moving medium from an instantaneous point source with non-isotropic diffusion is represented by:

$$C(x,y,z,t) = \frac{Q(t)}{(2\pi)^{3/2}\sigma_x(t)\,\sigma_y(t)\,\sigma_z(t)} \cdot \exp\left\{-\frac{1}{2}\left[\left(\frac{x-ut-x'}{\sigma_x(t)}\right)^2+\left(\frac{y-vt-y'}{\sigma_y(t)}\right)^2 + \left(\frac{z-xt-z'}{\sigma_z(t)}\right)^2\right]\right\} \tag{2}$$

where:

C = concentration (g cm^{-3})
Q = source strength (g sec^{-1})
t = time (sec)
u, v, w = velocities in x, y, z directions, respectively (cm sec^{-1})
$\sigma_x, \sigma_y, \sigma_z$ = standard deviation of diffusion cloud in three dimensions, respectively (cm)
x', y', z' = position of release

The development of Equation (2) into a diffusion model applicable to continuous point and area sources is divided below into three parts: standard deviation of cloud, point sources, and area sources.

Standard Deviation of Diffusing Cloud

Numerous schemes have been proposed for determining formulas and for determining the σ's in Equation (2). Most of these are based on G.I. Taylor's[16] original work. Among the investigators are Sutton,[6] Holland,[17] Kellogg,[18] Frenkiel and Katz,[19] Gifford,[20] Gifford and Pack,[21] Inoue,[22] and Hogstrom.[23]

Pasquill,[24, 25] using experimental data, formulated a set of rules for determining σ_y and σ_z for different atmospheric conditions. These have been widely used in estimating concentrations in diffusing plumes.

It is generally considered that the diffusion coefficients (i.e., the σ's) relating to a non-isotropic, non-homogeneous atmosphere depend upon atmospheric thermal stability, dynamic wind field, aerodynamic effects of roughness elements in the boundary, and the time of exposure of the plume to these conditions.

In the present model development a modification of the approach presented by Singer and Smith[26] was adopted. This method was judged to be well suited for a computational method using Equation (2) as the basis for an algorithm. The standard deviations of the diffusion cloud are given by:

$$\sigma_x = \sigma_{0x} + a\bar{u}\,(t - t')^p \tag{3a}$$

$$\sigma_y = \sigma_{0y} + a\bar{u}\,(t - t')^p \tag{3b}$$

$$\sigma_z = \sigma_{0z} + a\bar{u}\,(t - t')^p \tag{3c}$$

and

$$\sigma_{0x} = \sigma_{0y} \tag{4}$$

where $\bar{u}$ is the mean wind speed (cm sec^{-1}), a and p are dimensionless parameters depending on the intensity of turbulence and thermal stratification of the atmosphere, and $\sigma_{0x}, \sigma_{0y}, \sigma_{0z}$ (miles) depend on the characteristic geometry associated with an individual source of emission.

The values of a, σ_{0x}, σ_{0y}, and σ_{0z} were determined from parametric studies using observed data. Integration of Equation (2) was performed for continuous area sources for a number of combinations of values of these parameters and various wind speeds. (The method of integration will be discussed later.) When observed concentrations were compared with those computed from the integrations it was possible to delimit ranges for the values of the different parameters. Starting with the assumption that $p = 1$, it was found that values of $0.05 \leqslant a \leqslant 0.25$ gave satisfactory estimation of SO_2 concentrations for various atmospheric conditions. It was also similarly determined that $\sigma_{0x} = \sigma_{0y} = 0.001$ mile and $\sigma_{0z} = 0.01$ mile for continuous area sources in the metropolitan New York area. Figure 10-5 shows an example of computed SO_2 concentrations in the midtown Manhattan region for $a = 0.2$ at two different wind speeds. The points plotted are measured SO_2 concentrations.

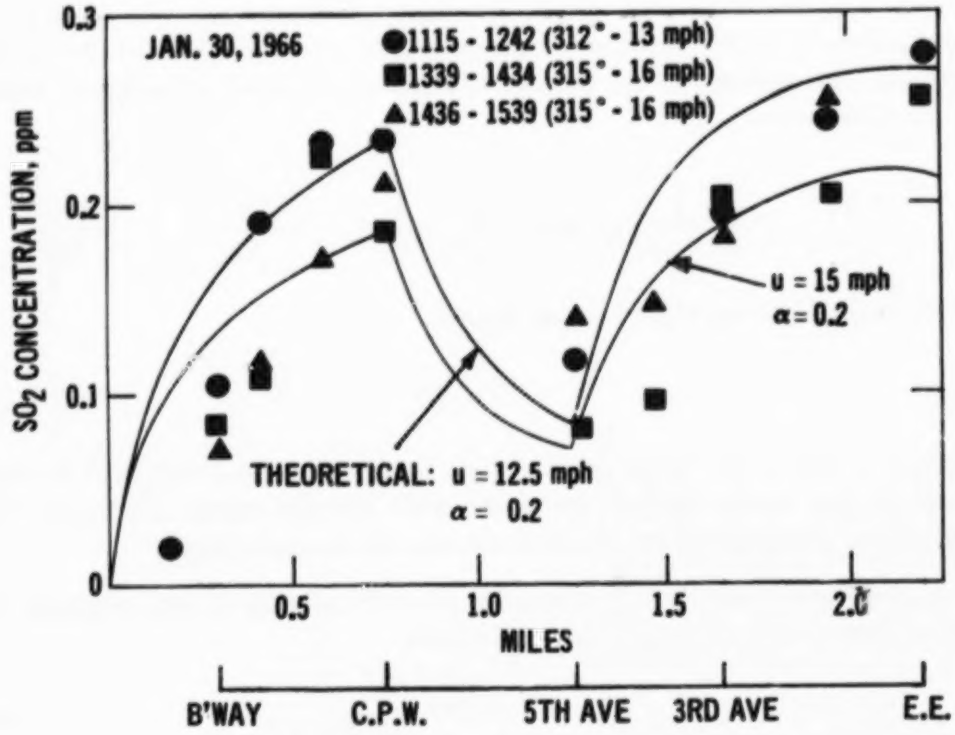

Figure 10-5. Computed SO_2 concentrations in 79th Street Manhattan with $\alpha = 0.2$ for two different wind speeds.

Since an inversion layer aloft is considered to be impenetrable by SO_2 injected below it, the value of σ_z is taken as constant when an inversion stratification is present. With the height of the base of the inversion layer as H (mi), the relationship, following Gifford,[27] is estimated as:

$$\sigma_z = \frac{H}{2}, \tag{5}$$

if σ_z as computed by Equation (3c) is greater than H/2.

Continuous Point Sources

Integration of Equation (2) over the time interval $[0,\infty]$ has been shown by Frenkiel[28] to give the following expression for the mean concentration from a continuous point source at ground level:

$$\frac{\bar{C}\,(x, y, z)}{Q} = \frac{1}{2\pi\,\sigma_y\,\sigma_z\,\bar{u}}\,\exp - \left[\frac{y^2}{2\sigma_y{}^2} + \frac{z^2}{2\sigma_z{}^2}\right] \tag{6}$$

where $\bar{u}$ is the mean wind speed. The equation applies for uniform flow in the x-direction. For emission from a source at height $\mathcal{H}$ (mi) above the ground and considering the ground as a perfect reflector of pollutant Equation (6) becomes

$$\frac{\bar{C}\,(x, y, z)}{Q} = \frac{1}{2\pi\,\sigma_y\,\sigma_z\,\bar{u}}\,\exp\,-\left(\frac{1}{2\sigma_y{}^2}\right)\exp\,-\left[\frac{(z-\mathcal{H})^2}{2\sigma_z{}^2} + \frac{(z+\mathcal{H})^2}{2\sigma_z{}^2}\right] \tag{7}$$

The height $\mathcal{H}$ is the effective stack height

$$\mathcal{H} = h + \Delta h \tag{8}$$

where h (mi) is the height of the stack from which the pollutant is emitted and Δh (mi) is the distance above the stack through which the plume rises by virtue of the buoyancy and exit velocity of the stack gases.

The expression used in this study for all point sources is that proposed by Brummage[29] for all atmospheric stabilities:

$$\Delta h = 0.047\,\frac{Q_h{}^{0.58}}{\bar{u}^{0.70}} \tag{9}$$

where Q_h is the emission rate of heat in cal $\sec^{-1}$. Simon[30] found this formula satisfactory to give plume heights for the Consolidated Edison Company stacks in New York City.

Continuous Area Sources

There is no known formula applicable to the emission from a continuous area source that is obtained by direct integration of Equation (2) over time and over fixed distances in both the x- and y-directions. A numerical method of integrating Equation (2) was developed for the present model. Examination of the results of the integration also led to a scheme that accurately but simply represents the emissions from a continuous area source.

With the ground as a perfect reflector of pollutant concentrations and a rectangular area source having sides 2a and 2b in the x- and y-directions centered at (x_0, y_0, z_0), the integral form of Equation (2) is:

$$C(x,x_0,\ y-y_0,\ z-z_0,t,t_0) = \int_{t=t_0}^{t} \frac{Q(t')}{(2\pi)^{3/2}\ \sigma_z(t-t')}$$

$$\cdot \left\{ \exp\left[-\tfrac{1}{2}\left(\frac{z-w\cdot(t-t')-z_0}{\sigma_z(t-t')}\right)^2\right]\right.$$

$$\left. + \exp\left[-\tfrac{1}{2}\left(\frac{z+w\cdot(t-t')+z_0}{\sigma_z(t-t')}\right)^2\right]\right\} \int_{x'=-a}^{a} \int_{y'=-b}^{b} \frac{1}{\sigma_x(t-t')\cdot\sigma_y(t-t')}$$

$$\cdot \exp\left\{-\tfrac{1}{2}\left[\frac{x-x_0-u\cdot(t-t')-x'}{\sigma_x(t-t')}\right]\right.$$

$$\left. -\tfrac{1}{2}\left[\frac{y-y_0-v\cdot(t-t')-y)}{\sigma_y(t-t')}\right]\right\} dx'\,dy'\,dt' \qquad (10)$$

where:

C = concentration ($g\ cm^{-3}$)

$Q(t')$ = source strength ($g\ cm^{-2}\ sec^{-1}$)

t = time (sec)

$(t-t')$ = time since emission (sec)

(x',y') = point of release measured from (x_0,y_0).

A schematic diagram representing the space referring to any point (x',y') and $(t-t')$ is given in Figure 10-6.

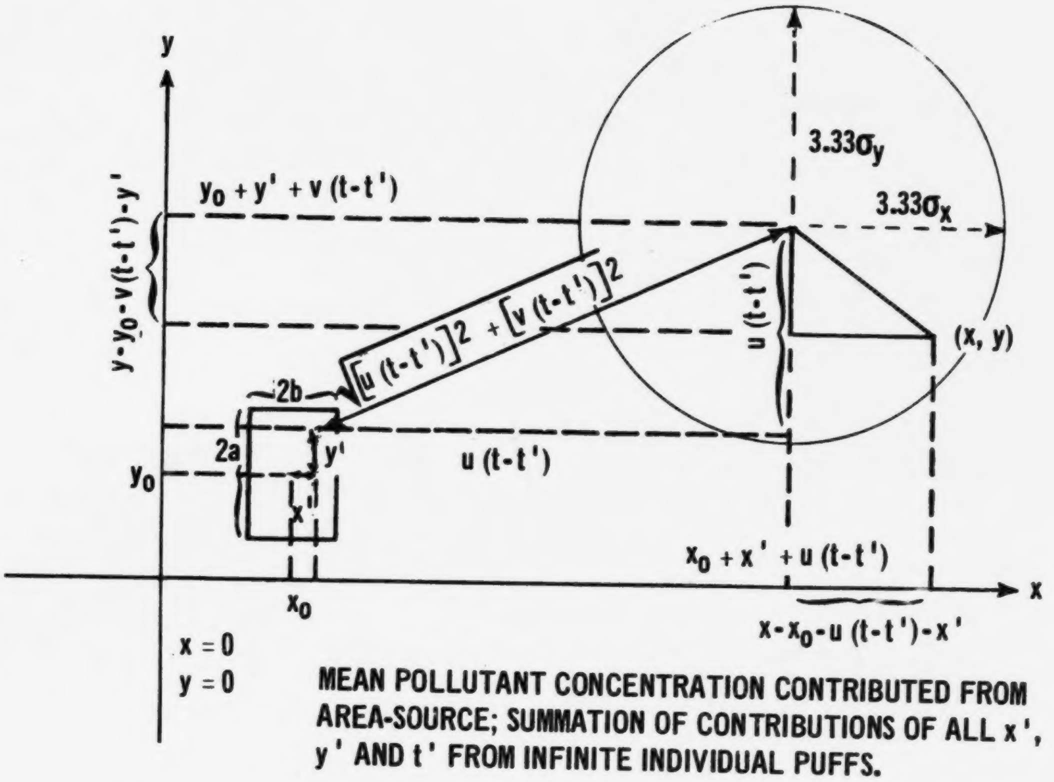
y
x
y₀ + y' + v (t-t')
y-y₀-v(t-t')-y'
3.33σy
3.33σx
(x, y)
√[u (t-t')]² + [v (t-t')]²
u (t-t')
2b
2a
y'
x'
y₀
u (t-t')
x₀ + x' + u (t-t')
x₀
x-x₀-u (t-t')-x'
x = 0
y = 0
MEAN POLLUTANT CONCENTRATION CONTRIBUTED FROM AREA-SOURCE; SUMMATION OF CONTRIBUTIONS OF ALL x', y' AND t' FROM INFINITE INDIVIDUAL PUFFS.

Figure 10-6. Schematic diagram showing how plume is computed from area source.

In order to simplify the integration of Equation (10), the following conditions were set:

(1) $a = b$;

(2) $t_0 = 0$, $t = 2$ hours;

(3) $v = w = 0$;

(4) u is constant over $(0, t)$;

(5) atmospheric stability and turbulent intensity are constant over $(0, t)$

(6) $Q(t') = Q$, a constant;

(7) $x_0 = y_0 = 0$.

In other words, the integration of Equation (10) is over a 2-hour interval during which emission rates and atmospheric conditions are steady, and over an area centered at the origin and oriented with one side parallel to the wind. These conditions along with the transformations:

$$X = \frac{x - u(t-t') - x'}{\sigma_x(t-t')} \tag{11}$$

and

$$Y = \frac{y-y'}{\sigma_y(t-t')} \tag{12}$$

reduce equation (10) to:

$$\frac{C}{Q} = \int_0^{2\ \mathrm{hr}} \frac{1}{(2\pi)^{1/2}\ \sigma_z(t-t')} \left\{ \exp\left[-\tfrac{1}{2}\left(\frac{z-z_0}{\sigma_t(t-t')}\right)^2\right] + \exp\left[-\tfrac{1}{2}\left(\frac{z+z_0}{\sigma_z(t-t')}\right)^2\right]\right\}$$

$$\left\{ \frac{1}{\sqrt{2\pi}} \int_{\frac{x-u\,\cdot\,(t-t')-a}{\sigma_x(t-t')}}^{\frac{x-u\,\cdot\,(t-t')+a}{\sigma_x(t-t')}} \exp\left[-\frac{X^2}{2}\right] dX \right\}$$

$$\left\{ \frac{1}{\sqrt{2\pi}} \int_{\frac{y-a}{\sigma_y(t-t')}}^{\frac{y+a}{\sigma_y(t-t')}} \exp\left[-\frac{Y^2}{2}\right] dY \right\} \quad dt' \tag{13}$$

In order to prevent accumulation of large errors in the double integration, a polynominal representation of the Gaussian probability function was applied for the integration over X and Y. To perform the integration over t', a refined two-part interval was used in a complicated application of Simpson's Rule. This prevented further undue accumulation of errors.

The integration in Equation (13) was carried out according to the procedure above for values of u, a, and a, within their possible limits; for various values of x, y, and z; for p= 1; and for z_0 = 100 ft., the assumed roof-top level characterizing metropolitan New York residential and small office buildings. At this point in the development it can be stated:

$$\frac{C}{Q_{Area}} = f(x, y, z, z_0, a, p, u, a, t, t_0). \qquad (14)$$

It is to be noted that (x, y) now represents the distance from the center of the area source.

Adaptation of Continuous Area Source Solution

In order to apply the result of the integration in Equation (10), represented by Equation (14), to the model, it is necessary to adopt the assumptions equivalent to those stated above. The 2-hour interval (0, t) is equivalent to the emission interval, Δt, over which contributions from the various sources are summed in the model. Emissions and meteorological conditions over the entire urban region are assumed to remain steady over the interval, Δt.

The are no actual data to support a non-zero value for w, and the theoretical knowledge of mesoscale phenomena, which would permit its calculation from other meteorological variables, is limited. It therefore seems reasonable to assume w = 0 everywhere in the region.

The assumption of v = 0 is equivalent to stating that the square area source elements have one side parallel to the mean wind. On the basis of computations on a simple grid, errors resulting from this assumption are judged to be small. With the above assumptions, Equation (14) can be used as the basis for modeling multiple area sources in urban localities. The quantity C/Q_{Area} is a tabulated function and could not be conveniently used in a numerical model in which a large number of area sources are considered. A set of conditions (some of which are approximations) that gave simple representations of the area source solutions and required reasonable computation time and memory storage capacity was found. The representations also preserved the features of the exact integration, with the conditions:

1. $\frac{\partial c}{\partial z} = 0;\ 0 \leqslant z \leqslant z_0$. This is commensurate with the notion that mechanical mixing dominates atmospheric turbulent diffusion in the vicinity of buildings and other bluff objects (see, for example, Halitsky.[31]) It was found empirically that σ_{0z} = 0.01 mile gave a reasonable approximation to the condition of uniform concentration between the ground and rooftop height, z_0.
2. In view of (1) the computed SO_2 concentrations at $z = z_0$ = 100 ft was used to represent those at ground level.

3. For $(t - t') > \Delta t$, and $p = 1$ the area source solution is approximated by a pseudo-Gassian distribution. The manner in which this is done will be discussed below.
4. $\dfrac{Cu}{Q_{Area}} \neq f(u)$. This condition will also be discussed below.

Using conditions (1) and (2) above, the solutions for area source emissions, Equation (14) becomes:

$$\frac{C}{Q_{Area}} = f(x, y, \alpha, p, u, a, t, t_0) \qquad (15)$$

Examination of the results of the integration in Equation (13) reveals that for $(t-t') \gg \Delta t$ the spatial concentration distribution approaches a shape that might be approximated by a Gaussian distribution, and the maximum concentration is far less than when $(t-t') \leqslant \Delta t$. An example of this is shown in Figure 10-7. It follows then, that the computation of the concentration field resulting from any area source can be divided into two formats. For $(t-t') \leqslant \Delta t$, i.e., during the interval in which the portion of the plume under study has been emitted from the source, one set of grid lines of the area sources is assumed to be parallel to the mean wind and the concentration field is computed directly from the tabulated value of C/Q_{Area} based on a chosen value of α, and $p = 1$ (Taylor's hypothesis). For $(t-t') > \Delta t$, i.e., for portions of the plume that were in the atmosphere at the beginning of interval, Δt, the field of concentration from an area source is represented in the following manner:

The distribution of concentrations is first assumed to be Gaussian. Then it is replaced by a simple uniform distribution within a rectangular parallelepiped with dimensions related to the σ's of the Gaussian distribution. This process is represented by the equality:

$$\int_{-\infty}^{\infty}\int_{-\infty}^{\infty}\int_{-\infty}^{\infty} \frac{Q}{(2\pi)^{3/2}\sigma_x\sigma_y\sigma_z}\, e^{-\frac{1}{2}\left[\left(\frac{x}{\sigma_x}\right)^2 + \left(\frac{y}{\sigma_y}\right)^2 + \left(\frac{z}{\sigma_z}\right)^2\right]}\, dx\,dy\,dz$$

$$= \frac{g(t)}{(4)^3\,\sigma_x\sigma_y\sigma_z} \qquad (15)$$

for $-2\sigma_x < x < 2\sigma_x,\ -2\sigma_y < y < 2\sigma_y,\ -2\sigma_z < z < 2\sigma_z$

where $g(t)$ is the total source output of a 2-hour period (g of SO_2). The dimensions of the parallelepiped are $4\sigma_x$, $4\sigma_y$, $4\sigma_z$. Accurate representations of the σ's in equation (16) were found to be the expressions;

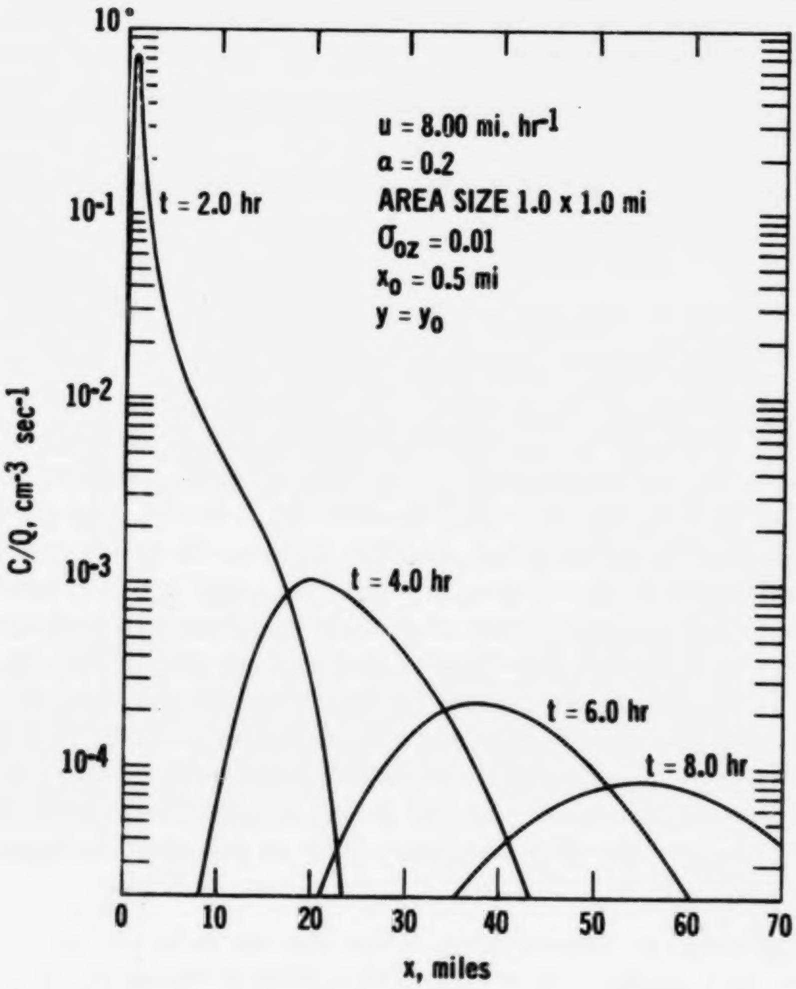

Figure 10-7. Time history of a plume from a continuous area-source.

$$
\begin{aligned}
\sigma_x &= \sigma_{0x} + \alpha\,\bar{u}\,(t - t') + \tfrac{1}{4}\,a + \tfrac{1}{4}\,\bar{u}\;(-t') \\
\sigma_y &= \sigma_{0y} + \alpha\,\bar{u}\,(t - t') + \tfrac{1}{4}\,a \\
\sigma_z &= \sigma_{0z} + \alpha\,\bar{u}\,(t - t') \\
\sigma_{z0} &= \sigma_{0y} \qquad (17)
\end{aligned}
$$

With the above conditions (3) the dependency of the tabular function C/Q_{Area} on p and the time, t and t_0, are removed and:

$$C/Q_{Area} = f(x, y, \alpha, u, a). \qquad (18)$$

Figure 10-8 illustrates the nature of this function for different values of the parameters.

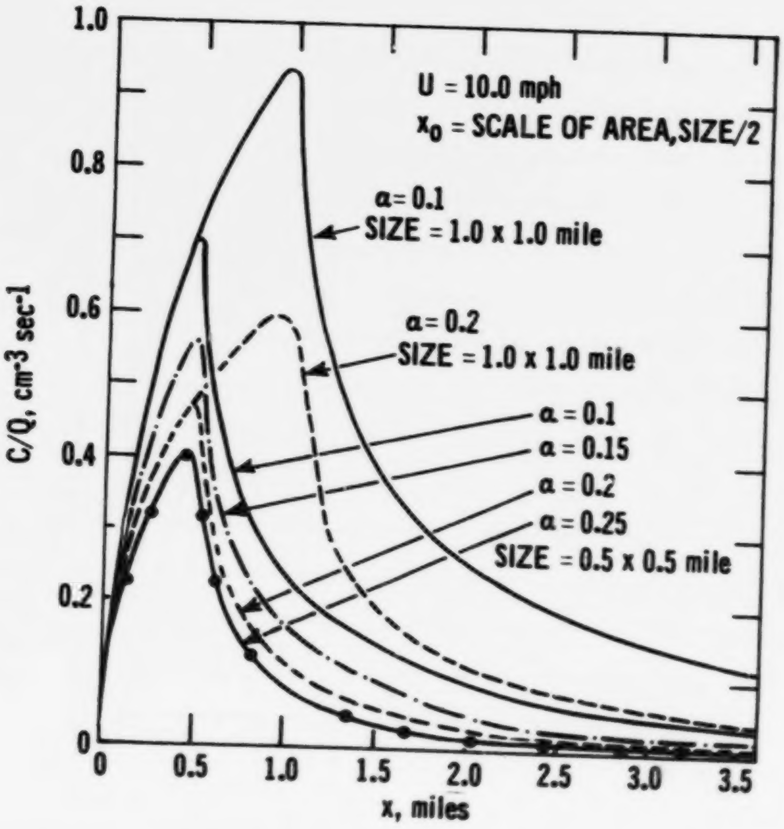

Figure 10-8. Downwind distribution of pollutant from area-sources ,parameterized by values of α.

Finally, by studying the integrated solution of Equation (13), it was found that:

$$\frac{C_u}{Q_{Area}} = f(x, y, \alpha; a). \qquad (18)$$

This is condition (4) above and is illustrated in Figure 10-9. This was a significant finding for it enables the model to handle a number of different source grid dimensions, a, while including the effect of various wind speeds.

Using all of the conditions discussed above, Equation (10) can be summed over all time intervals of duration Δt to obtain the contributions to the concentration of all "puffs" (each emitted during a different interval) at the point $(x-x_0, y-y_0)$ from an area source located at (x_0, y_0). The result is:

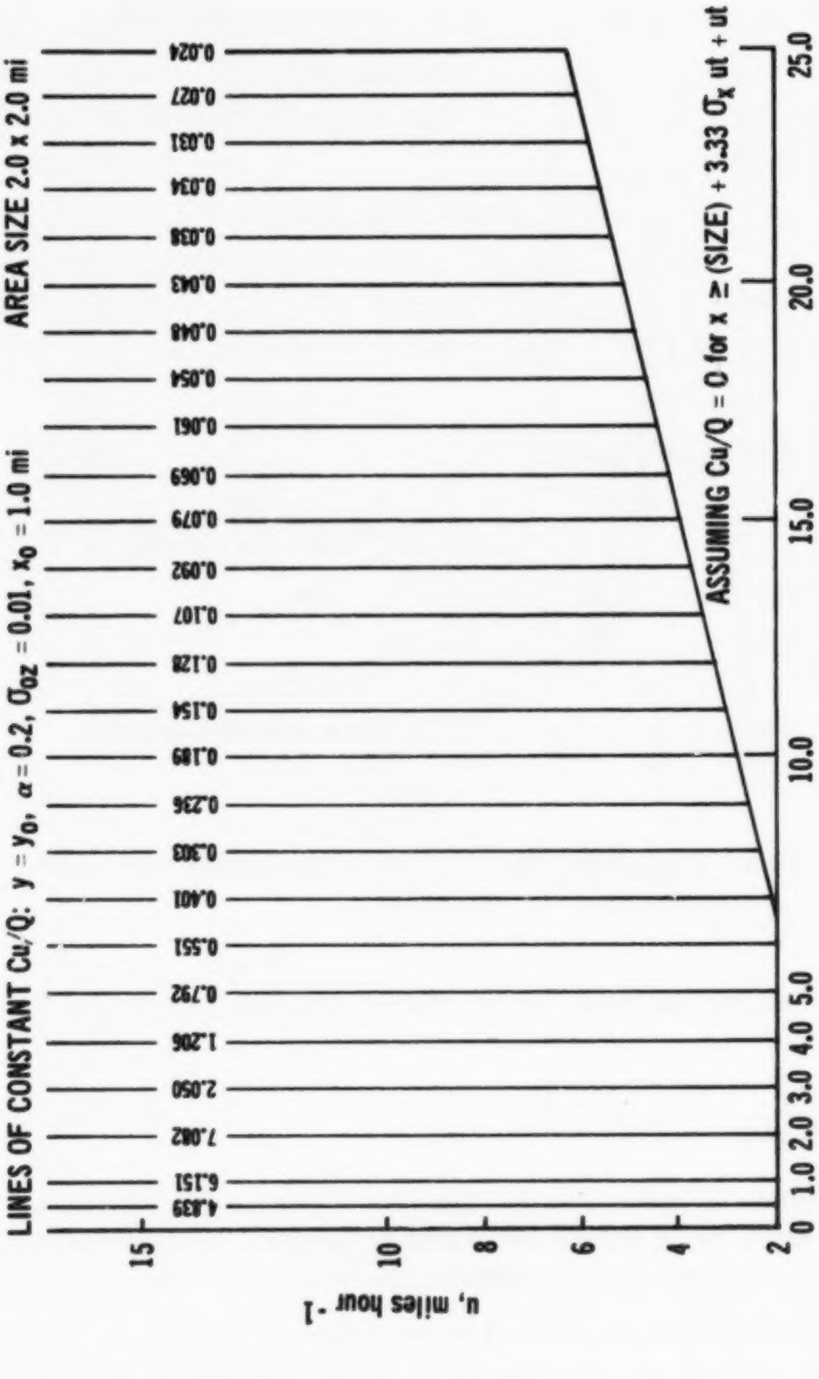

Figure 10-9. Illustrating that Cu/Q is independent of wind speed.

$$C(x-x_0, y-y_0, n\Delta t) = \sum_{t=n\Delta t}^{n\Delta t} \int_{t-n\Delta t}^{t-n\Delta t+\Delta t} \frac{2Q\left[\frac{2(N-n+1)-1}{2}\Delta t\right]}{(2\pi)^{3/2}\,\sigma_z(n\Delta t-t')}$$

$$\cdot \left\{\exp\left[-\tfrac{1}{2}\left(\frac{z_0}{\sigma_z\,(n\Delta t-t')}\right)^2\right]\right\} \cdot \int_{x'=-a}^{a} \int_{y'=-a}^{a} \frac{1}{\sigma_x(n\Delta t-t')\;\sigma_y(n\Delta t-t')}$$

$$\cdot\ \exp\left[-\tfrac{1}{2}\left\{\left(\frac{x-x_0-u(n\Delta t-t')-x'}{\sigma_x\,(n\Delta t-t')}\right)^2+\left(\frac{y-y_0-y'}{\sigma_y\,(n\Delta t-t')}\right)^2\right\}\right]\cdot dx'\,dy'\,dt' \qquad (20)$$

In this equation, N is the number of time intervals from the beginning of all emission to the present. When n = 1, the exact solution to Equation (10) is used, while for all of the remaining terms the center of gravity of the puff is advected according to the wind, and the pseudo-Gaussian distribution of Equations (16) and (17) are applied to compute the spatial distribution of concentrations. Finally, to complete the model construction, Equation (20) is summed over all x_0 and y_0 to obtain the concentrations contributed to a point (x,y) by all continuous area sources. This summed equation plus an equivalent one for point sources plus the tabular function Equation (19) represent the algorithm for the multiple-source model of dispersion and transport.

MODEL CONFIGURATION

To complete the model, a value of a, remained to be fixed, a grid representing area source emissions to be constructed and the computation grid to be specified. Based upon the parametric studies mentioned in earlier values of a in the range 0.1 to 0.25 were chosen, depending upon the thermal stratification.

Condition (4), in the preceeding section permitted simultaneous use of several different values of a, the dimension of the area-source grid. Figure 10-10 shows the area-source grid. The values of the dimension a used were 0.5, 1.0, 2.0, and 5.0 miles. The grid size at any particular location depends upon the source strengths and their spatial distributions, and on topographical and geographical factors. Generally the smallest grid size occurs in the central portion of the region where the annual emissions per unit area are the highest (Figure 10-2).

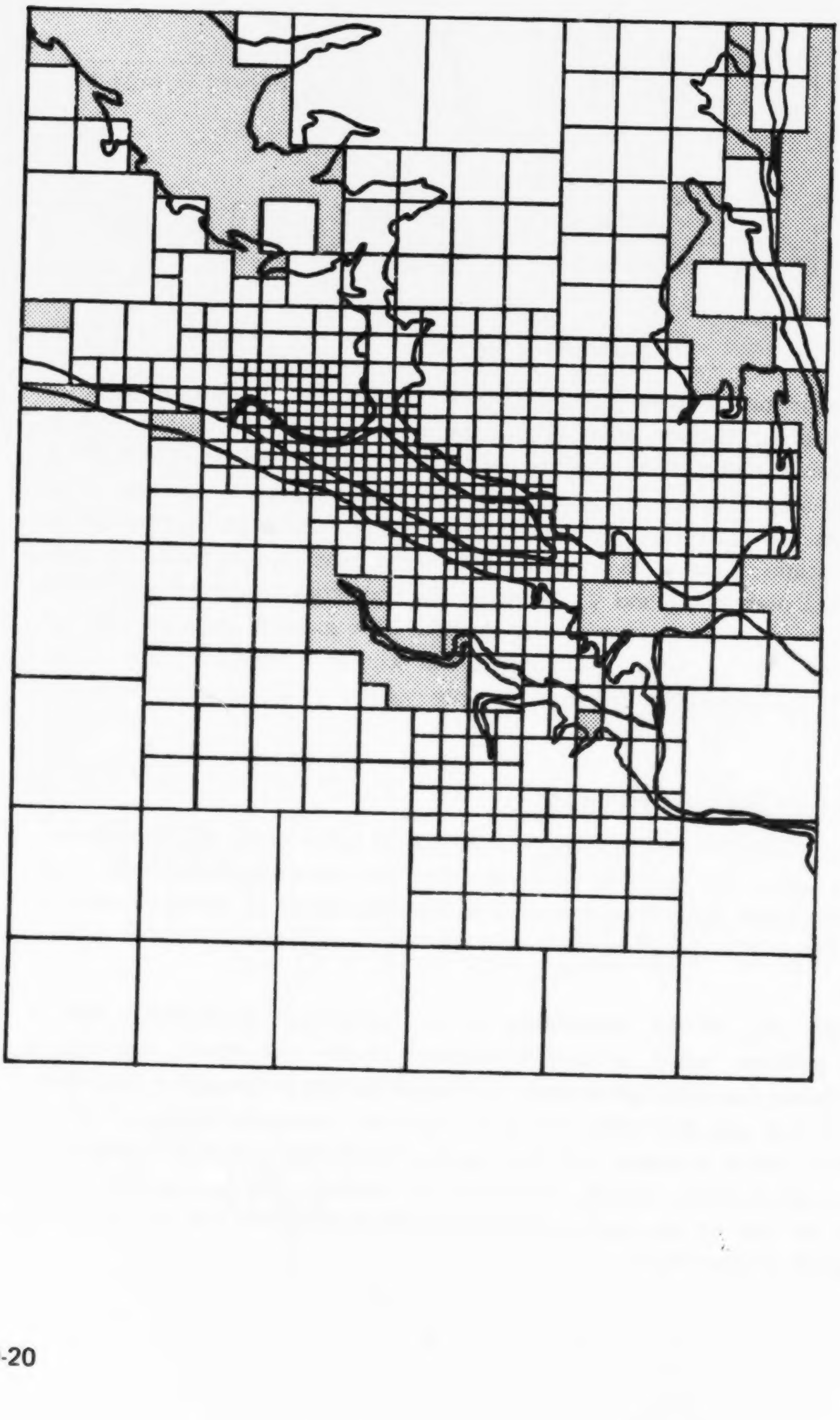

Figure 10-10. Area-source grid. Shaded areas represent zero emissions. Grid size depends on source strengths and spatial distribution, geographical and topographical factors.

Two computation grids (referring to x,y) with mesh sizes of 0.2 by 0.2 mile and 1.0 by 1.0 mile were used. The time interval, Δt, was 2 hours.

COMPUTATIONS AND VALIDATION

The computer methodology used in the computations representing the model is described elsewhere.[8]

The model was used to compute surface concentration patterns of SO_2 for the two test periods March 8-9, 1966, and November 15-16, 1966.

The computations were carried out by a CDC 6600 computer. The portion of the program dealing with winds and trajectories required 3 minutes of computer time for 24 time steps (48 hours) for source grid system consisting of 712 points (565 area sources and 148 point sources). The diffusion portion of the program computed the concentration field at more than 2000 points for each of the 24 time steps in a total computer time of 19 minutes.

Some exemplary results are shown in Figures 10-11 to 10-18, maps of concentration fields of SO_2 over Manhattan for various times during the test period, each using a 0.2 by 0.2 mile computational grid. Isolines with values less than 0.1 ppm are dashed. Zero time was at 00 hours on March 8 and November 15. Figure 10-19 is a map of a larger area computed for the same time as Figure 10-14, but using a 1.0 by 1.0 mile computation grid. It is clear that the coarser grid computation may miss several important small-scale features.

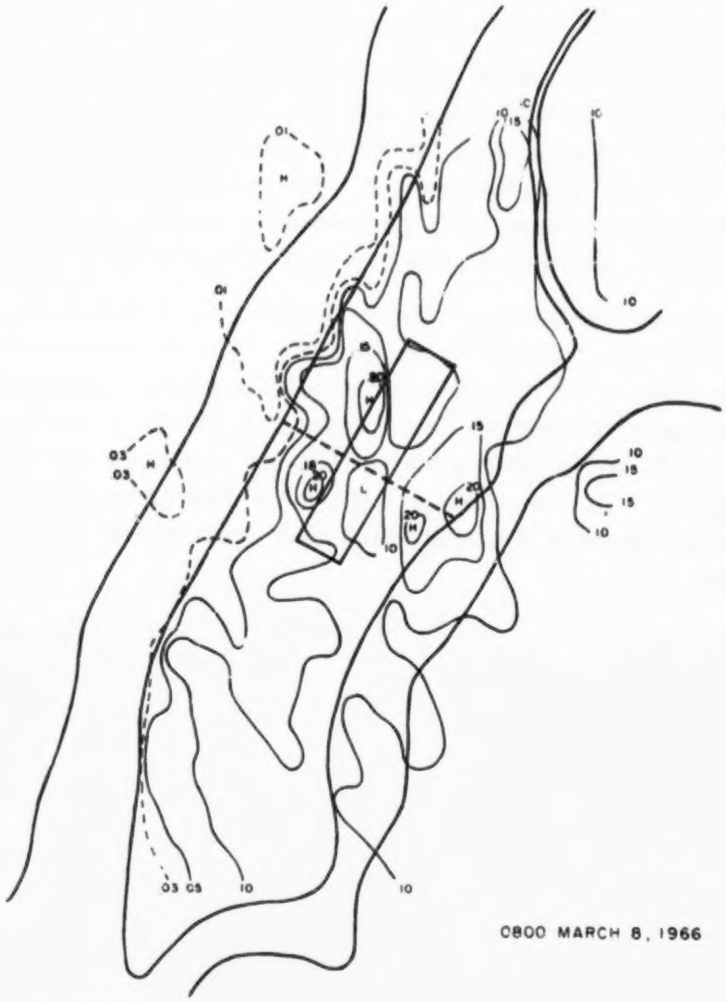
01
H
10
10
15
10
10
01
15
30
H
03
H
03
18
20
H
L
15
20
H
20
H
10
10
15
15
10
03
05
10
10

0800 MARCH 8, 1966

Figure 10-11. Predicted SO_2 concentration field (ppm), 0800 March 8, 1966, 0.2 x 0.2 mile computational grid.

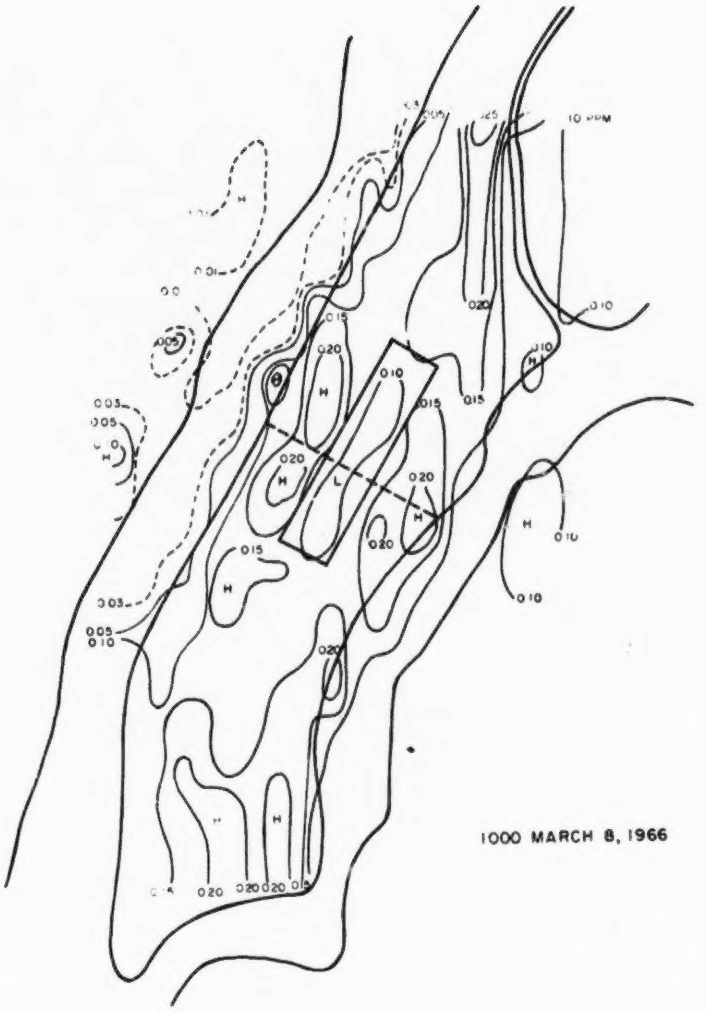
005
025
10 PPM
0 01
0 0
005
0 20
0 10
0 15
0 20
H
0 10
H
015
015
0 05
0 05
H
0 20
H
L
0 20
H
0 20
H
0 10
0 15
H
0 03
0 05
0 10
0 10
020
H
H
1000 MARCH 8, 1966
020
020 020
015

Figure 10-12. Predicted SO_2 concentration field (ppm), 1000 March 8, 1966, 0.2 x 0.2 mile computational grid.

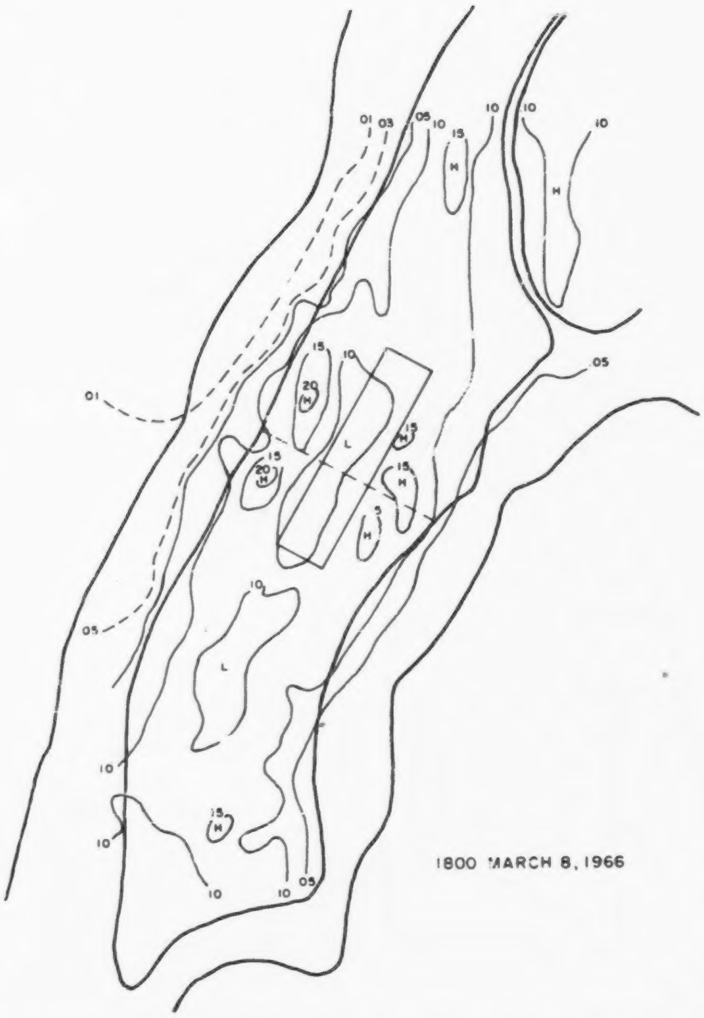
01
03
05
10
15
10
10
10
H
H
.05
01
15
10
20
H
L
15
H
15
20
H
15
H
5
H
10
05
L
10
15
H
10
10
10
05

1800 MARCH 8, 1966

Figure 10-13. Predicted SO_2 concentration field (ppm), 1800 March 8, 1966, 0.2 x 0.2 mile computational grid.

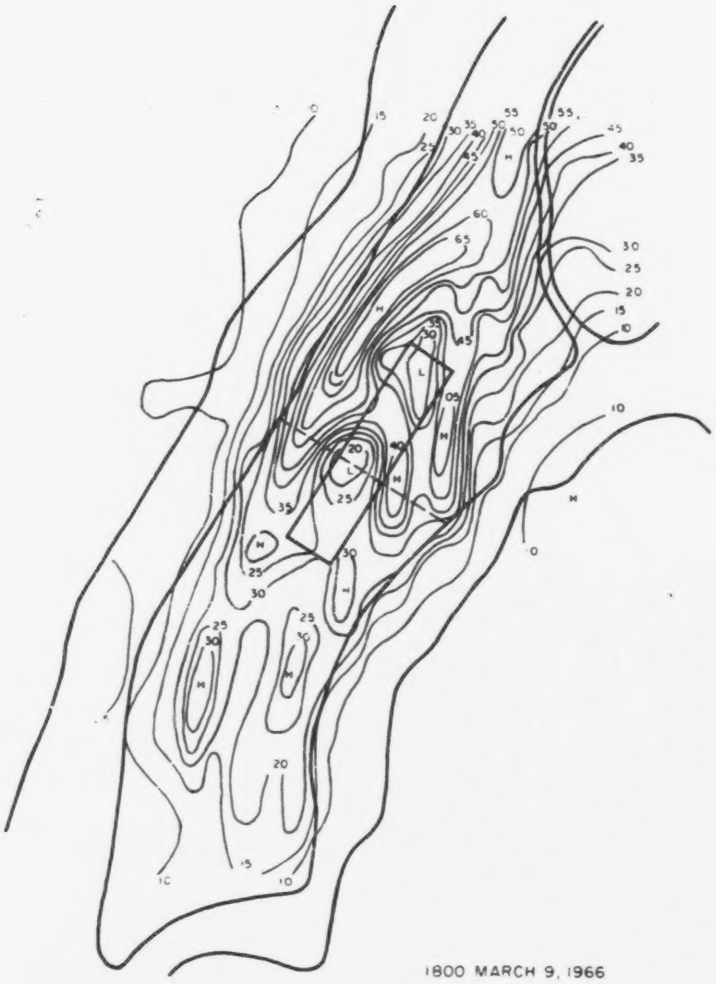

10
15
20
25
30
35
40
45
50
55
60
65
H
L
05
10
20
25
30
35
40
H
L
H
25
30
25
30
H
20
15
10
10

1800 MARCH 9, 1966

Figure 10-14. Predicted SO_2 concentration field (ppm), 1800 March 9, 1966, 0.2 x 0.2 mile computational grid.

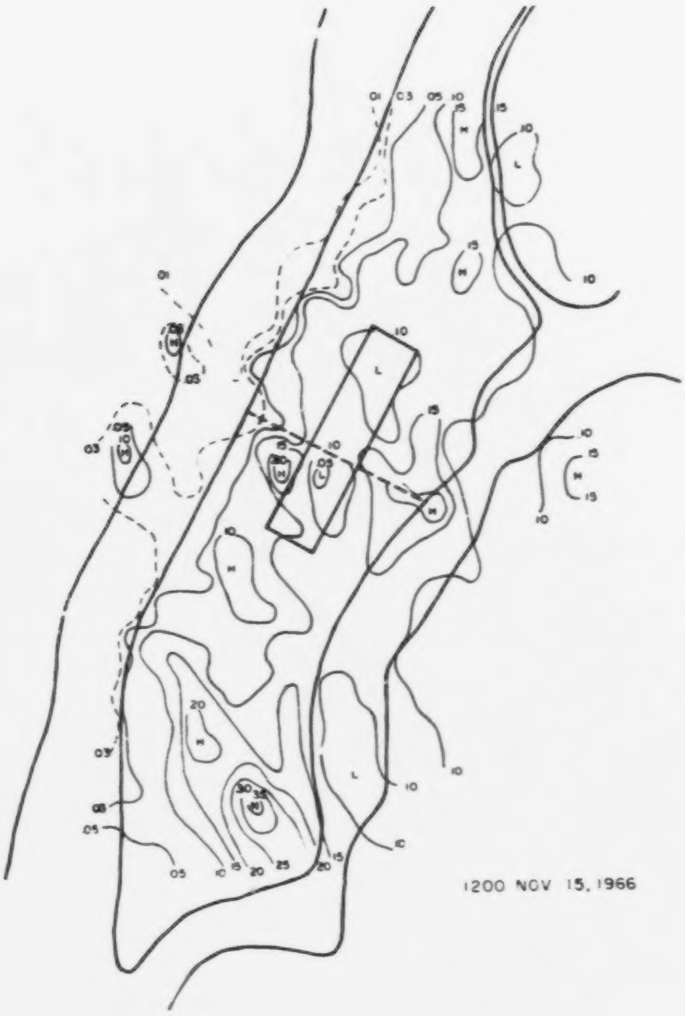
1200 NOV 15, 1966

Figure 10-15. Predicted SO_2 concentration field (ppm), 1200 November 15, 1966, 0.2 x 0.2 mile computational grid.

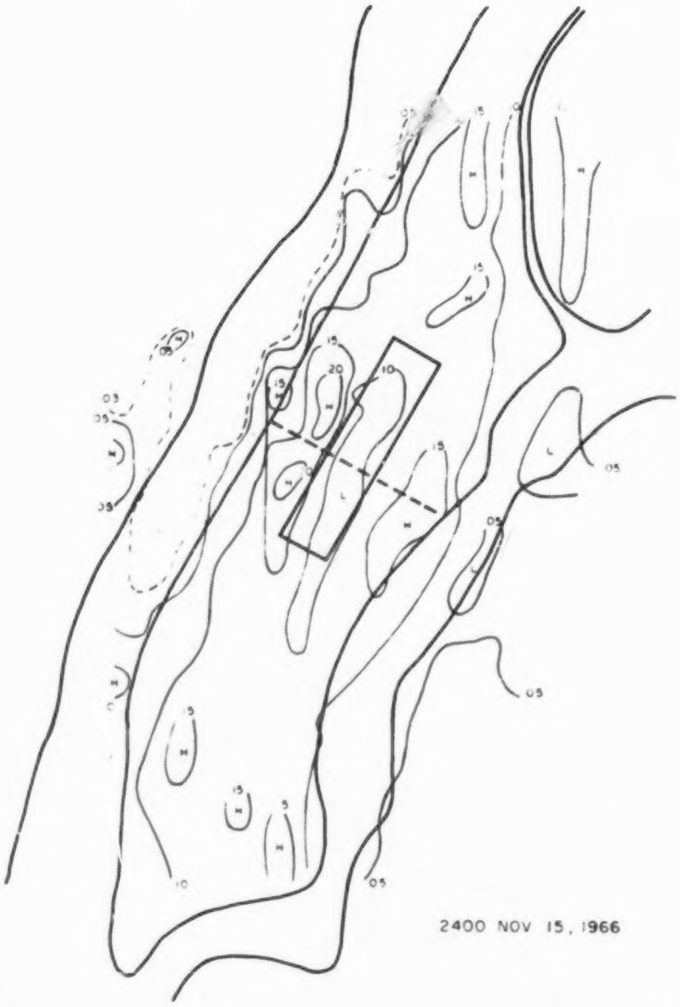
05
15
H
15
H
05
05
15
20
10
H
H
05
05
H
15
L
H
L
05
05
05
H
15
H
15
H
5
H
10
05

2400 NOV 15, 1966

Figure 10-16. Predicted SO_2 concentration field (ppm), 2400 November 15, 1966, 0.2 x 0.2 mile computational grid.

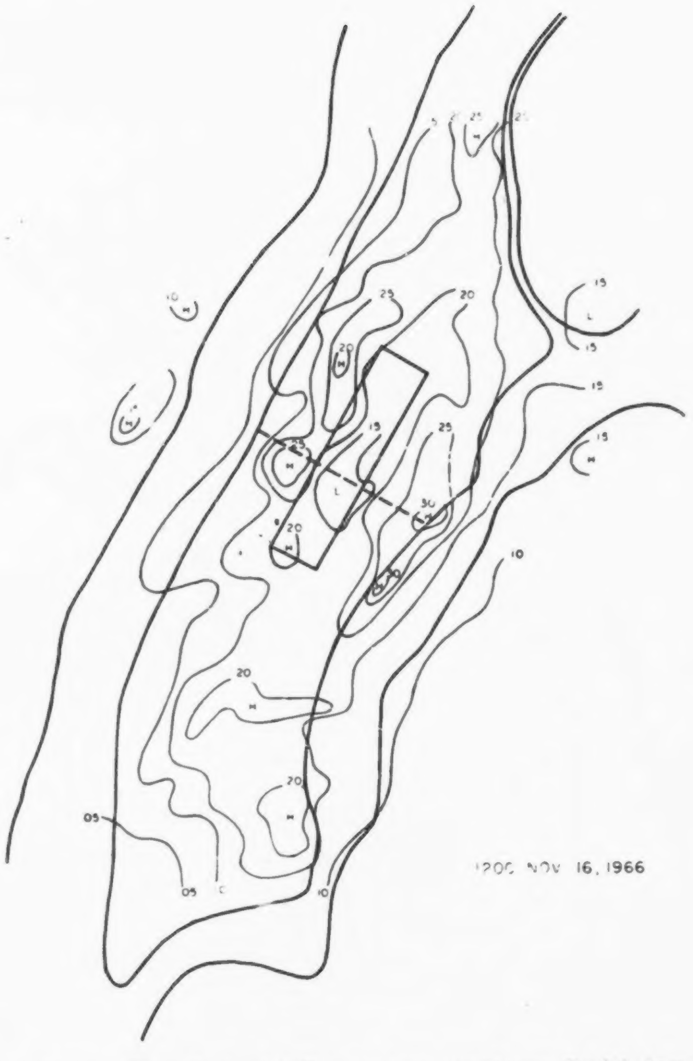
25
25
10
H
25
20
15
L
15
20
H
15
H
25
25
H
15
L
30
H
20
H
10
20
H
20
H
05
05
10
10
1200 NOV 16, 1966

Figure 10-17. Predicted SO_2 concentration field (ppm), 1200 November 16, 1966, 0.2 x 0.2 mile computational grid.

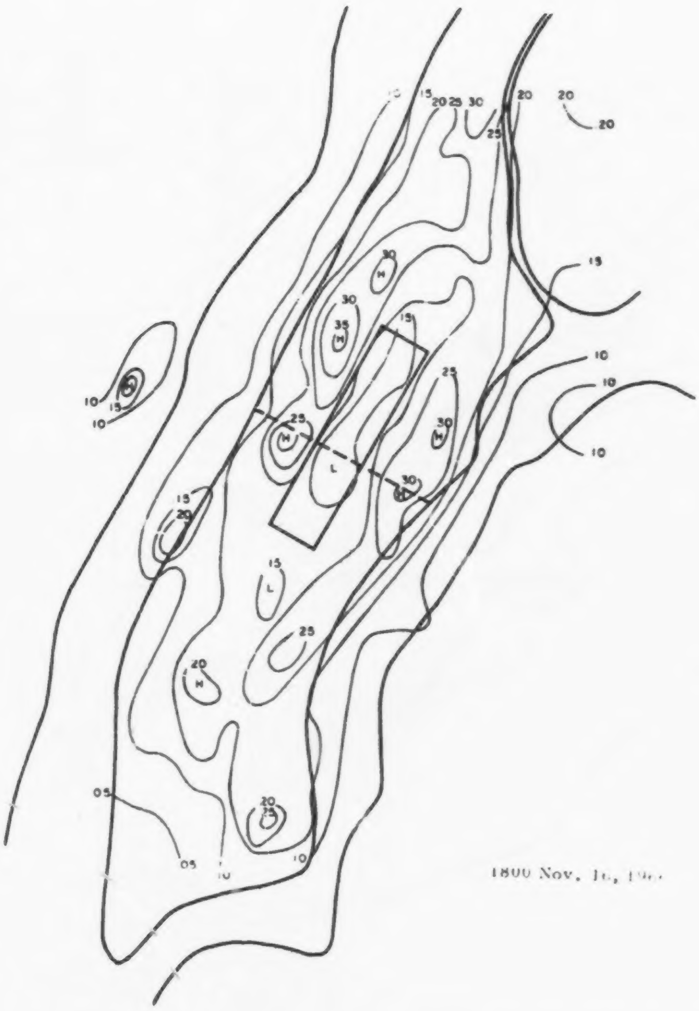
10
15
20
25
30
20
20
20
25
15
30
H
30
35
H
15
10
10
10
10
15
10
25
H
L
30
H
25
30
H
15
20
15
L
25
20
H
05
20
25
05
10
10
1800 Nov. 16, 1966

Figure 10-18. Predicted SO_2 concentration field (ppm), 1800 November 16, 1966, 0.2 x 0.2 mile computational grid.

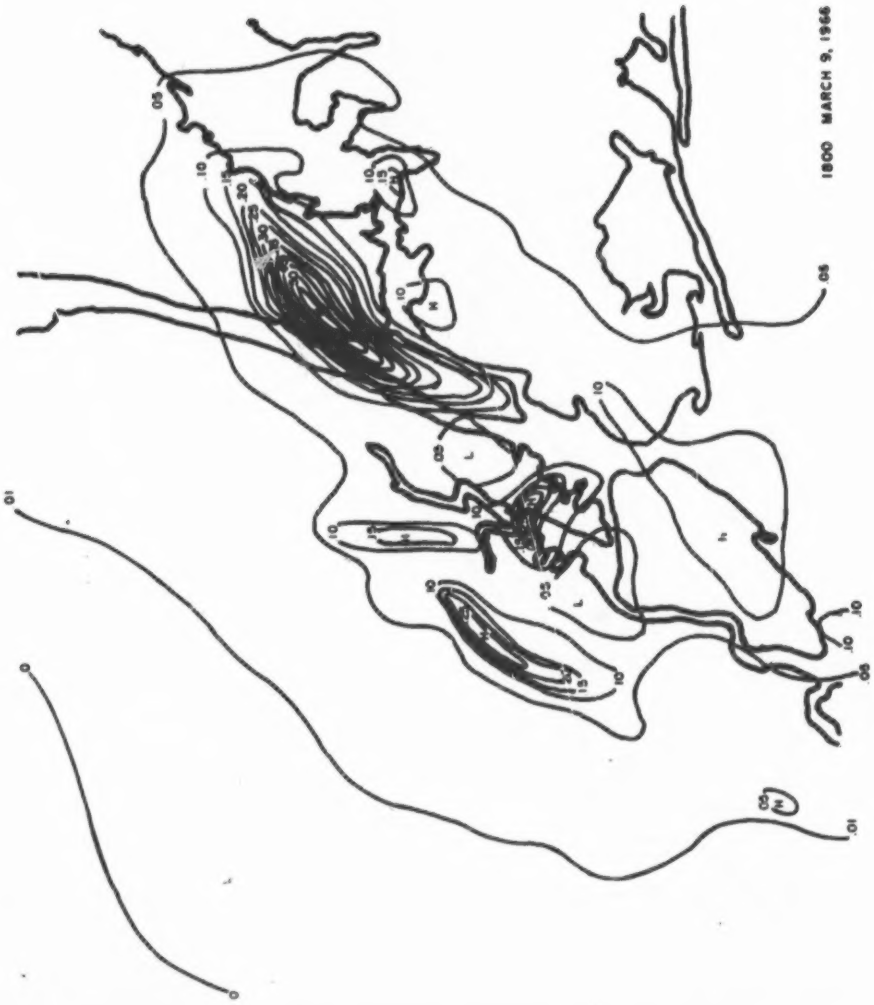
1800 MARCH 9, 1966
.01
0
.05
.10
.15
.20
H
L

Figure 10-19. Predicted SO_2 concentration field (ppm), 1800 March 9, 1966, 1.0 mile x 1.0 mile computational grid.

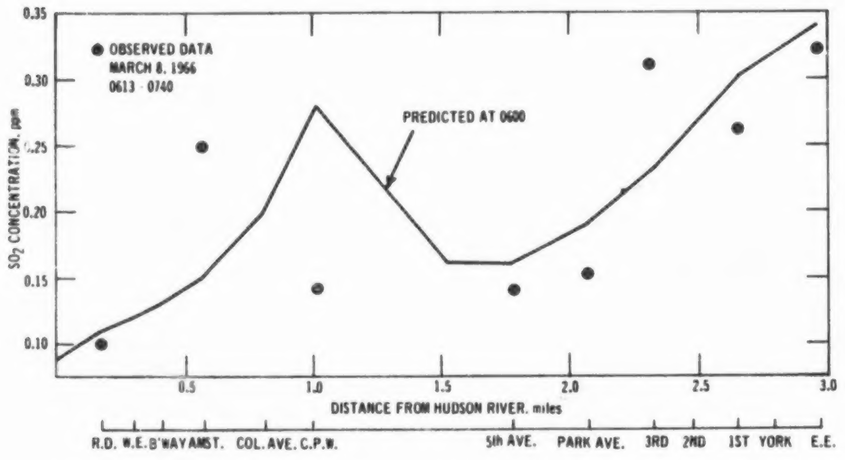

Figure 10-20. Observed and predicted variation of SO_2 concentration along the 79th Street crosstown transect at the indicated times.

A comparison of the computed results with observed concentrations is shown in Figures 10-20 to 10-23 that are cross town transects along 79th Street, of the concentration of SO_2 computed on a 0.2-mile grid. The lines represent the computed quantities while the observations are plotted as points.

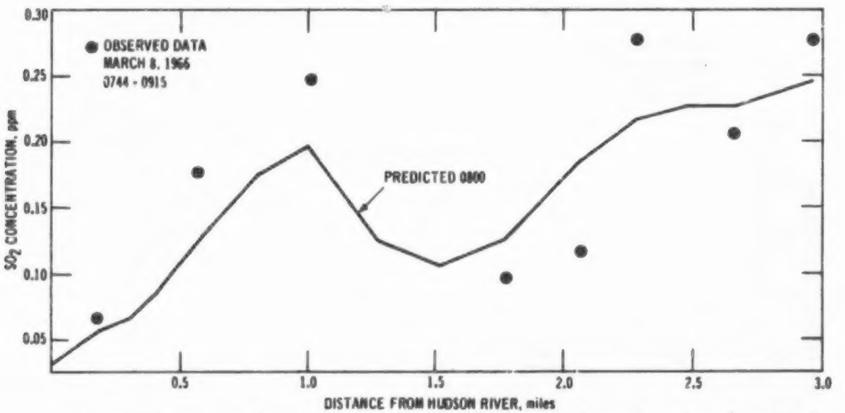

Figure 10-21. Observed and predicted variation of SO_2 concentration along the 79th Street crosstown transect at the indicated times.

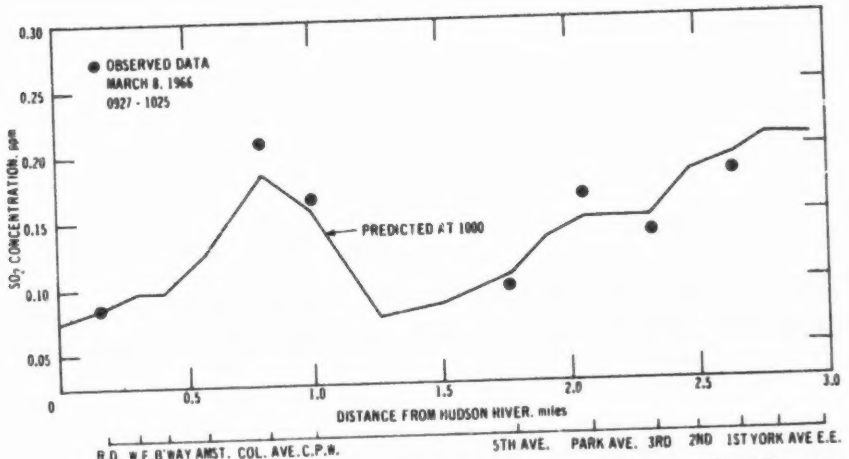

Figure 10-22. Observed and predicted variation of SO_2 concentration along the 79th Street crosstown transect at the indicated times.

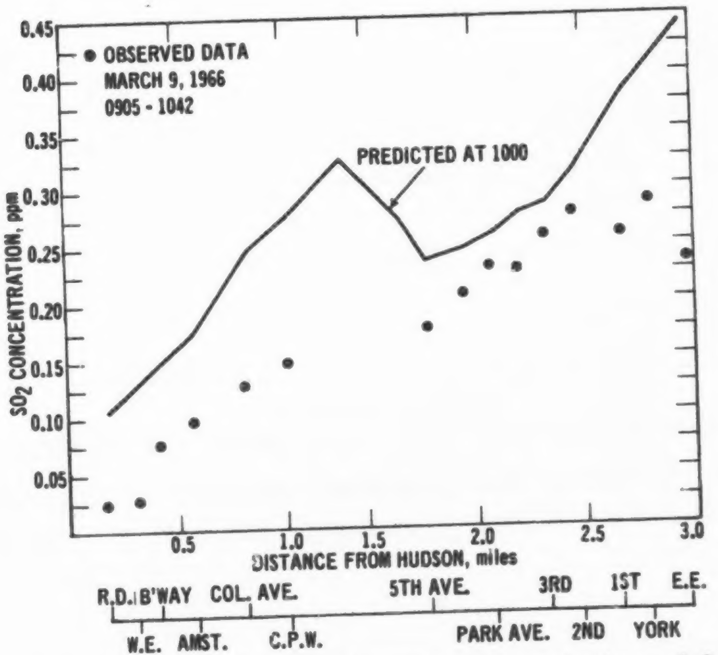

Figure 10-23. Observed and predicted variation of SO_2 concentration along the 79th Street crosstown transect at the indicated times.

While agreement is not perfect, the computed concentrations bear a discernible relationship to the observed concentrations. Figure 10-24 shows a transect for the same time as Figure 10-12, but it was computed using a 2.0 mile square area source grid over the entire region. It is evident that such a course representation of the area sources causes severe smoothing and distortion of the computed concentration field.

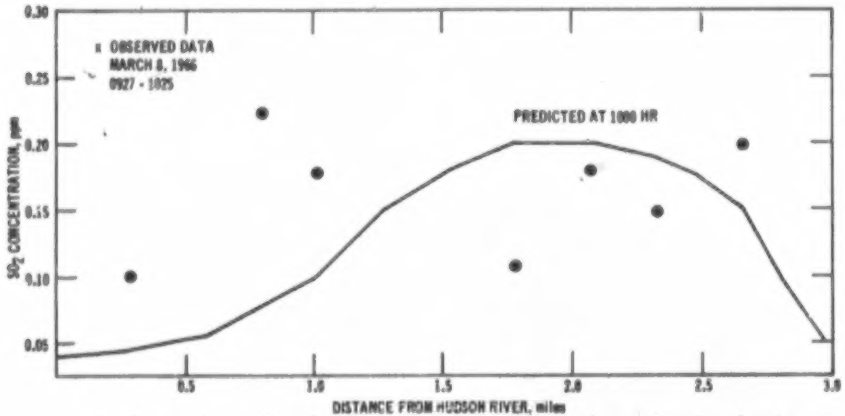

Figure 10-24. Observed and predicted variation of SO_2 concentration along 79th Street crosstown transect, same period as Figure 10-12, coarse grid 2.0 miles x 2.0 miles.

An objective estimate of the relationship between computed and observed concentrations for the two test periods is illustrated in Figure 10-25, a scatter diagram of observed versus computed values. The mean of the observed concentrations is 0.19 ppm, and the mean of the computed concentrations is 0.18 ppm. There are 121 data points in the diagram. The standard error of estimate is 0.09 ppm.

The situation depicted in Figures 10-14 and 10-19 for 1800 hours March 9 arose because of a complex wind field with a region of convergence over Manhattan Island. The wind field is shown in Figure 10-26. Because the SO_2 concentrations were computed using $w = 0$ everywhere, the values of concentrations shown are higher in the region of convergence than they would be if provision were made for non-zero values of w. The concentrations in the center of the convergence region are about twice as great as they should be.

A final point, illustrating the potential usefulness of the model, is seen in Figure 10-27, which shows the 1000-hour, March 8 SO_2 concentration field resulting from area source emissions only (compare with Figure 10-12).

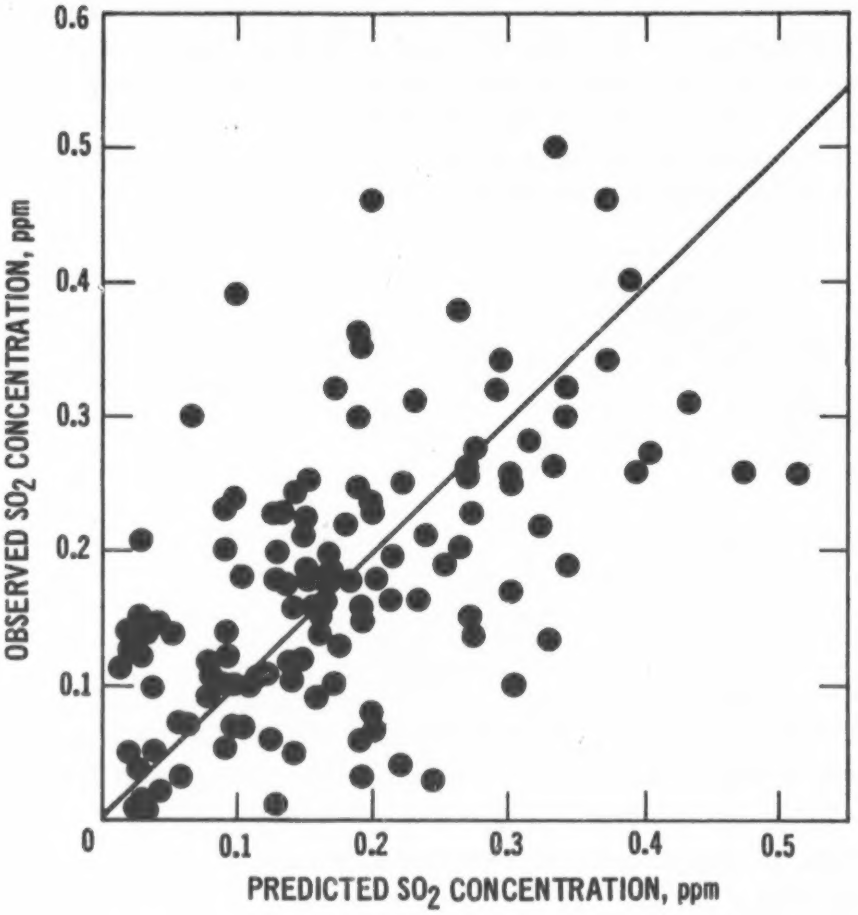

Figure 10-25. Plot of observed against predicted concentrations of SO_2. Mean observed and predicted concentrations, 0.19 and 0.18 ppm respectively. Standard error of estimate is 0.09 ppm.

DISCUSSION

A mathematical model for computing concentration in a multiple-source urban region has been developed. The model is three dimensional, accepts input data of meteorological conditions and source strengths that are functions of space and time, and computes pollutant concentration fields on a fine mesh grid (0.2 mile-square) over a 50-mile-square region at any given time. The framework of the model is general enough so that the vertical component of the wind could be included if it were known. To do this, however, the part of the algorithm giving the integrated expression for a continuous area source in tabular form (Equation 14) would have to be modified.

The adaptation of the model for the computations of SO_2 concentrations in the New York urban region involved assumptions of w = 0 and immediate uniform mixing of area source emissions between rooftop level and the ground. No removal factor was included. SO_2 reaching the ground was assumed to be reflected. These assumptions are, of course, possible causes of error in the computed concentration fields. Other sources of error are: coarseness of the meteorological observational network (Figure 10-1); poor data for source strength and inventory, particularly for manufacturing plant stacks; and unaccounted for topographical effects on dispersion.

Systems of the kind developed in this work are rarely amenable to *a posteriori* error analysis. The algorithm is based upon semi empirical theory, not derivable from known physical concepts. The sources of error as listed above are generally not readily controlled, and the assessment of their individual effects is difficult if not impossible.

The present status of the model is one of promising preliminary verification. Certainly a new effort in obtaining high-quality test data for periods up to 3 or 4 days in duration would be desirable. With such data further parametric studies could lead to improvement of the model.

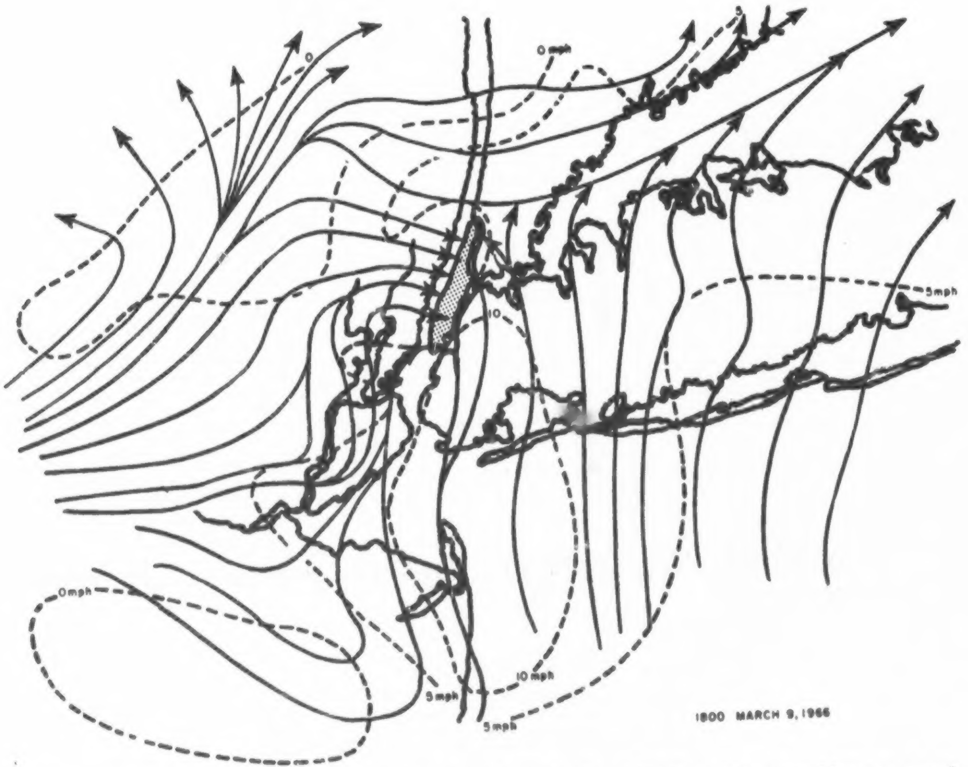

Figure 10-26. Wind field 1800 March 9, 1966. Streamlines and isotachs represented by solid and broken lines respectively. Convergence zone over Manhattan Island, shaded.

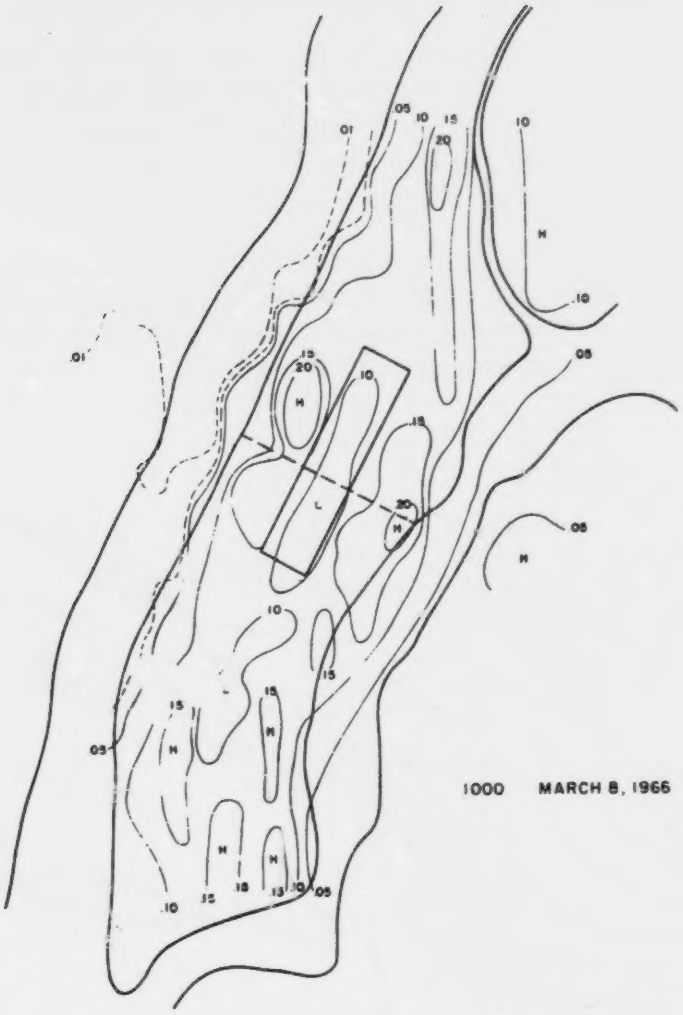
01
05
10
15
20
H
L
1000 MARCH 8, 1966

Figure 10-27. SO_2 concentration field, predicted from area sources only.

REFERENCES

1. Davidson, B. A Summary of the New York Urban Air Pollution Dynamics Research Program. J. Air Pollution Control Assoc. *17*:154-158, March 1967.
2. Davidson, B. et al. Mathematical Models of Urban Air Pollution Dynamics: Final Report. Vol. 2. New York University. 1969.
3. Scudder, B. Diagnosing the Mesoscale Wind Field over an Urban Area by Means of Synoptic Data. New York University. M. S. Thesis. 1965.
4. Druyan, L. M. A Comparison of Low-Level Trajectories in an Urban Atmosphere. J. Appl. Meteorol. *7*(4):583-590, August 1968.
5. Bornstein, R. Observations of the Urban Heat Island Effect in New York City. J. Appl. Meteorol. *7*(4):575-582, August 1968.
6. Sutton, O. G. Theory of Eddy Diffusion in the Atmosphere. Proc. Roy. Soc., Ser. A (London). *135*:143-165, February 1, 1932.
7. Frenkiel, F. N. Application of Statistical Theory of Turbulent Diffusion to Micrometeorology. J. Meteorol. *9*(4):252-259, August 1952.
8. Ogura, Y. Theoretical Distribution Functions of Matters Emitted from a Fixed Point. Meteorol. Soc. Japan J. *32*(Series II), January 1954.
9. Batchelor, G. K. Diffusion in a Field of Homogeneous Turbulence. I. Eulerian Analysis. Australian J. Sci. Research. *2*(4):437-450, December 1949.
10. Batchelor, G. K. Diffusion in a Field of Homogeneous Turbulence II. The Relative Motion of Particles. Proc. Cambridge Phil. Soc. (London). 48:345-362, April 1952.
11. Hay, J. S. and F. Pasquill. Diffusion from a Fixed Source at a Height of a Few Hundred Feet in the Atmosphere. J. Fluid Mech. *2*:299-310, May 1957.
12. Cramer, H. E., F. A. Record, and H. C. Vaughn. The Study of the Diffusion of Gases or Aerosols in the Lower Atmosphere. Massachusetts Institute of Technology. Cambridge. AFCRC-TR-58-239. 1958. 70 p.
13. Barad, M. L. and D. A. Haugen. A Preliminary Evaluation of Sutton's Hypothesis for Diffusion from a Continuous Point Source. J. Meteorol. *16*(1):12-20, February 1959.
14. Lin, C. C. and W. H. Reid. Turbulent Flow, Theoretical Aspects. In: Handbuch der Physik, Flugge, S. (ed.), Vol. 8/2. Berlin, Springer-Verlag, 1963. p. 438-523.
15. Moses, H. Mathematical Urban Air Pollution Models. National Center for Air Pollution Control, Chicago Dept. of Air Pollution Control, Argonne National Laboratory. Argonne, Ill. ANL/ES-RPY-001. April 1961. 69 p.
16. Taylor, G. I. Diffusion by Continuous Movements. Proc. London Math. Soc. *20*(Series 2):196-212, August 20, 1921.
17. Holland, J. Z. and R. F. Myers. A Meteorological Survey of the Oak Ridge Area. U.S. Weather Bureau, Oak Ridge, Tenn. U.S. Atomic Energy Commission, Technical Information Service, Final Report for 1948-1952. Report Number ORO-99. November 1953. 584 p.
18. Kellogg, W. W. Diffusion of Smoke in the Stratosphere. J. Meteorol. *13*(3): 241-250, June 1956.
19. Frenkiel, F. N. and I. Katz. Studies of Small Scale Turbulent Diffusion in The Atmosphere. J. Meteorol. *13*(4):388-394, August 1956.
20. Gifford, F. A., Jr. Atmospheric Diffusion from Volume Sources. J. Meteorol. *12*(3):245-251, June 1955.

    Gifford, F. A., Jr. Relative Atmospheric Diffusion of Smoke Puffs. J. Meteorol. *14*(5):410-414, October 1957.
21. Gifford, F., Jr. Statistical Properties of a Fluctuating Plume Dispersion Model. In: Advances in Geophysics, Landsberg, H. E. and J. Van Mieghem (eds.), Vol. 6. New York, Academic Press, 1959. p. 117-138.

22. Inoue, E. On the Shape of Stack Plumes. National Institute of Agriculture Sciences, Division of Meteorology, Meteorol. Res. Notes. Japan. Vol. 2, No. 5. 1960. p. 332-339.

23. Hogstrom, U. An Experimental Study on Atmospheric Diffusion. Tellus. *16*(2): 205-251, May 1964.

24. Pasquill, F. The Estimation of the Dispersion of Windborne Material. Meteorol. Mag. *90*(1063):33-49, February 1961.

25. Pasquill, F. Atmospheric Diffusion. London, D. Van Nostrand Co. Ltd., 1962. 297 p.

26. Smith, M. E. and I. A. Singer. An Improved Method of Estimating Concentration and Related Phenomena from a Point Source Emission. J. Appl. Meteorol. 5(5): 631-639, October 1966.

27. Gifford, F. A., Jr. Atmospheric Dispersion. Nucl. Safety. *1*:56-62, March 1960.

28. Frenkiel, F. N. Turbulent Diffusion: Mean Concentration Distribution in a Flow Field of Homogeneous Turbulence. In: Advances in Applied Mechanics, von Mises, R. and T. von Karman (eds.), Vol. III. New York, Academic Press Inc., 1953. p. 61-107.

29. Brummage, K. G. et. al. The Calculation of Atmospheric Dispersion from a Stack. Stichting, CONCAWE, The Hague, Netherlands. August 1966. 57 p.

30. Simon, C. Plume Rise and Plume Concentration Distribution from Consolidated Edison Plant in New York City. New York University. Technical Report Number 68-15. 1968.

31. Halitsky, J. (unpublished report) Effect of Turbulence on Gas Diffusion Around Obstacles. New York University. 1965.

APPENDIX – GLOSSARY OF SYMBOLS

a	dimensions of area-source grid
C	concentration
DD	number of degree days for date of interest
$g(t)$	total source output for a 2-hour period
h	height of stack from which pollutant is emitted
Δh	distance above stack through which plume rises by bouyancy and exit velocity of stack gases
H	height of base of inversion layer
$\mathcal{H}$	effective stack height
N	number of time intervals from beginning of all emissions to present
p	data based parameter to describe intensity of turbulence
Q	source strength
Q_h	heat emission rate
Q_{day}	daily total output of SO_2
Q_{year}	annual total output of SO_2
t	time
Δt	time interval
$(t - t')$	time since emission
u, v, w	velocities in x, y, z directions respectively
(x', y', z')	position of release
α	data based parameter to describe thermal stratification
$\sigma_x, \sigma_y, \sigma_z$	standard deviations of diffusing cloud in three dimensions respectively.

ABSTRACT

This paper presents a statistical approach to the analysis of multiple-station air sampling data in urban (i.e., multi-source) areas. Measured data values are considered to be composed of three contributions: an urban scale constituent, a contribution due to sources in the vicinity of the sampling station, and a contribution due to measurement and analysis errors. The significance of correlation coefficients calculated from paired data series and the influence of averaging several individual data series prior to calculating correlations is examined.

The data base for the present study is limited, but the following conclusions can be cited:

–The error contribution to the total variance in most field data series is significant.

–Correlations among single station data series, and between data from one station and an external predictor (such as a meteorological parameter), will be small in most cases. Errors and local phenomena in the data from a single station mask much of the urban scale variability that would correlate with most urban scale model predictors.

–An urban scale average, drawn from widely separated stations, is the best index of large scale air quality patterns.

–A maximum expected correlation coefficient can be calculated from the field data, and this value can serve as a criterion for the evaluation of air quality model projections.

–Whenever possible, a double set of instrumentation should be operated at one station within a sampling network. The redundant data provide an excellent measure of the expected error variance in the field observation.

AUTHORS

***JAMES R. MAHONEY** is Assistant Professor of Applied Meteorology at Harvard University, School of Public Health, and staff consultant at Environmental Research and Technology, Inc., Waltham, Massachusetts. He received a B.S. degree in physics from LeMoyne College (New York) in 1959 and a PH.D. degree in meteorology from Massachussetts Institute of Technology (M.I.T.) in 1966.*

***WILLIAM O. MADDAUS** is Water Resources Systems Engineer at Engineering-Science, Inc., Oakland, California. He received a B.S. degree in civil engineering from the University of California at Berkeley in 1967, and an M.S. in civil engineering degree, together with a C.E. degree from M.I.T. in 1969.*

***JOHN C. GOODRICH** is a teaching assistant in City Planning at Harvard University, Graduate School of Design, and staff consultant with Enviromental Research and Technology, Inc., Waltham, Massachusetts. He received the B.S. in civil engineering degree from Princeton University in 1966, and the Master of Regional Planning degree from Harvard in 1969.*

11. ANALYSIS OF MULTIPLE-STATION URBAN AIR SAMPLING DATA

JAMES R. MAHONEY, WILLIAM O. MADDAUS
AND JAMES C. GOODRICH

Harvard University

INTRODUCTION

Air pollution control depends upon adequate current data and projections describing concentrations of the important pollutants within the control region. Average concentrations, temporal and spatial variability, and concentrations during poor ventilation conditions must all be known.

Recently a large investment in time, effort and financial expenditure has been committed to the collection of multiple-station data in urban areas. Within the United States, several of the largest cities have instituted continuous monitoring for important local pollutants:

—The Los Angeles County Air Pollution Control Department instituted a program in 1947. Nine stations, all equipped to monitor carbon monoxide, oxides of nitrogen, ozone, hydrocarbons, sulfur dioxide and particulates, are operated throughout Los Angeles County.

—New York City recently activated a 38-station network, under the direction of the Air Resources Department. Each station records concentrations and surface meteorological data, and ten of the stations transmit data regularly to a central, computerized facility.

—Chicago has an active monitoring and projection program, operated with the cooperation of Argonne National Laboratories.

Many other cities have operated programs in response to local pollution problems. Pittsburgh, for example, has collected smoke shade data for more than 40 years. Its monitoring program was instituted to support that city's efforts to achieve a smokeless atmosphere.

In response to the requirements of the Air Quality Act of 1967, all of the states are currently establishing monitoring networks within federally designated air quality control regions. *All of the data collected is useful only when it is properly analyzed and made available for study and decision-making operations.* This paper presents a brief analysis of the uses and limitations of multiple-station air quality data collected in urban areas. The illustrative examples cited are drawn from an analysis for a ten-station SO_2 survey and a 20-station particulate survey conducted in the metropolitan Boston region in 1966 by the Massachusetts Department of Public Health.

The section headed "Design Specifications for a Multiple–Station System" summarizes the elements required for adequate specification of a sampling network. The section headed "Interstation Data Correlation Studies" contains the results of several interstation correlation studies for the Boston data. These results illustrate the degree of variability between simultaneous observations in various parts of the same urban region. The section captioned "Correlations between Air Quality Data and Meteorological Data" summarizes a correlation study of the same air quality data related to local meteorological data. Such correlation statistics must be developed to facilitate projections for special meteorological conditions and for changes in local emission rates. The section captioned "The Use Of Computer Generated Graphic Analyses for Air Quality Data" illustrates the use of computer generated graphic displays for the presentation of regional air quality data, and the concluding section contains recommendations for the establishment and analysis of multiple-station air sampling networks.

DESIGN SPECIFICATIONS FOR A MULTIPLE-STATION SYSTEM

Before a monitoring system can be established, several basic questions concerning its purposes must be resolved. The system criteria can be developed from an evaluation of the following topics. (Note that very similar specifications are required for the development of diffusion models intended to provide urban area concentration data.)

1. **Basic uses of the data.** Information concerning long term (annual) averages, monthly and seasonal variability, day-to-night variability, background levels, and frequencies and magnitudes of peak values will normally be desired. Also, observed concentrations during defined periods of poor atmospheric mixing are usually required.

2. **Spatial resolution.** Is it sufficient to report an average for the entire urban region, or for the "urban center" region? Will it be necessary to describe the variability among sub-regions of the urban area, and will an attempt be made to correlate local concentrations with local emission data?

3. **Time resolution.** Many instruments are capable of near-instantaneous observations, and a number of observing systems are providing data at 5-minute intervals. With few exceptions, hourly records of contaminant concentrations provide an adequate description of mean values and variability in the urban atmosphere. Higher frequency data reports usually contain significant noise caused by instrument errors and transient changes in local concentrations. For many purposes daily average values are adequate, and calibration difficulties frequently appear when the results of 24-hour observations are compared to corresponding averages of 24, one-hour observations.

4. **Projections based upon the data.** The required projections maybe either short-term forecasts for a single-day or a several-day episode, or long-term planning estimates, based upon expected changes in local emission sources or rates. When projections are desired, the air quality observations should be supplemented by surface and vertical profile meteorological data. The accuracy requirements for all data become more stringent when longer projections are prepared because small errors in time tendencies or spatial gradients will be magnified by the extrapolation process.

5. **Emergency action decisions based upon the data.** Some redundancy in measurements is desirable for the system if the output data is to be employed as the basis for wide-ranging emergency decisions.

6. **Compatability with data from other regions.** Although every reasonable effort should be made to develop uniform data collection and reporting programs, the physical variability within each urban area and the rapid development of observing instruments make complete standardization difficult.

When the purposes of the sampling network have been resolved, the detailed requirements for the network can be estimated: How many observing points are needed; how should they be located relative to one another and to the local geography; what sampling frequency and accuracy are necessary? The following sections are intended to provide some empirical information in response to these questions.

INTERSTATION DATA CORRELATION STUDIES

When several observing sites are used to characterize air quality in an urban area, the variations in the resulting data represent a mixture of instrumental error, local (or transient) phenomena, and large scale variability in contaminant concentrations. The best use of the field data results when estimates are available concerning the relative magnitudes of the observing errors, local phenomena, and urban-scale phenomena.

This section describes an approach to such estimates, based upon correlation studies and averaging techniques applied to the original field data. The analysis proceeds from the formal definition of the correlation coefficient, and it assumes that actual correlation statistics, calculated from field data, represent useful approximations to the "true" statistics which would be developed from very large data sets.

The illustrative examples cited in this section are drawn from the 1966 Boston Region Air Quality Study, conducted by the Massachusetts Department of Public Health. A general description of this study and its results appears in a state report;[3] only the SO_2 and smoke shade (Coefficient of haze, Coh) data are cited here.

Ten SO_2 observing locations were operated during the study period. These ten sites and ten additonal sites were employed for the collection of smoke shade data. The Boston region base map in Figure 11-1 indicates the locations of all 20 sites.

In the case of the SO_2 data, four-hour air samples were obtained, and the West-Gaeke method[1] was employed for all analyses. The monthly average diurnal variability for the ten-station average SO_2 data is shown in Figure 11-2 for the months of February, March, September and November. The observed diurnal pattern has the expected features: maximum concentrations in the early morning hours, and minima in the late afternoon. For the "winter" months, both the average concentrations and the average daily variability are greater. (December and January data samples were unavailable for use in the comparative study.) The November concentrations are probably higher than normal because of a prolonged stagnation episode between November 21, and 25, that year. Concentrations in the mid-summer months were all lower than the September data illustrated in the figure, and no diurnal pattern is evident for these months.

It should be noted that the concentrations observed on individual days frequently do not follow the pattern of the monthly averages shown in Figure 11-2. Mesoscale meteorological phenomena, having the time periods of one day or less, mask the tendency for day-time mixing and nighttime stability on many days.

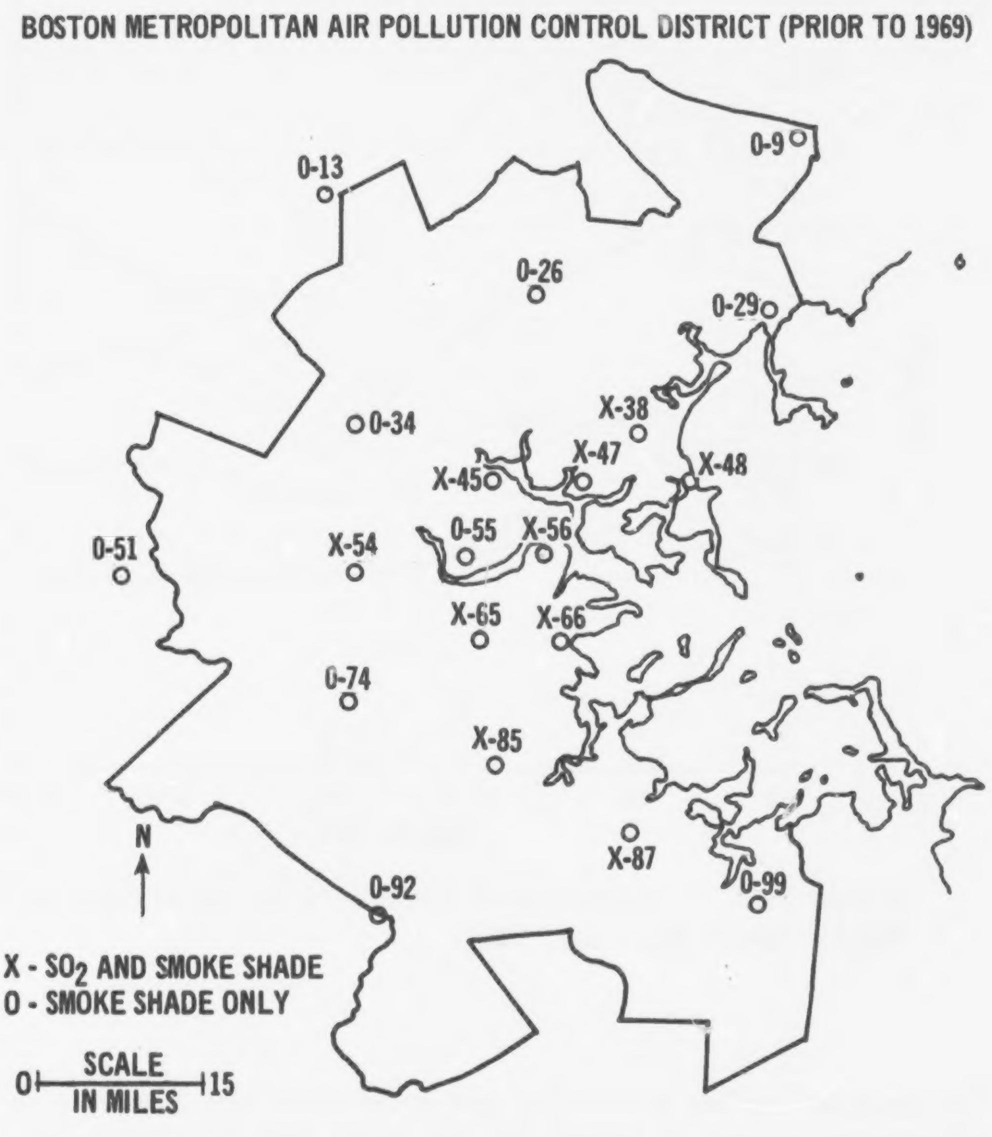
BOSTON METROPOLITAN AIR POLLUTION CONTROL DISTRICT (PRIOR TO 1969)
0-13
0-9
0-26
0-29
X-38
0-34
X-47
X-48
X-45
0-51
X-54
0-55
X-56
X-65
X-66
0-74
X-85
X-87
0-92
0-99
N
X - SO_2 AND SMOKE SHADE
0 - SMOKE SHADE ONLY
0
SCALE
IN MILES
15

Figure 11-1. Boston region base map indicating the ocean coast and the boundaries of the Boston Air Quality Control Region prior to 1969.

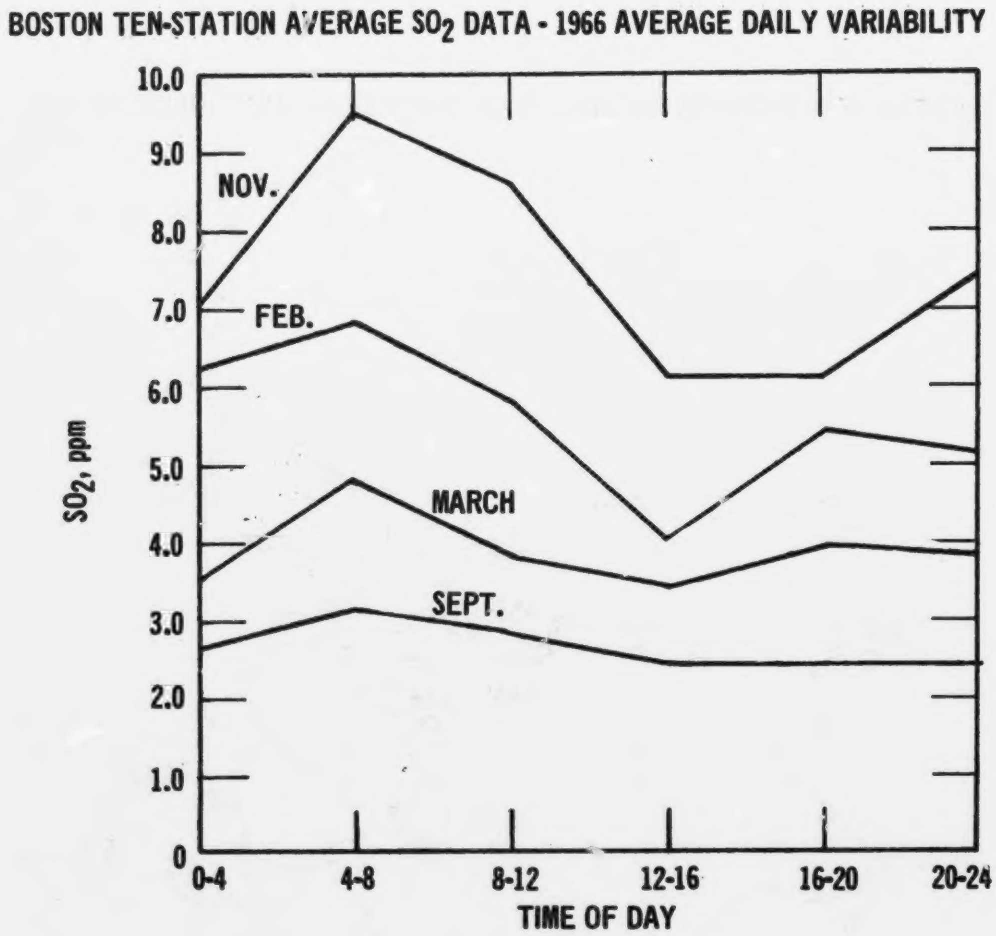

Figure 11-2. Average diurnal variability for the ten-station Boston region SO_2 data, 1966.

The statistical analysis of the SO_2 and smoke shade data is based upon calculated correlation coefficients for data series from individual stations, and groups of stations. The correlation coefficient R, for two data series x_i and y_i, having N members each, is

$$R = R_{x,y} = \frac{\Sigma[(x_i - \overline{x})\ (y_i - \overline{y})]}{\sqrt{\Sigma[(x_i - \overline{x})^2] \cdot \Sigma[(y_i - \overline{y})^2]}} \qquad (1)$$

where the overbar indicates the arithmetic average value for the series. The summation limits are $i = 1$ through $i = N$ in each case.

For this discussion the symbol V indicates the variance of a series, and C represents the covariance between two series:

$$V_x = \frac{\Sigma [(x_i - \bar{x})^2]}{N} \qquad (2)$$

$$C_{x,y} = \frac{\Sigma [(x_i - \bar{x})(y_i - \bar{y})]}{N} \qquad (3)$$

Then the correlation coefficient can be defined in terms of the variance and covariance forms

$$R_{x,y} = \frac{C_{x,y}}{V_x \cdot V_y} \qquad (4)$$

For this discussion the actual value of each field observation x_i (or y_i) in a time series is assumed to arise from an urban-wide contribution, a local scale contribution, and error due to measurement and analysis:

$$x_i = U_i + L_i^x + E_i^x \qquad (5)$$

where

x_i = a measured value of SO_2 concentration or smoke shade at one observing site,

U_i = contribution to x_i which is constant throughout the *urban* region,

L_i^x = contribution to x_i arising from sources in the *local* region of the measuring site,

E_i^x = contribution to x_i due to *errors* in measurement and analysis.

By the same definition an element of the time series y_i measured at another site within the urban area is

$$y_i = U_i + L_i^y + E_i^y \qquad (6)$$

Note that the urban scale contribution is equal (by definition) at each site.

With the aid of Equation (5) the variance and covariance of the x_i and y_i data series can be expressed in terms of the defined urban, local and error contributions:

$$V_x = \frac{\Sigma [(x_i - \bar{x})^2]}{N} = \frac{\Sigma [(U_i + L_i^x + E_i^x - \bar{U} - L^{\bar{x}} - \bar{E})^2]}{N}$$

$$= V_U + V_{L^x} + V_{E^x} + C_{U,L^x} + C_{U,E^x} + C_{L^x,E^x} \qquad (7)$$

But if the error contributions are random (i.e. uncorrelated with the urban plus local "real" variability, the Equation (7) reduces to

$$V_x = V_U + V_{L^x} + V_{E^x} + C_{U,L^x} \tag{8}$$

A similar result is obtained for the time series represented by the y_i terms:

$$V_y = V_U + V_{L^y} + V_{E^y} + C_{U,L^y} \tag{9}$$

The covariance between series x_i and y_i is

$$C_{x,y} = \frac{\Sigma[(U_i+L_i^x+E_i^x-\overline{U}-\overline{L^x}-\overline{E^x})\,(U_i+L_i^y+E_i^y-\overline{U}-\overline{L^y}-\overline{E^y})]}{N}$$

$$= V_U + C_{L^x,L^y} + C_{U,L^x} + C_{U,L^y} + C_{L^x,E^y} \tag{10}$$

$$+ C_{L^y,E^x} + C_{U,E^y} + C_{U,E^x} + C_{E^x,E^y}$$

Again, if the error contributions are uncorrelated to the real contributions, this becomes

$$C_{x,y} = V_U + C_{L^x,L^y} + C_{U,L^x} + C_{U,L^y} \tag{11}$$

Now Equations (4), (8), (9) and (11) can be used to write the correlation coefficient for the x_i and y_i series as

$$R_{x,y} = \frac{(V_U+C_{L^x,L^y}+C_{U,L^x}+C_{U,L^y})}{(V_U+V_{L^x}+V_{E^x}+C_{U,L^x})^{1/2}\,(V_U+V_{L^y}+V_{E^y}+C_{U,L^y})^{1/2}} \tag{12}$$

The remainder of this section is concerned with modifications of the general form expressed in Equation (12).

Case 1. Data from two sampling instruments operating at same site.

Two sampling instruments operated side-by-side can be used to estimate the magnitude of random measuring errors associated with the instruments. In this case the "urban" and "local" contributions to the measured concentrations are equal for each instrument. If the symbol T_i represents the true concentration at the observing site, then $T_i = U_i + L_i$, and Equation (12) reduces to the simpler, familiar form

$$R_{x,y} = \frac{V_T}{(V_T + V_{E^x})^{1/2}\ (V_T + V_{E^y})^{1/2}} \tag{13}$$

If the magnitude of the error variance associated with each instrument is assumed equal (i.e. $E^x = E^y \equiv E$), then

$$R_{x,y} = \frac{V_T}{(V_T + V_E)} \qquad (14)$$

Thus, for two instruments operating at the same location, the correlation coefficient for the paired data series represents the ratio of the "true" variance to the total (true plus error) variance.

As an example of this analysis, two tape stain samplers were operated side-by-side on the roof of a 50-foot-high building at the Harvard School of Public Health during part of 1968. Coh data obtained from the instruments operating on identical 2-hour sampling cycles during the months of June through August are summarized in Table 11-1.

If a value of R = 0.75 is adopted from Table 11-1 as typical for the sampling period, then the expected ratio of error variance to true variance for these instruments can be calculated. Equation (14) can be rewritten as

$$\frac{V_E}{V_T} = \left(\frac{1-R}{R}\right) ,$$

or (15)

$$\frac{V_E}{V_T} = \frac{1}{3} ,$$

based on data of Table 11-1. This significant contribution due to measuring errors must always be considered, particularly when the data from these instruments are used to make projections, or to estimate local gradients in concentrations,

Case 2. Data from two sampling instruments operated at different sites within urban area.

For separated sampling sites, the general Equation (12) must be adopted as the appropriate definition of the correlation coefficient for paired data series. Two limiting cases of Equation (12) may be considered, but they appear to be less interesting then the general case. In one limit, the "local" contribution can be assumed to be perfectly correlated to the "urban" contribution; this case reduces to Equation (14), discussed previously. In the other limit, the "local" contributions can be assumed to be completely uncorrelated to one another and to the urban scale contribution (i.e. $C_{U,Lx} = C_{U,Ly} = C_{Lx,Ly} = 0$); in this case the "local contribution can simply be considered as an additional error or "noise" term, and a form similar to Equation (14) is again appropriate.

An interesting approximation to Equation (12) can be developed from the assumption that the urban and local scale contributions to the measured data are uncorrelated (i.e. $C_{U,Lx} = C_{U,Ly} = 0$). If the error variances are also assumed to be equal ($V_{Ex} = V_{Ey} \equiv V_E$), then

$$R_{x,y} = \frac{(V_U + C_{Lx,Ly})}{(V_U + V_{Lx} + V_E)^{1/2}\ (V_U + V_{Ly} + V_E)^{1/2}} \qquad (16)$$

For this case the correlation coefficient represents approximately the ratio of the urban-scale variance plus the covariance of the local contributions to the total (urban plus local plus error) contributions.

Equation (16) is particularly interesting because the covariance term can be either positive or negative. An interpretation of this equation is suggested by the data illustrated in Figure 11-3. Monthly correlation coefficients for three station-pairs for February through November, 1966 are illustrated in this figure; the station locations are all indicated in the Boston base map, Figure 11-1. Stations 56 and 65 are central city locations, separated by a distance of only three miles. The covariance term $C_{Lx,Ly}$ might thus be expected to be positive for this pair. Conversely, stations 38 and 87 lie on opposite sides of the urban area, and on opposite sides of the major SO_2 emission areas. A negative covariance term $C_{Lx,Ly}$ for the local contributions at these stations is expected (i.e. when one station is upwind of the major sources, the other is downwind, and *vice versa*).

Equation (16) and the data of Figure 11-3 *suggest* the following interpretations:

a. The error variances for the station data series may be approximately one-half the magnitude of the real (urban scale plus local contributions) variances.

b. The urban scale contributions and the local contributions may be approximately equal in the data series.

c. For proximate station pairs (such as 56 and 65), and for station pairs with similar orientations relative to the local maximum emission regions (such as 56 and 85), the covariance between the station data series is expected to be positive. Calculated correlation coefficients for the data observed in conditions a, b, and c would be in the range of 0.25 to 0.5. Such results are obtained for most of the ten monthly calculations for both of these station pairs, is illustrated in Figure 11-3.

d. For station pairs on opposite sides of the major emission regions (such as 38 and 87), the covariance term $C_{Lx,Ly}$ in Equation (16) is expected to be negative. This would result in near-zero values for $R_{x,y}$, because the urban contribution variance term, V_U, is always positive. Figure 11-3 contains nine calculated monthly correlation coefficients for this pair of

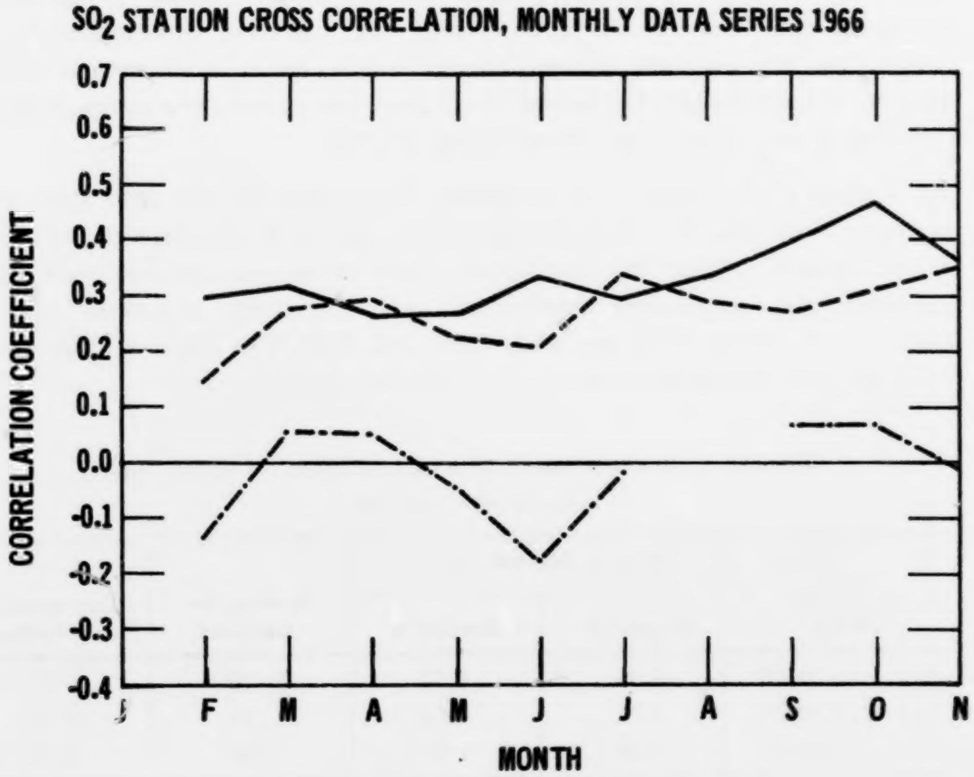

CODE	STATION CODES	ANNUAL AVERAGES
———	56 + 65	0.343
– – –	56 + 85	0.312
–·–·	38 + 87	0.016

Figure 11-3. SO_2 station correlation coefficients calculated for monthly data series.

stations, and the results are all small compared to the other station pairs. The average of the nine available monthly values is very nearly zero.

It should be stressed that the illustration described here is only suggestive. Many more data samples must be investigated to validate this statistical determination of the scale of urban pollution phenomena.

Case 3. Use of averaged data to reduce error variance.

Because of the error contribution to the data record from a single observing site, average values are frequently generated for use in model verification and projection applications, The averaging process can be carried out either along the time dimension, grouping data from a single source, or spatially, grouping data from separate observing sites operating simultaneously. In either case the averaging process always reduces the error variance contribution to the calculated correlation coefficient for paired data series. The real variance is also reduced by the averaging process.

An example of simple time averaging is provided by the tape stain data collected from the two samplers operating together at the Harvard School of Public Health. When the two-hourly data values are grouped into daily averages, the correlation coefficients for the three sequential periods described in Table 11-1 are 0.92, 0.95 and 0.94. The daily average values from the two samplers contain very little error contribution.

Table 11-1. TAPE STAIN DATA COLLECTED AT HSPH, 1968
(2-HOUR SAMPLES)

Sampling period	Average Coh per 10^3 ft		Number of data pairs	Correlation coefficient
	Sampler A	Sampler B		
6/21 – 6/30/68	0.85	0.92	56	0.73
7/1 – 7/10/68	0.72	0.68	93	0.73
7/11 – 8/6/68	1.00	1.01	269	0.78

When data from two or more observing sites are averaged, the correlation coefficient for the averaged data represents an improved measure of urban and local scale contributions, because of the reduction in random errors. The reduction in variance for an averaged set of data can be illustrated as follows. If X_i is defined as an average of two or more data series, then

$$X_i = \frac{1}{M} \sum_{j=1}^{M} x_{i,j}$$

$$= \frac{1}{M} \sum_{j=1}^{M} (U_i + L^x_{i,j} + E^x_{i,j}) \ , \qquad (17)$$

where M is the number of stations entering into the averaging process. The upper and lower limits for the variance V_x of the averaged data can be calculated: If the local contributions $L^x_{i,j}$ are perfectly correlated to one another, the *upper limit value* is

$$V_x = V_U + V_L x + C_{U,L} x + \frac{1}{M} V_E x \qquad (18)$$

If the local contributions are uncorrelated, the *lower limit value* is

$$V_x = V_U + \frac{1}{M} \left[V_L x + C_{U,L} x + V_E x \right] \qquad (19)$$

In practice the actual variance calculated for a set of averaged data lies between these two limits.

The variances enter the denominator of Equation (12) describing the constitution of the correlation coefficient, and the limiting cases described above suggest:

1. When averages are calculated from stations that are relatively close together, (a) the local contributions will be more highly correlated, (b) relatively large values of V_x will result, and (c) the correlation coefficient $R_{x,y}$ will be relatively small.
2. When averages are calculated from stations widely separated from one another, (a) the local contributions will be less correlated, (b) smaller values of V_x will result, and (c) the value of $R_{x,y}$ will be greater.

This pattern is illustrated in Table 11-2. The greatest correlation coefficient results when the middle and outer suburban stations are averaged. These stations are widely separated, and each is subjected to a variety of local scale contributions that do not affect the others. The inner city stations are more closely grouped, and the local scale contribution to these data is not filtered effectively by the averaging process.

Table 11-2. CALCULATED CORRELATION COEFFICIENTS FOR GROUPS OF TAPE STATION DATA, BOSTON, NOVEMBER 1 – 10, 1966

Station Grouping	Number of data pairs	R
Station 45 *vs* station 47	120	0.11
Station 54 *vs* inner city average	120	0.39
Inner-city[a] average *vs* middle-suburban[b] average	120	0.65
Middle-suburban average *vs* outer-suburban[c] average	120	0.82

[a] Inner-city stations: 45, 47, 55, 56, 65, 66

[b] Middle suburban stations: 26, 29, 34, 38, 48, 74, 85, 87

[c] Outer suburban stations: 9, 13, 51, 92, 99

Note that even for large groups of stations drawn from throughout the urban region (the middle and outer suburban data), the correlation coefficient is approximately 0.8. This value might be taken as an expected upper limit for correlations between field data and air quality model data, even when the field measurements and the model projections have been averaged to provide urban scale comparisons. For point-by-point comparisons of model projections and field data, significantly lower correlations must be expected.

CORRELATIONS BETWEEN AIR QUALITY DATA AND METEOROLOGICAL DATA

The time scale of several meteorological phenomena that influence urban air quality is less than 1 day (e.g. diurnal changes in stability, front passage, changes in "mean" wind direction, sea and lake breezes). The relationship between meteorological parameters and air quality indices must therefore be examined on a short-time period basis (e.g. 1-, 2-, 3-hour increments). This time period limitation often prevents the use of time averaging as a device to reduce the influence of errors in the data analysis. Spatial averaging, employing data from many stations, is , however, helpful in the examination of meteorological effects upon air quality.

Up to the present time the meteorological information available for most urban areas has been gathered at one primary observing site in each area. As a result, the most appropriate air quality index is often an urban-wide average value. Figure 11-4 illustrates the calculated correlations between observed SO_2 concentrations and wind speeds observed at Logan Airport, Boston during the 1966 study period. (Note that the ordinate scale in the figure is reversed. The calculated monthly correlation between wind speed and SO_2 concentration was always negative.) As expected, the ten-station average data relate best with the wind data. For the three individual stations illustrated, the correlation is lowest in the case of the coastal station number 48. Stations 56 and 65 are in urban-center locations.

In view of the error analysis developed in the preceeding section, it is likely that the correlation between a single meteorological parameter and an index of urban air quality may always be less than 0.5. This suggestion results from three considerations:

1. A single meteorological parameter (wind speed, stability, mixing depth) only partially describes the dilution capacity of the urban atmosphere.
2. The errors and the local influences reflected in the air quality observations are never completely filtered out of the data.
3. The representativeness of the meterological data is unknown in most cases. Usually a single observation, taken near the edge of the urban area, serves to characterize the meteorology of the entire area.

Several other air quality-meteorology studies by the authors, similar to the analysis summarized in Figure 11-4, have each resulted in correlation coefficients less than 0.4 for all data periods. Multiple parameter meteorological indices might result in larger correlations because of the better description they provide of the local ventilation capacity of the atmosphere. However, such indices were not considered in the present study.

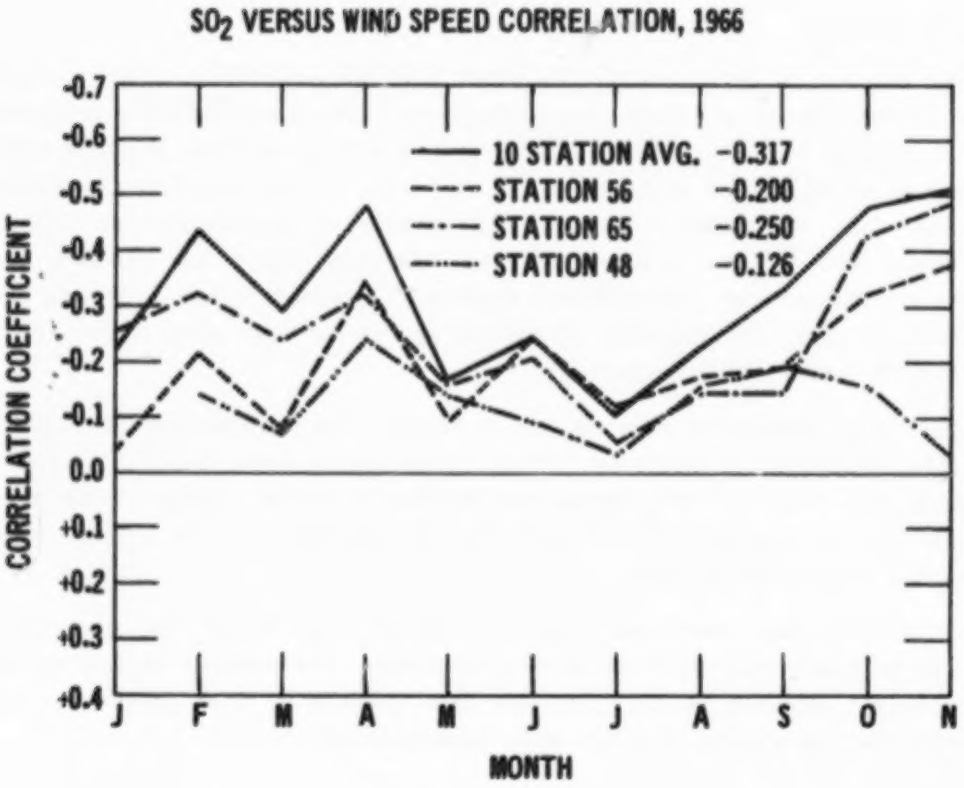

Figure 11-4. SO_2 concentration versus wind speed correlation coefficients calculated for monthly data series.

THE USE OF COMPUTER GENERATED GRAPHIC ANALYSES FOR AIR QUALITY DATA

Spatial variability in air quality observations is most effectively displayed on a geographic base map. This form of data presentation is desirable because the observations can be related directly to emission patterns, to human population, and to land-use distributions.

When the field data are stored in a computer-readable format (e.g., magnetic tape, punched cards, disks) the use of computer generated graphical displays of the data fields is particularly appropriate, with the advantages that:

–Maps can be produced rapidly and at minimum cost.

–The maps permit easy pattern recognition. Relationships between land use, emissions and air quality are quickly evident, and suspicious data points are often identified by the contour patterns.

—The interpolation scheme for evaluation of variables away from the observing locations is objective and repeatable.

The Laboratory for Computer Graphics and Spatial Analysis, of the Harvard Graduate School of Design, has adopted its SYMAP and SYMVU programs for presentation of air quality data, and examples of these mapping techniques are illustrated in Figures 11-5 and 11-6. In the two-dimensional-plan view maps, illustrated in Figure 11-5, shading is proportional to concentration. The left map is based upon an inadequate input data network, and the widespread high concentration regions are unrealistic. The right map was produced with the adoption of additional "background" data points, away from the important emission regions.

The three-dimensional view shown in Figure 11-6 represents an air quality (total suspended particulates) surface for Southern New England. The program that produces this display can produce a similar display of the same data for all possible lines of sight (i.e. all possible azimuth and elevation angles) toward the surface.

These maps are illustrated here to underline the importance of pattern display in the analysis of air quality field data. The mapping techniques are important adjuncts to the statistical data treatments; both approaches are useful for the analysis of urban scale concentration patterns.

RECOMMENDATIONS FOR THE ESTABLISHMENT AND ANALYSIS OF MULTIPLE STATION AIR SAMPLING NETWORKS

The data studies reported in this paper are limited, but they do offer a basis for several recommendations concerning sampling networks:

1. The intended purposes for the network data should be carefully developed before establishment of expansion of an air sampling network.
2. At least one redundant set of sampling equipment should be employed to evaluate the error contributions to the field data series which are obtained. The extra sets of sampling equipment might be installed in a mobile station and moved to each permanent field site on a scheduled basis to provide calibration checks upon all field equipment. A mobile unit could be used also, for special upwind-downwind studies near major emission areas.
3. Instead of equidistant spacing of sampling stations throughout an urban region, arrangements involving two or more stations in neighboring locations should be considered. Such arrangements may provide more useful data concerning urban and local scale variability in pollution concentrations.

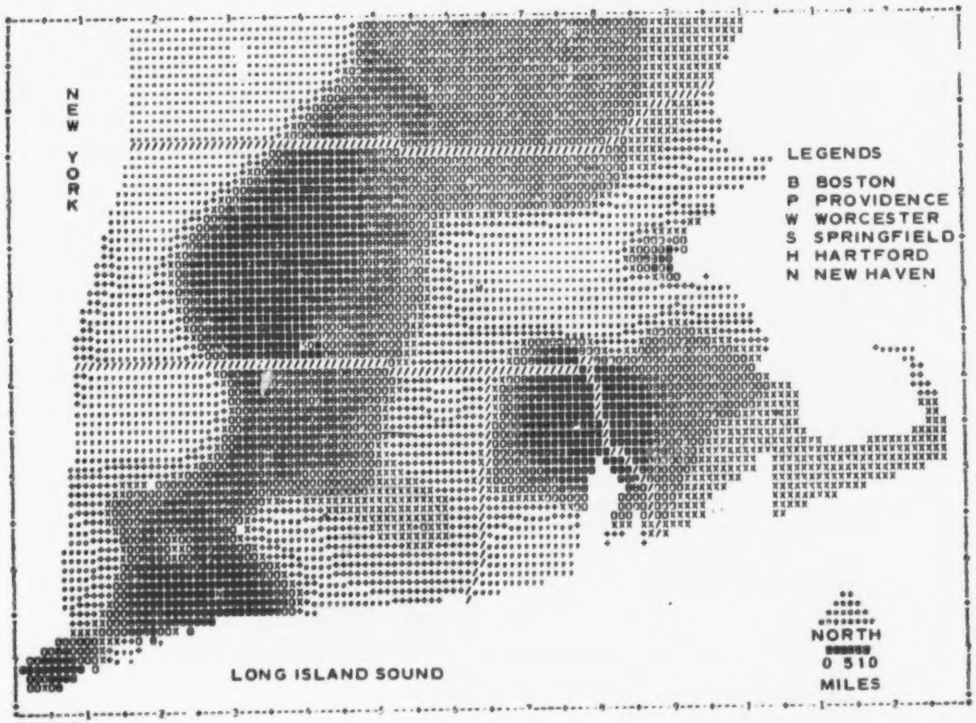
NEW YORK
LEGENDS
B BOSTON
P PROVIDENCE
W WORCESTER
S SPRINGFIELD
H HARTFORD
N NEW HAVEN
LONG ISLAND SOUND
NORTH
0 510
MILES

```
SYMAP
SOUTHERN NEW ENGLAND
1966 AIR QUALITY
SUSPENDED PARTICULATES (UG/M3) - YEARLY AVERAGE

ACTUAL DATA VALUE EXTREMES ARE    25.00    152.00
ARITHMATIC MEAN IS    75.57        STANDARDARD DEVIATION IS    25.77

TOTAL MISSING DATA POINTS IS    4
TOTAL SUPERIMPOSED DATA POINTS IS    2.  THESE OCCUR IN   1 LOCATIONS.

VALUE LIMITS FOR EACH LEVEL
   ('MAXIMUM' INCLUDED IN HIGHEST LEVEL ONLY)

MINIMUM  25.00  45.80  54.00  57.40  65.40  69.00  79.00  88.60   94.90  110.40
MAXIMUM  45.80  54.00  57.40  65.40  69.00  79.00  88.60  94.90  110.40  152.00

PERCENTAGE LIMITS FOR EACH LEVEL (BASED ON THE TOTAL VALUE RANGE)
   ('MAXIMUM' INCLUDED IN HIGHEST LEVEL ONLY)

MIMIMUM   0.00  16.38  22.83  25.51  31.81  34.65  42.52  50.08  55.04   67.24
MAXIMUM  16.38  22.83  25.51  31.81  34.65  42.52  50.08  55.04  67.24  100.00
```

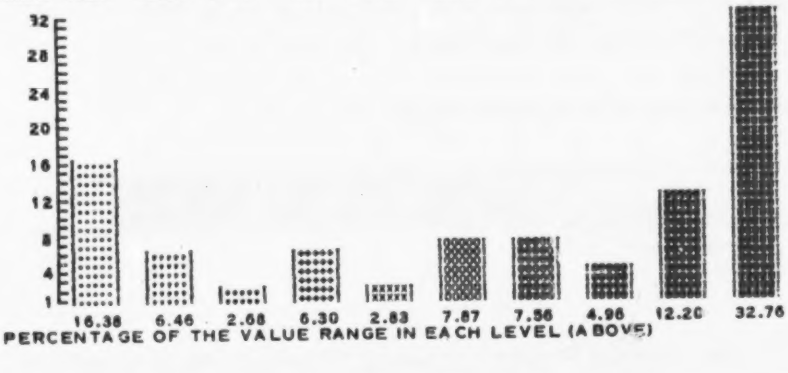

Figure 11-5a. SYMAP plot showing Southern New England particulate concentrations for 1966. Insufficient network -

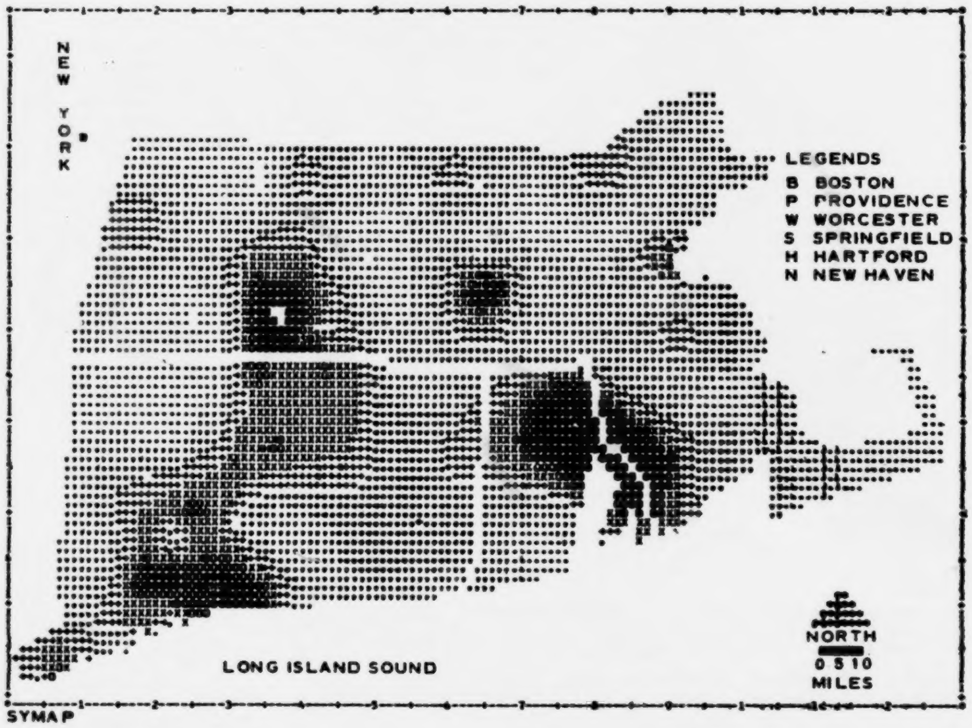
NEW YORK
LEGENDS
B BOSTON
P PROVIDENCE
W WORCESTER
S SPRINGFIELD
H HARTFORD
N NEW HAVEN
LONG ISLAND SOUND
NORTH
0 5 10
MILES
SYMAP

```
SOUTHERN NEW ENGLAND
1966 AIR QUALITY
SUSPENDED PARTICULATES (UG/M3) - YEARLY AVERAGE

DATA VALUE EXTREMES ARE     25.00    152.00

TOTAL MISSING DATA POINTS IS     5
TOTAL SUPERIMPOSED DATA POINTS IS      2.  THESE OCCUR IN    1 LOCATIONS.

ABSOLUTE VALUE RANGE APPLYING TO EACH LEVEL
   ('MAXIMUM' INCLUDED IN HIGHEST LEVEL ONLY)
                                                                              ABOVE
MINIMUM   BELOW  40.00  50.00  60.00  70.00  80.00   90.00  100.00  110.00  120.00  130.00
MAXIMUM  40.00   50.00  60.00  70.00  80.00  90.00  100.00  110.00  120.00  130.00

PERCENTAGE OF TOTAL ABSOLUTE VALUE RANGE APPLYING TO EACH LEVEL

                 11.11  11.11  11.11  11.11  11.11   11.11   11.11   11.11   11.11

FREQUENCY DISTRIBUTION OF DATA POINT VALUES IN EACH LEVEL

LEVEL      L       1      2      3      4      5       6       7       8       9       H

SYMBOLS    ■      ░      ░      ░      ▒      ▨       █       █       █       █

FREQ.      3      17     27     17     12     12       9       4       6       8       3

TIME = 0.0
```

Figure 11-5b. SYMAP plot showing Southern New England particulate concentrations. Additional stations.

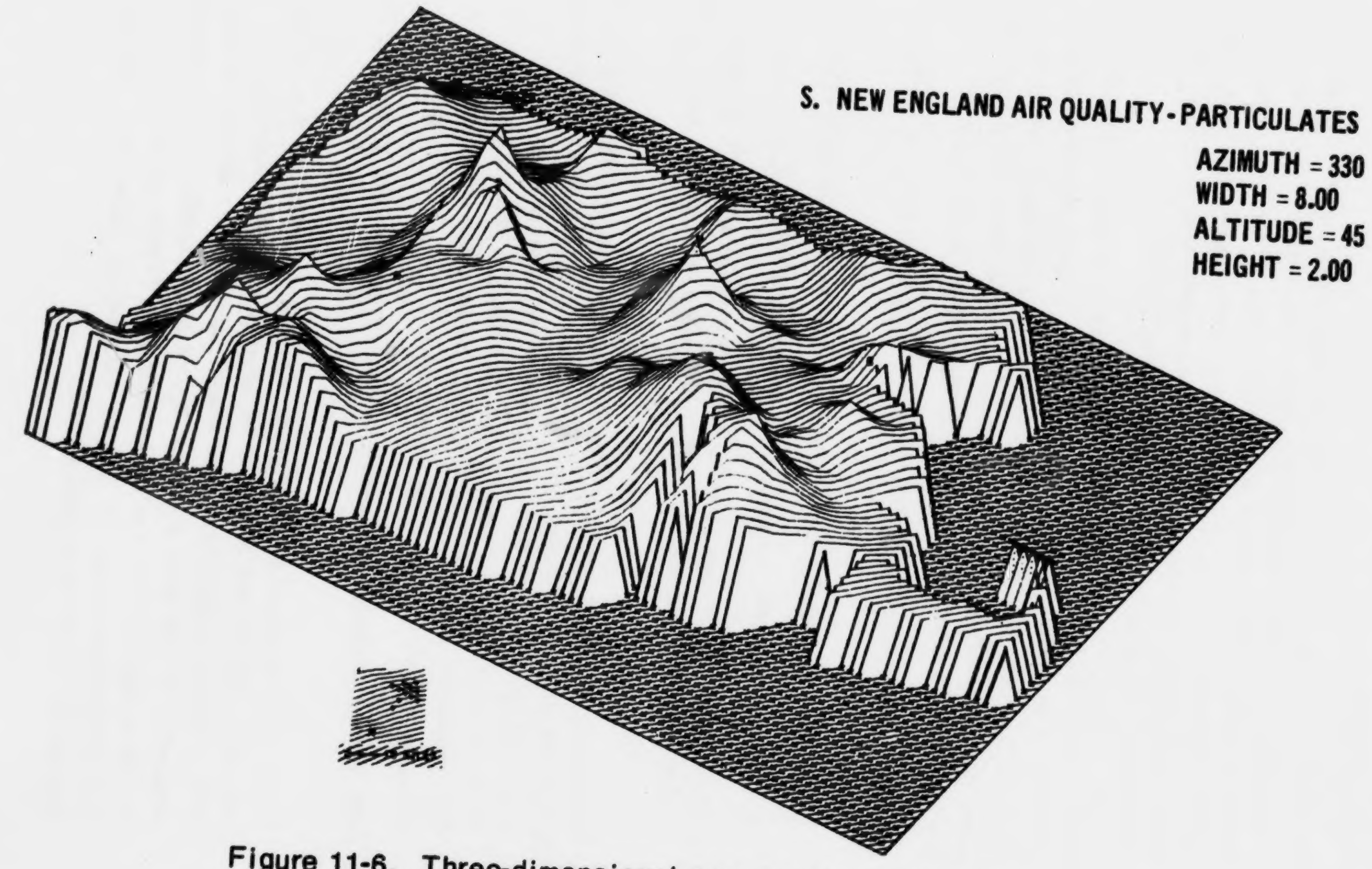
S. NEW ENGLAND AIR QUALITY-PARTICULATES
AZIMUTH = 330
WIDTH = 8.00
ALTITUDE = 45
HEIGHT = 2.00

Figure 11-6. Three-dimensional perspective view of the Southern New England particulate surface for 1966.

The following recommendations are concerned with data analysis techniques for sampling networks.

4. The best measure of urban scale concentrations is an average of simultaneous data from stations throughout the region. This technique minimizes both error variance and variance due to local sources. Correlation analysis involving single-location field-observation series and model projections (or meteorological parameters) will probably result in maximum correlation values of approximately 0.5.

5. When a large number of sampling stations are available, it is helpful to calculate two urban-wide averages, from non-overlapping sets of stations. The correlation coefficient for the two averages represents the upper limit correlation expected from any comparative study involving the field data. Examples of possible comparative studies include:

    a. Comparing time variability in the concentrations of two different pollutants,

    b. Relating pollutant concentrations to meteorological parameters,

    c. Comparing model calculations with actual field data.

6. When daily or longer-period data values are required, time averages of shorter term observations will usually be more reliable than single, long-period observations.

7. Computer-generated graphic displays of air quality fields should be employed as data analysis tools whenever practical. The repeatability of the computer-controlled interpolation scheme is essential for consistent interpretation of data. (As a corollary, it should be mentioned that improved interpolation schemes, based upon emission data and diffusion modeling, should be developed.)

The final recommendation represents a restatement of the theme for this paper:

8. All air quality observations include significant variability due to observing error and to the influence of sources near the observing site. All data analyses, projections, and model comparisons should include an evaluation of the error and local source contributions to the variability in the measured data. Performance indices ("skill scores") for models and projections must be judged relative to upper-limit correlation figures developed from the field data.

REFERENCES

1. Selected Methods for the Measurement of Air Pollutants. Division of Air Pollution. Cincinnati, Ohio. PHS Publication Number 999-AP-11. 1965.
2. Goodrich, J. C. Regional Planning and Air Pollution Analysis and Control: Methodology and Case Studies. Harvard University, Cambridge, Mass. M.S. Thesis. 1969.
3. Investigation and Study of Air Quality in the Metropolitan (Boston) Air Pollution Control District. Massachusetts Dept. of Public Health. 1968.

ACKNOWLEDGMENT

Mr. Maddaus carried out most of the Boston region correlation calculations, and the data maps are drawn from a recent Harvard Masters Thesis by Mr. Goodrich.[2] Other calculations and evaluations have been provided by Mr. B. A. Egan and Mr. E. I. White of the Harvard School of Public Health. The Massachusetts Department of Public Health provided all of the Boston Region data discussed in the paper.[3]

The preparation of this report was supported in part by the National Air Pollution Control Administration, Consumer Protection and Environmental Health Service, Public Health Service, U.S. Department of Health, Education, and Welfare, under Grant Number 1 RO1 APO1013-01.

APPENDIX – GLOSSARY OF SYMBOLS

C	covariance between two series
E_i^x	error contribution to X_i
i	iteration integer
L_i^x	constant contribution to X_i from measuring site locality
M	number of measuring stations entering into an averaging process
N	number of members
R	correlation coefficient
U_i	constant contribution to X_i from urban area
V	variance of a series
X_i	measured pollutant concentration at i
y_i	point in measured time series

Banquet Speech

12. PROGRESS + PROFITS + POPULATION = POLLUTION

MORRIS NEIBERGER
University of California, Los Angeles

Thank you very much, Dr. Stern. Or perhaps I shouldn't thank you, for I don't know why I let myself get into this situation. As I told the audience the only other time I got roped into giving a banquet speech, "It reminds me of Sam Goldwyn's comment, that anybody who pays good money to see a psychiatrist ought to have his head examined." Anyone who voluntarily undertakes to give an after-dinner talk at a technical conference certainly renders his sanity suspect. For, on the one hand, since ladies are present he has to be strictly non-technical, since being technical when ladies are present is even worse than being obsecene. About the technical aspects—I might mention that Francois Frenkiel saw me looking at a manuscript with equations today and said in a voice filled with horror, "You're not going to include equations in your talk tonight." When I replied "It will be only equations; I'm not going to include any words, just symbols in equations," Irv Singer said, "That's all right, as long as you limit yourself to equations my wife can understand." And when I asked what kind of equations his wife understands, he said, "None." So, technical talk is out!

On the other hand, the men in the audience will be bored and feel cheated if all they get for the price of the dinner ticket is some good food and a few jokes and platitudinous remarks. They feel that at least they should come away with some profound new ideas, stimulating insights that inspire them to attack the subject of the conference with increased energy, and predictions of the future of America and humanity that give them hope that their efforts will not be in vain.

On top of this, as I said in my previous dinner speech, the talk should be neither so humorous that the laughter is loud enough to awaken those who are using the time for an after-dinner snooze, nor so serious that it arouses thoughts that interfere with the digestive process.

Obviously, to succeed in this talk is impossible, so you may well ask: since I am aware of its impossibility, why did I undertake it? There is a simple answer. The only condition under which Arthur Stern would invite me to the conference was if I agreed to be an after-dinner speaker.

So, I promise that I will be only slightly technical, and not at all obscene, although it is with some reluctance that I forgo the latter. Knowing that one should always start an after-dinner speech with a little joke, I asked Dr. Clarenburg, who claims to know hundreds of them (though he says they are funny only in Dutch), and he recited a limerick that was very apropos of my subject, as he will see when I give the title of my talk. I would like very much to tell you this limerick; unfortunately, there are ladies present. Besides, I have already forgotten it.

About the new ideas, stimulating insights, and hopeful predictions I'm afraid that John Middleton, in his keynote speech for the conference, anticipated all the ideas I had intended to present, so I'll have to be satisfied to say things you already know, hoping that I can do so in ways that may possibly be fresh to some of you.

While considering the title I should give to my talk, I was very impressed by the slogan Walter Orr Roberts enunciated a few weeks ago, namely, "After the Moon, the Earth," and thought of stealing it as my topic. I certainly concur with the view that now that we have achieved the goal of reaching the moon we should divert a few billions from the space budget to augment the few millions now budgeted to study and protect our earthly enviroment. I have advocated making our federal expenditures more balanced in this regard for a long time. I have restrained my kleptomaniac tendency to steal Robert's subject, however, and following my pledge to Dr. Frenkiel, have chosen for the title of this presentation the equation:

PROGRESS + PROFITS + POPULATION = POLLUTION

It is just eight years since the conference on Air over Cities was held in Cincinnati, under the auspices of the Division of Air Pollution of the U.S. Department of Health, Education, and Welfare, Public Health Service. At the conference I chaired a session on dispersion and deposition of pollutants over cities. In my introduction to the session I pointed out the deficiencies in our knowledge of diffusion from multiple sources and area sources. I had hoped that the papers being presented at the present conference would be evidence of progress toward the elimination of these shortcomings. I fear that such evidence is not clear. But whether or not the solution of the problem has been attained, it is certainly true that the intervening 8 years have seen a tremendous increase in the concern and attention paid to air pollution. Whereas 8 years ago, air pollution was still regarded as a minor problem, serious for only a few unfortunate communities such as Los

Angeles; now, it competes with the Vietnam war, the racial question, and the student protest movement for first place in the attention of the country. Government bodies at all levels and civic organizations everywhere devote large amounts of time and effort to combating it. Whereas, at that time, it was regarded as an isolated problem, today it is recognized as an intrinsic part of the complicated impact civilization and technology are exerting on the environment.

In my talk this evening I wish to present some views about the root causes of the air pollution problem, and the relationship of this problem to some broader aspects of society. Just as education is frequently characterized as being founded in the three R's, I suggest that the roots of air pollution and other insults to the enviroment lie in the three P's: Progress, Profits, and Population. These three P's represent fetishes, which are heretical to question, like motherhood or patriotism. Unquestioning acceptance of them, however, will in the long run, lead to catastrophe.

As a starting point, suggesting why I am concerned with the three P's, I shall give an example from my home city. In Los Angeles the three P's are closely correlated: the measure of Progress has been the increase in Population, the expansion of industry, and above all, the Profits that have accrued to the real estate developers.

Some 15 years ago I gave a talk to the members of the research committee of the Los Angeles Chamber of Commerce. I told them that I did not know whether or not the salubrious climate of Los Angeles would have been able to destroy itself on its own; but with the energetic assistance of the Chamber of Commerce it had been achieved. By advertising the wonders of the Southern California climate and thereby attracting increasing numbers of people and industries, they transformed the clear blue skies, sparkling sunshine, bright green vegetation and the year round invigorating air into a murky brown smog that obscured the sun, withered the plant life, and irritated the eyes, noses and respiratory tracts of the people. I recommended to them that, until effective control measures were found, instead of trying to attract still more people and industries, they should sharply apply the brakes to the population growth of the area, using every means at their disposal to dissuade people and industries from moving to Los Angeles, and persuading those who were already there to move away.

Needless to say, such a heretical recommendation did not receive a favorable response from the Chamber of Commerce. Its promotional activities continued, for its primary motivation was and is the profits of its members, and not the protection of its surroundings. Progress prevailed and smog became more and more wide spread.

I have often been asked why the peak values of contaminant concentrations, registered in those years, have not been exceeded. To this my half-joking reply has been that you can't get automobiles much closer together than bumper to bumper. The tremendous increase in number of cars has meant larger and larger areas of high traffic concentrations, but no increase in peak concentrations of contaminants because the total emission in any given area has not increased.

Of course, that is only part of the story. The other part is that we have not yet had more severe meteorological conditions than those experienced in 1954 and 1955. One of these months, perhaps soon, a prolonged period of very light winds and low inversion will occur, and with it will come record-breaking levels of contaminant concentration, in spite of the measures that have been taken so far to reduce emission of pollutants. We can only hope that it will not be accompanied by a disastrous increase in illness and mortality. If it is, it will be one more reward for the prevalence of the three P's,

A great deal of attention has been paid, recently, to defining air quality standards in various communities and states, as well as nationally. These standards represent the maximum acceptable levels of concentration of particular pollutants from the standpoint of health, safety, and well-being. In some instances aesthetic considerations enter into the definition of standards with respect to particulates in the atmosphere. But, as all those attending this conference are aware, these air quality standards remain pious hopes until they are utilized to set maximum allowable emissions from the various types of sources. The multiple-source urban diffusion models that are the subject of this conference, offer, as one of their applications, the possibility of determining whether, under adverse meteorological conditions, the desired air quality standards could be met with existing sources of emissions and if not, how much reduction of emission rates would be required to achieve the standards. The models could also predict the effects of increased emissions due to expanding population, additional industrial sources, or the speading and redistribution of the urban areas. In places where the air quality standards are already exceeded frequently, the latter computations would seem almost superfluous.

One principle, which I think, is readily evident, and which I therefore expect to be confirmed by computation with these models, is the concept that emission control standards must be expressed on a per-unit-area basis rather than a per-source basis. This concept is most readily appreciated if one considers the present practice of expressing the allowable emissions in terms of the percentage of total concentration of effluent emitted from one source or the total emission from each individual source. In the former instance, if the rate of emission of the total effluent is increased, the permitted emission of pollution is correspondingly increased. In both cases, if in a given square-mile area the number of sources is multiplied, the total pollution allowed is correspondingly multiplied. The pollution from one or two sources in an industrial plant emitting maximum allowable concentrations might not exceed the air quality standards. If the same plant constructs a dozen more stacks, each emitting concentrations of contaminants individually acceptable, the total effect might well be to produce concentrations far in excess of the air quality standards. To prevent such excesses, the limit must be expressed in terms of total emission per unit area, whether the emission originates from one source or many.

This concept, which is so clear with respect to industrial stacks, applies likewise to vehicles. It is not adequate to set the emission limit in terms of individual cars without first estimating the consequences of this limit in terms of the total emission from all cars expected to be operating in a given area. As I pointed out before, and as has been experienced by drivers in all cities, this number of cars has a maximum, which is frequently reached when all lanes on all streets in the area are completely filled with bumper-to-bumper traffic.

The area-limit concept also applies to domestic sources, but if the allowable emissions are expressed on a per-capita basis there is no maximum similar to the automobile case, for modern apartment dwellings appear to have no upper-bound on the density of population which can be concentrated on small horizontal areas. While the vertical spread of high-rise apartments has some effect of spreading the emissions upwards also; the net effect of an increased number of people living in an area, is an increased amount of waste produced which must be disposed of, inevitably increasing the amount of pollution that enters the atmosphere.

I recognize that, at present, the limits to allowable emissions are not expressed on a per-capita basis, however democratic this basis may seem. Surely there is a sort of poetic justice in the idea that if I must share the unpleasant consequences of pollution with everyone, I should be permitted to contribute an equal share to everyone else's discomfort.

Whether or not the emission limits are expressed per-capita, it is self-evident that the amount of pollution is closely related to population. Each additional person in a community adds to the requirements for electric power, domestic heating, transportation, and waste disposal. If the pollution resulting is not proportional to the number of people, one may suspect that the deviation from proportionality is in favor of a more rapid increase in pollution than in population. Small towns generally have small pollution problems, and large metropolitan areas have gigantic ones. When regions are characterized by many metropolises their net pollution seems not merely additive, but combined in some non-linear fashion.

I shall return to the problem of population on a national and world-wide basis. Before considering it, however, I should like to expolore the effects of progress and profit in more detail.

Progress is often measured by the rise in the standard of living of the average citizen, but it might also be measured by the increase in power, which is associated with the rise in standard of living, or by the increase in number of appliances and machines, which are used to produce the rise in standard of living. Domestic cooling systems added to central heating, dryers in additon to washing machines, color TV in addition to radios, hi-fi systems and tape recorders, multiply the demand for power by a large factor. This increased demand leads to construction of more and larger electric generating plants, most of them using fossil fuel and emitting large amounts of contaminants into the air.

The natural demand for these additional comforts of life is augmented by intensive advertising campaigns by the manufacturers of the appliances and by the utility companies that distribute the fuel and electricity. Insofar as these industries are motivated by the purpose of rendering the lives of the citizens more comfortable, the labors of the housewives easier, and everyone's leisure more enjoyable, one would be led to commend them, while regretting the degree to which they miss their goal by also contributing to discomfort and illness with the pollution they introduce into the air. In addition to these high motives, however, or, in some instances, instead of them, the desire for profits enters strongly. Even when they know that additonal thermal electric generating plants will augment already objectionable levels of pollution, utility companies strive to increase the demand for electricity, using all sorts of promotional gimmicks to get customers to convert to all-electric homes, etc.

Two questions occur to me. One is whether the damage to the environment and the discomfort to the people, resulting from technological advances, should not be weighed against the conveniences produced in deciding whether these technological advances really represent progress. Perhaps on balance it would be preferable to forgo some of the benefits and be spared the accompanying disadvantages. The second question is whether, assuming the validity of asking the first, the decision about expansion of electric generating plants, for instance, should be based, as it is for the most part now, on whether expansion will yield a profit to the power companies. Shouldn't the public's welfare come first?

The automobile industry is perhaps the outstanding instance in which the desire for profits has dominated the public interest. Regretably, the recent agreement of the Department of Justice to a consent decree in its conspiracy suit against the auto makers has prevented the evidence in the case from becoming available to the public. But the agreement of the manufacturers to cease and desist, together with the fact that the court ruled that the evidence be impounded so that it could be available in damage suits, strongly suggest that they did indeed conspire to prevent and delay the development of air pollution control devices for motor cars.

Their motive has been stated clearly by Henry Ford II, in interviews quoted in *Fortune* magazine and in newspapers. In these interviews he said that the industry has too large an investment in equipment to make engine blocks, transmissions, and other parts of the internal combustion engine, for it to give a high priority to developing alternative power systems, such as an electric car. The billions of dollars of machinery owned by the auto industry act as a millstone, holding the people of our cities submerged in the pollution exhausted from internal combustion engines.

The same eagerness for profit has, of course, been responsible for the auto industry's failure to develop and introduce safety features until required to do so by federal legislation. Similarly, the profit motive has been responsible for the industry's disregard for such factors as the ease and costs of repairs and the protection of the car itself from damage in minor collisions.

The auto industry appears to judge its progress by the size of engine it can foist upon the public—500 cubic inches, this year. With the allowable emissions presently measured per unit volume of exhaust, it is clear that the increased cylinder capacity will represent increased amounts of pollution per car, which when added to the increased numbers of cars will offset the control measures. Pollution control considerations obviously did not enter the decision to put these mammoths on the market and feature them in the promotional advertising.

The internal combustion engine is, by its nature, an incomplete combusion engine. The automobile industry's answer to the requirements to reduce the products of that incomplete combustion, namely hydrocarbons and carbon monoxide, has been to promote further combustion in the exhaust system, where it produces no useful power. It has ignored the fact that, in that process, increased amounts of oxides of nitrogen are emitted.

It seems to me that the solution to the problem is to abandon the intrinsically inefficient internal combustion engine, and to develop an essentially pollution-free propulsion system in its place. It is inconceivable to me that the technological ingenuity that got man to the moon cannot get him from his home to work in a city without polluting the air.

The high rate of profit in the industry's operations can readily cover the cost to industry of developing a smog-free engine. I do not have recent figures at hand, but the American Institute of Management, in an article appearing in *The Corporate Director*, in July of 1956, reported that General Motors' net earnings, at the 1955 rate of profit, "were sufficient to recoup the company's entire net plant investment in 2 years." (Quoted by Ralph Nader in *The Progressive*, September 1968.)

From the standpoint of the profit motive, it is hard to understand the past reluctance of the auto industry to add air pollution control equipment to the internal combustion engines. The cost of this equipment has been added to the price of the car and you may be sure that in arriving at the price, it has been subject to the same profit margin as all other parts of the car, so that pollution control has increased the automobile industry's profits.

I have suggested that if the Federal, State, and municipal governments were to adopt laws setting a date after which no vehicle injecting any hydrocarbons, carbon monoxide, or oxides of nitrogen into the atmosphere might be sold in their jurisdictions, industry would accept the challenge and develop new propulsion systems to meet that requirement. In the California State Legislature, last year, such a bill was passed by the State Senate but was killed in a committee of the Assembly. When it came before the Senate, the lobbyists for industry apparently did not think anyone would take it seriously but once it passed in that body, the lobbyists exerted great pressure to prevent its consideration in the Assembly. Senator Petris plans to introduce it again at the next session, but with industry alerted I have no hope of its passage, even though the general public is more concerned about pollution than ever before.

That it is necessary to develop completely smog-free vehicles is clear, since, otherwise, whatever degree of reduction of emission is achieved, the increase in number of vehicles will rapidly make up for it and the levels of pollution of the atmosphere will continue to rise. Similarly, unless the emissions from power plants are completely eliminated, the rising demand for electric power due to population growth and increased per-capita use will offset individual emission limits, and the deterioration of the atmosphere will continue. The same applies, of course, to other industrial sources and to domestic sources. This situation is true on a local and statewide basis and, also, on a national and world-wide basis. The problems of urban areas in the more "advanced" countries are particularly acute because of the concentrations of population there. But the entire world is undergoing a population explosion, and in the developing countries there is also a power or energy explosion, which will increase as the people of Asia, Africa, and South America strive to attain the same levels of comfort, convenience, and mobility as Americans and Europeans have. Multiplying the world-wide population explosion by the prospective demands for power yields a potential for air pollution that staggers the imagination. It dramatizes the urgency for the development of completely pollution-free sources of energy and methods of transportation, and the need for contol of population.

I have previously pointed out that, even now, we do not know whether, on a world-wide basis, toxic contaminants are being put into the air faster than the natural cleansing processes of the atmosphere remove them. We know that pollution does not stay in the air; it is removed eventually. One way it is removed, for instance, is by getting into our eyes and respiratory systems and irritating them. It is also incorporated into the clouds and falls out in the form of rain, and it interacts with vegetation, and corrodes building materials. The question is whether the processes of removal are able to keep up with the rate of emission. We do know of one pollutant, though not a toxic one, of which there is an accumulation in the atmosphere. Carbon dioxide has been sampled long enough, and with enough accuracy, to show that the total amount is increasing steadily year by year. If the same thing is happening to toxic pollutants, such as carbon monoxide or nitrogen dioxide, eventually, the entire atmosphere will become so toxic that it will be necessary for people to go around in gas masks to survive. Alternatively, one can visualize people living in air conditioned vehicles, dealing with a complicated docking procedure similar to space vehicles, in going from building to automobile and vice versa. People could never venture out of doors, where they might be subject to "toxic fresh air."

Regardless of whether or not we are now putting toxic pollutants into the air faster than they are being removed; if the number of sources, stationary and vehicular, increases with the population and power explosion, that situation certainly will be reached, unless sufficently stringent controls on emissions per-source are put into effect, *and* unless the world population is stabilized.

There are, of course, other urgent reasons for being concerned about world population. To these is added the danger that the entire atmosphere will become too toxic to breathe because of the sheer number of people adding pollution to the air.

What is the solution? I believe that to find it, it is essential that we make some fundamental changes in social attitudes.

In the short run, of course, the present attempts to control sources of emission must be strengthened. More and more stringent standards of emission from stationary sources and from vehicles must be adopted. Rather than limiting the requirements by what is technically feasible, requirements should be set at levels that challenge technology to meet them.

In the longer run we must revise our attitudes about Progress, Profits, and Population. The concept of Progress must be amended to measure it in terms of the true amenities of life, including the enjoyment of clean air. The motivation of industry and commerce to maximize their profits must be restrained by the requirements of the safety and welfare of the people. Above all, we must take measures to limit population increase, and ultimately, to stabilize the population of the world.

I am not at all hopeful that we will be successful in any of these tasks. The concept that "bigger is better" is so ingrained in American attitudes that any move toward smaller automobiles, fewer appliances, and less people per square-mile will be regarded as retrogress rather than progress. Unless we find some way of having larger profits accrue to industry for building smaller cars, producing less electricity, and, in general, contributing less to pollution; industry and commerce will continue to enlarge their production of energy, commodities, and smog. As for the control of population, since it depends on the slow process of education about contraceptive methods and on producing motivation for their use, the prospects are remote indeed.

The prospects will remain remote until the nature of the problem is recognized. As I said at the beginning, I am encouraged by the increase in public awareness and concern in the past few years. If this increased concern can be focused on the roots of the problem, as typified by the three P's, there is a chance that new attitudes will develop, and solutions will be found.

AUTHOR

ARTHUR C. STERN, a mechanical engineer, is Professor of Air Hygiene at the University of North Carolina at Chapel Hill. He is the current President and Chairman of the Board of the Triangle Universities Consortium on Air Pollution, which involves Duke and North Carolina State Universities and the University of North Carolina at Chapel Hill. From 1935 to 1968 he was associated with the Federal Air Pollution Control Program, first in Cincinnati, Ohio, as the chief of its Research and Development Program; later, in Washington D.C., as the Assistant Director of NAPCA. He is perhaps best known as editor of the three-volume work, Air Pollution.

Symposium Summary

13. UTILIZATION OF AIR POLLUTION MODELS

ARTHUR C. STERN

University of North Carolina at Chapel Hill

It would serve you poorly to have me now recite a series of abstracts of the papers you have already read and heard, and of the discussion you have heard and will be able to read in final form in the Proceedings of this symposium. Rather, I can serve you best by assessing the impact of our deliberations.

If any one statement could characterize this symposium, it is that this was the one in which a "Gaussian" distribution was qualified by, "if that is not a dirty word." Those who had incorporated in their models, diffusional procedures developed to a state of increasing sophistication over the past 5 years were here on the defensive against those who, looking ahead, foresee newer procedures displacing them over the next 5 years.

This was the symposium at which people were first able to say to each other, "You have an elegant model, but is it the one we need? Does it meet our objectives for a model?" Yet statements of such objectives were alluded to only peripherally by the speakers and discussers.

NEEDS AND OBJECTIVES IN MODELING

Perhaps, the reason a statement of our needs and objectives in modeling did not come through loud and clear is that there is a complete spectrum of needs and objectives and that no single approach can satisfy all these needs, equally. We have heard of dimensional scales, ranging from the global scale, noted by our banquet speaker, to that of the single city block, discussed by several of you. Let us digress to look at the characteristics of these scales.

They have a unifying feature in that, as the horizontal scale is changed, there are corresponding changes in the vertical and temporal scales (Table 13-1).

Table 13-1. SCALES OF AIR POLLUTION SYSTEMS

System	Vertical scale	Temporal scale
Global	Atmosphere	decades
National	Stratosphere	years
State	Troposphere	months
Regional	Lowest mile	days
City block	Heights of buildings	hours

The time scale in Table 13-1 can be interpreted to mean either the time for effects to manifest themselves or the time inherent in taking effective, corrective action.

Purposes Served by Models

Beclouding a statement of objectives is the fact that models serve two quite diverse purposes. On one hand, models serve to test our understanding of the physical nature of the atmosphere and the sources we are modeling. If we can't model it, we don't understand it. A decade ago, we tended to say that we understood these phenomena, but lacked the programming, computational, and statistical capabilities to resolve the problem. Today, the tables are turned; we have programming, computational, and statistical capability far beyond our needs, but lack the physical inputs and concepts to fully exploit these capabilities. A model, thus serves to test these concepts and inputs. In this application models need to resolve fine detail and to have fine structure, otherwise they cannot test concepts and inputs.

On the other hand, models are used as an aid to decision making in air pollution control, and city and regional planning. In this application we could not care less about fine structure and fine detail. In fact, fine structure may obscure rather than elucidate, and we may have to seek ways to surpress the structure in the output in order to make it effectively useable for the decision-maker. It is small wonder that people talking about these two aspects of model making may have some problems communicating with one another.

Tactical and Strategic Models

Another thing that did not come through loud and clear in this Symposium was the differing tactical and strategic roles (Figure 13-1) that models are called upon to perform. Only by clearly delineating these differing roles and

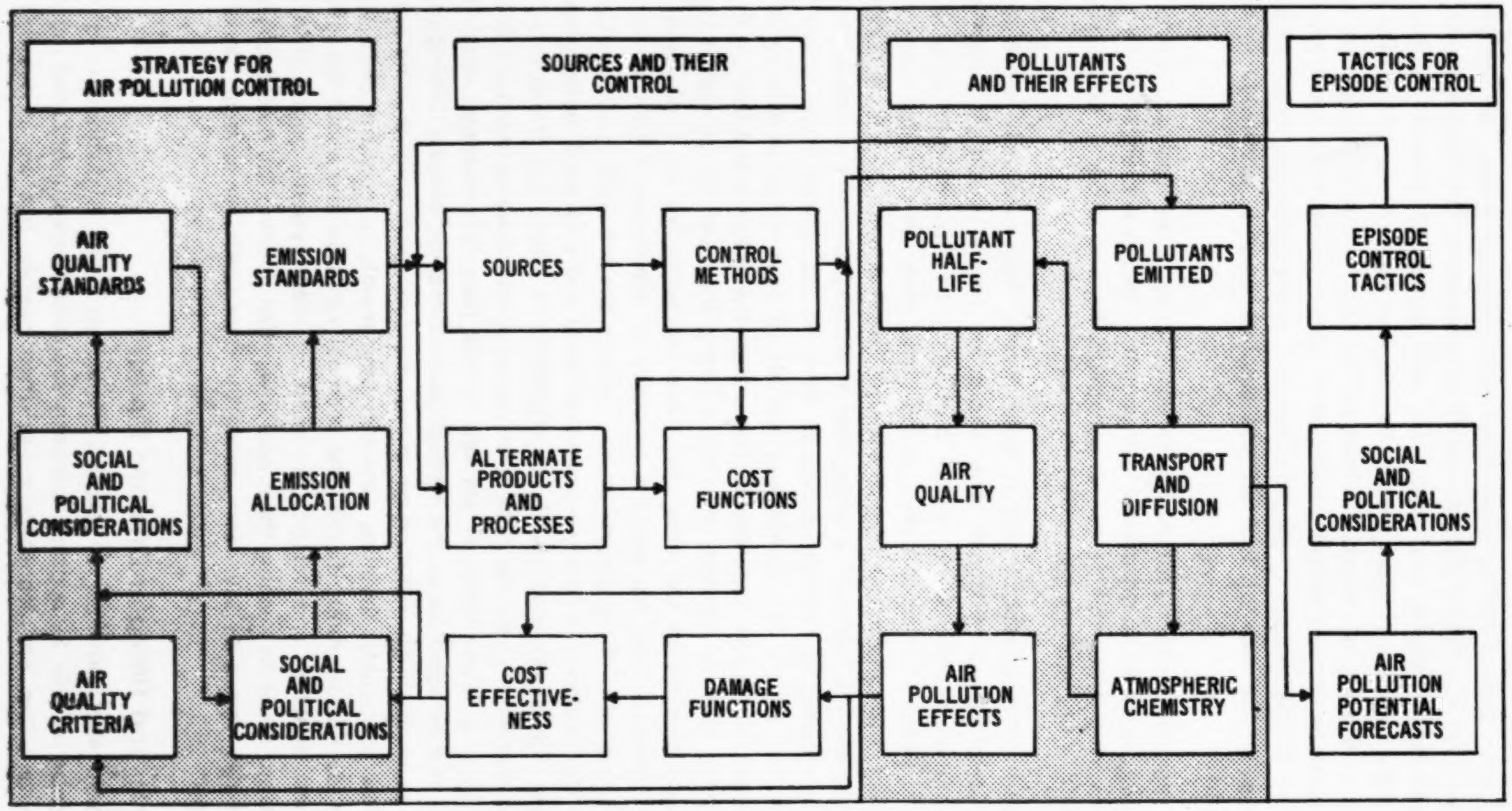
STRATEGY FOR AIR POLLUTION CONTROL
SOURCES AND THEIR CONTROL
POLLUTANTS AND THEIR EFFECTS
TACTICS FOR EPISODE CONTROL
AIR QUALITY STANDARDS
EMISSION STANDARDS
SOURCES
CONTROL METHODS
POLLUTANT HALF-LIFE
POLLUTANTS EMITTED
EPISODE CONTROL TACTICS
SOCIAL AND POLITICAL CONSIDERATIONS
EMISSION ALLOCATION
ALTERNATE PRODUCTS AND PROCESSES
COST FUNCTIONS
AIR QUALITY
TRANSPORT AND DIFFUSION
SOCIAL AND POLITICAL CONSIDERATIONS
AIR QUALITY CRITERIA
SOCIAL AND POLITICAL CONSIDERATIONS
COST EFFECTIVE-NESS
DAMAGE FUNCTIONS
AIR POLLUTION EFFECTS
ATMOSPHERIC CHEMISTRY
AIR POLLUTION POTENTIAL FORECASTS

Figure 13-1. A model of air pollution system.

recognizing their differing dimensional and temporal scales, can we plot a rational path for future diffusion-model development. The tactical model, or perhaps better stated, the model for the tactics of episode control, is inherently regional in scale, limited to a vertical scale of the lowest mile and a temporal scale of hours. In contrast to this, strategic models are best developed on state or national scales, since economic decisions and trade-offs inherent in the strategy of air pollution control are statewide, nationwide, or even (as in the case of fuel oil and gasoline supply) worldwide in their impact.

If a regional model is primarily tactical, rather than strategic, there are implications as to its diffusional component to be considered. Here, I would like to read into this record a paragraph from a paper I presented in Australia a few months ago.[1]

"Some of our regional air quality data systems may eventually prove to be white elephants, or whatever other expression we use to signify possessions entailing great expense out of all proportion to their usefullness to their owners. Some of these mistakes, which could have been avoided if the data needs of the jurisdiction had, themselves, been subject to proper systems analysis, are the result of a widespread misconception of the role of an air quality monitoring network during an alert. In the United States, there is a nationwide system for forecasting periods of high-meteorological-air-pollution potential, before they occur. The greater the extent and duration of the stagnation that is forecast, the more likely the readings at scattered air sampling stations in the area, the more representative the data from the central station, and the less the necessity to interrogate a multiplicity of remote stations. If the central station records the predicted rise in pollution levels (particularly in hourly-average-time data) and a forward meteorological forecast for a continuation of the stagnation is made, conditions exist for taking corrective measures. The existence of short-averaging-time-telemetered data from a multiplicity of stations would have corroborative value, but would not be essential to the tactical decision-making process. During other than extremely high-pollution situations, the data continually pouring out of complex continuous sampling networks tend mainly to confirm, daily, what is already known about diurnal and seasonal variation and about the effects of wind direction and velocity. In most of these systems, more time and effort are spent in keeping them operative, than in using the data acquired." I will have more to say, later, about the data needs for strategic decision-making.

Source- and Receptor-Oriented Models

We have also somehow or another, failed to make a distinction in our discussion at this Symposium between source-and receptor-oriented models. We have talked only about source-oriented models, but we all know that much work is under way on the receptor-oriented type. In the same paper referred to above,[1] I offered a rudimentary, statistical, air-quality receptor-oriented, model and, again, will quote:

"Both Larsen[2] and the author have discussed the properties of frequency distributions of air quality data and of the so-called arrowhead charts (Figure 13-2) that display them. However, until now, these data and charts have not been put to use to analyze the respective influences of source and weather on their make-up. If we were able to separate the source factors subject to human control, from the weather factors beyond such control, we would be able to synthesize the distributions of air quality data that would result from the application of specific control strategies. We would also be able to compare them with air quality objectives, expressed in like format, to determine which strategy comes closest to effecting a match.

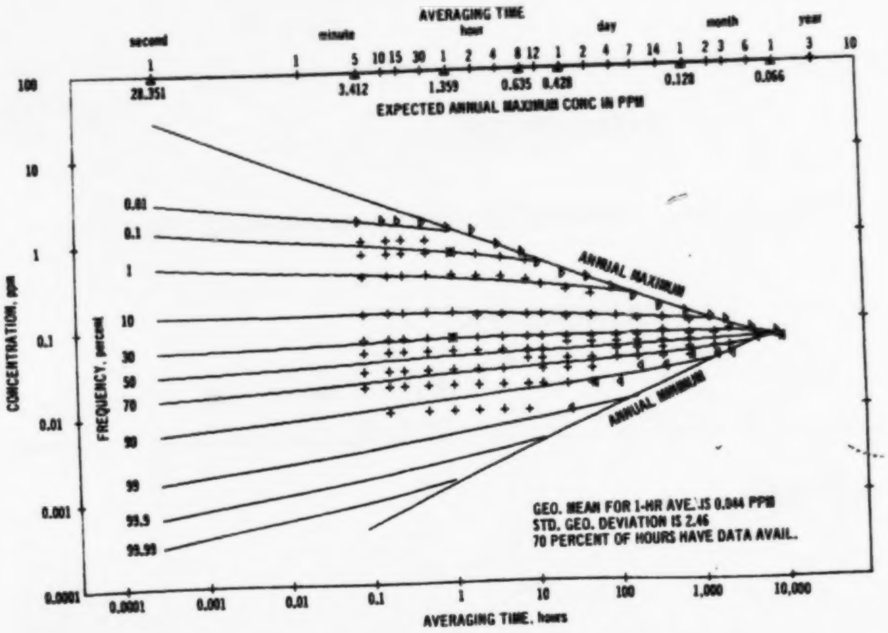

Figure 13-2. Arrowhead chart (produced by computer) for concentration vs. averaging time and frequency for nitrogen oxides in Washington, D. C. - - December 1, 1961 to December 1, 1964[2].

Figure 13-2 might have as its components, figures that look like Figures 13-3 and 13-4, respectively, the weather factors and the source factors. The analysis of Figure 13-4 for its individual components would be the converse of the emission inventory approach, in that the latter seeks to arrive at the same result through synthesis, whereas the approach just outlined seeks to

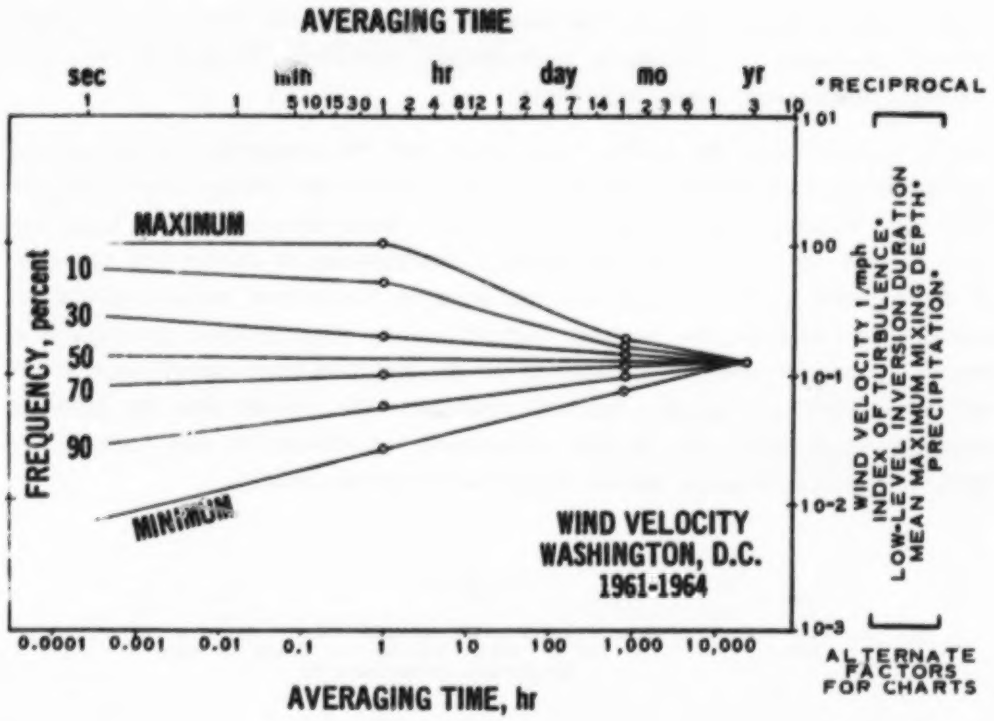

Figure 13-3. Weather factors in arrowhead chart.2

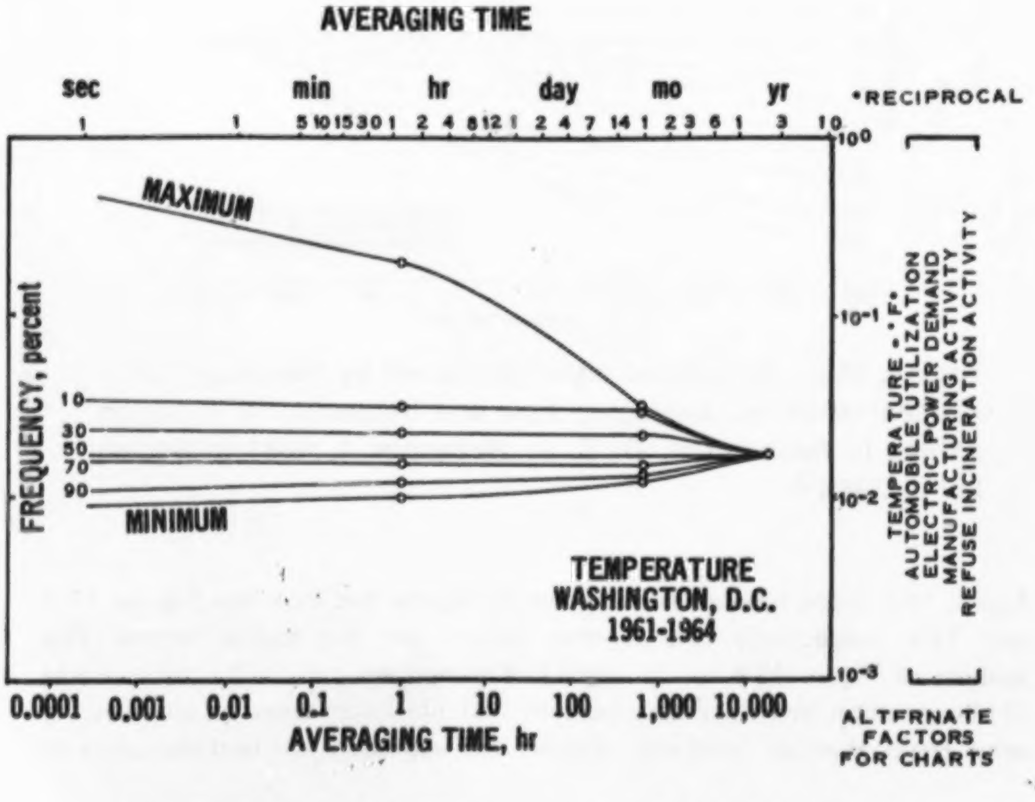

Figure 13-4. Source factors in arrowhead chart 2.

arrive at it through analysis. The two approaches should tend to check and reinforce each other, and thus improve our chances of determining the relative influence of various source categories across the averaging-time spectrum. This should give us useful leads to control strategies."

Averaging-Time Considerations

Having just shown a model that looks at the broad spectrum of averaging times, I would like to point out something we sometimes lose sight of, namely, that the adverse effects of air pollution have inherently different averaging times. The range is as follows:

Effect	Averaging time
Corrosion	year
Soiling	month
Health	day
Visibility	hour
Vegetation damage	minute
Odor	minute

It follows that the ideal strategic model will resolve all these averaging times, not just one of them. By the very nature of averaging time, once we resolve a relatively short one, all longer ones become available to us. Strategic models should, therefore, preferably resolve to averaging times, measurable in minutes.

In contrast to this, tactical models, being primarily concerned with protection of the health of a regional population from the effects of stagnation, need not resolve to such short averaging times.

CONCLUSION

In conclusion, let me repeat what our banquet speaker said last night. We have come a long way in our ability to model urban air pollution since our conference in Cincinnati on The Air Over Cities, a decade ago. We then started developing first-generation transport and diffusion models for first-generation computers. We are now developing second-generation models for third-generation computers. The computers have gained a generation on our use of them for modeling. It behooves us now to develop third-generation models to take full advantage of the generation of computers available to us. Yet, in doing so, let us heed the warnings we have heard at this symposium:

"It gains us naught, to apply better programming to inadequate physical input data and inadequate physical concepts."

REFERENCES

1. Larsen, R. I. A New Mathematical Model of Air Pollutant Concentration, Averaging Time, and Frequency. J. Air Pollution Control Assoc. *19*:24-30, January 1969.
2. Stern, A. C. The Systems Approach to Air Pollution Control. In: Proceedings of the Clean Air Conference of the Clean Air Society of Australia and New Zealand, New South Wales Dept. of Public Health, and New South Wales University, Vol. 2. Sydney, May 1969. p. 2.4.1. – 2.4.22.

AUTHORS

DARRYL RANDERSON, Ph.D. is a research meteorologist with the National Oceanic and Atmospheric Administration (NOAA) Air Resources Laboratory in Las Vegas, Nevada, and is responsible for the development of prediction techniques in forecasting atmospheric pollutant content.

RALPH C. SKLAREW, Ph.D. is a member of the Theoretical Sciences Division of Systems, Science, and Software, has engaged in applications of computer techniques to modeling high altitude chemistry, and transport and chemical interaction of air pollutants. He holds a Ph.D. in physics from the University of California.

LESTER MACHTA, Ph.D. is the Director of the NOAA Air Resources Laboratories, holds a Ph.D. in meteorology from the Massachussettes Institute of Technology. He has also worked for the U.S. Weather Bureau in the areas of radioactive fallout, atmospheric trajectories, and air pollution.

D. BRUCE TURNER, on assignment from the NOAA Air Resources Laboratories, serves as senior meteorologist for the Bureau of Critera and Standards at NAPCA. As a research meteorologist he was involved in developing dispersion models for urban areas with NAPCA's Division of Meteorology. He is a graduate of Carleton College and the University of Michigan.

J. E. CERMACK, Professor-in-Charge of the Fluid Mechanics Program at Colorado State University, is director of the Fluid Dynamics and Diffusion Laboratory. He earned a Ph.D. from Cornell in engineering mechanics and was awarded a NATO postdoctoral fellowship for study at Cambridge in 1962. He has pioneered the development of special wind tunnels for simulation of the lower atmosphere and directs a research program on low-level winds and diffusion over urban areas and complex topographies.

HARRY MOSES, a Meteorology Group Leader at the Argonne National Laboratory, holds an M.S. from the University of Chicago, a Diplomate in Meteorology from the University of Michigan and has been an Instructor at the University of Chicago, where he was also a member of the Thunderstorm Project, 1945.

L. A. CLARENBURG, Commissioner of Environmental Hygiene of the Rijnmond Authority in Rotterdam, has been head of the physical division of the chemical laboratory of the Belguim National Defense Research Council. He received his Ph.D. in theoretical chemistry in 1960 at the University of Utrecht.

BURTON FREEMAN, Vice-President of Systems, Science, and Software, is one of the founders of that company. He is an authority on large, computer code application to radiation flow and hydrodynamics. He holds a Ph.D. in physics from Yale.

DONALD H. PACK Deputy Director, NOAA Air Resources Laboratories, received his meteorology training at New York University, University of Chicago, and the University of Puerto Rico, and has worked in forecasting, turbulence, and air pollution research.

ROBERT E. STEWART, Assistant Professor of Enviromental Engineering, University of Florida, is the author of several papers on atmospheric and oceanic diffusion. He received a Ph.D. from the University of Waterloo in 1966.

14. DISCUSSIONS

INTRODUCTION

The following discussions were submitted in writing to the editor, subsequent to the Symposium. Attendees were given an open invitation to make comments on the Symposium topic and all of their responses are included in this chapter. Every author whose work was questioned was given an opportunity to read the question and to write a rebuttal if he felt one was needed. The chapter is divided into two sections; the first includes the discussions of Symposium papers and the second contains brief treatments of some additional approaches to multiple-source urban diffusion models.

RESPONSES TO INDIVIDUAL PAPERS

Lettau paper

Frank Pasquill

Regarding the effect on horizontal spread of the turning of wind with height, I would like to refer to a matter that is discussed in more detail in a paper that will shortly appear in the proceedings of a symposium on Recent Research in Air Pollution held by the Royal Society in November, 1968. Evidently, it is necessary to distinguish between the general distortion of a plume and the ultimate contribution of this distortion to enhanced spread at a *given level*. It turns out that there is a substantial time lag between these two phenomena. Examination of field data for stable conditions, available at the time of composing the foregoing paper, indicated that the effect on spread at a given level was unimportant in relation to the spread produced directly by the horizontal component of turbulence within about 5 km from an elevated source and about 12 km from a ground source.

Pasquill paper

Kenneth L. Calder

It may be appropriate to emphasize that, with very few exceptions, all urban pollution models developed in the past decade have been derived, with only minor modifications, from Dr. Pasquill's original broad estimates of spread made nearly 10 years ago and, frequently, without any serious attempt to modify his estimates for the effects of increased urban roughness or the urban heating. It seems very difficult to break with these long-standing affiliations with the Gaussian plume and $\sigma_y(x)$, $\sigma_z(x)$. In fact, there may be good reasons for not trying to, particularly since Dr. Pasquill now indicates how some appropriate modifications in the original estimate might be made to allow for urban factors. As Dr. G.D. Robinson has recently noted, it is also much easier to keep track of the conservation of mass in terms of modified Gaussian-plume (or puff) type models than in terms of theoretical models derived from the eddy-diffusity concept.

If some pessimism may have been caused among urban pollution modelers by Marsh and Withers' recent conclusions based on an attempt to model the SO_2 concentration distribution in Reading, England, then I think that Dr. Pasquill has provided the necessary antidote. Recognition of the random errors inherent in urban pollution models, such as those arising from inaccurate specification of wind direction, is very important. Dr. Pasquill's plea for more consideration of the modeling aspects for probability distributions of pollutant concentration, rather than just the spatial distribution of average values appears to be very timely.

Darryl Randerson

In the development of the Gaussian plume models one of the fundamental assumptions is that the diffusion is isotropic, so that the "exchange coefficients" do not vary spacially or temporally. Consequently, how do we justify utilizing variable σ values in the Gaussian plume models? Also, what justification is given for varying the atmospheric stability when another basic assumption of the model is that the atmosphere is neutrally stable?

Author's Reply

In my contribution to the general discussion I have included some general comments on the principle and practice of the 'Gaussian' assumption in dispersion models.

However, I must confess to being rather mystified by the emphasis in Mr. Randerson's question. I have certainly not had the impression that the assumption was necessarily prohibited either by *non-isotropic* turbulence or by non-neutral density stratification.

Sin'ichi Sakuruba

In the analysis of St. Louis dispersion data I think the vertical spread was overestimated. The tracer material, even if released from near the ground, tends to be lifted bodily, especially over an urban area. In the St. Louis case the overestimation of vertical spread of concentration is unavoidable, if the analysis is made assuming a constant height of the tracer-cloud. My inference is based on the result of dispersion data analysis made in Japan using the vertical concentration profile data.

Author's Reply

I am not sure whether Dr. Sakuruba's comment is offered primarily as an explanation of the discrepancy in the predicted and estimated values of vertical spread in daytime conditions or, generally, as a reason for questioning any apparent agreement. Clearly the mechanism to which he refers must be included in the complex of uncertainty that applies to values of vertical spread *inferred* from surface concentration, but there is, as yet, no quantitative indication of the significance of the effect in the cases analysed.

Calder Paper

Ralph C. Sklarew

Simple models, with universal applications, are much sought. Unfortunately, the relationship between averaging time and spatial resolution limits practical simplicity. A model so simple that the required calculations can be carried out by hand must, of necessity, have only gross, spatial resolution and a correspondingly long-period time average. In Dr. Gifford's model annual averages do, in fact, correspond to a spatial resolution consistent with hand calculational efforts. For abatement strategies and forecasting, where averages over shorter intervals are needed, finer spatial resolution is required, resulting in more lengthly computations.

A compromise may have been anticipated in two comments by Mr. Calder. The form of the transfer function, R, depends upon the path traversed, not just on the path length. Adopting this requirement and using a field or grid model would incorporate path dependence and, as a secondary benefit, eliminate the repetition of calculations necessary for each source-receptor pair. The second comment concerns the possible benefits to be gained from a parameter study with a large, complex model. A parameter study with such a model would indicate simplifications possible for each specific application. This, then, might become the third-generation model: a large, complex, grid model whose simplified offspring are uniquely adapted to a class of applications.

Johnson, Ludwig and Moon Paper

Kenneth Calder

Dr. Johnson has indicated that the area-source simulation used in his intra-urban model cannot be applied for very fine resolution of the concentration pattern, say on a scale of less than a city block, and that for the latter an entirely different modeling concept is necessary. This raises an important general question regarding the ultimate uses of the model and just how much knowledge of fine structure is really necessary, that is: what are the most important spatial and temporial scales in regard to damage effect or inhalation risk for the exposed population. Some clarification in terms of a system analysis will be necessary if there is to be any guarantee that the urban-diffusion modeling efforts are consistent with, and responsive to the characteristics of the overall system model. The sensitivity of the overall model to the urban diffusion model, when regarded as an input, should determine the detail and accuracy required for the latter.

Response by W. B. Johnson*

Dr. Calder's remarks are very appropriate, and I fully agree that the temporal and spatial scales treated by a diffusion submodel should be compatible with the objectives of any broader systems model of which it is part. The fundamental, practical reason why the fine scale must be treated in our model is that the only carbon monoxide (CO) data available for verification consist of point measurements near streets and buildings. The most generally available data are from Continuous Air Monitoring Program (CAMP) stations, which are located at streetside, usually at intersections. It is well known that these data strongly reflect siting effects, so much so that intercomparisons between cities are essentially meaningless.

We are attempting to design flexibility into our model so that different versions of it can be used for different purposes. Some specific foreseeable applications include the following:

1. Interpretation of the significance of existing air quality measurements (correction for siting effects)
2. Estimation of current urban-wide air quality patterns (augmentation of existing point measurements)
3. Selection of optimum control strategies (when used with a suitable systems model, which includes economic considerations)
4. Prediction of effects on future air quality of proposed or forecast changes in source distribution and strength.

The temporal and spatial scales in the completed model will be selectable to fit each of these applications.

[*] I would like to thank Mr. Wayne Ott of NAPCA and Mr. F. L. Ludwig of Stanford Research Institute for sharing their ideas on this subject with me.

In general, simulation models should probably deal with the temporal and spatial scales of pollutant concentrations that are most significant in terms of health and other effects. The provision of such air quality criteria is the domain of the medical and biological researchers and air quality management officals. Present knowledge of the time scale factor is presumably reflected in current air quality standards. However, the scale in space has not been similarly treated, nor does the definition of air quality include any spatial dimension. This situation is particularly serious when dealing with predominately ground-level sources, such as those of CO. Here, the location of a point measurement of air quality is all-important. The problem could be eased considerably if air quality were defined and measured in terms of line or area integrals. At the very least, there should be standards prescribing that point measurements be made at specific locations relative to local sources and buildings. This would substantially facilitate model verification, as well as air quality management.

Roberts, Croke, and Kennedy Paper

Kenneth L. Calder

Although this sophisticated model using superposition of instantaneous Gaussian puffs will hopefully mark the advent of a new generation of multiple-source pollution models, there may be some justification for the feeling that the trend has yet to be established. That is to say, an acceptable degree of agreement between the model predictions and observations may not be the only criterion. What is frequenty surprising in some applications is the closeness of the agreement in spite of the inherent inaccuracies of the model inputs and the extreme nature of the physical idealization involved. It is almost as though the condition for mass conservation, common to all models, in itself provided a very strong rather than an extremely weak constraint on the concentration field. Until it has been shown that such extreme complication of the present type of model is absolutely necessary in order to fit the practical observations with the required degree of accuracy, and that this complication is supported by sound physical principles, a case could be made for invoking Ockham's razor and continuing to use similar models.

Author's Response

We agree with Mr. Calder that, while the initial validation of our urban atmospheric pollution model is encouraging, there is as yet no demonstration that success is contingent upon the use of the integrated puff transport kernel. Because it is by nature a transient model, the integrated puff approach is particularly well-suited to regions characterized by significant diurnal cycling of windspeed and direction. For example, the work of Start and Markee,* with which we have recently become acquainted, indicates the importance of a puff model in evaluating dosages from hypothetical radioactivity releases in such regions. In this sense, Chicago may not be the optimal city to test the transient aspects of the model although diurnal variations in mixing-layer depth and periods of varying windspeed and direction seem to be modeled adequately. As suggested by Mr. Calder, we are currently investigating the sensitivity of our Chicago results to the choice of transport kernel.

In reference to "the extreme complication" of the model, it is important to note that the greatest demands on computer storage do not lie in the necessity for numerical integration of the dispersion kernel but are tied to the extensive efforts to establish seasonal and diurnal emission patterns and then link these refined estimates with hourly weather data and hourly estimates of mixing-layer depth to form the composite upon which the integrated puff kernel operates.

Lester Machta

It is my view that uncertainties involved in predicting weather elements six or so hours in advance raises serious questions about the usefulness of forecasts of air quality made a similar time in advance. The verification of low-level winds even in the simple terrain of suburban airports has not been particularly good; one would imagine that forecasts of wind direction and speed in a city setting would be even worse. Since the high-air-pollution episode normally involves a weak windspeed, the problem is even further complicated. Until it is demonstrated that forecasts of air quality can be provided six or so hours in advance I would be very loathe to advise air pollution control officials of such a possibility occuring in the near future.

Hilst Paper

Kenneth L. Calder

Dr. Hilst indicates that variations in windspeed were not considered in the sensitivity analysis since the dilution effect at the source and the time-of-flight effect in decay of pollutant would tend to cancel one another. This argument is not clear since we are considering a function of the form $u^{-1} \exp \left\{ \lambda x u^{-1} \right\}$. With the trajectory analysis that is involved in the TRC simulation model, it might be expected that the effects of errors in windspeed would be very complicated. If this is so, then I wonder about the validity of the conclusions regarding the decay parameter for SO_2 that enters the model in the combination $\lambda x u^{-1}$. I personally would feel that juggling with the half-life of SO_2 and reducing it from 3 hours to 1 hour in order to improve the agreement with observation is a rather risky business at this stage of the game, before a full error analysis has been made for windspeed.

---

*Start, G. E., and Markee, E. H. Jr., Relative Dose Factors from Long-Period Point Source Emissions of Atmospheric Pollutants, AECL–2787, Proc. USAEC Met. Info. Meeting, Chalk River, Ontario, 1967, pp 59–76.

Finally, although Dr. Hilst says that the TRC model has been extensively reported over the past 2 years, it is my feeling that the available accounts may not be sufficiently detailed to allow independent application of this model to other pollution problems. I would like to urge Dr. Hilst to publish, as soon as possible, a full technical report so that others are able to utilize this sophisticated model.

D. Bruce Turner

In additon to the eight errors listed by Dr. Hilst, I think there is a ninth, which might be called grid-size error. This is most noticeable when calculations made at grid-points are compared with measurements made at non-grid-point locations. Specific wind directions will cause individual pollution plumes to affect the measurement station, yet pass between grid-points and vice versa. This can be overcome by models able to calculate concentrations for any point. Where this effect was noticed, the model being used made calculations only at the center point of each grid square. This was because a technique had been developed to determine the concentration at the center point of an area-source square resulting from the emissions coming from within that square, but was not developed for points other than the center. Even with a model restricted to making computation at the center of each grid square this grid-size error can be made less noticeable if measurement stations used for model validation are also located as close to the center of grid squares as is practicable.

Sakuraba Paper

Frank Pasquill

The measurements of vertical spread described in Dr. Sakuraba's paper are obviously of considerable basic value and will no doubt be widely studied. However, one should be careful not to place a literal interpretation on the description of the observed vertical spread in terms of the stability categories that I have specified for use in the absence of more sophisticated data on diffusive conditions. As I noted in my own paper in this symposium these categories were specified for airflow, characteristic of a land surface with small to moderate roughness. On the other hand, it seems likely that Dr. Sakuraba's results also reflect the influence of sudden and appreciable changes of roughness on an air stream passing from the sea over a rather irregular coastline instead of the effect of stability differences alone.

Fortak Paper

Kenneth L. Calder

Dr. Fortak's discussion again emphasizes the point first raised by Dr. Pasquill at this meeting, that while a calculated spatial field of short-period average pollution concentration cannot be expected to agree very closely with that actually observed, the statistics obtained from an ensemble of such calculated concentration fields may well be in close agreement with reality.

As a small but important detail I was interested to see that Dr. Fortak has considered the numerical integration errors associated with the choice of grid size for the area-source specification. His conclusion that an area size of the order of 50 meters by 50 meters may be required for a satisfactory representation of a large number of point sources, is noteworthy, since, I believe, this is much smaller than the size used in some urban models currently being recommended for operational use.

Sheih, Davidson, and Friend Paper

Kenneth L. Calder

One point I found rather confusing in Drs. Sheih, Davidson, and Friend's paper was the initial statement that the model was derived from the statistical theory for turbulent diffusion, although later in the paper they stated that the model was semi-empirical and not derivable from known physical concepts. It would seem that the latter is a more true description since all the adjustable parameters and constants of the model are apparently derived by fitting observational data for sulfur dioxide in New York City. If this is so, then agreement between the model predictions and actual observations may be less impressive than for some other models where the parameter values are estimated independently.

The considerable effort made in this study to develop an adequate method for numerically integrating the emissions from a continuous area source is noteworthy and in strong contrast to the crude procedures used in many other models.

Mahoney, Maddaus, and Goodrich Paper

Harry Moses

One must bear in mind that the concentrations of a given pollutant such as SO_2, at a given station, is a function of several variables. Windspeed is one of these variables. It is possible in a multivariate system to find that several of the individual independent variables correlate poorly with the dependent variable, but when taken together, show a high multiple correlation.

It is also worth pointing out that the windspeed is a difficult variable to define. For example, at some distances from an elevated source such as a tall stack, an increase in windspeed is associated with an increase in pollutant concentration on the ground, because the stack plume rise is reduced during high winds. With a ground source an increase in windspeed results in lower concentrations downwind because of increased turbulent mixing. One must take such relations into account when using windspeed as a variable in a regression type model. Thus, it is not surprising to find that the zero order correlation of pollutant concentration with windspeed or even the reciprocal of windspeed is unimpressive, even though the windspeed has an ultimately important influence on the pollutant concentrations.

GENERAL DISCUSSION

Vertical Circulations and Eddy Diffusion Coefficients

James P. Friend

Until a dynamic meteorological model of urban atmospheres can produce circulations which are physically reasonable, attempts to incorporate circulations having vertical motions into the present dispersion models are equivalent to introducing new parameters to an already highly parameterized system.

It has been suggested that solving a diffusion equation with eddy diffusion coefficients (K's) would be more scientifically acceptable than application of Gaussian plume formulas. It seems to me, with the present state of knowledge, that this is equivalent to trading one set of parameters for another. We simply have no known physical laws by which values of the K's can be determined as functions of space, time, and meteorological conditions. There has been a plea by Dr. Pasquill and others here for more research in meteorological physics. One can do no better than to second that plea. Perhaps the resulting knowledge will eliminate the need to apply either of the two systems mentioned above.

Generalization of Vertical and Crosswind Spread

Frank Pasquill

I am, of course, primarily interested in the meteorological physics required in the design of systems for the prediction of air pollutant concentrations and in the need, which seems to be inevitable, for the adoption of some generalization about the vertical and crosswind spread of material.

Some models appear to generalize about the standard deviation of particle spread in vertical and horizontal directions, σ_y and σ_z, by using practical observations of the distribution of urban air pollutants. Although not unreasonable, it should be emphasised that such a procedure cannot be accepted automatically as justification for applying the model to flow and terrain conditions other than those obtaining in the pollutant survey. For the most useful generalization we must seek independent specifications of σ_y and σ_z in terms of meteorological parameters that can either be measured at the time in question or estimated from routine meteorological data.

The specification of σ_y and σ_z may be explicit (as from the statistical theory) or implicit (as from the gradient-transfer theory, and solution of the so-called classical equation of diffusion). It seems to be the view of some participants in this symposium that there is something conceptually superior in the use of the implicit classical diffusion equation. I find this view surprising in light of the essentially empirical nature of this approach both in principle and in application (i.e. no *a priori* specification of K is available to us). On the other hand, I have not claimed (as stated in one contribution to the discussion) that the K-approach is entirely unacceptable. In my own paper, however, I do argue that the approach is physically plausible and practically equivalent or superior to other approaches only for the case of *vertical* spread from a source that is *effectively* at ground level.

Finally on this question of the specification of σ_y and σ_z, it may be worth remembering that, in general, the most accurate specification appears to be possible for short ranges from continuous sources. On the other hand, the greatest uncertainty still seems to apply to the spread of an individual isolated puff.

Regarding the incorporation of estimates of spread in the prediction systems I have two other comments to offer. The first concerns the term *Gaussian*, to which there has been frequent reference in this symposium. It may be recalled that the Gaussian distribution follows from the classical diffusion equation *only when K is constant* and, consequently, the spread is proportional to the square root of the time. This latter relation has not been generally observed. Furthermore, the empirical support for the Gaussian shape comes only from *ensemble* averages of time-mean crosswind distributions from continuous sources, or of vertical distributions from effectively elevated sources. It has been noted, however, that the precise magnitude of crosswind spread seems unlikely to be of prime consequence in the distribution arising from a close network of multiple sources!

On the other hand, there is no real basis for assuming vertical Gaussian distribution from a ground-level source—instead the theoretical and empirical indications point to a shape between Gaussian and simple exponential. Furthermore, there is no reliable guidance available on the distribution in a puff. From all this it may seem rather irrelevant to attach great significance to the assumption of Gaussian distribution. The Gaussian shape may be convenient to use, but a 'center-concentrated' plume with a linear fall-off of concentration from the center may turn out to be just as satisfactory, in practice, for passive plumes or puffs. (It seems that the distribution in a hot plume or puff, initially dominated as it must be by the circulation and entrainment induced by relative motion, may, however, have a distribution much flatter than Gaussian).

My second comment concerns the suggestion that a 'sequential' puff representation of a *continuous* source may be desirable. While in principle this may seem preferable, permitting allowance for variable source strength and widely variable wind direction and diffusive conditions, I find it difficult to see how the approach can be advantageous in practice, unless it is in fact possible to specify the trajectory and spread of an individual puff. On the contrary, all experience points to the fact that the spreads of individual puffs in the same general airstream differ widely, and that reasonable accuracy in specification can be expected only on the basis of an *ensemble average*. In this context it does not seem to me to have been made clear how the envisaged 'puff' predictions are expected to be superior to those that would follow from considering the effects of continuous releases over arbitrary intervals of appreciable length.

Finally, there have been several references to pollutant movement within the confines of a street, and indeed one of the papers has considered some aspects thereof. It seems to me that there are two opposite extremes in the types of estimates that might be attempted. On one hand, as already in the general discussion, it may be possible to make a useful estimate by considering, on an individual basis, the effective enclosed volume of air available to accept the emission from some position in the street. It may be useful to add to this the refinement of a ventilation coefficient defining the rate at which this air is changed, so providing a more realistic estimate of the rate at which the pollutant concentration might build up. At the other extreme, for a statistical estimate of the effect over a complex of streets, it might be possible to make progress by developing a two-layer model on the following basis:

In the lower (street) layer one might reasonably assume that there is no advection of the air flow and the pollutant but only a vertical exchange with the upper (above roof) layer. Only in this upper layer can one reasonably expect the spread to follow the 'laws' previously specified for plumes. Essentially, the first requirement is to specify the distribution of sources in the upper layer and in the lower layer. The latter must then be represented as vertical fluxes at the boundary between the two layers. The concentration at any position in the lower layer will be determined by the concentration developed immediately overhead in the upper layer, by the local rate of (vertical) ventilation of the lower layer and by the local emission rate in the lower layer.

Physical-Scale Model Advantages

J. E. Cermack

A basic deficiency appears in all of the numerical models of urban diffusion presented in this Symposium—a deficiency of vital importance, particularly for the "source-based" models. This deficiency is the unrealistic representation by Gaussian plumes of diffusion from sources located within the urban complex. In particular, the diffusion of carbon monoxide from street-level sources is dominated by local geometry of the city and local meteorological conditions. The only feasible approach to reaching some understanding of this type of diffusion is through the study of physical models—scale models of typical city complexes placed in flows simulating thermally stratified atmospheres. Models on a scale of 1:200 to 1:1000 such as the 1:400 scale model of diffusion over Denver shown in a motion picture at this Symposium permit detailed diffusion measurements which can lead to some general conclusion on diffusion characteristics in city complexes. Utilizing even a modest amount of knowledge gained in this manner, the design of new numerical models should lead to gross improvement in their predictive capability. Physical models can be utilized to great advantage for "receptor-based" numerical models to help understand the relationship between source location and receptor response. This can be accomplished for particular urban settings under specified meteorological conditions.

In conclusion, I wish to emphasize that physical modeling of diffusion can be of great assistance in the operational aspects of air pollution control. This will be particularly true if the modeling is accomplished by a team composed of specialists in fluid dynamics and atmospheric sciences working in a meteorological wind tunnel of a type for which similarity of atmospheric flows has been verified.*

Second Generation Models—Finite Difference Approximations

Darryl Randerson

Several of my colleagues have expressed concern about the limitations in the Gaussian models and, consequently, forsee the advent of "second generation" prediction models. I would like to suggest that these new models will not be Gaussian models and will be free of the restraints inherent in such models. The new generation models will be both descriptive and conceptual and may represent finite-difference approximations to initial-value problems that arise in fluid dynamics. Special attention will be given to the calculation of time-dependent fields so that micrometeorological phenomena can be simulated in time and space and subsequently utilized to predict the

---

*Cermak, J. E. and Arya, S. P. S. Problems of Atmospheric Shear Flows and Their Laboratory Simulation. Int. Jl. of Boundary-Layer Meteorology *1*: 3-23 January 1970.

transport of effluvia over non-uniform terrain. Initial input for these new models will be generated from information and knowledge collected from past and future studies of urban meteorology. These new models will be closely related to meteorological parameters, to chemical behavior of effluvia in air and sunlight, to topographical effects, and to the generation of a representative source term. Consequently, these models may become quite complex; however, they should eventually lead to a rather fundamental model for predicting the transport and diffusion of matter through the atmosphere.

Tabluation Techniques

Harry Moses

A substantial amount of work has been carried out at the Argonne National Laboratory on a method called the Tabulation Prediction Scheme. Since it is relevant to the problem of developing and using multiple-source urban air pollution models, I should like to describe it briefly and show how it may be applied.

Description of Prediction Tables

This technique involves the use of a set of tables that show the relation between air pollutant concentrations and those meteorological variables that affect concentration levels. Hourly readings are used. The meteorological variables are arranged in an ordered sequence. For each entry the associated probability distribution of pollutant concentration is presented as shown in Table 14-1. For each combination of meteorological variables, sulfur dioxide (SO_2) concentrations are given, representing the minimum, the 25, 50, 75, 90, 95, 98, and 99 percentile values, and the maximum. The interquartile range, the difference in SO_2 concentrations between 75 and 95 percentiles; the mean; the standard deviation; and the number of cases for each entry are also presented. These data represent actual measurements obtained by the Chicago Telemetered Air Monitoring (TAM) stations during a 2-year period.

To arrange combinations of meteorological variables into an ordered sequence, appropriate group intervals must be selected for each.

Wind direction values may be grouped into three class intervals; time of day, also into three; windspeed into five; and so on. A number is assigned to each class interval, let us say, in increasing order. Any combination of meteorological variables corresponds to a equivalent-digit number. If letters are assigned to each class of each variable, then any combination would correspond to an equivalent-letter word. Since the combinations of meteorological variables are ordered, it is possible to look up any set of meteorological conditions just as one would look up a name in a telephone book or a word in a dictionary.

Table 14-1. TABULATION PREDICTION TECHNIQUE

Wind dir, degrees	Ceiling, feet	Wind sp, kt	Temp, deg F	Hour, CST	Percentile values of SO_2 (ppm) concentrations											Mean	St dev	Freq
					Min	25	50	75	90	95	98	99	Max	75-25	95-75			
0–140	7000–****	0– 3	70– 79	0– 3	0.0	0.0	0.0	0.0	0.0	0.0	0.0	0.0	0.0	0.0	0.0	0.0	0.0	0
0–140	7000–****	0– 3	70– 79	4–15	0.01	0.01	0.03	0.04	0.06	0.06	0.06	0.06	0.06	0.03	0.02	0.03	0.0183	6
0–140	7000–****	0– 3	70– 79	16–23	0.01	0.01	0.01	0.01	0.01	0.01	0.01	0.01	0.01	0.0	0.0	0.01	0.0	1
0–140	7000–****	0– 3	80– 89	0– 3	0.0	0.0	0.0	0.0	0.0	0.0	0.0	0.0	0.0	0.0	0.0	0.0	0.0	0
0–140	7000–****	0– 3	80– 89	4–15	0.02	0.02	0.02	0.03	0.03	0.03	0.03	0.03	0.03	0.01	0.0	0.02	0.0050	2
0–140	7000–****	0– 3	80– 89	16–23	0.02	0.02	0.02	0.02	0.02	0.02	0.02	0.02	0.02	0.0	0.0	0.02	0.0	1
0–140	7000–****	4– 7	10– 19	0– 3	0.01	0.01	0.02	0.02	0.02	0.02	0.02	0.02	0.02	0.01	0.0	0.02	0.0047	3
0–140	7000–****	4– 7	10– 19	4–15	0.0	0.0	0.0	0.0	0.0	0.0	0.0	0.0	0.0	0.0	0.0	0.0	0.0	0
0–140	7000–****	4– 7	10– 19	16–23	0.08	0.08	0.10	0.12	0.12	0.12	0.12	0.12	0.12	0.04	0.0	0.10	0.0200	2
0–140	7000–****	4– 7	20– 29	0– 3	0.02	0.02	0.02	0.02	0.02	0.02	0.02	0.02	0.02	0.0	0.0	0.02	0.0	1
0–140	7000–****	4– 7	20– 29	4–15	0.09	0.10	0.15	0.20	0.21	0.21	0.21	0.21	0.21	0.10	0.01	0.15	0.0460	4
0–140	7000–****	4– 7	20– 29	16–23	0.05	0.05	0.07	0.10	0.27	0.27	0.27	0.27	0.27	0.05	0.17	0.12	0.0864	4
0–140	7000–****	4– 7	30– 39	0– 5	0.01	0.01	0.03	0.04	0.05	0.06	0.08	0.08	0.08	0.03	0.02	0.02	0.0175	17
0–140	7000–****	4– 7	30– 39	4–15	0.01	0.02	0.04	0.09	0.13	0.15	0.28	0.29	0.30	0.07	0.06	0.06	0.0650	24

The probability distribution of SO_2 concentrations, based on past history, is given on the same line in the table as the combination of meteorological variables. In practice, the assigned letters or numbers are converted to actual ranges as shown in Table 14-1.

Applications of the Tabulation Prediction Scheme

The Tabulation Prediction Scheme may be used in at least three different ways:

1. As an adjunct to a source-oriented model.
2. As a means for monitoring changes in the source distribution over an area.
3. As a receptor-oriented urban air pollution model.

Use with a Source-Oriented Model

Assuming that the sources remain constant for the same hour of the day, the same season, and the same meteorological conditions, including air temperature, then the source-oriented model provides a single concentration value for each point on the calculation grid over an urban complex. The Tabulation Prediction Scheme shows that, historically, for example, during the past two years, not a single value but a distribution of values has been observed. The Tabulation Prediction Scheme thus provides a measure of the upper limit of accuracy obtainable, at least at the monitoring stations, by the source-oriented model. The source-oriented model may overcalculate in some parts of a city and undercalculate in others. Similarly, systematic errors may occur under some meteorological conditions such as different wind directions. The information provided by the tables of the Tabulation Prediction Scheme could, thus, serve as a basis for judiciously adjusting the calculations of the source-oriented models.

Monitoring Changes in the Source Distributions—The tables of the Tabulation Prediction Scheme must be continuously updated if they are to be used most effectively. One may accomplish this by comparing the distributions, obtained during a 1- or 2-month period, with the values in the tables. Appropriate tests for statistical significance may be used for this purpose. Automatic updating would, of course, be accomplished on a computer.

As a part of the updating program one might apply triangulation techniques to the data from two monitoring stations, to detect a significant change in the source strength over a given area. In Figure 14-1, for example, station 1 shows an increase in a ∠ 1, with respect to the base-line between stations 1 and 2. Similarly, station 2 shows an increase in the ∠ 2. Such an analysis indicates the area where the source inventory should be reexamined. When a network of monitoring stations is available, the lines from each station, indicating the direction in which a change in source strength occurred,

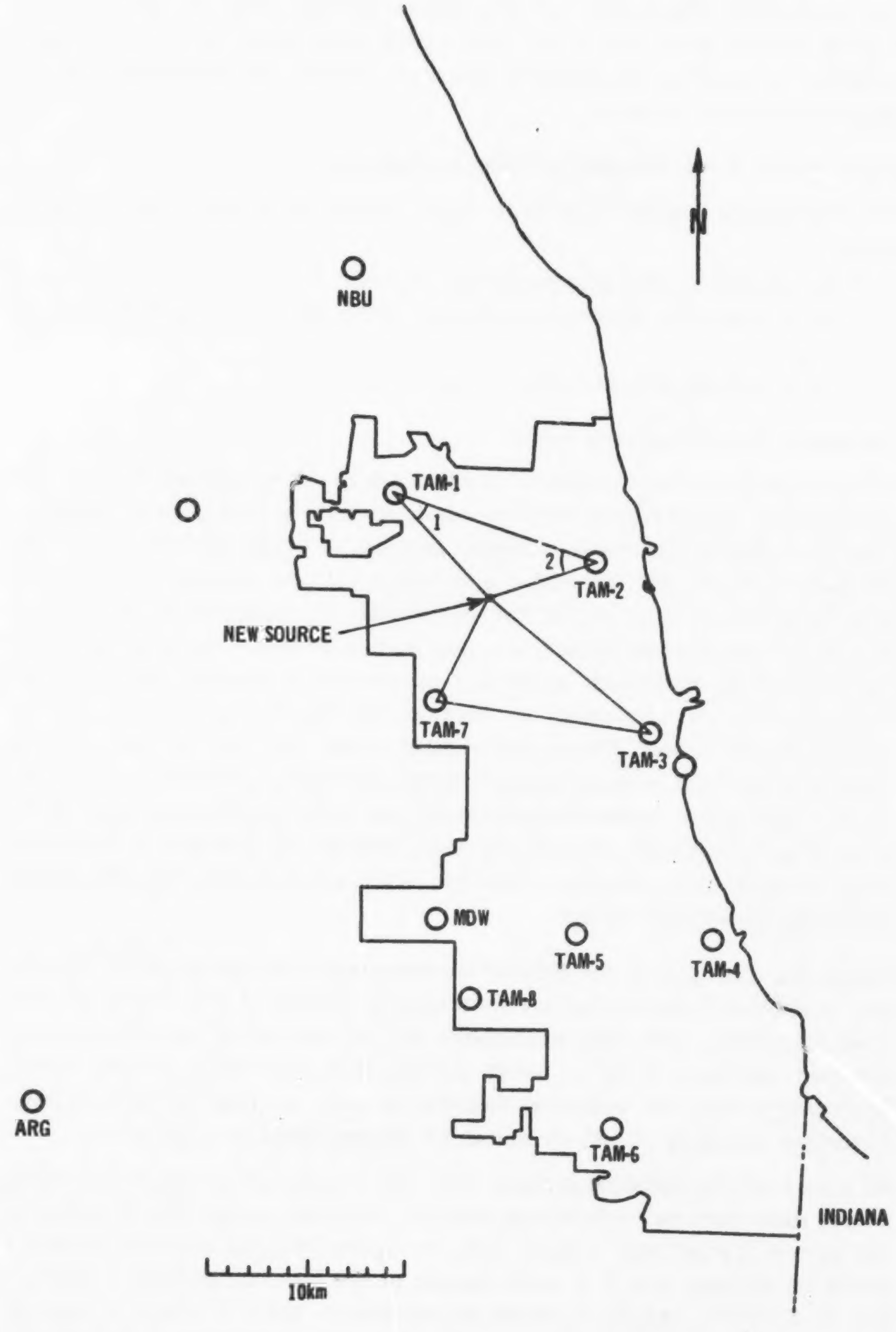
N
NBU
TAM-1
1
2
TAM-2
NEW SOURCE
TAM-7
TAM-3
MDW
TAM-5
TAM-4
TAM-8
ARG
TAM-6
INDIANA
10km

Figure 14-1. Identification of change in source inventory by triangulation techniques and tabulation prediction scheme.

delinate the area to be investigated in order to update the source inventory. This is yet another way in which this technique may be used with the source-oriented model.

Use as a Receptor-Oriented Urban Air Pollution Model—In cities with a network of pollutant monitoring stations, the Tabulation Prediction Scheme may be used to develop a receptor-oriented model. For example, for a given set of meteorological conditions, the 50th percentile SO_2 value may be determined from the tables, and lines of equal concentrations (isopleths) may be drawn. Areas showing values of SO_2 concentrations above a critical predetermined value such as 0.3 ppm would be delineated. Similarly, 75 or 90 percentile charts may be drawn. In this way, the Tabulation Prediction Scheme would serve as an urban air pollution model that would provide the basis for action by a municipal air pollution control office to request public utilities or other large users of coal to switch to gas where dual equipment existed. The Tabulation Prediction Scheme was used in this manner in a recent air pollution incident control test in Chicago, Illinois.*

A word of caution concerning the drawing of isopleths over a city where there are an insufficient number of stations is appropriate. The heterogeneity of pollutant concentrations over an urban complex coming from large, widely distributed, discrete sources, must be considered in drawing isopleths. For optimal use of the Tabulation Prediction Scheme information on the lack of uniformity or "lumpiness" in the pollutant concentrations should be obtained. Traverses with mobile air quality measuring equipment would provide such valuable insight into the spatial distribution of pollutants.

Computerized equipment to provide isopleths of a given variable over an area are described in the John, Ludwig, and Moon, and Mahoney, Maddaus, and Goodrich papers. These could be adapted for effective use with the Scheme. The Tabulation Prediction Scheme cables could be stored in a computer. Using forecasts of hourly values of the pertinent meteorological variables, prepared by a human forecaster as input, the computer can provide maps, either on a cathode ray oscilloscope or on paper, of the 50th, 75th, 90th or other percentile isopleths of a pollutant, for each hour of the forecast period.

Although the Tabulation Prediction Scheme is easy to use, a considerable amount of insight is necessary to develop an effective set of tables. The selection of appropriate meteorological variables or even the division of each variable into optimal group intervals requires a substantial amount of calculation. As an example: the levels of SO_2 in a residential area are closely related to temperature; the lower the temperatures, the more coal is burned, hence, the more SO_2 is produced. Hence, one is inclined to select temperature as one of the variables in the tabulations. The "cooling power," which is a function of temperature and windspeed, must also be considered before deciding whether this function, or the temperature, should be used.

---

*Croke, Edward J. and Samuel G. Booras, The Design of an Air Pollution Incident Control Plan, APCA No. 69-99. Presented before the 62nd Annual Meeting of the Air Pollution Control Administration, June 1969. New York, N. Y.

In spite of the work and skill required to construct an effective set of tables, their usefulness appears to be worth their cost. Every technique available should be used to provide the air pollution control official responsible to the public, with the best possible information to assist him in his decisions. The combination of the Tabulation Prediction Scheme with the source-oriented model results in a hybrid model, which appears to hold greater promise than the purely source-oriented or receptor-oriented models.

Mathematical Refinements

B. E. Freeman

During the Symposium we have heard a comprehensive exposition of the formulation and application of air pollution models to a number of urban areas via the plume and puff approximations. While many of the participants in the Symposium have pointed out shortcomings of these models and others have called for a more complete treatment of physical phenomena in the models, there has been no discussion of mathematical techniques to remedy these dificiencies. Fortunately, considerable experience has been gained with suitable methods of mathematical approximation which, in my mind, hold out substantial hope of removing many of the objections to the existing models. Clearly, it is not possible in these passing remarks to set out in detail the methods, which have been developed and are now being improved. Consequently, I shall attempt to summarize, briefly, the general characteristics of one refined model, its advantages, and its prospects.

Before I turn to the model itself, let me add another objection to those currently used; they are based on quasi-analytic solutions of *linear* equations for the evolutions of pollutant concentration. Now, in fact, many of the processes governing the fate of pollution are *nonlinear*; the reactions involving the components of photochemical smog, the micrometeorology of the urban basin, the modification of the eddy diffusion constants by the heat island of the city, and many others. These processes can only be taken into account in a mathematical framework more general than the plume and puff models.

The tested and successful method employed in many field problems is the grid or cell model, based on difference approximations to the partial differential equations governing the phenomena in question. In this approach, space and time are divided up into cells and the dependent variables are approximated through averages over the cells. If the cells are made to diminish in size in a suitably chosen manner, the solution of the difference equations will approach that of the differential equations.

The difference-equation grid model is not a new technique. In fact, this method was applied some 25 years ago by von Neumann to solve the hydrodynamical problem of the behavior of a nuclear explosive—one of the first applications of the digital computer. Since that time the difference-equation method has become much more sophisticated. With advances in the capacity and reliability of computing machinery and in numerical methods, it has become possible to attack an increasing number of physical problems —to mention only a few: astrophysicists model the evolution of the interior of stars and the characteristics of the radiations from the atmospheres of the stars; physicists describe nuclear explosion fireballs in the atmosphere and duplicate the hypervelocity impact of pellets on plates. The technique has been applied to the description of the natural enviroment, too. Of particular relevance is the progress, in recent years, on the dynamical modeling of global weather.

Now let me mention just a few of the characteristics of the model, that can be developed in modular fashion by adding new physical phenomena as warranted by our knowledge of them. First, the pollutants themselves are followed in space and time. The governing equations are the conservation equations for the several pollutant species necessary to describe urban pollution. The equations take account of the rate of change of the pollution concentrations in all of the cells of the urban basin due to (1) advection of the pollutant to neighboring cells by the wind field, (2) spread of pollutants through eddy diffusion, (3) injection of pollutants from the sources of pollution within the urban area, (4) chemical reactions which may take place within the cell, and (5) advection of pollutants from outside of the volume of interest. Each of these processes is modeled by adding an appropriate numerical term to some or all of the cells of the basin grid. The time history of pollution in the basin then evolves by time increments that simulate the actual temporal development. In such a field description of the pollutant concentrations, there is no difficulty added in accounting for nonlinear processes over linear ones.

With this model not only is it possible to take chemical reactions into account, but by supplying the wind field, diffusion coefficients, and sources in the usual way, the multi-source urban pollution application can also be solved, as in present models.

In successive modules it will be possible to take account of processes determining the wind field and the diffusion coefficients themselves. The meteorological equations, for example, can be solved by difference approximation, to predict the local modification of the wind field and thermal stratification by topography, diurnal solar heating, and heat sources within the city. The formulation is also compatible with the incorporation of models for the growth and decay of turbulence in order to evaluate eddy diffusivity as a field quantity. While it is to be expected that the modeling of the hydrodynamic equations will be quite expensive in computer time, in contrast to the nominal computer use required by the pollution grid model; some economics can be achieved by using implicit methods to increase the size of the time increment interval.

As in the case of the numerical weather model, we can only conjecture what the ultimate value of the grid model for air pollution will be. But to me it is clear that substantial improvements in physical and mathematical verisimitude can be achieved. As mathematical approximations are removed, the challenge will lie in taking advantage of the growing volume of urban pollution data to improve our understanding of the underlying physical processes. Only this way can we hope to make air pollution models quantitatively useful.

Consumer Applications

L. A. Clarenberg

I would like to approach the problem of multiple-source diffusion models from the consumers' point of view, that is from the standpoint of a person with some responsibility for the air quality in a region. After listening to the lectures given at this symposium I have the feeling that there may be a discrepancy between the model builders' aims and the consumers' needs.

The primary responsibility of an air pollution control authority is to see that standards set for a pollutant are not violated. Air pollution standards specify concentrations and corresponding percentages of the time these specified concentrations may be exceeded. This brings forth a need for maps on which iso-probability lines are drawn, that is lines of equal probability that a specified concentration has been exceeded, permitting an immediate evaluation of the air quality in a town or a region. The position of iso-probability lines is affected only by long-term (1-year) changes.

The models we have been discussing, thus far, calculate the joint contribution of a number of fixed sources to the concentration at a fixed site, e.g. a sampling station, for a given set of meteorological conditions. On a map the location of the sampling station with respect to any one source can be expressed exactly in terms of a downwind distance (x) and a lateral distance (y). I would like to name this a "space frame," in which all subsequent calculations are carried out. The result is a map covered with iso-concentration lines, pertinent to that particular set of conditions. For air quality control these lines are of little value, since their positions on the map change as meteorological conditions change. So, one might get the impression that model building has become a game—a word used by Dr. Roberts in this context—being played for its own sake, however, one that loses track of practical needs.

Turbulent diffusion is a process proceeding in time. Theories, describing the diffusion of a puff, are worked out in a "time frame." This means that one can predict the volume of a puff being transported through the atmosphere after a lapse of time, t; one cannot predict the exact position of the center of that puff relative to its origin. One can, however, predict the probability of finding the center after a time, t, in any one position relative to the origin.

If multiple-source urban diffusion models could be worked out in a pure time frame; then the concentration in any one location could be found by probability, for a given set of meteorological conditions, at the same time giving accurate prediction. By repeating the calculation for a great number of meteorological conditions and assigning the probability of occurrence, the most probable concentration distribution, to each set of conditions. From it is only a small step to produce iso-probability lines.

I have three reasons for advocating this idea. First, it seems to me that the input of meteorological data becomes much easier. Second, if ever models are to be made for pollutants other than sulfur dioxide—for example, oxidants— in which case one can neither locate nor specify the sources exactly, one would have to (as far as I can see) rely on "time-frame models." Last, but not least, results would be in better compliance with practical needs, especially when estimates of reliability are required for the predictions.

Uses, Limitations and Accuracy of Models

James R. Mahoney

A number of detailed, first generation, models for urban air contamination have been discussed at this meeting. In each case it would be desirable to have a statement of the specific *uses, limitations* and *accuracy* of the model. Such information would facilitate both applications of existing models and development of new models.

The following specific observations result from several of the technical discussions during the Symposium:

— The uses and limitations of the diffusion models can be stated in terms of the time and space scales appropriate for each model. Many of the early models have been applied to a wide spectrum of scales, from near-instantanous analysis to annual-average calculations in the time dimension, and from a few meters to tens of kilometers in the space dimension. Obviously the grid size for input data and for calculations should reflect the scale of the intended, model output data.

– The greatest deficiency in the present models is the lack of detailed meteorological data for the urban regions being described. It is futile to refine existing emission data and to reduce grid size in most of the model calculations when the windspeed and direction, atmospheric stability and mixing-depth data are all derived from a single observation site within the region. The new observation networks in some major urban areas have surface meteorological instruments at several sites; the data from such observations should be included in the model refinement process, whenever possible. Significantly improved *vertical* meteorological observations are also required for the development of improved models.

– Current models lack descriptions of chemical and photochemical transformations involving the various pollutants. Realistic, dynamic chemical models should be verified with detailed and extensive field observations; the first examples of such information are just now becoming available.

– Loss processes, particularly absorption and washout of pollutants, are not sufficiently understood for incorporation into existing models, but current field studies may provide some data on loss mechanisms that can be used in refined diffusion models.

– Model verification schemes, based upon comparisons with measured air quality, must be analyzed carefully. Errors and small-scale phenomena, reflected in air quality observations at single sites, may be as important as errors in the model input data. Whenever possible, model results should be compared to time and/or space averages of observed air quality data.

– It is possible that data from remote sensing instruments, presented in the form of average concentrations over extended horizontal paths, may be superior to data from individual observing sites for use in urban diffusion models. The use of spatial average concentration data would reduce the errors caused by local sources near the observing stations.

– Current models neglect the initial field of observed concentrations in the preparation of short-period (e.g. 1-day) forecasts. Model forecasts may improve if the *changes in concentration* from a known initial field are calculated as the predictive parameters.

– Many current diffusion models are used to describe regions containing an urban center and surrounding suburban and rural areas. When the spatial gradients of the emission rates are large only in one section of the model region (the central urban area), the use of *grid telescoping* in that limited section can improve model accuracy without imposing excessive computation time and data storage requirements.

– The expense and the importance of urban air-quality monitoring programs in operation, or in development, justify a significant effort toward the development of sophisticated advection-diffusion models that can make optimal use of the data being collected.

Approach to a Universal Model

Robert E. Stewart

I am somewhat disappointed by the current method of attack for solving the problem of urban air pollution prediction. I find that, for the most part, one has to postulate "not so good" assumptions in order to *make* the particular urban diffusion model fit the data. For example, the Gaussian distribution is a special solution to the semi-empirical diffusion equation, provided the standard deviations of concentration are related to their respective diffusion coefficients as given by Batchelor.* This implies homogeneous turbulence. Yet we stimpulate hypothetical, mathematical expressions for the standard deviations and, perhaps, even for the velocity vector as well. That is to say, we turn our backs on theory (ever so slightly) to arrive at a not-so-workable solution. If we can justify this then I suggest that we go all out and assume that the concentration field at a given time is a function of the important variables involved (i.e., vertical-temperature and velocity gradients, turbulence intensities, topographical parameters, stack conditions, pollutant parameters); and conduct a series of planned experiments, based on similarity theory, to arrive at a regression equation for urban areas. If we do have to revert to this type of approach, let us consult with systems analysts and experimental statisticians to arrive at a *universally acceptable model.*

In any event, it would be beneficial if a committee or a specialized group were set up to develop guidelines for future approaches to source-inventory, receptor-sampling, and urban diffusion modeling based on a review of the existing state of the art.

User-Oriented Design

D. H. Pack

We have heard of many advances in simulating the emission of pollutants, their transport and diffusion through the atmosphere, and the resulting concentrations. Dr. Hilst has advised us to consider carefully the purpose of any model during its design and not to expect all models to answer all questions.

It is profitable, I believe, to consider the use, and the users, of models in an organized way.

---

*Batchelor, G.K. Diffusion in a Field, of Homogeneous Turbulence. I. Eulerian Analysis Aust. J. Sci. Res. 2: 437-450. 1949.

Suppose, for example, we set up the following table for model application:

	Analyses	Prediction	Operations	Scales of:
Meteorologists				Time Space Information Resources
Control Agencies				
Planners				

A third dimension, scale, can be added for each combination of use and user.

The ultimate urban model could conceivably be used in all combinations but we must consider the paucity of information on sources and the deterioration of meteorological predictive skill with time.

It seems that, for some time to come, compromises will be necessary. To acknowledge them, each model builder should fill in the above boxes (or variants thereof) with his estimate of what the model will do and for whom it will work best. In the process, current information input, computer availability, and staff technical level should be considered among other criteria.

Such an exercise may well show that many of the models are already very successful. For unsuccessful models this approach can indicate where research effort must be applied.

General Discussion

D. Bruce Turner

Here are some miscellaneous comments that I would like to make:

— I would agree with Mr. Pack that the various models in use have been designed for different applications.

— Each researcher has verified his model in a slightly different manner making intercomparison of models difficult. Several methods of verification should be developed that could be used as standards for verification.

An additional problem in verification is that the concentrations calculated from the model represent something quite different from the concentrations measured by the sampling stations. In most models small sources are combined and calculations are made from one, uniform, area source for each grid square. The calculated concentrations are thus, more representative of an area. But measured concentrations are made at a single sampling point and are greatly influenced by nearby small sources especially those emitting at a height nearly level with the sampler intake probe . This difference between calculated and observed concentrations can be minimized by using the mean concentration from 3 or 4 sampling stations located hundreds of meters apart. The derived area-concentration may then be compared with the calculated concentration. An investigator will seldom expend his sampling equipment in this way, however, due to the cost of establishing and servicing stations.

– It appears to me that there is a "communication gap" between the researchers developing the models and those wanting to use them. There are indications that the prospective user is confusing the researchers' goals for the future uses of models with what can be done today. This may, in part, be due to the fact that the model verifications are stated in terms difficult for the laymen to understand readily.

– The spatial variation of air pollution is extremely complex because of the great number of air pollution sources in urban areas. Only the gross details of this variation can be revealed by air quality sampling because cost and manpower limit the number of samplers that can be applied. It is desirable to complement air quality monitoring with dispersion modeling to obtain isopleths of concentration. Since air quality is the product of the micro enviroment, it is always possible to go to a smaller scale and find many more details in the concentration field. Therefore, one has to decide on the space scale suitable for the detail one wants to observe and conduct the emission inventory, as well as the model computations, commensurate with that scale.

– The models that have been presented at this symposium haven't considered photochemistry. There is a need to have dispersion models that can be applied to reactive pollutants and their products. Since most models presented here assume that the contribution to the concentration at a receptor from each source can be determined independent of emissions from other sources, I doubt if these models will be useful for other than relatively unreactive substances. It appears that a different approach from normally distributed puffs or plumes is required to model reactive substances.

– A statement was made at this symposium to the effect that computer technology was available that had not yet been used. I would like to disagree with that statement because I know of a number of researchers who have used computers that could be considered in the category with the largest and fastest computers in this country, yet they have had to devise short cuts to use these computers to make calculations of air pollutant concentrations at reasonable cost and in a reasonable length of time. I believe that as advances in computer technology become available, they will be put to use by researchers formulating dispersion models.

– There is certainly room for more simplified models, especially in the area of community planning, where estimates of air quality for future decades is of interest. Models whose calculations can be made with desk calculators, for example, will find wide application when developed.

– A request was made to tailor dispersion model output to the user; specifically, to determine how frequently a given pollutant concentration is exceeded. Dr. Fortak's model for Bremen gives information of this type at specific points. I can certainly see its utility to control officials and planners.

– One item related to the success of dispersion modeling, which has not been mentioned at this symposium, is the computation of plume rise above the physical stack. Although several currently used plume rise equations do rather well when averaged over a number of trials, we still need improvement in hour-to-hour calculations of plume rise. Since many air pollution control strategies emphasize the difference between elevated and low-level sources, there is a critical need for models that can be used with equal reliability on both low-level and elevated sources. This, of course, gets one into all the difficulties involved in windspeed and direction, shear, and other measurements pointed out by Dr. Lettau.

15. APPENDIX
ATTENDANCE LIST

Dr. Donald D. Adrian
Civil Engineering Department
School of Engineering
University of Massachusetts
Amherst, Massachusetts 01003

Dr. Walter D. Bach, Jr.
Research Triangle Institute
Research Triangle Park, N. C. 27709

Dr. Eugene W. Bierly
Program Director of Meteorology
Atmospheric Sciences Section
National Science Foundation
Washington, D. C. 20550

Mr. F. T. Bodurtha
Senior Consultant
Environmental Control
Louviers Building
E. I. Du Pont de Nemours & Co.
Wilmington, Delaware 29898

Dr. W. A. Bowman
Lockheed Missiles & Space Co.
Huntsville Research and
Engineering Center
P. O. Box 1103 West Station
Huntsville, Alabama 35807

Dr. Al Boyer
Officer-in-Charge of Meteorology
Air Management Branch, Sixth Floor
Ontario Department of Energy and
Resources Management
1 St. Clair Avenue West
Toronto 195, Ontario

Mr. Edward W. Burt
Meteorologist
Air Pollution Control
Office
3820 Merton Drive
Raleigh, N. C. 27609

Mr. Kenneth L. Calder, ESSA
Chief Scientist
Division of Meteorology
Air Pollution Control
Office
3820 Merton Drive
Raleigh, N. C. 27609

Dr. J. E. Cermak
Engineering Mechanics
Department of Civil Engineering
Colorado State University
Fort Collins, Colorado 80521

Dr. Jack Chaddock
Chairman
Mechanical Engineering Department
Duke university
Durham, N. C. 27706

Mr. Anton Chaplin
Litton Systems, Inc.
Applied Technology Division
354 Dawson Drive
Camarillo, California 93101

Dr. L. A. Clarenburg
Rijnmond Authority
Schiedam
The Netherlands

Dr. Alan Cole
Earth Sciences Department
Northern Illinois University
De Kalb, Illinois 60115

Dr. H. E. Cramer
Director
Environmental Sciences Laboratory
GCA Technology
P. O. Box 15009
Salt Lake City, Utah 84115

Dr. Gabriel T. Csanady
Meteorology and Space Science
Building
The University of Wisconsin
1225 West Dayton Street
Madison, Wisconsin 53706

Mr. Margaret Day
Manager, Research Systems Analysis
Meteorology Research, Inc.
464 West Woodbury Road, Box 637
Altadena, California 91001

Mr. James L. Dicke
Meteorologist
Office of Manpower Development
Air Pollution Control
Office
Research Triangle Park, N. C. 27709

Dr. Authur Dodd
Meteorologist
Army Research Office
Duke University
Durham, North Carolina 27706

Dr. Rudolf J. Engelmann
Acting Chief
Fallout Studies Branch
Division of Biology and Medicine
U. S. Atomic Energy Commission
Washington, D. C. 20545

Dr. R. M. Felder
Department of Chemical Engineering
School of Engineering
North Carolina State University
Raleigh, N. C. 27607

Dr. Bruno Finzi-Contini
Istituto di Fisica Tecnica
Universita Degli Studi di Trieste
Facolta Di Ingegneria
Via Alfonso Valerio 10, Italy

Dr. Heinz Fortak
Institute fur Theoretische
Meteorologie
Der Freien Universitat Berlin
1 Berlin 33
Thielallsee 49
Federal Republic of Germany

Dr. David Fraser
Department of Environmental
Science & Engineering
School of Public Health
University of North Carolina
Chapel Hill, N. C. 27514

Dr. Burton Freeman
Vice-President
Systems, Science, & Software
P. O. Box 1620
La Jolla, California 92037

Mr. Francois N. Frenkiel
Naval Ship Research and
Development Center
Washington, D. C. 20007

Dr. James P. Friend
Atmospheric Chemistry
Department of Meteorology and
Oceanography
School of Engineering and Science
New York University
Geophysical Sciences Laboratory
2455 Sedgwick Avenue
Bronx, New York 10468

Dr. J. Gavis
Department of Environmental
Engineering
The Johns Hopkins University
Baltimore, Maryland 21218

Dr. F. A. Gifford, Jr.
Director, Air Resources Atmospheric
Turbulence and Diffusion
Laboratory
U. S. Department of Commerce
Post Office Box E
Oak Ridge, Tennessee 37830

Dr. James Halitsky
Senior Research Scientist
School of Engineering and Science
New York University
University Heights, Bronx, N. Y. 10453

Mr. Harry Hamilton
Engineering and Environmental
Sciences Division
Research Triangle Institute
P. O. Box 12194
Research Triangle Park, N. C. 27709

Mr. Steven Hanna
Air Resources Atmospheric
Turbulence and Diffusion
Laboratory
Cheyenne Hall Building
P. O. Box E
Oak Ridge, Tennessee 37831

Dr. George Herbert
President
Research Triangle Institute
P. O. Box 12194
Research Triangle Park, N. C. 27709

Dr. Glenn R. Hilst
Executive Vice-President
The Travelers Research Corporation
250 Constitution Plaza
Hartford, Connecticut 06103

Mr. G. C. Holzworth
Chief, Air Pollution Geophysics
Research Branch
Air Pollution Control
Office
3820 Merton Drive
Raleigh, N. C. 27609

Dr. Walter Hoydysh
School of Engineering & Science
New York University
Bronx, New York 10453

Mr. Harvey Jeffries
Department of Environmental Sciences
and Engineering
University of North Carolina
Chapel Hill, North Carolina 27514

Mr. Robert M. Jimeson
Physical Sciences Administration
Air Pollution Control
Office
801. N. Randolph St.
Arlington, Virginia 22203

Dr. Warren B. Johnson, Jr.
Senior Research Meteorologist
Aerophysics Laboratory
Stanford Research Institute
Menlo Park, California 94025

Mr. Edward W. Klappenbach
Senior Meteorologist
City of Chicago Department of
Air Pollution Control
320 North Clark Street
Chicago, Illinois 60610

Kr. Kenneth Knoerr
School of Forestry
Duke University
Durham, N. C. 27706

Dr. Richard J. Kopec
Department of Geography
University of North Carolina
Chapel Hill, N. C. 27514

Dr. Heinz H. Lettau
Department of Meteorology
University of Wisconsin
Meteorology and Space Science Bldg.
1225 West Dayton Street
Madison, Wisconsin 53076

Mr. Denis M. Lohman
Chief, Meteorology Section
Penn. Bureau of Air Pollution Control
P. O. Box 90
Harrisburg, Pennsylvania 17120

Dr. Lester Machta
Director, Air Resources Laboratories
Environmental Science Services
Administration
U. S. Department of Commerce
Silver Spring, Maryland 20910

Dr. James R. Mahoney
Assistant Professor of Applied
Meteorology
Harvard University School of
Public Health
Kresge Center for Environmental
Health
Department of Industrial Hygiene
665 Huntington Avenue
Boston, Massachusetts 02115

Dr. David B. Marsland
Department of Chemical Engineering
School of Engineering
North Carolina State University
Raleigh, N. C. 27607

Mr. Robert A. McCormick
Director Meteorology Program
Air Pollution Control
Office
3820 Merton Drive
Raleigh, N. C. 27609

Mr. Douglas L. McKay
Department of Environmental
Sciences and Engineering
University of North Carolina
Chapel Hill, North Carolina 27514

Dr. John T. Middleton
Commissioner
Air Pollution Control
Office
801 North Randolph Street
Arlington, Virginia 22203

Dr. David Moreau
Department of City and Regional
Planning
University of North Carolina
Chapel Hill, N. C. 27514

Mr. Paul Morgenstern
Environmental Sciences and Technology
Waldin Research Corporation
359 Allston Street
Cambridge, Massachusetts 02139

Dr. William J. Moroz
Director
Center for Air Environment Studies
Pennsylvania State University
226 Chemical Engineering II
University Park, Pennsylvania 16802

Mr. Harry Moses
Argonne National Laboratory
9700 South Cass Avenue
Argonne, Illinois 60439

Dr. J. C. Mulligan
Mechanical and Aerospace Engineering
North Carolina State University
Raleigh, N. C. 27607

Dr. R. E. Munn
Meteorological Branch
Department of Transport
315 Bloor Street, West
Toronto, 5, Ontario

Dr. C. R. Murthy
Physical Limnology Section
Department of Energy, Mines and
Resources
Canada Centre for Inland Waters
Great Lakes Division
P. O. Box 5050
867 Lakeshore Road
Burlington, Ontario

Dr. Charles O'Melia
Department of Environmental
Sciences and Engineering
University of North Carolina
Chapel Hill, N. C. 27514

Dr. Morris Neiburger
Department of Meteorology
University of California
Los Angeles, California 90024

Mr. Lawrence E. Niemeyer, ESSA
Assistant Director
Division of Meteorology
Air Pollution Control
Office
3820 Merton Drive
Raleigh, N. C. 27609

Mr. Donald H. Pack
Deputy Director
Air Resources Laboratory
Environmental Science Services
Administration
Silver Springs, Maryland 20910

Dr. Frank Pasquill
Meteorological Office
London Road
Bracknell, Berkshire, England

Mr. Francis Pooler
Chief, Boundary Layer Dynamic
Research Branch
Division of Meteorology
Air Pollution Control
Office
3820 Merton Drive
Raleigh, N. C. 27609

Dr. Darryl Randerson
ESSA-ARL
P. O. Box 14985
Las Vegas, Nevada 89114

Dr. John J. Roberts
Reactor Engineering Division
Argonne National Laboratory
9700 South Cass Avenue
Argonne, Illinois 60439

Dr. G. D. Robinson
Director, Environmental Physics
and Chemistry
The Travelers Research Corporation
250 Constitution Plaza
Hartford, Connecticut 06103

Dr. Shin'ichi Sakuraba
Meteorological Research Institute
Koenji Kita 4-35-8, Suginami-ku,
Tokyo, Japan

Dr. Walter J. Saucier
Department of Geosciences
North Carolina State University
Raleigh, N. C. 27607

Dr. Jabbar K. Sherwani
Department of Environmental
Sciences and Engineering
School of Public Health
University of North Carolina
Chapel Hill, N. C. 27514

Dr. L. J. Shieh
Scientific Center, IBM
2670 Hanover Street
Palo Alto, California

Mr. Conrad Simon
Senior Meteorologist
City of New York Department of
Air Resources
51 Astor Place
New York, N. Y. 10003

Mr. Irving A. Singer
Meteorology Group
Brookhaven National Laboratory
Associated Universities, Inc.
Upton, Long Island,
New York 11973

Dr. Ralph C. Sklarew
Systems, Science and Software
P. O. Box 1620
La Jolla, California 92037

Mr. David Slade
Fallout Studies Branch
Division of Biology and Medicine
U. S. Atomic Energy Commission
Washington, D. C. 20545

Dr. P. R. Slawson
Department of Mechanical Engineering
Faculty of Engineering
University of Waterloo
Waterloo, Ontario, Canada

Dr. William H. Snyder
Physical Scientist
Division of Meteorology
Air Pollution Control
Office
3820 Merton Drive
Raleigh, N. C. 27609

Dr. F. Y. Sorrell
Department of Engineering Mechanics
School of Engineering
North Carolina State University
Raleigh, N. C. 27607

Dr. Tom Stephens
Southern Research Institute
2000 9th Avenue, South
Birmingham, Alabama 35202

Prof. Arthur C. Stern
Department of Environmental Sciences
and Engineering
School of Public Health
University of North Carolina
Chapel Hill, N. C. 27514

Dr. Robert E. Stewart
Department of Environmental
Engineering
College of Engineering
University of Florida
Gainesville, Florida 32601

Dr. Gordon Strom
School of Engineering & Science
New York University
Bronx, New York 10453

Dr. John L. Sullivan
Environmental Engineering
Syracuse University
Syracuse, New York 13210

Dr. Hale Sweeny
Statistics Research Division
Engineering and Environmental
Sciences Division
Research Triangle Park, N. C. 27709

Dr. Peter A. Taylor
Department of Mathematics
University of Toronto
Toronto 5, Ontario, Canada

Mr. Joseph A. Tikvart
Meteorologist
Air Pollution Control
Office
3820 Merton Drive
Raleigh, N. C. 27609

Mr. Donald B. Turner
Meteorologist
Air Pollution Control
Office
3820 Merton Drive
Raleigh, N. C. 27609

Dr. Edward Ungar
Divisional Chief of Fluid and Gas
Dynamics
Battelle Institute
Columbus, Ohio 43201

Dr. Reginald I. Vachon
Mechanical Engineering Department
Auburn University
Auburn, Alabama 36830

Mr. E. A. Ward
TRW, Inc.
Washington Operations
1735 I Street, N. W.
Washington, D. C. 20006

Mrs. M. L. Weatherley
Warren Spring Laboratory
Ministry of Technology
Dudley House, Endell Street
London W. C. 2
England

Dr. Willis L. Webb
Atmospheric Sciences Laboratory
White Sands Missile Range
White Sands, New Mexico

Dr. Allen H. Weber
Department of Geosciences
North Carolina State University
Raleigh, N. C. 27607

Dr. Larry Wendell
Atomic Energy Commission
Box 2108
Idaho Falls, Idaho 83401

Dr. Daniel Werner
Mechanical Engineering
Duke University
Durham, N. C. 27706

Dr. James J. B. Worth
Associate Director of Engineering
Research Triangle Institute
Research Triangle Park, N. C. 27709